CHANGING PLANKTON COMMUNITIES: CAUSES, EFFECTS AND CONSEQUENCES

EDITED BY: Kristian Spilling, Letizia Tedesco, Riina Klais and Kalle Olli
PUBLISHED IN: Frontiers in Marine Science

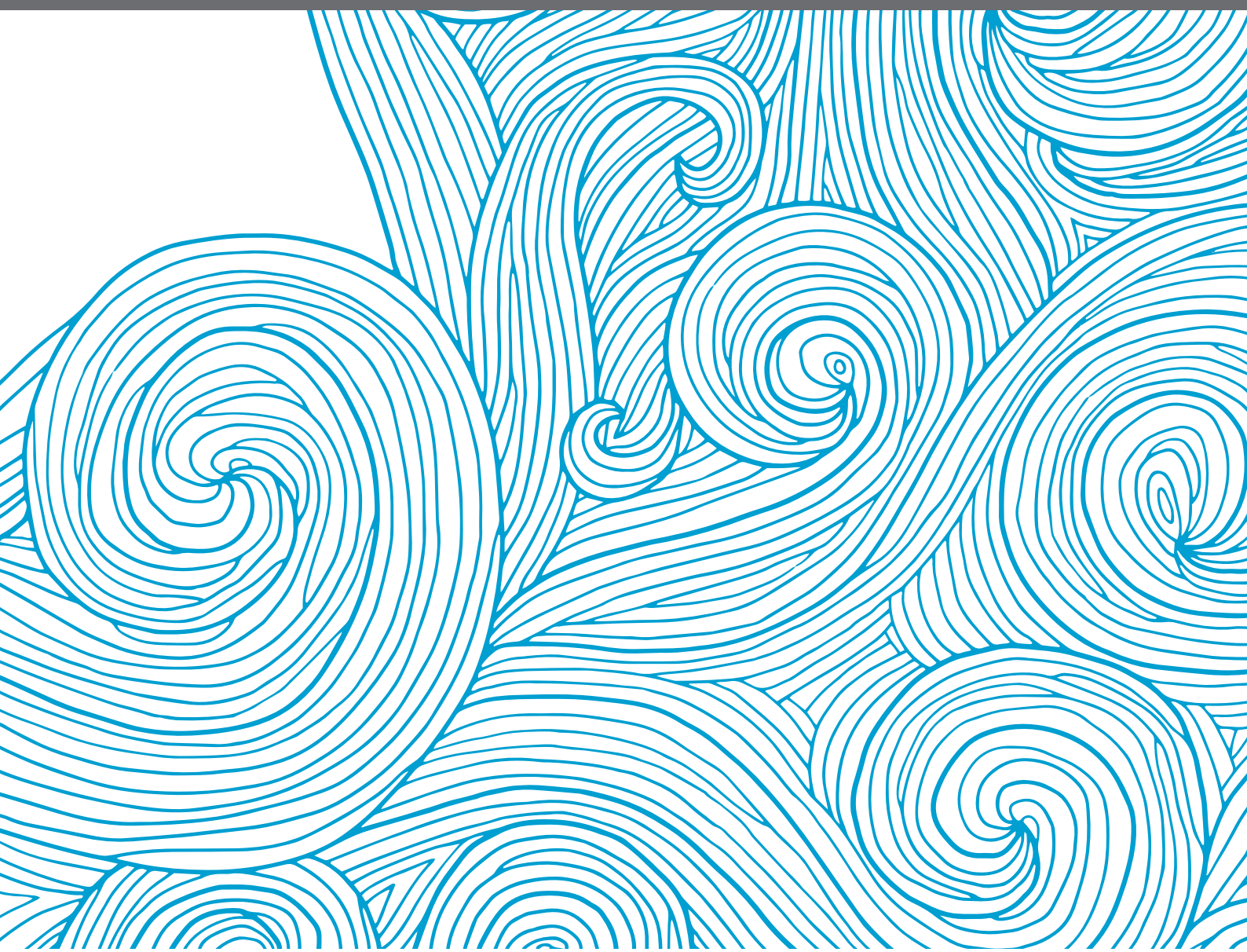

frontiers Research Topics

frontiers

ISSN 1664-8714
ISBN 978-2-88963-042-4
DOI 10.3389/978-2-88963-042-4

About Frontiers

Frontiers is more than just an open-access publisher of scholarly articles: it is a pioneering approach to the world of academia, radically improving the way scholarly research is managed. The grand vision of Frontiers is a world where all people have an equal opportunity to seek, share and generate knowledge. Frontiers provides immediate and permanent online open access to all its publications, but this alone is not enough to realize our grand goals.

Frontiers Journal Series

The Frontiers Journal Series is a multi-tier and interdisciplinary set of open-access, online journals, promising a paradigm shift from the current review, selection and dissemination processes in academic publishing. All Frontiers journals are driven by researchers for researchers; therefore, they constitute a service to the scholarly community. At the same time, the Frontiers Journal Series operates on a revolutionary invention, the tiered publishing system, initially addressing specific communities of scholars, and gradually climbing up to broader public understanding, thus serving the interests of the lay society, too.

Dedication to Quality

Each Frontiers article is a landmark of the highest quality, thanks to genuinely collaborative interactions between authors and review editors, who include some of the world's best academicians. Research must be certified by peers before entering a stream of knowledge that may eventually reach the public - and shape society; therefore, Frontiers only applies the most rigorous and unbiased reviews.
Frontiers revolutionizes research publishing by freely delivering the most outstanding research, evaluated with no bias from both the academic and social point of view. By applying the most advanced information technologies, Frontiers is catapulting scholarly publishing into a new generation.

What are Frontiers Research Topics?

Frontiers Research Topics are very popular trademarks of the Frontiers Journals Series: they are collections of at least ten articles, all centered on a particular subject. With their unique mix of varied contributions from Original Research to Review Articles, Frontiers Research Topics unify the most influential researchers, the latest key findings and historical advances in a hot research area! Find out more on how to host your own Frontiers Research Topic or contribute to one as an author by contacting the Frontiers Editorial Office: researchtopics@frontiersin.org

CHANGING PLANKTON COMMUNITIES: CAUSES, EFFECTS AND CONSEQUENCES

Topic Editors:
Kristian Spilling, Finnish Environment Institute (SYKE), University of Helsinki, Finland and University of Agder, Norway
Letizia Tedesco, Finnish Environment Institute (SYKE), Finland
Riina Klais, University of Tartu, Estonia
Kalle Olli, University of Tartu and Estonian University of Life Sciences, Estonia

Marine ecosystems are changing at an unprecedented rate. In addition to the direct effects of e.g. warming surface temperatures, the environmental changes also cause shifts in plankton communities. Plankton makes up the base of the marine food web and plays a pivotal role in global biogeochemical cycles. Any shifts in the plankton community composition could have drastic consequences for marine ecosystem functioning. This Research Topic focuses on causes, effects and consequences of such shifts in the plankton community structure.

Citation: Spilling, K., Tedesco, L., Klais, R., Olli, K., eds. (2019). Changing Plankton Communities: Causes, Effects and Consequences. Lausanne: Frontiers Media. doi: 10.3389/978-2-88963-042-4

Table of Contents

III. ZOOPLANKTON

IV. THEORY AND METHODS

frontiers in Marine Science

EDITORIAL
published: 28 May 2019
doi: 10.3389/fmars.2019.00272

Editorial: Changing Plankton Communities: Causes, Effects and Consequences

Kristian Spilling[1,2,3*], *Letizia Tedesco*[1], *Riina Klais*[4] and *Kalle Olli*[4,5]

[1] Finnish Environment Institute (SYKE), Helsinki, Finland, [2] Tvärminne Zoological Station, Faculty of Biological and Environmental Sciences, University of Helsinki, Hanko, Finland, [3] Faculty of Engineering and Science, University of Agder, Kristiansand, Norway, [4] Institute of Ecology and Earth Sciences, University of Tartu, Tartu, Estonia, [5] Institute of Agricultural and Environmental Sciences, Estonian University of Life Sciences, Tartu, Estonia

Keywords: phytoplankton, ciliates, zooplankton, marine bacteria, marine ecosystems, biogeochemical cycles, global change

Editorial on the Research Topic

Changing Plankton Communities: Causes, Effects and Consequences

Marine ecosystems are changing in response to multiple stressors such as global warming, increasing carbon dioxide (CO_2) and decreasing oxygen (O_2) concentrations and eutrophication of coastal waters, among others. The direct effects of these changes on plankton physiology have been studied for decades; less are known about possible effects these changes might have on the composition of plankton communities, and even less about what effects any such shift in plankton community composition will have on marine ecosystems. The plankton community makes up the base of the marine food web (i.e., primary producers, decomposers, and primary consumers) and plays a pivotal role in global biogeochemical cycles (e.g., Falkowski and Raven, 2013). Any change of the plankton community structure, driven by natural or human induced changes, may consequently have indirect effects on marine ecosystem functioning.

This Research Topic focused on causes, effects and consequences of changing composition of plankton communities. The 12 contributions to this volume include seven original research papers, one method paper, and four reviews; all touching the state-of-the-art in current plankton research, and each from a complementary angle.

Several of the original research papers deal with changing phytoplankton communities, environmental drivers and ecosystem effects. Fernández-Méndez et al. analyzed sea-ice ridges and the snow-ice interface, which are algal hotspots in the Arctic Ocean. Both sea-ice ridges and the snow-ice interface are projected to increase due to thinning of the ice, and Fernández-Méndez et al. described the algal communities, mostly dominated by different diatoms, in these habitats in the Arctic. von Scheibner et al. examined the phytoplankton and bacterioplankton response to short-term warming. Warming increased carbon availability for the bacterial community, but the ratio between bacterial and primary production was still relatively low, suggesting it is not much changed by short-term warming events. Cohen et al. described diatom transcriptional and physiological responses to changes in iron availability in the open Northeast Pacific Ocean and in the California upwelling system. They found species specific differences in gene expression to changes in nutrient availability and taxa specific strategies for coping with Fe stress. Ajani et al. investigated the realized niches of phytoplankton using a long-term data set collected off Eastern Australia. They demonstrated that the ecological niches can be dynamic and that climate change models cannot use fixed niches when forecasting the phytoplankton community composition.

Edited and reviewed by:
Angel Borja, Centro Tecnológico Experto en Innovación Marina y Alimentaria (AZTI), Spain

***Correspondence:**
Kristian Spilling
kristian.spilling@environment.fi

Specialty section:
This article was submitted to Marine Ecosystem Ecology, a section of the journal Frontiers in Marine Science

Received: *22 March 2019*
Accepted: *07 May 2019*
Published: *28 May 2019*

Citation:
Spilling K, Tedesco L, Klais R and Olli K (2019) Editorial: Changing Plankton Communities: Causes, Effects and Consequences. Front. Mar. Sci. 6:272. doi: 10.3389/fmars.2019.00272

There are three original research papers on zooplankton dynamics. Lips and Lips investigated the increasing importance of the mixotrophic ciliate *Mesodinium rubrum* in the Baltic Sea. The abundance of this species was higher in years of earlier warming and the authors suggest that it plays an important role in shaping the inorganic nutrient pools at the start of the summer (Lips and Lips). Haraguchi et al. studied the coupling between phytoplankton and ciliates in Danish waters over 2 years, and demonstrated a close coupling between these communities, suggesting top down control of the phytoplankton community by the ciliates. Karlsson and Winder examined ecosystem effects of two locally adapted populations of the filter feeding copepod *Eurytemora affinis* that differed in size. They demonstrated that morphologically divergent populations of the same species can perform different ecosystem functions through differences in quantitative and qualitative feeding, and by having different population response to changes in resource supply and the phytoplankton community composition.

In the method paper by Engel et al., they tested three different ways to manipulate species loss in natural phytoplankton communities. Dilution, filtration, and heat stress was used to remove rare, large and sensitive species, respectively, and this can be used as a method for non-random species manipulation in experiments. The majority of research on species loss has used the approach of random species removal, which may not be a suitable approach for studies of fragile species. The method development and standardization of approaches suggested by Engel et al. are essential for more realistic species loss modeling.

The review papers covered different aspects of plankton dynamics and trait-based approaches. Lindh and Pinhassi presented a comprehensive review of bacterioplankton communities in the Baltic Sea and environmental drivers for community changes based on field and experimental studies. Bartoli et al. reviewed the drivers of cyanobacterial blooms in the Curonian Lagoon (Baltic Sea), where cyanobacteria has benefitted from long term increase in the temperature and reduction in the inorganic N:P ratio. A comparison of the differences between freshwater and marine studies of phytoplankton traits and community assembly is presented by Weithoff and Beisner. Finally, Spilling et al. reviewed and synthesize state-of-the-art knowledge on the observed, long-term increase in dinoflagellate abundance in the Baltic Sea during spring bloom and the consequences the shift from diatom to dinoflagellate dominance has for biogeochemical cycles.

The topics of the papers published in this Research Topic ranged from heterotrophic bacteria, phytoplankton to zooplankton and covered different marine ecosystems. The potential shift in community composition may have dramatic effects on ecosystem functioning, for example on trophic transfer, and on biogeochemical fluxes through changes in export of organic material, i.e., the biological pump. One of the key challenges for predicting changes to the plankton community is to understand the various functional groups and their niche separation in combination with individual taxa's ability to acclimate, adapt and compete in a changing environment. This trait-based community ecology of plankton has started to gain traction (Litchman and Klausmeier, 2008; Litchman et al., 2013), and is a useful framework to investigate potential effects of environmental change on plankton community structure. In order to disentangle the potential consequences of shifts in plankton communities, more empirical studies of ecological interactions and export are needed. Hence, we consider the research papers in this Research Topic will be a valuable addition to the accumulating empirical evidence of how plankton communities are modulated by natural and human induced changes and the indirect effect this has on marine ecosystems.

AUTHOR CONTRIBUTIONS

All authors listed have made a substantial, direct and intellectual contribution to the work, and approved it for publication.

FUNDING

This editorial is a result of funding from the Academy of Finland (decisions no 259164, KS and LT), the Estonian Research Council (no 1574P, KO) and the EU BONUS program (grant agreement 2112932-1, LT).

ACKNOWLEDGMENTS

We thank all the contributing authors and reviewers to this Research Topic and the editorial team at Frontiers in Marine Sciences.

REFERENCES

Falkowski, P. G., and Raven, J. A. (2013). *Aquatic Photosynthesis, 2nd Edn.* Princeton, NJ: Princeton University Press.

Litchman, E., and Klausmeier, C. A. (2008). Trait-based community ecology of phytoplankton. *Annu. Rev. Ecol. Evo. Syst.* 39, 615–639. doi: 10.1146/annurev.ecolsys.39.110707.173549

Litchman, E., Ohman, M. D., and Kiørboe, T. (2013). Trait-based approaches to zooplankton communities. *J. Plankton Res.* 35, 473–484. doi: 10.1093/plankt/fbt019

Conflict of Interest Statement: RK was previously employed by the University of Tartu but is at present affiliated with the company EcoStat Ltd.

The remaining authors declare that the research was conducted in the absence of any commercial or financial relationships that could be construed as a potential conflict of interest.

frontiers in Marine Science

REVIEW
published: 10 October 2018
doi: 10.3389/fmars.2018.00361

Sensitivity of Bacterioplankton to Environmental Disturbance: A Review of Baltic Sea Field Studies and Experiments

Markus V. Lindh[1,2] *and Jarone Pinhassi*[1]*

[1] Centre for Ecology and Evolution in Microbial Model Systems—EEMiS, Linnaeus University, Kalmar, Sweden, [2] Swedish Meteorological and Hydrological Institute, Gothenburg, Sweden

Bacterioplankton communities regulate energy and matter fluxes fundamental to all aquatic life. The Baltic Sea offers an outstanding ecosystem for interpreting causes and consequences of bacterioplankton community composition shifts resulting from environmental disturbance. Yet, a systematic synthesis of the composition of Baltic Sea bacterioplankton and their responses to natural or human-induced environmental perturbations is lacking. We review current research on Baltic Sea bacterioplankton dynamics *in situ* (48 articles) and in laboratory experiments (38 articles) carried out at a variety of spatiotemporal scales. *In situ* studies indicate that the salinity gradient sets the boundaries for bacterioplankton composition, whereas, regional environmental conditions at a within-basin scale, including the level of hypoxia and phytoplankton succession stages, may significantly tune the composition of bacterial communities. Also the experiments show that Baltic Sea bacteria are highly responsive to environmental conditions, with general influences of e.g. salinity, temperature and nutrients. Importantly, nine out of ten experiments that measured both bacterial community composition and some metabolic activities showed empirical support for the *sensitivity* scenario of bacteria—i.e., that environmental disturbance caused concomitant change in both community composition and community functioning. The lack of studies empirically testing the *resilience* scenario, i.e., experimental studies that incorporate the long-term temporal dimension, precludes conclusions about the potential prevalence of resilience of Baltic Sea bacterioplankton. We also outline outstanding questions emphasizing promising applications in incorporating bacterioplankton community dynamics into biogeochemical and food-web models and the lack of knowledge for deep-sea assemblages, particularly bacterioplankton structure-function relationships. This review emphasizes that bacterioplankton communities rapidly respond to natural and predicted human-induced environmental disturbance by altering their composition and metabolic activity. Unless bacterioplankton are resilient, such changes could have severe consequences for the regulation of microbial ecosystem services.

Keywords: bacterial diversity, archaea, 16S rRNA, metabolic activity, ecosystem functioning, climate change

OPEN ACCESS

Edited by:
Kristian Spilling, Finnish Environment Institute (SYKE), Finland

Reviewed by:
Hermanni Kaartokallio, Finnish Environment Institute (SYKE), Finland
Stilianos Fodelianakis, King Abdullah University of Science and Technology, Saudi Arabia

***Correspondence:**
Jarone Pinhassi
jarone.pinhassi@lnu.se

Specialty section:
This article was submitted to Marine Ecosystem Ecology, a section of the journal Frontiers in Marine Science

Received: *03 May 2018*
Accepted: *19 September 2018*
Published: *10 October 2018*

Citation:
Lindh MV and Pinhassi J (2018) Sensitivity of Bacterioplankton to Environmental Disturbance: A Review of Baltic Sea Field Studies and Experiments. Front. Mar. Sci. 5:361. doi: 10.3389/fmars.2018.00361

BACTERIOPLANKTON COMMUNITY AND FUNCTIONAL DYNAMICS

Bacterioplankton communities have a remarkable capability in responding to environmental disturbances, such as changes in temperature, salinity and nutrients (Allison and Martiny, 2008; Logares et al., 2013; Cram et al., 2015; Salazar et al., 2016). Rapid responses are made possible thanks to relatively short generation times, and involve both adjustments in metabolic activity and restructuring of *community composition* (**Box 1**; Allison and Martiny, 2008; Brettar et al., 2016). There is now ample evidence that bacterioplankton activity and community composition play central roles in regulating biogeochemical cycles of elements, with particular focus on carbon in the form of dissolved organic matter (DOM) and dissolved organic carbon (DOC; Azam and Malfatti, 2007; Falkowski et al., 2008).

Given the importance of bacterioplankton-driven cycling of carbon, a fundamental question in microbial ecology is whether shifts in bacterioplankton community composition resulting from changes in environmental conditions also lead to changes in ecosystem functioning (Loreau, 2000, 2004; Langenheder et al., 2010; Comte and Del Giorgio, 2011; Beier et al., 2017). Bacterioplankton communities could, in theory, respond to environmental disturbances according to three scenarios termed *sensitivity*, *resistance*, and *resilience* [**Box 2**; *sensu* Allison and Martiny (2008); Shade et al. (2012)]. Each of these scenarios have distinctly different implications regarding how we interpret the consequences of environmental disturbances on the linkages between shifts in community composition and changes in community functioning. Ecosystem stability is linked with a community's response to disturbance. The stability depends on the *sensitivity*, *resistance* (insensitivity to disturbance), and the *resilience* (ability to return to original condition after disturbance) of the ecosystem (Shade et al., 2012). A disturbance is an event that can influence the community in pulses (discrete short-term events) or presses (long-term or continuous events). Shade et al. (2012) carried out a literature review to investigate bacterioplankton community responses to such disturbances in a variety of habitats. The authors identified that bacterioplankton communities are, in general, sensitive to disturbances but highlighted that empirical tests of *resilience*, i.e., studies that explicitly and comprehensively included the temporal dimension, were lacking.

THE BALTIC SEA AND PREDICTED CLIMATE CHANGE

The shallow brackish Baltic Sea system, with an average depth of ∼54 m, varies in both hydrology and physicochemical features; it consists of a 2,000 km long salinity gradient ranging from truly marine to freshwater conditions through several basins of which three are major (the *Baltic Sea Proper*, the *Bothnian Sea,* and the *Bothnian Bay*; Omstedt et al., 2014). In addition to strong shifts in salinity, Baltic Sea basins are affected by different magnitudes of river discharges, transferring freshwater, and terrestrial DOM, so-called allochthonous DOM (i.e., DOM transported into the sea from terrestrial sources; Kritzberg et al., 2004), to coastal waters, with seasonal variation (Omstedt et al., 2014; Rowe et al., 2018). The Baltic Sea is periodically affected by seasonal phytoplankton blooms, including typical diatom/dinoflagellate spring blooms and massive blooms of cyanobacteria in summer (Legrand et al., 2015), producing so-called autochthonous DOM (i.e., DOM produced *in situ* by e.g., phytoplankton; Kritzberg et al., 2004).

Projections of human-induced climate change in aquatic environments, with global temperature increases of 1.4–5.8°C and a global atmospheric CO_2 increase of 400 atm, resulting in lower pH by ∼0.4 units until 2,100, implicate that ecosystem changes of unparalleled extent will occur (Brettar et al., 2016). In the Baltic Sea region the Swedish meteorological and hydrological institute (SMHI) projects increased precipitation by up to 48% until 2,100, leading to lower salinities and increased output of allochthonous matter from river discharge (Meier, 2006). Moreover, cyanobacterial blooms are increasing in magnitude due to human-driven climate change and the hydrography of this semi-enclosed system (Omstedt et al., 2014; Legrand et al., 2015). Eutrophication brings excess nutrients to the microbial food web, stimulating phytoplankton blooms that in turn influence the bacteria, resulting in increased community respiration rates through the degradation of phytoplankton DOM that sinks and ultimately causes bottom water and sediment hypoxia (Tamelander et al., 2017). Decreasing oxygen levels (<2 mg ml^{-1} O_2) at the seafloor and in sediments of the Baltic Sea have been documented in the last 100 years and decreases are predicted to intensify in the future (Carstensen et al., 2014). Taken together, future selective forces in the marine environment will include, among others, increased sea surface temperatures, lower pH, eutrophication, hypoxia, increased allochthonous carbon inputs, decreased salinity, and massive cyanobacterial blooms (Andersson et al., 2015). Thus, the Baltic Sea offers a unique study system to investigate, in depth, both the causes and consequences of shifts in bacterioplankton community composition and functioning responding to environmental perturbations.

OVERVIEW OF BALTIC SEA BACTERIOPLANKTON STUDIES

We identified a total of 86 articles carrying out field studies and/or experiments focusing on bacterioplankton community composition in the Baltic Sea, as summarized in **Table 1** and **Figure 1**. Studies performed in the Skagerrak and Kattegatt seas were examined (**Supplementary Table 1**), but were not included in the main analyses. Among the Baltic Sea studies, 48 were categorized as research performed *in situ* and 38 were experimental studies at different scales (micro- or mesocosms; **Table 1**). Twenty-six articles included samples from deep-waters/sediments. Among all articles, one third ($n = 29$) included some form of activity measurement and among the *in situ* studies less than one fifth ($n = 9$) measured metabolic activity. A majority of the articles focus on spatial distributions for *in situ* data ($n = 27$; 56% of all *in situ* studies) and on the effect of nutrient additions for experimental data ($n = 22$; 58% of all experimental studies; **Table 1**). The conducted studies have been performed throughout the Baltic Sea and include empirical evidence of shifts

BOX 1 | Determining bacterioplankton community composition.

Marine bacteria and archaea, collectively known as *bacterioplankton*, are a fundamental part of the planktonic food-web and imperative for ecosystem functioning (Falkowski et al., 2008). *Bacterioplankton community composition* refers to the taxonomic identity of organisms and their frequency distribution in the ecosystem. However, phenotypic identification of bacterioplankton is problematic since only a small fraction of all bacterioplankton are easily cultivable and these typically do not mirror the complete bacterioplankton diversity (Pedros-Alio, 2006; Hagström et al., 2017). Microbial ecologists therefore use culture-independent genetic identification techniques to differentiate bacterioplankton taxa (see e.g., Hugerth et al., 2015; Sunagawa et al., 2015; Beier et al., 2017; Celepli et al., 2017). In general, identification of individual bacterioplankton taxa is done by sequencing of the 16S rRNA gene, ITS (Internal Transcribed Spacer) or similar genetic fragments, processing raw *sequence reads* using bioinformatic methods (see e.g., Edgar, 2013; Callahan et al., 2015) and clustering these into specific phylotypes or *operational taxonomic units* (OTUs), followed by taxon delineation at a specific sequence identity threshold (typically 97–99% sequence identity; Hugerth and Andersson, 2017). Taxonomic annotation of these OTUs is then performed by matching a type- or centroid sequence of the OTU cluster against a database with taxonomic information (see e.g., Quast et al., 2013).

Technical advances in the last decade in the form of high-throughput sequencing have increased the sequencing resolution and thereby the detection levels of individual OTUs by several orders of magnitude at rapidly decreasing costs (Poisot et al., 2013; Hugerth and Andersson, 2017). As a result, the field of microbial ecology has advanced from primarily describing major bacterioplankton groups or a few dominant populations to resolving the distribution of thousands of populations over different temporal and spatial scales. This makes bacterioplankton attractive also for monitoring and thus important for stakeholders and marine management.

BOX 2 | Bacterioplankton community responses to environmental disturbance

Below follows a brief description of three theoretical responses that bacterioplankton assemblages may undertake in the light of natural or human-induced changes in environmental conditions, *sensu* Allison and Martiny (2008), (Shade et al., 2012). The figure is laid so that it emphasizes the temporal dimension on the x-axis in the *resilience* scenario.

Sensitivity—when community composition is altered by environmental disturbance and the resulting community functioning (f_2) is typically different from the initial functioning (f_1).

Resistance—when community composition is not altered by environmental disturbance and community functioning (f_2) may be different from, or the same as the initial f_1.

Resilience—when community composition is initially altered by environmental disturbance but returns to the original composition and f_2 is typically temporally different from the initial f_1 but community functioning over time "returns to" f_3 similar to the initial f_1.

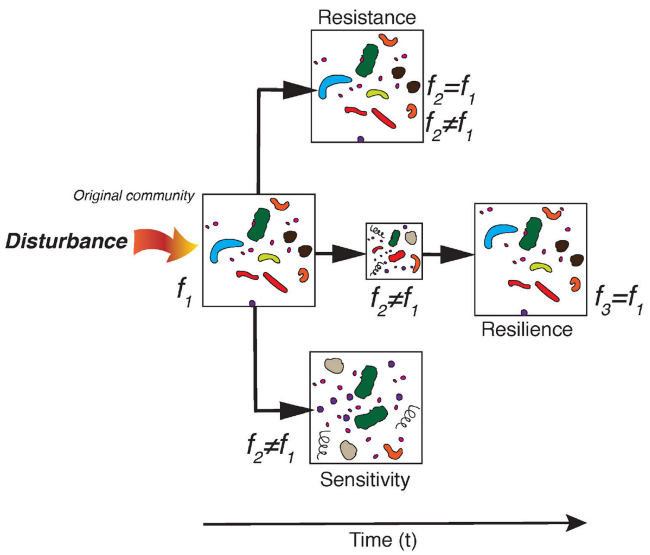

in bacterioplankton community composition in different basins (**Figure 1**). It is noteworthy that detailed temporal studies are typically limited to two sites in the Baltic Sea Proper (i.e., the Landsort Deep in the central Baltic Sea and at the Linnaeus Microbial Observatory off the coast of the island Öland in the Baltic Sea Proper) and that many deep-water/sediment samples have primarily been obtained from only two locations in the central Baltic Sea Proper (the Landsort and Gotland deeps in the central Baltic Sea; $n = 10$; 40% of all deep-water/sediment studies; **Figure 1**).

TEMPORAL AND SPATIAL VARIABILITY IN BACTERIOPLANKTON

Extended temporal studies are scarce in the Baltic Sea, but there are four published reports of bacterioplankton dynamics extending over ≥1 year at semi- to high-resolution (Pinhassi and Hagström, 2000; Riemann et al., 2008; Andersson et al., 2010; Lindh et al., 2015c). They all show pronounced shifts in bacterioplankton community composition with fairly distinct spring, summer and autumn communities. In general, Bacteroidetes dominate in spring during the diatom and dinoflagellate bloom. In summer, particular populations of e.g., Verrucomicrobia increase in abundance, associated with pronounced blooms of picocyanobacterial populations and filamentous Cyanobacteria. In autumn, actinobacterial populations proliferate, potentially following changes in temperature, mixing of the water column, and/or autumn phytoplankton blooms. Changes in temperature over the yearly cycle typically explain around 0.45 (Pearson r) of total variation in community composition (Andersson et al., 2010; Lindh et al., 2015c).

There have been three major transects studies of bacterioplankton community composition across the entire salinity gradient of the Baltic Sea, showing that changes in salinity is the major driver of the distribution of bacterial populations (OTUs) at large spatial scales in the Baltic Sea

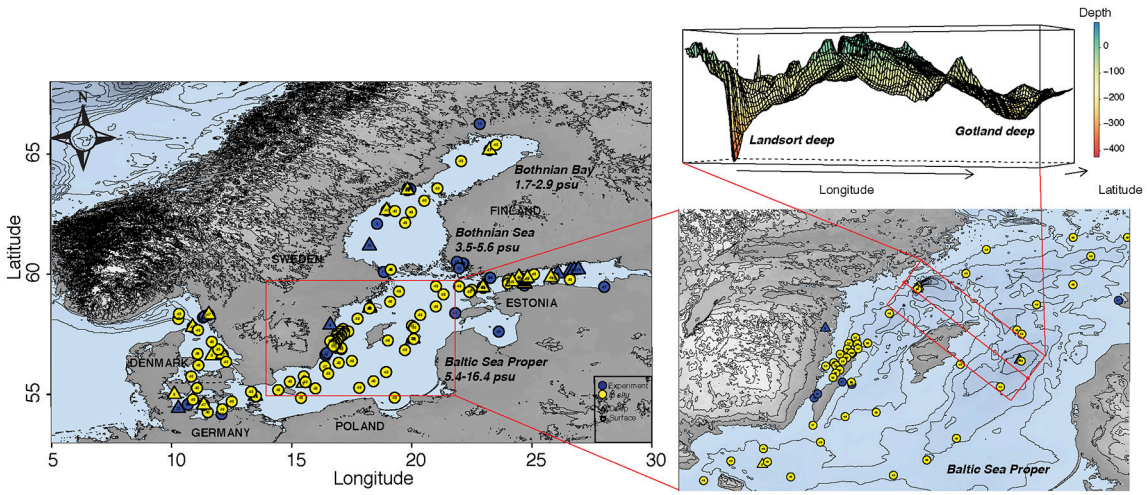

FIGURE 1 | Map showing *in situ* transects and temporally sampled stations (yellow symbols) and all stations that have been sampled for use in experimental studies with empirical evidence for the effect of natural or human-induced changes in environmental conditions on bacterioplankton community dynamics (blue symbols). Filled circles and triangles denote samples obtained from surface waters and from deep-water/sediment, respectively. Insert is a zoomed in map of the central Baltic Sea Proper with particularly many samples obtained, and a 3D rendition of the Gotland and Landsort Deep, frequently sampled to retrieve deep water and sediment samples. Dashed lines indicate boundaries for the three major basins; Bothnian Bay, Bothnian Sea and the Baltic Sea Proper. The map and bathymetry was produced using the package "marmap" (Pante and Simon-Bouhet, 2013) in R V.3.4.4 (R Core Development Team, 2017) and the bathymetry data was retrieved from NOAA (http://www.noaa.gov).

(Herlemann et al., 2011, 2016; Dupont et al., 2014; Larsson et al., 2014; Celepli et al., 2017). Notably, salinity explained almost all of the observed variation in bacterioplankton community composition with r values ranging from 0.78 to 0.97. In contrast, in a transect across one particular basin, the Baltic Sea Proper, Bunse et al. (2016a) found that, instead of salinity, the advancing phytoplankton spring bloom had a substantial influence in structuring the bacterial community (i.e., the distribution of specific OTUs). The authors emphasized how interactions between bacterioplankton and phytoplankton populations may influence carbon cycling to higher trophic levels thus extending the importance of bacterioplankton dynamics for ecosystem services. In addition, there have been several transects performed at high-resolution spatial scales of which two locations are particularly well-studied; the western Gotland Sea (Bertos-Fortis et al., 2016; Lindh et al., 2016, 2017) and the Gulf of Finland (Laas et al., 2014, 2015, 2016). For example, Bertos-Fortis et al. (2016) show that Cyanobacteria have plastic responses to changes in environmental conditions where opportunistic picocyanobacteria and N_2-fixing cyanobacteria may be able to utilize nutrients from filamentous Cyanobacteria during the summer bloom (Bertos-Fortis et al., 2016). An approach using metacommunity theory (Leibold et al., 2004) found that local environmental conditions rather than dispersal-driven assembly is the main mechanism for structuring bacterioplankton assemblages in the Baltic Sea (Lindh et al., 2016). Similarly, bacterioplankton communities in areas such as the Pacific Ocean and East China Sea are also mainly shaped by environmental factors and to a less extent by spatial factors (Yeh et al., 2015; Lindh et al., 2018). Moreover, deep-water bacterioplankton communities in the Gulf of Finland are structured by seasonally anoxic conditions where redox-specialized bacterioplankton populations proliferate (Laas et al., 2015). Surface seawater communities in that study, on the other hand, were largely assembled following variation in phytoplankton succession. Collectively, these studies indicate that whereas the salinity gradient sets the boundaries for bacterioplankton composition, regional environmental conditions at a within-basin scale, including the level of hypoxia and phytoplankton succession stages, may significantly tune the composition of bacterioplankton.

EXPERIMENTAL MANIPULATION OF ENVIRONMENTAL CONDITIONS

Salinity

The *in situ* studies described above dictate that grand scale spatial distributions of particular OTUs in the Baltic Sea are driven by changes in salinity. In accordance, manipulated changes in salinity in micro- and mesocosm experiments also show that salinity can significantly shape bacterioplankton community composition (Langenheder et al., 2003; Kaartokallio et al., 2005; Sjöstedt et al., 2012b; Lindh et al., 2015a). For example, shifts in bacterioplankton community structure occurred in response to salinity changes following the experimental melting of sea ice (Kaartokallio et al., 2005). Compositional shifts occurred in response to a change in salinity and DOM conditions using chemostats, showing how rare or inactive taxa already present in the "seed bank," proliferated over time (Sjöstedt et al., 2012b). Moreover, a transplant experiment showed how transfer of bacterioplankton assemblages from ambient to changed salinity (brackish compared to near freshwater) and DOM conditions

TABLE 1 | Summary of Baltic Sea bacterioplankton studies in which data on community composition is available ($n = 83$).

Study	Type		Water source[¶]	Include activity measurements?*	Factor tested	Total community or specific group
Glaubitz et al., 2009		△	Central Baltic Sea	YES	Dark CO_2 fixation	Total community
Holmfeldt et al., 2009	○		Northern Baltic Sea	YES	Spatial	Actinobacteria
Lindh et al., 2015c	○		Baltic Sea Proper	YES	Temporal	Total community
Pinhassi et al., 1997	○		Northern Baltic Sea	YES	Temporal	Total community
Piwosz et al., 2013	○		Baltic Sea Proper	YES	Temporal	Total community
Rieck et al., 2015	○		Baltic Sea	YES	Particle associated compared to free-living	Total community
Riemann et al., 2008	○		Central Baltic Sea	YES	Temporal	Total community
Andersson et al., 2010	○		Central Baltic Sea	NO	Temporal	Total community
Bengtsson et al., 2017	○		Western Baltic Sea	NO	Epibiont	Total community
Bergen et al., 2014	○		Baltic Sea	NO	Spatial	Spartobacteria
Bertos-Fortis et al., 2016	○		Baltic Sea Proper	NO	Spatiotemporal	Cyanobacteria
Brettar et al., 2012	○		Baltic Sea	NO	Spatial	Total community
Bunse et al., 2016a	○		Baltic Sea Proper	NO	Spatiotemporal	Total community
Buongiorno et al., 2017		△	Baltic Sea	NO	Molecular methods (Spatial)	Total community
Celepli et al., 2017	○	△	Baltic Sea	NO	Spatial	Cyanobacteria
Dupont et al., 2014	○	△	Baltic Sea	NO	Spatial	Total community
Eiler and Bertilsson, 2006	○		Baltic Sea	NO	Spatial	*Vibrio*
Eiler et al., 2006	○		Baltic Sea	NO	Spatiotemporal	*Vibrio*
Golebiewski et al., 2017	○		Baltic Sea Proper	NO	Spatial	Total community
Grote et al., 2012		△	Central Baltic Sea	NO	Spatial	*Sulfurimonas*
Hagström et al., 2000	○		Northern Baltic Sea	NO	Spatial	Total community
Herlemann et al., 2011	○	△	Baltic Sea	NO	Spatial	Total community
Herlemann et al., 2016	○	△	Baltic Sea	NO	Spatial	Total community
Hofle and Brettar, 1995	○		Central Baltic Sea	NO	Spatial	Total community
Hu et al., 2016	○		Baltic Sea	NO	Spatial	Total community
Kaartokallio et al., 2008	○		Northern Baltic Sea	NO	Temporal	Total community

(Continued)

TABLE 1 | Continued

Study	Type		Water source[¶]	Include activity measurements?*	Factor tested	Total community or specific group
Kisand and Wikner, 2003	●		Northern Baltic Sea	NO	Allochtonous DOM	Total community
Klier et al., 2018		▲	Baltic Sea	NO	Spatial	Total community
Koskinen et al., 2011	●		Northern Baltic Sea	NO	Spatiotemporal	Total community
Laas et al., 2016	●	▲	Gulf of Finland	NO	Spatiotemporal	Total community
Laas et al., 2014	●	▲	Gulf of Finland	NO	Spatiotemporal	Total community
Laas et al., 2015	●	▲	Gulf of Finland	NO	Spatial	Total community
Larsson et al., 2014	●	▲	Baltic Sea	NO	Spatial	Cyanobacteria
Lindh et al., 2016	●		Baltic Sea Proper	NO	Spatiotemporal	Total community
Lindh et al., 2017	●		Baltic Sea Proper	NO	Spatiotemporal	Total community
Lindroos et al., 2011	●		Northern Baltic Sea	NO	Spatiotemporal	Total community
Pinhassi and Hagström, 2000	●		Northern Baltic Sea	NO	Temporal	Total community
Rahlff et al., 2017	●		Baltic Sea	NO	Wind speed (spatial)	Total community
Reindl and Bolałek, 2017		▲	Baltic Sea Proper	NO	Methane production	Archaea
Reunamo et al., 2013	●		Baltic Sea Proper	NO	Petroleum hydrocarbon	Total community
Reyes et al., 2017		▲	Baltic Sea	NO	Fe and S Reducing Bacteria	Total community
Salka et al., 2008	●		Baltic Sea	NO	Spatial	Aerobic anoxygenic phototrophic bacteria
Salka et al., 2014	●		Baltic Sea	NO	Spatial	Actinobacteria
Simu and Hagström, 2004	●		Baltic Sea Proper	NO	Single cell life strategy	Oligotrophic bacteria
Stolle et al., 2011	●		Western Baltic Sea	NO	Bacterioneuston	Total community
Tiirik et al., 2014	●		Baltic Sea	NO	Antibiotic resistance (spatial)	Total community
Tuomainen et al., 2006	●		Gulf of Finland	NO	*Nodularia* sp. (Cyanobacteria) Aggregates	Total community
Zinke et al., 2017		▲	Baltic Sea	NO	Activity of deep sea microbes	Total community

(Continued)

TABLE 1 | Continued

Study	Type		Water source[¶]	Include activity measurements?*	Factor tested	Total community or specific group
Berg et al., 2013		▲	Central Baltic Sea	YES	Carbon substrate and trace metals	Total community
Berg et al., 2015		▲	Central Baltic Sea	YES	Ammonia oxidation	Archaea
Bergen et al., 2016	●		Western Baltic Sea	YES	Acidification	Total community
Brettar et al., 2006	●		Central Baltic Sea	YES	Denitrification	*Thiomicrospira denitrificans*
Camarena-Gómez et al., 2018	●		SW Coast of Finland	YES	Phytoplankton/ Autochtonous DOM	Total community
Dinasquet et al., 2013	●		Northern Baltic Sea	YES	DOC	Total community
Glaubitz et al., 2014		▲	Central Baltic Sea	YES	Carbon substrate	*Sulfurimonas*
Gomez-Consarnau et al., 2012	●		Baltic Sea Proper	YES	Carbon substrates	Total community
Grubisic et al., 2012	●		Northern Baltic Sea	YES	DOM and stratification depth	Total community
Hannig et al., 2007		▲	Central Baltic Sea	YES	Denitrification and anammox	Annamox bacteria
Herlemann et al., 2014	●		Western Baltic Sea	YES	Allochtonous DOM	Total community
Kaartokallio et al., 2005	●		Northern Baltic Sea	YES	Salinity	Total community
Labrenz et al., 2005		▲	Central Baltic Sea	YES	Different electron donor/acceptor combinations	Total community
Lindh et al., 2015a	●		Baltic Sea	YES	Salinity, Autochtonous and Allochtonous DOM	Total community
Reunamo et al., 2017		▲	Baltic Sea	YES	Petroleum hydrocarbon	Total community
Stolle et al., 2010	●		Western Baltic Sea	YES	Bacterioneuston, low wind	Total community
Tammert et al., 2012	●		Gulf of Finland	YES	Nutrient limitation and DOC	Total community
Traving et al., 2017	●		Northern Baltic Sea	YES	Allochtonous DOM	Total community
Vaquer-Sunyer et al., 2015	●		Baltic Sea Proper	YES	DON	Total community
Vaquer-Sunyer et al., 2016	●		Baltic Sea Proper	YES	Wastewater treatment plant effluent input	Total community

(Continued)

TABLE 1 | Continued

Study	Type	Water source¶	Include activity measurements?*	Factor tested	Total community or specific group
von Scheibner et al., 2014	●	Western Baltic Sea	YES	Temperature	Total community
von Scheibner et al., 2017	●	Western Baltic Sea	YES	Temperature	*Glaciecola sp.*
Anderson et al., 2013	▲	Central Baltic Sea	NO	Grazing	*Sulfurimonas*
Broman et al., 2017a	▲	Baltic Sea Proper	NO	Oxygen shifts	Total community
Broman et al., 2017b	▲	Baltic Sea Proper	NO	Oxygen shifts	Total community
Degerman et al., 2013	●	Northern Baltic Sea	NO	Increased temperature and nutrients	Total community
Eiler et al., 2007	●	Central Baltic Sea	NO	Temperature and DOM	*Vibrio*
Kisand et al., 2002	●	Northern Baltic Sea	NO	Allochtonous DOM	Total community
Langenheder et al., 2004	●	Northern Baltic Sea	NO	Allochtonous DOM	Total community
Langenheder et al., 2003	●	Northern Baltic Sea	NO	Salinity and allochtonous DOM	Total community
Lindh et al., 2015b	●	Northern Baltic Sea	NO	Allochtonous DOM and temperature	Total community
Lindh et al., 2013	●	Baltic Sea Proper	NO	Acidification and increased temperature	Total community
Sipura et al., 2005	●	Northern Baltic Sea	NO	Inorganic nutrient addition	Total community
Sjöstedt et al., 2012a	●	Baltic Sea Proper	NO	Increased temperature	Total community
Sjöstedt et al., 2012b	●	Baltic Sea	NO	Salinity and DOC	Total community
Tank et al., 2011	▲	Western Baltic Sea	NO	Temperature and salinity	Purple sulfur bacteria
Viggor et al., 2015	●	Gulf of Finland/Riga	NO	Petroleum hydrocarbon	Total community
Viggor et al., 2013	●	Baltic Sea Proper	NO	Petroleum hydrocarbon	Total community

Yellow symbols denote in situ transects and temporally sampled stations and blue symbols denote all stations that have been sampled for use in experimental studies with empirical evidence for the effect of natural or human-induced changes in environmental conditions on bacterioplankton community dynamics. Filled circles and triangles denote samples obtained from surface waters and from deep-water/sediments, respectively. The table is sorted according to (i) Field or experimental studies, (ii) include activity measurements, and (iii) author name.

¶ A water source from the "Baltic Sea" denotes multiple locations across different basins.

**Activity measurements encompass uptake rates such as ^{3}H-Leucine/Thymidine and enzymatic activities.*

(allochthonous compared to autochthonous) has a major impact on composition and metabolic activity (Lindh et al., 2015a). Still, how such changes in salinity affect bacterioplankton community functioning, with potential implications for ecosystem services, remains largely unknown.

Temperature and pH

Seasonal variation in temperature significantly affects bacterioplankton community dynamics in the Baltic Sea (Andersson et al., 2010; Lindh et al., 2015c). Empirical evidence from micro- and mesocosm experiments highlights temperature as a major driver of compositional shifts in bacterioplankton (Muren et al., 2005; Sommer et al., 2007; Hoppe et al., 2008; von Scheibner et al., 2014; Vaquer-Sunyer et al., 2015). Typically, OTUs affiliated with Gammaproteobacteria such as *Glaciecola* spp. proliferate at higher temperatures (von Scheibner et al., 2017). Gammaproteobacteria also increased in relative abundance in warming experiments of bacterioplankton amended with dissolved organic nitrogen sources and incubated in higher temperatures (Vaquer-Sunyer et al., 2015). Here it is also worthwhile to mention that cell size is influenced by increasing temperatures (Sjöstedt et al., 2012a), as also observed in other marine ecosystems (Morán et al., 2015).

Evidence for the effect of ocean acidification on Baltic Sea bacterioplankton community dynamics are few (Bergen et al., 2016). Still, there are some indications of synergistic effects between increased temperature and pCO_2 levels (Lindh et al., 2013). This is in line with analyses from other systems suggesting that ocean acidification could affect bacterioplankton growth and physiology both directly and indirectly, e.g., by affecting DOM release and composition originating from higher trophic levels (Vega Thurber et al., 2009; Joint et al., 2011; Bunse et al., 2016b; Sala et al., 2016). Therefore, increased sea surface temperatures together with acidification due to climate change will likely affect the dynamics of particular bacterioplankton populations either alone or synergistically with potential amplification effects.

Nutrient Inputs

The quality and composition of DOM is partly dependent on its origin, which can be either *allochthonous* or *autochthonous* (Kritzberg et al., 2004; Nagata, 2008). Since bacteria are the main contributors to the biological transformation of marine DOM, much attention has been put into uncovering the role of bacterial community composition in this biogeochemical process. In the Baltic Sea, particular opportunistic bacterioplankton populations are capable of successfully utilizing elevated concentrations of labile, low-molecular weight (LMW) compounds (Gomez-Consarnau et al., 2012). Moreover, multiple studies report important effects of allochthonous DOM on Baltic Sea bacterioplankton responses in community composition (Kisand et al., 2002; Grubisic et al., 2012; Herlemann et al., 2014). An important and intriguing future challenge is to determine the relationship between DOM composition and bacterioplankton community composition and functioning. Curiously, we found few studies reporting on the direct effects of inorganic nutrient enrichments on Baltic Sea Bacterioplankton communities (but see Tammert et al., 2012). This is perhaps surprising given the importance nitrogen and phosphorus plays in eutrophication of the Baltic Sea (Conley et al., 2009). Simple experiments with bacterioplankton assemblages and nitrogen and phosphorus additions will be a promising avenue of future research to couple changes in inorganic nutrients and DOM to shifts in bacterioplankton community structure and its relationship with Baltic Sea ecosystem function.

Opportunistic Gammaproteobacteria—Bottle Effects or True Dynamics?

OTUs affiliated with Gammaproteobacteria often increase in relative abundance in micro- and mesocosm experiments. Such dynamics are sometimes attributed to the so-called "bottle effect" in which confinement of water causes shifts in bacterioplankton community composition and physiological rates (Fuchs et al., 2000; Massana et al., 2001; Baltar et al., 2012). Such effects are typically detected by rapidly increasing proportions of copiotrophic gammaproteobacterial populations and metabolic activity (see e.g., Gomez-Consarnau et al., 2012; Sjöstedt et al., 2012b). However, we note that particular gammaproteobacterial OTUs also peak in relative abundance *in situ* (Andersson et al., 2010; Lindh et al., 2015c). This pattern does not only occur in the Baltic Sea but also in the North Sea and Mediterranean Sea (Fodelianakis et al., 2014; Alonso-Saez et al., 2015; Teeling et al., 2016). These findings suggest that Gammaproteobacteria could respond faster to environmental disturbances aided by their copiotrophic lifestyle and thus potentially become dominant more frequently due to increased incidence of perturbation *in situ*. It remains to be determined whether such changes would significantly alter microbial-driven carbon cycling or if these Gammaproteobacteria perhaps carry functional redundancy (see e.g., Pedler et al., 2014).

BACTERIOPLANKTON COMMUNITY FUNCTIONING IS CORRELATED WITH COMMUNITY DYNAMICS BUT DATA IS SCARCE

In this section we provide an overview of experimental studies that statistically tested the linkage between changes in bacterioplankton community composition and metabolic activity (i.e., functioning) upon environmental forcing (disturbance; **Table 2**). A few *in situ* studies have shown simultaneous shifts in bacterioplankton community composition and metabolic activity (Pinhassi et al., 1997; Riemann et al., 2008; Glaubitz et al., 2009; Holmfeldt et al., 2009; Piwosz et al., 2013; Lindh et al., 2015c; Rieck et al., 2015; **Table 1**), but as these measurements can be influenced by and/or auto-correlated to a number of undetermined environmental variables they were not included in the current analysis. A majority of experimental studies performed (non-quantitative) cluster-like analyses based on beta-diversity estimates that indicated shifts in composition (see e.g., Lindh et al., 2013; von Scheibner et al., 2014). Notably, most of the studies using cluster statistics methods show that functioning to some degree changes upon shift in composition. A number

TABLE 2 | Summary of Baltic Sea bacterioplankton studies in which experimental data with empirical testing of the effect of natural or anthropogenically induced disturbances on total bacterioplankton community composition and functioning have been determined concomitantly ($n = 10$).

Study*	Summary	Function change?	Composition shift?	Statistical tests	Indicated *p*-values
Bergen et al., 2016	Tested the effect of increased temperature and pCO2 levels on bacterioplankton communities. Found that warming and not pCO2 lead to changes in bacterioplankton community composition and metabolic activity.	YES	YES	Repeated measures ANOVA | PERMANOVA/ Linear discriminant effect size	≤0.01|0.001/LDA values>3.6 (LEfSe)
Camarena-Gómez et al., 2018	Tested how bacterial physiology and community structure were affected by changes in phytoplankton community composition.	YES	YES	Tukey's *b* | PERMANOVA	<0.05|<0.05
Dinasquet et al., 2013	Investigated how bacterioplankton communities respond to varying supply of bioavailable carbon (bDOC) and how this affected bacterioplankton community composition and functioning. Found that bDOC triggered a shift in community composition and changed the abundance of specific extracellular enzymes.	YES	YES	Factorial analysis of variance | Mantel's test	0.005|0.017
Grubisic et al., 2012	Tested the effect of changed DOM quality and concentrations and stratification depth on bacterioplankton communities. Bacterioplankton community composition were influenced both by stratification depth and DOM but only stratification depth affected bacterial heterotrophic production.	YES	YES	MANOVA | PLS analysis	<0.001|*VIP*-values >1 (PLS)
Herlemann et al., 2014	Investigated potential biodegradation of experimentally added riverine DOM by bacterioplankton communities. Found no evidence of a direct link between bacterioplankton composition and community functioning responding to riverine DOM.	NO	NO	Repeated measures ANOVA | two-way ANOSIM	>0.05|>0.05
Lindh et al., 2015a	Tested the impact of changed salinity and DOM quality on bacterioplankton communities, with a transplant experiment. Demonstrated shifts in bacterioplankton community composition coupled with changed metabolic activities responding to changes in the environmental conditions. After communities were re-transplanted to original environmental conditions they did not return to original composition nor functioning.	YES	YES	Repeated measures ANOVA | PERMANOVA/Mantel's test	0.001|0.001
Tammert et al., 2012	Tested the effects of nutrient limitation and bioavailable DOC additions on bacterioplankton communities. bDOC changed bacterial heterotrophic production and led to shifts in community composition.	YES	YES	Generalized least squares models | Permutations test	<0.001|<0.05
Traving et al., 2017	Investigated the effects of elevated levels of riverine DOM on bacterioplankton communities. DOM additions stimulated protease activity and specific operational taxonomic units responded significantly.	YES	YES	Linear mixed model | GLM analysis	<0.0002|<0.05
Vaquer-Sunyer et al., 2015	Investigated synergistic effects of simultaneous DON additions and warming on bacterioplankton communities. Bacterioplankton community composition and metabolic rates changed in relation to temperature and DON additions.	YES	YES	Mixed-effects model | Mantel's test	< 0.01|0.001
Vaquer-Sunyer et al., 2016	Tested the effects of wastewater treatment plant effluent inputs on bacterioplankton communities. Nutrient addition lead to shifts in bacterioplankton community composition linked with changed metabolic activity.	YES	YES	Repeated measures MANOVA | Mantel's test	<0.0001|<0.001

Statistical tests of significant effects and indicated p-values are given for bacterioplankton functioning followed by community composition separated by "|". All studies consisted of samples obtained from the surface and not from the deep-water or sediments. None of the studies measured shifts in bacterioplankton community composition and functioning over a longer period of time, therefore we can only determine initial sensitivity and not resilience.

**Only studies with total community and with statistical testing of observed effects were included in this qualitative analysis.*

of studies focused on changes in the relative or absolute abundance of particular taxa or groups of bacterioplankton such as *Sulfurimonas* GD-1, *Thiomicrospira denitrificans,* and *Glaciecola* spp. and also measured metabolic activity of these populations (Brettar et al., 2006; Glaubitz et al., 2014; von Scheibner et al., 2017). Importantly, shifts in abundance of these

particular populations were typically coupled to pronounced changes in metabolic activity when exposed to environmental disturbance.

Relatively few studies have carried out statistical assessments with quantitative data for changes in both the overall bacterioplankton community composition and bacterial functioning (e.g., using multivariate statistics such as Mantel's test, PERMANOVA, or similar). We analyze in detail these studies to reach a general understanding of current quantitative data. We note a lack of deep-water or sediments studies that in a strict sense target such quantitative assessments. Consequently, only studies with surface water samples were included in this analysis (**Table 2**). Nine out of ten studies with measurements of total bacterioplankton community composition and metabolic activity show empirical evidence of concomitant shifts in community composition and functioning. One study, by Herlemann et al. (2014), found no significant effects on bacterioplankton community dynamics responding to riverine DOM additions, including limited growth, nor links between composition and functioning. Thus, a majority of studies highlight bacterioplankton assemblages responding to disturbances following the *sensitivity* scenario (**Table 2**; **Box 2**).

The studies showing statistical support for concomitant shifts in community composition and functioning essentially investigated the effect of nutrient amendments on bacterioplankton community composition dynamics and metabolic activity (Grubisic et al., 2012; Tammert et al., 2012; Degerman et al., 2013; Lindh et al., 2015a; Vaquer-Sunyer et al., 2015, 2016; Bergen et al., 2016; Traving et al., 2017; Camarena-Gómez et al., 2018). The Bergen et al. (2016) study emphasized how temperature significantly alters community composition and heterotrophic bacterial production but that pCO2 had a more limited effect. The authors noted how these changes in bacterioplankton dynamics could be indicative of changed carbon fluxes in a future ecosystem where heterotrophy may become more important compared to today. Dinasquet et al. (2013) showed that bioavailable DOC triggered a shift in community composition and changed the abundance of specific extracellular enzymes suggesting that bacterioplankton communities can respond, following the sensitivity scenario, to varying supplies of DOC ultimately affecting heterotrophic respiration. Vaquer-Sunyer et al. (2015) also noted that nutrient inputs of dissolved organic nitrogen (DON) and changed temperature may lead to a more heterotrophic system. In a different study by Vaquer-Sunyer et al. (2016), they showed an effect of wastewater treatment plant effluent inputs on bacterioplankton dynamics, with an increase in the relative abundance of Cyanobacteria responding to the influx of wastewater with concomitant changes in metabolic activity. A recent study by Camarena-Gómez et al. (2018) investigated the relationship between phytoplankton bloom dynamics (different phytoplankton species) and bacterioplankton community function and taxonomic structure. Their work emphasized how bacterial metabolic activity and community composition were affected by changes in the phytoplankton community—in particular the divergent bacterial responses to phytoplankton dominated by diatoms compared to dinoflagellates. Amendment of a diatom dominated community resulted in a significantly changed bacterial heterotrophic production and shift in bacterioplankton community structure compared controls, while amendment of a dinoflagellate community had overall smaller impact on both community function and composition Camarena-Gómez et al., 2018). It is noteworthy how the addition of riverine DOM could result in changed ecosystem function from shifts in bacterioplankton community dynamics toward a more heterotrophic system (Degerman et al., 2013; Figueroa et al., 2016). Also in the Gulf of Finland enrichment with labile DOC changed bacterial production and led to shifts in community composition, promoting filamentous bacteria - the authors indicate that this DOC source may impact diversity, food-web structure and biogeochemical processing of carbon (Tammert et al., 2012). Only three specific studies have directly determined the correlation between shifts in community composition and metabolic activity responding to environmental perturbations (Lindh et al., 2015a; Vaquer-Sunyer et al., 2015, 2016). These studies indicated that variation in bacterioplankton community functioning is often significantly explained by changes in metabolic activity explaining up to around 0.65 of the variance (Pearson r).

Although environmental disturbances can influence bulk bacterioplankton community composition, the replacement of sensitive taxa will occur at the individual OTU level. For example, although Bergen et al. (2016) implicated limited effects on bulk community dynamics resulting from increased pCO_2, there was a substantial influence on particular populations with statistical support from linear discriminant effect size (LEfSe). Traving et al. (2017) performed statistical tests (generalized linear models) to determine the coupling between specific OTUs and amendment of riverine DOM where several OTUs were significantly correlated with changed environmental conditions. Although these shifts in the relative abundance of particular OTUs were not coupled directly to metabolic activity there were concomitant significant changes in protease activity. Taken together, the nine studies emphasize the *sensitivity* scenario of bacterioplankton communities in Baltic Sea, where particular populations respond to different sets of environmental forcing. The causal loop diagram in **Figure 2** summarizes the significant effects of changes in environmental conditions for community composition and functioning included in this review. Overall, the studies in this section highlight how changes in environmental forcing may significantly impact pelagic remineralization of organic carbon and result in a drastic reduction in the flow of organic matter through the microbial loop.

OUTSTANDING QUESTIONS

Although the Baltic Sea bacterial communities are fairly well studied, research to integrate bacterioplankton dynamics and its consequences in food-web and biogeochemical models is much needed. We infer that such integration is necessary to allow predictions and counter measures of detrimental future climate change effects on microbial food webs and their ecosystem services.

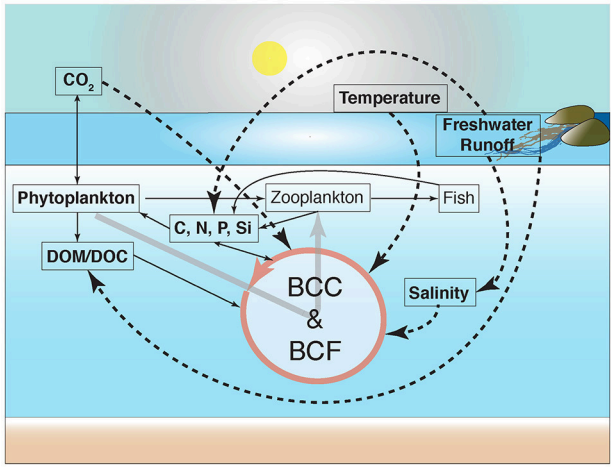

FIGURE 2 | Causal-loop diagram indicating potential ecosystem-wide effects in carbon cycling due to responses among bacterioplankton populations to natural and anthropogenic disturbances. Bacterioplankton community composition and functioning have been abbreviated to BCC and BCF, respectively. The figure is redrawn and modified from (Azam and Malfatti, 2007). Continuous and dashed arrows denote nutrient fluxes and changes in environmental variables with empirical evidence of significant effects on bacterioplankton community composition covered in this review, respectively. Changes in bacterioplankton community functioning, such as bacterial heterotrophic production and respiration, may occur due to increases in the availability of dissolved organic matter (DOM), resulting from, for example, increased freshwater runoff and phytoplankton blooms.

Recent work on bacterial populations and their activity at the seafloor of the Baltic Sea has shown a plethora of interesting dynamics and lifestyles including, an active community that was previously deemed unlikely (Glaubitz et al., 2009, 2014; Berg et al., 2013, 2015; Broman et al., 2017a,b; Reyes et al., 2017; Zinke et al., 2017). Detailed studies with concomitant measurements of bacterioplankton community composition and function are required in deep-waters and sediments of the Baltic Sea to determine the role of bacteria in key biogeochemical cycles (e.g., of C, N, P, and S) in general, and in relation to hypoxia in particular.

Seasonal *in situ* studies of bacterioplankton community dynamics have emphasized how communities return to a similar composition and functioning in specific seasons year after year (Fuhrman et al., 2006; Andersson et al., 2010; Lindh et al., 2015c). This could indicate that bacterioplankton communities are in fact resilient to recurrent pulse and press disturbances, but could also indicate that the environmental conditions over seasons are "repeated" and that the same bacterial populations are repeatedly selected for. Overall, there is a recognized need to incorporate the long-term temporal dimension when quantifying resistance and resilience of microbial communities (Shade et al., 2012; Fodelianakis et al., 2017; Liu et al., 2018). Only by including the temporal dimension can microbial ecologists fully understand the consequences of ocean change for bacterioplankton community dynamics, and we urgently need more information on changes occurring over time, preferably long-term studies. In particular, for experimental studies, there is a lack of data that empirically test the scenarios of resistance and resilience for Baltic Sea bacterioplankton communities. Nevertheless, in one study using a transplant and re-transplant experimental design (Lindh et al., 2015a), we showed how bacterioplankton community dynamics remain altered even after returning to the same environmental conditions as the original community experienced. One of the most important questions to address in future studies in the Baltic Sea will therefore be to empirically test whether bacterioplankton communities remain sensitive to an environmental disturbance or if the community can return to a similar original community structure and function following the *resilience* scenario. Presently, we observe that a majority of the Baltic Sea studies point toward the sensitivity scenario, and that it is necessary to await future research to make definite conclusions regarding the extent of resilience. Thus, within the time frame of 2 weeks, the studies indicate that sensitivity is more developed than resistance. Nevertheless, natural temporal changes in environmental conditions for time frames of more than a month will alter the composition and functioning of bacterioplankton communities, likely interfering with interpretations of the scenarios of sensitivity, resistance and resilience.

SUMMARY

A majority of the studies included in this review show that bacterioplankton community composition is sensitive to changes in environmental conditions, in particular salinity and nutrient inputs, with empirical support for simultaneous changes also in community functioning. As noted also in other aquatic environments, pronounced shifts in composition and bacterial heterotrophic production occur following spring diatom and dinoflagellate blooms and summer blooms of filamentous Cyanobacteria. The sensitivity scenario and its impact on the microbial loop is highlighted in **Figure 3A**. Salinity singles out as a principal determinant of the distribution of bacterioplankton populations across basin-wide spatial scales in the Baltic Sea. Nevertheless, at regional (within-basin) scales, changes in nutrient availability and both autochthonous and allochthonous DOM influence the bacterioplankton community composition. Hence, this review provides a roadmap as to what ecological consequences climate change could have on the Baltic Sea ecosystem if bacterioplankton dynamics changes. Yet, although bacterioplankton communities are initially sensitive we know very little about the potential of resilience due to the lack of empirical studies testing this scenario (**Figure 3B**).

For quantifying the level of *sensitivity* or *resilience* of bacterioplankton communities to natural and human-driven changes in environmental conditions it is essential to investigate particular bacterioplankton populations and their responses to alternate physicochemical conditions and specific (in)organic nutrient sources, e.g., different DOM and DOC compounds.

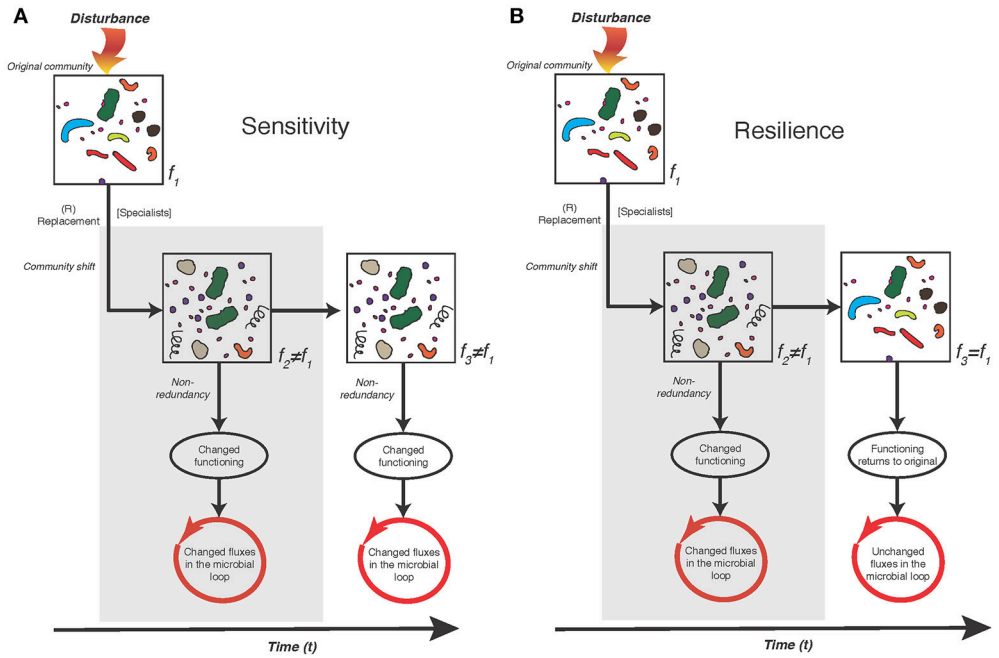

FIGURE 3 | Conceptual diagram of two possible scenarios of Baltic Sea bacterioplankton community dynamics, i.e., *sensitivity* **(A)**, and *resilience* **(B)**. In both the *sensitivity* and *resilience* scenario an environmental disturbance leads to the replacement of individual bacterioplankton populations and changed community functioning with potential impact on the microbial loop and carbon cycling. The scenarios differ in that over time the replacement of individual bacterioplankton populations and changed community functioning remains in **(A)**, but returns to similar individual bacterioplankton populations and community functioning as the original community in **(B)**. Scenarios with empirical evidence of significant effects on bacterioplankton community composition and functioning in the present review is the impact of dissolved organic nitrogen (DON) additions and increased temperatures Bergen et al. (2016), Vaquer-Sunyer et al. (2015). However, for Baltic Sea data, the lack of long-term studies precludes conclusions regarding whether the *sensitivity* or *resilience* scenario are the most prominent—currently studies have been designed primarily to determine the extent of the initial *sensitivity* (gray filled areas).

The *sensitivity* scenario has important implications for the Baltic Sea ecosystem: it dictates that environmental disturbances and climate change are likely to affect processes like the microbial-driven carbon pump and/or the general microbial regulation of energy and matter fluxes. We infer that knowledge of the linkages between bacterioplankton composition and bacterial cycling of carbon and other elements under varying environmental forcing is critically important for developing action plans to sustain microbial ecosystem services invaluable for all marine life.

AUTHOR CONTRIBUTIONS

ML and JP both participated in the study design, analysis, and writing of the article.

FUNDING

The research was supported by the Swedish Research Council FORMAS strong research programme EcoChange, the Linnaeus University Center for Ecology and Evolution in Microbial model Systems (EEMiS), and by grants from the Swedish Research Council VR. This work resulted from the BONUS BLUEPRINT project which was supported by BONUS (Art 185), funded jointly by the EU and FORMAS.

ACKNOWLEDGMENTS

This article was partly inspired by work done in the Ph.D. thesis by Lindh (2014), in particular the section on synthesis on bacterioplankton communities responding to natural and anthropogenically induced environmental disturbances. We also thank Carina Bunse, Mireia Bertos-Fortis, Hanna Farnelid, Catherine Legrand, Christofer Karlsson, Saraladevi Muthusamy, Federico Baltar, and Sandra Martinez-García for enthusing discussions that inspired writing this article.

SUPPLEMENTARY MATERIAL

The Supplementary Material for this article can be found online at: https://www.frontiersin.org/articles/10.3389/fmars.2018.00361/full#supplementary-material

REFERENCES

Allison, S. D., and Martiny, J. B. (2008). Resistance, resilience, and redundancy in microbial communities. *Proc. Natl. Acad. Sci. U.S.A.* 105(Suppl. 1), 11512–11519. doi: 10.1073/pnas.0801925105

Alonso-Saez, L., Diaz-Perez, L., and Moran, X. A. (2015). The hidden seasonality of the rare biosphere in coastal marine bacterioplankton. *Environ. Microbiol.* 17, 3766–3780. doi: 10.1111/1462-2920.12801

Anderson, R., Wylezich, C., Glaubitz, S., Labrenz, M., and Juergens, K. (2013). Impact of protist grazing on a key bacterial group for biogeochemical cycling in Baltic Sea pelagic oxic/anoxic interfaces. *Environ. Microbiol.* 15, 1580–1594. doi: 10.1111/1462-2920.12078

Andersson, A., Meier, H. E. M., Ripszam, M., Rowe, O., Wikner, J., Haglund, P., et al. (2015). Projected future climate change and Baltic Sea ecosystem management. *AMBIO* 44, 345–356. doi: 10.1007/s13280-015-0654-8

Andersson, A. F., Riemann, L., and Bertilsson, S. (2010). Pyrosequencing reveals contrasting seasonal dynamics of taxa within Baltic Sea bacterioplankton communities. *ISME J.* 4, 171–181. doi: 10.1038/ismej.2009.108

Azam, F., and Malfatti, F. (2007). Microbial structuring of marine ecosystems. *Nat. Rev. Microbiol.* 5, 782–791. doi: 10.1038/nrmicro1747

Baltar, F., Lindh, M. V., Parparov, A., Berman, T., and Pinhassi, J. (2012). Prokaryotic community structure and respiration during long-term incubations. *Microbiol Open* 1, 214–224. doi: 10.1002/mbo3.25

Beier, S., Shen, D., Schott, T., and Jürgens, K. (2017). Metatranscriptomic data reveal the effect of different community properties on multifunctional redundancy. *Mol Ecol.* 26, 6813–6826. doi: 10.1111/mec.14409

Bengtsson, M. M., Bühler, A., Brauer, A., Dahlke, S., Schubert, H., and Blindow, I. (2017). Eelgrass leaf surface microbiomes are locally variable and highly correlated with epibiotic eukaryotes. *Front. Microbiol.* 8:1312. doi: 10.3389/fmicb.2017.01312

Berg, C., Beckmann, S., Jost, G., Labrenz, M., and Juergens, K. (2013). Acetate-utilizing bacteria at an oxic-anoxic interface in the Baltic Sea. *FEMS Microbiol. Ecol.* 85, 251–261. doi: 10.1111/1574-6941.12114

Berg, C., Listmann, L., Vandieken, V., Vogts, A., and Juergens, K. (2015). Chemoautotrophic growth of ammonia-oxidizing Thaumarchaeota enriched from a pelagic redox gradient in the Baltic Sea. *Front. Microbiol.* 5:786. doi: 10.3389/fmicb.2014.00786

Bergen, B., Endres, S., Engel, A., Zark, M., Dittmar, T., Sommer, U., et al. (2016). Acidification and warming affect prominent bacteria in two seasonal phytoplankton bloom mesocosms. *Environ. Microbiol.* 18, 4579–4595. doi: 10.1111/1462-2920.13549

Bergen, B., Herlemann, D. P. R., Labrenz, M., and Jürgens, K. (2014). Distribution of the verrucomicrobial clade Spartobacteria along a salinity gradient in the Baltic Sea. *Environ. Microbiol. Rep.* 6:625–630. doi: 10.1111/1758-2229.12178

Bertos-Fortis, M., Farnelid, H. M., Lindh, M. V., Casini, M., Andersson, A., Pinhassi, J., et al. (2016). Unscrambling cyanobacteria community dynamics related to environmental factors. *Front. Microbiol.* 7:625. doi: 10.3389/fmicb.2016.00625

Brettar, I., Christen, R., and Hofle, M. G. (2012). Analysis of bacterial core communities in the central Baltic by comparative RNA-DNA-based fingerprinting provides links to structure-function relationships. *ISME J.* 6, 195–212. doi: 10.1038/ismej.2011.80

Brettar, I., Hoefle, M. G., Pruzzo, C., and Vezzulli, L. (2016). "Climate change effects on planktonic bacterial communities in the ocean - from structure and function to long-term and large-scale observations," in *Climate Change and Microbial Ecology: Current Research And Future Trends,* ed Jürgen Marxsen. (Giessen: Caister Academic Press), 23–40.

Brettar, I., Labrenz, M., Flavier, S., Botel, J., Kuosa, H., Christen, R., et al. (2006). Identification of a thiomicrospira denitrificans-like epsilonproteobacterium as a catalyst for autotrophic denitrification in the central Baltic Sea. *Appl. Environ. Microbiol.* 72, 1364–1372. doi: 10.1128/AEM.72.2.1364-1372.2006

Broman, E., Sachpazidou, V., Pinhassi, J., and Dopson, M. (2017a). Oxygenation of hypoxic coastal baltic sea sediments impacts on chemistry, microbial community composition, and metabolism. *Front. Microbiol.* 8:2453. doi: 10.3389/fmicb.2017.02453

Broman, E., Sjöstedt, J., Pinhassi, J., and Dopson, M. (2017b). Shifts in coastal sediment oxygenation cause pronounced changes in microbial community composition and associated metabolism. *Microbiome* 5:96. doi: 10.1186/s40168-017-0311-5

Bunse, C., Bertos-Fortis, M., Sassenhagen, I., Sildever, S., Sjoqvist, C., Godhe, A., et al. (2016a). Spatio-temporal interdependence of bacteria and phytoplankton during a baltic sea spring bloom. *Front. Microbiol.* 7:517. doi: 10.3389/fmicb.2016.00517

Bunse, C., Lundin, D., Karlsson, C. M. G., Akram, N., Vila-Costa, M., Palovaara, J., et al. (2016b). Response of marine bacterioplankton pH homeostasis gene expression to elevated CO_2. *Nat. Clim. Change.* 6, 483–487. doi: 10.1038/nclimate2914

Buongiorno, J., Turner, S., Webster, G., Asai, M., Shumaker, A. K., Roy, T., et al. (2017). Interlaboratory quantification of bacteria and archaea in deeply buried sediments of the Baltic Sea (IODP Expedition 347). *FEMS Microbiol. Ecol.* 93:fix007. doi: 10.1093/femsec/fix007

Callahan, B. J., Mcmurdie, P. J., Rosen, M. J., Han, A. W., Johnson, A. J., and Holmes, S. P. (2015). DADA2: high resolution sample inference from amplicon data. *Nat. Methods* 13, 581–583. doi: 10.1038/nmeth.3869

Camarena-Gómez, M. T., Lipsewers, T., Piiparinen, J., Eronen-Rasimus, E., Perez-Quemaliños, D., Hoikkala, L., et al. (2018). Shifts in phytoplankton community structure modify bacterial production, abundance and community composition. *Aquat. Microb. Ecol.* 81, 149–170. doi: 10.3354/ame01868

Carstensen, J., Andersen, J. H., Gustafsson, B. G., and Conley, D. J. (2014). Deoxygenation of the Baltic Sea during the last century. *Proc. Natl. Acad. Sci. U.S.A.* 111, 5628–5633. doi: 10.1073/pnas.1323156111

Celepli, N., Sundh, J., Ekman, M., Dupont, C. L., Yooseph, S., Bergman, B., et al. (2017). Meta-omic analyses of Baltic Sea cyanobacteria: diversity, community structure and salt acclimation. *Environ. Microbiol.* 19, 673–686. doi: 10.1111/1462-2920.13592

Comte, J., and Del Giorgio, P. A. (2011). Composition influences the pathway but not the outcome of the metabolic response of bacterioplankton to resource shifts. *PLoS ONE* 6:e25266. doi: 10.1371/journal.pone.0025266

Conley, D. J., Paerl, H. W., Howarth, R. W., Boesch, D. F., Seitzinger, S. P., Havens, K. E., et al. (2009). Controlling eutrophication: nitrogen and phosphorus. *Science* 323, 1014–1015. doi: 10.1126/science.1167755

Cram, J. A., Xia, L. C., Needham, D. M., Sachdeva, R., Sun, F., and Fuhrman, J. A. (2015). Cross-depth analysis of marine bacterial networks suggests downward propagation of temporal changes. *ISME J.* 9, 2573–2586. doi: 10.1038/ismej.2015.76

Degerman, R., Dinasquet, J., Riemann, L., De Luna, S. S., and Andersson, A. (2013). Effect of resource availability on bacterial community responses to increased temperature. *Aquat. Microbiol. Ecol.* 68, 131–142. doi: 10.3354/ame01609

Dinasquet, J., Kragh, T., Schroter, M.-L., Sondergaard, M., and Riemann, L. (2013). Functional and compositional succession of bacterioplankton in response to a gradient in bioavailable dissolved organic carbon. *Environ Microbiol.* 15, 2616–2628. doi: 10.1111/1462-2920.12178

Dupont, C. L., Larsson, J., Yooseph, S., Ininbergs, K., Goll, J., Asplund-Samuelsson, J., et al. (2014). Functional tradeoffs underpin salinity-driven divergence in microbial community composition. *PLoS ONE* 9: e89549. doi: 10.1371/journal.pone.0089549

Edgar, R. C. (2013). UPARSE: highly accurate OTU sequences from microbial amplicon reads. *Nat. Methods* 10, 996–998. doi: 10.1038/nmeth.2604

Eiler, A., and Bertilsson, S. (2006). Detection and quantification of Vibrio populations using denaturant gradient gel electrophoresis. *J. Microbiol. Methods* 67, 339–348. doi: 10.1016/j.mimet.2006.04.002

Eiler, A., Gonzalez-Rey, C., Allen, S., and Bertilsson, S. (2007). Growth response of *Vibrio cholerae* and other *Vibrio* spp. to cyanobacterial dissolved organic matter and temperature in brackish water. *FEMS Microbiol. Ecol.* 60, 411–418. doi: 10.1111/j.1574-6941.2007.00303.x

Eiler, A., Johansson, M., and Bertilsson, S. (2006). Environmental influences on *Vibrio* populations in northern temperate and boreal coastal waters (Baltic and Skagerrak Seas). *Appl. Environ. Microbiol.* 72, 6004–6011. doi: 10.1128/AEM.00917-06

Falkowski, P. G., Fenchel, T., and Delong, E. F. (2008). The microbial engines that drive earth's biogeochemical cycles. *Science* 320, 1034–1039. doi: 10.1126/science.1153213

Figueroa, D., Rowe, O. F., Paczkowska, J., Legrand, C., and Andersson, A. (2016). Allochthonous carbon—a major driver of bacterioplankton

production in the subarctic northern baltic sea. *Microb. Ecol.* 71, 789–801. doi: 10.1007/s00248-015-0714-4

Fodelianakis, S., Moustakas, A., Papageorgiou, N., Manoli, O., Tsikopoulou, I., Michoud, G., et al. (2017). Modified niche optima and breadths explain the historical contingency of bacterial community responses to eutrophication in coastal sediments. *Mol. Ecol.* 26, 2006–2018. doi: 10.1111/mec.13842

Fodelianakis, S., Papageorgiou, N., Pitta, P., Kasapidis, P., Karakassis, I., and Ladoukakis, E. D. (2014). The pattern of change in the abundances of specific bacterioplankton groups is consistent across different nutrient-enriched habitats in Crete. *Appl. Environ. Microbiol.* 80, 3784–3792. doi: 10.1128/AEM.00088-14

Fuchs, B. M., Zubkov, M. V., Sahm, K., Burkill, P. H., and Amann, R. (2000). Changes in community composition during dilution cultures of marine bacterioplankton as assessed by flow cytometric and molecular biological techniques. *Environ. Microbiol.* 2, 191–201. doi: 10.1046/j.1462-2920.2000.00092.x

Fuhrman, J. A., Hewson, I., Schwalbach, M. S., Steele, J. A., Brown, M. V., and Naeem, S. (2006). Annually reoccurring bacterial communities are predictable from ocean conditions. *Proc. Natl. Acad. Sci.* 103, 13104–13109. doi: 10.1073/pnas.0602399103

Glaubitz, S., Abraham, W.-R., Jost, G., Labrenz, M., and Juergens, K. (2014). Pyruvate utilization by a chemolithoautotrophic epsilonproteobacterial key player of pelagic Baltic Sea redoxclines. *FEMS Microbiol. Ecol.* 87, 770–779. doi: 10.1111/1574-6941.12263

Glaubitz, S., Lueders, T., Abraham, W. R., Jost, G., Jürgens, K., and Labrenz, M. (2009). 13C-isotope analyses reveal that chemolithoautotrophic Gamma- and *Epsilonproteobacteria* feed a microbial food web in a pelagic redoxcline of the central Baltic Sea. *Environ. Microbiol.* 11, 326–337. doi: 10.1111/j.1462-2920.2008.01770.x

Golebiewski, M., Calkiewicz, J., Creer, S., and Piwosz, K. (2017). Tideless estuaries in brackish seas as possible freshwater-marine transition zones for bacteria: the case study of the Vistula river estuary. *Environ. Microbiol. Rep.* 9, 129–143. doi: 10.1111/1758-2229.12509

Gomez-Consarnau, L., Lindh, M. V., Gasol, J. M., and Pinhassi, J. (2012). Structuring of bacterioplankton communities by specific dissolved organic carbon compounds. *Environ. Microbiol.* 14, 2361–2378. doi: 10.1111/j.1462-2920.2012.02804.x

Grote, J., Schott, T., Bruckner, C. G., Gloeckner, F. O., Jost, G., Teeling, H., et al. (2012). Genome and physiology of a model *Epsilonproteobacterium* responsible for sulfide detoxification in marine oxygen depletion zones. *Proc. Natl. Acad. Sci. U.S.A.* 109, 506–510. doi: 10.1073/pnas.1111262109

Grubisic, L. M., Brutemark, A., Weyhenmeyer, G. A., Wikner, J., Bamstedt, U., and Bertilsson, S. (2012). Effects of stratification depth and dissolved organic matter on brackish bacterioplankton communities. *Mar. Ecol. Prog. Ser.* 453, 37–48. doi: 10.3354/meps09634

Hagström, Å., Azam, F., Berg, C., and Zweifel, U. L. (2017). Isolates as models to study bacterial ecophysiology and biogeochemistry. *Aquat. Microbiol. Ecol.* 80, 15–27. doi: 10.3354/ame01838

Hagström, Å., Pinhassi, J., and Zweifel, U. L. (2000). Biogeographical diversity among marine bacterioplankton. *Aquat. Microbiol. Ecol.* 21, 231–244. doi: 10.3354/ame021231

Hannig, M., Lavik, G., Kuypers, M. M. M., Woebken, D., Martens-Habbena, W., and Juergens, K. (2007). Shift from denitrification to anammox after inflow events in the central Baltic Sea. *Limnol. Oceanogr.* 52, 1336–1345. doi: 10.4319/lo.2007.52.4.1336

Herlemann, D. P., Labrenz, M., Jürgens, K., Bertilsson, S., Waniek, J. J., and Andersson, A. F. (2011). Transitions in bacterial communities along the 2000 km salinity gradient of the Baltic Sea. *ISME J.* 5, 1571–1519. doi: 10.1038/ismej.2011.41

Herlemann, D. P. R., Lundin, D., Andersson, A. F., Labrenz, M., and Jürgens, K. (2016). Phylogenetic signals of salinity and season in bacterial community composition across the salinity gradient of the baltic sea. *Front. Microbiol.* 7:1883. doi: 10.3389/fmicb.2016.01883

Herlemann, D. P. R., Manecki, M., Meeske, C., Pollehne, F., Labrenz, M., Schulz-Bull, D., et al. (2014). Uncoupling of bacterial and terrigenous dissolved organic matter dynamics in decomposition experiments. *PLoS ONE* 9:e93945. doi: 10.1371/journal.pone.0093945

Hofle, M. G., and Brettar, I. (1995). Taxonomic diversity and metabolic-activity of microbial communities in the water column of the central baltic sea. *Limnol. Oceanogr.* 40, 868–874. doi: 10.4319/lo.1995.40.5.0868

Holmfeldt, K., Dziallas, C., Titelman, J., Pohlmann, K., Grossart, H. P., and Riemann, L. (2009). Diversity and abundance of freshwater *Actinobacteria* along environmental gradients in the brackish northern Baltic Sea. *Environ. Microbiol.* 11, 2042–2054. doi: 10.1111/j.1462-2920.2009.01925.x

Hoppe, H. G., Breithaupt, P., Walther, K., Koppe, R., Bleck, S., Sommer, U., et al. (2008). Climate warming in winter affects the coupling between phytoplankton and bacteria during the spring bloom: a mesocosm study. *Aquat. Microbiol. Ecol.* 51, 105–115. doi: 10.3354/ame01198

Hu, Y. O. O., Karlson, B., Charvet, S., and Andersson, A. F. (2016). Diversity of pico- to mesoplankton along the 2000 km salinity gradient of the Baltic Sea. *Front. Microbiol.* 7:679. doi: 10.3389/fmicb.2016.00679

Hugerth, L. W., and Andersson, A. F. (2017). Analysing microbial community composition through amplicon sequencing: from sampling to hypothesis testing. *Front. Microbiol.* 8:1561. doi: 10.3389/fmicb.2017.01561

Hugerth, L. W., Larsson, J., Alneberg, J., Lindh, M. V., Legrand, C., Pinhassi, J., et al. (2015). Metagenome-assembled genomes uncover a global brackish microbiome. *Gen. Biol.* 16:279. doi: 10.1186/s13059-015-0834-7

Joint, I., Doney, S. C., and Karl, D. M. (2011). Will ocean acidification affect marine microbes? *ISME J.* 5, 1–7. doi: 10.1038/ismej.2010.79

Kaartokallio, H., Laamanen, M., and Sivonen, K. (2005). Responses of Baltic Sea ice and open-water natural bacterial communities to salinity change. *Appl. Environ. Microbiol.* 71, 4364–4371. doi: 10.1128/AEM.71.8.4364-4371.2005

Kaartokallio, H., Tuomainen, J., Kuosa, H., Kuparinen, J., Martikainen, P. J., and Servomaa, K. (2008). Succession of sea-ice bacterial communities in the Baltic Sea fast ice. *Polar Biol.* 31, 783–793. doi: 10.1007/s00300-008-0416-1

Kisand, V., Cuadros, R., and Wikner, J. (2002). Phylogeny of culturable estuarine bacteria catabolizing riverine organic matter in the northern Baltic Sea. *Appl. Environ. Microbiol.* 68, 379–388. doi: 10.1128/AEM.68.1.379-388.2002

Kisand, V., and Wikner, J. (2003). Combining culture-dependent and -independent methodologies for estimation of richness of estuarine bacterioplankton consuming riverine dissolved organic matter. *Appl. Environ. Microbiol.* 69, 3607–3616. doi: 10.1128/AEM.69.6.3607-3616.2003

Klier, J., Dellwig, O., Leipe, T., Jürgens, K., and Herlemann, D. P. R. (2018). Benthic bacterial community composition in the oligohaline-marine transition of surface sediments in the Baltic Sea based on rRNA analysis. *Front. Microbiol.* 9:236. doi: 10.3389/fmicb.2018.00236

Koskinen, K., Hultman, J., Paulin, L., Auvinen, P., and Kankaanpää; H. (2011). Spatially differing bacterial communities in water columns of the northern Baltic Sea. *FEMS Microbiol. Ecol.* 75, 99–110. doi: 10.1111/j.1574-6941.2010.00987.x

Kritzberg, E., Cole, J. J., Pace, M. L., Granéli, W., and Bade, D. L. (2004). Autochthonous versus allochthonous carbon sources of bacteria: results from whole-lake C-13 addition experiments. *Limnol. Oceanogr.* 49, 588–596. doi: 10.4319/lo.2004.49.2.0588

Laas, P., Atova, E., Lips, I., Lips, U., Simm, J., Kisand, V., et al. (2016). Near-bottom hypoxia impacts dynamics of bacterioplankton assemblage throughout water column of the Gulf of Finland (Baltic Sea). *PLoS ONE* 11:e0156147. doi: 10.1371/journal.pone.0156147

Laas, P., Simm, J., Lips, I., Lips, U., Kisand, V., and Metsis, M. (2015). Redox-specialized bacterioplankton metacommunity in a temperate estuary. *PLoS ONE* 10:e0122304. doi: 10.1371/journal.pone.0122304

Laas, P., Simm, J., Lips, I., and Metsis, M. (2014). Spatial variability of winter bacterioplankton community composition in the Gulf of Finland (the Baltic Sea). *J. Mar. Syst.* 129, 127–134. doi: 10.1016/j.jmarsys.2013.07.016

Labrenz, M., Jost, G., Pohl, C., Beckmann, S., Martens-Habbena, W., and Jürgens, K. (2005). Impact of different *in vitro* electron donor/acceptor conditions on potential chemolithoautotrophic communities from marine pelagic redoxclines. *Appl. Environ. Microbiol.* 71, 6664–6672. doi: 10.1128/AEM.71.11.6664-6672.2005

Langenheder, S., Bulling, M. T., Solan, M., and Prosser, J. I. (2010). Bacterial biodiversity-ecosystem functioning relations are modified by environmental complexity. *PLoS ONE* 5:e10834. doi: 10.1371/journal.pone.0010834

Langenheder, S., Kisand, V., Lindstrom, E. S., Wikner, J., and Tranvik, L. J. (2004). Growth dynamics within bacterial communities in riverine and estuarine batch cultures. *Aquat. Microbiol. Ecol.* 37, 137–148. doi: 10.3354/ame037137

Langenheder, S., Kisand, V., Wikner, J., and Tranvik, L. J. (2003). Salinity as a structuring factor for the composition and performance of bacterioplankton degrading riverine DOC. *FEMS Microbiol. Ecol.* 45, 189–202. doi: 10.1016/S0168-6496(03)00149-1

Larsson, J., Celepli, N., Ininbergs, K., Dupont, C. L., Yooseph, S., Bergman, B., et al. (2014). Picocyanobacteria containing a novel pigment gene cluster dominate the brackish water Baltic Sea. *ISME J.* 8, 1892–1903. doi: 10.1038/ismej.2014.35

Legrand, C., Fridolfsson, E., Bertos-Fortis, M., Lindehoff, E., Larsson, P., Pinhassi, J., et al. (2015). Interannual variability of phyto-bacterioplankton biomass and production in coastal and offshore waters of the Baltic Sea. *AMBIO* 44, 427–438. doi: 10.1007/s13280-015-0662-8

Leibold, M. A., Holyoak, M., Mouquet, N., Amarasekare, P., Chase, J. M., Hoopes, M. F., et al. (2004). The metacommunity concept: a framework for multi-scale community ecology. *Ecol. Lett.* 7, 601–613. doi: 10.1111/j.1461-0248.2004.00608.x

Lindh, M., Sjöstedt, J., Casini, M., Andersson, A., Legrand, C., and Pinhassi, J. (2016). Local environmental conditions shape generalist but not specialist components of microbial metacommunities in the Baltic Sea. *Front. Microbiol.* 7:2078. doi: 10.3389/fmicb.2016.02078

Lindh, M. V. (2014). *Bacterioplankton Population Dynamics in a Changing Ocean.* Doctoral dissertation. Kalmar: Linnaeus University. Available online at: http://urn.kb.se/resolve?urn=urn:nbn:se:lnu:diva-38712

Lindh, M. V., Figueroa, D., Sjöstedt, J., Baltar, F., Lundin, D., Andersson, A., et al. (2015a). Transplant experiments uncover Baltic Sea basin-specific responses in bacterioplankton community composition and metabolic activities. *Front. Microbiol.* 6:223. doi: 10.3389/fmicb.2015.00223

Lindh, M. V., Lefebure, R., Degerman, R., Lundin, D., Andersson, A., and Pinhassi, J. (2015b). Consequences of increased terrestrial dissolved organic matter and temperature on bacterioplankton community composition during a Baltic Sea mesocosm experiment. *AMBIO* 44, S402–S412. doi: 10.1007/s13280-015-0659-3

Lindh, M. V., Maillot, B. M., Smith, C. R., and Church, M. J. (2018). Habitat filtering of bacterioplankton communities above polymetallic nodule fields and sediments in the Clarion-Clipperton zone of the Pacific Ocean. *Environ. Microbiol. Rep.* 10, 113–122. doi: 10.1111/1758-2229.12627

Lindh, M. V., Riemann, L., Baltar, F., Romero-Oliva, C., Salomon, P. S., Graneli, E., et al. (2013). Consequences of increased temperature and acidification on bacterioplankton community composition during a mesocosm spring bloom in the Baltic Sea. *Environ. Microbiol. Rep.* 5, 252–262. doi: 10.1111/1758-2229.12009

Lindh, M. V., Sjöstedt, J., Andersson, A. F., Baltar, F., Hugerth, L. W., Lundin, D., et al. (2015c). Disentangling seasonal bacterioplankton population dynamics by high-frequency sampling. *Environ. Microbiol.* 17, 2459–2476. doi: 10.1111/1462-2920.12720

Lindh, M. V., Sjöstedt, J., Ekstam, B., Casini, M., Lundin, D., Hugerth, L. W., et al. (2017). Metapopulation theory identifies biogeographical patterns among core and satellite marine bacteria scaling from tens to thousands of kilometers. *Environ. Microbiol.* 19, 1222–1236. doi: 10.1111/1462-2920.13650

Lindroos, A., Marta Szabo, H., Nikinmaa, M., and Leskinen, P. (2011). Comparison of sea surface microlayer and subsurface water bacterial communities in the Baltic Sea. *Aquat. Microbiol. Ecol.* 65, 29–42. doi: 10.3354/ame01532

Liu, Z., Cichocki, N., Bonk, F., Günther, S., Schattenberg, F., Harms, H., et al. (2018). Ecological stability properties of microbial communities assessed by flow cytometry. *mSphere* 3, *e*00564–17. doi: 10.1128/mSphere.00564-17

Logares, R., Lindstrom, E. S., Langenheder, S., Logue, J. B., Paterson, H., Laybourn-Parry, J., et al. (2013). Biogeography of bacterial communities exposed to progressive long-term environmental change. *ISME J.* 7, 937–948. doi: 10.1038/ismej.2012.168

Loreau, M. (2000). Biodiversity and ecosystem functioning: recent theoretical advances. *Oikos* 91, 3–17. doi: 10.1034/j.1600-0706.2000.910101.x

Loreau, M. (2004). Does functional redundancy exist? *Oikos* 104, 606–611. doi: 10.1111/j.0030-1299.2004.12685.x

Massana, R., Pedrós Alió, C., Casamayor, E. O., and Gasol, J. M. (2001). Changes in marine bacterioplankton phylogenetic composition during incubations designed to measure biogeochemically significant parameters. *Limnol. Oceanogr.* 46, 1181–1188. doi: 10.4319/lo.2001.46.5.1181

Meier, H. E. M. (2006). Baltic Sea climate in the late twenty-first century: a dynamical downscaling approach using two global models and two emission scenarios. *Climate Dyn.* 27, 39–68. doi: 10.1007/s00382-006-0124-x

Morán, X.A., Alonso-Sáez, L., Nogueira, E., Ducklow, H. W., González, N., López-Urrutia, Á., et al. (2015). More, smaller bacteria in response to ocean's warming? *Proc. R. Soc. Lond. B Biol. Sci.* 282:20150371. doi: 10.1098/rspb.2015.0371

Muren, U., Berglund, J., Samuelsson, K., and Andersson, A. (2005). Potential effects of elevated sea-water temperature on pelagic food webs. *Hydrobiol* 545, 153–166. doi: 10.1007/s10750-005-2742-4

Nagata, T. (2008). "Organic matter–bacteria interactions in seawater," in *Microbial Ecology of the Oceans,* ed D. Kirchman. (New York, NY: John Wiley & Sons, Inc.), 1668–1681.

Omstedt, A., Elken, J., Lehmann, A., Leppäranta, M., Meier, H. E. M., Myrberg, K., et al. (2014). Progress in physical oceanography of the Baltic Sea during the 2003–2014 period. *Progr. Oceanogr.* 128, 139–171. doi: 10.1016/j.pocean.2014.08.010

Pante, E., and Simon-Bouhet, B. (2013). marmap: a package for importing, plotting and analyzing bathymetric and topographic data in R. *PLoS ONE* 8:e73051. doi: 10.1371/journal.pone.0073051

Pedler, B. E., Aluwihare, L. I., and Azam, F. (2014). Single bacterial strain capable of significant contribution to carbon cycling in the surface ocean. *Proc Natl Acad Sci U.S.A.* 111, 7202–7207. doi: 10.1073/pnas.1401887111

Pedros-Alio, C. (2006). Marine microbial diversity: can it be determined? *Tr Microbiol* 14, 257–263. doi: 10.1016/j.tim.2006.04.007

Pinhassi, J., and Hagström, Å. (2000). Seasonal succession in marine bacterioplankton. *Aquat. Microbiol. Ecol.* 21, 245–256. doi: 10.3354/ame021245

Pinhassi, J., Zweifel, U. L., and Hagström, Å. (1997). Dominant marine bacterioplankton species found among colony-forming bacteria. *Appl. Environ. Microbiol.* 63, 3359–3366.

Piwosz, K., Salcher, M. M., Zeder, M., Ameryk, A., and Pernthaler, J. (2013). Seasonal dynamics and activity of typical freshwater bacteria in brackish waters of the Gulf of Gdansk. *Limnol. Oceanogr.* 58, 817–826. doi: 10.4319/lo.2013.58.3.0817

Poisot, T., Pequin, B., and Gravel, D. (2013). High-throughput sequencing: a roadmap toward community ecology. *Ecol. Evol.* 3, 1125–1139. doi: 10.1002/ece3.508

Quast, C., Pruesse, E., Yilmaz, P., Gerken, J., Schweer, T., Yarza, P., et al. (2013). The SILVA ribosomal RNA gene database project: improved data processing and web-based tools. *Nucleic Acids Res.* 41, D.590–596. doi: 10.1093/nar/gks1219

R Core Development Team (2017). *R: A Language and Environment for Statistical Computing.* Available online at: https://cran.r-project.org/

Rahlff, J., Stolle, C., Giebel, H. A., Brinkhoff, T., Ribas-Ribas, M., Hodapp, D., et al. (2017). High wind speeds prevent formation of a distinct bacterioneuston community in the sea-surface microlayer. *FEMS Microbiol. Ecol.* 93:fix041. doi: 10.1093/femsec/fix041

Reindl, A. R., and Bolałek, J. (2017). Biological factor controlling methane production in surface sediment in the polish part of the Vistula Lagoon. *Oceanol. Hydrobiol. Stud.* 46, 223–230. doi: 10.1515/ohs-2017-0022

Reunamo, A., Riemann, L., Leskinen, P., and Jorgensen, K. S. (2013). Dominant petroleum hydrocarbon-degrading bacteria in the Archipelago Sea in South-West Finland (Baltic Sea) belong to different taxonomic groups than hydrocarbon degraders in the oceans. *Mar. Poll. Bull.* 72, 174–180. doi: 10.1016/j.marpolbul.2013.04.006

Reunamo, A., Yli-Hemminki, P., Nuutinen, J., Lehtoranta, J., and Jørgensen, K. S. (2017). Degradation of crude oil and pahs in iron–manganese concretions and sediment from the northern Baltic Sea. *Geomicrobiol. J.* 34, 385–399. doi: 10.1080/01490451.2016.1197987

Reyes, C., Schneider, D., Thürmer, A., Kulkarni, A., Lipka, M., Sztejrenszus, S. Y., et al. (2017). Potentially active iron, sulfur, and sulfate reducing bacteria in skagerrak and bothnian bay sediments. *Geomicrobiol. J.* 34, 840–850. doi: 10.1080/01490451.2017.1281360

Rieck, A., Herlemann, D., Jürgens, K., and Grossart, H.-P. (2015). Particle-associated differ from free-living bacteria in surface waters of the Baltic Sea. *Front. Microbiol.* 6:1297. doi: 10.3389/fmicb.2015.01297

Riemann, L., Leitet, C., Pommier, T., Simu, K., Holmfeldt, K., Larsson, U., et al. (2008). The native bacterioplankton community in the central Baltic sea is influenced by freshwater bacterial species. *Appl. Environ. Microbiol.* 74, 503–515. doi: 10.1128/AEM.01983-07

Rowe, O. F., Dinasquet, J., Paczkowska, J., Figueroa, D., Riemann, L., and Andersson, A. (2018). Major differences in dissolved organic matter characteristics and bacterial processing over an extensive brackish water gradient, the Baltic Sea. *Mar. Chem.* 202, 27–36. doi: 10.1016/j.marchem.2018.01.010

Sala, M. M., Aparicio, F. L., Balagué, V., Boras, J. A., Borrull, E., Cardelús, C., et al. (2016). Contrasting effects of ocean acidification on the microbial food web under different trophic conditions. *ICES J. Mar. Sci.* 73, 670–679. doi: 10.1093/icesjms/fsv130

Salazar, G., Cornejo-Castillo, F. M., Benitez-Barrios, V., Fraile-Nuez, E., Alvarez-Salgado, X. A., Duarte, C. M., et al. (2016). Global diversity and biogeography of deep-sea pelagic prokaryotes. *ISME J.* 10, 596–608. doi: 10.1038/ismej.2015.137

Salka, I., Moulisova, V., Koblizek, M., Jost, G., Jürgens, K., and Labrenz, M. (2008). Abundance, depth distribution, and composition of aerobic bacteriochlorophyll a-producing bacteria in four basins of the central Baltic Sea. *Appl. Environ. Microbiol.* 74, 4398–4404. doi: 10.1128/AEM.02447-07

Salka, I., Wurzbacher, C., Garcia, S. L., Labrenz, M., Jürgens, K., and Grossart, H. P. (2014). Distribution of acI-actinorhodopsin genes in Baltic Sea salinity gradients indicates adaptation of facultative freshwater photoheterotrophs to brackish waters. *Environ. Microbiol.* 16, 586–597. doi: 10.1111/1462-2920.12185

Shade, A., Peter, H., Allison, S. D., Baho, D. L., Berga, M., Bürgmann, H., et al. (2012). Fundamentals of microbial community resistance and resilience. *Front. Microbiol.* 3:417. doi: 10.3389/fmicb.2012.00417

Simu, K., and Hagström, Å. (2004). Oligotrophic bacterioplankton with a novel single-cell life strategy. *Appl. Environ. Microbiol.* 70, 2445–2451. doi: 10.1128/AEM.70.4.2445-2451.2004

Sipura, J., Haukka, K., Helminen, H., Lagus, A., Suomela, J., and Sivonen, K. (2005). Effect of nutrient enrichment on bacterioplankton biomass and community composition in mesocosms in the Archipelago Sea, northern Baltic. *J. Plankt. Res.* 27, 1261–1272. doi: 10.1093/plankt/fbi092

Sjöstedt, J., Hagström, Å., and Zweifel, U. L. (2012a). Variation in cell volume and community composition of bacteria in response to temperature. *Aquat. Microbiol. Ecol.* 66, 237–246. doi: 10.3354/ame01579

Sjöstedt, J., Koch-Schmidt, P., Pontarp, M., Canback, B., Tunlid, A., Lundberg, P., et al. (2012b). Recruitment of members from the rare biosphere of marine bacterioplankton communities after an environmental disturbance. *Appl. Environ. Microbiol.* 78, 1361–1369. doi: 10.1128/AEM.05542-11

Sommer, U., Aberle, N., Engel, A., Hansen, T., Lengfellner, K., Sandow, M., et al. (2007). An indoor mesocosm system to study the effect of climate change on the late winter and spring succession of Baltic Sea phyto- and zooplankton. *Oecologia* 150, 655–667. doi: 10.1007/s00442-006-0539-4

Stolle, C., Labrenz, M., Meeske, C., and Jürgens, K. (2011). Bacterioneuston community structure in the southern Baltic sea and its dependence on meteorological conditions. *Appl. Environ. Microbiol.* 77, 3726–3733. doi: 10.1128/AEM.00042-11

Stolle, C., Nagel, K., Labrenz, M., and Jürgens, K. (2010). Succession of the sea-surface microlayer in the coastal Baltic Sea under natural and experimentally induced low-wind conditions. *Biogeosciences* 7, 2975–2988. doi: 10.5194/bg-7-2975-2010

Sunagawa, S., Coelho, L. P., Chaffron, S., Kultima, J. R., Labadie, K., Salazar, G., et al. (2015). Structure and function of the global ocean microbiome. *Science* 348:1261359. doi: 10.1126/science.1261359

Tamelander, T., Spilling, K., and Winder, M. (2017). Organic matter export to the seafloor in the Baltic Sea: drivers of change and future projections. *AMBIO* 46, 842–851. doi: 10.1007/s13280-017-0930-x

Tammert, H., Lignell, R., Kisand, V., and Olli, K. (2012). Labile carbon supplement induces growth of filamentous bacteria in the Baltic Sea. *Aquat. Biol.* 15, 121–134. doi: 10.3354/ab00424

Tank, M., Bluemel, M., and Imhoff, J. F. (2011). Communities of purple sulfur bacteria in a Baltic Sea coastal lagoon analyzed by puf LM gene libraries and the impact of temperature and NaCl concentration in experimental enrichment cultures. *FEMS Microbiol. Ecol.* 78, 428–438. doi: 10.1111/j.1574-6941.2011.01175.x

Teeling, H., Fuchs, B. M., Bennke, C. M., Krüger, K., Chafee, M., Kappelmann, L., et al. (2016). Recurring patterns in bacterioplankton dynamics during coastal spring algae blooms. *eLife* 5:e11888. doi: 10.7554/eLife.11888

Tiirik, K., Nõlvak, H., Oopkaup, K., Truu, M., Preem, J.-K., Heinaru, A., et al. (2014). Characterization of the bacterioplankton community and its antibiotic resistance genes in the Baltic Sea. *Biotechn. Appl. Biochem.* 61, 23–32. doi: 10.1002/bab.1144

Traving, S. J., Rowe, O., Jakobsen, N. M., Sorensen, H., Dinasquet, J., Stedmon, C. A., et al. (2017). The effect of increased loads of dissolved organic matter on estuarine microbial community composition and function. *Front. Microbiol.* 8:351. doi: 10.3389/fmicb.2017.00351

Tuomainen, J., Hietanen, S., Kuparinen, J., Martikainen, P., and Servomaa, K. (2006). Community structure of the bacteria associated with Nodularia sp. *(cyanobacteria)* aggregates in the Baltic Sea. *Microb. Ecol.* 52, 513–522. doi: 10.1007/s00248-006-9130-0

Vaquer-Sunyer, R., Conley, D. J., Muthusamy, S., Lindh, M. V., Pinhassi, J., and Kritzberg, E. S. (2015). Dissolved organic nitrogen inputs from wastewater treatment plant effluents increase responses of planktonic metabolic rates to warming. *Environ. Sci. Techn.* 49, 11411–11420. doi: 10.1021/acs.est.5b00674

Vaquer-Sunyer, R., Reader, H. E., Muthusamy, S., Lindh, M. V., Pinhassi, J., Conley, D. J., et al. (2016). Effects of wastewater treatment plant effluent inputs on planktonic metabolic rates and microbial community composition in the Baltic Sea. *Biogeosciences* 13, 4751–4765. doi: 10.5194/bg-13-4751-2016

Vega Thurber, R., Willner-Hall, D., Rodriguez-Mueller, B., Desnues, C., Edwards, R. A., Angly, F., et al. (2009). Metagenomic analysis of stressed coral holobionts. *Environ. Microbiol.* 11, 2148–2163. doi: 10.1111/j.1462-2920.2009.01935.x

Viggor, S., Joesaar, M., Vedler, E., Kiiker, R., Paernpuu, L., and Heinaru, A. (2015). Occurrence of diverse alkane hydroxylase alkB genes in indigenous oil-degrading bacteria of Baltic Sea surface water. *Mar. Poll. Bull.* 101, 507–516. doi: 10.1016/j.marpolbul.2015.10.064

Viggor, S., Juhanson, J., Joesaar, M., Mitt, M., Truu, J., Vedler, E., et al. (2013). Dynamic changes in the structure of microbial communities in Baltic Sea coastal seawater microcosms modified by crude oil, shale oil or diesel fuel. *Microbiol Res.* 168, 415–427. doi: 10.1016/j.micres.2013.02.006

von Scheibner, M., Doerge, P., Biermann, A., Sommer, U., Hoppe, H.-G., and Juergens, K. (2014). Impact of warming on phyto-bacterioplankton coupling and bacterial community composition in experimental mesocosms. *Environ. Microbiol.* 16, 718–733. doi: 10.1111/1462-2920.12195

von Scheibner, M., Sommer, U., and Jürgens, K. (2017). Tight coupling of *Glaciecola* spp. and diatoms during cold-water phytoplankton spring blooms. *Front. Microbiol.* 8:27. doi: 10.3389/fmicb.2017.00027

Yeh, Y.-C., Peres-Neto, P. R., Huang, S.-W., Lai, Y.-C., Tu, C.-Y., Shiah, F.-K., et al. (2015). Determinism of bacterial metacommunity dynamics in the southern East China Sea varies depending on hydrography. *Ecography* 38, 198–212. doi: 10.1111/ecog.00986

Zinke, L. A., Mullis, M. M., Bird, J. T., Marshall, I. P. G., Jørgensen, B. B., Lloyd, K. G., et al. (2017). Thriving or surviving? Evaluating active microbial guilds in Baltic Sea sediment. *Environ. Microbiol. Rep.* 9, 528–536. doi: 10.1111/1758-2229.12578

Conflict of Interest Statement: The authors declare that the research was conducted in the absence of any commercial or financial relationships that could be construed as a potential conflict of interest.

frontiers in Marine Science

ORIGINAL RESEARCH
published: 13 July 2018
doi: 10.3389/fmars.2018.00231

Phyto- and Bacterioplankton During Early Spring Conditions in the Baltic Sea and Response to Short-Term Experimental Warming

Markus von Scheibner[1], *Daniel P. R. Herlemann*[1,2], *Aleksandra M. Lewandowska*[3] *and Klaus Jürgens*[1]*

[1] Leibniz Institute for Baltic Sea Research Warnemünde, Rostock, Germany, [2] Center of Limnology, Estonian University of Life Sciences, Tartu, Estonia, [3] Tvarminne Zoological Station, University of Helsinki, Hanko, Finland

OPEN ACCESS

Edited by:
Riina Klais,
University of Tartu, Estonia

Reviewed by:
Raquel Vaquer-Sunyer,
Instituto Mediterráneo de Estudios Avanzados (IMEDEA), Spain
Jelena Godrijan,
Bigelow Laboratory For Ocean Sciences, United States

***Correspondence:**
Klaus Jürgens
klaus.juergens@io-warnemuende.de

Specialty section:
This article was submitted to Marine Ecosystem Ecology, a section of the journal Frontiers in Marine Science

Received: *10 January 2018*
Accepted: *14 June 2018*
Published: *13 July 2018*

Citation:
von Scheibner M, Herlemann DPR, Lewandowska AM and Jürgens K (2018) Phyto- and Bacterioplankton During Early Spring Conditions in the Baltic Sea and Response to Short-Term Experimental Warming. Front. Mar. Sci. 5:231. doi: 10.3389/fmars.2018.00231

Predicted increases in sea surface temperatures are expected to shift the balance between autotrophic production and the heterotrophic degradation of organic matter toward a more heterotrophic system. For early phytoplankton spring blooms at low water temperature the impact of rising temperatures has been mainly investigated in mesocosm experiments, while field observations are scarce. During a Baltic Sea research cruise we examined early spring bloom conditions, characterized by low temperatures (0–3°C), and performed on-board warming experiments to compare the responses of phyto- and bacterioplankton production to an increase in temperature. In the northern Baltic Sea, the low phytoplankton biomass indicated pre-bloom conditions. In the southern Baltic Sea, a diatom-dominated phytoplankton bloom with increased primary production (PP) occurred. Associated with this bloom were increases in bacterial production (BP) and bacterial abundance as well as shifts in bacterial community composition toward an increased proportion of *Gammaproteobacteria* and *Bacteroidetes*. However, the low BP/PP ratios (average: 1.2 ± 0.14%) indicated weak coupling between the bacterial and phytoplankton communities. Short-term warming (6 h, Δ+6°C) significantly enhanced PP (mean Q_{10} 1.4) and especially BP (mean Q_{10} 2.3). Hence, the higher water temperature increased both carbon flow into the bacterial community and bacterial processing of organic matter, thereby confirming previous experimental studies. By contrast, BP/PP ratios remained relatively low after warming (average: 1.7 ± 0.5%), unlike in previous mesocosm experiments performed at comparable temperatures and with similar plankton communities. Overall, these results imply that bacterial activities are suppressed during early phytoplankton blooms at low temperatures in the Baltic Sea and are not substantially altered by short-term warming events.

Keywords: phytoplankton spring bloom, bacteria, primary production, bacterial production, temperature, global warming, Baltic Sea, bacterial community composition

INTRODUCTION

Under various greenhouse gas emission scenarios, ocean surface temperatures are predicted to increase 2–5°C by the end of this century (IPCC, 2013). Rising temperatures directly and indirectly impact pelagic organisms and aquatic food webs, leading to changes in the structure and functioning of marine ecosystems (Boyd and Doney, 2002; Sarmiento et al., 2004). Phytoplankton account for ∼50% of global net primary production (PP) and are the main energy source for aquatic ecosystems (Field et al., 1998). The major consumers of phytoplankton-derived organic matter are heterotrophic bacteria present in the upper water layers of aquatic ecosystems. The coupling of phytoplankton dissolved organic carbon (DOC) production with DOC consumption by heterotrophic prokaryotes (mostly bacteria) plays a central role in the biogeochemistry of pelagic food webs (Azam, 1998; Ducklow, 2000). The phytoplankton-bacteria relationship and the coupling between the two components is generally analyzed by comparing primary production to bacterial production (BP) rates (Hoppe et al., 2002; Morán et al., 2002, 2013) or, more comprehensively, to bacterial carbon demand (BCD), thereby also including bacterial respiration (del Giorgio et al., 1997; Rivkin and Legendre, 2001). The degree of coupling between autotrophic producers and heterotrophic decomposers in planktonic systems has a strong impact on the fate of organic matter and its partitioning into different pathways, such as microbial utilization, transfer to higher trophic levels, or accumulation and export (Wohlers et al., 2009). The DOC production by phytoplankton also shapes the succession of bacterial taxa and their specific functions (Sarmento and Gasol, 2012; Teeling et al., 2012), and the amount and the composition of the released DOM strongly depend on phytoplankton species and the physiological status of this cell (Nagata, 2000; Thornton, 2014).

In principle, all biological processes are modulated by temperature but the observed effects on metabolism in marine plankton are generally stronger for heterotrophic than for autotrophic organisms (Pomeroy and Deibel, 1986; Morán et al., 2006). The metabolic theory of ecology (Brown et al., 2004) predicts that respiration increases at higher rate than photosynthesis with increasing temperature, due to the lower activation energy of autotrophs (Harris et al., 2006). Moreover, phytoplankton are most often limited by light or nutrient levels (Tilzer et al., 1986), which diminishes the temperature sensitivity of growth (Edwards et al., 2016). The effects of temperature are reflected in reduced bacterial growth during phytoplankton spring blooms at low temperatures (e.g., polar regions), which may temporarily uncouple heterotrophic DOC consumption from autotrophic organic matter production (Pomeroy and Deibel, 1986; Kirchman et al., 2009). Conversely, an increase in water temperature has the potential to intensify the degree of phytoplankton-bacterioplankton coupling by stimulating bacterial growth and substrate consumption more than for the phytoplankton. Therefore, an increase in temperature potentially shifts the balance of autotrophic production and heterotrophic consumption toward the latter (Hoppe et al., 2002; López-Urrutia et al., 2006; Morán et al., 2006; O'Connor et al., 2009; Degerman et al., 2013).

Over the last decade, the impact of temperature changes on phyto-bacterioplankton coupling and the consequences for the marine carbon cycle have mainly been investigated in mesocosm studies that included experimental warming (e.g., Morán et al., 2006; O'Connor et al., 2009; Lindh et al., 2012). For example, the effect of sea surface warming on food web dynamics and pelagic carbon flow patterns has been investigated in several indoor-mesocosm experiments using natural spring plankton communities from the Baltic Sea (Sommer et al., 2012; Wohlers-Zöllner et al., 2012). Among other results, a temperature increase was repeatedly shown to strongly stimulate bacterial abundance, bacterial production (BP), and bacterial respiration, resulting in an increased processing of phytoplankton-derived organic matter by heterotrophic bacteria and a higher carbon flow into the microbial food web (Hoppe et al., 2008; Wohlers et al., 2009; von Scheibner et al., 2014). The results of other experiments, performed both in the Baltic Sea (Müren et al., 2005; Eriksson Wiklund et al., 2009; Degerman et al., 2013; Vaquer-Sunyer et al., 2015) and in other marine areas (e.g., Keller et al., 1999; O'Connor et al., 2009), also revealed that an increase in temperature increases planktonic respiration and intensifies the coupling of primary producers and heterotrophic consumers. Overall, warming-induced increases in heterotrophic activities resulted in a higher net consumption of DOC and subsequently in a reduced net consumption of dissolved inorganic carbon (DIC), thus constituting a positive feedback response to global warming (Wohlers et al., 2009).

However, current knowledge of the underlying mechanisms by which surface water warming influences food web dynamics and phyto-bacterioplankton coupling is still limited, and it is not clear whether the results from mesocosm studies can be extrapolated to *in situ* conditions. This is due to a paucity of field studies investigating the coupling of phyto- and bacterioplankton production under the *in situ* conditions of the early spring bloom, when water temperatures are low and the phytoplankton development depends on a first and generally weak stratification of the water column.

The Baltic Sea is a brackish, semi-enclosed shelf sea, with pronounced phytoplankton blooms in spring and autumn. In the southern Baltic, the phytoplankton spring bloom normally occurs between late February and early April whereas in northern regions it often begins later and extends until May, depending on the intensity of the surface irradiance, water stratification, and ice cover (Spilling and Markager, 2008; Wasmund et al., 2008; Klais et al., 2013). The spring blooms are typically dominated by diatoms (e.g., *Chaetoceros* spp. and *Skeletonema costatum*) although in some parts of the Baltic Sea (e.g., the central Baltic Sea) cold-water dinoflagellates may be dominant, especially after warmer winters (Wasmund et al., 2008, 2011; Klais et al., 2011, 2013). A strong increase in annual mean surface temperature is predicted for the Baltic Sea, with pronounced winter warming by up to 6°C expected by the end of this century (HELCOM, 2013).

The aim of this study was to investigate the phyto-bacterioplankton coupling during early spring bloom conditions at low water temperatures in the Baltic Sea, and to examine

their response to short-term warming. We hypothesized that at these low temperatures the activity and production of planktonic bacteria would be suppressed compared to phytoplankton. For this purpose, we collected water samples from different stations in the northern and southern Baltic Sea, assessed phyto- and bacterioplankton composition and measured primary and bacterial production. Additionally, we performed shipboard incubations, where PP and BP levels in response to an increase in temperature were measured. Some of the results confirmed those of previous mesocosm warming studies, but striking differences with respect to the strength of phyto-bacterioplankton coupling became also obvious.

MATERIALS AND METHODS

Sampling

Water samples were taken at eight stations (stations 1–8), extending from the Gulf of Finland to the southern Baltic Sea, during a research cruise of the *R/V* Alkor between March 4 and 11, 2009 (**Figure 1**). Surface water samples were collected directly after sunrise using a rosette comprising 24 10-L bottles equipped with a conductivity/temperature/depth (CTD) sensor (SeaBird 911) and sensors for fluorescence. The concentrations of inorganic nutrients were determined as described by Grasshoff et al. (1999). To collect microbial biomass for DNA extraction, water samples of 1–1.5 L were filtered onto 0.2-μm polycarbonate filters (without pre-filtration) and stored frozen at −80°C. DNA was extracted as described in Weinbauer et al. (2002). For phytoplankton, 250-mL samples were fixed with Lugol's iodine and a subsample was later counted using an inverted microscope (Utermöhl, 1958). Phytoplankton species identification was performed in agreement with the HELCOM COMBINE protocol and the Checklist of Baltic Sea Phytoplankton Species (Baltic Sea Environment Proceedings No. 95, Helsinki Commission). Phytoplankton cell volumes were calculated after an approximation to geometric standards and converted to phytoplankton biomass (μg C L^{-1}) according to HELCOM recommendations (Olenina et al., 2006).

Heterotrophic and autotrophic picoplankton were analyzed by flow cytometry using a FACScalibur (Becton & Dickinson) with a constant flow rate (35 μL min^{-1}) and yellow-green latex beads (0.5 μm, Polysciences), which served as an internal standard. Duplicates of unfiltered 4-mL samples were fixed with 400 μL of 1% paraformaldehyde and 0.05% glutaraldehyde (final concentration), shock frozen in liquid nitrogen, and stored at −20°C. Smaller autotrophic cells, including *Synechococcus* as well as pico- und nanoeukaryotic phytoplankton (<5 μm), were distinguished by size and fluorescence (chlorophyll-*a* and phycoerythrin). Heterotrophic cells were analyzed after staining with 2.5 μM (final concentration) SYBR Green (Molecular Probes). Bacteria were detected by their characteristic position in a plot of side scatter (SSC) vs. green fluorescence (FL1) and were further divided into high nucleic acid (HNA) and low nucleic acid (LNA) bacterial cells as described by Gasol and del Giorgio (2000).

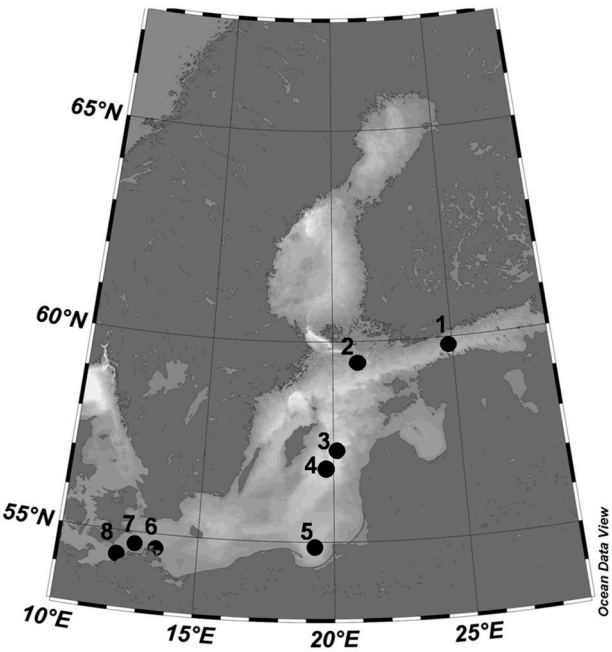

FIGURE 1 | Map of the Baltic Sea, showing the study area and the position of the eight sampling stations. According to the GPS coordinates, the station map was plotted using Ocean Data View (Schlitzer, 2011).

Primary Production and Bacterial Secondary Production

The first CTD in the morning (7:30 a.m. for all stations except stations 1, 5, and 8, 10:30 a.m.) was used to collect surface water (1–2.5 m) for the experimental incubations and the PP and BP measurements at *in situ* and experimentally increased (+6°C) temperatures. PP was measured using the [^{14}C]-bicarbonate incorporation method of Gragas (1975), with 200 μL of [^{14}C]-bicarbonate (10 μCi/mL) per 250-mL sample and three different light intensities (100, 75, and 50% of *in situ* light irradiation) to simulate the first few meters of the surface water layer. Triplicate samples of each light intensity and of one sample subjected to dark conditions (covered with aluminum foil) were incubated in a closed transparent incubator for 6 h on the deck of the ship at two different temperatures (Δ0°C and Δ+6°C) (Figure S1). The temperature was carefully adjusted to Δ+6°C using a thermostatic water bath according to the measured ambient water temperature (**Table 1**). The reactions were terminated by immediately filtering the samples through cellulose-nitrate filters (0.2 μm) and then exposing them to HCl fumes for 10 min before they were fixed with Lumagel scintillation cocktail (Packard). The PP values were used to calculate the surface water production rates (μg C $m^{-}3$). Due to technical problems in gathering data of daily rates of photosynthetically active radiation (PAR), daily production rates were roughly estimated by doubling the values for the half-day incubations (6 h) (Wasmund et al., 2001).

BP was measured based on [^{3}H]-leucine (306 mCi $mmol^{-1}$) incorporation as described by Simon and Azam (1989). Triplicate

TABLE 1 | Overview of the baseline parameters for all sampled stations in the Baltic Sea.

Station no.	Temperature [°C]	Salinity	NO_3^- [μmol L^{-1}]	PO_4^{3-} [μmol L^{-1}]	Phytoplankton [μg C L^{-1}]	Bacteria [10^6 ml^{-1}]
1	0.1	5.24	6.78	0.85	50.9	–
2	1.4	6.33	6.45	0.88	16.9	0.59
3	3.1	7.33	1.89	0.57	14.4	0.43
4	3.2	7.40	4.01	0.57	–	0.47
5	2.8	7.51	5.32	0.6	104.0	0.90
6	2.5	8.35	0.93	0.45	201.1	0.74
7	2.8	8.45	1.02	0.45	169.8	0.73
8	2.6	10.1	0	0.24	378.1	0.64

10-mL aliquots of the unfiltered samples and of one blank were incubated in dark with [^{3}H]-leucine (100 nM final concentration) at two different temperatures (Δ0°C and Δ+6°C) for 2 h before the reactions were stopped by the incorporation of formaldehyde (1% final concentration). The blank consisted of a sample in which formaldehyde was added before the addition of [^{3}H]-leucine. The same thermostatic water bath, as for the PP, was used to adjust the temperature to Δ+6°C. All samples were filtered onto 0.2-μm polycarbonate filters (Millipore) and rinsed with 10 mL of cold 5% trichloroacetic acid. The filters were dissolved in 4 mL of scintillation cocktail (Lumagel Plus) and the incorporated label subsequently counted in a scintillation counter (Packard). BP was calculated, assuming a leucine to carbon conversion factor of 1.5 kgC mol^{-1} leucine (Kirchman, 2001). Bacterial carbon demand (BCD) was estimated based on BP and an estimate of bacterial respiration, using the models proposed by Rivkin and Legendre (2001) as well as by del Giorgio and Cole (1998), **Table 2**.

Activation energy for metabolic rates (PP and BP) was derived from the Arrhenius equation by

$$\ln(k_2/k_1) = E_a/R^*(1/T_1 - 1/T_2) \quad (1)$$

where k_1 and k_2 are the metabolic rates at *in situ* and elevated temperature, respectively, T_1 and T_2 are the corresponding *in situ* and elevated incubation temperatures in Kelvin (K) and R is the gas constant (8.314472 mol^{-1} K^{-1}). The Q_{10} (the relative change in a metabolic rate expected for a 10 K temperature increase) was calculated by using the equation of Raven and Geider (1988):

$$Q_{10} = e^{10Ea/RT2} \quad (2)$$

where Ea is the activation energy, R is the gas constant and T is the mean temperature in Kelvin.

Analysis of Bacterial Community Composition

DNA was amplified using the bacterial 16S rRNA gene primers Bakt_341F (CCTACGGGNGGCWGCAG) and Bakt_805R (GACTACHVGGGTATCTAATCC) (Herlemann et al., 2011) and sequenced using pyrosequencing technology. For data analysis, the resulting sequences were assembled using QIIME 1.9.1 (Caporaso et al., 2010) and the "joins paired-end Illumina reads" function with default settings to merge forward and reverse sequences with an overlap of at least 30 bp. Sequences without overlap were discharged. After converting fastq to fasta using the "convert_fastaqual_fastq" function, the resulting sequences were evaluated using the SILVA NGS pipeline (Klindworth et al., 2013) with default settings. This automated pipeline aligns the reads to a curated database using the SINA aligner (Pruesse et al., 2012), in which problematic reads such as PCR artifacts (including potential chimeras) and non-ribosomal reads are filtered out. The reads were quality filtered with the following settings: reads <50 aligned nucleotides and reads with >2% ambiguities, >2% homopolymers, or low alignment quality. After alignment, the sequences were dereplicated by clustering according to their 98% sequence identity with each other (pairwise distance and single linkage clustering) using CD-HIT (Li and Godzik, 2006). The longest read in each cluster was BLAST searched against SILVA SSU Ref 128 for the classification of sequences. The resulting classification of the reference sequence of a cluster was mapped to all members of the respective cluster as well as to their replicates. Similar classifications (approximately resembling genus level) were merged to operational taxonomic units (OTUs). Closest related sequences in the SILVA SSU Ref 128 database to the sequence with most abundant reads are shown for the dominant OTUs in Table S1. Sequences having an average BLAST alignment coverage and alignment identity of <93% were considered as unclassified and assigned to the group "no relative." OTU counts were rarefied to 1000 reads per sample using the single_rarefraction.py script implemented in Qiime version 2.0 (Caporaso et al., 2010). The 16S rRNA gene sequences were part of a previous study (Herlemann et al., 2016). The raw sequencing data were deposited at the Short Sequence Archive under accession number PRJEB14590.

Statistical Analyses

PP and BP data sets were statistically analyzed using the paired *t*-test to determine the significance of the temperature effects at the *in situ* (Δ0°C) and elevated (Δ+6°C) temperatures. The significance level was set at $p < 0.05$ (IBM SPSS Statistics 20). To compare the dominant taxa between stations, the relative abundances of the >75% most abundant OTUs (>40 reads)

TABLE 2 | Daily primary production (PP), bacterial production (BP), and the resulting BP/PP ratios for Δ0°C and Δ+6°C and derived Q10 values for PP and BP.

Station No.	PP [µg C L^{-1} d^{-1}]		BP [µg C L^{-1} d^{-1}]		BP/PP [%]		BCD_1 [µg C L^{-1} d^{-1}]		BCD_2 [µg C L^{-1} d^{-1}]		BCD/PP [%]		Q_{10}	
	(Δ0°C)	(Δ6°C)	(Δ0°C)	(Δ6°C)	(Δ0°C)	(Δ6°C)	(Δ0°C)	(Δ6°C)	(Δ0°C)	(Δ6°C)	(Δ0°C)	(Δ6°C)	PP	BP
1	9.7 ± 2.6	11.2 ± 3.0	0.76 ± 0.07	1.21 ± 0.10	7.8 ± 0.7	10.8 ± 0.9	3.3 ± 0.1	4.0 ± 0.2	2.0 ± 0.2	3.8 ± 0.3	20.5 ± 1.8	34.1 ± 2.7	1.3	2.2
2	2.0 ± 0.8	4.0 ± 1.7	0.74 ± 0.08	1.11 ± 0.11	36.4 ± 4, 1	27.4 ± 2.6	3.3 ± 0.1	4.0 ± 0.2	2.2 ± 0.2	3.9 ± 0.4	105 ± 11.3	95.5 ± 8.8	3.1	1.9
3	8.3 ± 4.2	29.2 ± 5.6	0.95 ± 0.09	1.21 ± 0.02	11.5 ± 1.1	4.1 ± 0.1	3.6 ± 0.2	4.0 ± 0.2	2.6 ± 0.3	4.2 ± 0.4	32 ± 3.3	14.2 ± 1.5	8.2	1.5
4	19.2 ± 10	42.7 ± 10.8	0.59 ± 0.04	0.88 ± 0.08	3.1 ± 0.2	2.1 ± 0.2	3.0 ± 0.1	3.7 ± 0.1	1.8 ± 0.1	3.5 ± 0.3	9.4 ± 0.6	8.3 ± 0.6	3.8	1.9
5	327.5 ± 43.7	370.4 ± 69.2	4.38 ± 0.23	7.80 ± 0.45	1.3 ± 0.1	2.1 ± 0.1	8.6 ± 0.3	13.9 ± 0.7	12.4 ± 0.7	27.9 ± 1.6	3.8 ± 0.2	7.5 ± 0.4	1.2	2.6
6	201.7 ± 15.5	235.9 ± 60.1	1.94 ± 0.15	2.09 ± 0.39	1.0 ± 0.1	0.9 ± 0.2	4.5 ± 1.3	5.7 ± 0.6	4.3 ± 2.2	6.1 ± 1.1	2.1 ± 1.1	2.6 ± 0.4	1.3	1.1
7	181.4 ± 16.7	219.6 ± 20.8	2.14 ± 0.16	3.30 ± 0.19	1.2 ± 0.1	1.5 ± 0.1	5.2 ± 0.1	7.2 ± 0.3	6.9 ± 0.2	9.5 ± 0.6	3.8 ± 0.1	4.3 ± 0.3	1.4	2.1
8	303.2 ± 55.0	413.8 ± 66.2	3.84 ± 0.29	7.04 ± 0.54	1.3 ± 0.1	1.7 ± 0.1	7.0 ± 0.3	12.7 ± 0.7	9.1 ± 0.7	17.6 ± 1.2	3.0 ± 0.2	4.2 ± 0.3	1.7	2.8

Bacterial carbon demand (BCD) was estimated according to the models by del Giorgio and Cole (1998) (BCD_1) and Rivkin and Legendre (2001) (BCD_2). BCD_2 was used for the calculation of BCD/PP ratios.

were visualized in a heatmap. Explicet (Robertson et al., 2013) was used to estimate richness and Shannon diversity for the eight stations. Bacterial OTUs that significantly differed in their relative abundances between stations were identified using a linear discriminant analysis effect size (LEfSe) analysis (Segata et al., 2011) with the default settings, except the "One against all" strategy, for multi-class analysis.

RESULTS

In Situ Conditions of the Baltic Sea

During the cruise in early March, the *in situ* water temperatures were between 0.1° and 3.2°C (**Figure 1**, **Table 1**). Within the first part of the transect (hereafter called "northern stations"), extending from the Gulf of Finland (station 1) to those in the central Baltic Sea (stations 3–4), there was no indication of an ongoing phytoplankton spring bloom. Phytoplankton biomass (5.1–39.2 µg C L^{-1}) (**Figure 2A**, **Table 1**) and production (**Figure 3A**) levels in the surface waters were very low, with no sign of nutrient depletion (**Table 1**). The phytoplankton community was dominated by the dinoflagellate *Scrippsiella* sp., which at station 1, for example, contributed ∼95% to total phytoplankton biomass (**Figure 2A**, Table S2). Several large ciliates (mainly *Lohmaniella* sp.) were also identified. By contrast, at stations in the southern Baltic Sea (5–8), developing phytoplankton blooms were evidenced by biomass and PP levels up to 10 times higher than at the northern stations (PP: 180–330 vs. 2–20 µg C L^{-1} day^{-1}, respectively; **Figures 2A**, **3A**) and by the depletion of nutrient concentrations, particularly nitrate (**Table 1**). The phytoplankton communities at the southern stations were dominated by the diatom *Skeletonema costatum* (59–93% of phytoplankton biomass), with minor contributions by the dinoflagellate *Gymnodinium* ssp. and other diatoms (*Chaetoceros* spp., *Thalassiosira rotula*) (**Figure 2A**). Overall, 26 different phytoplankton species within nine phyla (e.g., Dinophyta or Heterokontophyta) were detected over the whole transect (Table S2).

Heterotrophic bacterial abundance was also higher at the southern (0.64–0.90 × 10^6 cells mL^{-1}) than at the northern (0.43–0.59 × 10^6 cells mL^{-1}) stations but the increase was relatively modest (**Figure 2B**). HNA bacteria accounted for 0.13–0.16 × 10^6 cells mL^{-1} at the northern and 0.24–0.35 × 10^6 cells mL^{-1} at the southern stations (average 30 ± 4% and 39 ± 3% of total prokaryotes, respectively) (**Figure 2B**). The difference in BP was much stronger, as the rates measured at the southern stations were 8-fold higher (**Figure 3B**). Picocyanobacteria (mainly *Synechococcus*), picoeukaryotes, and nanoeukaryotes, enumerated by flow cytometry, did not show a similarly clear pattern. Their abundance was highest at station 5 and lowest at station 2 (**Figure 2B**).

Temperature Effect on Bacteria-Phytoplankton Coupling

The experimental temperature rise of △+6°C resulted in a significant increase in PP at all stations (paired *t*-test, $p = 0.008$, $n = 8$) (**Figure 3A**). This warming-dependent increase in PP was recorded for incubations at 100 and 75% light intensity, while

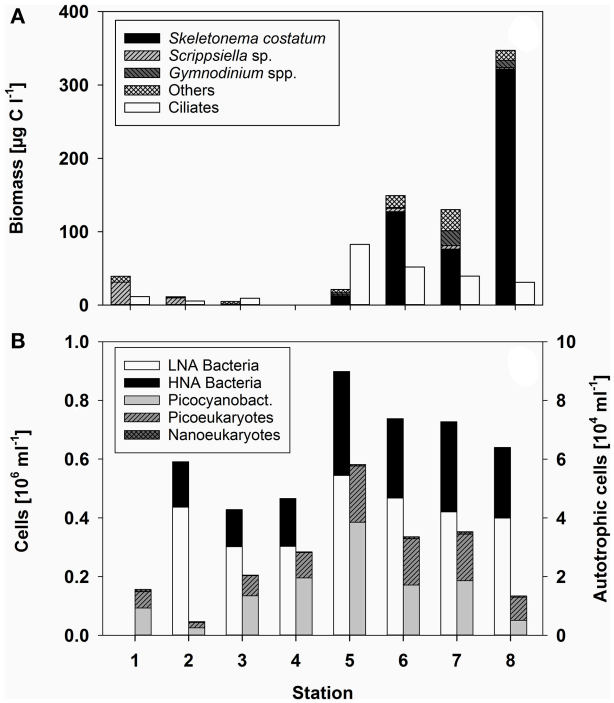

FIGURE 2 | (A) Biomass of the dominant phytoplankton taxa or taxonomic groups, as well as that of ciliates (µg C L^{-1}) according to the different stations. No data were obtained for station 4. **(B)** Bacterial abundance (10^6 mL^{-1}) at the different stations. Heterotrophic bacteria were distinguished according to their low and high nucleic acid (LNA and HNA) content. Autotrophic cells, determined by flow cytometry, are divided into *Synechococcus*, picoeukaryotes, and nanoeukaryotes (gray bars).

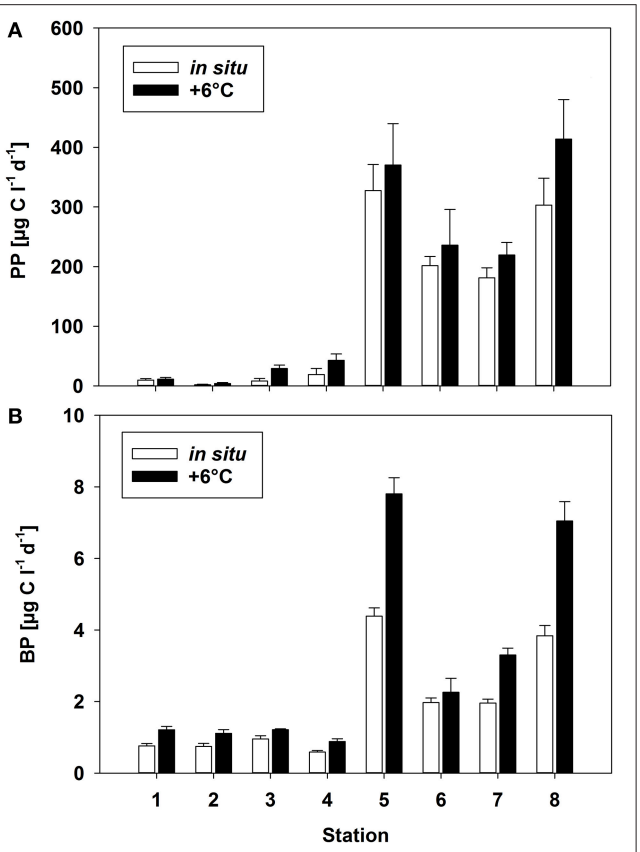

FIGURE 3 | (A) Primary production (PP) and **(B)** bacterial production (BP) rates [µg C L^{-1} $days^{-1}$] at two different temperatures (Δ0°C and Δ+6°C) at the different stations. Mean (±SD) of three replicate measurements.

at 50% light intensity PP remained almost constant (Figure S3). The temperature increase of Δ+6°C led to a stronger relative increase in PP at stations with a low phytoplankton biomass and a low rate of PP (stations 1–4; up to 250% at station 3) than at stations with high PP rates (stations 5–8). The increase at the latter stations during the incubation period was only 20% on average (**Figure 3A**, **Table 2**), with the strongest increase (36%) at station 8. The calculated Q_{10} values were in the range of 1.2–1.7 for the southern, high-PP stations and 1.3–8.2 for the northern, low-PP stations (**Figure 2A**; **Table 2**). However, for the northern stations these values should be interpreted with caution as the PP values were very low and the measured increases were in some cases close to the detection limit.

With a warming of Δ+6°C, BP also increased significantly (paired *t*-test, $p = 0.008$, $n = 8$), although with a high variability (mean increase 59 ± 31%) (**Figure 3B**). At both the northern and the southern stations BP increased by 2- to 4-fold (**Figure 3B**, **Table 2**). The resulting Q_{10} for bacterial production ranged between 1.1 and 2.8 (mean 2.2 ± 0.7) at high-PP stations (5–8) and were comparable with BP at low-PP stations which ranged between 1.5 and 2.2 (mean 1.9 ± 0.3 (**Table 2**). The calculated ratios of BP/PP and BCD/PP were much lower at the southern stations (5–8), where the phytoplankton blooms had developed, than at the northern non-bloom stations (1–4) (**Table 2**). This was independent of the chosen model for calculating BCD (**Table 2**). The experimental temperature increase did not result in significantly different ratios of BP/PP and BCD/PP at any of the northern stations (paired *t*-test, $p = 0.798$, $n = 8$) (**Table 2**). However, for the southern stations only, warming resulted in clearly increased BP/PP and BCD/PP ratios.

Bacterial Community Composition

The northern stations (1–4) of the Baltic Sea were dominated by *Actinobacteria* (13.4–26.7% of the total sequences), *Alphaproteobacteria* (18.7–24.5%), and *Bacteroidetes* (10.5–13.9%) (**Figure 4**). At the southern stations (5–8), where the diatom-dominated phytoplankton spring bloom occurred, the same phyla/classes predominated but the proportion of *Bacteroidetes* was much larger (15.5–40%). The contribution of *Cyanobacteria* (mainly *Synechococcus*) was maximal at station 5 (17.9%) and decreased with increasing phytoplankton biomass in the southern Baltic Sea (stations 7 and 8). This pattern was consistent with the cell counts of picocyanobacteria determined by flow cytometry (**Figure 2B**). Compared to the northern stations (1–4), the proportions of *Bacteroidetes* and *Gammaproteobacteria* nearly doubled at the southern stations (5–8), whereas those of *Betaproteobacteria*, *Planctomycetes*, and

Verrucomicrobia decreased (**Figure 4**). In addition, the bacterial α-diversity decreased with increasing phytoplankton biomass (number of bacterial genera, Shannon index; Figure S2).

Among the 75% most abundant bacterial OTUs, LEfSe analysis identified 14 that differed significantly between stations with a high (stations 5–8) and low (stations 1–4) phytoplankton biomass (**Figure 5**). In the phytoplankton-dominated samples of the southern stations, several OTUs belonging to *Flavobacteria* (unclassified Cryomorphaceae, *Ulvibacter*, unclassified Flavobacteriaceae) were particularly abundant, with OTU NS3a reaching a relative abundance of 16.8% at station 8 (**Figure 5**). LEfSe analysis also identified the enrichment of *Candidatus* Aquiluna (*Actinobacteria*) as well as representatives from the unclassified PeM15 group (*Actinobacteria*) and the BAL58 group (*Betaproteobacteria*) at the southern stations. The dominant OTUs from the northern stations were more diverse and included representatives from the *Alphaproteobacteria*, *Betaproteobacteria*, *Acidobacteria*, and *Chloroflexi* but also from the flavobacterial NS9 group. Additionally, several OTUs occurred in higher abundance at all eight of the investigated stations (**Figure 5**).

DISCUSSION

Early Spring Plankton Development in the Baltic Sea

The Baltic Sea is characterized by annual phytoplankton spring blooms. These occur during late February to early April in the southern parts but may last into May in the northern parts (Groetsch et al., 2016). Sufficient light is essential for the onset of phytoplankton blooms. Diminished vertical mixing and the associated earlier onset of thermal stratification depend on the balance of surface warming and wind energy. In the Baltic Sea, there is a strong inter-annual variation in the springtime water temperature, which ranges between −1° and +5°C (HELCOM, 2013). In the northern Baltic, low water temperatures prevent thermal stratification such that the phytoplankton spring bloom generally does not start before April (Spilling and Markager, 2008). However, short-term warming periods can result in a temporal stratification, warmer surface temperatures, and the initiation of smaller, earlier phytoplankton blooms (e.g., Wasmund et al., 1998). Recent trends of ongoing sea surface warming have already been shown to impact the phytoplankton spring bloom in the Baltic Sea, in the form of earlier bloom onsets and changes in community composition (Klais et al., 2011, 2013; Wasmund et al., 2011). For example, during recent winter periods, the earlier stratification of the water column due to the increasing sea surface temperature frequently led to changes in phytoplankton composition and abundance, such that the proportions of cold-water species, including *Diatomophyceae*, declined and those of warm-water species, such as *Dinophyceae* and *Cyanophyceae*, increased.

Our study missed the beginning of the early spring bloom at the northern Baltic Sea stations, where we encountered pre-bloom conditions, but it did encompass a typical diatom-dominated spring bloom (mainly *Skeletonema costatum*), which developed in late February and reached a peak in early March (Wasmund et al., 2013; Groetsch et al., 2016), at the sea's southern stations. Hence, this study detected the normal phytoplankton spring succession, whereby stations 5–7 probably covered the initial phase and station 8 the maximum of the spring bloom. Here the diatoms were probably already experiencing nutrient limitation, especially by nitrate availability (**Table 1**). This high phytoplankton biomass of 347 μg C L^{-1} at station 8 was in accordance with previous phytoplankton peaks observed during springtime in the Baltic Sea (e.g., Wasmund et al., 2008). The dominance of one or few taxa during the phytoplankton spring blooms in the Baltic Sea, as observed here for *Skeletonema costatum* (e.g., ∼95% of total phytoplankton

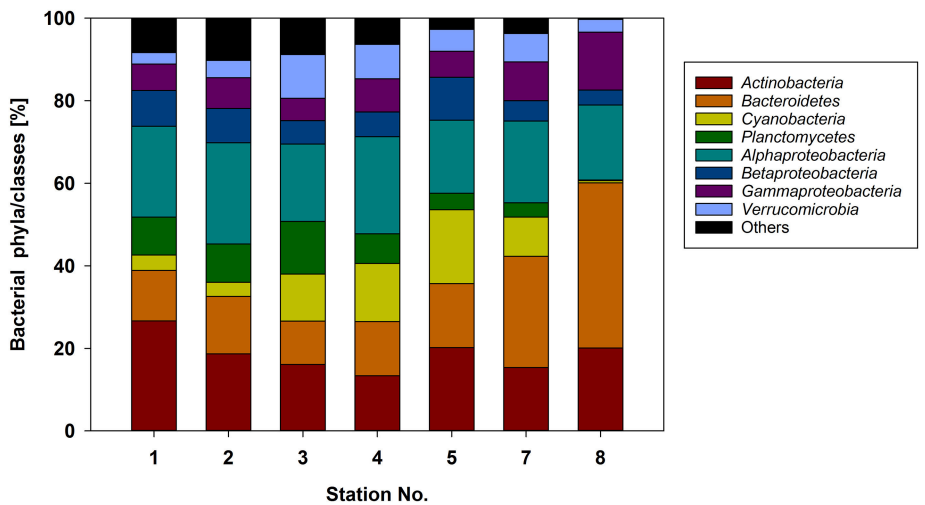

FIGURE 4 | Relative abundance of the major bacterial phyla/classes at the different stations sampled based on 16S rRNA gene analysis.

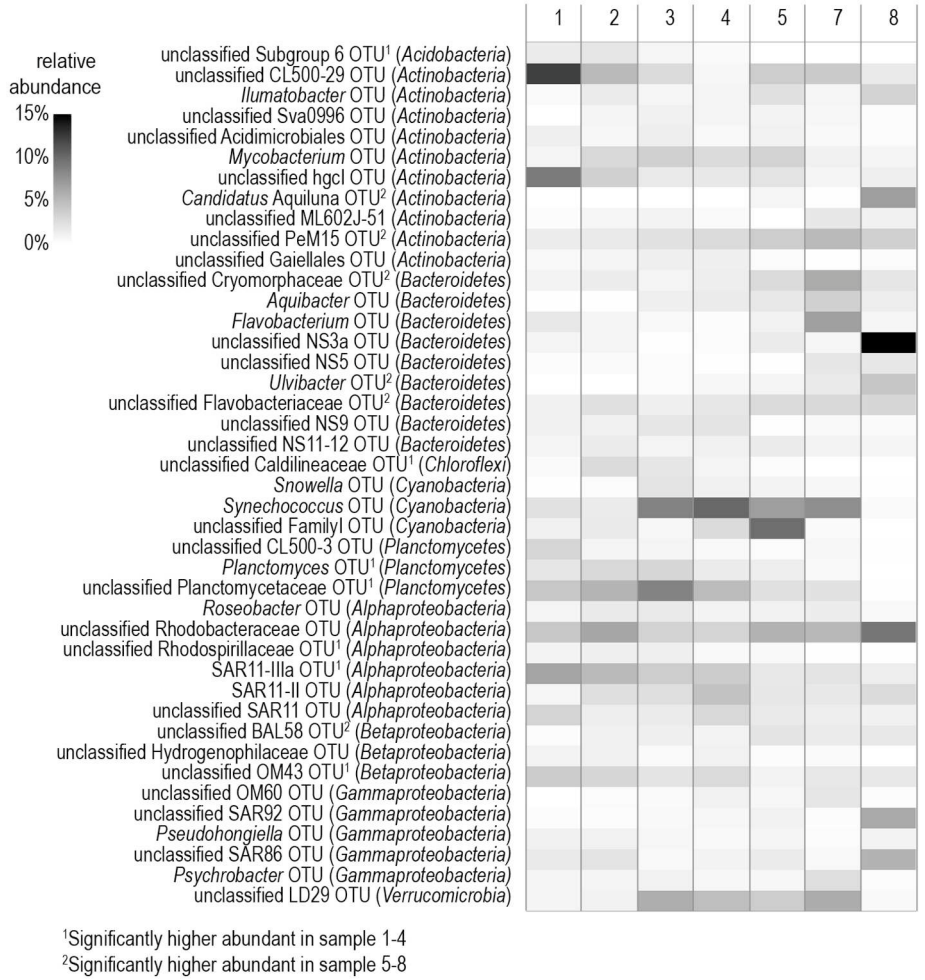

FIGURE 5 | Heatmap of the 75% most abundant operational taxonomic units (OTUs) detected in samples from the different stations. The affiliation with the respective phylum is shown in parentheses.

biomass at station 8) is also a typical feature (Wasmund et al., 2013). Phytoplankton provides labile organic carbon, either directly through the exudation of DOC (which resembles dissolved PP) or indirectly through grazers or viral lysis, thereby activating the bacterioplankton community and triggering the growth of adapted bacterial taxa (Sarmento and Gasol, 2012; Teeling et al., 2012; Wear et al., 2015). However, at very low temperatures bacterial growth can be suppressed or delayed despite organic matter production by the phytoplankton spring blooms (Pomeroy and Deibel, 1986). The latter presumption has been challenged by studies that demonstrated considerable bacterial activity at low temperatures (Yager et al., 2001; Kirchman et al., 2009). Interactive effects between temperature and substrate supply complicate predictions of the response to temperature by bacterioplankton communities (Pomeroy and Wiebe, 2001; Hall and Cotner, 2007; Kritzberg et al., 2010).

In our field study, where the temperature at all stations was in the 0–3°C range, activation of the bacterial communities by blooming phytoplankton was apparent at stations with high PP (**Figures 2B**, **3B**). Here, increases in bacterial abundance and production, as well as in the proportion of HNA bacteria, a common indicator of more active bacterial cells (Gasol et al., 1999), were recorded. A similar temperature experiment revealed that *in situ* BP and BR were positively related to temperature but BR responded more strongly to temperature than BP, indicating that increased temperature may result in a higher bacterial carbon demand and decreased growth efficiency (Kritzberg et al., 2010). Thus, overall there is considerable evidence that increasing temperature results in a higher carbon turnover in surface waters during phytoplankton spring blooms.

At the level of the main phylogenetic phyla/classes, there were only minor differences in bacterial community composition (BCC) across the stations sampled (**Figure 4**) whereas larger differences were visible at the genus level based OTU composition (**Figure 5**). Although salinity is a dominant factor for BCC in the Baltic Sea, major shifts occur when salinities drop to <3 or rise to >10 (Herlemann et al., 2011). Modest changes in main bacterial phyla in our study area can be explained by

the fact that only stations in a salinity range of 5.2–10 were covered. Temperature is another strong factor for the BCC, but since the conditions of the sampled stations were also relatively similar in terms of temperature (0–3°C), we assume that the presence of phytoplankton was probably the main driver for the differences in the dominating OTUs at the different stations. Both bacterial richness (here, the number of different OTUs) and the Shannon index decreased with increasing phytoplankton biomass (Figure S2), indicating that adapted bacteria became more dominant. OTUs belonging to *Gammaproteobacteria* and *Bacteroidetes*, which became more dominant at the stations with high phytoplankton biomass, are characteristic for diatom-dominated phytoplankton blooms (Teeling et al., 2012; Buchan et al., 2014; Bunse et al., 2016). For example, at station 8 with the phytoplankton bloom peak, one OTU of the NS3a marine group within the *Flavobacteriales* dominated. The same taxon occurred in high abundance in a previous mesocosm experiment with a comparable diatom-dominated phytoplankton bloom (clone-157; 16% of all 16S rRNA clones; von Scheibner et al., 2014) as well as in another field study carried out in the same area of the Baltic Sea during a spring bloom (OTU_000022; 16% of all 16S rRNA gene sequences; Bunse et al., 2016). This suggests a key role for this flavobacterial taxa in carbon processing during early diatom spring blooms in the Baltic Sea. Most of the other abundant OTUs in our study differed from those reported by Bunse et al. (2016), perhaps due to the fact that those authors encountered a higher phytoplankton biomass, with a different phytoplankton composition in the northern Baltic than was the case in our study. Generally, the OTUs that were abundant during the phytoplankton bloom at station 8 were more closely related to the OTUs from the southern Baltic Sea in the study of Bunse et al. (2016).

Phyto-Bacterioplankton Coupling and the Impact of Warming

Although bacterial abundance and production were elevated at the southern stations (5–8), characterized by high PP rates, proportionally much stronger increases in phytoplankton and lower BP/PP ratios (1.0%–1.3%) than generally known for phytoplankton blooms were recorded. Despite our measurements of PP are probably only rough estimates of daily production, as changes in light and radiation could not be considered, and PP may change from day to day, we do not think that more extensive PP measurements would have provided very different BP/PP ratios. For example, the incubations at stations 1, 5 and 8 started later in the morning, and higher radiance over midday may have resulted in higher PP values, BP increased equivalent to PP, resulting in comparable BP/PP values. The Q10 values have to be interpreted with caution as the calculation was based on only two temperatures. However, the obtained Q10 values are well within the range of reported values from experimental warming experiments.

According to global observations, water temperature correlates positively with BP/PP ratios, which increase from 2 to 10% in cold and temperate climate zones up to roughly 40% at lower latitudes (Carlson and Ducklow, 1996; Ducklow et al., 1999; Hoppe et al., 2002). This suggests that the low temperature in our study area suppressed bacterial growth and therefore prevented stronger phytoplankton-bacteria coupling. The low BP/PP ratios are comparable to those reported in other studies of low temperature waters, in which ratios < 10% were interpreted as evidence of "uncoupled" BP and PP (Cole et al., 1988; Nielsen and Richardson, 1989). The low water temperatures during early spring blooms in the Baltic Sea probably delay the bacterial degradation of phytoplankton-derived organic matter and may result in the gradual temporal accumulation of DOC. A temporal delay of bacteria-phytoplankton coupling is often recorded at these low water temperatures, since the bacterioplankton peak follows the phytoplankton bloom peak often with a delay of 1–2 weeks and could be a critical factor for the low bacterial abundance and production in this study (e.g., Hoppe et al., 2008). Furthermore, high grazing pressure is often observed for controlling the bacterial growth during phytoplankton spring blooms at low temperatures and could be another factor for the reduction in phytoplankton-bacteria coupling (Lignell et al., 1992; von Scheibner et al., 2014).

Bacterial growth is more dependent on dissolved primary production (DPP) than on particulate primary production (PPP) (e.g., Morán et al., 2002). Data concerning the percent extracellular release (PER) of PP in the Baltic Sea during phytoplankton spring blooms are scarce, but studies from other systems indicate that PER is usually <20% of total PP (Nagata, 2000; Teira et al., 2001; Marañón, 2005; Morán et al., 2013). At a PER of 20%, the estimated BCD at the northern stations would exceed DPP whereas at the southern stations BCD could be entirely fueled by DPP. However, other mechanisms also contribute to the transfer of phytoplankton carbon to bacteria, such as sloppy feeding by zooplankton or viral lysis. As we did not measure DPP, we used PPP as a proxy for phytoplankton organic carbon production, which can fuel the microbial loop. Although BP/PP ratios are insufficient to completely describe the pelagic carbon flow, they are indicators of the current relation between autotrophic production and heterotrophic consumption of organic matter. Including measurements of DPP, bacterial respiration, and grazing rates in assessments of the carbon flow during the phytoplankton spring bloom would lead to more precise estimates but probably would not change the overall finding of low phytoplankton-bacteria coupling.

Warming (Δ+6°C) stimulated both PP and BP, with distinctly higher average Q_{10} values for BP (2.1 ± 0.7) than for PP (1.4 ± 0.2) during phytoplankton bloom conditions at the southern stations (**Table 2**). This positive effect of higher temperature on bacterial production rates is in agreement with many previous studies in the Baltic Sea and other marine locations in this climate zone (Vázquez-Domínguez et al., 2007; Hoppe et al., 2008; Panigrahi et al., 2013). However, in some studies the Q_{10} for BP even exceeded the normal range of 2–3 known for heterotrophic organisms during phytoplankton spring blooms (Vaquer-Sunyer et al., 2015). PP increased significantly with higher temperatures in all samples, resulting in Q_{10} values between 1.2 and 8.2 (**Table 2**). These were within the range reported in other field studies (e.g., Panigrahi et al., 2013) and in marine mesocosm experiments in the Baltic Sea (Hoppe et al., 2008; von Scheibner

et al., 2014). In our study, the warming-related increase in PP suggested light saturation of phytoplankton, since light-limited rates of PP are insensitive to temperature changes (Tilzer et al., 1986), as also shown in mesocosm studies of marine plankton (e.g., Lewandowska and Sommer, 2010; Lewandowska et al., 2012; Sommer et al., 2012). Q_{10} values between 1.2 and 1.7 at stations with high PP rates indicated that short-term warming did not greatly disturb biochemical processes. In addition, these values are in accordance with those of previous studies demonstrating lower temperature-sensitivity of phytoplankton growth and production (Marañón et al., 2014). A more detailed picture would be obtained by measuring not only the response of particulate but also that of dissolved primary production (e.g., Morán et al., 2006) as this is expected to be more related to bacterial substrate utilization. However, other temperature-sensitive factors, such as grazing pressure (Duarte et al., 2005; Aberle et al., 2007), qualitative and quantitative aspects of phytoplankton exudation (Zlotnik and Dubinsky, 1989; Morán et al., 2006), and substrate affinity (Nedwell, 1999), can strongly interfere with phytoplankton-bacteria interactions and will have to be considered for a more comprehensive understanding of the effects of temperature. Their inclusion would also help to explain the absence of a temperature effect on the BCD/PP ratio in samples obtained from the non-bloom conditions of the northern Baltic Sea (stations 1–4). In these waters, temperature more strongly stimulated PP than BP, such that carbon flow to heterotrophic decomposers was reduced by ∼1% per 1°C. The high proportion of *Dinophyceae* (e.g., *Scrippsiella* sp.), which often establish a high biomass at low temperature in the northern Baltic Sea (Kremp, 2000; Kremp et al., 2008), may have been responsible for the reduced carbon flow to bacterioplankton. However, at these very low PP and BP rates, carbon budget calculations should be interpreted with caution, since small changes, close to the detection limit, nonetheless strongly impact BP/PP ratios.

Comparison of Field Data With Experimental Warming Experiments

Our results from the Baltic Sea are consistent with those of other field studies performed at a similar cold temperature range (Hoppe et al., 2002; Morán et al., 2002; Duarte et al., 2005). They suggest that only a small fraction of the fixed carbon of phytoplankton enters the heterotrophic bacterial community during early bloom conditions at cold temperatures. Previous mesocosm studies of Baltic Sea spring communities, examined at a temperature range similar to that tested in the present work, showed that BP during phytoplankton spring bloom conditions was strongly stimulated by warming (Wohlers et al., 2009; von Scheibner et al., 2014), leading to a closer temporal coupling of autotrophic and heterotrophic processes as the temperature rose (Wohlers-Zöllner et al., 2012). The mean Q_{10} of 2.2 for the bacterial response in our study was nearly identical to that reported in a previous experimental warming experiment ($Q_{10} =$ 2.4) (Hoppe et al., 2008).

However, bacterial stimulation by warming was much less in this field study than in previous mesocosm studies mentioned above, as BP/PP ratios were low (0.9–2.1%) even during the diatom blooms at the southern stations (**Table 2**), implying that BP was largely uncoupled from PP also at the elevated experimental temperatures. By contrast, in the mesocosm experiments the BCD/PP ratio during the bloom peak was ∼19% at the *in situ* temperature (∼2°C) and ∼24% in response to a warming of +6°C (von Scheibner et al., 2014). Major differences with our field study were the higher phytoplankton biomass (1,000–1,500 μg C L^{-1}) and PP in the mesocosm experiments (Hoppe et al., 2008; Wohlers et al., 2009; Lewandowska and Sommer, 2010), significant grazing by mesozooplankton and a longer duration. This might have provided higher substrate supply from phytoplankton origin for heterotrophic bacteria. Several studies already highlighted that bacterial growth is rather depended on the supply of dissolved PP than to particulate PP. Moreover, in experimental warming study with slight temperature increase of 2°C resulted in massive increase of dissolved PP, whereas the particulate PP nearly stable (Morán et al., 2006). In the more unstable physical conditions of the Baltic Sea (e.g., higher vertical mixing or drifting), phytoplankton biomass is much lower (**Table 1**). This could explain the differences in the carbon flow patterns between the mesocosm experiments vs. *in situ* conditions in our study. Another reason for the distinct differences in phyto-bacterioplankton coupling might be that the duration of warming in this study was not sufficient to allow acclimatization of the bacterial communities to a similar extent as in the mesocosm studies, which were generally conducted for several weeks.

CONCLUSIONS

Overall, the appearance of diatom-dominated phytoplankton blooms in the southern Baltic Sea led to a strong activation of the bacterial communities, in contrast to the northern Baltic Sea, where the phytoplankton biomass was low and dominated by dinoflagellates. The experimental temperature increase during the phytoplankton bloom significantly enhanced both PP and, especially, BP. This partially confirmed our hypothesis and previously published considerations that warming results in a stronger stimulation of bacterioplankton than of phytoplankton communities under cold-water conditions. However, according to the low BP/PP ratios, bacteria were still relatively uncoupled from phytoplankton growth, a situation that remained essentially unchanged after a temperature increase of 6°C. This is in contrast to results from previous mesocosm experiments and suggests that during the early spring bloom in the Baltic Sea increased sea surface temperatures will not strengthen bacterio-phytoplankton coupling to a similar extent as in mesocosm experiments. The clear differences in carbon flow pattern between field conditions and experimental studies could be due to different factors such as physical conditions, food web structure and acclimation, which remain to be examined. The temporal response patterns of microbial communities to warming as well as possible bacterial adaptations are important avenues for future field and experimental research. By careful comparisons of the results of experimental mesocosm with those of *in situ* studies, including

the different time scales, a more realistic picture of the effects of global warming on the marine carbon budget will be obtained.

AUTHOR CONTRIBUTIONS

MvS and KJ planned, initiated and conducted the study and wrote the first draft of the manuscript. All authors discussed the results and edited the manuscript. DH analyzed bacterial community composition and AL assessed phytoplankton composition and biomass.

FUNDING

This work was funded by the German Science Foundation (DFG), grants JU367/7-3 (priority program AQUASHIFT) and JU 367/15-1 to KJ. DH was supported by the grant MOBTT24 (Estonian Research Council, and European Union).

ACKNOWLEDGMENTS

We thank the crew and captain of the *RV Alkor* (AL332) for support during the cruise, and Marco Nack for technical assistance during the incubation experiments, as well as Annett Grüttmüller for flow cytometry analysis.

SUPPLEMENTARY MATERIAL

The Supplementary Material for this article can be found online at: https://www.frontiersin.org/articles/10.3389/fmars.2018.00231/full#supplementary-material

REFERENCES

Aberle, N., Lengfellner, K., and Sommer, U. (2007). Spring bloom succession, grazing impact and herbivore selectivity of ciliate communities in response to winter warming. *Oecologia* 150, 668–681. doi: 10.1007/s00442-006-0540-y

Azam, F. (1998). Microbial control of oceanic carbon flux: the plot thickens. *Science* 280, 694–696. doi: 10.1126/science.280.5364.694

Boyd, P. W., and Doney, S. C. (2002). Modelling regional responses by marine pelagic ecosystems to global climate change. *Geophys. Res. Lett.* 29, 53-1–53-4. doi: 10.1029/2001GL014130

Brown, J. H., Gillooly, J. F., Allen, A. P., Savage, V. M., and West, G. B. (2004). Toward a metabolic theory of ecology. *Ecology* 85, 1771–1789. doi: 10.1890/03-9000

Buchan, A., LeCleir, G. R., Gulvik, C. A., and González, J. M. (2014). Master recyclers: features and functions of bacteria associated with phytoplankton blooms. *Nat. Rev. Microb.* 12, 686–698. doi: 10.1038/nrmicro3326

Bunse, C., Bertos-Fortis, M., Sassenhagen, I., Sildever, S., Sjoqvist, C., Godhe, A., et al. (2016). Spatio-temporal interdependence of bacteria and phytoplankton during a Baltic Sea spring bloom. *Front. Microbiol.* 7:517.

Caporaso, J., Kuczynski, J., Stombaugh, J., Bittinger, K., Bushman, F. D., Costello, E. K., et al. (2010). QIIME allows analysis of high-throughput community sequencing data. *Nat. Methods* 7, 335–336. doi: 10.1038/nmeth.f.303

Carlson, C. A., and Ducklow, H. W. (1996). Growth of bacterioplankton and consumption of dissolved organic carbon in the Sargasso Sea. *Aquat. Microb. Ecol.* 10, 69–85. doi: 10.3354/ame010069

Cole, J. J., Findlay, S., and Pace, M. L. (1988). Bacterial production in fresh and saltwater ecosystems: a cross-system overview. *Mar. Ecol. Prog. Ser.* 43, 1–10. doi: 10.3354/meps043001

Degerman, R., Dinasquet, J., Riemann, L., Sjöstedt de Luna, S., and Andersson, A. (2013). Effect of resource availability on bacterial community responses to increased temperature. *Aquat. Microb. Ecol.* 68, 131–142. doi: 10.3354/ame01609

del Giorgio, P. A., and Cole, J. J. (1998). Bacterial growth efficiency in natural aquatic systems. *Annu. Rev. Ecol. Syst.* 29, 503–541. doi: 10.1146/annurev.ecolsys.29.1.503

del Giorgio, P. A., Cole, J. J., and Cimbleris, A. (1997). Respiration rates in bacteria exceed phytoplankton production in unproductive aquatic systems. *Nature* 385, 148–151. doi: 10.1038/385148a0

Duarte, C. M., Agust,í, S., Vaqué, D., Agawin, N. S. R., Felipe, J., Casamayor, E. O., et al. (2005). Experimental test of bacteria-phytoplankton coupling in the Southern Ocean. *Limnol. Oceanogr.* 50, 1844–1854. doi: 10.4319/lo.2005.50.6.1844

Ducklow, H. W. (2000). "Bacterial production and biomass in the oceans," in *Microbial Ecology of the Oceans*, ed D. L. Kirchman (New York, NY: Wiley), 85–120.

Ducklow, H. W., Carlson, C. A., and Smith, W. O. (1999). Bacterial growth in experimental plankton assemblages and seawater cultures from the Phaeocystis antarctica bloom in the Ross Sea, Antarctica. *Aquat. Microb. Ecol.* 19, 215–227. doi: 10.3354/ame019215

Edwards, K. F., Thomas, M. K., Klausmeier, C. A., and Litchman, E. (2016). Phytoplankton growth and the interaction of light and temperature. *Synth. Species Community Level. Limnol. Oceanogr.* 61, 1232–1244. doi: 10.1002/lno.10282

Eriksson Wiklund, A. K., Dahlgren, K., Sundelin, B., and Andersson, A. (2009). Effects of warming and shifts of pelagic food web structure on benthic productivity in a coastal marine system. *Mar. Ecol. Prog. Ser.* 396, 13–25. doi: 10.3354/meps08290

Field, C. B., Behrenfeld, M. J., Randerson, J. T., and Falkowski, P. G. (1998). Primary production of the biosphere. *Integr. Terres. Oceanic Compon. Sci.* 281, 237–240. doi: 10.1126/science.281.5374.237

Gasol, J. M., and del Giorgio, P. A. (2000). Using flow cytometry for counting natural planktonic bacteria and understanding the structure of planktonic bacterial communities. *Sci. Mar.* 64, 197–224. doi: 10.3989/scimar.2000.64n2197

Gasol, J. M., Zweifel, U. L., Peters, F., Fuhrman, J. A., and Hagström, Å. (1999). Significance of size and nucleic acid content heterogeneity as measured by flow cytometry in natural planktonic bacteria. *Appl. Environ. Microbiol.* 65, 4475–4483.

Gragas, E. (1975). A manual for phytoplankton primary production studies in the Baltic. *Baltic Marine Biol.* 3, 1–88.

Grasshoff, K., Kremling, K., and Ehrhardt, M. (1999). *Methods of Seawater Analysis*. Weinheim: Wiley-VCH Verlag GmbH.

Groetsch, P. M. M., Simis, S. G. H., Eleveld, M. A., and Peters, S. W. M. (2016). Spring blooms in the Baltic Sea have weakened but lengthened from 2000 to 2014. *Biogeoscience* 13, 4959–4973. doi: 10.5194/bg-13-4959-2016

Hall, E. K., and Cotner, J. B. (2007). Interactive effect of temperature and resources on carbon cycling by freshwater bacterioplankton communities. *Aquat. Microb. Ecol.* 49, 35–45. doi: 10.3354/ame01124

Harris, L. A., Duarte, C. M., and Nixon, S. W. (2006). Allometric laws and prediction in estuarine and coastal ecology. *Estuar. Coasts* 29, 340–344. doi: 10.1007/BF02782002

HELCOM (2013). "Climate change in the Baltic Sea Area: HELCOM thematic assessment in 2013," in *Balt. Sea Environ. Proc. No. 137*.

Herlemann, D. P. R., Labrenz, M., Jürgens, K., Bertilsson, S., Waniek, J. J., and Andersson, A. F. (2011). Transitions in bacterial communities along the 2000 km salinity gradient of the Baltic Sea. *ISME J.* 5, 1571–1579. doi: 10.1038/ismej.2011.41

Herlemann, D. P. R., Lundin, D., Andersson, A. F., Labrenz, M., and Jürgens, K. (2016). Phylogenetic signals of salinity and season in bacterial community composition across the salinity gradient of the Baltic Sea. *Front. Microbiol.* 7:1883. doi: 10.3389/fmicb.2016.01883

Hoppe, H.-G., Breithaupt, P., Walther, K., Koppe, R., Bleck, S., Sommer, U., et al. (2008). Climate warming in winter affects the coupling between phytoplankton

and bacteria during the spring bloom. A mesocosm study. *Aquat. Microb. Ecol.* 51, 105–115. doi: 10.3354/ame01198

Hoppe, H.-G., Gocke, K., Koppe, R., and Begler, C. (2002). Bacterial growth and primary production along a north-south transect of the Atlantic Ocean. *Nature* 416, 168–171. doi: 10.1038/416168a

IPCC (2013). *Intergovernmental Panel on Climate Change 2013 - The Physical Science Basis*. Cambridge: Cambridge University Press.

Keller, A. A., Oviatt, C. A., Walker, H. A., and Hawk, J. D. (1999). Predicted impacts of elevated temperature on the magnitude of the winter-spring phytoplankton bloom in temperate coastal waters. A mesocosm study. *Limnol. Oceanogr.* 44, 344–356. doi: 10.4319/lo.1999.44.2.0344

Kirchman, D. L. (2001). Measuring bacterial biomass production and growth rates from leucine incorporation in natural aquatic environments. *Meth. Microbiol.* 30, 227–237. doi: 10.1016/S0580-9517(01)30047-8

Kirchman, D. L., Morán, X. A. G., and Ducklow, H. W. (2009). Microbial growth in the polar oceans - role of temperature and potential impact of climate change. *Nat. Rev. Microbiol.* 7, 451–459. doi: 10.1038/nrmicro2115

Klais, R., Tamminen, T., Kremp, A., Spilling, K., and Olli, K. (2011). Decadal-scale changes of dinoflagellates and diatoms in the anomalous Baltic Sea spring bloom. *PLoS ONE* 6:e21567. doi: 10.1371/journal.pone.0021567

Klais, R., Tamminen, T., Kremp, A., Spilling, K., and Woong, A. B. (2013). Spring phytoplankton communities shaped by interannual weather variability and dispersal limitation. Mechanisms of climate change effects on key coastal primary producers. *Limnol. Oceanogr.* 58, 753–762. doi: 10.4319/lo.2013.58.2.0753

Klindworth, A., Pruesse, E., Schweer, T., Peplies, J., Quast, C., Horn, M., et al. (2013). Evaluation of general 16S ribosomal RNA gene PCR primers for classical and next-generation sequencing-based diversity studies. *Nucleic Acids Res.* 41, e1. doi: 10.1093/nar/gks808

Kremp, A. (2000). Factors regulating germination of resting cysts of the spring bloom dinoflagellate Scrippsiella hangoei from the northern Baltic Sea. *J. Plankton Res.* 22, 1311–1327. doi: 10.1093/plankt/22.7.1311

Kremp, A., Tamminen, T., and Spilling, K. (2008). Dinoflagellate bloom formation in natural assemblages with diatoms. Nutrient competition and growth strategies in Baltic spring phytoplankton. *Aquat. Microb. Ecol.* 50, 181–196. doi: 10.3354/ame01163

Kritzberg, E. S., Duarte, C. M., and Wassmann, P. (2010). Changes in Arctic marine bacterial carbon metabolism in response to increasing temperature. *Polar Biol.* 33, 1673–1682. doi: 10.1007/s00300-010-0799-7

Lewandowska, A. M., Breithaupt, P., Hillebrand, H., Hoppe, H.-G., Jürgens, K., and Sommer, U. (2012). Responses of primary productivity to increased temperature and phytoplankton diversity. *J. Sea Res.* 72, 87–93. doi: 10.1016/j.seares.2011.10.003

Lewandowska, A. M., and Sommer, U. (2010). Climate change and the spring bloom. A mesocosm study on the influence of light and temperature on phytoplankton and mesozooplankton. *Mar. Ecol. Prog. Ser.* 405, 101–111. doi: 10.3354/meps08520

Li, W., and Godzik, A. (2006). Cd-hit: a fast program for clustering and comparing large sets of protein or nucleotide sequences. *Bioinformatics* 22, 1658–1659. doi: 10.1093/bioinformatics/btl158

Lignell, R., Kaitala, S., and Kuosa, H. (1992). Factors controlling phyto- and bacterioplankton in late spring on a salinity gradient in the northern Baltic. *Mar. Ecol. Prog. Ser.* 84, 121–131. doi: 10.3354/meps084121

Lindh, M. V., Riemann, L., Baltar, F., Romero-Oliva, C., Salomon, P. S., Granéli, E., et al. (2012). Consequences of increased temperature and acidification on bacterioplankton community composition during a mesocosm spring bloom in the Baltic Sea. *Environ. Microbiol.* 5, 252–262. doi: 10.1111/1758-2229.12009

López-Urrutia, Á., San Martin, E., Harris, R. P., and Irigoien, X. (2006). Scaling the metabolic balance of the oceans. *Proc. Natl. Acad. Sci. U.S.A.* 103, 8739–8744. doi: 10.1073/pnas.0601137103

Marañón, E. (2005). Phytoplankton growth rates in the Atlantic subtropical gyres. *Limnol. Oceanogr.* 50, 299–310. doi: 10.4319/lo.2005.50.1.0299

Marañón, E., Cermeño, P., Huete-Ortega, M., López-Sandoval, D. C., Mouriño-Carballido, B., and Rodríguez-Ramos, T. (2014). Resource supply overrides temperature as a controlling factor of marine phytoplankton growth. *PLoS ONE* 9:e99312. doi: 10.1371/journal.pone.0099312

Morán, X. A. G., Ducklow, H. W., and Erickson, M. (2013). Carbon fluxes through estuarine bacteria reflect coupling with phytoplankton. *Mar. Ecol. Prog. Ser.* 489, 75–85. doi: 10.3354/meps10428

Morán, X. A. G., Estrada, M., Gasol, J. M., and Pedrós-Ali,ó, C. (2002). Dissolved primary production and the strength of phytoplankton- bacterioplankton coupling in contrasting marine regions. *Microb. Ecol.* 44, 217–223. doi: 10.1007/s00248-002-1026-z

Morán, X. A. G., Sebastián, M., Pedrís-Alií, C., and Estrada, M. (2006). Response of Southern Ocean phytoplankton and bacterioplankton production to short-term experimental warming. *Limnol. Oceanogr.* 51, 1791–1800. doi: 10.4319/lo.2006.51.4.1791

Müren, U., Berglund, J., Samuelsson, K., and Andersson, A. (2005). Potential effects of elevated sea-water temperature on pelagic food webs. *Hydrobiologia* 545, 153–166. doi: 10.1007/s10750-005-2742-4

Nagata, T. (2000). "Production mechanisms of dissolved organic matter," in *Microbial Ecology of the Oceans*, ed D. L. Kirchman (New York, NY: Wiley), 121–152.

Nedwell, D. (1999). Effect of low temperature on microbial growth: lowered affinity for substrates limits growth at low temperature. *FEMS Microbiol. Ecol* 30, 101–111. doi: 10.1111/j.1574-6941.1999.tb00639.x

Nielsen, T. G., and Richardson, K. (1989). Food chain structure of the North Sea plankton communities: seasonal variations of the role of the microbial loop. *Mar. Ecol. Prog. Ser.* 56, 75–87. doi: 10.3354/meps056075

O'Connor, M. I., Piehler, M. F., Leech, D. M., Anton, A., and Bruno, J. F. (2009). Warming and resource availability shift food web structure and metabolism. *PLoS Biol.* 7:e1000178. doi: 10.1371/journal.pbio.1000178

Olenina, I., Hajdu, S., Edler, L., Andersson, A., Wasmund, N., Busch, S., et al. (2006). "Biovolumes and size-classes of phytoplankton in the Baltic Sea, Helsinki," in HELCOM *Balt. Sea Environ. Proc. No. 106*, 144pp. hdl:10013/epic.39031.d001

Panigrahi, S., Nydahl, A., Anton, P., and Wikner, J. (2013). Strong seasonal effect of moderate experimental warming on plankton respiration in a temperate estuarine plankton community. *Estuar. Coast. Shelf Sci.* 135, 269–279. doi: 10.1016/j.ecss.2013.10.029

Pomeroy, L. R., and Deibel, D. (1986). Temperature regulation of bacterial activity during the spring bloom in newfoundland coastal waters. *Sci.* 233, 359–361. doi: 10.1126/science.233.4761.359

Pomeroy, L. R., and Wiebe, W. J. (2001). Temperature and substrates as interactive limiting factors for marine heterotrophic bacteria. *Aquat. Microb. Ecol.* 23, 187–204. doi: 10.3354/ame023187

Pruesse, E., Peplies, J., and Glöckner, F. O. (2012). SINA: accurate high-throughput multiple sequence alignment of ribosomal RNA genes. *Bioinformatics* 28, 1823–1829. doi: 10.1093/bioinformatics/bts252

Raven, J. A., and Geider, R. J. (1988). Temperature and algal growth. *N. Phytol.* 110, 441–461. doi: 10.1111/j.1469-8137.1988.tb00282.x

Robertson, C. E., Harris, J. K., Wagner, B. D., Granger, D., Browne, K., Tatem, B., et al. (2013). Explicet: graphical user interface software for metadata-driven management, analysis and visualization of microbiome data. *Bioinformatics* 29, 3100–3101. doi: 10.1093/bioinformatics/btt526

Rivkin, R. B., and Legendre, L. (2001). Biogenic carbon cycling in the upper ocean: effects of microbial respiration. *Science* 291, 2398–2400. doi: 10.1126/science.291.5512.2398

Sarmento, H., and Gasol, J. M. (2012). Use of phytoplankton-derived dissolved organic carbon by different types of bacterioplankton. *Environ. Microbiol.* 14, 2348–2360. doi: 10.1111/j.1462-2920.2012.02787.x

Sarmiento, J. L., Slater, R., Barber, R., Bopp, L. P., Doney, S. C., Hirst, A. C., et al. (2004). Response of ocean ecosystems to climate warming. *Global Biogeochem. Cycles* 18, 1–23. doi: 10.1029/2003GB002134

Segata, N., Izard, J., Waldron, L., Gevers, D., Miropolsky, L., Garrett, W. S., et al. (2011). Metagenomic biomarker discovery and explanation. *Genome Biol.* 12:R60. doi: 10.1186/gb-2011-12-6-r60

Schlitzer (2011). *Ocean Data View*. Available online at: https://odv.awi.de/

Simon, M., and Azam, F. (1989). Protein content and protein synthesis rates of planktonic marine bacteria. *Mar. Ecol. Prog. Ser.* 51, 201–213. doi: 10.3354/meps051201

Sommer, U., Aberle, N., Lengfellner, K., and Lewandowska, A. M. (2012). The Baltic Sea spring phytoplankton bloom in a changing climate. An experimental approach. *Mar. Biol.* 159, 2479–2490. doi: 10.1007/s00227-012-1897-6

Spilling, K., and Markager, S. (2008). Ecophysiological growth characteristics and modeling of the onset of the spring bloom in the Baltic Sea. *J. Mar. Syst.* 73, 323–337. doi: 10.1016/j.jmarsys.2006.10.012

Teeling, H., Fuchs, B. M., Becher, D., Klockow, C., Gardebrecht, A., Bennke, C. M., et al. (2012). Substrate-controlled succession of marine bacterioplankton populations induced by a phytoplankton bloom. *Science* 336, 608–611. doi: 10.1126/science.1218344

Teira, E., José Paz,ó, M., Serret, P., and Fernández, E. (2001). Dissolved organic carbon production by microbial populations in the Atlantic Ocean. *Limnol. Oceanogr.* 46, 1370–1377. doi: 10.4319/lo.2001.46.6.1370

Thornton, D. C. O. (2014). Dissolved organic matter (DOM) release by phytoplankton in the contemporary and future ocean. *Eur. J. Phycol.* 49, 20–46. doi: 10.1080/09670262.2013.875596

Tilzer, M. M., Elbrächter, M., Gieskes, W. W., and Beese, B. (1986). Light-temperature interactions in the control of photosynthesis in Antarctic phytoplankton. *Polar Biol.* 5, 105–111. doi: 10.1007/BF00443382

Utermöhl, H. (1958). "Zur Vervollkommnung der quantitativen Phytoplankton-Methodik," in *Mitteilungen Internationale Vereinigung Theoretische und Angewandte Limnologie,* Vol. 9 (German), 1–38.

Vaquer-Sunyer, R., Conley, D. J., Muthusamy, S., Lindh, M. V., Pinhassi, J., and Kritzberg, E. S. (2015). Dissolved organic nitrogen inputs from wastewater treatment plant effluents increase responses of planktonic metabolic rates to warming. *Environ. Sci. Technol.* 49, 11411–11420. doi: 10.1021/acs.est.5b00674

Vázquez-Domínguez, E., Vaqué, D., and Gasol, J. M. (2007). Ocean warming enhances respiration and carbon demand of coastal microbial plankton. *Global Change Biol.* 13, 1327–1334. doi: 10.1111/j.1365-2486.2007.01377.x

von Scheibner, M., Dörge, P., Biermann, A., Sommer, U., Hoppe, H.-G., and Jürgens, K. (2014). Impact of warming on phyto-bacterioplankton coupling and bacterial community composition in experimental mesocosms. *Environ. Microbiol.* 16, 718–733. doi: 10.1111/1462-2920.12195

Wasmund, N., Andrushaitis, A., Łysiak-Pastuszak, E., Müller-Karulis, B., Nausch, G., Neumann, T., et al. (2001). Trophic status of the south-eastern Baltic Sea. A comparison of coastal and open areas. *Estuar. Coast Shelf Sci.* 53, 849–864. doi: 10.1006/ecss.2001.0828

Wasmund, N., Göbel, J., and Bodungen, B. V. (2008). 100-years-changes in the phytoplankton community of Kiel Bight (Baltic Sea). *J. Mar. Syst.* 73, 300–322. doi: 10.1016/j.jmarsys.2006.09.009

Wasmund, N., Nausch, G., and Feistel, R. (2013). Silicate consumption. An indicator for long-term trends in spring diatom development in the Baltic Sea. *J. Plankton Res.* 35, 393–406. doi: 10.1093/plankt/fbs101

Wasmund, N., Nausch, G., and Matthäus, W. (1998). Phytoplankton spring blooms in the southern Baltic Sea - spatio-temporal development and long-term trends. *J. Plankton Res.* 20, 1099–1117. doi: 10.1093/plankt/20.6.1099

Wasmund, N., Tuimala, J., Suikkanen, S., Vandepitte, L., and Kraberg, A. (2011). Long-term trends in phytoplankton composition in the western and central Baltic Sea. *J. Mar. Syst.* 87, 145–159. doi: 10.1016/j.jmarsys.2011.03.010

Wear, E. K., Carlson, C. A., James, A. K., Brzezinski, M. A., Windecker, L. A., and Nelson C. E. (2015). Synchronous shifts in dissolved organic carbon bioavailability and bacterial community responses over the course of an upwelling-driven phytoplankton bloom. *Limnol. Oceanogr.* 60, 657–677. doi: 10.1002/lno.10042

Weinbauer, M. G., Fritz, I., Wenderoth, D. F., and Höfle, M. G. (2002). Simultaneous extraction from bacterioplankton of total RNA and DNA suitable for quantitative structure and function analyses. *Appl. Environ. Microbiol.* 68, 1082–1087. doi: 10.1128/AEM.68.3.1082-1087.2002

Wohlers, J., Engel, A., Zöllner, E., Breithaupt, P., Jürgens, K., Hoppe, H.-G., et al. (2009). Changes in biogenic carbon flow in response to sea surface warming. *PNAS* 106, 7067–7072. doi: 10.1073/pnas.0812743106

Wohlers-Zöllner, J., Biermann, A., Engel, A., Dörge, P., Lewandowska, A. M., von Scheibner, M., et al. (2012). Effects of rising temperature on pelagic biogeochemistry in mesocosm systems. A comparative analysis of the AQUASHIFT Kiel experiments. *Mar. Biol.* 159, 2503–2518. doi: 10.1007/s00227-012-1958-x

Yager, P. L., Connelly, T. L., Mortazavi, B., Wommack, K. E., Bano, N., Bauer, J. E., et al. (2001). Dynamic bacterial and viral response to an algal bloom at subzero temperatures. *Limnol. Oceanogr.* 46, 790–801. doi: 10.4319/lo.2001.46.4.0790

Zlotnik, I., and Dubinsky, Z. (1989). The effect of light and temperature on DOC excretion by phytoplankton. *Limnol. Oceanogr.* 34, 831–839.

Conflict of Interest Statement: The authors declare that the research was conducted in the absence of any commercial or financial relationships that could be construed as a potential conflict of interest.

frontiers in Marine Science

ORIGINAL RESEARCH
published: 14 November 2017
doi: 10.3389/fmars.2017.00360

Diatom Transcriptional and Physiological Responses to Changes in Iron Bioavailability across Ocean Provinces

*Natalie R. Cohen[1], Kelsey A. Ellis[1], Robert H. Lampe[1], Heather McNair[2], Benjamin S. Twining[3], Maria T. Maldonado[4], Mark A. Brzezinski[2], Fedor I. Kuzminov[5], Kimberlee Thamatrakoln[5], Claire P. Till[6,7], Kenneth W. Bruland[6], William G. Sunda[1], Sibel Bargu[8] and Adrian Marchetti[1]**

[1] Department of Marine Sciences, University of North Carolina at Chapel Hill, Chapel Hill, NC, United States, [2] The Marine Science Institute and the Department of Ecology Evolution and Marine Biology, University of California, Santa Barbara, Santa Barbara, CA, United States, [3] Bigelow Laboratory for Ocean Sciences, East Boothbay, ME, United States, [4] Department of Earth, Ocean, and Atmospheric Sciences, University of British Columbia, Vancouver, BC, Canada, [5] Department of Marine and Coastal Sciences, Rutgers, the State University of New Jersey, New Brunswick, NJ, United States, [6] Department of Ocean Sciences, University of California, Santa Cruz, Santa Cruz, CA, United States, [7] Chemistry Department, Humboldt State University, Arcata, CA, United States, [8] Department of Oceanography and Coastal Sciences, College of the Coast and Environment, Louisiana State University, Baton Rouge, LA, United States

OPEN ACCESS

Edited by:
Kristian Spilling, Finnish Environment Institute (SYKE), Finland

Reviewed by:
Ulisses Miranda Azeiteiro, University of Aveiro, Portugal
Penelope Ann Ajani, University of Technology Sydney, Australia

***Correspondence:**
Adrian Marchetti
amarchetti@unc.edu

Specialty section:
This article was submitted to Marine Ecosystem Ecology, a section of the journal Frontiers in Marine Science

Received: *13 August 2017*
Accepted: *26 October 2017*
Published: *14 November 2017*

Citation:
Cohen NR, Ellis KA, Lampe RH, McNair H, Twining BS, Maldonado MT, Brzezinski MA, Kuzminov FI, Thamatrakoln K, Till CP, Bruland KW, Sunda WG, Bargu S and Marchetti A (2017) Diatom Transcriptional and Physiological Responses to Changes in Iron Bioavailability across Ocean Provinces. Front. Mar. Sci. 4:360. doi: 10.3389/fmars.2017.00360

Changes in iron (Fe) bioavailability influence diatom physiology and community composition, and thus have a profound impact on primary productivity and ecosystem dynamics. Iron limitation of diatom growth rates has been demonstrated in both oceanic and coastal waters of the Northeast Pacific Ocean and is predicted to become more pervasive in future oceans. However, it is unclear how the strategies utilized by phytoplankton to cope with low Fe bioavailability and resupply differ across these ocean provinces. We investigated the response of diatom communities to variable Fe conditions through incubation experiments performed in the Fe mosaic of the California Upwelling Zone and along a natural Fe gradient in the Northeast Pacific Ocean. Through coupling gene expression of two dominant diatom taxa (*Pseudo-nitzschia* and *Thalassiosira*) with biological rate process measurements, we provide an in-depth examination of the physiological and molecular responses associated with varying Fe status. Following Fe enrichment, oceanic diatoms showed distinct differential expression of gene products involved in nitrogen assimilation, photosynthetic carbon fixation, and vitamin production compared to diatoms from low-Fe coastal sites, possibly driven by the chronic nature of Fe stress at the oceanic site. Genes of interest involved in Fe and N metabolism additionally exhibited divergent expression patterns between the two diatom taxa investigated, demonstrating that diverse diatoms may invoke alternative strategies when dealing with identical changes in their environment. We report here several mechanisms used distinctly by coastal or oceanic diatom communities as well as numerous taxa-specific strategies for coping with Fe stress and rearranging nutrient metabolism following Fe enrichment.

Keywords: diatoms, *Thalassiosira*, *Pseudo-nitzschia*, iron, metatranscriptomics, California Upwelling Zone, Northeast Pacific Ocean

INTRODUCTION

Phytoplankton growth is limited by iron (Fe) availability in ∼30–40% of the ocean (Moore et al., 2001, 2004). The subarctic Northeast (NE) Pacific Ocean is one of the most well-characterized of these high-nutrient, low chlorophyll (HNLC) regions. Productivity in the NE Pacific Ocean remains low as a result of low Fe concentrations regardless of sufficient nitrate (NO_3^-) levels and is typically dominated by small cells such as the cyanobacterium *Synechococcus* and eukaryotic picophytoplankton (Varela and Harrison, 1999). In this region, Fe is supplied to surface waters mainly through atmospheric deposition of dust from arid continental regions and volcanic emissions, with Fe inputs from continental margin sediments fueling winter phytoplankton blooms when atmospheric deposition is low (Lam et al., 2006; Lam and Bishop, 2008). A gradient in surface nutrient concentrations is observed from this oceanic region eastwards toward the continent; bioavailable Fe increases and supports higher phytoplankton biomass while NO_3^- concentrations in the upper mixed layer decrease to limiting levels on the continental shelf (Taylor and Haigh, 1996; Harris et al., 2009; Ribalet et al., 2010).

Iron-limited growth of phytoplankton may also occur in coastal waters, notably in regions of the California Upwelling Zone (CUZ; Hutchins et al., 1998; Bruland et al., 2001). These regions of the CUZ are characterized by high concentrations of upwelled macronutrients, but relatively low dissolved Fe (dFe) such that phytoplankton blooms ultimately become Fe-stressed. Low Fe levels result from the lack of Fe inputs from rivers and narrow continental shelves that prevent mixing of upwelled water with Fe derived from Fe-rich shelf sediments (Johnson et al., 1999; Bruland et al., 2001) and consequently, the primary Fe source in the CUZ is winter river sediment deposition (Hutchins et al., 2002; Chase et al., 2005).

Phytoplankton that subsist in Fe-limited environments are equipped with strategies to sustain growth during periods of physiological Fe stress and to rapidly respond to sudden increases in bioavailable Fe. Strategies employed by phytoplankton include replacement of Fe-containing proteins with Fe-independent ones to decrease cellular Fe requirements (La Roche et al., 1996; Peers and Price, 2006; Allen et al., 2008; Lommer et al., 2012), increasing Fe uptake rates through induction of high affinity Fe uptake systems (Maldonado and Price, 2001; Morrissey et al., 2015) and using Fe storage through specialized proteins or vacuoles (Marchetti et al., 2009; Nuester et al., 2012). In some diatom laboratory isolates and natural communities, these low-Fe strategies are rapidly reversed when Fe concentrations increase (Kustka et al., 2007; Lommer et al., 2012), whereas in others these strategies are permanent adaptations (Lommer et al., 2010; Marchetti et al., 2012). Phytoplankton species from low-Fe oceanic environments generally have lower growth requirements for cellular Fe than species from higher Fe coastal waters, largely linked to differences in Fe-containing photosynthetic proteins and complexes (Sunda and Huntsman, 1995; Strzepek and Harrison, 2004; Peers and Price, 2006; Behrenfeld and Milligan, 2013). While we have an understanding of how a few phytoplankton species alter their nutrient metabolism in response to chronic Fe limitation from laboratory experiments, how the nutrient strategies invoked by intermittently Fe-limited coastal taxa might differ from those used by species residing in chronically Fe-limited regions of the open ocean has not been directly compared.

A large amount of genetic diversity exists among diatom taxa, possibly due to differences in environmental pressures at the time of evolutionary emergence (Sims et al., 2006; Armbrust, 2009; Rabosky and Sorhannus, 2009). A genomic comparison between the evolutionarily older centric *Thalassiosira pseudonana* and the more recently evolved pennate *Phaeodactylum tricornutum* demonstrates the two diatoms share only 57% of their genes with each other, suggesting a tremendous amount of genomic diversity exists between members of these two diatom lineages (Bowler et al., 2008). Furthermore it is often observed that pennate diatoms, especially those belonging to the genus *Pseudo-nitzschia,* tend to dominate large Fe-induced blooms in HNLC waters (de Baar et al., 2005; Marchetti et al., 2012). These observations may suggest that the pennate diatoms have evolved distinct strategies for optimizing their potential for rapid growth when transitioning from low to relatively high Fe conditions, resulting in a competitive advantage over older lineages of diatoms as well as other types of phytoplankton.

To better understand whether major diatom genera from coastal and oceanic regions differ in their gene expression responses to changes in Fe availability, a comparative analysis across distinct nutrient regimes was performed through a combination of metatranscriptomic and physiological approaches. Microcosm incubation experiments were conducted at geographically diverse sites with different Fe regimes, macronutrient concentrations, and phytoplankton community compositions—at an Fe-limited oceanic site and a coastal site in the subarctic NE Pacific Ocean, and at three biogeochemically distinct sites within the Fe mosaic of the coastal CUZ. For our study, we focused on the changes in gene expression patterns between two dominant taxa across all sites—the pennate diatom *Pseudo-nitzschia* and the centric diatom *Thalassiosira*. These two taxa were classified by the *Tara Oceans* circumnavigation expedition to be two of the eight most abundant diatom genera in the global ocean (Malviya et al., 2016). Given the large amount of genetic and physiological variation observed between major diatom groups (Bowler et al., 2008; Marchetti et al., 2009; Sutak et al., 2012; Alexander et al., 2015), differences in molecular responses to changing Fe availabilities across the NE Pacific Ocean and CUZ were anticipated.

MATERIALS AND METHODS

Experimental Design

Incubation experiments were conducted on two separate cruises: within regions of the CUZ during July 3–26th 2014 onboard the *R/V Melville* and along the Line-P transect of the subarctic NE Pacific Ocean during June 7–23rd 2015 onboard the *Canadian Coast Guard Ship (CCGS) John P. Tully* (**Figure 1**). The incubated phytoplankton community response was assessed using a combination of physiological measurements and metatranscriptomics to examine the effects of Fe status

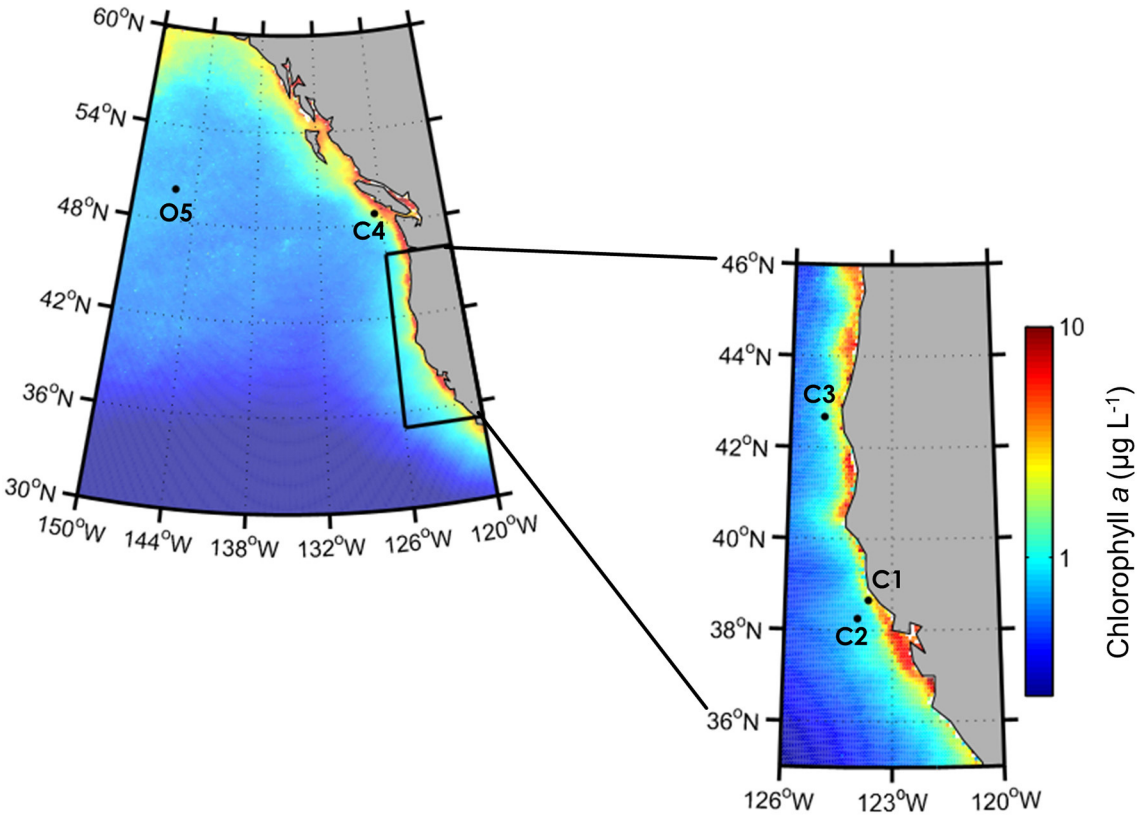

FIGURE 1 | Locations of incubation experiments in the California Upwelling Zone (C1, C2, C3) and along Line P (C4, O5) in the Northeast Pacific Ocean. Color bar indicates climatological-averaged chlorophyll *a* concentrations (μg L^{-1}) from SeaWiFS (1997-2010).

on diatom physiology and gene expression. Each experiment included three treatments: (1) a 5 nmol L^{-1} $FeCl_3$ addition (Fe), (2) a 200 nmol L^{-1} desferroxamine B (DFB) addition, and (3) an unamended control (Ctl), each sampled at two time points.

During the CUZ cruise, three incubation experiments were performed at separate locations corresponding to distinct Fe and macronutrient regimes (Supplementary Table 1), including sites of high dFe, macronutrients, and phytoplankton biomass (C1: 38°39.30 N, 123°39.87 W), relatively low dFe, high macronutrients and high phytoplankton biomass (C2: 38°15.31 N, 123°57.98 W), and low dFe with high macronutrients and low phytoplankton biomass (C3: 42°40.00 N, 125°0.00 W) (**Figure 1**). Near-surface seawater was collected from a depth of ∼15 m using a trace-metal clean sampling system consisting of a tow-fish sampler attached to Kevlar™ line, PFA Teflon tubing, and a Teflon dual-diaphragm pump that pumped seawater directly into a positive pressure trace-metal clean bubble. The seawater was placed in a large 200 L acid-cleaned HDPE drum for homogenization before being distributed into 10 L flexible acid-cleaned polyethylene cubitainers (Hedwin Corporation). Cleaning protocols for the cubitainers included successive soaks in 1.2 mol L^{-1} hydrochloric acid (reagent grade) for 3 days, 1.2 mol L^{-1} hydrochloric acid (trace metal grade) for 1 week and 0.1 mol L^{-1} acetic acid (trace-metal grade) until use. Prior to filling the cubitainers with seawater, the dilute acetic acid was removed and the cubitainers were rinsed thoroughly three times with ambient seawater from the collection site. The primary objective of these experiments was to elucidate the responses of target diatom genera and the phytoplankton community to variable Fe conditions. Therefore, sites were targeted that would ensure adequate macronutrient concentrations to support phytoplankton growth. However, at C2, 15 μmol L^{-1} of $Si(OH)_4$ was added to all cubitainers to support growth of diatoms due to the initially low $Si(OH)_4$ concentration (<4.7 μmol L^{-1}).

During the Line-P cruise, incubation experiments were conducted at the low NO_3^- coastal station P4 (48°39 N, 126°40 W; referred to as C4 in this analysis) and at the chronically Fe-limited, HNLC oceanic station P26, also known as Ocean Station Papa (OSP, 50°00 N, 145°00 W; Harrison, 2002; referred to as O5). Seawater was collected at depths corresponding to ∼30% of incident irradiance (8–12 m) at both stations using a trace-metal clean sampling system consisting of a Teflon air bellows pump and PTFE lined Kevlar™ tubing attached to a Kevlar™ line. The seawater was pumped directly into 10 L acid-cleaned polyethylene cubitainers placed within an on-deck trace-metal clean positive pressure flowhood. At site C4, 10 μmol L^{-1} of NO_3^- was added to all cubitainers to support growth of diatoms due to the initially low NO_3^- concentration (<1.5 μmol L^{-1}).

At the start of the experiments, ambient seawater was filtered for all initial measurements (T_0). For each incubation experiment, cubitainers were filled to serve as a control (Ctl) or amended with $FeCl_3$ or DFB just prior to dawn. All cubitainers were placed in on-deck Plexiglass incubators with flow-through seawater to maintain near-ambient surface water temperatures. Incubators were covered with neutral density screening to achieve ∼30% of the incident irradiance (Supplementary Figure 1). Following 24–96 h of incubation (Supplementary Table 1; depending on the measured macronutrient drawdown) the cubitainers for a specific time point were removed from the incubators and filtered immediately. The goal for each time point was to achieve measureable drawdowns in macronutrients that would infer stimulation of phytoplankton growth without complete macronutrient depletion. However, for some experiments and time points, depletion of NO_3^- or other macronutrients occurred. All filtrations were conducted at dawn. Subsamples for dissolved and particulate nutrients, size-fractionated uptake rates of dissolved inorganic carbon (DIC) and NO_3^-, size-fractionated chlorophyll *a*, $F_v/F_{m,}$ and RNA were collected at T_0 and from each cubitainer according to the protocols described below.

Nutrient Concentrations, Uptake Rates, and Biogenic Silica Concentrations

For CUZ experiments, dissolved nitrate and nitrite (NO_3^- + NO_2^-), phosphate (PO_4^{3-}), and silicic acid (H_4SiO_4) concentrations were measured onboard using a Lachat Quick Chem 8000 Flow Injection Analysis system (Parsons et al., 1984) with detection limits of 0.05 μM for NO_3^- + NO_2^-, 0.03 μM for PO_4^{3-}, and 0.2 μM for H_4SiO_4 (Bruland et al., 2008). Particles were removed by filtration through a Whatman GF/F filter (25 mm). Reference standards for nutrients in seawater were run for quality control. During Line-P sampling, ∼15 mL of seawater was filtered through a Whatman GF/F filter into acid-rinsed polypropylene tubes and frozen at −20°C in aluminum blocks until onshore analysis. Shortly following the cruise, the dissolved NO_3^- + NO_2^-, PO_4^{3-}, and H_4SiO_4 concentrations were determined using an Astoria nutrient analyzer (Barwell-Clarke and Whitney, 1996). Nutrient detection limits were 0.2 μM for NO_3^- + NO_2^-, 0.02 μM for PO_4^{3-}, and 0.5 μM for H_4SiO_4 (Frank Whitney and Mark Belton [IOS], pers. comm.).

For biogenic silica (bSi) measurements, 335 mL (CUZ) or 250 mL (Line P) of seawater was filtered onto polycarbonate filters (1.2 μm pore size for CUZ and 0.6 μm pore size for Line-P, 25 mm), digested with NaOH in Teflon tubes, and measured with the colorimetric ammonium molybdate method (Krause et al., 2013).

Size-fractionated particulate nitrogen (PN), particulate carbon (PC), and NO_3^- uptake rates were obtained by adding ^{15}N-$NaNO_3$ to 618 mL subsample of experimental seawater placed within clear polycarbonate bottles. The concentration of NO_3^- added was no more than 10% of ambient NO_3^- level within CUZ incubations, and was 1 μmol L^{-1} within Line-P incubations (corresponding to NO_3^- levels of 68% at T_0 and 10% within NO_3^--amended incubations at C4, and ∼10% at O5). DIC uptake within Line-P incubations was measured by additionally spiking subsamples with 120 μmol L^{-1} $NaH^{13}CO_3$. Bottles were incubated in the same flow-through Plexiglass incubators where cubitainers were kept. Following 8 h of incubation, seawater samples were filtered in series through a polycarbonate filter (5 μm pore size, 47 mm) via gravity filtration, and then through a pre-combusted (450°C for 5 h) GF/F filter by gentle vacuum (<100 mg Hg). Particulates collected on the 5 μm polycarbonate filter were then rinsed onto a separate pre-combusted GF/F filter using an artificial saline solution. Filters were stored at −20°C until onshore analysis. In the laboratory, filters were heated to 60°C for 24 h and pelletized in tin capsules (Elemental Microanalysis) in preparation for analysis of the atom % ^{15}N, atom % ^{13}C (for Line-P), particulate nitrogen (PN), and particulate carbon (PC) using an elemental analyzer paired with an isotope ratio mass spectrometer (EA-IRMS). Biomass-normalized NO_3^- uptake rates (PN-*V*NO_3) and DIC uptake rates (PC-*V*DIC) for the Line-P experiments were obtained by dividing the measured NO_3^- and DIC biological uptake rates by PN and PC concentrations, respectively.

To quantify *V*DIC in CUZ incubations, incorporation of ^{14}C was determined using a protocol adapted from Taylor et al. (2013). Briefly, 60 mL of seawater from each cubitainer was distributed into acid-cleaned light and dark polycarbonate bottles. In each bottle, 1.2 μCi of $NaH^{14}CO_3$ was added. Bottles were incubated in the same flow-through Plexiglass incubators where cubitainers were kept for 6.5–8 h. Following incubation, samples were filtered through stacked 47 mm polycarbonate filters (5 and 1 μm) separated with a mesh spacer during filtration. Filters were vacuum dried, placed in 7 mL scintillation vials containing 0.5 mL of 6 M HCl and permitted to degas for 24 h. Disintegrations per minute (DPM) retained on the filters were measured using a Beckman Coulter LS 6500 scintillation counter. Reported values are light bottle DPMs minus dark bottle DPMs. To obtain *V*DIC, DIC uptake rates were normalized to PC concentrations obtained as part of the NO_3^- uptake measurements within each incubation and size fraction.

Dissolved Iron Concentrations

Seawater samples for Fe analysis within the CUZ were acidified at sea with the equivalent of 4 mL 6 N quartz-distilled HCl per L of seawater (pH ∼ 1.7) and stored in acid-cleaned LDPE bottles for at least 2 months prior to analysis. Samples were analyzed using an adaption of Biller and Bruland (2012) as described in Parker et al. (2016). Briefly, this method involves preconcentrating the Fe from buffered (pH 6.0) seawater on Nobias-chelate PA1 resin and eluting with 1 N quartz-distilled HNO_3. The eluent was analyzed with a Thermo-Element high resolution XR ICP-MS in counting mode. Line-P dissolved Fe samples were stored in acid-cleaned LDPE bottles, acidified post-cruise with Optima-grade HCl (1 mL 12 N HCl per L of seawater), and allowed to sit for >3 months. Dissolved Fe was measured via ICP-MS by P. Morton at Florida State University following resin preconcentration using the protocol of Milne et al. (2010).

Chlorophyll *a*

Four hundred milliliters of seawater was gravity-filtered through a polycarbonate filter (5 μm pore size, 47 mm diameter) followed by vacuum filtration through a GF/F filter (0.7 μm nominal pore size, 25 mm diameter) using a series filter cascade for size fractionation. Filters were frozen at −80°C until analysis. Chlorophyll *a* extraction was performed using 90% acetone at −20°C for 24 h and the extracted Chl *a* was quantified by fluorometry with a Turner Designs 10-AU fluorometer using the acidification method (Parsons et al., 1984).

Domoic Acid

Approximately 250 mL of seawater from each CUZ site was filtered through GF/F filters (25 mm) via vacuum pressure (<100 mm Hg) and the filters were frozen at −80°C. The filters were extracted with 20% methanol (MeOH) in water. The mixture was sonicated in an ice bath for 2 min at 30–40 W with a Sonicator 3000, followed by centrifugation (10 min, 1,399 × g). The supernatant was collected and passed through a 0.22 μm syringe filter. Samples were stored at −20°C until analysis. Concentrations with a detection limit of 0.01 μg L^{-1} were obtained using an enzyme-linked immunosorbent assay (Abraxis, Warminster, PA, USA) following the manufacturer's protocol, including running each sample in duplicate at several dilutions. Final concentrations (pg DA mL $extract^{-1}$) were calculated using the manufacturer supplied analysis spreadsheet.

Photophysiology

The maximum photochemical yield of PSII (F_v/F_m) was measured by fast repetition rate fluorometry (FRRF) using a custom-built fluorescence-induction and relaxation system (Kolber et al., 1998; Gorbunov and Falkowski, 2004). Before each measurement, a 5 mL subsample of seawater from each cubitainer was acclimated to low light for 20 min. A saturating pulse (20,000 μmol photons m^{-2} s^{-1}) of blue light (450 nm) was applied to dark-acclimated cells for a duration of 100–200 μs. Measurements were obtained using the single-turnover flash (STF) setting with the average of 50 iterations for the CUZ experiments, and a single iteration for the Line-P experiments. Data were blank corrected using 0.2 μm filtered seawater.

RNA Extraction and Bioinformatic Analysis

Phytoplankton in seawater samples were filtered onto 0.8 μm Pall Supor filters (142 mm) via peristaltic pumping, immediately flash frozen in liquid nitrogen and stored at −80°C until extraction onshore. The filters were briefly thawed on ice before being extracted individually using the ToTALLY RNA Kit (Ambion). The extraction procedure followed manufacturer protocols with the modified first step of glass bead addition and vortexing to facilitate disruption of cells. Removal of DNA was performed with one round of DNAse I (Ambion) incubation. For the Line P experiments, due to low yields in treatments, RNA from the triplicate cubitainers was pooled prior to sequencing. Within CUZ experiments all triplicate incubation samples were sequenced separately. At the oceanic site O5, RNA yields were too low to successfully sequence metatranscriptomes at the T_1 timepoint, and consequently, transcriptomic analyses were performed using the T_0, T_2 Fe, and T_2 Ctl treatments. Metatranscriptomic library preparation was performed with the Illumina TruSeq Stranded mRNA Library Preparation Kit and HiSeq v4 reagents. Samples were barcoded and run across three lanes of Illumina HiSeq 2000 (125 bp, paired-end) yielding on average 23 million paired-end reads per sample (Supplementary Table 2). The RNA-seq data reported here has been deposited in the National Center for Biotechnology (NCBI) sequence read archive (SRA) under the BioProject accession no. PRJNA320398 and PRJNA388329.

Raw reads were trimmed for quality bases and removal of adapters using Trimmomatic v0.32 (paired-end mode, adaptive quality trim with 40 bp target length, and strictness of 0.6, minimum length of 36 bp; Bolger et al., 2014). Trimmed paired reads were merged into single reads with BBMerge v8.0. For each site, the resulting merged pairs and non-overlapping paired-end reads were assembled using ABySS v1.5.2 with a multi-kmer approach (Birol et al., 2009). The different k-mer assemblies were merged to remove redundant contigs using Trans-ABySS v1.5.3 (Robertson et al., 2010). Read counts were obtained by mapping raw reads to assembled contigs with Bowtie2 v2.2.6 (end-to-end alignment; Langmead and Salzberg, 2012). Alignments were filtered by mapping quality score (MAPQ) of 10 or higher as determined by SAMtools v1.2 (Li et al., 2009). Taxonomic and functional annotations were assigned based on sequence homology to reference databases via BLASTx v2.3.0 with an e-value cutoff of 10^{-3} (Altschul et al., 1990). Functional annotations were assigned according to the top hit using the Kyoto Encyclopedia of Genes and Genomes (KEGG; Release 75), while taxonomic assignments were obtained according to the top hit using MarineRefII (Laboratory of Mary Ann Moran, University of Georgia), a custom-made database comprised of protein sequences of marine prokaryotes and eukaryotes including all sequenced transcriptomes from Marine Microbial Eukaryote Transcriptome Sequencing Project (MMETSP) (Keeling et al., 2014). Taxonomic information was obtained from NCBI's Taxonomy Database (each isolate in MarineRefII is assigned a NCBI taxonomic ID). The information from NCBI was manually curated to ensure proper assignment and use of common phytoplankton taxonomic ranks. For our analysis, we have grouped diatom-associated sequences at the genus level. Therefore, the patterns in gene expression observed could be driven by one dominant species or many equally distributed species belonging to a genus within each site.

All diatom-assigned counts were summed to both the genus taxonomic rank and KEGG Orthology (KO) functional annotation level. For genes of interest without a KO assignments but with an annotated gene definition (i.e., ISIPs and rhodopsin), raw counts corresponding to KEGG gene definitions were summed. EdgeR v3.12.0 was used to calculate *Pseudo-nitzschia*- or *Thalassiosira*-specific normalized fold change and counts-per-million (CPM) from pairwise comparisons using the exactTest (Robinson and Smyth, 2008; Robinson and Oshlack, 2010; Robinson et al., 2010; Klingenberg and Meinicke, 2017). Significance ($p < 0.05$) was calculated with edgeR's estimate of tagwise dispersions across all samples within CUZ sites. Heatmaps were produced with the R package

pheatmap v1.0.8, and dendrograms created using Euclidean distance and hierarchical clustering. Assembled contigs, read counts, and functional annotations of contigs are available at marchettilab.web.unc.edu/data.

In order to directly compare transcript abundance across locations for principal component analyses (PCA), the assemblies for all sites were merged with Trans-ABySS. The removal of redundant contigs was verified with GenomeTools v.1.5.1. Counts were obtained by aligning raw reads against this merged metatranscriptome using Salmon v.0.7.3-beta. Normalized counts were then obtained with edgeR v3.12.0. PCA biplots were created using log-transformed normalized counts for genes of interest with ggbiplot v.0.5.

Phylogenetic Analysis of Environmental Sequences

Environmental *Pseudo-nitzschia* and *Thalassiosira* contigs functionally annotated as RubisCO (*RBCL*), rhodopsin (*RHO*), or superoxide dismutase (*SOD*) and containing a large number of mapped reads were compared to diatom reference sequences for phylogenetic characterization. Diatom sequences used in reference alignments were obtained through a sequence homology search using BLASTx v2.2.28 with *Pseudo-nitzschia RBCL, RHO,* and *SOD* against the database MMETSP using an E-value cutoff of 10^{-5} (Altschul et al., 1990). Sequences were aligned using MUSCLE within Geneious v5.6.4 software (Edgar, 2004).

RESULTS

Nutrient Regimes of Experimental Sites

CUZ site C1 (**Figure 1**) was characterized by high macronutrient and dFe concentrations in the mixed layer supporting a high biomass, nutrient-replete phytoplankton community. The community was dominated by phytoplankton cells in the >5 μm chlorophyll *a* (chl *a*) size fraction, constituting 88% of the total chl *a* concentration (**Figure 2B**; Supplementary Table 1). Macronutrient concentrations were rapidly consumed during the first 24 h of incubation (T_1), with near complete depletion of the NO_3^- (≤1 μmol L^{-1} remaining by 48 h [T_2]; **Figure 2A**). The initially Fe-replete phytoplankton community (dFe: 3.57 nmol L^{-1}) was mostly unaffected by the additions of Fe or DFB as demonstrated through relatively constant F_v/F_m, phytoplankton biomass, particulate nitrogen (PN)-specific nitrate uptake rates (VNO_3, or nitrate assimilation rates), and particulate carbon (PC)-specific dissolved inorganic carbon uptake rates ($VDIC$, or carbon assimilation rates) across treatments at each time point (**Figures 2B–E**). Furthermore, the NO_3:Fe ratio of the initial (T_0) seawater (3.8 μmol:nmol. Supplementary Table 1) was substantially below the predicted threshold ratio for eventual Fe stress of 12 μmol:nmol for phytoplankton in this region as proposed by King and Barbeau (2007), albeit this ratio is subject to variation as a function of phytoplankton iron demands (Bruland et al., 2001), suggesting this phytoplankton community was not likely to be driven into Fe limitation prior to complete NO_3^- utilization. However, indications of molecular-level responses to Fe and DFB additions were observed; 74 genes were differentially expressed ($p < 0.05$) in *Pseudo-nitzschia* between the Fe and DFB treatments (Supplementary Figure 2A). Fe-stress bioindicator genes (*FLDA*, *PETE,* and *ISIP2A;* Whitney et al., 2011; Morrissey et al., 2015; Graff van Creveld et al., 2016) increased in expression following the addition of DFB relative to the added Fe treatment, suggesting the onset of Fe stress following the addition of DFB by the end of the first time point.

CUZ site C2 was located in close geographical proximity to C1 (**Figure 1**), yet exhibited different mixed layer properties in relation to phytoplankton biomass, silicic acid ($Si[OH]_4$) and dFe concentrations (0.44 nmol L^{-1}). Nitrate and ortho-phosphate (PO_4^{3-}) concentrations were similarly high (10.3 and 0.96 μmol L^{-1}, respectively) as found at site C1, although $Si(OH)_4$ levels were appreciably lower (4.7 μmol L^{-1}) and possibly growth-limiting to certain diatoms (Nelson et al., 1996). Therefore, incubations were amended with 15 μmol L^{-1} $Si(OH)_4$ to support potential diatom growth with added Fe (Brzezinski, 1985). Although the chl *a* concentration in the >5 μm size fraction was initially <1 μg L^{-1} and biogenic silica (bSi) concentrations were <3 μmol L^{-1}, by 48 h (T_1) the >5 μm chl *a* fraction reached 5–8 μg L^{-1}, and bSi increased to 10–15 μmol L^{-1} in all treatments, accompanied by appreciable decreases in NO_3^-, PO_4^{3-}, and $Si(OH)_4$ concentrations (**Figures 2A,B**). Since this community quickly depleted NO_3^- concentrations during the experimental period, this site presented an opportunity to couple the physiological indicators of NO_3^- stress with N-related transport and assimilation genes observed to be elevated in NO_3-starved laboratory diatom cultures (Hildebrand, 2005; Song and Ward, 2007; Bender et al., 2014; Rogato et al., 2015). Apart from F_v/F_m reaching relatively low values in the DFB treatments, indications of Fe stress in bulk physiological measurements across treatments were absent (**Figure 2C**). However, the initial seawater NO_3:Fe ratio of 23.4 μmol:nmol suggests this community may have been driven into Fe limitation provided sufficient $Si(OH)_4$ was present. Additionally, a total of 414 *Pseudo-nitzschia*–associated genes were differentially expressed ($p < 0.05$) by T_1 between the Fe and DFB treatments (Supplementary Figure 2). This greater number of differentially expressed genes in *Pseudo-nitzschia* when compared to C1 suggests the C2 diatom community in the DFB treatment experienced a higher degree of Fe stress during the incubation period. The initially low dissolved $Si(OH)_4$:NO_3 ratio at this site furthermore implies a possible increase in the Si:N ratios of Fe-stressed diatoms (Hutchins and Bruland, 1998; Marchetti and Cassar, 2009; Brzezinski et al., 2015). Interestingly, concentrations of domoic acid (DA), a neurotoxin produced by *Pseudo-nitzschia*, was 90 pg mL^{-1} in initial seawater (T_0) and exceeded 3,000 pg mL^{-1} in the control treatment by T_1 (Supplementary Figure 3). This increase in DA concentration may be linked to both the increase in *Pseudo-nitzschia* abundance and depletion of $Si(OH)_4$ resulting in Si-limited cells which has been shown to greatly enhance DA production (Pan et al., 1996).

Site C3 (**Figure 1**) contained the lowest dFe concentrations (0.31 nmol L^{-1}) among the CUZ sites along with high macronutrient concentrations [17 μmol L^{-1} NO_3^-, 19 μmol L^{-1} $Si(OH)_4$, and 1.5 μmol L^{-1} PO_4^{3-}; **Figure 2A**]. The corresponding NO_3:Fe ratio of the initial seawater was

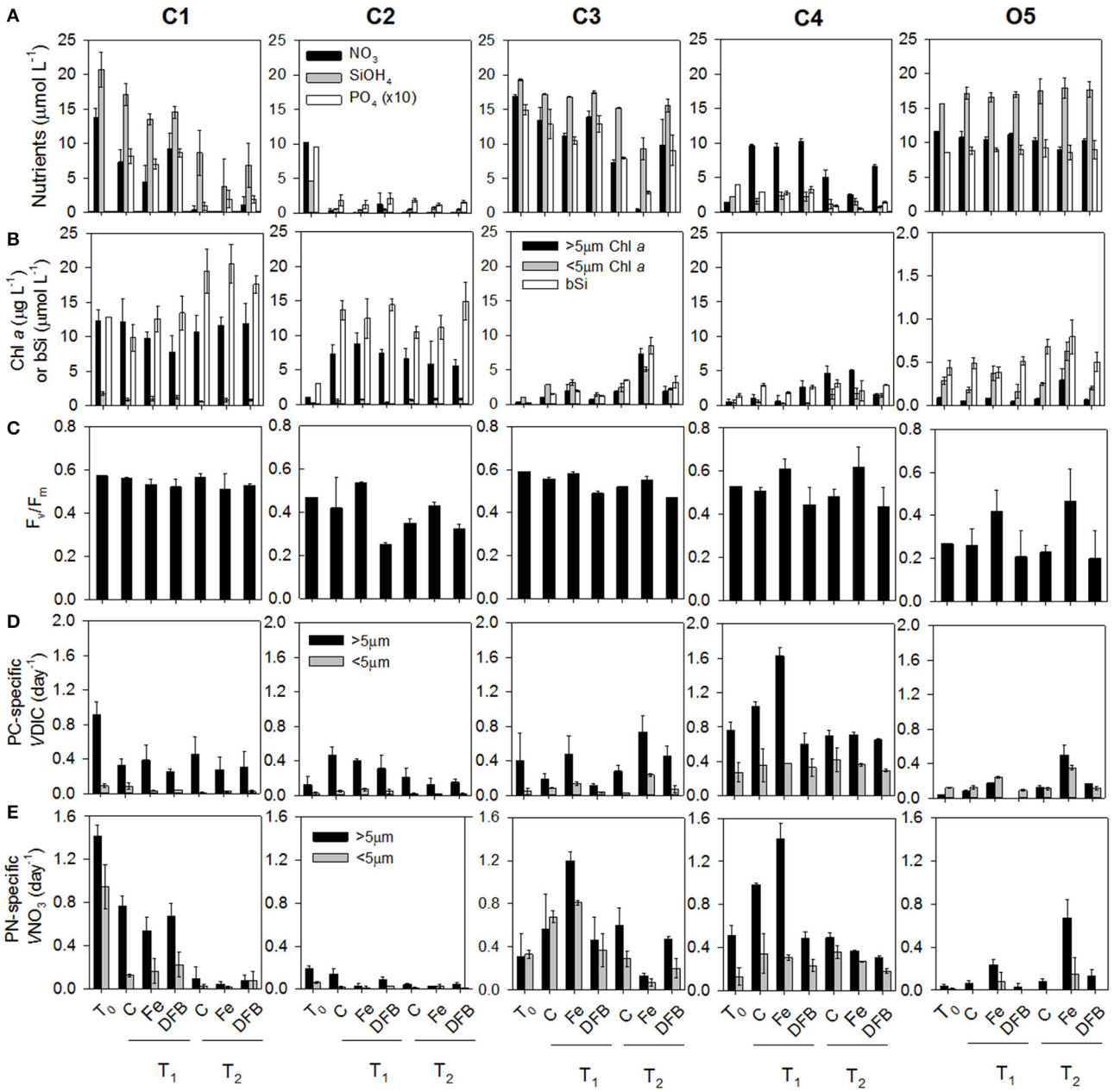

FIGURE 2 | Dissolved macronutrient concentrations: nitrate (NO_3^-), silicic acid ($SiOH_4$), and ortho-phosphate (PO_4^{3-}) **(A)**, Size-fractionated chlorophyll *a* ($\mu g\ L^{-1}$) within the large (>5 µm) and small (<5 µm) size fractions or biogenic silica ($\mu mol\ L^{-1}$) **(B)**, Maximum photochemical yield of PSII (F_v/F_m) **(C)**, Particulate carbon (PC)-specific dissolved inorganic carbon (DIC) uptake rates [*V*DIC (day^{-1})] within the large and small size fractions **(D)**, and particulate nitrogen (PN)-specific nitrate uptake rates [VNO_3 (day^{-1})] within the large and small size fractions **(E)** in each treatment and sample time points across sites (see Supplementary Table 1). Where present, error bars represent the standard deviation associated with the mean of triplicate incubations.

~54.9 µmol:nmol (Supplementary Table 1). Following incubation, the chl *a*, bSi, PN-specific VNO_3, and PC-specific *V*DIC were all higher in the Fe-amended treatment relative to the unamended control by T_1 (**Figures 2B,D,E**). By 72 h, NO_3^- was completely drawn down within the Fe treatment (T_2). Despite the pronounced influence of Fe enrichment on bulk parameters, F_v/F_m values were only slightly higher in the Fe treatment than the control, but they were substantially higher than in the DFB treatment (**Figure 2C**). This is likely a reflection of the different phytoplankton composition at this location compared to site C2, which did not show indications of an Fe-addition response on the measured bulk parameters, but did demonstrate elevated F_v/F_m values in the added Fe treatment. Site C3 represented the only phytoplankton community in

the CUZ that displayed a definite physiological response to Fe addition relative to the control treatment (Supplementary Table 1). The Fe-induced molecular response in diatoms was demonstrated by the differential expression of 458 genes in *Pseudo-nitzschia* and 1,223 genes in *Thalassiosira* between the Fe and DFB treatments (Supplementary Figure 2C), and 365 genes in *Pseudo-nitzschia* and 837 genes in *Thalassiosira* between the Fe and Ctl treatments ($p < 0.05$).

Coastal site C4 was located at station P4 of the Line-P transect in the subarctic NE Pacific Ocean (**Figure 1**). Initial mixed-layer seawater properties were characterized by low concentrations of macronutrients and dFe, which supported a low phytoplankton biomass. Nitrate concentrations were initially 1.5 μmol L^{-1} (**Figure 2A**). To facilitate a potential phytoplankton growth response to added Fe, 10 μmol L^{-1} of NO_3^- was added to each treatment. $Si(OH)_4$ concentrations were also initially low (2.2 μmol L^{-1}) and incubation concentrations dropped to <2 μmol L^{-1} in most treatments by the second time point (T_2; **Figure 2A**). These low concentrations restricted biomass accumulation as bSi (**Figure 2B**) and it is likely that the resulting diatom community experienced $Si(OH)_4$ limitation by the end of the incubation period. Despite its relatively close proximity to land and relatively high dFe concentration (0.64 nmol L^{-1}), there was a pronounced response to Fe addition at C4 as demonstrated through higher F_v/F_m, PN-specific VNO_3, and PC-specific *V*DIC in the Fe treatment compared to values in the unamended control by T_1 (**Figures 2D,E**; Supplementary Table 1). The NO_3:Fe ratio following artificial NO_3^- addition was 18.8 μmol:nmol, sufficiently high to cause Fe stress with phytoplankton growth following an increase in phytoplankton biomass.

Oceanic site O5 was located at Ocean Station Papa (OSP), station P26 of the Line-P transect (**Figure 1**). This site demonstrated characteristically high macronutrients and low dFe (0.05 nmol L^{-1}), resulting in the highest NO_3:Fe ratio observed across all experimental sites (234 μmol:nmol; Supplementary Table 1). Phytoplankton biomass was initially low, consistent with historical observations from this well-characterized Fe-limited region (**Figure 2A**; Supplementary Table 1; Boyd and Harrison, 1999). In contrast to most of the coastal sites, the majority of the phytoplankton biomass was dominated by picophytoplankton and other small cells (<5 μm) initially and throughout the incubation period (Supplementary Table 1; **Figure 2B**). Biogenic Si concentrations only increased after 96 h with similar responses in controls and Fe treatments (**Figure 2B**). Both large and small chl *a* size fractions, F_v/F_m, PN-specific VNO_3, and PC-specific *V*DIC were higher in the Fe treatment than in the unamended control (Ctl), confirming that the phytoplankton community in the initial seawater and in all incubation treatments without added Fe were experiencing Fe limitation (**Figures 2B–E**).

Community Composition across Sites

Metatranscriptomic assembly of sequence data and subsequent taxonomic annotation yielded the relative transcript proportions of phytoplankton functional groups (**Figure 3**). The CUZ site C1 was predominantly comprised of diatom transcripts at T_0; however, there was a 26% decrease in diatom transcripts in both the Fe and DFB treatments by T_1, accompanied by genus-level shifts within the diatoms. In contrast, CUZ site C2 initially yielded a phytoplankton community transcript pool dominated equally by diatoms (30%) and prasinophytes (28%), with diatoms remaining a dominant taxa following incubation (26–28%) and prasinophyte transcripts substantially decreasing from 28 to 3–8% in both Fe and DFB incubations. CUZ site C3 contained a phytoplankton community transcript pool almost equally represented by diatoms, prasinophytes, haptophytes, and dinoflagellates with little change in community composition among treatments following incubation. The coastal subarctic Pacific site C4 yielded an initial phytoplankton community transcript pool dominated by dinoflagellate-assigned sequences (24%), although these sequences decreased by ∼10% in the Fe treatment, concurrent with a 9% increase in diatom transcripts. At the oceanic site O5, there were initially equal proportions of prasinophyte (22%) and haptophyte (23%) transcripts, with little representation by diatoms (4%). However, diatom-assigned transcripts constituted 9% of the community transcript pool by T_2 in the Fe addition treatment. *Pseudo-nitzschia* and *Thalassiosira* were among the top five diatom genera at all sites examined based on relative transcript abundance (**Figure 3**). These two genera together constituted between 9 and 53% of the transcript proportions in the initial diatom communities, and 25–58% of the Fe-enriched diatom communities.

Gene Expression Responses to Fe Status across Sites

Gene expression responses among sites were compared using Euclidian distance similarity analyses between Fe and DFB treatments (Fe/DFB, Fe/Ctl for O5) within the diatom genera *Pseudo-nitzschia* and *Thalassiosira* (**Figure 4**). Expression responses within coastal sites clustered together, while the oceanic site O5 displayed distinctly different patterns in both taxa. At site O5, 83 out of 1,334 KEGG Orthology genes (KOs) in *Pseudo-nitzschia* demonstrated >16-fold higher expression in the added Fe treatment than in the Fe-limited control treatment (**Figure 4**, Supplemental Table 4). By comparison, 155 out of 1,241 KOs in *Thalassiosira* showed >16-fold higher expression in the added Fe treatment compared to the low Fe control treatment. The most highly differentially expressed genes in oceanic *Pseudo-nitzschia* following Fe enrichment were ferritin (*FTN*, 290-fold), a metal transporter (*CNNM*, 32-fold), a putative bicarbonate (HCO_3) transporter (*ICTB*, 133-fold), and an NADPH-dependent glutamate synthase (*GLT*; 146-fold). In oceanic *Thalassiosira*, highly differentially expressed genes included ferredoxin-dependent sulfite reductase (*Fd-SIR*, 74-fold) and ferredoxin-dependent glutamate synthase (*Fd-GLT*; 416-fold). Fe addition induced both genera to increase the expression of several genes involved in photosynthesis by >16-fold exclusively at this location. Both taxa overexpressed gene products involved in vitamin biosynthesis, including the Fe-dependent vitamin B_7 synthesis protein biotin synthase (*BIOB*), which increased expression in the Fe enriched treatment by 84- and 49-fold in *Pseudo-nitzschia* and *Thalassiosira,* respectively.

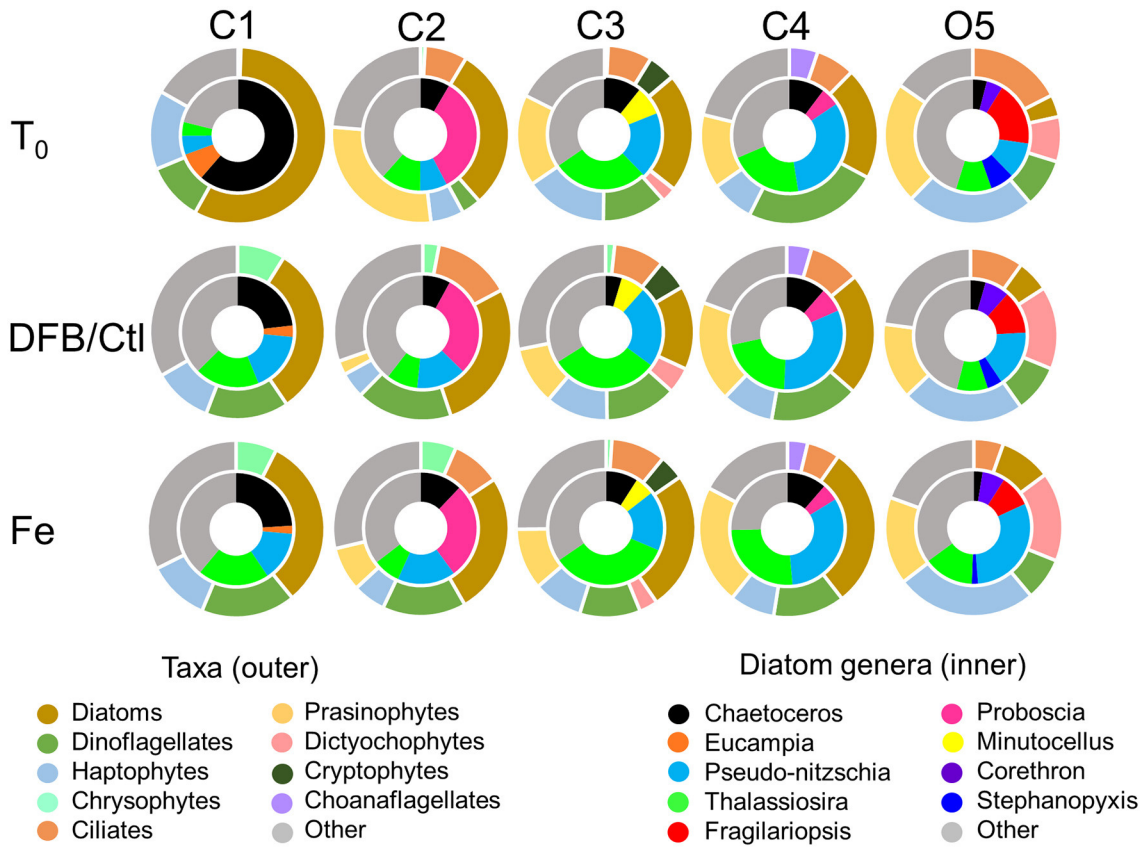

FIGURE 3 | The average transcript proportions of phytoplankton taxa (outer charts) and diatom genera (inner charts) from initial seawater (T_0) and during the first time point (T_1; see Supplementary Table 1) within the Fe addition (Fe) and DFB addition (DFB) treatments at each site. Note that for site O5, the T_2 control (Ctl) treatment is provided as the Fe-limited comparison.

Furthermore, *Pseudo-nitzschia* increased expression of the vitamin B_1 (thiamine) biosynthetic gene *THIC* (by 179-fold) and vitamin B_6 (pyridoxine) biosynthetic genes pyridoxine kinase (*PDXK*; by 74-fold) and pyridoxine 4-dehydrogenase (*PLDH*; by 152-fold) following Fe enrichment at the oceanic site.

A number of genes demonstrated higher expression in the Fe-limited control treatment at O5. Forty-eight out of 1,334 genes in *Pseudo-nitzschia* and 77 out of 1,241 genes in *Thalassiosira* showed >16-fold higher expression in the Ctl treatment than in the added Fe treatment, patterns that were not found in diatoms from the examined coastal sites (**Figure 4**). In *Thalassiosira*, these genes encode proteins such as the copper (Cu)/zinc (Zn) superoxide dismutase (*Cu-Zn SOD*), an enzyme that removes toxic superoxide radicals by dismuting them into molecular oxygen and hydrogen peroxide, and a divalent metal transporter belonging to the ZIP family (ZIP7) (Marchetti and Maldonado, 2016). In both taxa, ribulose-1,5-bisphosphate carboxylase oxygenase (RubisCO; large subunit; *RBCL*), which catalyzes C-fixation in the Calvin cycle, had ≥24-fold higher expression in the Ctl treatment at O5.

Influence of Fe Availability on Fe Metabolism

The expression of genes involved in cellular growth and function, including N and C assimilation, vitamin synthesis, Fe-related metabolism, and trace metal acquisition, were compared in the dominant diatom genera *Pseudo-nitzschia* and *Thalassiosira* between the Fe and DFB/Ctl treatments (**Figure 5**). Genes encoding proteins involved in metal transport were detected at all locations, with expression patterns varying depending on site and taxa. *Pseudo-nitzscha* increased expression of the Fe transporter *ABC.FEV.S* by >2-fold under Fe enrichment at all locations where incubated communities showed a physiological Fe effect (C3, C4, O5; Supplementary Table 1). Transcripts for another Fe uptake protein, the high affinity iron permease *FTR*, were generally more abundant in the DFB/Ctl treatments in *Thalassiosira*, although the gene was more highly expressed following Fe enrichment in *Pseudo-nitzschia* at sites C2, C3, and O5 (**Figure 5**). The putative metal transporter *CNNM* was 32-fold more highly expressed following Fe enrichment in *Pseudo-nitzschia* at the oceanic site, but was not detected in *Thalassiosira*. Conversely, the non-specific metal transporter *ZIP7* was 21-fold more highly expressed under Fe-limiting conditions in

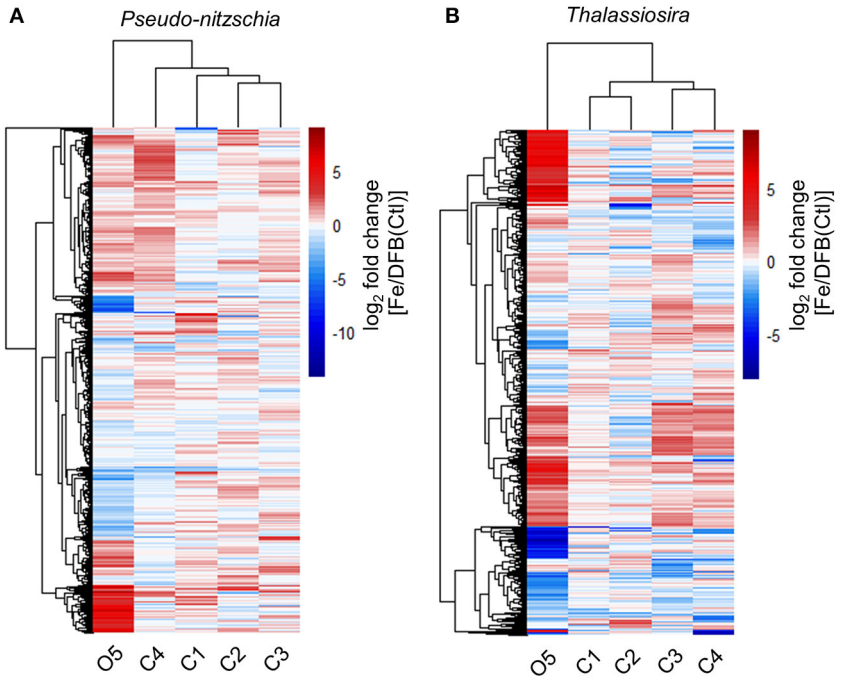

FIGURE 4 | Differential expression response of shared KEGG Orthologs (KOs) between the Fe and DFB treatments at T_1 in the diatom genera *Pseudo-nitzschia* **(A)** and *Thalassiosira* **(B)**. Heatmap represents the $\log_2$ fold change in gene expression within the Fe addition treatment relative to the DFB addition treatment at each site. For site O5, the T_2 control (Ctl) treatment is used as the Fe-limited comparison. Only KOs with transcript abundances >5 $\log_2$ CPM are included. Dendrograms reflect similarity in expression responses among sites (columns) or KOs (rows).

oceanic *Pseudo-nitzschia* and similarly not detected in oceanic *Thalassiosira*. Transcripts for Fe starvation induced proteins (*ISIP*s), including the recently-identified Fe acquisition protein *ISIP2A* that binds Fe at the cell surface and is thought to be involved in intracellular Fe transport (Morrissey et al., 2015), were highly abundant in Fe-stressed treatments (e.g., DFB and/or Ctl depending on the site) across all sites and in both taxa (**Figure 5**). Although their specific functions in diatoms are unclear, other *ISIP*s were markedly abundant and differentially expressed in the DFB/Ctl treatments, with *ISIP1* one of the most differentially expressed genes between Fe-replete and Fe-limited treatments at each experimental site and in both taxa (Supplementary Figure 2).

Other Fe-related metabolic processes similarly varied depending on both site and taxa. Differences in expression patterns between taxa were generally greater for these Fe-related genes than in the N- and C-related genes investigated (**Figure 5**). At most sites, transcripts for the Fe storage protein ferritin (*FTN*) were higher in the Fe addition treatments than in the DFB/Ctl treatments. However, at two sites (C2 and C4), *FTN* transcripts were more abundant in the DFB treatment compared to the Fe addition treatment for one of the two genera (e.g., at site C2, 3.5-fold higher in *Pseudo-nitzschia*, $p = 1 \times 10^{-3}$ and at site C4, 90-fold higher in *Thalassiosira*). *SOD*s were additionally differentially expressed, but they showed different expression patterns depending on the enzymes' metal cofactor(s) and the diatom genus. *Cu-Zn SOD*, which contains both Cu and Zn at its active site, showed a >100-fold higher expression in *Thalassiosira* in the Fe-limited control than in the added Fe treatment at the Fe-limited site O5. In contrast, in the same Fe-limited control treatment at this location, *Pseudo-nitzschia* demonstrated 2-fold higher expression of *Fe-Mn SOD*, which contains either Fe or manganese (Mn) as its metal cofactor. Based on the presence of Mn-coordinating amino acids at sites G-77 and Q-146 of the most highly expressed *Fe-Mn SOD* contigs, this *Pseudo-nitzschia* SOD was determined to specifically utilize Mn as its metal cofactor (Crowley et al., 2000; Groussman et al., 2015) (Supplementary Figure 4C).

Transcriptional responses of genes encoding Fe-dependent proteins and their functional replacements in photosynthetic electron transport were examined in both diatom genera (**Figure 5**). Transcripts for the Fe-independent protein flavodoxin (*FLDA*), which functionally replaces the Fe-protein ferredoxin (*PETF*) in photosynthetic electron transport, were generally more abundant in the DFB/Ctl treatments than in the Fe treatments in both genera (**Figure 5**). Conversely, transcripts of *PETF* were >2-fold higher in the high-Fe treatment only in *Thalassiosira* and across all sites. In *Pseudo-nitzschia*, *PETF* transcripts were either constitutively expressed (C3 and C4), more highly expressed in the DFB treatment (C1), or not present (C2 and O5) (**Figure 5**). Transcripts of cytochrome c_6 (*PETJ*) and its functional non-Fe replacement, the copper-protein plastocyanin, also showed differences in gene expression. *PETJ* transcripts were more abundant in the high Fe treatment at

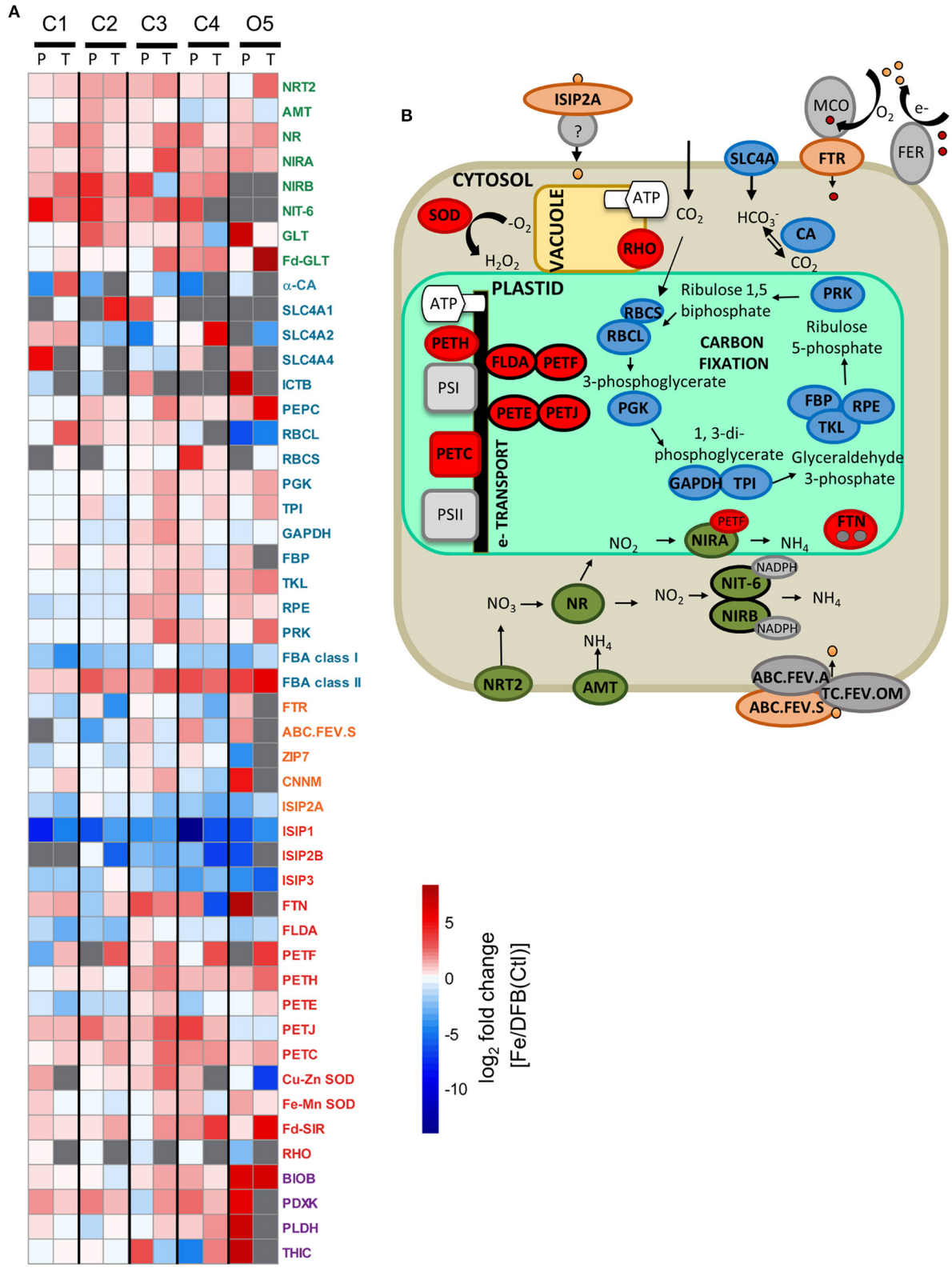

FIGURE 5 | Differential expression responses of select genes involved in nitrogen (N; green), carbon (C; blue), metal transport (orange), iron (Fe; red), and vitamin (purple)-related processes between the T_1 Fe and DFB/Ctl treatments within the diatom genera *Pseudo-nitzschia* (P) and *Thalassiosira* (T) **(A)**. Heatmap represents

(Continued)

FIGURE 5 | Continued
the $\log_2$ fold change of gene expression within the Fe addition treatment relative to the DFB treatment at each site. For site O5, the T_2 control (Ctl) treatment is used as the Fe-limited comparison. Gray boxes indicate transcripts were not detected in either treatment. White boxes signify no change in expression between treatments. A schematic representation of select N, C, Fe, metal transport, and vitamin-related processes within a diatom cell, color-coded by genes of interest included in **(A)** is provided **(B)**. Adjacent proteins with black borders indicate similar cellular functions (e.g., *FLDA, PETF*). Gene abbreviations are NRT2, nitrate transporter; AMT, ammonium transporter; URTA, urea transporter; NR, nitrate reductase; NIRA, ferredoxin-nitrite reductase; NIRB, nitrite reductase; NIT-6, nitrite reductase; GLT, glutamate synthase; Fd-GLT, ferredoxin-glutamate synthase; α-CA, carbonic anhydrase (α family); SLC4A, solute carrier family (bicarbonate transporters); ICTB, putative bicarbonate transporter; PEPC, phosphoenolpyruvate carboxylase; RBCL, RubisCO large subunit; RBCS, RubisCO small subunit; PGK, phosphoglycerate kinase; TPI, triseophosphate isomerase; GAPDH, glyceraldehyde 3-phosphate dehydrogenase; FBP, fructose-1,2-bisphosphatase I; TKL, transketolase; RPE, ribulose-phosphate 3-epimerase; PRK, phosphoribulokinase; FBA class I, fructose bisphosphate aldolase (class I); FBA class II, fructose bisphosphate aldolase (classII); FTR, high affinity iron permease; ABC.FEV.S: iron complex transport system substrate-binding protein; ZIP7, zinc transporter 7; CNNM, metal transporter; ISIP2A, iron starvation induced protein 2A; ISIP1, iron starvation induced protein 1; ISIP2B, iron starvation induced protein 2B; ISIP3, iron starvation induced protein 3; FTN, ferritin; FLDA, flavodoxin I; PETF: ferredoxin; PETH, ferredoxin-NADP+ reductase; PETE, plastocyanin; PETJ, cytochrome c_6; PETC, cytochrome b_6f complex; Cu-Zn SOD, superoxide dismutase containing Cu and Zn as cofactors; Fe-Mn SOD, superoxide dismutase containing Fe or Mn as cofactor; Fd-SIR, ferredoxin-sulfite reductase; RHO, rhodopsin (note the localization of RHO within the vacuole membrane is speculative); BIOB, biotin synthase; PDXK, pyridoxal kinase; PLDH, pyridoxal 4-dehydrogenase; THIC, phosphomethylpyrimidine synthase.

all sites and in both genera, except O5, where it was slightly more abundant in the Fe-limited control treatment (**Figure 5**). By contrast, transcripts for plastocyanin (*PETE*) displayed inconsistent expression trends in response to Fe status across sites, being relatively more abundant following Fe enrichment in both genera at C3 (1.4-fold in *Pseudo-nitzschia*; 1.9-fold in *Thalassiosira*, $p = 5 \times 10^{-4}$) and at the initially Fe-limited oceanic site, O5 (1.4-fold in *Thalassiosira*; **Figure 5**). At all other locations *PETE* transcripts were either more abundant under DFB conditions or not detected.

Transcripts for the proton-pumping protein rhodopsin (*RHO*) furthermore demonstrated differences in expression patterns among genera. This protein can supplement Fe-intensive photosynthesis in the light-driven production of membrane proton gradients and ATP in some diatoms (Marchetti et al., 2015). Rhodopsin was not detected in *Thalassiosira* at any location while its expression increased in *Pseudo-nitzschia* by >2-fold in the DFB/Ctl treatments relative to the Fe treatment at the two lowest dFe sites [C3 ($p = 0.01$) and O5; **Figure 5**; Supplementary Table 1]. At the other sites *RHO* expression was constitutive. These rhodopsin contigs were structurally similar to diatom rhodopsins identified within the MMETSP database (≥55% similarity; Supplementary Figure 4B).

Relationships among Fe-related transcript abundance, experimental site and treatment were determined using Principal Components Analysis (PCA) individually for each diatom genus. Principle components P1 and P2 explained 54% of the variation in transcript abundance in *Pseudo-nitzschia* and 76% in *Thalassiosira* (**Figure 6C**). In *Pseudo-nitzschia*, transcripts for the photosynthetic genes ferredoxin-NADP+ reductase (*PETH*), *PETJ*, a cytochrome b_6/f complex protein (*PETC*), *FTN*, and *Cu-Zn SOD* were in higher relative abundance within Fe addition treatments while *RHO*, *ISIPs*, *FLDA*, *PETE,* and *FTR* were generally more abundant in the Ctl and/or DFB treatments, as the principle component P1 separated these samples based on Fe treatment. In *Thalassiosira*, a similar response was observed, although *RHO* was not detected, and *PETF,* which was sporadically found and not abundant in *Pseudo-nitzschia,* strongly co-varied with the other genes highly expressed in the treatments where Fe was added (**Figure 6C**).

Influence of Fe Availability on N Metabolism

Genes involved in N transport and metabolism were investigated to assess the influence of varying Fe status on N assimilation. Transcripts for genes encoding nitrate (*NRT2*) and ammonium (*AMT*) transporters were detected at all locations, with *NRT2* increasing in expression by >2-fold in response to Fe addition relative to the DFB/Ctl treatment at the majority of sites in both taxa, while *AMT* expression varied depending on site (**Figure 5**). For instance, C4 was the only location with a >2-fold increase in *AMT* expression in the DFB treatment in both *Pseudo-nitzschia* and *Thalassiosira*. Transcripts corresponding to genes encoding components of NO_3^- assimilation, including nitrate (*NR*) and nitrite reductases (*NIRA, NIRB, NIT-6*) were generally more abundant in the treatments with added Fe, although *NIRA* and *NIRB* displayed opposite expression patterns in *Pseudo-nitzschia* and *Thalassiosira* at site C3 (**Figure 5**). Furthermore *Pseudo-nitzschia* increased gene expression of one group of nitrite reductases [*NIRB* and *NIT-6*, which use NADPH as the reductant (Brown et al., 2009)] by 11- and 3.6-fold, respectively, following added Fe while *Thalassiosira* conversely increased *NIRB* expression by 3.7-fold in the DFB treatment (**Figure 5**). In addition, *Thalassiosira* increased gene expression of another form of nitrite reductase (*NIRA*, which uses ferredoxin/flavodoxin as reductant; Brown et al., 2009) by 8-fold ($p = 3 \times 10^{-22}$) following Fe enrichment while *Pseudo-nitzschia* constitutively expressed *NIRA* at this location. Noticeably, transcripts for the genes encoding *NIRB* and *NIT-6* were present in at least one of the two diatom taxa examined at all sites except the oceanic site, O5.

The relationships among transcript abundance for N uptake and assimilation-related genes, experimental sites, treatments and PN-specific VNO_3 measurements within the >5 μm size fraction of the phytoplankton community were examined via PCA bi-plots. Principle components P1 and P2 explained 86% of the variation in N-related transcript abundance in *Pseudo-nitzschia* and 88% in *Thalassiosira* (**Figure 6A**). Sites generally contained high transcript abundances of *NRT2* and *NR* in the added Fe treatment, with the two genes strongly co-varying with one another in both *Pseudo-nitzschia* and *Thalassiosira.* Furthermore, the Fe addition treatments at two

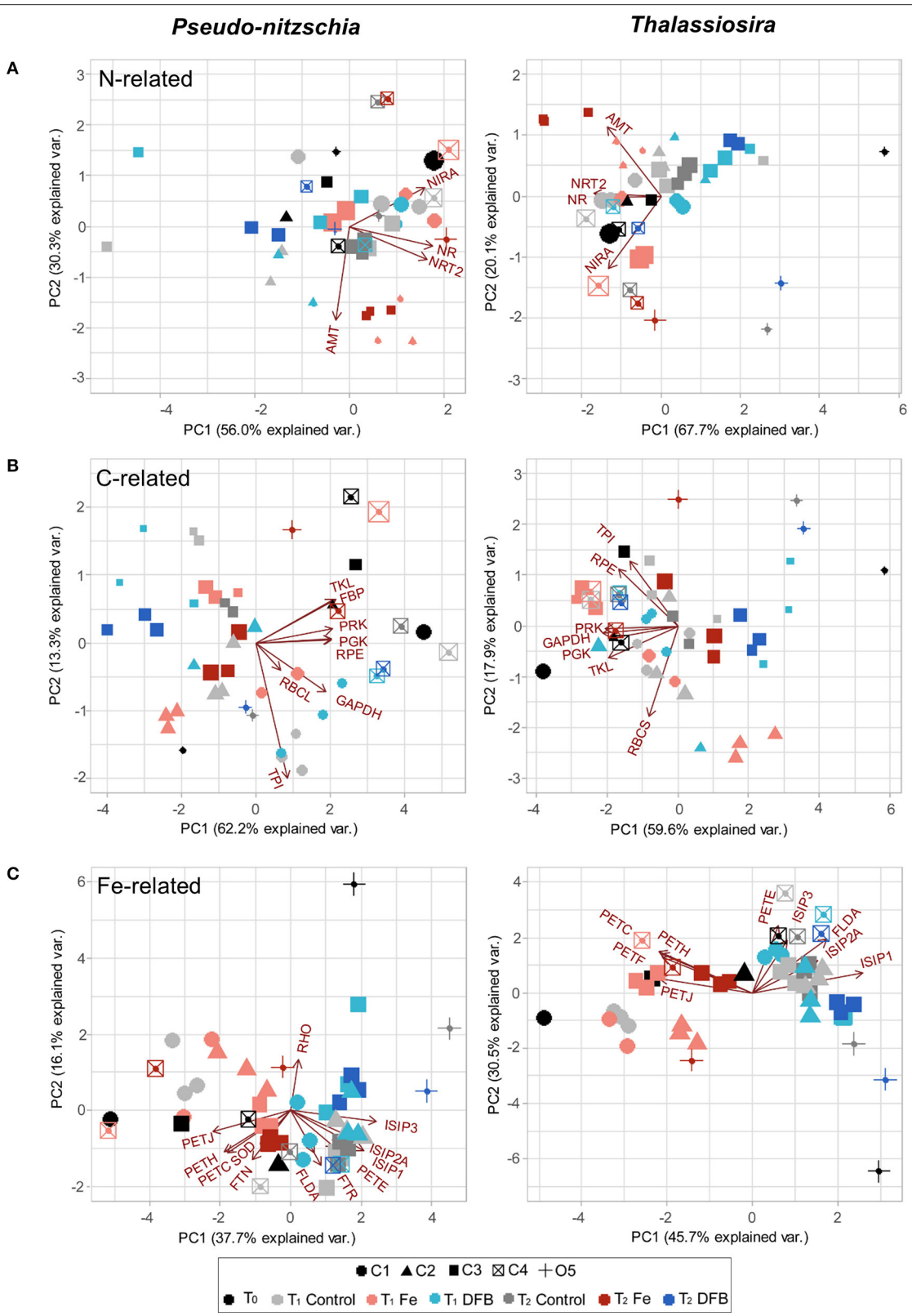

FIGURE 6 | PCA bi-plots depicting the relationship between treatment (color), site (shape), and biomass-normalized N and C rates for transcript abundances of genes involved in N, C, and Fe-related processes in *Pseudo-nitzschia* (left) and *Thalassiosira* (right). Size of points scales with increasing PN-specific VNO_3 (day^{-1}) from 0.04 to 1.63 day^{-1} **(A)**, and with increasing PC-specific *V*DIC (day^{-1}) from 0.01 to 1.50 day^{-1} **(B).** For the Fe-related genes transcript abundance PCA bi-plot, sizes remain constant across samples **(C)**. See **Figure 5** for the list of gene abbreviations.

sites that experienced NO_3^- depletion following incubation, C2 and C3, clustered together and contained the highest *AMT* transcript abundance at T_1 and T_2, respectively. Phytoplankton communities within these incubation treatments concomitantly displayed low PN-specific VNO_3 (0.03–0.13 day^{-1}; **Figure 6A**). The highest PN-specific VNO_3 were observed in the added Fe treatment at site C4 at T_1 and at C1 within the initial (T_0) phytoplankton community (1.4 day^{-1}), which coincided with high abundances of *NIRA* transcripts in both genera at these locations.

Influence of Fe Availability on C Metabolism

To further gain insight into how variable Fe status influences macronutrient resource utilization and regional biogeochemistry, genes involved in C transport and fixation were examined among sites and between diatom genera. Transcripts corresponding to a carbonic anhydrase belonging to the α-family (*α-CA*), involved in the carbon concentrating mechanism (CCM) within photosynthetic eukaryotes (Reinfelder, 2011), were either constitutively expressed, not detected, or more highly expressed in the DFB treatment at all locations apart from C1, where expression was 7-fold higher following Fe addition in *Thalassiosira* (**Figure 5**).

Members of the solute carrier (SLC) family of bicarbonate transporters (*SLC4A-1*, *-2*, and *-4*), which import bicarbonate ions from the environment also thought to be involved in the CCM (Nakajima et al., 2013), were detected intermittently among sites, though in low transcript abundance (**Figure 5**). These genes share sequence homology with the *P. tricornutum* genes *PtSLC4-1*, *-2,* and *-4* (BLASTP; $E < 2 \times 10^{-69}$) and displayed inconsistent patterns of gene expression with each another, with no clear relationship to carbon assimilation rates. Another putative bicarbonate transporter (*ICTB*) was detected intermittently across sites and solely in *Pseudo-nitzschia*, where it was notably more highly expressed by 128-fold following Fe addition at O5. Conversely in *Thalassiosira*, the gene encoding phosphoenolpyruvate carboxylase (*PEPC*), which is part of a C_4-CCM in some species of this genus (Reinfelder, 2011), was more highly expressed by 73-fold following Fe addition at O5.

Gene expression of RubisCO (*RBCL*) was higher by >24-fold in the Fe-limited control treatment in both genera at site O5 while at other sites the gene was either constitutively expressed, increased expression in the added Fe treatment, or not detected (**Figure 5**). In addition, other genes involved in the Calvin Cycle, including phosphoglycerate kinase (*PGK*), transketolase (*TKL*), ribulose-phosphate 3-epimerase (*RPE*), and phosphoribulokinase (*PRK*), generally increased in expression following Fe addition compared to the DFB/Ctl treatment at one or more of the three sites experiencing some degree of Fe limitation (C3, C4, and O5; Supplementary Table 1; **Figure 5**). At the CUZ sites C1 and C2, transcripts for these genes were either not differentially expressed or were more abundant in the DFB treatment within both diatom genera. Fructose-bisphosphate aldolases (FBA), involved in the Calvin Cycle, glycolysis, and gluconeogenesis, demonstrated strong Fe-dependent transcriptional patterns regardless of site and taxa (**Figure 5**). Transcripts corresponding to class II FBA, likely a metal-dependent aldolase, increased by 1.5 to 69-fold in the added Fe treatment as compared to DFB treatments with the largest fold change attributed to *Pseudo-nitzschia* from O5. Class II FBA has been previously demonstrated to be abundant under high-Fe conditions in diatoms and is hypothesized to contain Fe^{2+} as a metal cofactor (Horecker et al., 1972; Allen et al., 2012; Lommer et al., 2012). Transcripts corresponding to class I FBA, the metal-independent version of class II FBA, conversely increased by 1.3 to 16-fold in DFB compared to Fe treatments.

The relationships in transcript abundance among C fixation-related genes, experimental sites, incubated treatments and PC-specific *V*DIC measurements were assessed using PCA bi-plots. Principle components P1 and P2 together explained 80% of the variation in C-related transcript abundance in *Pseudo-nitzschia* and 78% in *Thalassiosira* (**Figure 6B**). Site C4 contained some of the highest PC-specific *V*DIC measurements within the >5 μm size fraction (0.65–1.6 day^{-1}), and coincided with the highest transcript abundances of *PGK*, *PRK*, *FBP*, *TKL*, *RPE*, and *GAPDH* in *Pseudo-nitzschia* (**Figure 6B**). Conversely, Fe-limited treatments from C3 and O5 had the lowest transcript abundances of these genes in both *Pseudo-nitzschia* and *Thalassiosira*, with principle component P1 separating these samples from other sites and treatments (**Figure 6C**). Fe-limited sites C3 and O5 phytoplankton communities additionally displayed some of the lowest PC-specific *V*DIC observed (0.11–0.17 day^{-1}).

DISCUSSION

Prior to this study, our understanding of the strategies utilized by phytoplankton to cope with low Fe bioavailability and resupply across different coastal and oceanic regions was limited. Furthermore, whether diverse diatom genera from identical environments would respond similarly when exposed to changes in Fe availability was unresolved. The gene expression patterns presented here demonstrate that the cosmopolitan diatom genera *Pseudo-nitzschia* and *Thalassiosira* rely on diverse sets of strategies to handle Fe stress, and that oceanic diatoms from both groups are highly responsive to changes in Fe availability with a greater degree of differentially expressed genes involved in nitrate assimilation, carbon fixation, and vitamin production compared to their coastal counterparts.

Iron-Related Gene Expression Responses across Sites

Differences in gene expression patterns in response to Fe status were observed between the coastal (C1-C4) and oceanic sites (O5) examined in this study. This included the >16-fold higher expression of genes in the added Fe treatment relative to the Fe-limited control encoding proteins involved in B_7 synthesis (*BIOB*) in both taxa, and B_1 (*THIC*) and B_6 (*PDXK, PDLH*) synthesis in *Pseudo-nitzschia*. These increases are consistent with previous field observations demonstrating that Fe enrichment of previously Fe-limited oceanic diatom communities stimulates B-vitamin transcript production (Cohen et al., 2017). Genes encoding an Fe storage protein (ferritin [*FTN*]) and components of amino acid metabolism (glutamate

synthase [*GLT*] in *Pseudo-nitzschia*; ferredoxin-dependent glutamate synthase [*Fd-GLT*] in *Thalassiosira*) were similarly more highly expressed by >16-fold following Fe addition exclusively at site O5. Conversely, in the Fe-limited control, we observed the >16-fold higher expression of genes encoding the proteins Cu-Zn superoxide dismutase (Cu-*Zn SOD*) and RubisCO (*RBCL*), in either one or both taxa investigated. These distinct transcriptomic patterns of genes involved in diverse metabolic processes reflect differences in environmental factors selecting for diatom growth between the chronically Fe-limited open ocean and sporadically Fe-limited coastal regions.

In contrast, many photosynthetic genes were highly expressed following Fe addition regardless of location. A subset of these genes displayed distinct expression responses depending on whether the incubated communities experienced Fe limitation of growth rate (e.g., C3 and O5) or only Fe stress (C4; Supplementary Table 1). One such gene encodes the putative Fe transporter *ABC.FEV.S*, in which expression increased following Fe addition in *Pseudo-nitzschia* only at sites C3, C4, and O5. Additional genes include flavodoxin *(FLDA)* and plastocyanin *(PETE),* in which transcripts were generally more abundant in the DFB or Fe-limited Ctl treatments, consistent with flavodoxin's role as an Fe-independent photosynthetic electron carrier and plastocyanin's role as a Cu-dependent replacement for Fe-dependent cytochrome c_6. At the Fe-stressed CUZ site C3 however, *FLDA* was either constitutively expressed or slightly more abundant after Fe addition, depending on the diatom genus. Plastocyanin (*PETE)* transcripts were similarly more abundant after Fe addition in both diatom genera at C3 and in *Thalassiosira* at O5. This pattern suggests coastal diatoms from higher-Fe systems tend to temporarily replace Fe-dependent photosynthetic proteins with Fe-independent ones, while certain diatoms in chronically Fe-limited environments may rely exclusively on the Fe-free alternatives (Marchetti et al., 2012).

Fe-Related Gene Expression Responses Between Diatom Taxa

Pseudo-nitzschia and *Thalassiosira* demonstrated several distinct responses to changes in Fe status despite co-existing under identical environmental conditions. Ferredoxin (*PETF*), ferredoxin-dependent glutamate synthase (*Fd-GLT*), and ferredoxin-dependent sulfite reductase (*Fd-SIR*) transcripts were more abundant in *Thalassiosira* at oceanic site O5 following Fe addition with these responses absent in *Pseudo-nitzschia*. In contrast, ferredoxin-related transcripts in oceanic *Pseudo-nitzschia* were constitutively expressed or not detected. These patterns may suggest oceanic *Thalassiosira* strongly utilizes ferredoxin and ferredoxin-dependent proteins following Fe addition while *Pseudo-nitzchia* relies on Fe-independent machinery. Site O5 was additionally the only location in which *Thalassiosira* increased gene expression of *Cu-Zn SOD* under Fe-limitation. This pattern was not evident in oceanic *Pseudo-nitzschia,* where gene expression of this protein was constitutive, or by either genus at coastal sites, suggesting that the oceanic *Thalassiosira* species have distinctly evolved to rely on this Cu- and Zn-containing enzyme as the preferred superoxide dismutase in their Fe-limited environment. *Pseudo-nitzschia* conversely increased expression of *Mn SOD* following Fe addition, likely as a result of iron-induced increases in photosynthetic rates and photosynthetic production of superoxide radicals (Asada, 2006). These patterns highlight differences in preferred metal cofactors as a function of Fe status and transcriptional tendencies between the two taxa.

Transcripts corresponding to rhodopsin (*RHO)* increased in abundance within *Pseudo-nitzschia* in the DFB/Ctl treatments at the two sites experiencing pronounced Fe limitation (C3 and O5), but were not identified in *Thalassiosira* at any location. This is consistent with rhodopsin being undetected in sequenced *Thalassiosira* spp. transcriptomes (Marchetti et al., 2015) and supports the notion that *Pseudo-nitzschia* may have a competitive advantage over non-rhodopsin containing taxa, allowing for an Fe-independent alternative to photosynthesis for ATP generation during times of Fe stress. Ferritin (*FTN)* gene expression patterns furthermore diverged between the two taxa at the coastal sites C4 (Line-P) and C2 (CUZ). This supports laboratory findings suggesting *FTN* may exhibit different expression patterns among diverse phytoplankton (Marchetti et al., 2009; Botebol et al., 2015), even between taxa residing in the same location. Lastly, *ABC.FEV.S*, encoding a membrane Fe transport system protein, displayed divergent expression patterns between the examined genera with only *Pseudo-nitzschia* increasing *ABC.FEV.S* expression after Fe addition in all incubations exhibiting signs of iron limitation (C3, C4, and O5).

Taken together, these patterns in gene expression demonstrate that members of the pennate diatom genus *Pseudo-nitzschia* and the centric diatom genus *Thalassiosira* restructure their functional metabolisms in response to changes in Fe availability in distinct manners, possibly allowing both species to co-exist in the same environment. Both taxa are equipped with strategies to sustain growth under chronic Fe limitation in the open ocean, as supported by their equal transcript abundance during initial sampling. Following pulse Fe additions however, oceanic *Pseudo-nitzschia* relies in part on the strategies discussed above to gain a competitive advantage over *Thalassiosira* and quickly dominates the phytoplankton community. It remains unclear however which combination of environmental factors in the NE Pacific Ocean would select for the preferential growth of *Thalassiosira* over *Pseudo-nitzschia.* We conclude that substantial differences in molecular responses to changes in Fe status are observed across taxonomic groups, and patterns in gene expression should not be assumed universal across diverse taxa or environments.

Nitrogen-Related Gene Expression as a Function of Fe Status

The majority of N transport and assimilation genes investigated increased in expression following Fe addition in both *Pseudo-nitzschia* and *Thalassiosira*. Several site- and taxa-specific patterns were identified, with some trends also possibly explained by each site's initial NO_3^- concentration. For example, most gene copies encoding the NO_3^- transporter, *NRT2,* have been demonstrated in laboratory cultures to increase in expression in NO_3-stressed diatoms (Bender et al., 2014; Rogato et al., 2015), and transcripts corresponding to this gene were some of

the most abundant in both *Pseudo-nitzschia* and *Thalassiosira* at C2—the CUZ site where NO_3^- concentrations were depleted in all incubations by the first sampling time point. This gene also showed expression trends that correlated with Fe status; *NRT2* transcripts were more abundant after Fe addition at all locations, regardless of initial NO_3^- concentrations. Based on these observations, *NRT2* in diatoms also appears to be linked to Fe status and follows the expression of other N-related genes involved in Fe-dependent NO_3^- assimilation, including those encoding nitrate reductase (*NR)* and nitrite reductase (*NIRA*; Marchetti et al., 2012).

Diatoms were perhaps relying on NH_4 in place of NO_3^- as a source of N based on gene expression patterns at several CUZ sites. Fe-enriched treatments at C2 contained the lowest NO_3^- after 48 h of incubation (0.06 μmol L^{-1}), and the genes encoding the ammonium transporters *AMTs* concomitantly increased in expression in the Fe relative to DFB treatment (**Figure 6**). Furthermore at C3, Fe-enriched communities entered NO_3^- stress by the end of the incubation period, and *AMT* expression simultaneously increased in both *Pseudo-nitzschia* and *Thalassiosira*. This negative relationship between NO_3^- concentrations and *AMT* transcript abundance in natural diatom assemblages is consistent with those in laboratory *Pseudo-nitzschia multiseries* and *Fragilariopsis cylindrus* cultures (Bender et al., 2014; Rogato et al., 2015), and is reported here as one of the first observations of this relationship in natural phytoplankton communities.

High *AMT* transcript abundance at some of these locations may also represent NH_4 rather than NO_3^- being preferred as an N source by Fe-stressed diatoms conserving their cellular Fe supply, as NO_3^- assimilation depends on various Fe-dependent processes (Milligan and Harrison, 2000). This is supported by the increased expression of *AMT* transcripts in both *Pseudo-nitzschia* and *Thalassiosira* from the Fe-stressed coastal Line-P incubations at C4. *Pseudo-nitzschia* from the Fe-limited site O5 also exhibited this pattern whereas *Pseudo-nitzschia* from C3 and *Thalassiosira* from both C3 and O5 did not, suggesting other environmental parameters aside from Fe status are influencing whether diatoms utilize NH_4- or NO_3-specific N uptake pathways.

Similar to our Fe-related gene expression results, several N-related genes demonstrated divergent expression responses between *Pseudo-nitzschia* and *Thalassiosira.* Expression of the NO_2^- reductase genes, *NIRA* and *NIRB*, displayed opposite patterns between the two genera at the CUZ site where Fe-stress occurred in incubations (C3), with *Pseudo-nitzschia* highly expressing the gene encoding non-ferredoxin-utilizing NO_2^- reductase (*NIRB*) following Fe addition, and *Thalassiosira* highly expressing the gene encoding the ferredoxin-utilizing nitrite reductase (*NIRA*). Furthermore at site O5, *Pseudo-nitzschia* increased expression of *AMT* and NADPH-dependent glutamate synthase (*GLT*) following Fe addition while *Thalassiosira* increased expression of *NRT2* and ferredoxin-dependent glutamate synthase (*Fd-GLT*). These transcriptomic patterns may suggest *Pseudo-nitzschia* continues to rely on the non-Fe requiring metabolic pathways for assimilating N once Fe becomes available (*AMT, NIRB*, *GLT*), whereas *Thalassiosira* shifts over to Fe-dependent ones (*NRT2, NIRA, Fd-GLT*) upon Fe resupply.

These expression patterns furthermore support that substantial variations exist between the two diatom taxa in terms of N acquisition and assimilation strategies following changes in Fe supply. Both *Pseudo-nitzschia* and *Thalassiosira* are equipped with distinct strategies to compete under a variety of Fe and N conditions, and this may contribute to how multiple diatom species relying upon the same limiting resources in identical environments co-exist (i.e., paradox of the plankton; Hutchinson, 1961). These patterns are consistent with previous reports of resource partitioning among diatoms based on N and phosphate utilization (Alexander et al., 2015). Varying environmental pressure likely maintain populations of diverse diatom genera in the open ocean, with certain species outcompeting others depending on specific sets of external factors, including both macro- and micronutrients (Godhe and Rynearson, 2017).

Carbon-Related Gene Expression Responses as a Function of Fe Status

Genes encoding proteins involved in C uptake and assimilation were surveyed in order to determine the influence of Fe addition or stress on C metabolism. We observed site-specific expression patterns of the diatom RubisCO large subunit protein (*RBCL),* where gene expression was substantially elevated at site O5 in the Fe-limited control treatment relative to the Fe addition response in both diatom genera. A sequence analysis of RubisCO contigs obtained across experimental sites demonstrates that O5 protein sequences are structurally less similar to known *Pseudo-nitzschia* and *Thalassiosira* RubisCO protein sequences within the MMETSP database than those at the four coastal sites (Supplementary Figure 4A; Supplementary Table 3). This distinction in both protein structure and transcriptional expression may indicate a distinct adaptation and utilization of RubisCO in the oceanic diatoms than in those from high-Fe coastal waters. Phylogenetically diverse diatom species have been demonstrated to vary in their RubisCO enzyme kinetics in laboratory cultures, with their RubisCO content inversely linked to the strength of their carbon concentrating mechanism (CCM; Young et al., 2016). The CCM increases CO_2 concentrations in chloroplast stroma in the vicinity of RubisCO and is fueled by the energy (ATP) generated from the Fe-intensive process of photosynthesis (Reinfelder, 2011; Young et al., 2016). We hypothesize that chronically Fe-limited oceanic diatoms are ATP-limited by the scarcity of Fe needed to support photosynthesis, and instead increase their RubisCO protein content to maintain high rates of carbon fixation rather than allocate scarce energy resources to the CCM. Furthermore, the genes encoding a putative bicarbonate transporter (*ICBT*) and a C_4-CCM component (*PEPC;* Reinfelder et al., 2000; Sage, 2004; Reinfelder, 2011) were highly expressed following Fe addition in *Pseudo-nitzschia* and *Thalassiosira*, respectively, exclusively at O5. This supports that diatoms may be capable of shuffling energy pools into either the CCM or RubisCO production depending on Fe bioavailability. Interestingly, in

laboratory-based proteomic analyses with cultures of the coastal diatom *T. pseudonana*, RubisCO was similarly more highly expressed under Fe limitation, while PEPC protein levels were higher under Fe-replete conditions (Nunn et al., 2013). Consistent with our hypothesis, Hopkinson et al. (2010) attributed increases in biomass following CO_2-enrichment of an Fe-limited phytoplankton community in the HNLC Northeast Pacific Ocean to downregulation of the CCM in order to conserve iron and photosynthetically-produced energy. Laboratory-based RubisCO kinetic work with cultured diatom isolates is needed to confirm whether diatoms from HNLC regions minimize their photosynthetic demand for Fe by synthesizing more RubisCO enzymes rather than allocating scarce energy resources into the CCM.

Other C fixation-related gene expression patterns were largely consistent with C assimilation rates, and generally varied as a function of both Fe status and ocean province. The genes *PGK*, *TKL*, *RPE*, and *PRK* did not exhibit site-specific expression patterns similar to *RBCL*, and instead increased in expression following Fe enrichment at sites where Fe addition increased C assimilation rates (C3, C4, and O5). Increased expression of these genes is expected with Fe stimulation of C-fixation and growth. These expression patterns are in agreement with laboratory cultures of the diatom *P. tricornutum*, which increased expression of genes involved in C fixation during the light portion of their diel cycle, when DIC is being taken up to support photosynthesis (Chauton et al., 2013).

CONCLUSION

Gene expression characterization coupled with biological rate processes across geographically diverse communities suggests regional and taxa-specific strategies are utilized by diatoms when rapidly responding to variations in environment. Our analysis demonstrates that chronically Fe-limited oceanic diatoms will restructure Fe, N, and C metabolism in a distinctive manner following Fe addition when compared to the response of coastal diatom communities that receive inherently more variable Fe inputs. *Pseudo-nitzschia* and *Thalassiosira*, two cosmopolitan diatom taxa found at all locations investigated, at times demonstrated divergent transcriptomic responses to changes in Fe status in terms of photosynthetic processes and N metabolism, even under identical environmental conditions.

Potential limitations to our approach include gene expression analyses being conducted on specific diatom genera while the physiological rate process measurements correspond to bulk phytoplankton communities. We therefore assumed the physiological characteristics to be representative of all phytoplankton members present. Furthermore, the metatranscriptomic approach used here consisted of analyzing cumulative expression responses of pooled gene copies; however, distinct gene copies have been shown to vary in their transcriptional response to environmental conditions within a single organism (Bender et al., 2014; Levitan et al., 2015; Rogato et al., 2015). In order to gain further resolution, we recommend laboratory-based studies be performed investigating the direct relationships between nutrient uptake rates and expression of specific gene copies encoding proteins involved in nutrient assimilation in distinct members from each of the genera *Pseudo-nitzschia* and *Thalassiosira*.

The findings presented here support the notion that a tremendous degree of genetic diversity is contained within the diatom lineage, and this may strongly influence the abundance and distribution of phytoplankton communities. Since Fe bioavailability to phytoplankton is predicted to change with increasing temperature and acidification of surface seawater (Shi et al., 2010; Sunda, 2010; Capone and Hutchins, 2013; Hutchins and Boyd, 2016), these findings will aid in predicting the consequences of changing ocean conditions on phytoplankton productivity and community growth dynamics.

AUTHOR CONTRIBUTIONS

AM, BT, and KB designed the study; NC, KE, BT, and AM performed the incubation experiments; NC conducted the metatranscriptomic and physiological analysis; RL provided bioinformatic support; FK and KT obtained photophysiological measurements onboard the *R/V Melville*; MB and HM quantified biogenic silica; MM provided primary productivity measurements; CT and BT quantified trace metals; WS contributed to iron metabolism interpretations; SB quantified domoic acid; NC and AM wrote the manuscript. All authors contributed to intellectual content and approved the final manuscript.

FUNDING

Research was funded through National Science Foundation grants OCE-1334935 to AM, OCE-1334632 to BT, OCE-1334387 to MB, OCE-1333929 to KT, and OCE-1259776 to KB, as well as through Discovery NSERC grant 261521-13 to MM.

ACKNOWLEDGMENTS

We thank J. Roach (UNC), S. Haines (UNC), W. Gong (UNC), M. Kanke (UNC), S. Davies (UNC), and M. Love (UNC) for sequencing analysis advice and guidance. P. Morton (FSU) analyzed the dissolved Fe samples from the Line P cruise (C4 and O5). Dissolved nutrients were analyzed by T. Coale (SIO) onboard the *R/V Melville* (C1-C3), and by M. Belton (IOS) onboard the *CCGS J.P. Tully* (C4 & O5). Z. Li (Duke) provided climatological remote sensing images in **Figure 1**. We are grateful to the scientists and crew of the *CCGS J.P. Tully* (Line-P cruise 2015-09) and the *R/V Melville* (cruise 1405) for their support and assistance at sea. RNA-Seq data was processed using UNC's Research Computing clusters. Finally, we would like to thank Carolyn Duckham for her help collecting and processing samples for DIC uptake rates at stations C1–C3.

SUPPLEMENTARY MATERIAL

The Supplementary Material for this article can be found online at: https://www.frontiersin.org/articles/10.3389/fmars.2017.00360/full#supplementary-material

REFERENCES

Alexander, H., Jenkins, B. D., Rynearson, T. A., and Dyhrman, S. T. (2015). Metatranscriptome analyses indicate resource partitioning between diatoms in the field. *Proc. Natl. Acad. Sci. U.S.A.* 112, E2182–E2190. doi: 10.1073/pnas.1421993112

Allen, A. E., LaRoche, J., Maheswari, U., Lommer, M., Schauer, N., Lopez, P. J., et al. (2008). Whole-cell response of the pennate diatom *Phaeodactylum tricornutum* to iron starvation. *Proc. Natl. Acad. Sci. U.S.A.* 105, 10438–10443. doi: 10.1073/pnas.0711370105

Allen, A. E., Moustafa, A., Montsant, A., Eckert, A., Kroth, P. G., and Bowler, C. (2012). Evolution and functional diversification of fructose bisphosphate aldolase genes in photosynthetic marine diatoms. *Mol. Biol. Evol.* 29, 367–379. doi: 10.1093/molbev/msr223

Altschul, S. F., Gish, W., Miller, W., Myers, E. W., and Lipman, D. J. (1990). Basic local alignment search tool. *J. Mol. Biol.* 215, 403–410. doi: 10.1016/S0022-2836(05)80360-2

Armbrust, E. V. (2009). The life of diatoms in the world' s oceans. *Nature* 459, 185–192. doi: 10.1038/nature08057

Asada, K. (2006). Production and scavenging of reactive oxygen species in chloroplasts and their functions. *Plant Physiol.* 141, 391–396. doi: 10.1104/pp.106.082040

Barwell-Clarke, J., and Whitney, F. (1996). *Institute of Ocean Sciences Nutrient Methods and Analysis*. Canadian Technical Report of Hydrography and Ocean Sciences no. 182. Available online at: http://linep.waterproperties.ca/2012-13/documents/Barwell-Clarke_Whitney_1996.pdf

Behrenfeld, M. J., and Milligan, A. J. (2013). Photophysiological expressions of iron stress in phytoplankton. *Annu. Rev. Mar. Sci.* 5, 217–246. doi: 10.1146/annurev-marine-121211-172356.

Bender, S., Durkin, C., Berthiaume, C., Morales, R., and Armbrust, E. V. (2014). Transcriptional responses of three model diatoms to nitrate limitation of growth. *Front. Mar. Sci.* 1:3. doi: 10.3389/fmars.2014.00003

Biller, D. V., and Bruland, K. W. (2012). Analysis of Mn, Fe, Co, Ni, Cu, Zn, Cd, and Pb in seawater using the Nobias-chelate PA1 resin and magnetic sector inductively coupled plasma mass spectrometry (ICP-MS). *Mar. Chem.* 130–131, 12–20. doi: 10.1016/j.marchem.2011.12.001

Birol, I., Jackman, S. D., Nielsen, C. B., Qian, J. Q., Varhol, R., Stazyk, G., et al. (2009). *De novo* transcriptome assembly with ABySS. *Bioinformatics* 25, 2872–2877. doi: 10.1093/bioinformatics/btp367

Bolger, A. M., Lohse, M., and Usadel, B. (2014). Trimmomatic: a flexible trimmer for Illumina sequence data. *Bioinformatics* 30, 2114–2120. doi: 10.1093/bioinformatics/btu170

Botebol, H., Lesuisse, E., Sutak, R., Six, C., Lozano, J.-C., Schatt, P., et al. (2015). Central role for ferritin in the day/night regulation of iron homeostasis in marine phytoplankton. *Proc. Natl. Acad. Sci. U.S.A.* 112, 1–6. doi: 10.1073/pnas.1506074112

Boyd, P., and Harrison, P. J. (1999). Phytoplankton dynamics in the NE subarctic Pacific. *Deep-Sea Res. II* 46, 2405–2432. doi: 10.1016/S0967-0645(99)00069-7

Bowler, C., Allen, A. E., Badger, J. H., Grimwood, J., Jabbari, K., Kuo, A., et al. (2008). The Phaeodactylum genome reveals the evolutionary history of diatom genomes. *Nature* 456, 239–244. doi: 10.1038/nature07410

Brown, K. L., Twing, K. I., and Robertson, D. L. (2009). Unraveling the regulation of nitrogen assimilation in the marine diatom *Thalassiosira pseudonana* (Bacillariophyceae): diurnal variations in transcript levels for five genes involved in nitrogen assimilation. *J. Phycol.* 45, 413–426. doi: 10.1111/j.1529-8817.2009.00648.x

Bruland, K. W., Lohan, M. C., Aguilar-Islas, A. M., Smith, G. J., Sohst, B., and Baptista, A. (2008). Factors influencing the chemistry of the near-field Columbia River plume: Nitrate, silicic acid, dissolved Fe, and dissolved Mn. *J. Geophys. Res. Ocean.* 113:C00B02. doi: 10.1029/2007JC004702

Bruland, K. W., Rue, E. L., and Smith, G. J. (2001). Iron and macronutrients in California coastal upwelling regimes: implications for diatom blooms. *Limnol. Oceanogr.* 46, 1661–1674. doi: 10.4319/lo.2001.46.7.1661

Brzezinski, M. A. (1985). The Si:C:N ratio of marine diatoms: interspecific variability and the effect of some environmental variables. *J. Phycol.* 21, 347–357. doi: 10.1111/j.0022-3646.1985.00347.x

Brzezinski, M. A., Krause, J. W., Bundy, R. M., Barbeau, K. A., Franks, P., Goericke, R., et al. (2015). Enhanced silica ballasting from iron stress sustains carbon export in a frontal zone within the California Current. *J. Geophys. Res. Ocean.* 120, 4654–4669. doi: 10.1002/2015JC010829

Capone, D. G., and Hutchins, D. A. (2013). Microbial biogeochemistry of coastal upwelling regimes in a changing ocean. *Nat. Geosci.* 6, 711–717. doi: 10.1038/ngeo1916

Chase, Z., Hales, B., Cowles, T., Schwartz, R., and van Geen, A. (2005). Distribution and variability of iron input to Oregon coastal waters during the upwelling season. *J. Geophys. Res. C Ocean.* 110, 1–14. doi: 10.1029/2004JC002590

Chauton, M. S., Winge, P., Brembu, T., Vadstein, O., and Bones, A. M. (2013). Gene regulation of carbon fixation, storage, and utilization in the diatom phaeodactylum tricornutum acclimated to light/dark cycles. *Plant Physiol.* 161, 1034–1048. doi: 10.1104/pp.112.206177

Cohen, N. R., Ellis, K. A., Burns, W. G., Lampe, R. H., Schuback, N., Johnson, Z., et al. (2017). Iron and vitamin interactions in marine diatom isolates and natural assemblages of the Northeast Pacific Ocean. *Limnol. Oceanogr.* 62, 2076–2096. doi: 10.1002/lno.10552

Crowley, J. D., Traynor, D. A., and Weatherburn, D. C. (2000). Enzymes and proteins containing manganese: an overview. *Met. Ions Biol. Syst.* 37, 209–278.

de Baar, H. J. W., Boyd, P. W., Coale, K. H., Landry, M. R., Tsuda, A., Assmy, P., et al. (2005). Synthesis of iron fertilization experiments: from the iron age in the age of enlightenment. *J. Geophys. Res. C Ocean.* 110, 1–24. doi: 10.1029/2004JC002601

Edgar, R. C. (2004). MUSCLE: multiple sequence alignment with high accuracy and high throughput. *Nucleic Acids Res.* 32, 1792–1797. doi: 10.1093/nar/gkh340

Godhe, A., and Rynearson, T. (2017). The role of intraspecific variation in the ecological and evolutionary success of diatoms in changing environments. *Philos. Trans. R. Soc. B Biol. Sci.* 372:20160399. doi: 10.1098/rstb.2016.0399

Gorbunov, M. Y., and Falkowski, P. (2004). "Fluorescence Induction and Relaxation (FIRe) technique and instrumentation for monitoring photosynthetic processes and primary production in aquatic ecosystems," in *13th International Congress of Photosynthesis, Vol. 2*, eds A. van der Est and D. Bruce (Montreal, QC: Allen Press), 1029–1031.

Graff van Creveld, S., Rosenwasser, S., Levin, Y., and Vardi, A. (2016). Chronic iron limitation confers transient resistance to oxidative stress in marine diatoms. *Plant Physiol.* 172, 968–979. doi: 10.1104/pp.16.00840

Groussman, R. D., Parker, M. S., and Armbrust, E. V. (2015). Diversity and evolutionary history of iron metabolism genes in diatoms. *PLoS ONE* 10:e0129081. doi: 10.1371/journal.pone.0129081

Harris, S. L., Varela, D. E., Whitney, F. W., and Harrison, P. J. (2009). Nutrient and phytoplankton dynamics off the west coast of Vancouver Island during the 1997/98 ENSO event. *Deep Sea Res. Part II Top. Stud. Oceanogr.* 56, 2487–2502. doi: 10.1016/j.dsr2.2009.02.009

Harrison, P. J. (2002). Station papa time series: insights into ecosystem dynamics. *J. Oceanogr.* 58, 259–264. doi: 10.1023/A:1015857624562

Hildebrand, M. (2005). Cloning and functional characterization of ammonium transcporters fromt he marine diatom Cylindrotheca fusiformis (Bacillariophyceae). *J. Phycol.* 41, 105–113. doi: 10.1111/j.1529-8817.2005.04108.x

Hopkinson, B. M., Xu, Y., Shi, D., McGinn, P. J., and Morel, F. M. M. (2010). The effect of CO_2 on the photosynthetic physiology of phytoplankton in the Gulf of Alaska. *Limnol. Oceanogr.* 55, 2011–2024. doi: 10.4319/lo.2010.55.5.2011

Horecker, B. L., Tsolas, O., and Lai, C.-Y. (1972). "6 Aldolases," in *The Enzymes*, ed P. D. Boyer (San Diego, CA: Academic Press), 213–258.

Hutchins, D. A., and Boyd, P. W. (2016). Marine phytoplankton and the changing ocean iron cycle. *Nat. Clim. Change* 6, 1072–1079. doi: 10.1038/nclimate3147

Hutchins, D. A., and Bruland, K. W. (1998). Iron-limited diatom growth and Si:N uptake ratios in a coastal upwelling regime. *Nature* 393, 561–564. doi: 10.1038/31203

Hutchins, D. A., DiTullio, G. R., Zhang, Y., and Bruland, K. W. (1998). An iron limitation mosaic in the California upwelling regime. *Limnol. Oceanogr.* 43, 1037–1054. doi: 10.4319/lo.1998.43.6.1037

Hutchins, D. A., Hare, C. E., Weaver, R. S., Zhang, Y., Firme, G. F., DiTullio, G. R., et al. (2002). Phytoplankton iron limitation in the humboldt current and peru upwelling. *Limnol. Oceanogr.* 47, 997–1011. doi: 10.4319/lo.2002.47.4.0997

Hutchinson, G. E. (1961). The paradox of the plankton. *Am. Nat.* 95, 137–145.

Johnson, K. S., Chavez, F. P., and Friederich, G. E. (1999). Continental-shelf sediment as a primary source of iron for coastal phytoplankton. *Nature* 398, 697–700. doi: 10.1038/19511

Keeling, P. J., Burki, F., Wilcox, H. M., Allam, B., Allen, E. E., Amaral-Zettler, L. A., et al. (2014). The Marine Microbial Eukaryote Transcriptome Sequencing Project (MMETSP): illuminating the functional diversity of eukaryotic life in the oceans through transcriptome sequencing. *PLoS Biol.* 12:e1001889. doi: 10.1371/journal.pbio.1001889

King, A. L., and Barbeau, K. (2007). Evidence for phytoplankton iron limitation in the southern California Current System. *Mar. Ecol. Prog. Ser.* 342, 91–103. doi: 10.3354/meps342091

Klingenberg, H., and Meinicke, P. (2017). How to normalize metatranscriptomic count data for differential expression analysis. *bioRxiv*. doi: 10.1101/134650

Kolber, Z. S., Prášil, O., and Falkowski, P. G. (1998). Measurements of variable chlorophyll fluorescence using fast repetition rate techniques: defining methodology and experimental protocols. *Biochim. Biophys. Acta* 1367, 88–106. doi: 10.1016/S0005-2728(98)00135-2

Krause, J. W., Brzezinski, M. A., Villareal, T. A., and Wilson, C. (2013). Biogenic silica cycling during summer phytoplankton blooms in the North Pacific subtropical gyre. *Deep Sea Res. Part I Oceanogr. Res. Pap.* 71, 49–60. doi: 10.1016/j.dsr.2012.09.002

Kustka, A. B., Allen, A. E., and Morel, F. M. M. (2007). Sequence analysis and transcriptional regulation of iron acquisition genes in two marine diatoms. *J. Phycol.* 43, 715–729. doi: 10.1111/j.1529-8817.2007.00359.x

La Roche, J., Boyd, P. W., McKay, R. M. L., and Geider, R. J. (1996). Flavodoxin as an *in situ* marker for iron stress in phytoplankton. *Nature* 382, 802–805. doi: 10.1038/382802a0

Lam, P. J., and Bishop, J. K. B. (2008). The continental margin is a key source of iron to the HNLC North Pacific Ocean. *Geophys. Res. Lett.* 35, 1–5. doi: 10.1029/2008GL033294

Lam, P. J., Bishop, J. K. B., Henning, C. C., Marcus, M. A., Waychunas, G. A., and Fung, I. Y. (2006). Wintertime phytoplankton bloom in the subarctic Pacific supported by continental margin iron. *Global Biogeochem. Cycles* 20, 1–12. doi: 10.1029/2005GB002557

Langmead, B., and Salzberg, S. L. (2012). Fast gapped-read alignment with Bowtie 2. *Nat. Methods* 9, 357–359. doi: 10.1038/nmeth.1923

Levitan, O., Dinamarca, J., Zelzion, E., Lun, D. S., Guerra, L. T., Kim, M. K., et al. (2015). Remodeling of intermediate metabolism in the diatom *Phaeodactylum tricornutum* under nitrogen stress. *Proc. Natl. Acad. Sci. U.S.A.* 112, 412–417. doi: 10.1073/pnas.1419818112

Li, H., Handsaker, B., Wysoker, A., Fennell, T., Ruan, J., Homer, N., et al. (2009). The sequence alignment/map format and SAMtools. *Bioinformatics* 25, 2078–2079. doi: 10.1093/bioinformatics/btp352

Lommer, M., Roy, A.-S., Schilhabel, M., Schreiber, S., Rosenstiel, P., and LaRoche, J. (2010). Recent transfer of an iron-regulated gene from the plastid to the nuclear genome in an oceanic diatom adapted to chronic iron limitation. *BMC Genomics* 11:718. doi: 10.1186/1471-2164-11-718

Lommer, M., Specht, M., Roy, A.-S., Kraemer, L., Andreson, R., Gutowska, M. A., et al. (2012). Genome and low-iron response of an oceanic diatom adapted to chronic iron limitation. *Genome Biol.* 13:R66. doi: 10.1186/gb-2012-13-7-r66

Maldonado, M. T., and Price, N. M. (2001). Reduction and transport of organically bound iron by *Thalassiosira oceanica* (Bacillariophyceae). *J. Phycol.* 37, 298–310. doi: 10.1046/j.1529-8817.2001.037002298.x

Malviya, S., Scalco, E., Audic, S., Vincent, F., Veluchamy, A., Poulain, J., et al. (2016). Insights into global diatom distribution and diversity in the world's ocean. *Proc. Natl. Acad. Sci. U.S.A.* 113, E1516–E1525. doi: 10.1073/pnas.1509523113

Marchetti, A., and Cassar, N. (2009). Diatom elemental and morphological changes in response to iron limitation: a brief review with potential paleoceanographic applications. *Geobiology* 7, 419–431. doi: 10.1111/j.1472-4669.2009.00207.x

Marchetti, A., Catlett, D., Hopkinson, B. M., Ellis, K., and Cassar, N. (2015). Marine diatom proteorhodopsins and their potential role in coping with low iron availability. *ISME J.* 9, 2745–2748. doi: 10.1038/ismej.2015.74

Marchetti, A., and Maldonado, M. T. (2016). "Iron," in *The Physiology of Microalgae*, eds M. A. Borowitzka, J. Beardall, and J. A. Raven (Cham: Springer International Publishing), 233–279.

Marchetti, A., Parker, M. S., Moccia, L. P., Lin, E. O., Arrieta, A. L., Ribalet, F., et al. (2009). Ferritin is used for iron storage in bloom-forming marine pennate diatoms. *Nature* 457, 467–470. doi: 10.1038/nature07539

Marchetti, A., Schruth, D. M., Durkin, C. A., Parker, M. S., Kodner, R. B., Berthiaume, C. T., et al. (2012). Comparative metatranscriptomics identifies molecular bases for the physiological responses of phytoplankton to varying iron availability. *Proc. Natl. Acad. Sci. U.S.A.* 109, E317–E325. doi: 10.1073/pnas.1118408109

Milligan, A. J., and Harrison, P. J. (2000). Effects of non-steady-state iron limitation on nitrogen assimilatory enzymes in the marine diatom *Thalassiosira weissflogii* (Bacillariophyceae). *J. Phycol.* 36, 78–86. doi: 10.1046/j.1529-8817.2000.99013.x

Milne, A., Landing, W., Bizimis, M., and Morton, P. (2010). Determination of Mn, Fe, Co, Ni, Cu, Zn, Cd and Pb in seawater using high resolution magnetic sector inductively coupled mass spectrometry (HR-ICP-MS). *Anal. Chim. Acta* 665, 200–207. doi: 10.1016/j.aca.2010.03.027

Moore, J. K., Doney, S. C., Glover, D. M., and Fung, I. Y. (2001). Iron cycling and nutrient-limitation patterns in surface waters of the World Ocean. *Deep. Res. II* 49, 463–507. doi: 10.1016/S0967-0645(01)00109-6

Moore, J. K., Doney, S. C., and Lindsay, K. (2004). Upper ocean ecosystem dynamics and iron cycling in a global three-dimensional model. *Global Biogeochem. Cycles* 18:GB4028. doi: 10.1029/2004GB002220

Morrissey, J., Sutak, R., Paz-Yepes, J., Tanaka, A., Moustafa, A., Veluchamy, A., et al. (2015). A novel protein, ubiquitous in marine phytoplankton, concentrates iron at the cell surface and facilitates uptake. *Curr. Biol.* 25, 364–371. doi: 10.1016/j.cub.2014.12.004

Nakajima, K., Tanaka, A., and Matsuda, Y. (2013). SLC4 family transporters in a marine diatom directly pump bicarbonate from seawater. *Proc. Natl. Acad. Sci. U.S.A.* 110, 1767–1772. doi: 10.1073/pnas.1216234110

Nelson, D. M., DeMaster, D. J., Dunbar, R. B., and Smith, W. O. (1996). Cycling of organic carbon and biogenic silica in the Southern Ocean: estimates of water-column and sedimentary fluxes on the Ross Sea continental shelf. *J. Geophys. Res.* 101, 18519. doi: 10.1029/96JC01573

Nuester, J., Vogt, S., and Twining, B. S. (2012). Localization of iron within centric diatoms of the genus Thalassiosira. *J. Phycol.* 48, 626–634. doi: 10.1111/j.1529-8817.2012.01165.x

Nunn, B. L., Faux, J. F., Hippmann, A. A., Maldonado, M. T., Harvey, H. R., Goodlett, D. R., et al. (2013). Diatom proteomics reveals unique acclimation strategies to mitigate Fe limitation. *PLoS ONE* 8:e75653. doi: 10.1371/journal.pone.0075653

Pan, Y., Subba Roa, D. V., Mann, K. H., Brown, R. G., and Pocklington, R. (1996). Effects of silicate limitation on production of domoic acid, a neurotoxin, by the diatom Pseudo- nitzschia m ultiseries. I. Batch culture studies. *Mar. Ecol. Prog. Ser.* 131, 225–233. doi: 10.3354/meps131235

Parker, C. E., Brown, M. T., and Bruland, K. W. (2016). Scandium in the open ocean: a comparison with other group 3 trivalent metals. *Geophys. Res. Lett.* 43, 2758–2764. doi: 10.1002/2016GL067827

Parsons, T. R., Maita, Y., and Lalli, C. M. (1984). *A Manual of Chemical and Biological Methods for Seawater Analysis*. Oxford; New York, NY: Pergamon Press.

Peers, G., and Price, N. M. (2006). Copper-containing plastocyanin used for electron transport by an oceanic diatom. *Nature* 441, 341–344. doi: 10.1038/nature04630

Rabosky, D. L., and Sorhannus, U. (2009). Diversity dynamics of marine planktonic diatoms across the Cenozoic. *Nature* 457, 183–186. doi: 10.1038/nature07435

Reinfelder, J. R. (2011). Carbon concentrating mechanisms in eukaryotic marine phytoplankton. *Annu. Rev. Mar. Sci.* 3, 291–317. doi: 10.1146/annurev-marine-120709-142720

Reinfelder, J. R., Kraepiel, A. M. L., and Morel, F. M. M. (2000). Unicellular C4 photosynthesis in a marine diatom. *Nature* 407, 996–999. doi: 10.1038/35039612

Ribalet, F., Marchetti, A., Hubbard, K. A., Brown, K., Durkin, C. A., Morales, R., et al. (2010). Unveiling a phytoplankton hotspot at a narrow boundary between coastal and offshore waters. *Proc. Natl. Acad. Sci. U.S.A.* 107, 16571–16576. doi: 10.1073/pnas.1005638107/-/DCSupplemental

Robertson, G., Schein, J., Chiu, R., Corbett, R., Field, M., Jackman, S. D., et al. (2010). *De novo* assembly and analysis of RNA-seq data. *Nat. Methods* 7, 909–912. doi: 10.1038/nmeth.1517

Robinson, M. D., McCarthy, D. J., and Smyth, G. K. (2010). edgeR: a Bioconductor package for differential expression analysis of digital gene expression data. *Bioinformatics* 26, 139–140. doi: 10.1093/bioinformatics/btp616

Robinson, M. D., and Oshlack, A. (2010). A scaling normalization method for differential expression analysis of RNA-seq data. *Genome Biol.* 11:R25. doi: 10.1186/gb-2010-11-3-r25

Robinson, M. D., and Smyth, G. K. (2008). Small-sample estimation of negative binomial dispersion, with applications to SAGE data. *Biostatistics* 9, 321–332. doi: 10.1093/biostatistics/kxm030

Rogato, A., Amato, A., Iudicone, D., Chiurazzi, M., Ferrante, M. I., and d'Alcalà, M. R. (2015). The diatom molecular toolkit to handle nitrogen uptake. *Mar. Genomics* 24 (Pt 1), 95–108. doi: 10.1016/j.margen.2015.05.018

Sage, R. F. (2004). The evolution of C4 photosynthesis. *New Phytol.* 161, 341–370. doi: 10.1111/j.1469-8137.2004.00974.x

Shi, D., Xu, Y., Hopkinson, B. M., and Morel, F. M. M. (2010). Effect of ocean acidification on iron availability to marine phytoplankton. *Science* 327, 676–679. doi: 10.1126/science.1183517

Sims, P. A., Mann, D. G., and Medlin, L. K. (2006). Evolution of the diatoms: insights from fossil, biological and molecular data. *Phycologia* 45, 361–402. doi: 10.2216/05-22.1

Song, B., and Ward, B. B. (2007). Molecular cloning and characterization of high-affinity nitrate transporters in marine phytoplankton. *J. Phycol.* 43, 542–552. doi: 10.1111/j.1529-8817.2007.00352.x

Strzepek, R. F., and Harrison, P. J. (2004). Photosynthetic architecture differs in coastal and oceanic diatoms. *Nature* 431, 689–692. doi: 10.1038/nature02954

Sunda, W. G. (2010). Iron and the carbon pump. *Science* 327, 654–655. doi: 10.1126/science.1186151

Sunda, W. G., and Huntsman, S. A. (1995). Iron uptake and growth limitation in oceanic and coastal phytoplankton. *Mar. Chem.* 50, 189–206. doi: 10.1016/0304-4203(95)00035-P

Sutak, R., Botebol, H., Blaiseau, P.-L., Léger, T., Bouget, F.-Y., Camadro, J.-M., et al. (2012). A comparative study of iron uptake mechanisms in marine microalgae: Iron binding at the cell surface is a critical step. *Plant Physiol.* 160, 2271–2284. doi: 10.1104/pp.112.204156.

Taylor, F. J. R., and Haigh, R. (1996). Spatial and temporal distributions of microplankton during the summers of 1992–1993 in Barkley Sound, British Columbia, with emphasis on harmful species. *Can. J. Fish. Aquat. Sci.* 53, 2310–2322. doi: 10.1139/f96-181

Taylor, R. L., Semeniuk, D. M., Payne, C. D., Zhou, J., Tremblay, J.-É., Cullen, J. T., et al. (2013). Colimitation by light, nitrate, and iron in the Beaufort Sea in late summer. *J. Geophys. Res. Ocean.* 118, 3260–3277. doi: 10.1002/jgrc.20244

Varela, D. E., and Harrison, P. J. (1999). Effect of ammonium on nitrate utilization by Emiliania huxleyi, a coccolithophore from the oceanic northeastern Pacific. *Mar. Ecol. Prog. Ser.* 186, 67–74.

Whitney, L. P., Lins, J. J., Hughes, M. P., Wells, M. L., Chappell, P. D., and Jenkins, B. D. (2011). Characterization of putative iron responsive genes as species-specific indicators of iron stress in thalassiosiroid diatoms. *Front. Microbiol.* 2:234. doi: 10.3389/fmicb.2011.00234

Young, J. N., Heureux, A. M. C., Sharwood, R. E., Rickaby, R. E. M., Morel, F. M. M., and Whitney, S. M. (2016). Large variation in the Rubisco kinetics of diatoms reveals diversity among their carbon-concentrating mechanisms. *J. Exp. Bot.* 67, 3445–3456. doi: 10.1093/jxb/erw163

Conflict of Interest Statement: The authors declare that the research was conducted in the absence of any commercial or financial relationships that could be construed as a potential conflict of interest.

frontiers in Marine Science

CORRECTION
published: 05 April 2018
doi: 10.3389/fmars.2018.00115

Corrigendum: Diatom Transcriptional and Physiological Responses to Changes in Iron Bioavailability across Ocean Provinces

*Natalie R. Cohen[1], Kelsey A. Ellis[1], Robert H. Lampe[1], Heather McNair[2], Benjamin S. Twining[3], Maria T. Maldonado[4], Mark A. Brzezinski[2], Fedor I. Kuzminov[5], Kimberlee Thamatrakoln[5], Claire P. Till[6,7], Kenneth W. Bruland[6], William G. Sunda[1], Sibel Bargu[8] and Adrian Marchetti[1]**

[1] Department of Marine Sciences, University of North Carolina at Chapel Hill, Chapel Hill, NC, United States, [2] The Marine Science Institute and the Department of Ecology Evolution and Marine Biology, University of California, Santa Barbara, Santa Barbara, CA, United States, [3] Bigelow Laboratory for Ocean Sciences, East Boothbay, ME, United States, [4] Department of Earth, Ocean, and Atmospheric Sciences, University of British Columbia, Vancouver, BC, Canada, [5] Department of Marine and Coastal Sciences, Rutgers, The State University of New Jersey, New Brunswick, NJ, United States, [6] Department of Ocean Sciences, University of California, Santa Cruz, Santa Cruz, CA, United States, [7] Chemistry Department, Humboldt State University, Arcata, CA, United States, [8] Department of Oceanography and Coastal Sciences, School of the Coast and Environment, Louisiana State University, Baton Rouge, LA, United States

OPEN ACCESS

Approved by:
Marine Science Editorial Office, Frontiers, Switzerland

***Correspondence:**
Adrian Marchetti
amarchetti@unc.edu

Specialty section:
This article was submitted to Marine Ecosystem Ecology, a section of the journal Frontiers in Marine Science

Received: 16 March 2018
Accepted: 19 March 2018
Published: 05 April 2018

Citation:
Cohen NR, Ellis KA, Lampe RH, McNair H, Twining BS, Maldonado MT, Brzezinski MA, Kuzminov FI, Thamatrakoln K, Till CP, Bruland KW, Sunda WG, Bargu S and Marchetti A (2018) Corrigendum: Diatom Transcriptional and Physiological Responses to Changes in Iron Bioavailability across Ocean Provinces. Front. Mar. Sci. 5:115. doi: 10.3389/fmars.2018.00115

Keywords: diatoms, *Thalassiosira*, *Pseudo-nitzschia*, iron, metatranscriptomics, California upwelling zone, Northeast Pacific Ocean

A corrigendum on

Diatom Transcriptional and Physiological Responses to Changes in Iron Bioavailability across Ocean Provinces

by Cohen, N. R., Ellis, K. A., Lampe, R. H., McNair, H., Twining, B. S., Maldonado, M. T., et al. (2017). Front. Mar. Sci. 4:360. doi: 10.3389/fmars.2017.00360

In the original Acknowledgments of this article, we neglected to thank Carolyn Duckham for her help collecting and processing samples for DIC uptake rates at stations C1-C3. The authors regret this oversight. This error does not change the scientific conclusions of the article in any way.

The original article has been updated.

Conflict of Interest Statement: The authors declare that the research was conducted in the absence of any commercial or financial relationships that could be construed as a potential conflict of interest.

frontiers in Marine Science

ORIGINAL RESEARCH
published: 12 March 2018
doi: 10.3389/fmars.2018.00075

Algal Hot Spots in a Changing Arctic Ocean: Sea-Ice Ridges and the Snow-Ice Interface

Mar Fernández-Méndez[1], Lasse M. Olsen[1], Hanna M. Kauko[1], Amelie Meyer[1], Anja Rösel[1], Ioanna Merkouriadi[1], Christopher J. Mundy[2], Jens K. Ehn[2], A. Malin Johansson[3], Penelope M. Wagner[4], Åse Ervik[5,6], Brian K. Sorrell[7], Pedro Duarte[1], Anette Wold[1], Haakon Hop[1,8] and Philipp Assmy[1]*

[1] Norwegian Polar Institute, Fram Centre, Tromsø, Norway, [2] Centre for Earth Observation Science, University of Manitoba, Winnipeg, MB, Canada, [3] Department of Physics and Technology, UiT The Arctic University of Norway, Tromsø, Norway, [4] Norwegian Ice Service, Norwegian Meteorological Institute, Tromsø, Norway, [5] Sustainable Arctic Marine and Coastal Technology, Centre for Research-based Innovation, Norwegian University of Science and Technology, Trondheim, Norway, [6] The University Centre in Svalbard, Longyearbyen, Norway, [7] Department of Bioscience, Aarhus University, Aarhus, Denmark, [8] Department of Arctic and Marine Biology, Faculty of Biosciences, Fisheries and Economics, UiT The Arctic University of Norway, Tromsø, Norway

OPEN ACCESS

Edited by:
Letizia Tedesco, Finnish Environment Institute (SYKE), Finland

Reviewed by:
Urania Christaki, Université du Littoral Côte d'Opale, France
Kevin Arrigo, Stanford University, United States
Maria A. Van Leeuwe, University of Groningen, Netherlands

***Correspondence:**
Mar Fernández-Méndez
mar.fdez.mendez@gmail.com;
mar@npolar.no

Specialty section:
This article was submitted to Marine Ecosystem Ecology, a section of the journal Frontiers in Marine Science

Received: *15 July 2017*
Accepted: *20 February 2018*
Published: *12 March 2018*

Citation:
Fernández-Méndez M, Olsen LM, Kauko HM, Meyer A, Rösel A, Merkouriadi I, Mundy CJ, Ehn JK, Johansson AM, Wagner PM, Ervik Å, Sorrell BK, Duarte P, Wold A, Hop H and Assmy P (2018) Algal Hot Spots in a Changing Arctic Ocean: Sea-Ice Ridges and the Snow-Ice Interface. Front. Mar. Sci. 5:75. doi: 10.3389/fmars.2018.00075

During the N-ICE2015 drift expedition north-west of Svalbard, we observed the establishment and development of algal communities in first-year ice (FYI) ridges and at the snow-ice interface. Despite some indications of being hot spots for biological activity, ridges are under-studied largely because they are complex structures that are difficult to sample. Snow infiltration communities can grow at the snow-ice interface when flooded. They have been commonly observed in the Antarctic, but rarely in the Arctic, where flooding is less common mainly due to a lower snow-to-ice thickness ratio. Combining biomass measurements and algal community analysis with under-ice irradiance and current measurements as well as light modeling, we comprehensively describe these two algal habitats in an Arctic pack ice environment. High biomass accumulation in ridges was facilitated by complex surfaces for algal deposition and attachment, increased light availability, and protection against strong under-ice currents. Notably, specific locations within the ridges were found to host distinct ice algal communities. The pennate diatoms *Nitzschia frigida* and *Navicula* species dominated the underside and inclined walls of submerged ice blocks, while the centric diatom *Shionodiscus bioculatus* dominated the top surfaces of the submerged ice blocks. Higher light levels than those in and below the sea ice, low mesozooplankton grazing, and physical concentration likely contributed to the high algal biomass at the snow-ice interface. These snow infiltration communities were dominated by *Phaeocystis pouchetii* and chain-forming pelagic diatoms (*Fragilariopsis oceanica* and *Chaetoceros gelidus*). Ridges are likely to form more frequently in a thinner and more dynamic ice pack, while the predicted increase in Arctic precipitation in some regions in combination with the thinning Arctic icescape might lead to larger areas of sea ice with negative freeboard and subsequent flooding during the melt season. Therefore, these two habitats are likely to become increasingly important in the new Arctic with implications for carbon export and transfer in the ice-associated ecosystem.

Keywords: Arctic ecosystem, ice algae, phytoplankton, infiltration communities, sea-ice ridges, community composition, climate change

INTRODUCTION

Current changes in sea-ice conditions have consequences for algal biomass and growth, with bottom-up cascading effects on the Arctic marine food web (Wassmann et al., 2011). The significant decline in sea-ice extent and thickness during the last 30 years has caused an increase in the light available for phytoplankton (Arrigo and van Dijken, 2011; Bélanger et al., 2013) and, thus, an increase in phytoplankton net annual primary production (Arrigo and van Dijken, 2015). Likewise, there have been several reports of under-ice phytoplankton blooms in the recent years enabled by the increased light transmission through melt ponds (e.g., Mundy et al., 2009; Arrigo et al., 2012) or through leads (Assmy et al., 2017). In contrast, ice algal areal production is probably decreasing on a pan-Arctic scale due to the loss of sea-ice habitat (Dupont, 2012). In addition, biomass standing stocks are low in young ice compared to the disappearing older ice, probably limited by recruitment, adding to the reduction in sea-ice algal areal production (Lange et al., 2017a; Olsen et al., 2017). As the ice edge retreats further north each summer, ice algae will be limited to the stratified deep basins of the Central Arctic with more oligotrophic conditions compared to the more productive shelves (Barber et al., 2015). The trend toward earlier ice melt and later ice formation may furthermore cause a mismatch in the timing between primary and secondary producers, diminishing the amount of carbon and energy transferred up the food chain (Søreide et al., 2010; Leu et al., 2011; Ji et al., 2013).

Diatoms typically dominate both the phytoplankton and the sea-ice spring blooms, while flagellates, dinoflagellates, and picoeukaryotes usually dominate in late summer (Tremblay et al., 2009; Moran et al., 2012; van Leeuwe et al., 2018). Some diatom species, such as *Shionodiscus bioculatus* (formerly *Thalassiosira bioculata)* (Alverson et al., 2006) and *Fragilariopsis cylindrus*, are sea-ice associated and have been observed both in the water column and in the ice (von Quillfeldt, 2000). Other sea-ice specialists such as *Nitzschia frigida* and *Melosira arctica* grow attached to the ice, while *Chaetoceros gelidus* (formerly *Chaetoceros socialis*) (Chamnansinp et al., 2013), *Fragilariopsis oceanica* and the haptophyte *P. pouchetii* are typically found in the water column (Booth and Horner, 1997). Current estimates of algal biomass and production in the ice-covered Arctic Ocean generally include phytoplankton and less often sea-ice algae (Gosselin et al., 1997; Sakshaug et al., 2004). Only recent studies have quantified the contribution of other sea-ice related environments, such as melt ponds (Mundy et al., 2011; Lee et al., 2012; Fernández-Méndez et al., 2015), and other more elusive forms of algal accumulations under the ice such as floating algal aggregates (Assmy et al., 2013; Fernández-Méndez et al., 2014).

There are few observations of ice algae growing in ridges (Syvertsen, 1991; Hegseth, 1992; Legendre et al., 1992) and at the snow-ice interface in the Arctic (Buck et al., 1998; McMinn and Hegseth, 2004; von Quillfeldt et al., 2009). Ridges are known to be hot spots for biological activity since they act as shelters for ice fauna and ice-associated zooplankton (Hop and Pavlova, 2008; Gradinger et al., 2010) and juvenile polar cod (Gulliksen and Lønne, 1989). Ridges have also been recently identified as locations of high algal biomass using under-water remotely operated vehicles (Lange et al., 2017b). However, due to the sampling challenges that these complex structures pose, algae have only been sampled sporadically. Snow infiltration communities growing at the snow-ice interface, have been widely described for Antarctic pack ice (Horner et al., 1988; Spindler, 1994; Robinson et al., 1997; Kristiansen et al., 1998; Garrison et al., 2003), where they contribute substantially to sea-ice primary production (Arrigo et al., 1997). In the few observations obtained from the Arctic, the dominant species reported are mostly phytoplankton such as *P. pouchetii* in pack ice north of Svalbard and Svalbard fjords (McMinn and Hegseth, 2004; von Quillfeldt et al., 2009), and unidentified pennate and centric diatoms in Disco Island, Greenland (Buck et al., 1998).

Despite these important observations, algal communities growing in ridges and at the snow-ice interface are understudied in the Arctic. Published studies of these two environments mainly focused on a qualitative assessment of the algal species present (especially in ridges), and the photosynthetic performance of the snow infiltration community in the study by McMinn and Hegseth (2004). During the Norwegian young sea ICE (N-ICE2015) drift expedition, we followed the evolution of these communities over 6 weeks and were able to characterize the physical-chemical environment in which these algal communities thrive, and we explain why these environments are suitable habitats for Arctic microalgae.

The aim of this study is to characterize sea-ice ridges and snow-ice interfaces as potential habitats and refuges for algae in the Arctic Ocean. In particular, we assess the importance of their biomass compared to adjacent environments, we define the light and nutrient regimes that these communities experience, we assess their photosynthetic activity, and we describe the species present. Furthermore, we discuss the role of these environments for hosting algae in the future Arctic Ocean against the background of the ongoing and predicted changes in the Arctic icescape.

MATERIALS AND METHODS

Sampling

All samples were collected during the N-ICE2015 drift expedition that took place between January and June 2015 in ice-covered waters north-west of Svalbard (Granskog et al., 2016). In total four ice floes were occupied and monitored during the expedition. Data presented in this study were obtained during drifts of Floe 3 and 4 (**Figure 1A**). Sea-ice algae present in ridges were sampled during the drift of Floe 3 between 10 May and 3 June 2015. Between 10 and 18 May, scuba divers using a slurp gun (modified 3.5 L Trident® suction gun) collected samples from the surface of the submerged ledges on the thin ice side every other day (side labeled with a star in **Figures 1B**, **2**). These samples were used for algal biomass, physiology, and community analysis. Slurp gun sampling can potentially lead to loss of algal biomass, however it can be considered the most appropriate method to sample these surface-attached algal layers. To use these samples quantitatively, the area sampled on the ledge's surface was measured (0.05 ×

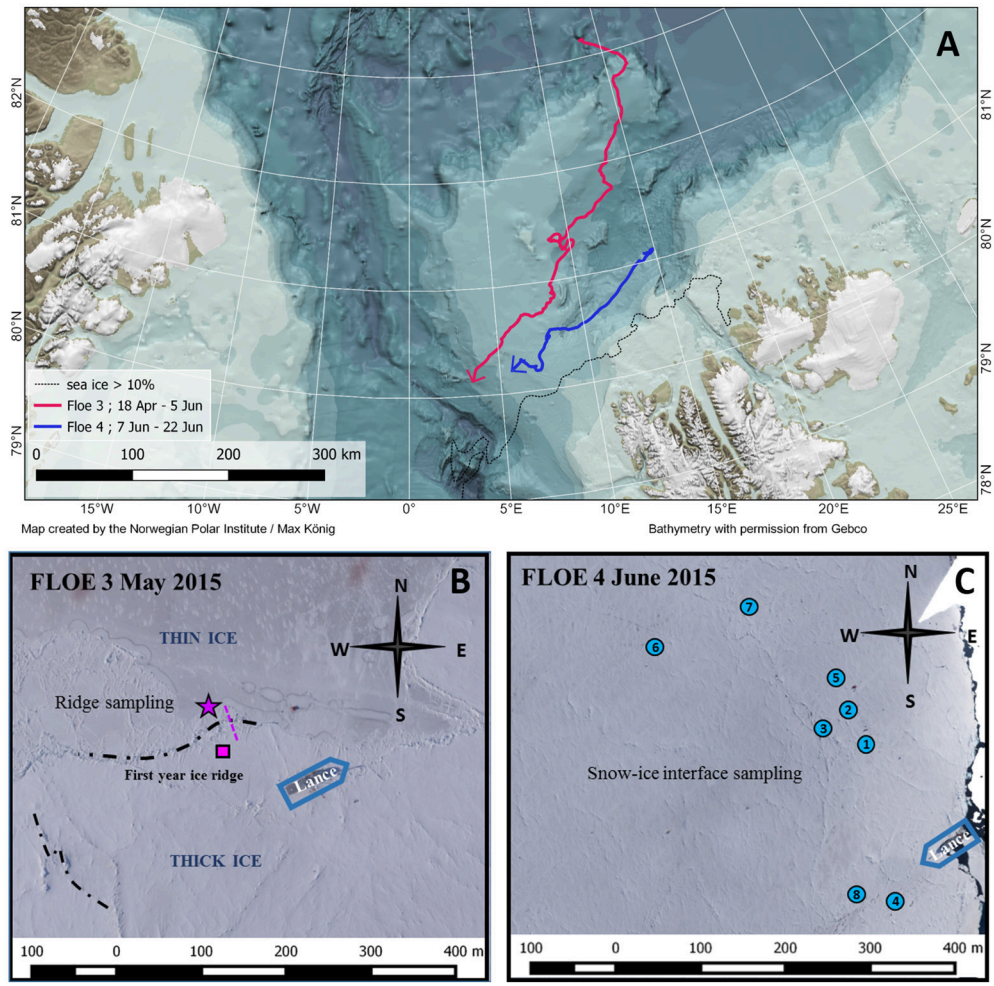

FIGURE 1 | (A) Study area with bathymetry for the N-ICE2015 expedition. The drift trajectories are shown in thick magenta (Floe 3) and blue (Floe 4) lines. The black dotted line indicates the ice edge (>10% ice coverage) position on 25 May 2015. Map created by Max König for the Norwegian Polar Institute. Bathymetry with permission from IBCAO (Jakobsson et al., 2012). **(B)** Aerial image of the study area during Floe 3 (image taken on 23 May 2015) and location of ridge sampling. The pink line indicates the transect sampled across the ridge and the star the sampling site from which the videos were recorded and the biomass estimates calculated. The pink square indicates the low biomass side of the ridge. **(C)** Aerial image of the study area during Floe 4 (image taken on 14 June 2015) and locations of snow-ice interface sampling. Vasilii Kustov and Sergey Semenov (Arctic and Antarctic Research Institute. St. Petersburg. Russia).

0.54 m) and used to estimate areal biomass. On 28 May, 31 May and 3 June, sea-ice algae at the ridge were sampled by ice coring with a 9-cm diameter ice corer (Mark II coring system, KOVACS Enterprise, Roseburg, USA). Bottom and top 0.1 m of the cores were collected on 28 May and entire cores of submerged sea-ice ledges were collected in three pieces with the ice corer on 30 May and 3 June for chlorophyll (Chl) *a* measurements and quantitative taxonomic analysis at both sides of the ridge. Melting of the ice cores occurred in the dark without addition of filtered seawater to avoid the addition of nutrients.

Algae growing at the snow-ice interface were sampled on Floe 4 between 9 and 18 June. Snow was removed with a shovel to search for brownish coloration as an indicator for algae at random areas with negative freeboard and high snow accumulation. In a radius of 500 m around the ship, we found and sampled these dense algae accumulations at eight different locations, usually along cracks in the ice (**Figures 1C**, **3**). Samples for qualitative analysis were taken with a snow shovel and melted in clean wide-necked plastic buckets. On 9 June, samples for quantitative analyses were taken using the bottom part of the ice corer and a plastic plate to close the bottom once it was filled with slush.

Characterization of the Physical Setting: Sea Ice and Snow

The ridge we chose for this study was a typical first-year ice (FYI) ridge (based on the characterization of its physical properties by Ervik et al., under review) that had formed adjacent to a refrozen lead as we started sampling Floe 3 in late April. We were able to follow its progression for a month. The internal ridge structure

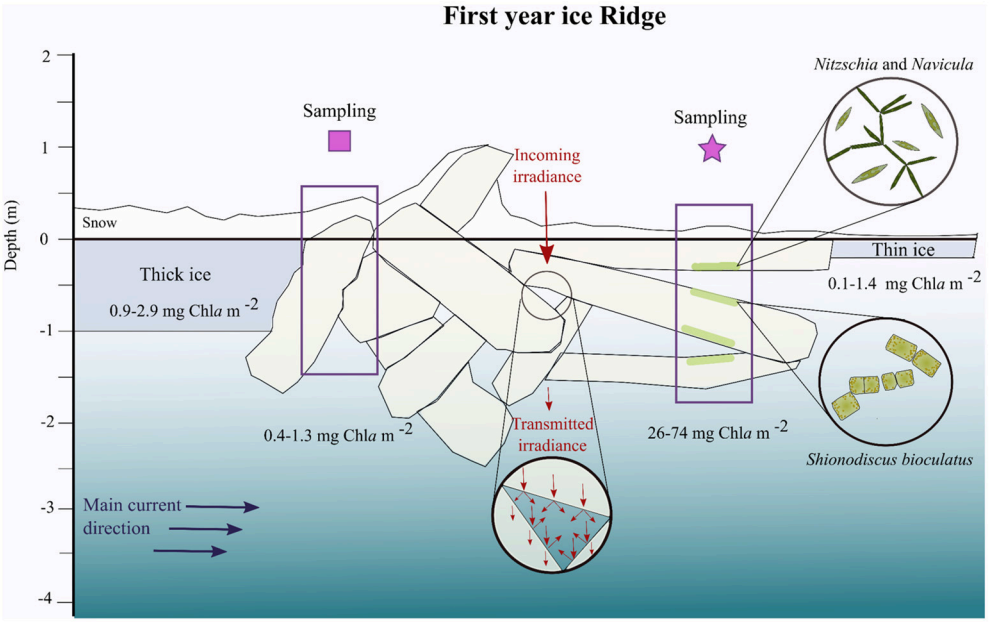

FIGURE 2 | Scheme of a first-year ice ridge based on observations and measurements performed during May 2015. The square and star correspond to the sampling sites indicated on **Figure 1B**. The main water current below the ice is a simplification from **Figure 5C**. The transmitted irradiance is depicted in a qualitative way to show the reflections that occur inside ridge cavities where the light might be higher than below the ridge itself. The most abundant algal species at the distinct surfaces of the ledges are depicted in the circles to the right based on **Figure 3**.

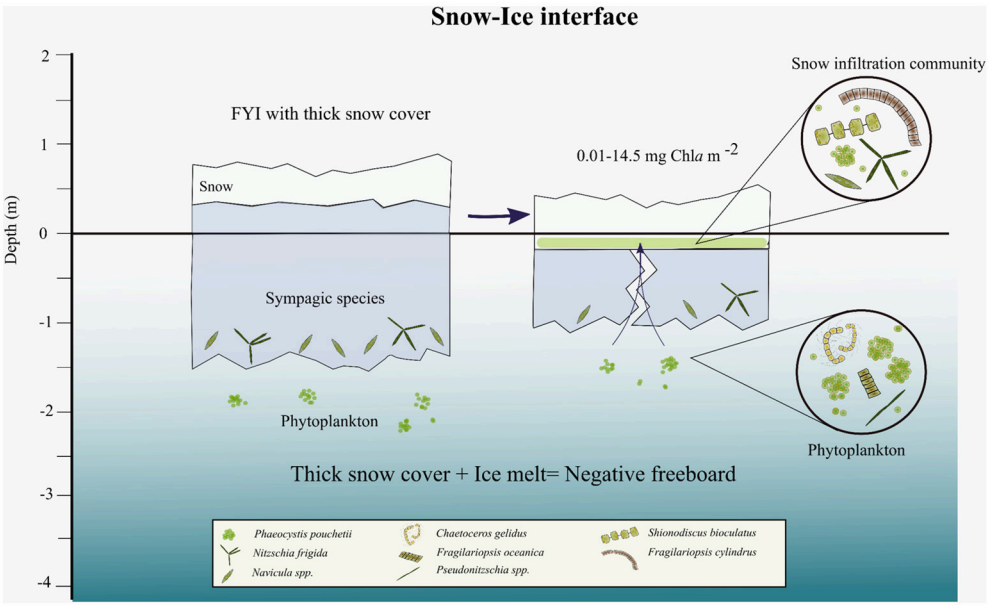

FIGURE 3 | Scheme of snow-ice interface habitat with algal biomass and simplified taxonomic composition. The snow infiltration community is established when thin ice with a thick snow cover starts melting and cracks appear in the ice that enable seawater to infiltrate into the snow-ice slush layer.

was determined by drilling holes with a 0.051 m auger along a transect perpendicular to the ridge length, as described in Ervik et al. (under review). To calculate the ridge macro-porosity (ratio of voids filled with water or slush to the total thickness of the ice) of the unconsolidated part (rubble), we added up the lengths of all the voids inside the rubble ice and divided by the total lengths of all the drill holes inside the rubble. Six videos of the underwater part of the ridge were recorded with a GoPro Hero black on 25

and 28 May (a compilation of these videos can be found in the Supplementary Material).

Ridge and rubble ice coverage, as well as smooth ice, new ice and open water percentages were assessed from satellite scenes. Five Radarsat-2 scenes of areas located within 10 km of the research vessel's position from 25 May until 15 June were processed and the percentage of deformed ice was estimated (Table S1, Figure S1). Radarsat-2 scenes use the standard frequency (C-band) for operational sea-ice monitoring and have successfully been used to separate deformed, FYI and multiyear ice (MYI) (Casey et al., 2014). The satellite imagery used here are fully polarimetric scenes with a high spatial resolution (5 m). The scenes were radiometrically calibrated using the included metadata calibration information (MacDonald, 2016), and subsequently segmented using the "extended polarimetric feature space" algorithm (Doulgeris and Eltoft, 2010; Doulgeris, 2013). The segmentation algorithm separated each image into distinct categories based on the statistical properties of the texture features. The identification and classification into open water, new and young ice, smooth ice, and ridges and rubble ice followed procedures used by operational ice analysts and documented in MANICE [Canadian Ice Service (CIS) Meteorological Service of Canada, 2005]. The total percentage of each category type was estimated once the segments had been combined into classified areas.

Water currents below the ice close to the ridge were measured with a medium-range vessel-mounted broadband 150 kHz acoustic Doppler current profiler (ADCP; Teledyne RD Instruments, Poway, CA, USA). Profiles were averaged hourly in 8-m vertical bins with the first bin centered at 23 m (Meyer et al., 2017). Current speed and direction at 23 m depth were used to analyze the current dynamics relative to the ridge during Floe 3 based on the ship's navigation data. The 23 m depth current data from the vessel-mounted ADCP were the shallowest current data set available for the study time period and were validated by comparing with near surface (1 m depth) current speed available for part of the time period from Acoustic Doppler Velocimeter instruments (ADV; Sontek Xylem, San Diego, CA, USA).

Snow depth and ice thickness on Floe 4 were determined using an electromagnetic instrument (EM31) in combination with a GPS-snow probe as described in Rösel et al. (2018). Negative freeboard areas that could potentially be flooded through cracks in the ice were estimated based on data from snow and ice thickness transects within a radius of 5 km around the ship (Rösel et al., 2016a,b) and drill hole data (Rösel and King, 2017). Additionally, a snow pit was dug and analyzed on 13 June at the first location (SI1) (**Figure 1C**), where we sampled the snow infiltration communities. Density, temperature, hardness and grain size of the snow were determined at 0.1 m intervals (Gallet et al., 2017).

Light Measurements and Calculations

Transmitted irradiance below ridges was measured during Floe 3 with a vLBV300 remotely operated vehicle (ROV) (SeaBotix.Inc, San Diego, CA, USA). The amount of transmitted photosynthetically active radiation (PAR) available below the studied ridge was measured using a cosine-corrected hyperspectral irradiance sensor (HyperOCR, Satlantic, Halifax, Canada) mounted on the upper part of the ROV. The same type of sensor was mounted on the surface of the ice looking upwards to measure incoming irradiance. Simultaneous measurements with both sensors allowed for transmittance estimates. In total, 334 radiation measurements at <5 m depth below the ridge were performed during 7, 18, and 20 May. Moreover, based on the observations by divers and the videos from the ROV's camera (600TVL color), as well as with an underwater camera attached to a pole and deployed through a hole in the ice, we could qualitatively assess the light field inside the ridge.

In addition, we used the following modification of the equation by Light et al. (2008) to calculate light transmitted (PAR_z) through the ridge with three overlaid ice ledges, separated by voids with water:

$$PAR_z = (1-R)\times PAR_{surface}\times\exp[-K_{snow}\times Z_{snow} - K_{ice}\times(Z_{ice_1}+Z_{ice_2}+Z_{ice_3}) - K_{water}\times(Z_{water_1}+Z_{water_2})]$$

where R is the specular reflection that happens at the surface (5%) (Perovich, 1989), $PAR_{surface}$ is the incoming *PAR* from a Trios-Sensor located at the weather station on the ice camp (Hudson et al., 2016), K_{snow} is the snow light attenuation coefficient for PAR (14.82 m^{-1}), K_{ice} is the ice light attenuation coefficient (0.93 m^{-1}), K_{water} is the water light attenuation coefficient (0.1 m^{-1}), and *Z* is thickness of the three different ledges or the depth of the water voids in between them. The snow attenuation coefficient was calculated from time series of incident and transmitted *PAR* and the sea-ice light attenuation coefficient was taken from Light et al. (2008). To compare with the ROV under-ice measurements, we calculated the light transmitted at the side of the ridge facing the refrozen lead (marked with a star in **Figures 1B**, **2**) from 23 April to 5 June, using its minimum (0.07 m) and maximum (0.11 m) snow depths measured on 28 May. In addition, to obtain an idea of the spatial variability of light transmitted through the ridge, we calculated *PAR* transmitted at 1-m intervals where we measured snow depth, ice thickness and water voids on 24 and 31 May.

The amount of light available for the snow infiltration communities was measured with a scalar Mini PAR logger (JFE MKV-L, Japan). In addition, we calculated the transmitted irradiance below 0.2–0.7 m of snow using the measured incoming irradiance and the snow attenuation coefficient mentioned above.

Chemical and Biological Analysis

Inorganic nutrients (nitrate, phosphate, and silicic acid) were sampled at 5 m below the ridge and at the snow-ice interface, collected in 20 mL scintillation vials, fixed with 0.2 mL chloroform and stored refrigerated until sample analysis ∼6 months later. Nutrients were measured spectrophotometrically on a modified Scalar auto-analyzer following Bendschneider and Robinson (1952) for nitrate, and Grasshoff (1965), for phosphate and silicic acid. The measurement uncertainty was 10% or less for all nutrients. Ammonium, which can reach very high concentrations in sea ice, was unfortunately not measured in these samples. In order to elucidate nitrogen remineralization in

these high algal biomass environments, it should be measured in future studies. Nutrient concentrations in the water column at 5 m depth are available at the Norwegian Polar Data Centre (Assmy et al., 2016).

For chlorophyll *a* (Chl *a*) and particulate organic carbon and nitrogen (POC and PON) 10–200 mL of sample (depending on the coloration of the melted sea-ice sample) were filtered through GFF and pre-combusted GFF filters (diameter 25 mm; Whatman, GE Healthcare, Little Chalfont, UK), respectively. Chl *a* was extracted in 5 mL of 100% methanol at 5°C in the dark for 12 h and measured fluorometrically using a Turner 10-AU Fluorometer (Turner Designs, San Jose, USA). POC and PON samples were analyzed with continuous-flow mass spectrometry (CF-IMRS) using a Roboprep/tracermass mass spectrometer (Europa Scientific, UK).

To calculate the percentage of algal biomass that each environment was contributing to the total sea-ice biomass we multiplied the percentage of surface that each environment (e.g., ridges and deformed ice, deformed edges next to open water or young ice, flooded FYI; non-flooded FYI or second-year ice (SYI) and young ice) covered by the range of biomass measured in each environment.

To calculate nutrient demand we followed Cota et al. (1987) and used our measured Chl *a* concentrations, the N:Chl *a* and Si:Chl *a* ratios, and the calculated growth rate based on Chl *a* measurements taken over consecutive days. Furthermore, we calculated the nutrient replenishment rate (mmol m^{-2} d^{-1}) by multiplying the measured nutrient concentrations in the under-ice water (transformed from per cubic meter to per square meter) by the measured water current velocity below the ice.

The physiological status of the photosynthetic apparatus of the algae was assessed with Pulse Amplitude Modulation (PAM) fluorometry using a Phyto-PAM Phytoplankton Analyzer (Walz, Eiffeltrich, Germany). Samples from the ridge were carefully collected by divers every 2 days between 10 and 18 May using a slurp gun, and between 28 and 31 May by scraping the surface of the ice core (the top and the bottom) into filtered seawater. Snow-ice infiltration layer samples for PhytoPAM analysis were collected with a clean bucket on the 9, 10, 11, 13, and 14 June. The quantum yield (Φ_{PSII}) of photosystem II fluorescence was determined on 30-min dark-acclimated samples from the ratio of variable and maximal fluorescence (Fv/Fm). In addition, Rapid Light Curves (RLCs) were performed with 20 sec pulses of actinic light ranging between 1 and 900 μmol photons m^{-2} s^{-1} in 13 steps. The relative photosynthetic electron transport rate (rETR) was calculated as the product of Φ_{PSII}, the theoretical absorption of PSII and the scalar irradiance of PAR at each pulse. The RLCs were fitted using the equation of Webb et al. (1974) to yield data from which the initial slope (α), the maximum rETR, and the photoacclimation parameter (E_k) were derived. There was no evidence of photoinhibition in any RLCs, so no photoinhibitory modification was included in the model. Only photosynthetic parameters obtained from the blue excitation channel (470 nm) were used, to optimize the signal-to-noise ratio and due to the strong absorption by Chl *c*, fucoxanthin and carotenoids in blue light by diatoms, which were the dominant algal group in our samples (Walz, 2003; Johnsen and Sakshaug, 2007). To statistically test for differences in the photosynthetic parameters of the different algal communities in the ridges we used the ANCOVA test for comparison of regression lines; (Sokal and Rohlf, 2012).

An additional approach used to test whether the diatoms found in the ridges and the snow-ice interface were actively growing was the silica stain method (McNair et al., 2015). We added 100 μL of the fluorescent dye 2-(4-pyridyl)-5-((4-(2-dimethylaminoethylaminocarbamoyl) -methoxy)phenyl)oxazole (PDMPO) (1 mM PDMPO in dimethylsulphoxide (DMSO) solution; ThermoFisher Scientific, Waltham, MA, USA) to 70 mL of each sample. After incubating in transparent plastic cell culture bottles *in situ* for 24 h, the samples were observed and photographed under an inverted Nikon TS100 light microscope (Nikon, Tokyo, Japan) on board. We show a selection of these images taken on board in the Supplementary Material to demonstrate the *in situ* uptake of silicate by the diatoms. Unfortunately, the preservation of these samples was unsuccessful and therefore further quantitative analysis could not be performed.

For algal taxonomy analysis, 190 mL of melted sample were filled into brown glass bottles and fixed with an aldehyde mixture of hexamethylenetetramine-buffered formaldehyde and glutaraldehyde at 0.1 and 1% final concentration, respectively. Quantitative estimates of each species were performed using an inverted Nikon Ti-U light microscope (Nikon TE300 and Ti-S, Tokyo, Japan) using the Utermöhl (1958) method, as described in Olsen et al. (2017). Furthermore, a variant of the Imaging FlowCytobot (IFCB) (Sosik and Olson, 2007) was used to obtain digital micrographs of algae from ridge-surface samples (slurp gun and scrapes) in the nano- and micro-size fraction (Olsen et al., 2017). These images of algae were assigned to taxonomical groups manually using custom software written by S. R. Laney at Woods Hole Oceanographic Institution and were used for quantitative analysis for the slurp gun and scrape samples from the ridge.

Ice fauna samples collected by divers with a suction pump (Lønne, 1988) below the ridge were preserved in 4% hexamethylenetetramine-buffered formaldehyde solution immediately after sampling. Organisms were identified under a Leica M80 stereo-microscope (Leica Microsystems, Wetzlar, Germany), equipped with an ocular micrometer.

RESULTS

Sea-Ice Ridge Properties

The ridge chosen for the study was formed during a storm between 26 and 30 April 2015 from FYI next to a refrozen lead, as observed from the vessel. Based on its physical properties we characterized the ridge as a FYI ridge. MYI ridges, which were not the object of this study, are usually more consolidated than FYI ridges and have lower macro-porosity. The percentage of deformed ice (including ridges and rubble ice) in the area studied between 26 and 31 May 2015, was 50.9 ± 3.2% based on classifications of surface types in three 25 × 25 km Radarsat 2 scenes (Table S1). The percentage of deformed edges next to leads was 2.8–7.4%. At the two sides of the ridge, where we

cored for biological analysis (**Figure 1B**), we encountered three ledges on top of each other with voids between them. The three ledges at the star sampling point (**Figure 2**), from top to bottom were 1.29, 0.88, and 1.69 m thick on 28 May, and 0.23, 0.80, and 0.55 m on 31 May. The decrease in thickness was probably a combination of melting and spatial variability. In general, across the ridge, from 24 to 31 May, both snow depth and sea-ice thickness decreased (**Figure 4**). The rubble macro-porosity of the unconsolidated submerged part of the ice, which represents the percentage of voids in between the ice ledges, was 25% on 24 May and decreased to 16% on 31 May. On 28 May, snow thickness was 0.13–0.22 m on the thick ice side (square) of the ridge, while it was 0.07–0.11 m on the refrozen lead side (star) (**Figure 2**).

Incoming PAR averaged from 7, 18 and 20 May was 786 ± 21 μmol photons m^{-2} s^{-1} (average and standard deviation). PAR transmitted through the ridge varied between 0.1 and 8.5% of the incoming PAR. The average transmitted PAR below the ridge was 24 ± 10 μmol photons m^{-2} s^{-1} ($n = 334$) (n is the number of samples), i.e., about 3% of the average incoming PAR, based on ROV measurements at 0–5 m below the ridge. This was higher than light transmitted through the thicker ice (Average 0.37 ± 0.08 μmol photons m^{-2} s^{-1}, $n = 44638$) and lower than through the thin refrozen lead (Average 114 ± 69 μmol photons m^{-2} s^{-1}, $n = 55$) measured during the N-ICE2015 expedition (Taskjelle et al., 2016; Kauko et al., 2017; Olsen et al., 2017). However, from the videos we observed that transmitted light was highly variable and patchy inside the ridge structure. Bright spots were observed inside the ridge in between the ledges (see Video in Supplementary Material).

Since light transmission measurements below ridged areas were scarce, we also attempted to model in a simplistic way the *PAR* transmitted through the ridge based on the snow and ice thickness and based on optical properties (cf. section Light Measurements and Calculations). The *PAR* transmitted through the thick-ice side of the ridge was lower (average on 24 May: 9 μmol photons m^{-2} s^{-1}; average on 31 May: 59 μmol photons m^{-2} s^{-1}) than through the thin-ice side (average on 24 May: 62 μmol photons m^{-2} s^{-1}; average 31 May: 274 μmol photons m^{-2} s^{-1}; **Figure 4**). This coincides with higher snow accumulation on the thick side of the ridge compared to the thin ice side. On 28 May, snow depth ranged between 0.07 and 0.11 m at the thin ice side of the ridge, so we calculated the theoretical minimum and maximum light transmitted through that specific spot from 23 April to 3 June to estimate temporal variability according to measured incoming irradiance (**Figure 5A**). The calculated transmitted *PAR* at one spot, without taking into account changes in snow and ice light attenuation coefficients as the melt season progressed, was generally one order of magnitude lower than the measured PAR with the ROV, except on 7 May when they

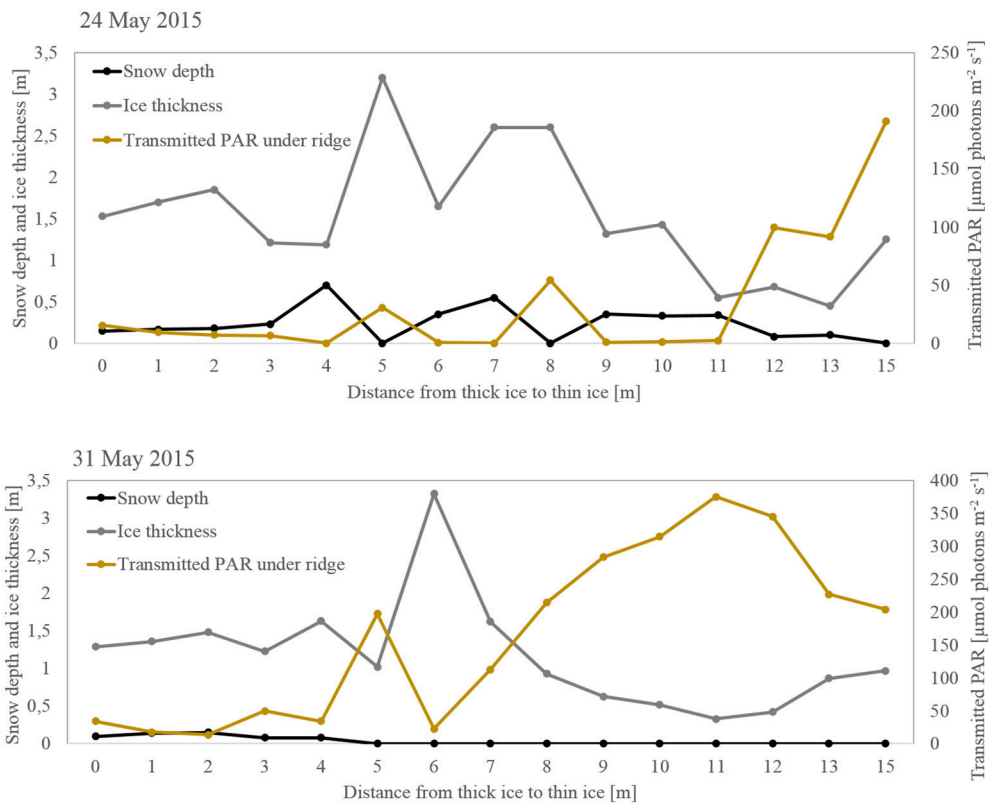

FIGURE 4 | Transect of light transmitted through the FYI ridge from the thick ice to the thin-ice side. Snow depth (black), total sea ice thickness (gray), and the estimated light transmitted below the ridge (yellow).

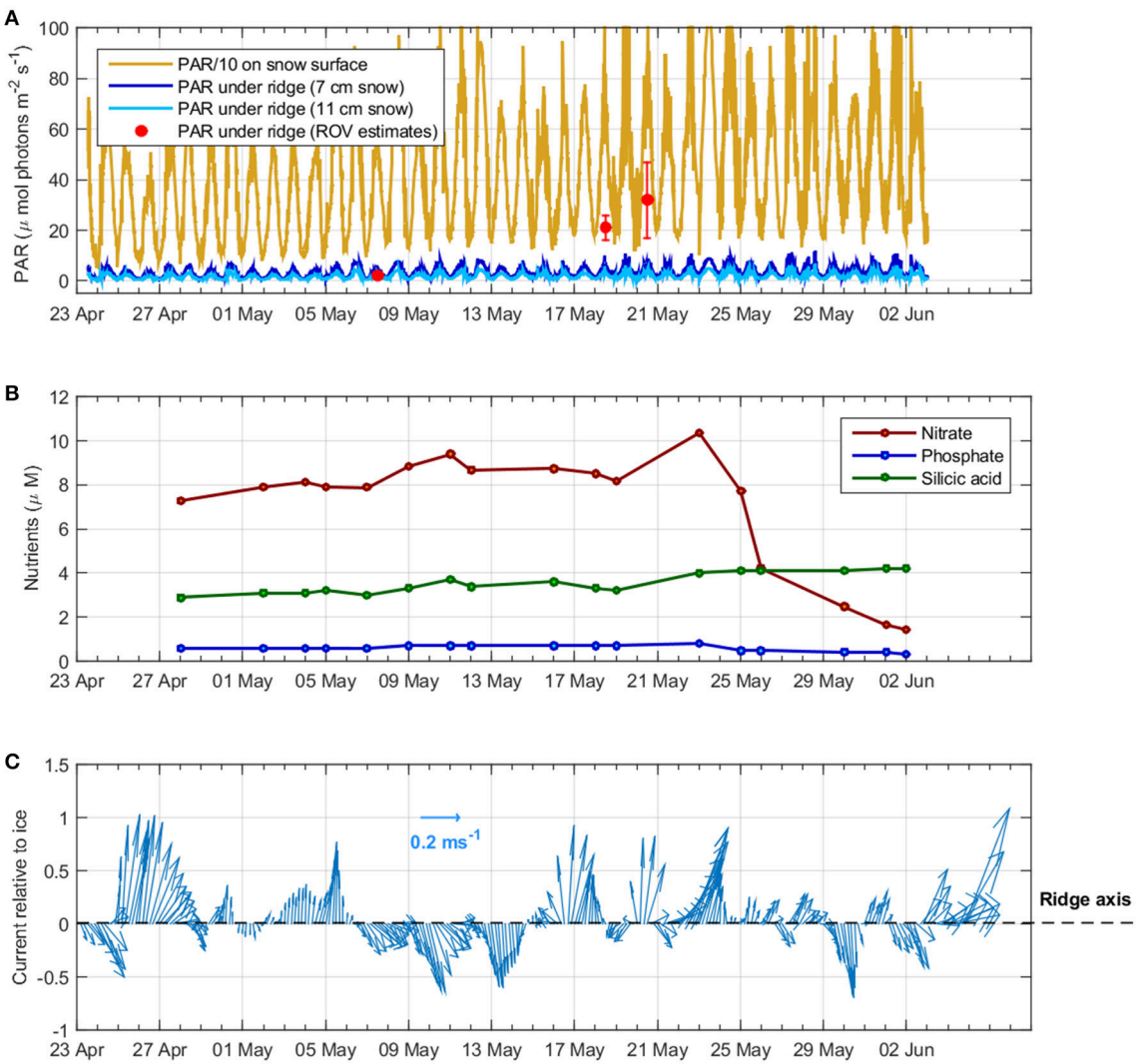

FIGURE 5 | Overview of the conditions during Floe 3 with time series of **(A)** incoming Photosynthetically active radiation (PAR) measured above the ice (yellow) and calculated below the ridge for two snow thicknesses (dark blue: 0.07 m and light blue: 0.11 m) and the ice ledge thickness on 31 May. The red dots represent average and standard deviation of ROV measurements performed on 7, 18, and 20 May; note that PAR values above the ice (yellow) have been scaled down by a factor of 10 for clarity purposes; **(B)** Nutrient concentrations (nitrate, phosphate, and silicic acid) at 5 m depth below the ice; **(C)** Ocean current speed relative to the ice depicted by the arrows size and direction relative to the ridge axis at 23 m depth depicted in the y-axis (from vessel-mounted ADCP).

compared well (**Figure 5A**). The ROV measurements covered a wide area below the ridge and included lateral light sources since measuring depth was up to 5 m below the ridge (Katlein et al., 2016). Therefore, when comparing the measurements with the transmitted *PAR* calculated across the ridge we do encounter similar values, especially toward the thin ice side where the influence of the refrozen lead allowed more light to penetrate. The spatial variability of calculated light transmitted across the ridge (**Figure 4**) indicates that changes in snow depth and ice thickness were the major drivers of light-transmission variability.

Nutrient concentrations in the water column (at 5 m depth) between 28 April and 25 May were 8.4 ± 0.8 μM nitrate, 3.4 ± 0.4 μM silicic acid and 0.6 ± 0.1 μM phosphate (average and standard deviation) (**Figure 5B**). After the development of a *Phaeocystis*-dominated under-ice bloom in the water column (26 May–2 June) (Assmy et al., 2017), nitrate concentrations were reduced to 2.4 ± 1.2 μM and phosphate to 0.4 ± 0.1 μM, while silicic acid increased slightly to 4.1 ± 0.1 μM (**Figure 5B**) as we drifted into more Atlantic-influenced waters.

Overall currents were weak, averaging 0.1 m s^{-1} relative to the ice, and came from various directions during the study period (23 April–5 June). However, over the period from 30 May to 5 June, current speeds larger than 0.2 m s^{-1} were observed with a mean relative current speed of 0.3 m s^{-1} flowing in a north-east direction (32°) (Figure S2) that crossed the ridge from the thick-ice side toward the thin refrozen lead side (**Figure 5C**). Thus, the

part of the ridge facing the refrozen lead was on the lee side of the stronger currents (**Figure 2**).

Algal Communities in FYI Ridges

Dense accumulations of algae were observed by naked eye on the top and bottom of the ledges during the entire sampling period (10 May to 3 June; **Figure 7** and Video in Supplementary Material). When sampling these surfaces communities, a clear distinction became apparent between the bottom of the ledges and their vertical surfaces, and the top of submerged ledges. The bottom and the vertical wall communities were dominated by the pennate sea-ice diatoms *Nitzschia frigida* and *Navicula* species, while the top community was dominated by *Shionodiscus bioculatus* (**Figure 6A**). Pennate diatoms of the genus *Navicula* increased their dominance from 10 to 31 May. The fluffy algal layer that accumulated on the top of submerged ledges and was dominated by *S. bioculatus* could be easily washed off by divers. A more diverse community was revealed in the ice cores taken from the ridge (**Figure 6B**). The three species that dominated the internal ice community on 31 May were *F. cylindrus*, *N. frigida,* and *Pseudo-nitzschia* sp. Three days later, on 3 June, the percentage of dinoflagellate cysts increased from <10% to >25%. On that day, the most abundant diatoms were *Pseudo-nitzschia* sp. and *N. frigida* (**Figure 6B**).

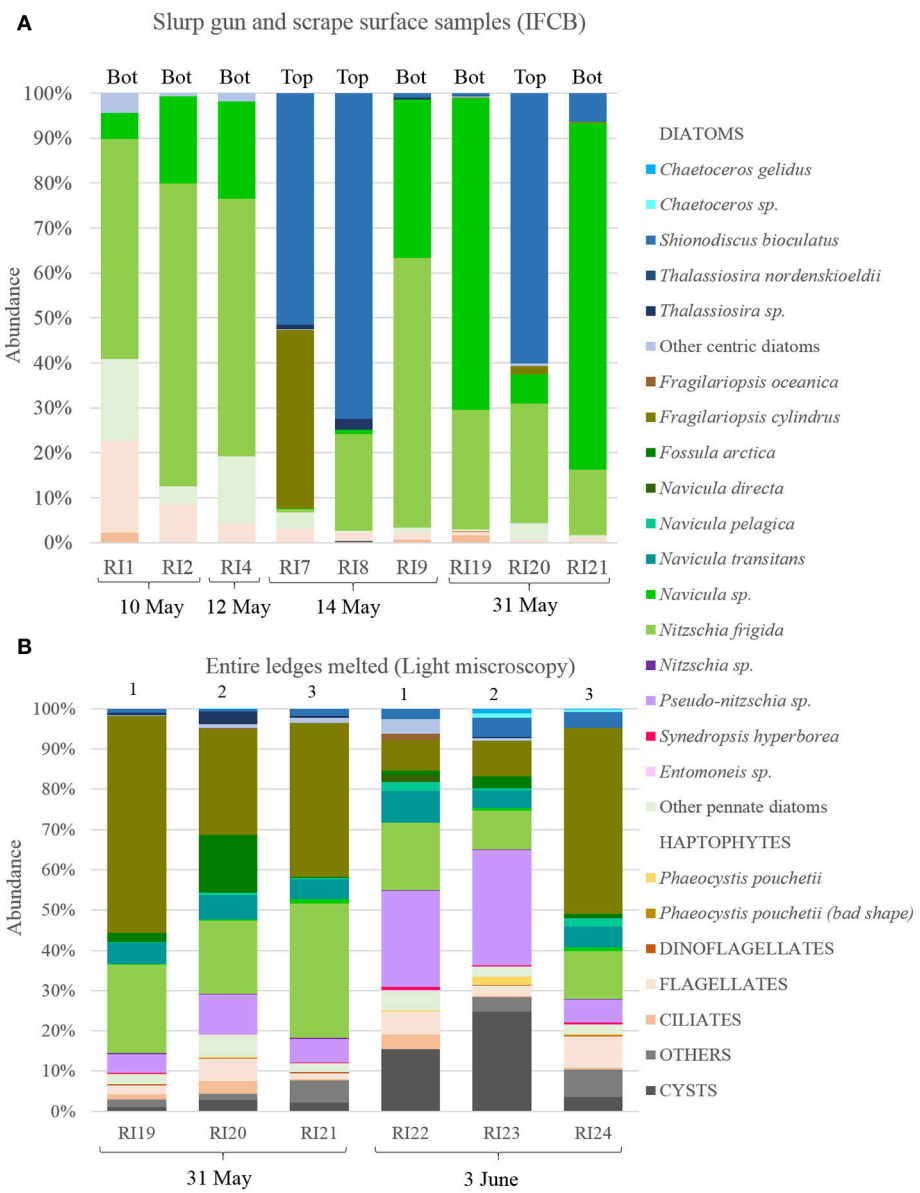

FIGURE 6 | Relative composition of ridge communities **(A)** Surface of the ice ledge samples collected with the slurp gun or by coring and then scraping the bottom (Bot) or top (Top) of the ice core. Samples analyzed with the imaging FlowCytoBot (IFCB). **(B)** Entire ledges melted. Numbers at the top correspond to the order of the ledges from top to bottom and the dates of sampling are indicated below. Samples analyzed by light microscopy enabling a higher taxonomic resolution.

TABLE 1 | Compilation of most abundant algal species, biogeochemical and photophysiological parameters of ridge individual samples collected on Floe 3.

Sample ID	Date (2015)	Sample type	Most abundant algal species	Ice thickness sampled	Chl *a*	POC	PON	BSi	C:N molar	N:Si molar	Quantum yield of photosystem II (Φ_{PSII})	Pmax (rETR)	Initial slope (α)	E_k
Units				(m)	(mg m^{-2})	(mg m^{-2})	(mg m^{-2})	(mg m^{-2})	(–)	(–)	(–)	(–)	[mol e-(mol photon)$^{-1}$]	[μmol photons m^{-2} s^{-1}]
RI1	10 May	Slurp gun Bottom	*Nitzschia frigida*	surface	0.31	10.3	3.6	–	3.32	–	–	–	–	–
RI2	10 May	Slurp gun Bottom	*Nitzschia frigida*	surface	2.97	42.0	10.0	–	4.91	–	0.54	42.6	0.08	533
RI3	10 May	Slurp gun Bottom	–	surface	4.67	315.3	35.4	–	10.4	–	0.61	45.8	0.25	183
RI4	12 May	Slurp gun Bottom	*Nitzschia frigida*	surface	4.23	73.1	14.4	–	5.92	–	–	–	–	–
RI5	12 May	Slurp gun Bottom	–	surface	1.60	39.7	9.7	–	4.80	–	0.31	18.6	0.13	143
RI6	12 May	Slurp gun Bottom	–	surface	2.76	21.9	6.5	–	3.91	–	–	–	–	–
RI7	14 May	Slurp gun Top	*Shionodiscus bioculatus*	surface	3.33	63.5	16.7	–	4.44	–	0.47	36.9	0.09	410
RI8	14 May	Slurp gun Top	*Shionodiscus bioculatus*	surface	2.17	39.1	12.6	–	3.61	–	0.46	40.2	0.15	268
RI9	14 May	Slurp gun Bottom	*Nitzschia frigida*	surface	9.87	154.4	40.1	–	4.50	–	0.49	82.7	0.09	919
RI10	16 May	Slurp gun Top	–	surface	–	–	–	–	–	–	0.56	40.1	0.30	189
RI11	18 May	Slurp gun Top	–	surface	–	–	–	–	–	–	0.34	27.3	0.13	210
RI12	18 May	Slurp gun Top	–	surface	–	–	–	–	–	–	0.28	27.8	0.11	253
RI13	18 May	Slurp gun Bottom	–	surface	–	–	–	–	–	–	0.19	35.6	0.07	509
RI14	18 May	Slurp gun Bottom	–	surface	–	–	–	–	–	–	0.28	19.1	0.08	239
RI15	28 May	Ledge 1 Bottom (star)	*Pseudo-nitzschia sp. Fragilariopsis cylindrus*	0.1	2.29	92.2	13.7	–	7.84	–	0.18	24.5	0.09	272
RI16	28 May	Ledge 2 Top (star)	*Nitzschia frigida. Shionodiscus bioculatus*	0.1	3.76	101.6	18.1	–	6.56	–	0.1	15.9	0.05	318
RI17	28 May	Ledge 1 Bottom (square)	*Fragilariopsis cylindrus* and flagellates	0.1	1.13	75.1	9.4	–	9.32	–	–	–	–	–
RI18	28 May	Ledge 2 Top (square)	Resting spores	0.1	0.40	30.2	3.1	–	11.4	–	–	–	–	–

(Continued)

TABLE 1 | Continued

Sample ID	Date (2015)	Sample type	Most abundant algal species	Ice thickness sampled	Chl *a*	POC	PON	BSi	C:N molar	N:Si molar	Quantum yield of photosystem II (Φ_{PSII})	Pmax (rETR)	Initial slope (α)	E_k
Units				(m)	(mg m^{-2})	(mg m^{-2})	(mg m^{-2})	(mg m^{-2})	(–)	(–)	(–)	(–)	[mol e-(mol photon)$^{-1}$]	[µmol photons m^{-2} s^{-1}]
Rl19	31 May	Ledge 1	*Fragilariopsis cylindrus. Nitzschia frigida*	1.29	27.87	1071.0	143.6	76.7	8.70	3.74	–	–	–	–
Rl20	31 May	Ledge 2	*Fragilariopsis cylindrus. Nitzschia frigida*	0.88	19.18	537.5	78.4	20.6	8.00	7.63	0.39	30	0.04	750
Rl21	31 May	Ledge 3	*Fragilariopsis cylindrus. Nitzschia frigida*	1.69	26.95	638.8	92.7	59.5	8.04	3.12	–	–	–	–
Rl22	3 June	Ledge 1	*Pseudo-nitzschia sp.*	0.23	6.78	230.2	29.1	9.0	9.23	6.46	–	–	–	–
Rl23	3 June	Ledge 2	*Pseudo-nitzschia sp.* and resting spores	0.80	11.04	564.3	75.3	26.8	8.74	5.60	–	–	–	–
Rl24	3 June	Ledge 3	*Fragilariopsis cylindrus*	0.55	8.58	339.7	50.2	53.9	7.90	1.86	–	–	–	–

Samples taken at the ridge and the biogeochemical and photosynthetic parameters measured are summarized in **Table 1**. Chl *a* concentrations in the slurp gun samples from the beginning of May ranged between 0.3 and 9.9 mg m^{-2}. In late May and early June, the volumetric Chl *a* concentrations, from melting entire cores from the ledges, ranged between 13.8 and 29.4 mg m^{-3} ($n = 6$) at the thin ice side, which correspond to an integrated Chl *a* stock of 26–74 mg Chl *a* m^{-2}. The thick ice side had lower Chl *a* concentrations (4–11 mg m^{-3}, $n = 2$) which correspond to 0.4–1.3 mg Chl *a* m^{-2} based on one bottom and one top 10-cm section (**Table 1**); therefore the biomass in the thick ice is probably underestimated. The integrated POC on the thin ice side of the ridge was 1,134–2,247 mg C m^{-2} (94–187 mmol C m^{-2}), the PON 154–314 mg N m^{-2} (11–22 mmol N m^{-2}), and the biogenic silica 9–77 mg Si m^{-2} (0.3–2.7 mmol Si m^{-2}). The C:Chl *a* weight ratio of the integrated biomass in the three ledges was 35.8 ± 9.6, the C:N molar ratio of the organic material was 8.4 ± 0.5, and the N:Si molar ratio 4.7 ± 2.1 ($n = 6$) (**Table 1**). The maximum nutrient demand of the integrated ridge community on 31 May was 15.7 mmol N m^{-2} d^{-1} and 38.9 mmol Si m^{-2} d^{-1} based on an estimated growth rate of 0.7 d^{-1} (derived from Chl *a* measurements on 31 May and 3 June) and the measured N:Chl *a* w:w ratio of 4.25 and the Si:Chl *a* ratio of 2.11.

The photosynthetic acclimation of the diatoms to the prevailing light climate was assessed with photosynthetic parameters obtained from RLCs. The maximum dark-adapted quantum yield (φ) of the slurp gun and scrape samples was 0.40 ± 0.16 ($n = 9$) for *Nitzschia*-dominated bottoms of the ledge, and 0.42 ± 0.11 ($n = 5$) for the *Shionodiscus*-dominated top part of the ledge (**Table 1**). Variability was very high (range: 0.19–0.61), but most samples were photosynthetically healthy with no evidence of chronic photoinhibition in the dark-adapted yield data. In addition, on-board observations of silica stain uptake samples revealed that the *N. frigida* bottom community and the *S. bioculatus* surface community were growing and taking up silicate at the time of sampling (Figures S3A–D). The photoacclimation parameter (E_k), calculated from electron transport with the PhytoPAM, was higher but highly variable for *Nitzschia*-dominated communities (421 ± 295 µmol photons m^{-2} s^{-1}) and slightly lower with less variability for *Shionodiscus*-dominated communities (266 ± 86 µmol photons m^{-2} s^{-1}). No statistically significant differences were detected in the light-response parameters between these two communities (ANCOVA test for comparison of regression lines; Sokal and Rohlf, 2012).

The sympagic amphipod *Apherusa glacialis* was the most dominant ice fauna species. Other amphipods present were *Themisto libellula, Gammarus wilkitzkii, Onisimus glacialis,* and *Eusirus holmi*. Some zooplankton species, such as the copepods *Oithona similis*, *Calanus glacialis* and undetermined Harpacticoida were present, although in lower numbers (Table S2).

Snow-Ice Interface Properties

When we arrived on Floe 4 on 11 June, the wider surrounding was mainly composed of FYI with a modal ice thickness of 1.0 m and an average snow depth of 0.25 ± 0.17 m on top.

TABLE 2 | Compilation of biogeochemical parameters of the snow-infiltration communities (SI).

Sample ID	Date (2015)	Chl *a*	POC	PON	C:N molar	Salinity	Nitrite	Nitrate	Phosphate	Silicic acid
Units		(mg m^{-3})	(mg m^{-3})	(mg m^{-3})	(–)	(–)	(μM)	(μM)	(μM)	(μM)
SI1	09 June	110.85	3170.0	435.7	8.49	10.90	n.d.	n.d.	n.d.	n.d.
SI1	09 June	135.46	3683.5	522.2	8.23	6.50	n.d.	n.d.	n.d.	n.d.
SI1	10 June	362.46	15002.4	2102.1	8.33	18.00	0.13	1.09	1.90	1.85
SI1	13 June	111.50	6701.6	1078.1	7.25	17.70	0.20	2.21	4.91	4.74
SI2	15 June	14.93	4616.4	608.4	8.85	17.50	0.11	0.40	2.73	8.97
SI3	15 June	2.61	3870.6	414.1	10.91	15.30	0.15	1.03	1.92	5.84
SI4	17 June	1.62	907.8	99.1	10.69	13.80	0.07	1.06	0.29	1.01
SI5	17 June	38.11	5701.3	680.9	9.77	21.10	0.46	0.40	3.12	3.52
SI6	18 June	0.37	692.6	59.0	13.71	10.00	0.06	0.64	0.18	0.70
SI7	18 June	42.25	552.9	74.7	8.64	12.10	0.06	0.40	2.45	6.49
SI8	18 June	46.06	2663.3	317.5	9.79	10.80	0.13	1.48	3.62	11.58

By 18 June, the modal ice thickness decreased to 0.8 m due to a strong bottom melting event, while the snow thickness remained in the same range (Rösel et al., 2018). Penetrating swell caused a breakup of the icepack into scattered 100–200 m pieces on the morning of 19 June. The snow depth at the first snow-ice interface sampled (0.7 m) was thicker than the mean snow depth of 0.32 ± 0.20 m on Floe 4 (Rösel et al., 2018). When the relation between ice thickness and snow thickness exceeded the hydrostatic equilibrium, the thick snow cover pushed the ice below sea level creating areas of negative freeboard. Based on drill hole measurements, 53% of the area of Floe 4 had negative freeboard (Rösel and King, 2017).

According to the snow pit performed on 13 June at SI1 (Figure S4), the top 0.3 m of the snow pack was hard wind slab of 0.5 mm grain size. The bottom 0.5 m consisted of refrozen melt layers of larger grain size (1.0 mm). The snow hardness decreased toward the bottom of the snow pack, close to the slush where the algae had accumulated (Figure S4). The temperature profile across the snow showed values around 0°C in the upper 0.3 m and <0°C in the lower 0.5 m (−0.1 to −1.2°C). Compiling the information from the eight locations sampled (**Figure 1C**), the slush where the algae were found had thickness of 0.04–0.2 m, temperature of −1.2 to −1.7°C, and bulk salinity of 6.5 to 21.1 (practical salinity unit, henceforth unitless) (average 13.9 ± 4.3, $n = 11$; **Table 2**) in the melted slush depending on the amount of seawater that had percolated to the snow-ice interface. Snow infiltration communities were typically found in areas with thick snow (0.2–0.7 m), thin ice (0.4–0.9 m) in an advanced stage of melt, and were usually associated with cracks in the ice. Seawater percolated through the cracks in the ice toward the flooded snow-ice interface. Algae were found along the cracks and spreading ∼0.5 m to either side of the crack (**Figures 7B,C**).

The PAR transmittance through 0.2–0.4 m snow cover was 3–14% of the incoming irradiance based on measurements on 11 June at SI1 using a scalar PAR sensor. When using the average estimated snow light attenuation coefficient of 14.82 m^{-1} for Floe 3, the calculated transmitted *PAR* was one order of magnitude lower than *in situ* measurements. This is due to the fact that the scalar PAR sensor collects light from all directions, while

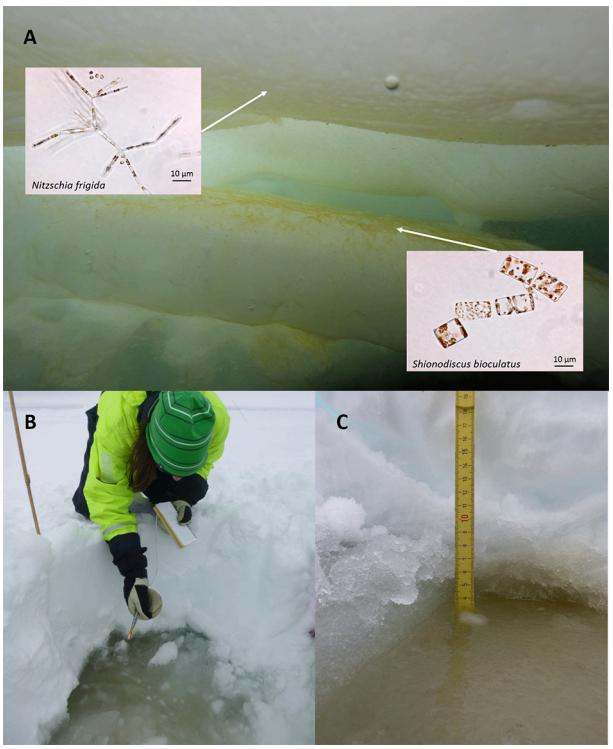

FIGURE 7 | (A) Underwater photograph of FYI ridge sampled on 31 May indicating the most abundant species of the bottom and top of the ledges. Microscopy images of the bottom of the first ledge shows the pennate diatom *Nitzschia frigida* (RI19) and the top of the second ledge shows the centric diatom *Shionodiscus bioculatus* (RI20). **(B)** Photo of the snow infiltration community SI1 found below 0.7 m of snow on 9 June 2015. **(C)** Photo of the snow-ice interface SI1 with a metric tape in cm scale to give an idea of its thickness.

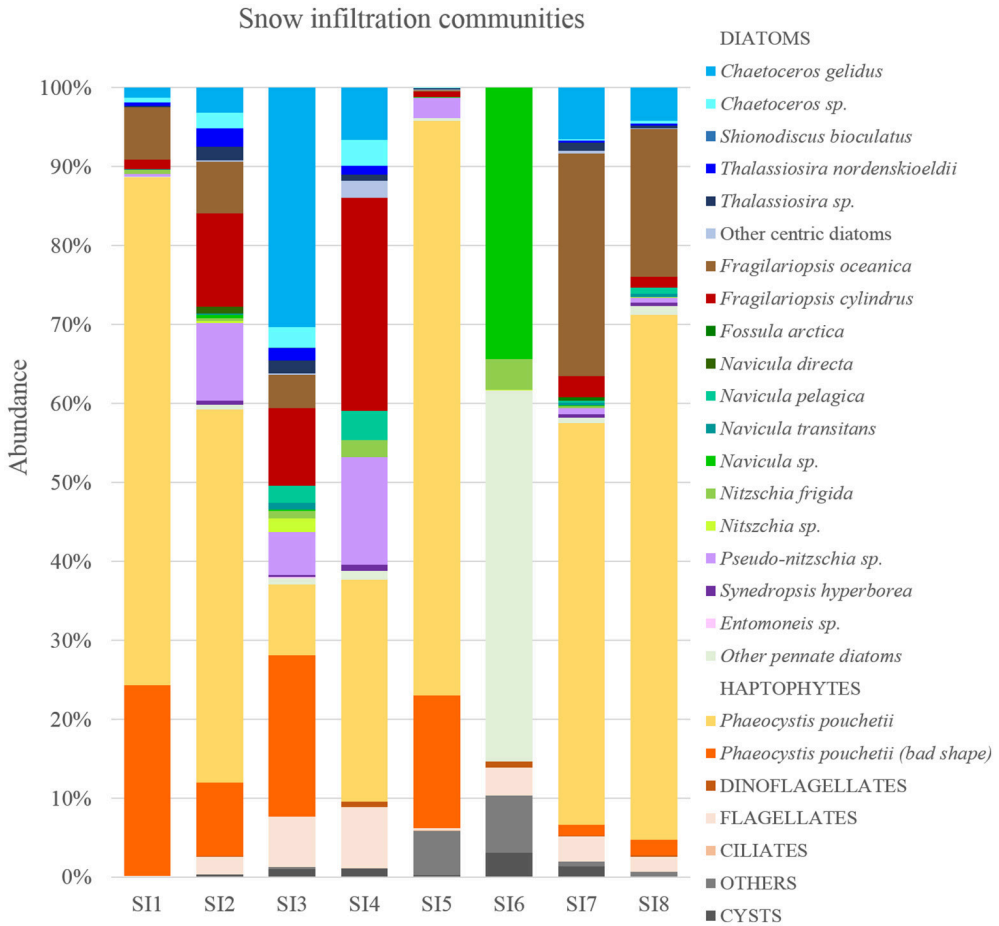

FIGURE 8 | Relative composition of eight different snow infiltration communities based on cell abundance. Samples analyzed by light microscopy.

our calculations assume a downwelling light field. On an average sunny day (1,200 μmol photons m^{-2} s^{-1} incoming PAR), algae below 0.2 m of snow would receive 62 μmol photons m^{-2} s^{-1} and 0.03 μmol photons m^{-2} s^{-1} below 0.7 m of snow. This corresponds to 0.0025–5% transmitted PAR.

Algal Communities at the Snow-Ice Interface

Snow infiltration communities were found at eight different spots on Floe 4 between 9 and 18 June (**Figure 1C**). The taxonomic composition of the snow-infiltration communities was very diverse and included both pelagic and ice-associated species. Besides a small percentage of flagellates, ciliates and dinoflagellates (sum of the three groups 3.4 ± 2.8%), the snow infiltration communities were dominated by the haptophyte *P. pouchetii* (51 ± 31%) and diatoms (42 ± 27%; **Figure 8**). *Phaeocystis pouchetii*, which was the dominating species of the under-ice phytoplankton bloom taking place at the same time, was present in the snow infiltration communities (8.3×10^5-8.7×10^7 cells L^{-1}) in similar concentrations as in the water column (8.6×10^5-9.9×10^7 cells L^{-1}; Assmy et al., 2017). The dominant pelagic diatoms present were *F. oceanica*, *C. gelidus*, *Pseudo-nitzschia* sp. and *Thalassiosira* spp.; and the main ice-associated diatoms were *F. cylindrus, Navicula* sp. and *Nitzschia* sp. (**Figure 7**). However, some species such as *F. oceanica* and *F. cylindrus* can be quite abundant in both sea ice and the water column making the pelagic vs. ice-associated distinction difficult. In terms of diatoms, most snow-ice interface communities were dominated by a typical pelagic algal composition except for SI6 that had a more ice-algal composition (**Figure 7**). This sample had very low counts and a higher percentage of resting spores than all the others, indicating a senescent stage. Also, in many of the snow-ice interface communities, a high percentage of the *P. pouchetii* colonies observed were decaying and contained very few cells (3–70% of the community was *P. pouchetii* cells in bad shape), indicating that this species infiltrated from the water column but was not performing optimally in its new habitat.

The Chl *a* concentration in the slush collected at the snow-ice interface ranged three orders of magnitude: from 0.37 to 362 mg m^{-3} (Average: 69 ± 115 mg m^{-3}, $n = 11$; **Table 2**). The POC was 552–15,000 mg C m^{-3} and the PON 59–2,102 mg N m^{-3} ($n = 11$) (**Table 2**). The average C:N molar ratio of the algal biomass was 9.7 ± 1.8. Despite being in the middle of the productive season, some of the nutrients present in the melted slush, such as

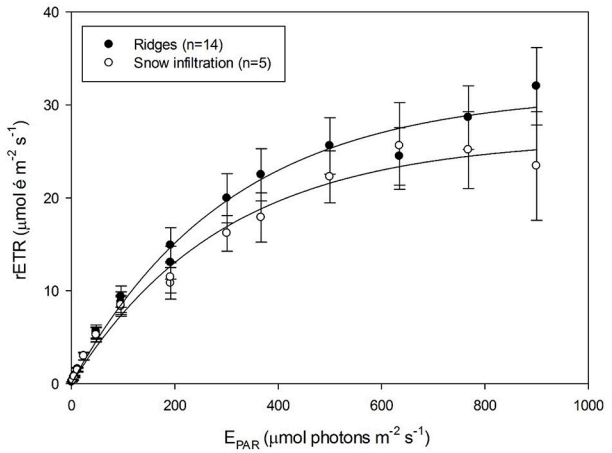

FIGURE 9 | Rapid light curves from ridge (black circles) and snow infiltration (white circles) communities measured with PhytoPAM. The relative electron transfer rate (rETR) is plotted against photosynthetically active radiation (E_{PAR}). Average and standard deviation for each light step are shown and the Webb et al. (1974) model was used to fit the average curve.

phosphate, had very high concentration. Nitrate ranged between 0.4 and 2.2 µM, phosphate between 0.2 and 4.9 µM, and silicic acid between 0.7 and 11.6 µM ($n = 11$) (**Table 2**). The maximum nitrate demand of the snow-ice interface community was 17.8 mmol N m^{-2} d^{-1} at a growth rate of 0.62 d^{-1} (calculated with Chl *a* values from 9 and 10 June in SI1) and a N:Chl *a* ratio of 5.7.

On-board observations of silica stain uptake samples revealed that the diatoms were growing and taking up silicic acid at the time of sampling (Figures S3E, F), while light microscopy analysis revealed a high percentage of decaying *P. pouchetii* cells. This variability in the physiological status of the algae at the snow-ice interface was reflected in the photosynthetic activity measurements performed with the PhytoPAM. The Φ_{PSII}, at SI1 during 5 days (9, 10, 11, 13, and 14 June), ranged between 0.22 and 0.46 ($n = 5$) indicating that only part of the snow-ice infiltration community was healthy. The low salinities at SI1 (6–18) could be responsible for the decaying *P. pouchetii* cells. The photoadaptation parameter (E_k) ranged between 156 and 453 µmol photons m^{-2} s^{-1}. When comparing the snow-ice interface community with the ridge communities, we found that ridge communities had significantly higher light saturation level (ANCOVA test for homogeneity of regression curves; Sokal and Rohlf, 2012), implying that these communities were acclimated to higher light intensities than the snow infiltration community (**Figure 9**).

DISCUSSION AND CONCLUSIONS

Contribution of FYI Ridges and Snow-Ice Interfaces to Arctic Algal Biomass and Sampling Challenges

Algal accumulations in complex structures such as ridges and in hidden layers at the snow-ice interface are understudied in the Arctic Ocean and thus have not been accounted for in sea-ice algal biomass estimates. In this study, we have estimated the contribution of ridge and snow infiltration communities to the total ice algal biomass for the first time (**Table 3**) based on RadarSat-2 satellite scene ice-type classification (Figure S1), *in situ* negative freeboard measurements, and the measured Chl *a* in each sea-ice environment.

Ridges and rubble ice could contribute 36–96% of the total sea-ice biomass, assuming that all of this area would sustain the same amount of biomass as the thin ice side of the ridge we sampled (**Table 3**). In reality, the percent contribution was probably lower since not all ridges are FYI ridges close to a refrozen lead. Indeed, in our study region, only 2.8–7.4% were deformed edges next to open water or young ice (**Table 3**). If only this particular type of ridge would host algal biomass as we observed in the thin ice side of our study ridge (26–74 mg Chl *a* m^{-2}) and the rest of the ridges and deformed areas would only host as much biomass as we observed on thick ice side of the ridge (0.4–1.3 mg Chl *a* m^{-2}), their contribution would be 34–75% of the total sea-ice biomass (**Table 3**). Nevertheless, compared to other sea-ice environments (FYI, new, and young ice), ridges and deformed ice areas, can account for most of the sea-ice related biomass. This is in agreement with large-scale under-ice ROV surveys that point toward ridges as relevant for algal biomass accumulation (Lange et al., 2017b). It is therefore critical that ridges are examined more closely and included in biomass and productivity estimates for Arctic sea ice.

Snow infiltration communities, which in the Antarctic can be responsible for most of the ice-associated production (Arrigo et al., 1997) and biomass (0.5–30 mg Chl *a* m^{-2}; Arrigo and Thomas, 2004), seem to have a smaller contribution in the Arctic. Assuming a minimum thickness of the slush layer of 0.04 m, the integrated Chl *a* was 0.01–14 mg m^{-2}. On a larger scale, if all areas with negative freeboard would be inhabited by these communities, algal standing stocks on flooded sea ice could potentially reach 0.1–3.4 mg Chl *a* m^{-2} and contribute 9–32% to the total sea-ice integrated Chl *a* (**Table 3**). The minimum percent contribution of snow infiltration communities (9%) to total ice algal standing stocks was tenfold higher than the minimum contribution of ice algal biomass in level FYI and SYI (0.9%). Thus, including snow infiltration communities in sea-ice biomass and productivity estimates is relevant, especially during the late productive season when the ice starts melting and bottom sea-ice production decreases (Leu et al., 2015). However, these communities were usually only found along cracks in the ice and not in all flooded areas. Unfortunately, there is currently no way to quantify the percentage of the flooded area covered by cracks in the ice, so the estimate provided is just a potential maximum of the real contribution.

Ridge and snow infiltration algal communities have not been extensively studied in the Arctic, likely due to the difficulties in sampling and detecting them. Ridges are complex ice structures that are challenging to sample using the regular ice-core drilling techniques (Timco and Burden, 1997; Gradinger et al., 2010; Lange et al., 2017a). In our study, the ridge algal community was very loosely attached to the surfaces of the ledge and is therefore, partially lost when sampling the entire core by drilling. Slurp gun

samples collected by divers, in otherwise inaccessible cavities and structures of the ridges, seem to be better suited for determining the dominant algal species concentrated at the surface of the submerged ledges compared to ice coring. The latter will likely result in the loss of loosely attached surface communities, such as the fluffy layer of *S. bioculatus*, during core retrieval. Coring of the entire ridge on the other hand will provide information on the internal ice community structure and biomass. Thus, a combination of ice coring and slurp gun sampling or ice coring from below by divers would be the best approach to assess both qualitatively and quantitatively the algal community in ridges.

ROVs can be used to study the optical properties and derive algal biomass from light transmission. However, ROVs are likely to get entangled in complicated under-ice structures and therefore, measurements are usually taken several meters below the ridge (Lange et al., 2016), integrating light from a broad area under the ridge. Smaller ROVs with better maneuverability might be a solution to map the spatial variability in light penetration and algal biomass inside the ridge structure, but divers are needed to obtain measurements inside specific structures. In addition, specific modeling approaches need to be developed to describe the complex light regime inside the ridge structure, since simple 1D vertical models, like the one we used, fail to reproduce the observed complex light field inside the ridge.

The challenge in the case of snow infiltration communities is to detect them since they are covered by snow and therefore not readily visible from the surface, except at the edge of ice floes (von Quillfeldt et al., 2009). In addition, upscaling of the potential habitat suitable for snow infiltration communities requires a good knowledge of the percentage of the ice floe that has negative freeboard. In this study, we based our estimates on *in situ* observations from several kilometer long transects with EM31 (Rösel et al., 2016a), the snow probe (Rösel et al., 2016b), and drill holes (Rösel and King, 2017). Satellites cannot detect infiltration layers at the snow-ice interface (Ackley et al., 2008). Detecting potential zones of surface flooding is challenging due to the difficulties in differentiating wet melting snow from surface flooding (Onstott, 1992). It is therefore necessary to be either in person in the field or have autonomous instruments such as Ice Mass Balance buoys deployed on the ice to qualitatively observe rapid sea-ice melt events. However, knowing the potentially flooded area does not give any information on where the snow infiltration communities grow. Our observations indicate that they concentrate along cracks in the ice, and these are difficult to detect when covered with snow, and therefore, difficult to upscale. Despite the potential local importance of snow infiltration communities, their upscaling is challenging and this study is just a first attempt to estimate their contribution to ice-associated algal biomass that needs to be further refined.

TABLE 3 | Biomass upscaling of sea-ice environments on Floe 3 and 4 based on satellite (Radarsat 2) estimates of percentage cover of different ice types.

	Floe 3 (May)				Floe 4 (June)			
Environment	**Chl *a* [mg m^{-2}]**	**% cover from RDS-2**	**Chl *a* [mg km^{-2}]**	**% of total sea ice Chl *a***	**Chl *a* [mg m^{-2}]**	**% cover from RDS-2**	**Chl *a* [mg km^{-2}]**	**% of total sea ice Chl *a***
Ridges and deformed ice	0.3–74	50.9	1.5×10^5–3.7×10^7	36–96	0.3–74	46.3	1.4×10^5–3.4×10^7	34–90
Deformed edges next to open water or young ice	26–74	2.8–7.4	1.9×10^6–5.4×10^6	34–75	–	–	–	–
Sea ice flooded (FYI)	–	–	–	–	0.01–14	21.6	1.3×10^5–3.4×10^6	9–32
Sea ice non flooded (FYI and SYI)	0.6–2.9	43.3	2.6×10^5–1.2×10^6	3–62	0.6–1.7	21.6	1.3×10^5–3.7×10^5	0.9–32
Young ice	0.14–2.4	3.9	5.4×10^3–9.3×10^4	0.2–1.3	0.14–2.4	5.1	7.4×10^3–1.2×10^5	0.3–1.7

The Role of Ridges and the Snow-Ice Interface as Algal Safe Havens: Irradiance, Nutrients, and Grazing Pressure

The high algal biomass encountered in ridges and at the snow-ice interface during the 2015 productive season in the high Arctic indicates that these two environments provide shelter

and favorable conditions for algal accumulation and potentially growth.

Newly formed FYI ridges with complex ice structures offer plenty of cavities and surfaces for attachment and deposition (16–25% voids). The complex structure of sea ice piled up in ridges creates an extensive habitat for sea-ice algae which exceeds other sea-ice related environment in terms of its total surface area, with the exception of Antarctic platelet ice. Indeed, other studies have reported higher macro-porosity values of 30–35% (Høyland, 2007; Strub-Klein and Sudom, 2012). In addition, the lee side of ridges provide algal communities protection from under-ice water currents, particularly for those algae that are loosely attached to ice surfaces such as the communities dominated by *S. bioculatus*. Therefore, higher biomass concentrations are expected on the lee side or hydrodynamic shadow of ridges. This effect has been suggested to explain accumulation of diatoms (Melnikov and Bondarchuk, 1987; Krembs et al., 2002), algal aggregates (Katlein et al., 2015b), as well as ice fauna (Hop and Pavlova, 2008; Kiko et al., 2017) in sheltered areas of ridges. Indeed, ridges are hot spots for accumulation of sea-ice fauna (Gradinger et al., 2010) since the organisms can graze on the abundant surface-attached sea-ice algae. For example, *A. glacialis*, which was the most abundant ice-associated amphipod in this study, has been shown to actively feed on ice algae, which can be a main contribution to its diet (Werner, 2000; Brown et al., 2017).

The snow-ice interface on the contrary provides shelter from grazing since only small ciliates were observed grazing on the snow infiltration community (**Figure 8**). In addition, the low salinity in the slush (6–21) would reduce the grazing activity of potential grazers that could reach this layer. This lack of strong metazoan grazing pressure in the infiltration community environment could have favored the accumulation of algal biomass. Processes of physical concentration of algal biomass in the slush could also be responsible for the high accumulation of biomass. Since the highest algal biomass accumulations occurred within half a meter around cracks in the ice, we hypothesize that infiltrated communities concentrated in these areas, trapped in the porous snow-ice slush as water percolates to the rest of the floe.

The accumulation of snow on the side of ridges (Chapters 3 and 4 in Thomas, 2017) has likely led to the assumption that light transmission through ridges is very low. However, according to our observations, inside the complex ridge structure there are cavities that appear as bright areas inside the ridge. Bright areas were present especially in ridges associated with leads and thin ice (**Figure 2** and Videos in the Supplementary Material). Furthermore, cracks at the sides of ridges (Katlein et al., 2015a), as well as often snow-free portions of high points in a ridge due to wind erosion (Sturm and Massom, 2010) have been suggested to transmit more light than adjacent level thick ice (Lange et al., 2017a). In addition, the side with less snow and close to the thin ice received more light and could therefore support higher algal growth rates, assuming light limitation at the thick-ice side (**Table 1**).

Snow infiltration communities received more light (PAR transmittance 3–14%) than ridge algal communities (PAR transmittance 0.06–8.5%) according to *in situ* measurements depending on the snow depth. This transmittance values were similar to those measured below ridges by an ROV in the Central Arctic (up to 5%) (Lange et al., 2017b), and lower than the PAR transmittance in the thin ice next to the ridge (5–40%) (Kauko et al., 2017). However, *in situ* measurements below the snow might be affected by lateral spreading of radiation and light scatter when removing part of the snow cover to introduce the sensor. Calculated *PAR* transmittance at the snow-ice interface (0.0025–5%) is generally lower than at the ridges (0.12–71%, range from transects in **Figure 4**) especially at the thin ice side. In some cases, the snow-ice interface received one order of magnitude more light than the water column below thick ice (Olsen et al., 2017). This implies that the snow-ice interface, when flooded, might provide an advantage for infiltrated pelagic diatoms that were growing at low rates in the water column at that time (Assmy et al., 2017).

The other key factor for algal growth is nutrient availability. The algal communities growing on the surfaces of submerged ledges in ridges have direct access to the nutrients in the sea water (**Figure 2**), while the ones in the snow-ice interface are dependent on the nutrients available *a priori* in the snow-ice layer and those percolating upwards from the water column (**Figure 3**). The observed currents below the ice crossed the ridge from the thick-ice side to the thin-ice side most of the time, especially toward the end of May, when stronger currents were observed (Figure S2). Before we drifted into the under-ice phytoplankton bloom (Assmy et al., 2017), the currents could have provided a constant flux of nutrients to the ridge surface-attached communities. Diatoms are able to store nutrients intracellularly without using them for growth immediately (Kamp et al., 2011; Fernández-Méndez et al., 2015). Based on our nutrient and current measurements, before 25 May (pre-bloom) one centimeter water layer moving below the ice provided 1.56×10^3-7.78×10^3 mmol N m^{-2} d^{-1} and 5.18×10^3-2.59×10^3 mmol Si m^{-2} d^{-1}, which is two orders of magnitude more than the calculated nutrient demand for these communities (15.7 mmol N m^{-2} d^{-1} and 38.9 mmol Si m^{-2} d^{-1}) using the method explained in Cota et al. (1987) and our own measured ratios and growth rates. This calculation suggests that the algae fixed to the ridge surfaces are flushed with enough nutrients to support their growth demands. Nevertheless, the currents and nutrient uptake dynamics inside the ridge and at the ice-water interface would need to be resolved better in order to assess the reality of the nutrient supply and limitations. The high C:N ratio (8.4 ± 0.5, $n = 6$) of the integrated biomass in the entire ledges might be due to the higher fraction of dead cells and/or detritus inside the ice as compared to the surface layers.

Nutrient concentrations in the melted slush at the snow-ice interface were highly variable, yet did reach surprisingly high concentrations, especially phosphate (up to 5 μM) and silicic acid (up to 12 μM). Nitrate was lower probably due to active consumption by *P. pouchetii* in the water column (Assmy et al., 2017). The high phosphate concentrations compared to the water column could be due to leakage of nutrients previously stored inside the algal cells (Needoba and Harrison, 2004; Kamp et al., 2011), active remineralization by bacteria (Arrigo and Thomas, 2004; Cowie et al., 2014) or atmospheric deposition with snow

precipitation (Nomura et al., 2010). A re-supply of nutrients can eventually come from the infiltrated surrounding seawater. At the time when the snow-ice infiltration communities were observed, nitrate concentrations in the water column were relatively low due to uptake by the under-ice *P. pouchetii* bloom (**Figure 4B**). However, if the ice had been previously flooded, nutrients from a different water mass could have been trapped in this layer. During the winter months of the N-ICE expedition, snow-ice formation was observed in February-March in ice floes of the same area and similar conditions (Granskog et al., 2017; Merkouriadi et al., 2017). Nutrient concentrations in the snow/slush sampled in March 2015 reached values up to 17 μM nitrate, 1 μM phosphate and 4 μM silicate. This amount of nitrate could yield 42 mg Chl *a* m^{-3}, which is one order of magnitude less than the maximum Chl *a* concentrations observed in the slush layer (362 mg Chl *a* m^{-3} SI1, **Table 2**). This indicates that the winter pre-formed nutrients are insufficient to explain the high biomass observed at the snow-ice interface.

In addition, the fact that we found several species of pelagic diatoms growing in the snow-ice interface points toward a flooding of the ice and establishment of the infiltration community in a different water mass with a more diatom-dominated phytoplankton community than the one we observed. Backtracking of Floe 4 (Olsen et al., 2017, **Figure 1**) indicates that the floe was closer to the shelf break some weeks earlier and these waters might have hosted a different phytoplankton community than the *P. pouchetii* dominated community observed on the Yermak Plateau. Indeed, the presence of abundant pelagic diatoms in surface waters on 8 June (Assmy et al., 2017) could explain the presence of pelagic diatoms in the snow-ice interface. On the other hand, the haptophyte *P. pouchetii*, despite being present in high cell abundance, was not performing well, indicated by the high amount of disintegrated cells and colonies observed under the microscope (**Figure 8**). These dead cells might be the reason for the high C:N ratio.

Distinct Algal Communities Occupy Different Ridge Surfaces

One interesting aspect of understudied ridge environments is that they seem to favor specific algal communities. Inside ridges, two clearly distinct communities were observed at the bottom and at the top of the submerged ledges (**Figure 7A**). A mixture of sea-ice pennate diatoms dominated by *N. frigida* and *Navicula* species at the bottom of the ledges is in accordance with previous observations of FYI and MYI, in which these species are dominating the bottom of the sea ice (Syvertsen, 1991; Melnikov et al., 2002). Sea-ice pennate diatoms excrete extracellular polymeric substances that enable them to attach inside brine channels at the under-side of the ice (Krembs et al., 2000, 2011; Bowman, 2013). On the contrary, the centric diatom *S. bioculatus* seems to have a clear advantage for colonizing the top of ledges (von Quillfeldt et al., 2009) as a fluffy algal layer since this species is not able to actively attach to the ice. This fluffy layer can be easily washed off by strong currents which agrees with previous observations of Arctic ridge communities (Hegseth, 1992; Ambrose et al., 2005). Furthermore, their presence supports the protective role of interior ridge cavities from currents (**Figure 2**).

The difference in the photoacclimation parameter (E_k) between the *Nitzschia* (421 μmol photons m^{-2} s^{-1} on average) and the *Shionodiscus*-dominated communities (266 μmol photons m^{-2} s^{-1} on average) might indicate that different parts of the submerged ledges receive on average different light intensities that favor different species that are able to acclimate to those light conditions. For example, *S. bioculatus* is more light sensitive and better shade adapted since it usually performs poorly under high light environments such as melt ponds (Assmy et al., 2013). Small-scale light measurements inside ridges and a spatially resolved light transmission model for complex under-ice structures are needed to further confirm this hypothesis.

Diatoms vs. *Phaeocystis* at the Snow-Ice Interface

The snow-ice interface had no distinct biotopes within the slush layer. Nevertheless it is interesting to compare the species that accumulated in the infiltration layer with the ones in the water column, which in this study was the source of the snow infiltration community. In the literature there are examples of snow-ice interface layers dominated by *Phaeocystis* (McMinn and Hegseth, 2004), by diatoms (Buck et al., 1998), or by a mixture of both (Kristiansen et al., 1998). During our study, we encountered five snow infiltration communities dominated by *P. pouchetii* (SI1, SI2, SI5, SI7, and SI8), and three dominated by diatoms (SI3, SI4, and SI6), although both groups were present in all of them. Differences in *Phaeocystis* vs. diatom dominance could reflect differences in phytoplankton composition in the source waters when infiltration occurred through the cracks in the ice or the time since flooding occurred at a particular site, the latter on the scale of community succession. *Phaeocystis pouchetii* was the most abundant species based on cell numbers in the water column at the time of sampling (Assmy et al., 2017), which is consistent with its presence in the infiltration community. This species is supposed to be very plastic since it can adapt its photosynthetic efficiency to the rapidly changing light regime (Palmisano et al., 1986; Cota et al., 1994; McMinn and Hegseth, 2004). However, during a side experiment, in which we removed the snow on top of SI1 and sampled it 24 h later, we could observe a decrease in the healthy cell numbers of *Phaeocystis* and an increase in poor-quality cell numbers, with no significant change in the diatom composition (Figure S5). This indicates that *P. pouchetii* could not deal with the rapid increase in irradiance and that diatom frustules are more resistant to decay. The average E_k of SI1 was 331 ± 125 μmol photons m^{-2} s^{-1} ($n = 5$) and the measured E_d(PAR) below 0.2–0.7 m of snow ranged between 1 and 162 μmol photons m^{-2} s^{-1}. The difference between E_k and E_d indicates that the cells are adapted to a higher light intensity than what they were experiencing in the snow-ice interface at the time we measured light intensity below the snow. In general, the higher light intensities experienced in the snow-ice interface compared to the water column (<1% of incoming irradiance;

Assmy et al., 2017), as well as the low salinities at the snow-ice interface (6.5–21), might have negatively affected part of the *P. pouchetii* population, while not having as deleterious impact on the diatom portion of the community due to their rigid silica frustules. Similar findings have been observed in ice melt processing studies with respect to flagellate versus diatom species (Buck et al., 1998; Garrison et al., 2003). Pelagic diatoms such as *F. oceanica*, *C. gelidus*, and *Pseudo-nitzschia* sp. which were not abundant in the water column at the time of sampling but might have infiltrated previously, managed to rapidly accumulate in the snow-ice interface (**Figure 8** and Figure S3).

Future Predictions and Implications

With the ongoing changes in the Arctic icescape due to anthropogenic climate change, a shift in community composition and productivity of sea-ice algae is expected (Dupont, 2012; Fernández-Méndez et al., 2015; Hardge et al., 2016; Olsen et al., 2017). During May-June 2015, the percentage of ridge and deformed ice cover was very high (46–51%), in agreement with recent airborne surveys indicating that ridged ice can make up a substantial fraction of the pack ice (Haas et al., 2010). For example, in Fram Strait from 1990 to 2011 ridges contributed 66% of the mean thickness of sea ice (Hansen et al., 2014). In the coming decades, as the ice gets thinner and more dynamic due to increased temperatures and wind (Spreen et al., 2011; Renner et al., 2014), an increase in FYI pressure ridge formation is expected (Wadhams and Toberg, 2012). As we have shown in this study, FYI ridges close to refrozen leads can host high biomass of healthy algal communities and could therefore play an important role in the Arctic icescape's future productivity. We encourage future studies to focus on pressure ridges despite the sampling challenges, since they are an important and under-quantified part of the Arctic icescape.

The mean snow thickness observed on FYI on Floe 4 was 0.32 ± 0.20 m (Rösel et al., 2018), which is in the same range given in the Warren-Climatology based on observations from snow on thick MYI (snow of 0.33 m; Warren et al., 1999). Sea-ice and snow thicknesses have changed toward a thinner, FYI-dominated ice cover that had less time to collect snow than older ice (Gallet et al., 2017; Merkouriadi et al., 2017). The combination of thin and rapidly melting sea ice and a relatively thick snow cover, led to negative freeboard and flooding of approximately half of Floe 4. This situation might become more frequent in the future, as sea-ice thickness continues to decrease (Maslanik et al., 2007; Stroeve et al., 2012), while precipitation falling on sea ice has been predicted to increase north of Greenland and in the Eurasian basin of the high Arctic where the remaining ice will reside (Bintanja and Selten, 2014). In addition, in the Atlantic sector, the influence of an increasingly warm Atlantic water inflow will contribute to faster ice melt from below (Polyakov et al., 2017). Thus, the contribution of snow to sea-ice mass balance could increase (Granskog et al., 2017), with flooding events in early spring (Granskog et al., 2017; Provost et al., 2017). These conditions favor the accumulation of algae at the snow-ice interface. These snow-infiltration communities have been frequently observed in the Antarctic, where the ratio of snow-to-sea ice thickness is high. We hypothesize that this "Antarctification" of the Arctic icescape will lead to more frequent accumulation of sea-ice algae at the snow-ice interface, especially in the Atlantic sector, and that snow infiltration communities might play a similarly important role in sea-ice related productivity in the future Arctic, as in the Antarctic (Arrigo et al., 1997).

The consequences of more algae accumulating in these two environments are still unknown, but we can hypothesize that ridges will become hot spots of biomass that will fuel the ice-associated food chain, since they will be accessible for grazers (Gradinger et al., 2010) and their carbon will be transferred to upper trophic levels (Falk-Petersen et al., 2009). On the contrary, snow infiltration communities will remain largely inaccessible for larger grazers during the productive season, although some grazers have been observed at the ice surface in Antarctic sea ice (Schnack-Schiel et al., 2001), and will likely sink when the ice melts, strengthening the sympagic-benthic coupling (Søreide et al., 2013) if they are not being decomposed and remineralized by bacteria. Moreover, the different algal species accumulating in these environments will influence how much carbon is exported to the seafloor, given that diatoms are more efficient carbon exporters than *P. pouchetii* (Reigstad and Wassmann, 2007). In terms of timing, while snow infiltration communities seem to appear only at the end of the productive season linked to ice melt, ridge communities are likely important year-round but particularly during the summer melt season when most ice algal biomass is lost from level sea ice. Thus, pressure ridges might act as refuges for the ice-associated flora and fauna during times of rapid melt and as an algal seed bank for newly formed ice.

The key points of this study are:

- Ridge algal communities can account for most of the sea-ice biomass when compared with other sea-ice environments, while the snow infiltration communities are difficult to upscale since they occur below thick snow along cracks, but they are locally important for sea-ice biomass estimates at the end of the productive season.
- Ridges are a favorable environment for algal growth because they provide extensive surfaces for attachment, shelter from strong currents, light conduits and a sufficient nutrient supply.
- Snow ice interfaces present high accumulations of algal biomass probably due to physical accumulation, higher irradiance than below the ice and shelter from grazers.
- Ridges host distinct algal communities with different light acclimation parameters and attachment strategies. Pennate sea-ice diatoms are found in the bottom part of the ledges, while *S. bioculatus* forms a fluffy layer on the top part of the ledges.
- Infiltration communities were dominated by the haptophyte *P. pouchetii* and pelagic chain-forming diatoms which were performing better than *P. pouchetii*.

We conclude that both, ridges and the snow-ice interface are important and understudied environments in the Arctic ecosystem. This study provides a comprehensive description of these two environments and, thus, can be used as a baseline for more extensive studies in the future. An assessment of the role of

FYI ridges and snow infiltration communities for Arctic sea-ice biomass and productivity will become more important in the future with the ongoing trends of sea-ice thinning and increase in precipitation.

AUTHOR CONTRIBUTIONS

All coauthors contributed to data collection, analysis, and interpretation. The conception and design of the study was led by PA, PD, HH, CM, and MF-M. Writing of the manuscript was done by MF-M with input from all coauthors.

FUNDING

This study was supported by the Centre of Ice, Climate and Ecosystems at the Norwegian Polar Institute through the N-ICE2015 project. PA, PD, LO, HK, CM, BS, and HH were supported by the Research Council of Norway (project Boom or Bust no. 244646). MF-M, PA, CM, AR, and HH were supported by the Ministry of Foreign Affairs, Norway, through the ID Arctic project. AJ was funded by the Norwegian Research Council (NFR) through the NORRUSS program (NFR project no. 233896) and we were thankful for using resources developed under CIRFA (NFR number 237906). The ROV purchase was funded by the Canada Foundation for Innovation (CFI) grant to CM and JE.

ACKNOWLEDGMENTS

We would like to thank the captain and crew of the RV *Lance* and the polar bear guards for making the sampling possible. We acknowledge the work of Max König and George Roth with **Figure 1A** map and Vasilii Kustov for the AUV aerial pictures of Floes 3 and 4 in **Figures 1B,C**. Radarsat-2 data was provided by NSC/KSAT under the Norwegian-Canadian Radarsat agreement 2015. We recognize the efforts of Max König (NPI) and Thomas Kræmer (UiT) for making the co-located satellite image acquisitions possible.

SUPPLEMENTARY MATERIAL

The Supplementary Material for this article can be found online at: https://www.frontiersin.org/articles/10.3389/fmars.2018.00075/full#supplementary-material

The video for this article can be found online at: https://figshare.com/s/d31c7742e889e31c6b32

REFERENCES

Ackley, S. F., Lewis, M. J., Fritsen, C. H., and Xie, H. (2008). Internal melting in Antarctic sea ice: development of "gap layers." *Geophys. Res. Lett.* 35, 1–5. doi: 10.1029/2008GL033644

Alverson, A. J., Kang, S.-H., and Theriot, E. C. (2006). Cell wall morphology and systematic importance of *Thalassiosira ritscheri* (Hustedt) Hasle, with a description of *Shionodiscus* gen. nov. *Diatom Res.* 21, 251–262. doi: 10.1080/0269249X.2006.9705667

Ambrose, W. G. Jr., von Quillfeldt, C., Clough, L. M., Tilney, P. V. R., and Tucker, T. (2005). The sub-ice algal community in the Chukchi sea: large- and small-scale patterns of abundance based on images from a remotely operated vehicle. *Polar Biol.* 28, 784–795. doi: 10.1007/s00300-005-0002-8

Arrigo, K. R., and Thomas, D. N. (2004). Large scale importance of sea ice biology in the Southern Ocean. *Antarct. Sci.* 16, 471–486. doi: 10.1017/S0954102004002263

Arrigo, K. R., and van Dijken, G. L. (2015). Continued increases in Arctic Ocean primary production. *Progr. Oceanogr.* 136, 60–70. doi: 10.1016/j.pocean.2015.05.002

Arrigo, K. R., and van Dijken, G. L. (2011). Secular trends in Arctic Ocean net primary production. *J. Geophys. Res.* 116:C09011. doi: 10.1029/2011JC007151

Arrigo, K. R., Perovich, D. K., Pickart, R. S., Brown, Z. W., van Dijken, G. L., Lowry, K. E., et al. (2012). Massive phytoplankton blooms under Arctic sea ice. *Science* 336, 1408. doi: 10.1126/science.1215065

Arrigo, K. R., Worthen, D. L., Lizotte, M. P., Dixon, P., and Dieckmann, G. (1997). Primary production in Antarctic sea ice. *Science* 276, 394–397. doi: 10.1126/science.276.5311.394

Assmy, P., Duarte, P., Dujardin, J., Fernández-Méndez, M., Fransson, A., Hodgson, R., et al. (2016). *N-ICE2015 Water Column Biogeochemistry*. Norwegian Polar Institute.

Assmy, P., Ehn, J. K., Fernández-Méndez, M., Hop, H., Katlein, C., Sundfjord, A., et al. (2013). Floating ice-algal aggregates below melting arctic sea ice. *PLoS ONE* 8:e76599. doi: 10.1371/journal.pone.0076599

Assmy, P., Fernández-Méndez, M., Duarte, P., Meyer, A., Randelhoff, A., Mundy, C. J., et al. (2017). Leads in Arctic pack ice enable early phytoplankton blooms below snow-covered sea ice. *Sci. Rep.* 7:40850. doi: 10.1038/srep40850

Barber, D. G., Hop, H., Mundy, C. J., Else, B., Dmitrenko, I. A., Tremblay, J.-E., et al. (2015). Selected physical, biological and biogeochemical implications of a rapidly changing Arctic Marginal Ice Zone. *Progr. Oceanogr.* 139, 122–150. doi: 10.1016/j.pocean.2015.09.003

Bélanger, S., Cizmeli, S. A., Ehn, J., Matsuoka, A., Doxaran, D., Hooker, S., et al. (2013). Light absorption and partitioning in Arctic Ocean surface waters: impact of multi year ice melting. *Biogeosciences* 10, 5619–5670. doi: 10.5194/bgd-10-5619-2013

Bendschneider, K., and Robinson, R. I. (1952). A new Spectrophotometric method for the determination of nitrite in seawater. *J. Mar. Res.* 2, 87–96.

Bintanja, R., and Selten, F. M. (2014). Future increases in Arctic precipitation linked to local evaporation and sea-ice retreat. *Nature* 509, 479–482. doi: 10.1038/nature13259

Booth, B. C., and Horner, R. A. (1997). Microalgae on the Arctic Ocean Section, 1994: species abundance and biomass. *Deep Sea Res. Part II* 44, 1607–1622. doi: 10.1016/S0967-0645(97)00057-X

Bowman, J. P. (2013). "Sea-ice microbial communities," in *The Prokaryotes-Prokaryotic Communities and Ecophysiology*, eds E. Rosenberg, E. F. DeLong, S. Lory, E. Stackebrandt, and F. Thompson (Berlin; Heidelberg: Springer), 139–161.

Brown, T., Assmy, P., Hop, H., Wold, A., and Belt, S. (2017). Transfer of ice algae carbon to ice-associated amphipods in the high-Arctic pack ice environment. *J. Plankton Res.* 39, 664–674. doi: 10.1093/plankt/fbx030

Buck, K. R., Nielsen, T. G., Hansen, B. W., Gastrup-Hansen, D., and Thomsen, H. A. (1998). Infiltration phyto- and protozooplankton assemblages in the annual sea ice of Disko Island, West Greenland, spring 1996. *Polar Biol.* 20, 377–381. doi: 10.1007/s003000050317

Canadian Ice Service (CIS) Meteorological Service of Canada, Environment Canada (2005). *Manual of Standard Procedures for Observing and Reporting Ice Condition (MANICE),* Revised 9th Edition. Canadian Ice Service (CIS) Meteorological Service of Canada, Environment Canada.

Casey, J. A., Beckers, J., Busche, T., and C. H. (2014). "Towards the retrieval of multi-year sea ice thickness and deformation state from polarimetric C- and X-band SAR observations," in *IEEE International Geoscience and Remote Sensing Symposiym (IGARSS)* (Quebec City, QC).

Chamnansinp, A., Li, Y., Lundholm, N., and Moestrup, O. (2013). Global diversity of two widespread, colony-forming diatoms of the marine plankton, *Chaetoceros socialis* (syn. *C. radians)* and *Chaetoceros gelidus* sp. nov. *J. Phycol.* 49, 1128–1141. doi: 10.1111/jpy.12121

Cota, G. F., Prinsenberg, S. J., Bennett, E. B., Loder, J. W., Lewis, M. R., Anning, J. L., et al. (1987). Nutrient fluxes during extended blooms of Arctic ice algae. *Arctic* 92, 1951–1962. doi: 10.1029/JC092iC02p01951

Cota, G. F., Smith, W. O., and Mitchell, B. G. (1994). Photosynthesis of *Phaeocystis* in the Greenland Sea. *Limnol. Oceanogr.* 39, 948–953. doi: 10.4319/lo.1994.39.4.0948

Cowie, R., Williams, G., Maas, E., Voyles, K., and Ryan, K. (2014). Antarctic sea-ice microbial communities show distinct patterns of zonation in response to algal-derived substrates. *Aquat. Microb. Ecol.* 73, 123–134. doi: 10.3354/ame01710

Doulgeris, A. P. (2013). "A simple and extendable segmentation method for multi-polarisation SAR Images," in *POLinSAR 2013* (Frascati).

Doulgeris, A. P., and Eltoft, T. (2010). Scale mixture of Gaussian modelling of polarimetric SAR data. *EURASIP J. Appl. Signal Proc.* 2010:874592. doi: 10.1155/2010/874592

Dupont, F. (2012). Impact of sea-ice biology on overall primary production in a biophysical model of the pan-Arctic Ocean. *J. Geophys. Res.* 117, C00D17. doi: 10.1029/2011JC006983

Falk-Petersen, S., Haug, T., Hop, H., Nilssen, K. T., and Wold, A. (2009). Transfer of lipids from plankton to blubber of harp and hooded seals off East Greenland. *Deep Sea Res. Part II* 56, 2080–2086. doi: 10.1016/j.dsr2.2008.11.020

Fernández-Méndez, M., Katlein, C., Rabe, B., Nicolaus, M., Peeken, I., Bakker, K., et al. (2015). Photosynthetic production in the central Arctic Ocean during the record sea-ice minimum in 2012. *Biogeosciences* 12, 3525–3549. doi: 10.5194/bg-12-3525-2015

Fernández-Méndez, M., Wenzhöfer, F., Peeken, I., Sørensen, H. L., Glud, R. N., and Boetius, A. (2014). Composition, buoyancy regulation and fate of ice algal aggregates in the Central Arctic Ocean. *PLoS ONE* 9:e107452. doi: 10.1371/journal.pone.0107452

Gallet, J.-C., Merkouriadi, I., Liston, G. E., Polashenski, C., Hudson, S., Rösel, A., et al. (2017). Spring snow conditions on Arctic sea ice north of Svalbard, during the Norwegian young sea ICE (N-ICE2015) expedition. *J. Geophys. Res. Atmos.* 122, 10820–10836. doi: 10.1002/2016JD026035

Garrison, D. L., Jeffries, M. O., Gibson, A., Coale, S. L., Neenan, D., Fritsen, C., et al. (2003). Development of sea ice microbial communities during autumn ice formation in the Ross Sea. *Mar. Ecol. Progr. Ser.* 259, 1–15. doi: 10.3354/meps259001

Gosselin, M., Levasseur, M., Wheeler, P. A., Horner, R. A., Boothg, B. C., and Booth, B. C. (1997). New measurements of phytoplankton and ice algal production in the Arctic Ocean. *Deep Sea Res. Part II* 44, 1623–1644. doi: 10.1016/S0967-0645(97)00054-4

Gradinger, R., Bluhm, B., and Iken, K. (2010). Arctic sea-ice ridges — Safe heavens for sea-ice fauna during periods of extreme ice melt? *Deep. Res. Part II* 57, 86–95. doi: 10.1016/j.dsr2.2009.08.008

Granskog, M. A., Assmy, P., Gerland, S., Spreen, G., Steen, H., and Smedsrud, L. H. (2016). Arctic research on thin ice: consequences of Arctic sea ice loss. *Eos* 97. doi: 10.1029/2016EO044097

Granskog, M. A., Rösel, A., Dodd, P. A., Divine, D. V., Gerland, S., Martama, T., et al. (2017). Snow contribution to first-year and second-year Arctic sea ice mass balance north of Svalbard. *J. Geophys. Res. Ocean.* 122, 2539–2549. doi: 10.1002/2016JC012398

Grasshoff, K. (1965). *On the Automatic Determination of Phosphate, Silicate and Fluoride in Seawater*. ICES Hydrographic Committee Report, 129.

Gulliksen, B., and Lønne, O. J. (1989). Distribution, abundance, and ecological importance of marine sympagic fauna in the Arctic. *Reun. Cons. Int. Explor. Mer.* 188, 133–138.

Haas, C., Hendricks, S., Eicken, H., and Herber, A. (2010). Synoptic airborne thickness surveys reveal state of Arctic sea ice cover. *Geophys. Res. Lett.* 37:L09501. doi: 10.1029/2010GL042652

Hansen, E., Ekeberg, O. C., Gerland, S., Pavlova, O., Spreen, G., and Tschudi, M. (2014). Variability in categories of Arctic sea ice in Fram Strait. *J. Geophys. Res. Ocean.* 119, 7175–7189. doi: 10.1002/2014JC010048

Hardge, K., Peeken, I., Neuhaus, S., Lange, B. A., Stock, A., Stoeck, T., et al. (2016). The importance of sea ice for exchange of habitat-specific protist communities in the Central Arctic Ocean. *J. Mar. Syst.* 165, 124–138. doi: 10.1016/j.jmarsys.2016.10.004

Hegseth, E. N. (1992). Sub-ice algal assemblages of the Barents Sea: Species composition, chemical composition, and growth rates. *Polar Biol.* 12, 485–496. doi: 10.1007/BF00238187

Hop, H., and Pavlova, O. (2008). Distribution and biomass transport of ice amphipods in drifting sea ice around Svalbard. *Deep Sea Res. Part II Top. Stud. Oceanogr.* 55, 2292–2307. doi: 10.1016/j.dsr2.2008.05.023

Horner, R. A., Syvertsen, E. E., Thomas, D. P., and Lange, C. (1988). Proposed terminology and reporting units for sea ice algal assemblages. *Polar Biol.* 8, 249–253. doi: 10.1007/BF00263173

Høyland, K. (2007). Morphology and small-scale strength of ridges in the North-western Barents Sea. *Cold Reg. Sci. Technol.* 48, 169–187. doi: 10.1016/j.coldregions.2007.01.006

Hudson, S. R., Cohen, L., and Walden, V. P. (2016). *N-ICE2015 Surface Broadband Radiation Data*. Norwegian Polar Institute.

Jakobsson, M., Mayer, L., Coakley, B., Dowdeswell, J. A., Forbes, S., Fridman, B. et al. (2012). The international bathymetric chart of the Arctic Ocean (IBCAO) version 3.0. *Geophys. Res. Lett.* 39:L12609. doi: 10.1029/2012GL052219

Ji, R., Jin, M., and Øystein, V. (2013). Sea ice phenology and timing of primary production pulses in the Arctic Ocean. *Glob. Chang. Biol.* 19, 734–741. doi: 10.1111/gcb.12074

Johnsen, G., and Sakshaug, E. (2007). Biooptical characteristics of PSII and PSI in 33 species (13 pigment groups) of marine phytoplankton, and the relevance for pulseamplitude-modulated and fast-repetition-rate fluorometry. *J. Phycol.* 43, 1236–1251. doi: 10.1111/j.1529-8817.2007.00422.x

Kamp, A., de Beer, D., Nitsch, J. L., Lavik, G., and Stief, P. (2011). Diatoms respire nitrate to survive dark and anoxic conditions. *Proc. Natl. Acad. Sci. U.S.A.* 108, 5649–5654. doi: 10.1073/pnas.1015744108

Katlein, C., Arndt, S., Nicolaus, M., Perovich, D. K., and Jakuba, M., V (2015a). Influence of ice thickness and surface properties on light transmission through Arctic sea ice. *J. Geophys. Res. Ocean.* 120, 5932–5944. doi: 10.1002/2015JC010914

Katlein, C., Fernández-Méndez, M., Wenzhöfer, F., and Nicolaus, M. (2015b). Distribution of algal aggregates under summer sea ice in the Central Arctic. *Polar Biol.* 38, 719–731. doi: 10.1007/s00300-014-1634-3

Katlein, C., Perovich, D. K., and Nicolaus, M. (2016). Geometric effects of an inhomogeneous sea ice cover on the under ice light field. *Front. Earth Sci.* 4:6. doi: 10.3389/feart.2016.00006

Kauko, H. M., Taskjelle, T., Assmy, P., Pavlov, A. K., Mundy, C., Duarte, P., et al. (2017). Windows in Arctic sea ice: light transmission and ice algae in a refrozen lead. *J. Geophys. Res. Biogeosci.* 122, 1486–1505. doi: 10.1002/2016JG003626

Kiko, R., Kern, S., Kramer, M., and Mütze, H. (2017). Colonization of newly forming Arctic sea ice by meiofauna: a case study for the future Arctic? *Polar Biol.* 40, 1277–1288. doi: 10.1007/s00300-016-2052-5

Krembs, C., Eicken, H., and Deming, J. W. (2011). Exopolymer alteration of physical properties of sea ice and implications for ice habitability and biogeochemistry in a warmer Arctic. *Proc. Natl. Acad. Sci. U.S.A.* 108, 3653–3658. doi: 10.1073/pnas.1100701108

Krembs, C., Gradinger, R., and Spindler, M. (2000). Implications of brine channel geometry and surface area for the interaction of sympagic organisms in Arctic sea ice. *J. Exp. Mar. Bio. Ecol.* 243, 55–80. doi: 10.1016/S0022-0981(99)00111-2

Krembs, C., Tuschling, K., and v. Juterzenka, K. (2002). The topography of the ice-water interface – its influence on the colonization of sea ice by algae. *Polar Biol.* 25, 106–117. doi: 10.1007/s003000100318

Kristiansen, S., Farbrot, T., Kuosa, H., Myklestad, S., and von Quillfeldt, C. H. (1998). Nitrogen uptake in the infiltration community, an ice algal community in Antarctic pack-ice. *Polar Biol.* 19, 307–315. doi: 10.1007/s003000050251

Lange, B. A., Flores, H., Michel, C., Beckers, J. F., Bublitz, A., Casey, J. A., et al. (2017a). Pan-Arctic sea ice-algal chl a biomass and suitable habitat are largely underestimated for multi-year ice. *Glob. Chang. Biol.* 23, 4581–4597. doi: 10.1111/gcb.13742t

Lange, B. A., Katlein, C., Castellani, G., Fernández-Méndez, M., Nicolaus, M., Peeken, I., et al. (2017b). Characterizing spatial variability of ice algal chlorophyll *a* and net primary production between sea ice habitats using horizontal profiling platforms. *Front. Mar. Sci.* 4:349. doi: 10.3389/fmars.2017.00349

Lange, B. A., Katlein, C., Nicolaus, M., Peeken, I., and Flores, H. (2016). Sea ice algae chlorophyll *a* concentrations derived from under-ice spectral radiation profiling platforms. *J. Geophys. Res. Ocean.* 121, 8511–8534. doi: 10.1002/2016JC011991

Lee, S. H., Stockwell, D. A., Joo, H., Son, Y. B., Kang, C., and Whitledge, T. E. (2012). Phytoplankton production from melting ponds on Arctic sea ice. *J. Geophys. Res.* 117, 1–11. doi: 10.1029/2011JC007717

Legendre, L., Ackley, S., Dieckmann, G., Gulliksen, B., Horner, R., Hoshiai, T., et al. (1992). Ecology of sea ice biota. *Polar Biol.* 12, 429–444. doi: 10.1007/BF00243114

Leu, E., Mundy, C. J., Assmy, P., Campbell, K., Gabrielsen, T. M., Gosselin, M., et al. (2015). Arctic spring awakening— Steering principles behind the phenology of vernal ice algal blooms. *Progr. Oceanogr.* 139, 151–170. doi: 10.1016/j.pocean.2015.07.012

Leu, E., Søreide, J. E., Hessen, D. O., Falk-Petersen, S., and Berge, J. (2011). Consequences of changing sea-ice cover for primary and secondary producers in the European Arctic shelf seas: timing, quantity, and quality. *Progr. Oceanogr.* 90, 18–32. doi: 10.1016/j.pocean.2011.02.004

Light, B., Grenfell, T. C., and Perovich, D. K. (2008). Transmission and absorption of solar radiation by Arctic sea ice during the melt season. *J. Geophys. Res.* 113:C03023. doi: 10.1029/2006JC003977

Lønne, O. J. (1988). A diver-operated electric suction sampler for sympagic (=under-ice) invertebrates. *Polar Res.* 6, 135–136. doi: 10.3402/polar.v6i1.6854

MacDonald, Dettwiler, and Associates Ltd. (2016). *Radarsat-2 Product Description. RN-SP-52-1238*. MacDonald, Dettwiler, and Associates Ltd.

Maslanik, J. A., Fowler, C., Stroeve, J., Drobot, S., Zwally, J., Yi, D., et al. (2007). A younger, thinner Arctic ice cover: increased potential for rapid, extensive sea-ice loss. *Geophys. Res. Lett.* 34:L24501. doi: 10.1029/2007GL032043

McMinn, A., and Hegseth, E. N. (2004). Quantum yield and photosynthetic parameters of marine microalgae from the southern Arctic Ocean, Svalbard. *J. Mar. Biol. Assoc.* 84, 865–871. doi: 10.1017/S0025315404010112h

McNair, H. M., Brzezinski, M. A., and Krause, J. W. (2015). Quantifying diatom silicification with the fluorescent dye, PDMPO. *Limnol. Oceanogr. Methods* 13, 587–599. doi: 10.1002/lom3.10049

Melnikov, I. A., and Bondarchuk, L. L. (1987). Ecology of mass accumulations of colonial diatom algae under drifting Arctic ice. *Oceanology* 27, 233–236.

Melnikov, I. A., Kolosova, E. G., Welch, H. E., and Zhitina, L. S. (2002). Sea ice biological communities and nutrient dynamics in the Canada Basin of the Arctic Ocean. *Deep Sea Res. Part I Oceanogr. Res. Pap.* 49, 1623–1649. doi: 10.1016/S0967-0637(02)00042-0

Merkouriadi, I., Gallet, J.-C., Liston, G. E., Polashenski, C., Graham, R. M., and Gerland, S. (2017). Winter snow conditions on Arctic sea ice north of Svalbard, during the Norwegian young sea ICE (N-ICE2015) expedition. *J. Geophys. Res. Atmos.* 122, 10837–10854. doi: 10.1002/2017JD026753

Meyer, A., Sundfjord, A., Fer, I., Provost, C., Villacieros Robineau, N., Koenig, Z., et al. (2017). Winter to summer oceanographic observations in the Arctic Ocean north of Svalbard. *J. Geophys. Res. Oceans* 122, 6218–6237. doi: 10.1002/2016JC012391

Moran, S. B., Lomas, M. W., Kelly, R. P., Gradinger, R., Iken, K., and Mathis, J. T. (2012). Seasonal succession of net primary productivity, particulate organic carbon export and autotrophic community composition in the eastern Bering Sea. *Deep. Res. Part II* 65–70, 84–97. doi: 10.1016/j.dsr2.2012.02.011

Mundy, C. J., Gosselin, M., Ehn, J., Gratton, Y., Rossnagel, A., Barber, D. G., et al. (2009). Contribution of under-ice primary production to an ice-edge upwelling phytoplankton bloom in the Canadian Beaufort Sea. *Geophys. Res. Lett.* 36, 1–5. doi: 10.1029/2009GL038837

Mundy, C. J., Gosselin, M., Ehn, J. K., Belzile C., Poulin, M., Alou, E., et al. (2011). Characteristics of two distinct high-light acclimated algal communities during advanced stages of sea ice melt. *Polar Biol.* 34, 1869–1886. doi: 10.1007/s00300-011-0998-x

Needoba, J. A., and Harrison, P. J. (2004). Influence of low light and a light: dark cycle on NO_3 uptake, intracellular NO_3, and nitrogen isotope fractionation by marine phytoplankton. *J. Phycol.* 40, 505–516. doi: 10.1111/j.1529-8817.2004.03171.x

Nomura, D., Nishioka, J., Granskog, M. A., Krell, A., Matoba, S., Toyota, T., et al. (2010). Nutrient distributions associated with snow and sediment-laden layers in sea ice of the southern Sea of Okhotsk. *Mar. Chem.* 119, 1–8. doi: 10.1016/j.marchem.2009.11.005

Olsen, L. M., Laney, S. R., Duarte, P., Kauko, H. M., Fernández-Méndez, M., Mundy, C. J., et al. (2017). The seeding of ice-algal blooms in Arctic pack ice: the multiyear ice seed repository hypothesis. *J. Geophys. Res. Biogeosci.* 122, 1529–1548. doi: 10.1002/2016JG003668

Onstott, R. G. (1992). "SAR and scatterometer signatures of sea ice," *in Microwave Remote Sensing of Sea Ice,* ed F. D. Carsey (Washington, DC: American Geophysical Union), 73–104.

Palmisano, A. C., SooHoo, J. B., SooHoo, S. L., Kottmeier, S. T., Craft, L. L., and Sullivan, C. W. (1986). Photoadaptation in *Phaeocystis pouchetii* advected beneath annual sea ice in McMurdo Sound, Antarctica. *J. Plankton Res.* 8, 891–906. doi: 10.1093/plankt/8.5.891

Perovich, D. K. (1989). *Two-Stream Multilayer, Spectral Radiative Transfer Model for Sea Ice.* Defense Technical Information Center.

Polyakov, I. V., Pnyushkov, A. V., Alkire, M. B., Ashik, I. M., Baumann, T. M., Carmack, E. C., et al. (2017). Greater role for Atlantic inflows on sea-ice loss in the Eurasian Basin of the Arctic Ocean. *Science* 356, 285–291. doi: 10.1126/science.aai8204

Provost, C., Sennéchael, N., Miguet, J., Itkin, P., Rösel, A., Koenig, Z., et al. (2017). Observations of flooding and snow-ice formation in a thinner Arctic sea ice regime during the N-ICE2015 campaign: influence of basal ice melt and storms. *J. Geophys. Res. Ocean.* 122, 7115–7134. doi: 10.1002/2016JC012011

Reigstad, M., and Wassmann, P. (2007). Does *Phaeocystis* spp. contribute significantly to vertical export of organic carbon? *Biogeochemistry* 83, 217–234. doi: 10.1007/s10533-007-9093-3

Renner, A. H. H., Gerland, S., Haas, C., Spreen, G., Beckers, J. F., Hansen, E., et al. (2014). Evidence of Arctic sea ice thinning from direct observations. *Geophys. Res. Lett.* 41, 5029–5036. doi: 10.1002/2014GL060369

Robinson, D. H., Kolber, Z., and Sullivan, C. W. (1997). Photophysiology and photoacclimation in surface sea ice algae from McMurdo Sound, Antarctica. *Mar. Ecol.* 147, 243–256. doi: 10.3354/meps147243

Rösel, A., and King, J. (2017). *N-ICE2015 Ice Thickness, Snow Thickness, and Freeboard from Thickness Drillings [Data set]*. Norwegian Polar Institute.

Rösel, A., Divine, D., King, J. A., Nicolaus, M., Spreen, G., Itkin, P., et al. (2016a). *N-ICE2015 Total (Snow and Ice) Thickness Data from EM31 [Data set]*. Norwegian Polar Institute.

Rösel, A., Itkin, P., King, J., Divine, D., Wang, C., Granskog, M. A., et al. (2018). Thin sea ice, thick snow and widespread negative freeboard observed during N-ICE2015 north of Svalbard. *J. Geophys. Res. Oceans*. doi: 10.1002/2017JC012865. [Epub ahead of print].

Rösel, A., Polashenski, C. M., Liston, G. E., King, J. A., Nicolaus, M., Gallet, J., et al. (2016b). *N-ICE2015 Snow Depth Data with Magnaprobe [Data set]*. Tromsø: Norwegian Polar Institute.

Sakshaug, E., Stein, R., and Macdonald, R. W. (2004). "Primary and secondary production in the Arctic Seas," in *The Organic Carbon Cycle in the Arctic Ocean*, eds R. Stein and R. W. Macdonald (Berlin: Springer), 57–82.

Schnack-Schiel, S., Thomas, D. N., Haas, C., Dieckmann, G. S., and Alheit, R. (2001). The occurrence of the copepods *Stephos longipes* (Calanoida) and *Drescheriella glacialis* (Harpaticoida) in summer sea ice in the Weddell Sea, Antarctica. *Antarct. Sci.* 13, 150–157. doi: 10.1017/S0954102001000232

Sokal, R. R., and Rohlf, F. J. (2012). *Biometry: the Principles and Practice of Statistics in Biological Research*. New York, NY: W.H. Freeman and Company.

Søreide, J. E., Carroll, M. L., Hop, H., Ambrose Jr, W. G., Hegseth, E. N., and Falk-Petersen, S. (2013). Sympagic-pelagic-benthic coupling in Arctic and Atlantic waters around Svalbard revealed by stable isotopic and fatty acid tracers. *Mar. Biol. Res.* 9, 831–850. doi: 10.1080/17451000.2013.775457

Søreide, J. E., Leu, E., Berge, J., Graeve, M., and Falk-Petersen, S. (2010). Timing of blooms, algal food quality and *Calanus glacialis* reproduction and growth in a changing Arctic. *Glob. Chang. Biol.* 16, 3154–3163. doi: 10.1111/j.1365-2486.2010.02175.x

Sosik, H. M., and Olson, R. J. (2007). Automated taxonomic classification of phytoplankton sampled with imaging-in-flow cytometry. *Limnol. Oceanogr. Methods* 5, 204–216. doi: 10.4319/lom.2007.5.204

Spindler, M. (1994). Notes on the biology of sea ice in the Arctic and Antarctic. *Polar Biol.* 14, 319–324. doi: 10.1007/BF00238447

Spreen, G., Kwok, R., and Menemenlis, D. (2011). Trends in Arctic sea ice drift and role of wind forcing: 1992 – 2009. *Geophys. Res. Lett.* 38:L19501. doi: 10.1029/2011GL048970

Stroeve, J. C., Kattsov, V., Barrett, A., Serreze, M., Pavlova, T., Holland, M., et al. (2012). Trends in Arctic sea ice extent from CMIP5, CMIP3 and observations. *Geophys. Res. Lett.* 39:L16502. doi: 10.1029/2012GL052676

Strub-Klein, L., and Sudom, D. (2012). A comprehensive analysis of the morphology of first-year sea ice ridges. *Cold Reg. Sci. Technol.* 82, 94–109. doi: 10.1016/j.coldregions.2012.05.014

Sturm, M., and Massom, R. A. (2010). "Snow and sea ice," in *Sea Ice*, eds G. S. Dieckmann and D. N. Thomas (Oxford, UK: Blackwell Publishing Ltd.), 153–204.

Syvertsen, E. E. (1991). Ice algae in the Barents Sea: types of assemblages, origin, fate and role in the ice-edge phytoplankton bloom. *Polar Res.* 10, 277–287.

Taskjelle, T., Hudson, S. R., Pavlov, A., and Granskog, M. A. (2016). *N-ICE2015 Surface and Under-Ice Spectral Shortwave Radiation Data*. Norwegian Polar Institute.

Thomas, D. N. (ed.). (2017). *Sea Ice*, *3rd Edn.* West Sussex: Wiley-Blackwell.

Timco, G. W., and Burden, R. P. (1997). An analysis of the shapes of sea ice ridges. *Cold Reg. Sci. Technol.* 25, 65–77. doi: 10.1016/S0165-232X(96)00017-1

Tremblay, G., Belzile, C., Gosselin, M., Poulin, M., Roy, S., and Tremblay, J.-É. (2009). Late summer phytoplankton distribution along a 3500 km transect in Canadian Arctic waters: strong numerical dominance by picoeukaryotes. *Aquat. Microb. Ecol.* 54, 55–70. doi: 10.3354/ame01257

Utermöhl, H. (1958). Zur Vervollkommung der quantitativen Phytoplankton-Methodik. *Mitt. Int. Ver. Theor. Angew. Limnol.* 9, 1–38.

van Leeuwe, M. A., Tedesco, L., Arrigo, K. R., Assmy, P., Campbell, K., Meiners, K. M., et al. (2018). Microalgal community structure and primary production in Arctic and Antarctic sea ice: a synthesis. *Elem. Sci. Anth.* 6:4. doi: 10.1525/elementa.267

von Quillfeldt, C. H. (2000). Common diatom species in Arctic spring blooms : their distribution and abundance. *Bot. Mar.* 43, 499–516. doi: 10.1515/BOT.2000.050

von Quillfeldt, C. H., Hegseth, E. N., Sakshaug, E., Johnsen, G., and Syvertsen, E. E. (2009). "Ice algae," in *Ecosystem Barents Sea*, eds E. Sakshaug, G. Johnsen, and K. M. Kovacs (Trondheim: Tapir Aacademic Press), 285–302.

Wadhams, P., and Toberg, N. (2012). Changing characteristics of arctic pressure ridges. *Polar Sci.* 6, 71–77. doi: 10.1016/j.polar.2012.03.002

Walz, H. (2003). *Phytoplankton Analyzer Phyto-PAM and Phyto-Win software V 1.45, System Components and Principles of Operation*. Available online at: http://www.walz.com/downloads/manuals/phyto-pam/phyto_4e.pdf

Warren, S. G., Rigor, I. G., Untersteiner, N., Radionov, V. F., Bryazgin, N. N., Aleksandrov, Y. I., et al. (1999). Snow depth on arctic sea ice. *J. Climate* 12, 1814–1829.

Wassmann, P., Duarte, C. M., Agustí, S., and Sejr, M. K. (2011). Footprints of climate change in the Arctic marine ecosystem. *Glob. Chang. Biol.* 17, 1235–1249. doi: 10.1111/j.1365-2486.2010.02311.x

Webb, W. L., Starr, M., and Duane, N. (1974). Carbon dioxide exchange of *Alnus rubra*: a mathematical model. *Oecologia* 17, 281–291. doi: 10.1007/BF00345747

Werner, I. (2000). Faecal pellet production by Arctic under-ice amphipods – transfer of organic matter through the ice/water interface. *Hydrobiologia* 426, 89–96. doi: 10.1023/A:1003984327103

Conflict of Interest Statement: The authors declare that the research was conducted in the absence of any commercial or financial relationships that could be construed as a potential conflict of interest.

frontiers in Marine Science

ORIGINAL RESEARCH
published: 17 August 2018
doi: 10.3389/fmars.2018.00285

Phytoplankton Realized Niches Track Changing Oceanic Conditions at a Long-Term Coastal Station off Sydney Australia

Penelope A. Ajani[1]*, *Niall McGinty*[2], *Zoe V. Finkel*[3†] and *Andrew J. Irwin*[2†]

[1] Climate Change Cluster (C3), University of Technology, Sydney, NSW, Australia, [2] Department of Mathematics and Computer Science, Mount Allison University, Sackville, NB, Canada, [3] Environmental Science Program, Mount Allison University, Sackville, NB, Canada

OPEN ACCESS

Edited by:
Kristian Spilling,
Finnish Environment Institute (SYKE), Finland

Reviewed by:
Andrew M. Fischer,
University of Tasmania, Australia
Alena S. Gsell,
Netherlands Institute of Ecology (NIOO-KNAW), Netherlands

***Correspondence:**
Penelope A. Ajani
Penelope.Ajani@uts.edu.au

†Present Address:
Zoe V. Finkel,
Department of Oceanography, Dalhousie University, Halifax, NS, Canada
Andrew J. Irwin,
Department of Mathematics and Statistics, Dalhousie University, Halifax, NS, Canada

Specialty section:
This article was submitted to Marine Ecosystem Ecology, a section of the journal Frontiers in Marine Science

Received: 30 April 2018
Accepted: 25 July 2018
Published: 17 August 2018

Citation:
Ajani PA, McGinty N, Finkel ZV and Irwin AJ (2018) Phytoplankton Realized Niches Track Changing Oceanic Conditions at a Long-Term Coastal Station off Sydney Australia. Front. Mar. Sci. 5:285. doi: 10.3389/fmars.2018.00285

Phytoplankton dynamics are closely linked to the ocean-climate system with evidence that changing ocean conditions are substantially altering phytoplankton biogeography, abundance and phenology. Using phytoplankton community composition and environmental data spanning 1965 to 2013 from a long-term Pacific Ocean coastal station offshore from Sydney, Australia (Port Hacking 100 m), we used the Maximum Entropy Modelling framework (MaxEnt) to test whether phytoplankton realized niches are fixed or shift in response to changing environmental conditions. The mean niches of phytoplankton closely tracked changes in mean temperature, while the mean salinity and mixed layer depth realized niches were consistently at the extreme range of available conditions. Prior studies had shown a fixed niche for nitrate in some phytoplankton species at a site where nitrate concentration was decreasing and potentially limiting; however, at Port Hacking nitrate and silicate niches increased more rapidly than environmental conditions, apparently in response to periodic occurrences of elevated nutrient concentrations. This study provides further evidence that climate change model projections cannot assume fixed realized niches of biotic communities, whilst highlighting the importance of sustained ocean measurements from the southern hemisphere to enhance our understanding of global ocean trends.

Keywords: Port Hacking, climate change, MaxEnt, nitrate, species distribution models

INTRODUCTION

Warming of the Earth's ocean and atmosphere due to anthropogenic CO_2 emissions has seen a global average increase in surface air temperature of 0.85°C over the past century (IPCC, 2014), with the upper ocean trapping the majority of the anthropogenic heating (IPCC, 2013). Atmospheric warming is associated with a decrease in pH and acidification of ocean waters (Rost et al., 2008; Beaufort et al., 2011). It is in these upper, sunlit waters of the global ocean that phytoplankton flourish, producing ~ 45 Gt a^{-1} of organic carbon (Falkowski et al., 1998; Field et al., 1998). Phytoplankton are a critical food source for higher trophic levels, sustaining marine food webs, which culminate in important fish stocks (Falkowski et al., 2004; Doney, 2006; Richardson and Poloczanska, 2008).

The flow-on effects that changes in climate and phytoplankton communities may have on ocean food webs and global biogeochemical cycles are poorly understood yet potentially profound and include the potential for harmful algal bloom intensification (Edwards and Richardson, 2004; Gobler et al., 2017). Moreover, establishing links between climate change and trends in the structure of phytoplankton assemblages is challenging, as phytoplankton have been shown to exhibit orders-of-magnitude variability over seasonal, inter-annual and inter-decadal time scales (Zingone et al., 2010).

With the potential for rapid dispersal, high reproduction rates and unexpected genetic structuring (Koester et al., 2013), both the fundamental niche of phytoplankton species and the ecological space or realized niche occupied in a particular community (Hutchinson, 1957) may be adaptable to changing ocean conditions. The set of all abiotic and biotic conditions in which a species can persist is called the fundamental niche and is usually determined experimentally in controlled conditions. Observational studies of natural communities can be used to document the realized niche where a species actually occurs, which can be thought of as a modification of the fundamental niche resulting from competition and biotic interactions. Various niche characteristics (e.g., niche position, breadth, overlap, plasticity, and conservatism) have been estimated under varying single- or multi-stressor conditions both in the laboratory (Collins et al., 2014; Boyd et al., 2015; Thomas et al., 2016; Ji et al., 2017) and the field (Irwin et al., 2012; Brun et al., 2015). However, understanding the organismal tolerance and plasticity that will drive evolutionary change remains uncertain, with model projections of biotic communities under climate change still assuming fixed realized niches (Chivers et al., 2017).

Recent approaches have used many species with different trait values to seed marine ecosystem models to examine emergent biogeography of microbial communities (Follows et al., 2007). Field based observations have been used to compare the changes in biogeography of different functional groups of phytoplankton and zooplankton to the velocity of climate change (isotherm movement) (Chivers et al., 2017). Combined with species distribution modeling (SDM), field observations have been used to model phytoplankton biogeography between historical and projected future ocean conditions (Barton et al., 2016) and to track species over time at a single location (Irwin et al., 2015). In the latter example, modeled phytoplankton data from a long-term coastal station CARIACO (Carbon Retention in a Colored Ocean) off the coast of Venezuela, revealed that species niches were not stable over decadal time periods, but were able to exhibit some adaptive capacity to changes in environmental conditions. Many questions remain, however, as we assess the importance and generality of this phenomenon. Little is known about how quickly species respond to environmental changes, if some species or functional groups are particularly flexible or resistant to changes, and what is the potential for contrasting effects of individual environmental drivers or directional changes. More time series are needed to resolve these open questions.

The Port Hacking 100 m (at a depth of 100 m) coastal monitoring station (hereafter PH_{100m}), located on the east coast of Australia, is one of the longest established coastal stations in the Southern Hemisphere. Located 5 km from Sydney, this station has been the focus of many short-term phytoplankton and hydrological investigations since its inception in 1954, with its disparate phytoplankton datasets only recently assembled (Ajani et al., 2016). In 2009, this station became one of nine National Reference Stations located around Australia maintained by the Integrated Marine Observing System (IMOS) to monitor long-term changes in Australia's ocean (Lynch et al., 2014). PH_{100m} is located within a very complex oceanographic setting, dominated by the East Australian Current (EAC), which originates in the Coral Sea to the north and brings warm, oligotrophic waters into more temperate latitudes (Ridgway and Dunn, 2003). The EAC has strengthened and moved poleward (Ridgway and Hill, 2012; Wu et al., 2012) with long-term increases in temperature, salinity, and nitrate and a decline in silicate recorded at this station over the past 60 years (Thompson et al., 2009).

While no concomitant shift in total phytoplankton abundance has been reported at this station over the past 60 years, species composition over the past decade has seen a decline in dinoflagellates compared to diatoms toward the present. There is also an emerging dominance of two tropical species *Trichodesmium erythraeum* (cyanobacterium) and *Bacteriastrum* spp. (diatom) at this station (Ajani et al., 2014a,b). This shift in composition, however, has only been reported over the most recent decade, when water temperatures declined amidst a long-term warming signal.

With this in mind, we studied the realized niches of phytoplankton species at PH_{100m} to address the following questions. Do realized niches change in response to environmental change, or are they primarily conserved resulting in a restructuring of communities and changes in biogeography as environmental conditions change? The changes in physical and chemical conditions at PH_{100m} allowed us to test for changes in realized niches over time, so we refined this question by examining how rapidly realized niches change. Another refinement recognizes that the realized niche for some environmental variables may be much more plastic than for others, so we investigate if niches change at different rates for different variables. Many environmental conditions and changes in conditions are correlated, so we investigate if these correlations are reflected in the realized niches and their changes. Finally, we investigate if species respond to changes in the mean environmental conditions, or if more detailed information about the distribution of environmental conditions is required to anticipate changes to realized niches.

MATERIALS AND METHODS

Five disparate phytoplankton sampling campaigns were conducted at the PH_{100m} coastal station (34°7'3.36"E, 151°13'5.52"S, **Figure 1**) over the period from 1965 to 2013 (approximately ∼20 years of sampling over a ∼50 year period). These were coded OSL (1965–1966), HALLE (1978–1979), AJANI97 (1997–1998) AJANI98 (1998–2009), and NRS (2009–2013) and their sampling frequencies, methodologies and

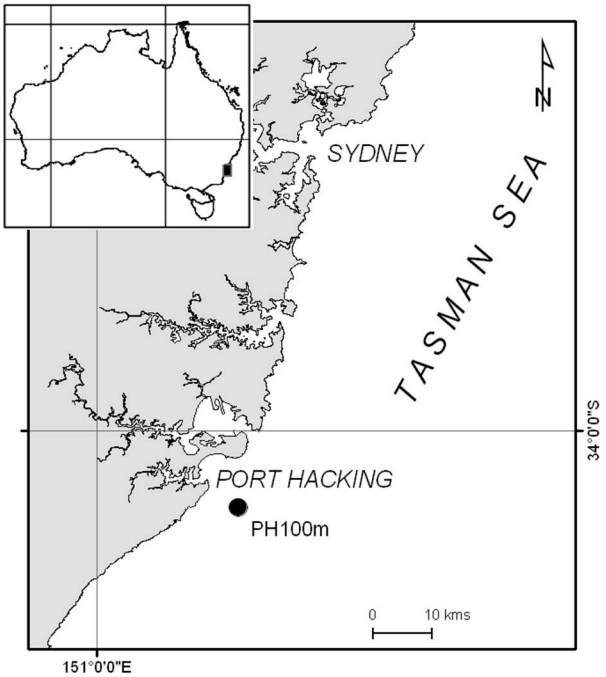

FIGURE 1 | Map of study area showing southeast Australia (inset) and the coastal monitoring station Port Hacking 100 m (PH_{100m}) indicated by black circle.

references are summarized in **Table 1**. In brief, phytoplankton samples were collected approximately weekly to monthly using either discrete bottle samples or phytoplankton mesh nets (20 or 37 μm) and preserved before microscopic examination. Cells were identified to the lowest possible taxon using light microscopy and where identification to species level was not possible, cells were assigned to genus level only (e.g., *Chaetoceros* spp., *Thalassiosira* spp. etc.). For comparability across sampling campaigns, certain taxa were pooled to genus level. Simultaneous meaurements of several environmental parameters including temperature (°C), salinity, oxidized nitrogen (μmol L^{-1} nitrate and nitrite, hereafter "nitrate"), and dissolved reactive silicate (μmol L^{-1}; hereafter "silicate") occurred during these sampling campaigns (refer to references in **Table 1** for all environmental collection and analytical methodologies).

All phytoplankton abundance data were pooled across 0–50 m except for AJANI97 and AJANI98 which were 0–100 m and converted to simple records of species presence, while all environmental parameters were averaged across the upper 50 m. To assess if the phytoplankton were tracking changes in thermal stratification at this location, we also calculated the mixed-layer depth (MLD) over the sampling duration. This was defined as the depth where the temperature was more than 0.5°C lower than the surface temperature (Levitus, 1982).

Differences in sampling methodology and frequency can introduce a sampling bias and effect model performance when performing niche models (Kramer-Schadt et al., 2013). Although this concern is largely focused on spatial distribution modeling, similar problems could arise from temporal models collected at a single station. Temporal filtering of weekly data to monthly reduced the number of viable species to model, but for those retained we found significant positive correlations ($r = 0.78$ to 0.93) between the filtered and unfiltered species in terms of how each species track their niche. Similarly, a comparison between the two principal modes of sample collection (net hauls and discrete bottle samples) during 2009, found that while cell counts were significantly lower in the bottle samples, over 72% of the species were collected by both methods and the five most abundant species were the same. We therefore did not correct for changes in sampling frequency or method. For sampling frequency in particular, the spatial filtering would have resulted in a significant loss of modeled species and our tests suggest there would be no change to the overall conclusions.

Tracking Changes in Phytoplankton Niches

To investigate whether phytoplankton niches have adapted to changing environmental conditions on a decadal scale at PH_{100m}, we divided the combined dataset into three distinct periods representing different thermal regimes.The first period, P1, represented four years of stable colder temperatures before the rapid warming during the mid 1990s, and included data from the years 1964, 1965, 1978, and 1979. The second period, P2, which included data from 1997 to 2004, showed no abrubt step-wise changes in environmental conditions but did exhibit a significant decline in ocean temperatures. The final period, P3, showed evidence of renewed warming and included data collected from 2005 to 2013. We chose the end of year midpoint as the division for the two periods separating the data into an initial post El Niño cooling phase (P2) and a cooler period with renewed warming (P3).

Secondly, we investigated how quickly phytoplankton track changes environmental conditions by observing the rate at which the niche changed on a rolling annual basis. We limited this analysis to the years between 1997 and 2013 due to the large gaps present between the earlier four years of data. We calculated a running mean niche of each species using a 4-year moving window which provided a possible total of 14 niche measurements (i.e., 1997–2001, 1998–2002, …, 2010–2013). For both analyses, species that were found to occur at least 15 times in at least one period (P1, P2, and P3), or within one 4-year window, were retained for subsequent niche modeling.

Statistical Analysis

We used the Maximum Entropy Modelling framework (MaxEnt, Phillips and Dudik, 2008) to estimate the logistic probability of finding a particular species in univariate or multivariate niche space by comparing the environmental conditions where a taxon is present with the measured background environment of all sampling events. MaxEnt has become one of the most popular algorithms used to model species distributions. It has consistently been found in comparative studies to give robust estimates and to perform as one of the best algorithms available (Elith and Leathwick, 2009). Our focus is on using MaxEnt to describe the realized niches of phytoplankton and to test for changes over time in these niches. Alternative modeling frameworks could be used

TABLE 1 | Phytoplankton sampling campaign codes, frequency, duration, methodology and reference from PH_{100m} coastal station (IMOS = Integrated Marine Observing System; NRS = National Reference Station).

Code	Period	Sampling frequency	Sampling methodology	Number of samples	Counting methodology	Reference
OSL	P1 Apr 1965–Apr 1966	Weekly	4.5 L using van Dorn sampler; discrete 0,10, 20 m pooled "surface"; 30 and 50 m pooled "intermediate"; 75 and 100 m pooled "bottom"	42	Diluted subsamples counted in gridded chamber to between 100 and 500 per ml range	Grant and Kerr, 1970
HALLE	P1 Apr 1978–Apr 1979	Weekly	24 L-duplicate casts with twin 6 L water sampler (Jitts, 1964); discrete 0, 10, 20, 30, 40, 50, 75, and 100 m;	38	Utermohl chamber and whole bottom counted at x200 magnification for rare and large species; 10–30 random fields counted for abundant diatoms and small flagellates	Hallegraeff, 1981
AJANI97	P2 Apr 1997–Apr 1998	Weekly	100 m vertical net haul – 37 μm mesh (Heron, 1982)	49	Lund cell and light microscope x400 magnification	Ajani et al., 2001
AJANI98	P2 and P3 Sept 1998–Dec 2009	Monthly	50 m vertical net haul-20 μm mesh	113	Lund cell and light microscope x400 magnification	Ajani et al., 2014a,b
NRS	P3 Feb 2009–Dec 2013	Monthly	Niskin bottles- integrated sample 0–50 m	44	Sedgewick-Rafter x200 magnification for large diatoms and dinoflagellates; 500–600x magnification for nanoplankton species	imos.aodn.org.au

P1, P2, and P3 refer to the 3 periods of analyses used in this manuscript; P3 starts in 2005 (see methods for additional detail).

ranging from regression to machine learning. MaxEnt is both highly flexible, with weak *a priori* assumptions about the response of each species to each condition, and highly interpretable in contrast with some "black-box" machine learning techniques. For each MaxEnt model run, a total of 100 bootstrap re-sampling runs were performed. Threshold and hinge responses were disabled as our focus is primarily on the mean niche conditions for each species and to reduce the likelihood of overfitting of the model (Elith et al., 2011). Model performance was evaluated by examining the area under the curve (AUC) of the receiving operator characteristic, where values approaching one suggest a higher probability that a model will correctly identify a species presence. Using the AUC as a single measure for evaluating model performance can be prone to several biases (Yackulic et al., 2013). Nevertheless, by raising the minimum AUC for inclusion of a model to 0.7, we successfully removed the most poorly fitted models that may have biased our results. We used the permutation importance to measure the contribution of each variable to the total AUC on a percentage scale by permuting the values of one variable at a time at random and observing the decrease in model performance. A large decrease in the AUC indicates that the variable is very important in the characterisation of the species' niche.

To investigate whether phytoplankton niches have adapted to changing conditions on a decadal scale, we focused on each environmental variable individually and used the probability response curves to calculate the mean realized niche of each modeled species for each period (P1, P2, P3) or 4-year moving window during the period 1997–2013. For the decadal analysis, the background data were sampled from all observations. For the moving window approach, the background data were sampled from the years included in the moving window. For both analyses, only species that were found to occur at least 15 times in at least one period (P1, P2, and P3), or within one 4-year window were examined. The 100 bootstrap samples provided an estimate of 95% confidence intervals of the mean niche for each species. We restricted our analysis to environmental conditions that were common to all periods and removed extreme values present within individual periods of the time series. Had they been included these extreme values could have had an effect on the species niche calculation, where a difference in niches would be found largely due to the change in available background conditions.

We performed several tests to examine the effect of the changing environment on the realized niches. For each environmental variables, we calculated the community average mean niche for all species within a period as well as the background environmental conditions. We hypothesize that the magnitude and direction of the changes in the niche and environmental differences will be similar. We also hypothesized that the degree of niche change is dependent upon the initial niche and its distance from the mean environmental conditions. To test this, we first examined species that were found in two or more periods and used a linear regression model to examine

the pair-wise relationship between the mean niche of the earliest period and the change in mean niches between the two periods. We then examined the rate at which changes to a species niche occurred. We computed the correlations between the running mean of the background environmental conditions and the running mean of the mean niche for all species that were modeled in at least 5 of the 14 time steps. To test for a delay in the response of the community to environmental change, we computed these correlations on simultaneous measures and with a lag of 1–4 years between the environmental conditions and the estimated mean niches. Since some of the changes in niches did not seem to be directly proportional to changes in the mean environmental conditions, we compared the distance between the mean niche and mean environmental conditions to the standard deviation of the environmental conditions in each 4-year moving window.

RESULTS

Phytoplankton Niche Modelling

A total of 34 species were present in at least two periods with a mean AUC of 0.7 or greater (**Supplementary Table 1**). The variation in mean AUC was low with a standard deviation of < 0.1 across all three periods (P1: 0.71 ± 0.089; P2: 0.81 ± 0.063; P3: 0.72 ± 0.061). Four environmental variables (temperature, salinity, mixed layer depth, and nitrate concentration) allowed comparisons across all three periods while comparisons for silicate concentration were only possible between the latter time periods P2–P3 (**Table 2**). A total of 16 species were present in both periods P1 and P2 and 31 species were present in periods P2 and P3 (**Supplementary Tables 2**, **3**). We found changes in the community average mean niches and the mean environmental conditions were always in the same direction for temperature, MLD and nitrate concentration between P1 and P2 and between P2 and P3. Changes in the community average mean niches exceeded changes in the environmental conditions for temperature, nitrate and silicate concentration (**Table 2**). Salinity and mixed layer depth changes were very small or not significantly different from the environment and mean niche between both pairs of periods. A few niche changes nominally in the opposing direction to changes in the environment all corresponded to small, non-significant changes in environmental conditions. Changes in the mean niches for each species were in the same direction as the environmental change for almost all species (**Supplementary Tables 2**, **3**). For each species, the magnitude of niche change was negatively associated with their initial niches, indicating that species with niches in the initial period (P1 or P2) farthest from new conditions in the second period (P2 or P3) exhibited the largest change in their mean niche (**Figure 2**). We interpreted this as a signal of direct pressure on the realized niche due to changes in environmental conditions.

The most important variables determining a species' niche varied between the three periods examined (**Table 3**). In P1, temperature was the most important variable for all species overall (with a mean permutation importance of 36%), with nitrate concentration (21%) being marginally more important than the two remaining variables (silicate was not available for this period). For P2 temperature was the third most important variable (18%) having been supplanted by the added variable silicate concentration (32%) as most important and nitrate concentration (20%) as the second most important. Period P3

TABLE 2 | Mean environmental conditions (top) and niches (bottom), 95% confidence interval on the mean, and change in means between two periods for temperature, mixed layer depth (MLD), salinity, nitrate and silicate concentrations over time (P1: 1965–1979, P2: 1997–2004, and P3: 2005–2009) at the Port Hacking monitoring station.

Variables	P1 Mean	P1 95% CI	P2–P1 Δ	P2 Mean	P2 95% CI	P3–P2 Δ	P3 Mean	P3 95% CI
ENVIRONMENT								
Temperature (°C)	18.58	(18.14–19.28)	**0.7**	19.28	(18.89–19.67)	**−0.47**	18.81	(18.49–19.14)
MLD (m)	28.59	(23.48–33.61)	−3.3	25.29	(21.01–29.63)	−3.14	22.15	(18.02–26.28)
Salinity	35.51	(35.48–35.54)	−0.02	35.49	(35.47–35.51)	−0.07	35.42	(35.40–35.44)
Nitrate (μmol L^{-1})	2.02	(1.73–2.31)	**−0.51**	1.51	(1.25–1.82)	**0.45**	1.96	(1.66-2.26)
Silicate (μmol L^{-1})	NA	NA	NA	1.31	(1.15–1.47)	−0.08	1.23	(1.16–1.4)
NICHES								
Temperature (°C)	18.23	(18.11–18.34)	**1.62**	19.85	(19.78–19.92)	**−1.11**	18.74	(18.62–18.86)
MLD (m)	73.1	(68.9–75.3)	−15.44	57.66	(51.66–61.66)	−4.96	52.7	(51.6–53.8)
Salinity	35.16	(35.13–35.19)	**0.13**	35.29	(35.25–35.33)	**−0.08**	35.21	(34.19–35.23)
Nitrate (μmol L^{-1})	3.59	(3.56–3.82)	**−1.72**	1.87	(1.64–2.0)	**1.88**	3.75	(3.69–3.81)
Silicate (μmol L^{-1})	NA	NA	NA	1.42	(1.31–1.53)	**1.15**	2.57	(2.39–2.75)

Differences between periods shown in bold are statistically significant ($P < 0.05$).

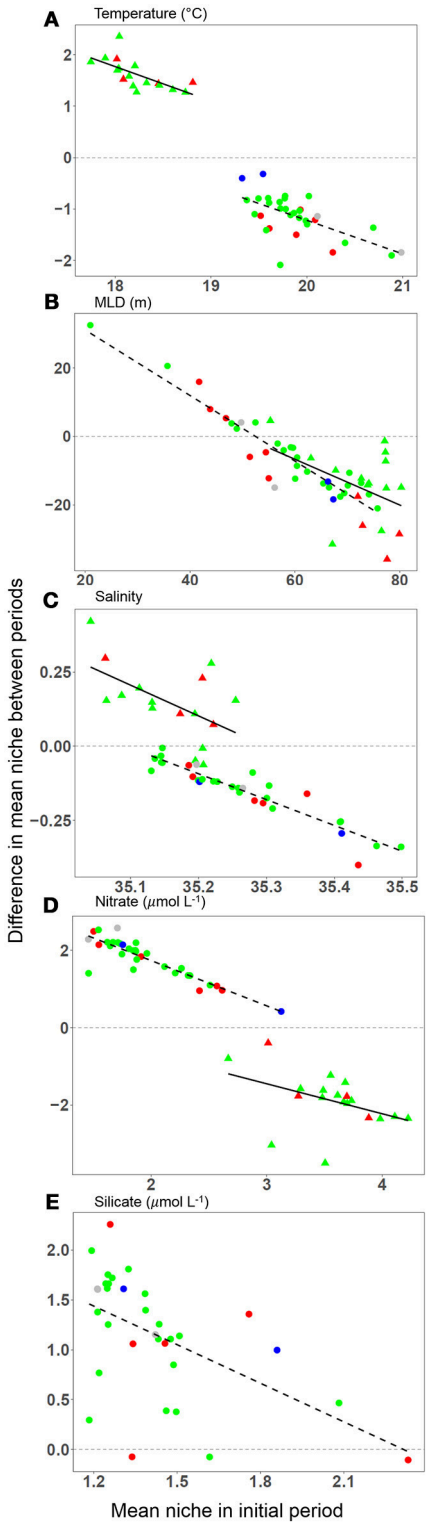

FIGURE 2 | Changes in the mean realized niche as a function of the mean niche in an initial period. Each panel displays changes for one variable between periods P1 and P2 (triangles) and between periods P2 and P3 (circles): **(A)** temperature (°C), **(B)** mixed layer depth (m), **(C)** salinity, **(D)** nitrate concentration (μmol L^{-1}), **(E)** silicate concentration (μmol L^{-1}). Each symbol *(Continued)*

FIGURE 2 | represents a single species. Regression lines illustrate that the greatest changes in the realized niche occur in species with an initial niche that is most dissimilar from the average conditions in the second period (P1–P2, solid line; P2–P3, dashed line). See **Table 2** for changes in mean environmental conditions and niches. Silicate niches were not available in P1, so the first difference is not shown in panel **(E)**. Colours correspond to the phytoplankton groups coccolithophores (gray), diatoms (green), dinoflagellates (red), and silicoflagellates (blue).

showed an increase in the importance of salinity (22%) and a slight decrease in importance for both nutrient variables (**Table 3**). Overall, all the predictors played an important role in determining the realized niches of species on average, with no clear signal in which one variable dominated the information characterizing the niches.

Tracking Change in Phytoplankton Niches

A total of 33 species appeared in suitable numbers of samples to model the niche at least once during the period 1997–2013 (**Supplementary Table 4**). There were strong positive correlations found between changes in environmental conditions and each species niche and the average niches of all species (**Figure 3**). We found no evidence of any lagged responses, meaning that the changes in mean niche likely occurred within one year of the corresponding change in the environment. The time-series analysis revealed three different patterns in the differences between the mean environment and mean realized niches and how they changed over time. For temperature, the mean niche was approximately equal to the mean temperature in the environment, changing at a similar rate and in the same direction. For salinity and mixed layer depth, the mean niches were at extreme values of the distributions of environmental conditions, corresponding to low (relatively fresh) salinity and large (relatively deep) mixed layer depths. Changes in environmental conditions and mean niches were relatively small for both of these variables (summarized in **Table 2**, **Supplementary Table 3**). A third pattern was observed for nitrate and silicate concentrations. Mean niches increased more rapidly than corresponding changes in the mean environmental conditions from 2000 to 2007. The changes arrested in the second half of the study from 2007 to 2013. Despite the increases in silicate niches, there was a steady decrease in the mean silicate concentrations between 1997 and 2013. We computed the difference between the community average mean niche and the mean environmental conditions for each variable. This separation between niches and environmental conditions was close to 0 for temperature, approximately constant for salinity and mixed layer depth, and increased rapidly for nitrate and silicate concentration. Since the mean environmental conditions was not predictive of this difference, we compared the difference to the standard deviation of the environmental conditions (**Figure 4**). Nitrate and silicate concentrations both showed strongly positive correlations demonstrating that changes in the distribution of environmental conditions (represented here by changes in the standard deviation, but likely due the increasing frequency of higher nutrient concentrations) led to the changes

TABLE 3 | The relative importance (Mean, %) and 95% confidence interval (CI) of each of the five environmental variables within each of the three periods (P1: 1964, 1965, 1978, 1979; P2: 1997–2004; P3:2005–2013) averaged over all species analyzed.

	P1		P2		P3	
Variable	**Mean**	**CI**	**Mean**	**CI**	**Mean**	**CI**
Temperature (°C)	36	(31.5–39.5)	17.8	(13.4–22.2)	20.8	(19.9–22.7)
MLD (m)	18.1	(15.3–21.9)	12.6	(9.4–15.8)	12.5	(10.9–14.1)
Salinity	21.4	(19.5–25.9)	16.7	(14.5–19.9)	24.1	(21.5–26.6)
Nitrate (μmol L^{-1})	23.9	(19–26.2)	20.1	(18.3–23)	18.8	(17–20.6)
Silicate (μmol L^{-1})	––	–	31.6	(26.5–36.7)	22.8	(19.5–26.1)

in the mean niches. No such relationship was found for the other environmental variables (dotted lines in **Figure 4**) Each variable is analyzed in a separate panel of **Figure 4** and the final panel **F** overlays all the variables, standardized to zero mean and unit variance in each axis to facilitate comparison across variables. The community was dominated by diatoms so we attempted to determine if the silicate effect was stronger in diatoms compared to other functional types, but the small number of species of other groups made a careful taxonomic analysis inconclusive.

Correlations in the Environment and Niche Interpretations

Correlations among environmental variables are ubiquitous in the ocean and always have the potential to complicate the analysis of observational data. Our focus has been on univariate species distribution models and the mean realized niche rather than on a multivariate model which might be selected to get the most explanatory power to be used for prediction. Univariate niches are generally easier to interpret (Elith et al., 2011; Irwin et al., 2012). The correlations among our predictors are generally small in this time series, and only significantly different from 0 for three pairs of variables: temperature and nitrate concentration, silicate and nitrate concentration, and a very small correlation between silicate concentration and salinity (**Table 4**). The sign of these correlations agrees with the relative changes in mean realized niches, but the relative changes in temperature and nitrate niches relative to changes in the mean environmental conditions are very different, indicating that there is an independent signal observed in changes in the temperature and nitrate realized niches.

DISCUSSION

The Port Hacking coastal monitoring station (PH_{100m}) is one of the longest running ocean time series in the Southern Hemisphere (**Figure 1**). The hydrography of the region exhibits complexity at several time scales (Hallegraeff and Jeffrey, 1993; Ajani et al., 2001, 2016; Pritchard et al., 2003). Over the last 60 years there has been a long-term increase in temperature (0.75°C $century^{-1}$), salinity (0.23 $century^{-1}$), and nitrate concentration (0.56 μmol L^{-1} $century^{-1}$) and decline in silicate concentration (−1.97 μmol L^{-1} $century^{-1}$) (Thompson et al., 2009). Superimposed on these multi-decadal trends are seasonal, annual, and decadal variations. In recent years (1997–2013) there has been a decline in salinity, likely due to an increase in rainfall, a modest decline in sea surface temperatures, a decline in mixed layer depth, an increase in annual average nitrate concentrations and a decline in silicate concentrations. Climate predictions for Australia include warmer ocean temperatures and more intense rainfall events across the nation, although annual-average rainfall is projected to decline (www.csiro.au/state-of-the-climate). Australian climate patterns are also influenced by the long-term increasing trend in global air and ocean temperatures (http://www.bom.gov.au). It has been hypothesized that the decline in silicate and other environmental conditions will lead to changes phytoplankton community composition at this site (Ajani et al., 2014a,b). Phytoplankton are rapid and effective indicators of changes in the oceanic environment (Richardson and Schoeman, 2004). Here we determine the capacity of the realized niche of phytoplankton at this coastal site to track changes in their environment conditions since 1965, with an emphasis on the years from 1997 through 2013.

Microbes may have a high capacity to adapt to climate change through selection on standing diversity and *de novo* mutation, although there may be limits on the ability of species to adapt to multiple stressors (Collins, 2013). In the laboratory, evolutionary change has been demonstrated in numerous microbial species including *Escherichia coli*, *Trichodesmium, Chlamydomonas*, and *Emiliania*, often in less than a thousand generations, indicating that marine phytoplankton may be able to adapt to climate change nearly as rapidly as it occurs (Frank and Slatkin, 1990; Collins and Bell, 2004; Benner et al., 2013; Collins, 2013; Hutchins et al., 2015; Walworth et al., 2016). Despite this evidence, many researchers assume that the physiological traits and niches of phytoplankton are fixed as this facilitates projections of the effects of climate change and there remain few studies documenting changes in phytoplankton niches over time, especially in the field (Thomas et al., 2004, 2012; Flombaum et al., 2013; Barton et al., 2016).

The fundamental niche is the full set of environmental conditions under which a species can persist, and for phytoplankton, this is typically defined in the laboratory. In the field, species are influenced by the interaction of multiple environmental conditions and simultaneous, competition and other biotic interactions, all of which are rarely examined in the lab and as a result, their realized niche is generally a limited subset of their fundamental niche. At a tropical site

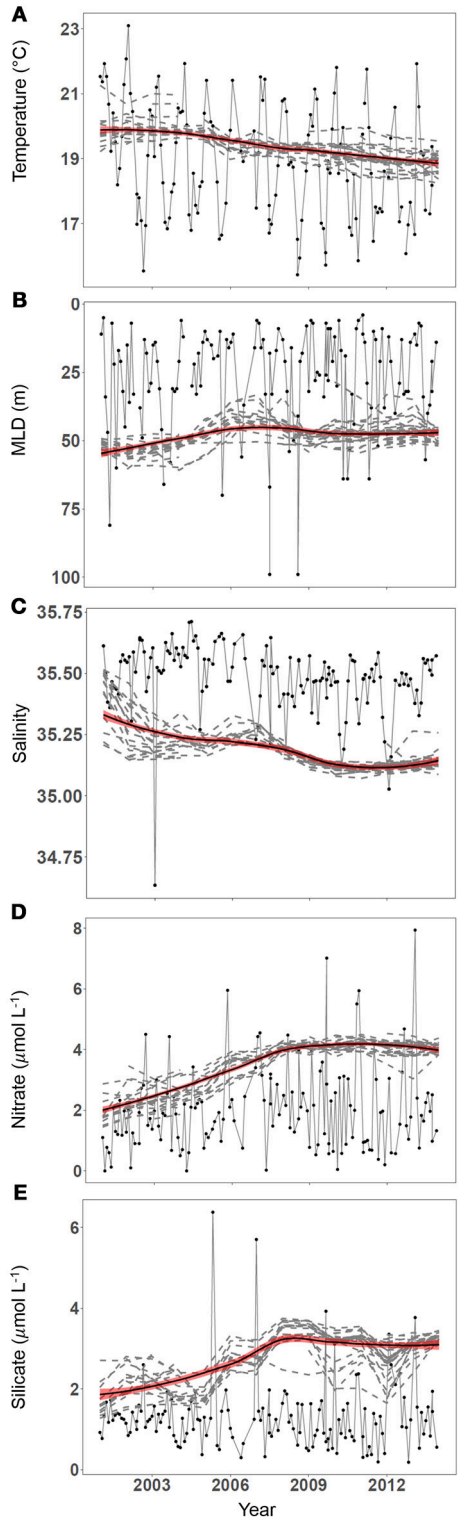

FIGURE 3 | Mean realized niches change over time in response to changes in mean environmental conditions and their distributions. Running mean niches are compared to environmental conditions in panels **(A–E)**. Monthly environmental conditions are shown (black line, filled circles) for **(A)** temperature (°C), **(B)** mixed layer depth (m), **(C)** salinity, **(D)** nitrate concentration (μmol L^{-1}), and **(E)** silicate concentration (μmol L^{-1}). The 4-year running mean of the mean realized niche for species found in at least 4 of the 15 periods between 1997 and 2013 (dashed lines) and a loess smoother (black, thick line) with a shaded region 1 standard error wide (red) are overlaid on these panels.

(Continued)

in coastal Venezuelan waters (Station CARIACO) over a 15 year period (1995–2011), we observed changes in the realized niches of 67 phytoplankton species in response to warming of about 1.3°C and a decrease in nitrate concentration of about 0.7 μmol L^{-1} (Irwin et al., 2015). While changes in the realized temperature niche closely tracked changes in average conditions in the environment, we observed two distinct responses in the nitrate niches. Some species tracked the decrease in nitrate concentration while others retained an essentially fixed realized niche. We do not know if these results are typical of changes in phytoplankton at other sites, how rapidly the changes occurred, or the reason for the differences we observed in temperature and nitrate niche changes.

The evidence from the Port Hacking coastal station is that realized niches of phytoplankton track changes in environmental conditions (**Figure 2**, **Table 2**). We observed three patterns of changes in the realized environmental niches that we believe to be a result of mismatch between the fundamental niches and available environmental conditions. For temperature, the mean niche, averaged over all species, is very close to the mean environmental conditions and the mean niche closely tracks changes in the environment. The changes in mean niche have the same sign but are slightly larger than changes in ocean temperature, whether we examine changes from one period to the next (**Table 2**) or changes in the running-mean estimate over time (**Figure 3A**). This is expected, since the fundamental temperature niche for many species is generally wide compared to the ranges of temperatures observed at PH_{100m} (Boyd et al., 2013; Brun et al., 2015). In addition, ocean currents can be expected to have exposed the drifting phytoplankton communities arriving at PH_{100m} to large temperature fluctuations, which will have helped retain species with wide temperature niches (Doblin and van Sebille, 2016), although in some cases currents may promote local adaptations and barriers to gene flow (Rynearson and Armbrust, 2005). By contrast, mean niches are biased relative to the environment for salinity and mixed layer depth, with salinity niches being smaller (fresher) by about 0.25 psu compared to the environment and mixed layer depth niches being larger (deeper) by about 30 m. Mean niches for both these variables are generally at an extreme edge of the distribution of the environmental conditions, indicating an increased probability of finding phytoplankton species in general at one end of the distribution of these variables. Changes in environmental conditions between periods (**Table 2**) are not significant, and changes in mean niche are near zero but significant (for salinity) or not significant (for mixed layer depth). As with temperature, inter-annual variability in these environmental conditions is much larger than the changes over the time-series in mean niche (**Figures 3B,C**). More dramatic changes in mean salinity and mixed layer depth could be expected

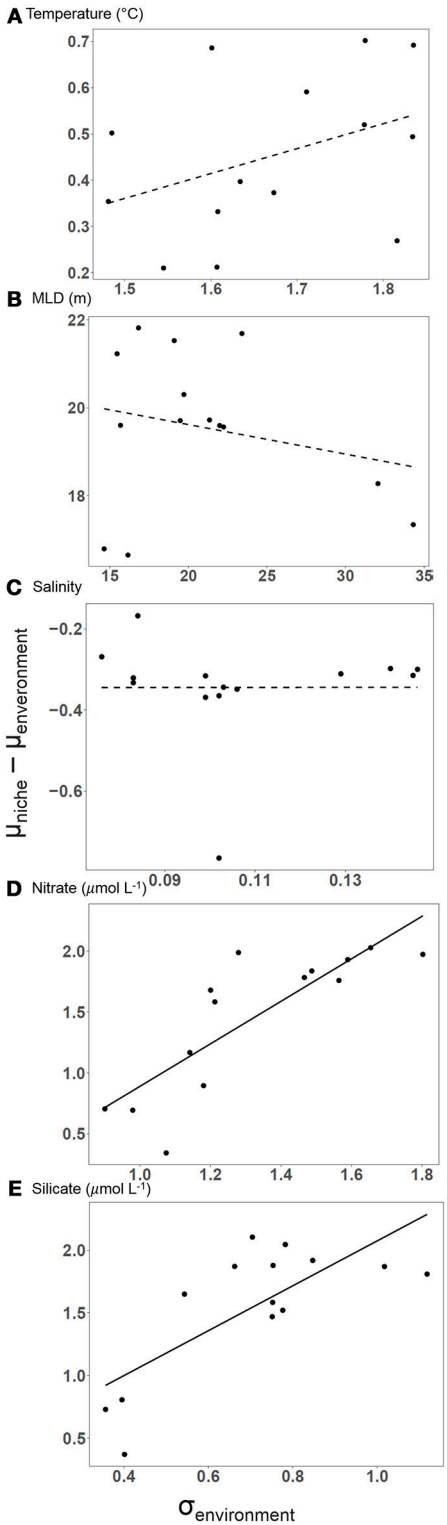

FIGURE 4 | The difference between the community average of mean realized niches and the mean environmental conditions for each 4-year window as a function of the standard deviation of environmental conditions. For nitrate and silicate concentration (D, E) increasing variability in the environment led to larger differences between mean environmental conditions and mean realized

(Continued)

FIGURE 4 | niches (linear regressions, black line, $p < 0.05$). The relationship was non-significant (dashed line, $p > 0.05$) for temperature, mixed layer depth, and salinity **(A–C)** revealing close tracking of the mean or an extreme value of the environmental conditions for these variables.

TABLE 4 | The correlation matrix between the five environmental variables for all observations between 1997 and 2013. Significant ($P < 0.05$) correlations are in bold.

	Temperature	MLD	Salinity	Nitrate
Temperature (°C)	–			
MLD (m)	−0.15	–		
Salinity	−0.12	0.18	–	
Nitrate (μmol L^{-1})	**−0.47**	−0.18	−0.16	–
Silicate (μmol L^{-1})	−0.16	−0.13	**−0.21**	**0.56**

to change the corresponding niches, but the ability of species to persist at the edge of the distribution of these variables allowed the realized niches to remain largely unaffected over the study period. A third pattern is observed for nitrate and silicate concentrations. Relatively small changes in mean concentrations in the ocean (**Table 2**, **Figures 3D,E**) appear to have resulted in considerably larger changes in the mean niches, and for silicate concentration, the change is in the opposite direction (although the environmental change was not significantly different from zero). These three different kinds of changes in realized niches may be related to the mismatch between the fundamental niche and the available environmental conditions at this site.

Unlike Station CARIACO, where many phytoplankton species displayed a fixed niche for nitrate, the realized niche for nitrate concentration at PH_{100m} tracks an increase in nitrate concentration at the site. Also somewhat surprisingly, for several variables, most notably nitrate and silicate concentration, the mean realized niche over all species, at times, increases more rapidly than the mean concentration in the environment (**Figure 3**). Differences in the concentration and temporal dynamics in nitrate concentrations between the two locations may account for the different phenomena at the two sites. The average monthly nitrate concentration at Station CARIACO was <1 μmol L^{-1}, indicating that nitrate may be the limiting resource for many phytoplankton species at this location, whilst the higher concentrations observed at PH_{100m} ($\sim$2 μmol L^{-1}) may not be limiting for many species. Diatoms are known to thrive under variable conditions at PH_{100m}, often taking advantage of nutrient pulses (Hallegraeff and Reid, 1986; Ajani et al., 2014a,b). Increasing nitrate loading in the coastal ecosystem offshore from Sydney is predicted to continue in future years, with more frequent upwelling events anticipated and an increase in anthropogenic nutrient loading via river discharges and ocean outfalls (Pritchard et al., 2003). How phytoplankton will react to this further increase in nitrate concentration will require further investigation over longer time scales and highlights the importance of Australia's National Reference Stations to monitor long-term changes in Australia's ocean.

Because of mismatch between fundamental and realized niche, the consequences of environmental changes on some of

the realized niches are not sufficiently well described by changes in the mean conditions. Nitrate and silicate concentrations exhibit increasing frequency of relatively high concentrations over the 1997–2013 time series, starting most noticeably around 2005 (**Figures 3D,E**). The standard deviation of nutrient concentrations, measured over a calendar year, captures this increase and can be used to explain why mean realized niches increase more rapidly than mean environmental conditions (**Table 2**, **Figures 4**, **Supplementary Tables 3**, **4**). The difference between mean realized niche and mean environmental condition is correlated with the standard deviation of the environmental conditions; all measured on a calendar year for nitrate and silicate concentrations (**Figure 4**). The corresponding relationship for temperature, salinity, and mixed layer depth was not significant.

The realized niches of phytoplankton changed rapidly in response to changes in environmental conditions at Port Hacking. We evaluated the lag-times associated with the mean realized environmental niches and environmental conditions and found the correlation was highest with no lag, demonstrating that there was no evidence of a lag even as small as 1 year between environmental change and corresponding changes in the realized niche. Analyses between non-overlapping periods in this study (**Table 2**, **Figure 2**) and a previous study at Station CARIACO showed changes in realized niches between periods but did not address the question of how quickly realized niches changed. This rapid change in realized niche suggests that niche tracking arises from rapid processes such as gene frequency change in the population caused by ecological selection or immigration of new ecotypes. We do not anticipate that physiological plasticity is responsible for these changes in realized niche, except possibly for temperature, since the interannual variation in environmental conditions is much larger than longer-term changes that we are emphasizing. If plasticity was responsible, then the niches would likely be much broader and uniform across species, encompassing the full range of environmental conditions (Irwin et al., 2015). Moreover, since the realized niche for temperature is very close to the mean conditions and tracks the mean very closely, it is possible that some of the species at Port Hacking have broad temperature niches relative to the range of environmental conditions.

Our analysis of phytoplankton realized niches at Port Hacking has demonstrated that realized niches for the species observed at this site approximately track changes in environmental conditions and that these changes happen with a time lag of less than 1 year. This reinforces results observed at Station CARIACO which showed that phytoplankton realized niches adapt to changing ocean conditions. Our analysis at PH_{100m} provides a second, independent test of this idea. The longer time record at Port Hacking included some changes in environmental conditions in opposing directions compared to those observed at Station CARIACO, and some reversals, for example an increase in temperature (and niche) between 1965 and 79 (P1) and 1997–2004 (P2) followed by a decrease between 1997 and 2004 (P2) and 2005–2013 (P3). Our results also extend the previous analysis by illustrating that changes in mean conditions may not always be sufficient to explain the changes in the mean niche. Episodic increases in macronutrient concentrations were sufficient at Port Hacking to enable disproportionate increases in the corresponding realized niches, as phytoplankton exploited these new conditions. Furthermore, the East Australian Current is intensifying (poleward extension of approximately 350 km) and continuing to undergo significant warming (2.28°C/century) (Ridgway and Hill, 2012). This latitudinal shift and warming trend is predicted to cause shifts in phytoplankton abundance, distribution and composition along the east Australian coast with the emergence of tropical species into more temperate waters already documented (Hallegraeff et al., 2012; Ajani et al., 2014a,b). This spatial restructuring of the plankton may in turn cause changes in biotic interactions (predation, competition), with potential impacts on biogeochemical cycling, higher trophic levels, and biodiversity (Chivers et al., 2017). Taken together, these studies and the details of rates and magnitude of changes in realized niche, emphasize the need to expect changes in phytoplankton niches when designing ecosystem models used to project biotic responses to climate change. This study provides further evidence that climate change model projections cannot assume fixed realized niches of biotic communities, and highlights the importance of sustained ocean measurements from the southern hemisphere (as well as the northern hemisphere) to enhance our understanding of global ocean trends. Moreover, future work to test the proposed mechanisms for the observed niche flexibility should combine population genetics and microbial experimental evolution to allow for a mechanistic understanding how changes in realized niches can be predicted and thereby taken into account in climate change projections.

AUTHOR CONTRIBUTIONS

PA, ZF, and AI are responsible for the conceptualisation of this work. PA, NM, and AI performed the analysis. All authors (PA, NM, ZF, and AI) are responsible for the writing, reviewing, and editing of this manuscript.

ACKNOWLEDGMENTS

We acknowledge all contributors, past and present to the PH_{100m} time-series dataset especially Professor Gustaaf Hallegraeff, Ms Alex Coughlan, Professor Anthony Richardson, Dr Tim Ingleton, and Dr Andrew Allen. National Reference Station data are sourced from the Integrated Marine Observing System (IMOS). IMOS is a national collaborative research infrastructure, supported by the Australian Government. Finally, PA would like to thank the University of Technology Sydney Chancellor's Postdoctoral Fellowship scheme for funding; ZF and AI thank the Natural Science and Engineering Research Council (NSERC) Canada for funding. This work was supported by grants from the Simons Foundation (549935, AI; 549937 ZF).

SUPPLEMENTARY MATERIAL

The Supplementary Material for this article can be found online at: https://www.frontiersin.org/articles/10.3389/fmars.2018.00285/full#supplementary-material

REFERENCES

Ajani, P., Hallegraeff, G., Allen, D., Coughlan, A., Richardson, A. J., Armand, L., et al. (2016). Establishing baselines: a review of eighty years of phytoplankton diversity and biomass in southeastern Australia. *Oceanogr. Mar. Biol.* 54, 387–412. doi: 10.1201/9781315368597-9

Ajani, P., Lee, R., Pritchard, T., and Krogh, M. (2001). Phytoplankton dynamics at a long-term coastal station off Sydney, Australia. *J. Coast. Res.* 34, 60–73.

Ajani, P.A., Allen, A. P., Ingleton, T., and Armand, L. (2014b). Erratum: a decadal decline in relative abundance and a shift in phytoplankton composition at a long-term coastal station off southeast Australia. *Limnol. Oceanogr.* 59, 2240–2242. doi: 10.4319/lo.2014.59.6.2240

Ajani, P. A., Allen, A. P., Ingleton, T., and Armand, L. (2014a). A decadal decline in relative abundance and a shift in microphytoplankton composition at a long-term coastal station off southeast Australia. *Limnol. Oceanogr.* 59, 519–531. doi: 10.4319/lo.2014.59.2.0519

Barton, A. D., Irwin, A. J., Finkel, Z. V., and Stock, C. A. (2016). Anthropogenic climate change drives shift and shuffle in North Atlantic phytoplankton communities. *Proc. Natl. Acad. Sci. U.S.A.* 113, 2964–2969. doi: 10.1073/pnas.1519080113

Beaufort, L., Probert, I., de Garidel-Thoron, T., Bendif, E. M., Ruiz-Pino, D., Metzl, N., et al. (2011). Sensitivity of coccolithophores to carbonate chemistry and ocean acidification. *Nature* 476, 80–83. doi: 10.1038/nature 10295

Benner, I., Diner, R. E., Lefebvre, S. C., Li, D., Komada, T., Carpenter, E. J., et al. (2013). *Emiliania huxleyi* increases calcification but not expression of calcification-related genes in long-term exposure to elevated temperature and pCO(2). *Philos. Trans. R. Soc. Lond. B Biol. Sci.* 368:20130049. doi: 10.1098/rstb.2013.0049

Boyd, P. W., Lennartz, S. T., Glover, D. M., and Doney, S. C. (2015). Biological ramifications of climate-change-mediated oceanic multi-stressors. *Nat. Clim. Chang.* 5, 71–79. doi: 10.1038/nclimate2441

Boyd, P. W., Rynearson, T. A., Armstrong, E. A., Fu, F., Hayashi, K., Hu, Z., et al. (2013). Marine phytoplankton temperature versus growth responses from polar to tropical waters–outcome of a scientific community-wide study. *PLoS ONE* 8:e63091. doi: 10.1371/journal.pone.0063091

Brun, P., Vogt, M., Payne, M. R., Gruber, N., O'Brien, C. J., Buitenhuis, E. T., et al. (2015). Ecological niches of open ocean phytoplankton taxa. *Limnol. Oceanogr.* 60, 1020–1038. doi: 10.1002/lno.10074

Chivers, W. J., Walne, A. W., and Hays, G. C. (2017). Mismatch between marine plankton range movements and the velocity of climate change. *Nat. Commun.* 8:14434. doi: 10.1038/ncomms14434

Collins, S. (2013). New model systems for experimental evolution. *Evolution* 67, 1847–1848. doi: 10.1111/evo.12116

Collins, S., and Bell, G. (2004). Phenotypic consequences of 1,000 generations of selection at elevated CO2 in a green alga. *Nature* 431, 566–569. doi: 10.1038/nature02945

Collins, S., Rost, B., and Rynearson, T. A. (2014). Evolutionary potential of marine phytoplankton under ocean acidification. *Evol. Appl.* 7, 140–155. doi: 10.1111/eva.12120

Doblin, M. A., and van Sebille, E. (2016). Drift in ocean currents impacts intergenerational microbial exposure to temperature. *Proc. Natl. Acad. Sci. U.S.A.* 113, 5700–5705. doi: 10.1073/pnas.1521093113

Doney, S. C. (2006). Oceanography-Plankton in a warmer world. *Nature* 444, 695–696. doi: 10.1038/444695a

Edwards, M., and Richardson, A. J. (2004). Impact of climate change on marine pelagic phenology and trophic mismatch. *Nature* 430, 881–884. doi: 10.1038/nature02808

Elith, J., and Leathwick, J. R. (2009). Species distribution models: ecological explanation and prediction across space and time. *Annu. Rev. Ecol. Evol. Syst.* 40, 677–697. doi: 10.1146/annurev.ecolsys.110308.120159

Elith, J., Phillips, S. J., Hastie, T., Dudik, M., Chee, Y. E., and Yates, C. J. (2011). A statistical explanation of MaxEnt for ecologists. *Divers. Distrib.* 17, 43–57. doi: 10.1111/j.1472-4642.2010.00725.x

Falkowski, P. G., Barber, R. T., and Smetacek, V. (1998). Biogeochemical controls and feedbacks on ocean primary production. *Science* 281, 200–206.

Falkowski, P. G., Katz, M. E., Knoll, A. H., Quigg, A., Raven, J. A., Schofield, O., et al. (2004). The evolution of modern eukaryotic phytoplankton. *Science* 305, 354–360. doi: 10.1126/science.1095964

Field, C. B., Behrenfeld, M. J., Randerson, J. T., and Falkowski, P. (1998). Primary production of the biosphere: integrating terrestrial and oceanic components. *Science* 281, 237–240.

Flombaum, P., Gallegos, J. L., Gordillo, R. A., Rincon, J., Zabala, L. L., Jiao, N., et al. (2013). Present and future global distributions of the marine *Cyanobacteria Prochlorococcus* and *Synechococcus*. *Proc. Natl. Acad. Sci. U.S.A.* 110, 9824–9829. doi: 10.1073/pnas.1307701110

Follows, M. J., Dutkiewicz, S., Grant, S., and Chisholm, S. W. (2007). Emergent biogeography of microbial communities in a model ocean. *Science* 315, 1843–1846. doi: 10.1126/science.1138544

Frank, S. A., and Slatkin, M. (1990). The distribution of allelic effects under mutation and selection. *Genet. Res.* 55, 111–117. doi: 10.1017/S0016672300025350

Gobler, C. J., Hattenrath-Lehmann, T. K., Doherty, O. M., Griffith, A. W., Kang, Y., and Litaker, R. W. (2017). Reply to Dees et al.: Ocean warming promotes species-specific increases in the cellular growth rates of harmful algal blooms. *Proc. Natl. Acad. Sci. U.S.A.* 114, E9765–E9766. doi: 10.1073/pnas.1715749114

Grant, B. R., and Kerr, J. D. (1970). Phytoplankton numbers and species at Port Hacking station and their relationship to the physical environment. *Austr. J. Mar.Freshw. Res.* 21, 35–45. doi: 10.1071/MF9700035

Hallegraeff, G., Beardall, J., Brett, S., Doblin, M., and Thompson, P.,. (2012). "Phytoplankton," in *A Marine Climate Change Impacts and Adaptation Report Card for Australia 2012*, eds E. S. Poloczanska, A. J. Hobday, and A.J. Richardson (Brisbane, QLD: CSIRO Marine and Atmospheric Research), 227–240.

Hallegraeff, G. M. (1981). Seasonal study of phytoplankton pigments and species at a coastal station off Sydney: importance of diatoms and the nanoplankton. *Mar. Biol.* 61, 107–118. doi: 10.1007/BF00386650

Hallegraeff, G. M., and Jeffrey, S. W. (1993). Annually recurrent diatom blooms in spring along the New South Wales coast of Australia. *Austr. J. Mar.Freshw. Res.* 44, 325–334. doi: 10.1071/MF9930325

Hallegraeff, G. M., and Reid, D. D. (1986). Phytoplankton species successions and their hydrological environment at a coastal station off Sydney. *Austr. J. Mar.Freshw. Res.* 37, 361–377. doi: 10.1071/MF9860361

Heron, A. C. (1982). A vertical free fall plankton net with no mouth obstructions. *Limnol. Oceanogr.* 27, 380–383. doi: 10.4319/lo.1982.27.2.0380

Hutchins, D. A., Walworth, N. G., Webb, E. A., Saito, M. A., Moran, D., McIlvin, M. R., et al. (2015). Irreversibly increased nitrogen fixation in *Trichodesmium* experimentally adapted to elevated carbon dioxide. *Nat. Commun.* 6:8155. doi: 10.1038/ncomms9155

Hutchinson, G. E. (1957). Cold spring harbor symposium on quantitative biology. *Concluding Remarks* 22, 415–427.

IPCC (2013). "Climate change 2013: the physical science basis," in *Contribution of Working Group I to the Fifth Assessment Report of the Intergovernmental Panel on Climate Change,* eds T.F. Stocker, D. Qin, G. K. Plattner, M. Tignor, S.K. Allen, J. Boschung, A. Nauels, Y. Xia, V. Bex and P.M. Midgley (Cambridge, UK; New York, NY: Cambridge University Press).

IPCC (2014). "Climate Change 2014: Synthesis Report," in *Contribution of Working Groups I, II and III to the Fifth Assessment Report of the Intergovernmental Panel on Climate Change*, ed R. K. Pachauri and L. A. Meyer (IPCC, Geneva: Core Writing Team).

Irwin, A. J., Finkel, Z. V., Muller-Karger, F. E., and Troccoli Ghinaglia, L. (2015). Phytoplankton adapt to changing ocean environments. *Proc. Natl. Acad. Sci. U.S.A.* 112, 5762–5766. doi: 10.1073/pnas.1414752112

Irwin, A. J., Nelles, A. M., and Finkel, Z. V. (2012). Phytoplankton niches estimated from field data. *Limnol. Oceanogr.* 57, 787–797. doi: 10.4319/lo.2012.57.3.0787

Ji, X., Verspagen, J. M. H., Stomp, M., and Huisman, J. (2017). Competition between cyanobacteria and green algae at low versus elevated CO2: who will win, and why? *J. Exp. Bot.* 68, 3815–3828. doi: 10.1093/jxb/erx027

Jitts, H. R. (1964). A twin six-litre plastic water sampler. *Limnol. Oceonogr.* 9:452. doi: 10.4319/lo.1964.9.3.0452

Koester, J. A., Swanson, W. J., and Armbrust, E. V. (2013). Positive selection within a diatom species acts on putative protein interactions and transcriptional regulation. *Mol. Biol. Evol.* 30, 422–434. doi: 10.1093/molbev/mss242

Kramer-Schadt, S., Niedballa, J., Pilgrim, J. D., Schröder, B., Lindenborn, J., Reinfelder, V., et al. (2013). The importance of correcting for sampling bias in MaxEnt species distribution models. *Divers. Distribut.* 19, 1366–1379. doi: 10.1111/ddi.12096

Levitus, S. (1982). *Climatological Atlas of the World Ocean*. NOAA Prof. Paper No. 13. Washington, DC. US Government Printing Office.

Lynch, T. P., Morello, E. B., Evans, K., Richardson, A. J., Rochester, W., Steinberg, C. R., et al. (2014). IMOS national reference stations: a continental-wide physical, chemical and biological coastal observing system. *PLoS ONE* 9:e113652. doi: 10.1371/journal.pone.0113652

Phillips, S. J., and Dudik, M. (2008). Modeling of species distributions with Maxent: new extensions and a comprehensive evaluation. *Ecography* 31, 161–175. doi: 10.1111/j.0906-7590.2008.5203.x

Pritchard, T., Lee, R., Ajani, P., Rendell, P., Black, K., and Koop, K. (2003). Phytoplankton responses to nutrient sources in coastal waters off southeastern Australia. *Aquat. Ecosyst. Health Manag.* 6, 105–117. doi: 10.1080/14634980301469

Richardson, A. J., and Poloczanska, E. S. (2008). Ocean science - Under-resourced, under threat. *Science* 320, 1294–1295. doi: 10.1126/science.1156129

Richardson, A. J., and Schoeman, D. S. (2004). Climate impact on plankton ecosystems in the Northeast Atlantic. *Science* 305, 1609–1612. doi: 10.1126/science.1100958

Ridgway, K., and Hill, K. (2012). "East Australian current," in *A Marine Climate Change Impacts and Adaptation Report Card for Australia 2012*, eds E. S. Poloczanska, A. J. Hobday, and A. J. Richardson. Available online at: http://www.oceanclimatechange.org.au

Ridgway, K. R., and Dunn, J. R. (2003). Mesoscale structure of the mean East Australian current system and its relationship with topography. *Prog. Oceanogr.* 56, 189–222. doi: 10.1016/S0079-6611(03)00004-1

Rost, B., Zondervan, I., and Wolf-Gladrow, D. (2008). Sensitivity of phytoplankton to future changes in ocean carbonate chemistry: current knowledge, contradictions and research directions. *Mar. Ecol. Progr. Ser.* 373, 227–237. doi: 10.3354/meps07776

Rynearson, T. A., and Armbrust, E. V. (2005). Maintenance of clonal diversity during a spring bloom of the centric diatom *Ditylum brightwellii*. *Mol. Ecol.* 14, 1631–1640. doi: 10.1111/j.1365-294X.2005.02526.x

Thomas, C. D., Cameron, A., Green, R. E., Bakkenes, M., Beaumont, L. J., Collingham, Y. C., et al. (2004). Extinction risk from climate change. *Nature* 427, 145–148. doi: 10.1038/nature02121

Thomas, M. K., Kremer, C. T., Klausmeier, C. A., and Litchman, E. (2012). A global pattern of thermal adaptation in marine phytoplankton. *Science* 338, 1085–1088. doi: 10.1126/science.1224836

Thomas, M. K., Kremer, C. T., and Litchman, E. (2016). Environment and evolutionary history determine the global biogeography of phytoplankton temperature traits. *Global Ecol. Biogeogr.* 25, 75–86. doi: 10.1111/geb.12387

Thompson, P. A., Baird, M. E., Ingleton, T., and Doblin, M. A. (2009). Long-term changes in temperate Australian coastal waters: implications for phytoplankton. *Mar. Ecol. Prog. Ser.* 394, 1–19. doi: 10.3354/meps08297

Walworth, N. G., Fu, F. X., Webb, E. A., Saito, M. A., Moran, D., McLlvin, M. R., et al. (2016). Mechanisms of increased *Trichodesmium* fitness under iron and phosphorus co-limitation in the present and future ocean. *Nat. Commun.* 7:12081. doi: 10.1038/ncomms12081

Wu, L., Cai, W., Zhang, L., Nakamura, H., Timmermann, A., Joyce, T., et al. (2012). Enhanced warming over the global subtropical western boundary currents. *Nat. Clim. Change* 2, 161–166. doi: 10.1038/nclimate1353

Yackulic, C. B., Chandler, R., Zipkin, E. F., Royle, J. A., Nichols, J. D., Grant, E. H. C., et al. (2013). Presence-only modelling using MAXENT: when can we trust the inferences? *Methods Ecol. Evol.* 4, 236–243. doi: 10.1111/2041-210x.12004

Zingone, A., Dubroca, L., Iudicone, D., Margiotta, F., Corato, F., d'Alcala, M. R., et al. (2010). Coastal phytoplankton do not rest in winter. *Estuaries Coasts* 33, 342–361. doi: 10.1007/s12237-009-9157-9.

Conflict of Interest Statement: The authors declare that the research was conducted in the absence of any commercial or financial relationships that could be construed as a potential conflict of interest.

frontiers in Marine Science

REVIEW
published: 19 September 2018
doi: 10.3389/fmars.2018.00327

Shifting Diatom—Dinoflagellate Dominance During Spring Bloom in the Baltic Sea and its Potential Effects on Biogeochemical Cycling

Kristian Spilling[1,2], Kalle Olli[3,4], Jouni Lehtoranta[1], Anke Kremp[1], Letizia Tedesco[1], Tobias Tamelander[2], Riina Klais[3], Heikki Peltonen[1] and Timo Tamminen[1]*

[1] Finnish Environment Institute (SYKE), Helsinki, Finland, [2] Tvärminne Zoological Station, Faculty of Biological and Environmental Sciences, University of Helsinki, Hanko, Finland, [3] Institute of Ecology and Earth Sciences, University of Tartu, Tartu, Estonia, [4] Institute of Agricultural and Environmental Sciences, Estonian University of Life Sciences, Tartu, Estonia

The Baltic Sea is affected by a range of human induced environmental pressures such as eutrophication. Here we synthesize the ongoing shift from diatom dominance toward more dinoflagellates in parts of the Baltic Sea during the spring bloom and its potential effects on biogeochemical cycling of key elements (e.g., C, N, and P). The spring bloom is the period with the highest annual primary production and sinking of organic matter to the sediment. The fate of this organic matter is a key driver for material fluxes, affecting ecosystem functioning and eutrophication feedback loops. The dominant diatoms and dinoflagellates appear to be functionally surrogates as both groups are able to effectively exhaust the wintertime accumulation of inorganic nutrients and produce bloom level biomass that contribute to vertical export of organic matter. However, the groups have very different sedimentation patterns, and the seafloor has variable potential to mineralize the settled biomass in the different sub-basins. While diatoms sink quickly out of the euphotic zone, dinoflagellates sink as inert resting cysts, or lyse in the water column contributing to slowly settling phyto-detritus. The dominance by either phytoplankton group thus directly affects both the summertime nutrient pools of the water column and the input of organic matter to the sediment but to contrasting directions. The proliferation of dinoflagellates with high encystment efficiency could increase sediment retention and burial of organic matter, alleviating the eutrophication problem and improve the environmental status of the Baltic Sea.

Keywords: eutrophication, pelagic-benthic coupling, ecosystem functioning, community composition, plankton sedimentation, carbon sink

OPEN ACCESS

Edited by:
Michael Arthur St. John, Technical University of Denmark, Denmark

Reviewed by:
Maren Voss, Leibniz Institute for Baltic Sea Research (LG), Germany
Bernd Wemheuer, University of New South Wales, Australia

****Correspondence:***
Kristian Spilling
kristian.spilling@environment.fi

Specialty section:
This article was submitted to Marine Ecosystem Ecology, a section of the journal Frontiers in Marine Science

Received: *30 April 2018*
Accepted: *27 August 2018*
Published: *19 September 2018*

Citation:
Spilling K, Olli K, Lehtoranta J, Kremp A, Tedesco L, Tamelander T, Klais R, Peltonen H and Tamminen T (2018) Shifting Diatom—Dinoflagellate Dominance During Spring Bloom in the Baltic Sea and its Potential Effects on Biogeochemical Cycling. Front. Mar. Sci. 5:327. doi: 10.3389/fmars.2018.00327

INTRODUCTION

Global change is causing drastic changes to the lowest levels of the marine food web (Halpern et al., 2008; Duarte, 2014), with evidence of shifting community composition of primary producers in e.g., the North Atlantic (Leterme et al., 2005), the North Sea (Hinder et al., 2012), parts of the Mediterranean Sea (Mercado et al., 2007) and the Baltic Sea (Klais et al., 2011). The main drivers/pressures for this change are warming of the surface water, changes in stratification, eutrophication, ocean acidification, overfishing, loss of biodiversity, spreading of non-indigenous species and increasing UV exposure (e.g., Hallegraeff, 2010; Duarte, 2014).

Different species of phytoplankton have different traits (Litchman and Klausmeier, 2008), most notably size and shape, growth rate, life history, and behavior such as motility that together determine their ecological niche and preferred environmental conditions, and phytoplankton is a major driver for global carbon fixation and biogeochemical cycles. State-of-the-art biogeochemical models typically have several functional groups of phytoplankton, but as the models become more advanced we need empirical studies to disentangle what effect the observed shifts in phytoplankton communities have on ecosystem functioning (Fennel and Neumann, 2014).

The Baltic Sea is among the shelf seas projected to change most rapidly, due to its close interaction with land and reduced alkalinity (Niiranen et al., 2013; BACCI, 2015). Eutrophication is one of the main threats to the Baltic Sea ecosystem (e.g., HELCOM, 2009), but also ocean acidification (Havenhand, 2012; Omstedt et al., 2014), global warming (Belkin, 2009; Meier et al., 2014) and pollutants (HELCOM, 2010) greatly affect this ecosystem and pose challenges for effective management of natural habitats (Elmgren et al., 2015).

Long-term eutrophication in the Baltic Sea has led to accumulation of phosphorus (P), particularly in the sediment, to an extent that internal loading off-sets reduction in nutrient loading from the catchment (Gustafsson et al., 2012). Spread of hypoxia in the bottom water and sediments directly affect the cycling of the main elements (Conley et al., 2011; Carstensen et al., 2014), which in turn affects the community of primary producers when bottom water is transported to the surface during seasonal turnover or upwelling (Cloern, 2001).

Global warming is projected to reduce the sea ice coverage, ice thickness and increase water temperature in the Baltic Sea (Thomas et al., 2017). Expected increase in precipitation in the Northern Baltic catchment will affect freshwater inflow and nutrient run-off (Andersson et al., 2015). Changes to both temperature and freshwater inflow have the potential to change stratification of water layers, with direct implications for vertical transport of O_2 and for planktonic life forms, in particular during the build-up of stratification in spring (Stipa, 2004). Input of freshwater will also influence the concentration of dissolved organic matter with implication for light dependent phytoplankton (Andersson et al., 2018). At present, freshwater induced stratification is important for the initial start of the spring bloom, but thermal stratification may become more important in the future (Hordoir and Meier, 2012). Warming of the Baltic Sea has already caused temporal shifts in the phytoplankton distribution during the highly productive spring, with earlier and more prolonged spring bloom (Groetsch et al., 2016; Kahru et al., 2016). In addition, long-term monitoring data suggest that the phytoplankton community is changing during spring in some areas of the Baltic Sea from diatom to dinoflagellates dominance (Klais et al., 2011), as a consequence of the ongoing climate change (Klais et al., 2013).

We have some understanding of how ongoing environmental changes affect the phytoplankton community, but much less is known how phytoplankton community composition feeds back into ecosystem functioning. Using the Baltic Sea as a case study, we review the present knowledge of the ongoing diatom—dinoflagellate shift, and provide a synthesis of the existing knowledge of how the phytoplankton community composition directly affects ecosystem functioning through species-specific sedimentation, life cycle changes and yields of resting stages. We argue that the diatom to dinoflagellate shift has the potential to induce substantial changes in pelagic and benthic ecosystem functioning, and we provide a conceptual model of how this change could affect biogeochemical cycling of key elements. The ratio of diatoms to dinoflagellates was recently suggested to be a new environmental indicator, with a high ratio being associated with good environmental status as diatoms have historically dominated the spring bloom (Wasmund et al., 2017). However, a clear understanding of how this shift may affect the environment is still missing, and we argue that this shift could increase burial of organic matter, which would alleviate the eutrophication problem and improve the environmental status of the Baltic Sea.

IMPORTANCE OF THE SPRING BLOOM FOR BIOGEOCHEMICAL CYCLES IN THE BALTIC SEA

Long term Chl-*a* data from western Gulf of Finland indicates a doubling in the biomass peak during spring from early 1970s to mid-1980s; the trend has somewhat reversed after the early 1990s (Raateoja et al., 2005), but it is clear that much of the increased algal production resulting from eutrophication takes place during spring. In the most eutrophied parts of the Baltic Sea such as the Gulf of Finland (**Figure 1**), 40–60% of annual carbon fixation takes place during the spring bloom. This covers only 3–5 weeks of the year, and a large fraction of this fixed carbon sinks to the seafloor (Lignell et al., 1993; Heiskanen, 1998).

The onset of the spring bloom is related to salinity stratification and warming of the surface water (Stipa, 2004). It typically starts in the Southern Baltic Sea in February/March and moves northwards like a mosaic of patches (Kahru and Nõmmann, 1990; Kahru et al., 1990). It reaches the Gulf of Finland in April and the Bothnian Sea and Bothnian Bay in May/June, but in the Bothnian Bay the biomass amplitude is much lower than for most other parts of the Baltic Sea. Two recent papers examining time series of the spring bloom timing point toward an earlier start and a longer bloom with lower biomass amplitude (Groetsch et al., 2016; Kahru et al., 2016) in agreement with modeling scenarios (Thomas et al., 2017). This was attributed to the general warming of the climate where the periods with warm water had expanded temporally over the main Baltic basins (Kahru et al., 2016). Kahru et al. (2016) also reported that the summer community of phytoplankton is becoming more abundant than the spring community based on satellite observations of Chl *a*. However, the Chl *a* determination from remote sensing is difficult to estimate (Darecki and Stramski, 2004), and recent direct measurements of Chl *a*, covering large parts of the Baltic Sea, demonstrate that the Chl *a* concentration during spring is still much higher than during summer in the main basins of the Baltic Sea (Simis et al., 2017).

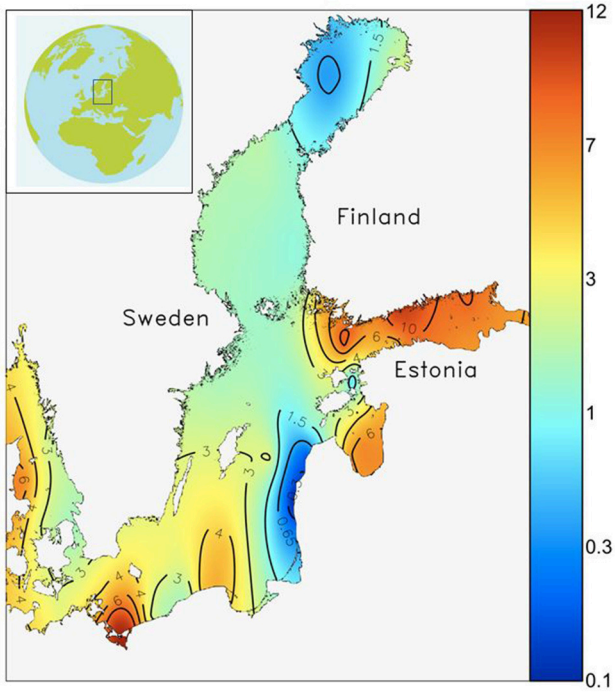

FIGURE 1 | Spatial variability of the spring bloom peak biomass (wet weight, mg L^{-1}) in the Baltic Sea. High biomass (>6 mg L^{-1}) is found in the most eutrophied basins (e.g., Gulf of Finland), mid-level biomass (1.5–3 mg L^{-1}) is found in the larger basins (e.g., Northern Baltic Proper, Bothnian Sea) and low biomass (<1.5 mg L^{-1}) is found in the most oligotrophic parts (e.g., Bothnian Bay) of the Baltic Sea. The map has been modified from Klais et al. (2011).

The spring bloom in the Baltic Sea (with the exception of Bothnian Bay that is P-limited) is terminated when inorganic nitrogen has been depleted, i.e., the community is N-limited (Wulff et al., 2001; Tamminen and Andersen, 2007). The cascading effect of increased spring blooms during the last decades has led to a regime-shift-like development, i.e., non-linear change, when inorganic P pools of the Baltic Proper and Gulf of Finland have remained at elevated levels (>0.1 umol L^{-1}) after the spring bloom (Spilling, 2007b; Raateoja et al., 2011). Low, hardly detectable phosphate concentrations were as a rule observed prior to mid-1990s, although N limitation of the spring bloom was demonstrated even then (Tamminen, 1995). Similar changes have also been reported in the Bothnian Sea (Lundberg et al., 2009; Rolff and Elfwing, 2015). The loading of P from the catchment in these areas has decreased after mid-1990s, seemingly a paradox, but the reason for this increase in P concentrations is attributed to the release of P from the sediment and exchange between sub-basins, which masks the realized reductions in the P loading (Pitkänen et al., 2001; Kiirikki et al., 2006; Stigebrandt et al., 2014; Lehtoranta et al., 2017). The sediment release of P might be much larger than loading from land in parts of the Baltic Sea (Conley et al., 2002), and the observed regime shift in P availability has seemingly affected both the magnitude and source of the P loading.

Diatoms is the only major phytoplankton group to take up substantial quantities of dissolved silicate (DSi) in addition to N and P. DSi is used to build their cell walls in the form of biogenic silicate (BSi) (Martin-Jézéquel et al., 2000). The DSi originates mainly from natural processes such as weathering of rock, and human activities such as damming of rivers have reduced the natural supply DSi to the Baltic Sea (Humborg et al., 2008). In addition, eutrophication has been suggested to affect the DSi concentration; if the elevated input of N and P increases the biomass of fast growing diatoms, the flux of BSi to the seafloor could increase where it is potentially buried (Schelske and Stoermer, 1971; Conley et al., 1993). However, in the Gulf of Finland the release of DSi from the bottom and back to the water column forms a large part of the pelagic DSi pool (Tallberg et al., 2017).

The concentration of DSi is important as it may influence the competition between diatoms and others phytoplankton groups such as dinoflagellates. For example, the increased N:DSi ratio associated with eutrophication favors non-siliceous phytoplankton (Officer and Ryther, 1980). A molar N:DSi ratio >2 (Gilpin et al., 2004), or absolute concentrations of <2 μmol DSi L^{-1} (Egge and Aksnes, 1992) have been suggested to favor flagellates over diatoms. However, some diatoms can acclimate to DSi stress and sustain high growth rates despite low DSi concentrations (Olsen and Paasche, 1986; Brzezinski et al., 1990).

In the Baltic Sea, there has been a long term decrease in DSi concentration that has leveled off after the 2000s (Papush and Danielsson, 2006). There is a difference between the sub-basins in terms of silicate budget and most of the accumulation of BSi takes place in the Gulfs of Bothnia, Finland and Riga (Papush et al., 2009), but the spring bloom diatoms are at present not DSi limited (Wasmund et al., 2013), perhaps with the exception of Gulf of Riga (Olli et al., 2008). Shifting nutrient stoichiometry could shift the competitive balance to non-siliceous phytoplankton in the future (Danielsson et al., 2008). However, many of the dominant Baltic Sea diatoms seem to be less silicified in terms of the N:Si ratio than the Redfield ratio (Spilling et al., 2010) and consequently less sensitive to low DSi concentration. An exception are their resting spores that typically have thicker frustules than the vegetative forms, and the spore formation could be affected by low DSi concentration at the end of the spring bloom (Kremp et al., 2008).

Changing Phytoplankton Community

The phytoplankton community during the highly productive spring is dominated by diatoms and dinoflagellates in most of the Baltic Sea (Niemi, 1975; Heiskanen, 1993; Wasmund et al., 1998; Höglander et al., 2004; Tamelander and Heiskanen, 2004; Jaanus et al., 2006). Diatoms are generally very successful during periods of high new production (i.e., production based on accumulated nitrate), like the spring bloom, as their higher growth rate enables them to outcompete e.g., dinoflagellates (Reynolds, 2006). This is also the case for the spring phytoplankton community in the Baltic Sea, where the dinoflagellates are not able to achieve growth rates comparable to diatoms under controlled lab conditions (Spilling and Markager, 2008). Rather, the recruitment, affecting abundances before the spring bloom start, seem to govern the success of dinoflagellates during spring bloom (Kremp et al., 2008). Additionally, certain sequences

of weather conditions, particularly stratification periods at the onset of the spring bloom have been related to subsequent dinoflagellate dominance (Heiskanen, 1998; Höglander et al., 2004; Klais et al., 2013). Stratification beneath the ice may serve as a platform for dinoflagellates to build up high biomass already during winter (Spilling, 2007a). In addition, some dinoflagellates are mixotrophs (uptake or feeding on organic components), which may supplement C fixation during light limited conditions (Carlsson and Graneli, 1998; Legrand and Carlsson, 1998; Rintala et al., 2007).

In spite of varying dominance of diatoms and dinoflagellates during the spring bloom period, both of the groups are able to effectively exhaust the wintertime accumulation of inorganic N, and produce bloom-level biomasses, and they thus appear to be functional surrogates (Kremp et al., 2008). However, the stoichiometry of the sinking material varies depending on the species composition, as diatom-dominated communities have a higher C: N: P ratio than mixed or dinoflagellate-dominated communities (Spilling et al., 2014). Changes in C: N: P ratio may have consequences for food quality and remineralization in the pelagic and benthic systems of the Baltic Sea. Grazing pressure is relatively low during the spring bloom (Lignell et al., 1993), which is the reason why much of the biomass sink to the seafloor. However, the planktonic grazer communities can be affected as changes in spring bloom composition influence the quality of food available for the emerging copepod populations (Vehmaa et al., 2011), and increasing temperature may boost heterotrophic activity and reduce the export of phytoplankton to the seafloor in the future (Tamelander et al., 2017).

The phytoplankton community composition may also affect the structure of the sinking biomass that may influence the benthic biogeochemistry. Diatoms are worldwide known to be important vehicles for transporting fixed carbon from the atmosphere to great depths (Doney, 1997; Smetacek, 1998). In the relatively shallow Baltic Sea, a large fraction of this carbon sinks to the seafloor. The majority of vegetative dinoflagellate cells lyse, in contrast to diatoms, leading to remineralization in the pelagic zone or forming of slow sinking phytodetritus (Heiskanen, 1998; Tamelander and Heiskanen, 2004). Dinoflagellates can also constitute a major fraction of the sedimentation flux, with sharp peaks during mass encystment, depending on the species and their respective encystment strategies. Built for long-term survival, the cysts that do settle, do not contribute to the benthic oxygen demand (Spilling and Lindström, 2008), although they have a similar carbon content (roughly 50% of the dry weight). Diatoms also have resting stages called spores, and there is a large variation in the amount of resting spores being produced after the bloom depending on the species, ranging from virtually none to most of the cells forming spores (e.g., Kuosa et al., 1997). The different life history traits have also been suggested to impact sedimentation of phytoplankton biomass quantitatively, with higher vertical export from diatom dominated blooms (Heiskanen, 1998). However, vertical export estimates of phytoplankton and total particulate organic carbon (POC) export vary greatly among years characterized by diatom or dinoflagellate dominance (Heiskanen, 1993, 1995; Tallberg and Heiskanen, 1998; Tamelander and Heiskanen, 2004), with no consistent trend. Conceivably, both intact cells (diatoms, spores, and cysts) and detritus (mainly from vegetative dinoflagellate cells) may settle but the share of resting stages will depend on environmental effects on cyst/spore formation and deposition, and on the life cycle strategy of the prevailing species (Kremp et al., 2009; Warns et al., 2012).

Consequently, the phytoplankton composition during the spring bloom may affect both the summertime nutrient pools of the water column, and the input of labile organic matter to the bottom sediments. In the case of diatom dominance, drawdown of nutrients to the bottom is efficient and leaves impoverished nutrient stocks for summertime regenerated production in the euphotic zone. During dinoflagellate dominance, more organic material may be available for remineralization in the productive surface layer, supporting recycling through the microbial loop. However, a complicating factor, which may counteract this assumption, is the active release of dissolved organic matter that is more prevalent during diatom dominance (Camarena-Gómez et al., 2018). This can be done for several reasons (e.g., Thornton, 2014), for example stimulating bacterial growth, which may provide some benefits in return for phytoplankton like the production of B12 vitamin (Kazamia et al., 2012), or be a way to dissipate excess light energy (Zlotnik and Dubinsky, 1989).

CHANGING SPECIES COMPOSITION–A FUNCTIONAL SHIFT IN THE MAKING?

In the last few decades, the proportion of dinoflagellates in the spring bloom biomass has increased in the northern Baltic Sea, most notably in the Gulf of Finland. For example, monitoring data from the waters off the city of Helsinki (see Olli et al., 2011 for description of data), reveal that in spite of substantial variation, the proportion of dinoflagellates has increased from 10 to 20% in the 1970s up to around 80% by the turn of the century (**Figure 2**). The increase of the dinoflagellate proportion has been, with varying strength, a common phenomenon in large parts of the Gulf of Finland, including the north-western part of the Gulf (e.g., archipelago off the Hanko peninsula), but also in the eastern parts of the Gulf (Klais et al., 2011). Overall, the previously diatom dominated spring blooms in the eutrophied Gulf of Finland have incrementally shifted to dinoflagellate dominated blooms in just three decades, but with large inter-annual variation. The inter-annual variation is partly climate driven (Klais et al., 2013), but the reason for the decrease of dinoflagellates in the 1990s outside Helsinki (**Figure 2**) is not yet resolved, suggesting other variables affecting the population dynamics e.g., the timing of recruitment is important for dinoflagellate development (Kremp et al., 2008).

In spite of the general increase in the dinoflagellate proportion in the Gulf of Finland, opposing decadal scale trends have occurred in other sub-basins. In the central Baltic Proper, where the proportion of dinoflagellates was ca. 80–90% for many decades, a slow decrease have been observed (Wasmund et al., 1998). Wasmund and Uhlig (2003) reported a weak increase of spring bloom dinoflagellate biomass in the southern Baltic Sea, but gave no data on proportions. In the eutrophied

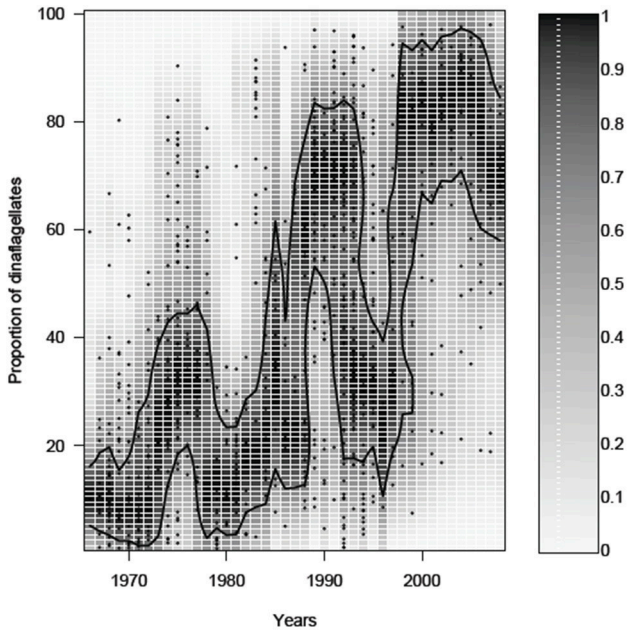

FIGURE 2 | Temporal change in the proportion of dinoflagellates from the sum of diatoms plus dinoflagellates in the spring bloom outside the city of Helsinki (Gulf of Finland). The symbols show the proportion of dinoflagellates in a particular sample. The gray scale shows the probability of having a particular dinoflagellate proportion, obtained by a kernel density estimate of a particular year. The contour line shows the 75% probability level.

Gulf of Riga, strong spring blooms of heavily silicified diatom species exhausted the dissolved silicate stocks in mid 1990s (Olli et al., 2008), giving rise to a short period of high dinoflagellate proportions, in the otherwise diatom dominated basin.

Dinoflagellates

The dinoflagellate spring bloom community includes several species that can reach high biomasses depending on conditions and location. Single-celled, medium-sized, oval-shaped dinoflagellates regularly reach high abundances in the northern basins and the central Baltic Sea. These were previously considered as one species, *Scrippsiella hangoei*, but high resolution scanning electron microscopy and rDNA analyses revealed that this entity is represented by at least three different species belonging to different dinoflagellate orders: *Biecheleria baltica* (syn *Woloszynskia halophila*), *Apocalathium malmogiense* (syn *S. hangoei*), and *Gymnodinium corollarium* (Larsen et al., 1995; Kremp et al., 2005; Moestrup et al., 2009). Records of their specific resting cysts suggest that *B. baltica* is mainly found in the northern basins, particularly the Gulf of Finland (Olli and Trunov, 2010), while *G. corollarium* has its main distribution in the central Baltic Sea (Sundström et al., 2009). *A. malmogiense* cysts are rare in Baltic surface sediments, suggesting that this species is of a minor importance in the spring dinoflagellate community (Kremp et al., 2018). In addition to the three single-celled species, the chain forming, arctic *Peridiniella catenata* can reach high abundances in some years during spring and it has a wide distribution in the Baltic Sea. If *B. baltica* prevails in the Gulf of Finland, the shift to dinoflagellate dominated spring blooms can be ascribed to the proliferation of this species alone (**Figure 3**). To the best our knowledge, *B. baltica* has not been found in any other water body and its origin remains thus enigmatic, but it seems to have a center of expansion in the western Gulf of Finland, from where it has in recent decades spread east- and westwards. Due to the potential of *B. baltica* to completely take over the spring bloom in just a few decades, its unique life history traits, recruitment preferences, and biogeochemical consequences of dominance are of great interest (see below). Despite the conspicuous expansion of *B. baltica* in the northern Baltic Sea, the species is virtually absent in the neighboring Gulf of Riga (Olli and Heiskanen, 1999), suggesting that local hydrography can act as an efficient dispersal barrier.

The major spring bloom dinoflagellates differ from each other in several functional traits, which may affect biogeochemical pathways, e.g., different life cycle strategies may affect sedimentation rate of the population. Formation and subsequent sedimentation of cysts now known to be produced by *B. baltica* at the end of the spring bloom can contribute up to 45% of the total vertical POC flux (Heiskanen, 1993) Notable cyst fluxes have also been documented for *G. corollarium* from the Bornholm and Gotland basins (Sundström et al., 2009). For *P. catenata,* it has been established that most of the biomass produced by this species during spring disintegrates in the water column at the end of the bloom (Heiskanen and Kononen, 1994), and only a minor part of the population undergoes encystment (Kremp, 2000; Spilling et al., 2006; Olli and Trunov, 2010).

Species-specific life cycle strategies, involving fundamentally different mechanisms leading to the respective transitions, likely affect biogeochemical processes. High cyst yields are triggered by different environmental factors and physiological processes (Kremp et al., 2009). Depending on the dominant species, specific temperature and inorganic nutrient dynamics during spring will induce different life cycle responses, with different outcomes regarding vertical fluxes of cyst bound carbon. This has been demonstrated by simulations of numerical models that explicitly consider the regulation of life cycle transitions (Warns et al., 2013). Species-specific differences also exist in germination efficiencies of cysts, which may affect the fate of cyst-bound carbon in the sediment. Of the *B. baltica* cysts produced, only 10–20% will germinate under optimal conditions the following spring (Kremp, 2000), which implies that *B. baltica* blooms could support long-term organic carbon storage in the sediments.

The behavioral adaptations of the vernal bloom influence the biogeochemical cycling within the water column. At the late phase of the spring bloom, the vertically migrating dinoflagellate cells (Olli et al., 1998) descend below the euphotic layer (30–40 m depth), where cyst formation takes place (Spilling et al., 2006). If only a few percent of the cells encyst at most, the bulk of the biomass disintegrates and contributes to the DOM and slowly sinking phytodetrital pools in mid-depths of the water column. This resource, re-mineralized nutrients and organic

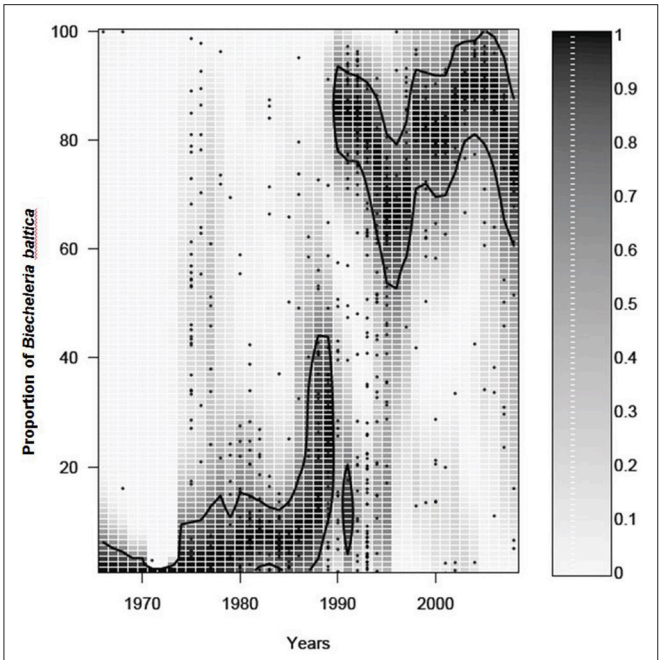

FIGURE 3 | Temporal change in the proportion of *Biecheleria baltica* from the total dinoflagellate biomass. All other notions as in **Figure 2**.

carbon substrate, will only have restricted availability to the organisms in the euphotic layer, as the rapidly establishing thermocline effectively segregates the water column. The single cell dinoflagellates, i.e., *Biecheleria* complex, was not found to migrate vertically in the coastal Gulf of Finland (Olli et al., 1998), but was shown to do so in the open waters of the north-western Baltic Proper, as a result of mineral nutrient depletion of the surface layer (Höglander et al., 2004). Thus the behavioral adaptations are not only species-specific, but probably also reflect regional variations in hydrodynamics and nutrient availability.

Diatoms

The diatom community tends to be more diverse during bloom conditions, compared to dinoflagellates, and functions more as a guild of complementing species (Smayda and Reynolds, 2003). This is also the case in the Baltic Sea where there are more diatom species present than dinoflagellates, but only a few species occur throughout the Baltic Sea during spring, making up a large fraction of the diatom biomass. Some of these diatoms are also present during winter in connection to the ice (Ikävalko and Thomsen, 1997), and can also be found in the Arctic, e.g., *Achnanthes taeniata* and *Melosira arctica*. These two and *Thalassiosira levanderi* are generally abundant in the initial phase of the spring bloom. Other abundant diatoms during the main bloom phase are *Chaetoceros wighamii*, *C. holsaticus*, *Diatoma tenuis, T. baltica,* and *Skeletonema marinoi*, where the latter typically become relatively more dominating after the peak of the spring bloom in the Gulf of Finland (Spilling, 2007b). Although some of these species occur also outside the Baltic Sea, the strong salinity gradient seems to be an effective barrier for gene exchange (Sjöqvist et al., 2015).

Diatom spores are less studied than dinoflagellate cysts in the Baltic Sea, but they seem to share many of the same characteristics. The fraction of the population that goes through the life-cycle change to form spores is highly species-specific and affected by environmental conditions (Heiskanen and Kononen, 1994; Kuosa et al., 1997). For example, *A. taeniata*, *C. holsaticus,* and *M. arctica* may settle to the seafloor primarily as spores, but the spore formation is affected e.g., by the availability of DSi, and the spore formation could be lower under less favorable conditions (Kuosa et al., 1997; Heiskanen, 1998). The functional role of diatom spores is similar to dinoflagellate cysts, i.e., long term survival in the sediment, and would thus have very much the same traits in terms of how they affect biogeochemical cycles. They can be buried and can be a useful tool for studies of paleoenvironmental changes (Witak et al., 2011). Interestingly, some spores (and also dinoflagellate cysts) are able to survive for up to a century in the sediment, enabling genetic comparison with present day strains (Härnström et al., 2011; Kremp et al., 2018). To our knowledge, there are no good estimates of how much carbon and nutrients are buried in the sediments in the form of diatom spores annually, but it is clear that the community composition is one of the key components determining this.

LINKING SEDIMENTATION OF PHYTOPLANKTON TO MICROBIAL MINERALIZATION PROCESSES

The main driver of sediment nutrient cycling is organic matter serving the energy source for heterotrophic microorganisms (Berner, 1974; Froelich et al., 1979). In addition to the organic matter, the availability of electron acceptors (O_2, NO_3, Mn, and Fe oxides and SO_4) create the premises for the pathways of organic carbon mineralization. In the Baltic Sea, availability of organic matter and electron acceptors vary in the bottoms of the different sub-basins. For example, the sediments of the Gulf of Bothnia are organic poor compared to the Gulf of Riga, the Baltic Proper and the Gulf of Finland (Lehtoranta et al., 2008; Aigars et al., 2015; Egger et al., 2015). The Bothnian Bay is oxic down to the seafloor and O_2 may penetrate centimeters into the sediment (Slomp et al., 2013). The sediment of the Gulf of Riga is oxic as well, but the penetration depth varies considerably throughout the year (Aigars et al., 2015). In the oxic areas, the bottoms can use the entire set of electron acceptors to mineralize settled phytoplankton.

In contrast to the Gulf of Bothnia, the basins of the Baltic Proper suffer from long-term hypoxia and anoxia, and the O_2 penetrates into the sediment only in the shallow slopes with oxic water and after major Baltic inflow events (Almroth-Rosell et al., 2015; Mohrholz et al., 2015). Further north, at the entrance of the Gulf of Finland, anoxic periods vary inter-annually and seasonally, being most common in summer (Lehtoranta et al., 2017). The pore-water concentrations of dissolved Fe are low in the sediments of this region (Lehtoranta and Heiskanen, 2003; Jilbert et al., 2011), but, the concentration of sulfate is twice as

high as in the Bothnian Bay. So in the Baltic Proper and the Gulf of Finland microbes have reduced access to O_2, NO_3, and Fe(III), but a continuous contact to abundant sulfate.

To summarize, the ability of the benthic systems to mineralize the settled phytoplankton, their cysts, spores, and detritus is sub-basin specific in the Baltic Sea. The marked changes in the pelagic ecosystem or in the hydrodynamics have the potential to induce sub-basin specific shifts in the mineralization pathways which regulate the cycles of C, N, P, Fe, Mn, and S in the sediments.

Settling Spring Bloom Biomass and Mineralization of N and P

Nitrate (NO_3) can be used as a nutrient in the pelagic zone and as an oxidant in mineralization and in oxidation of reduced substances such as Fe^{2+}, HS^-, H_2S, and CH_4 leading to formation of N_2 gas in sediments. In the oxic sediments of the Baltic Sea, the coupled nitrification-denitrification takes place right below the interface between oxic and anoxic layers, and is considered to be the major pathway for denitrification in the Baltic Sea (Hietanen and Kuparinen, 2008). The organic N is mineralized first to ammonium (NH_4) and then oxidized in the presence of O_2 to nitrite (NO_2) and subsequently to NO_3 which feeds the denitrification process. This process forms a link between settled organic matter, nitrogen, and respiration because organic C is oxidized by NO_3 to CO_2 and nitrate is denitrified to N_2 gas.

Denitrification is often seen as a negative feedback mechanism for eutrophication processes as it removes N from the system. Oxic conditions are needed to maintain the stock of NO_3 for the coupled nitrification-denitrification, but anoxic condition is obligatory for denitrification. Vahtera et al. (2007a) suggested that the increase in size of hypoxic area in the Baltic Sea is linked to the decrease in storage of N through removal of N by denitrification. However, stratification and excess organic matter may deplete O_2, which inhibits the formation of NO_3 and may lead to accumulation of NH_4 and decrease the N removal through denitrification in sediments (Jäntti and Hietanen, 2012). There is an alternative pathway for N removal through ammonium oxidation coupled to nitrite reduction, also leading to the production of gaseous forms of N (mainly N_2 but also NO and N_2O) (Kuypers et al., 2003). This N removing mechanism, anammox, requires one oxidized N species (NO_2^-) for every N_2 molecule made, which is half the requirement of denitrification. Anammox bacteria grow relatively slowly and the lack of NO_2^- will also stop the anammox process. However, N removal might in this case take place further up in the water column in the Baltic Proper (Dalsgaard et al., 2013), but this is a process that is not very pronounced in other sub basins such as the Gulf of Finland (Jäntti and Hietanen, 2012).

The cycling of sediment P is intimately linked to the mineralization of the settling phytoplankton and detritus. Phosphate itself is not a redox-sensitive substance, but there is commonly a strong, negative correlation between O_2 and phosphate concentrations. This relationship can largely be explained with the coupling of P to the Fe cycling (Einsele, 1938). Based on literature and the tests with estuarine sediments from the Gulf of Finland, it is evident that the mineralization through Fe(III) oxides and Fe reduction by H_2S (or HS^-) may result in markedly different outcomes regarding cycling of P in different sub-basins (Lehtoranta et al., 2009).

In the Bothnian Bay, the concentrations of dissolved Fe^{2+} and P in pore water indicate that the microbial Fe reduction may maintain the coupled cycling of Fe and P in the sediments (Blomqvist et al., 2004; Slomp et al., 2013). The Bothnian Bay, therefore, has a great potential to capture the P mineralized from settled phytoplankton and detritus to newly forming Fe(III) oxides in the oxic zone of the sediment. Also the burial of the reduced Fe phosphate mineral vivianite ($Fe_3(PO_4)_2 8H_2O$), may enhance the P binding in the methanogenic zone of the Gulf of Bothnia (Slomp et al., 2013; Egger et al., 2015). In contrast to the Bothnian Bay, the formation of solid Fe sulfide minerals may block the cycling of Fe in the Baltic Proper and the Gulf of Finland (Lehtoranta et al., 2008). In these areas the dominance of sulfate reduction creates sulfidic conditions and the P mineralized from phytoplankton and Fe(III) oxides may freely escape from the sediment to water without sequestration by Fe. From a water quality perspective, the formation of Fe sulfides rapidly deteriorates environmental conditions as the ability of the sediment to sorb P into Fe is largely lost. This is the situation in the Baltic Proper and the Gulf of Finland where the sediments ability to capture P originating from settling algae has been reduced or lost.

It is evident that the amount of settled phytoplankton and detritus has direct consequences for the cycling of N and P in the Baltic Sea ecosystem. What is less apparent is the qualitative aspect of the settling biomass and what electron acceptor may be used in the mineralization process. Spilling and Lindström (2008) added different cultures of spring bloom algae to a natural sediment, and found that they produced very different responses in the sediment, depending on species-specific life cycle change. In short, a dinoflagellate that produced cysts did not contribute to oxygen depletion, NH_4 formation and P release. The vegetative stages, in contrast, (of both a diatom and another dinoflagellate) quickly turned the sediment anoxic with the formation of Fe sulfides, NH_4 and release of P. This highlights the qualitative aspect of the settling material, i.e., not all of the phytoplankton settled is easily mineralized, and this is to our knowledge not taken into account in any models of biogeochemical cycling.

Resting stages, being cysts or spores, are built to survive for a long time in the sediment. The qualitative aspect of the settling biomass cannot be divided into dinoflagellates or diatoms as such, but is linked to life cycle changes. However, the amount of resting stages made after the spring bloom is species-specific, and dinoflagellates tend to produce more carbon bound to resting stages than diatoms. In particular *B. baltica* and *G. corollarium* go through mass encystment and because their germination success is low the following year, they are effective vehicles for carbon burial in the sediment. At least *B. baltica* has increased its biomass substantially over the past decades, and if this continues a larger share of the biomass produced during spring could be buried permanently at the seafloor.

Sediment Thresholds Controlling Nutrient Dynamics

With increasing transport of phytoplankton to the seafloor, there will generally be successive, non-linear thresholds that change the mineralization pathways and geochemical conditions in the sediment. The first threshold takes place when stratification decreases the transport rate of O_2 downwards, or there is an excess of organic C input enhancing the oxygen consumption. Both cases lead to anoxia first in the sediment and then in overlying water. Under these conditions, the coupled nitrification-denitrification is blocked and the NO_3 flux from water to sediment starts to control the denitrification, which is the case in the Gulf of Riga (Aigars et al., 2015). Without oxidation of NH_4 only few micromoles of labile carbon served by phytoplankton is required to deplete NO_3 as the near-bottom water concentration of NO_3 varies commonly from 2 to 10 μmol L^{-1} in the Gulf of Finland. Eventually the anoxic conditions result in the accumulation of NH_4 in the near-bottom water. Then the oxidation of released NH_4 to NO_3 may occur only in the chemocline between oxic and anoxic water layers and the formed NO_3 may be denitrified with organic matter and sulfides present in anoxic water as in the Gotland Basin (Dalsgaard et al., 2013). We have modified the conceptual model of Vahtera et al. (2007a) to include the threshold regarding the cycling of N (**Figure 4**). Although part of the N removal may occur above the seafloor (Dalsgaard et al., 2013), the potential termination of N-removal could form a positive feedback loop for eutrophication.

After depletion of NO_3 and in the presence of labile organic C in the sediment, the system is pushed toward a second threshold when microbe-driven Fe(III) reduction results in and simultaneous release of Fe and P to the near-bottom water. When Fe is diffused or transported during vertical mixing or upwelling events to an oxic environment, the newly formed Fe(III) oxides have the capacity to resorb P originating from the settled phytoplankton.

The concentration of poorly crystalline Fe(III) is suggested to control the Fe reduction rate. Four moles of Fe is needed to oxidize one mole of organic carbon and without re-oxidation by oxygen, NO_3, and Mn oxides, the pool of bioavailable Fe(III) oxides can be consumed within days in organic rich marine sediments, but large regional differences are evident (Rysgaard et al., 2001; Canfield et al., 2005). The depletion of bioavailable Fe(III) oxides leads to a third threshold, where sulfate reduction is the dominant mineralization pathway for settled phytoplankton biomass. The passing of the third threshold forms enough sulfides capable to precipitate with reactive Fe and block its cycling. Under the sulfidic conditions, the sediment and water column has poor ability to bind P to Fe, which results in a large release of Fe bound P and organic P and a minor release of Fe to the overlaying water. Thus, in the Baltic Sea the large pulse of P in the sulfidic conditions is explained by the dissolution of Fe(III) oxide bound P and the mineralization of fresh organic P that may be released within a short period of time compared to "old" organic P, which may take years to remineralization in sediments (Ahlgren et al., 2006). Additionally, the high amount of labile C and abundance of SO_4 maintains sulfate reduction and leads to accumulation of free sulfides in the water column as found in the bottom water of the Baltic Proper and occasionally in the Gulf of Finland. The oxidation of these sulfides in the chemocline consumes O_2, NO_3, Mn(IV), and Fe(III) present in the water column, delaying the recovery of the sedimentary system of the Baltic Sea. Typically, there is too little Fe to bind P in the water and the ability of the sediment to resorb P to Fe(III) oxides depends on the re-oxidation of the reduced Fe(II). The oxidation of Fe by O_2 in the water takes place at a very thin surface layer, but may be extended with the help of benthic animals that burrows into the sediment, such as *Marenzelleria* spp., an alien species that has spread to large bottom areas in the Baltic (Norkko et al., 2012; Maximov et al., 2015).

Modeling of biogeochemical fluxes relies on the information of sediment processes and our understanding of these sediment thresholds as eutrophication increases the amount of sinking phytoplankton. We have concentrated on solving how easily degraded organic matter consume the various electron acceptors in the sediment, and how this affects material fluxes through the sediment-water interface. However, the qualitative aspect of the settling material as described above should be taken into consideration (Stolpovsky et al., 2015), in particular under the scenario with changing composition of the sinking organic matter. Another important biological process to consider is bioturbation by benthic animals, which will affect sediment processes e.g., by increasing oxygen penetration depth into the sediment (Norkko et al., 2012). Understanding the complex interplay between settling phytoplankton biomass, its quality (labile, semi-labile, or refractory) and biological activity in the sediment is the target of ongoing modeling efforts (e.g., Stolpovsky et al., 2018). In the Baltic Sea, an important step would be to better predict the quantity of the settling organic matter that will trigger the three sediment thresholds described above, taking the qualitative aspect of the biomass and bioturbation into consideration.

PELAGIC NUTRIENT DYNAMICS—FROM SPRING TO SUMMER

One of the highly visible effects of the eutrophication problem in the Baltic Sea is the increased biomass of diazotrophic cyanobacteria during summer (Elmgren et al., 2015). The prevailing N limitation at the end of the spring bloom leads to a low N:P ratio during summer, which favors N-fixing cyanobacteria during warm, calm summer months (Niemi, 1979; Wasmund et al., 2005). The cyanobacterial blooms directly affect the eutrophication problem, as their fixation of N is comparable in magnitude with anthropogenic loading of N in parts of the Baltic Sea (Savchuk, 2005; Wasmund et al., 2005). In addition to the cyanobacterial biomass, the part of the newly fixed N is released and may be taken up by other components in the plankton food web (Adam et al., 2016), and this may start right after the spring bloom when the water is still relatively cold (10°C) (Svedén et al., 2015). The cyanobacterial input of N might have a self-enforcing nature by increasing the biomass load reaching the sediment, aggravating oxygen consumption and increasing release of P (Tamminen and Andersen, 2007; Vahtera et al., 2007a). However, we argue that the species composition

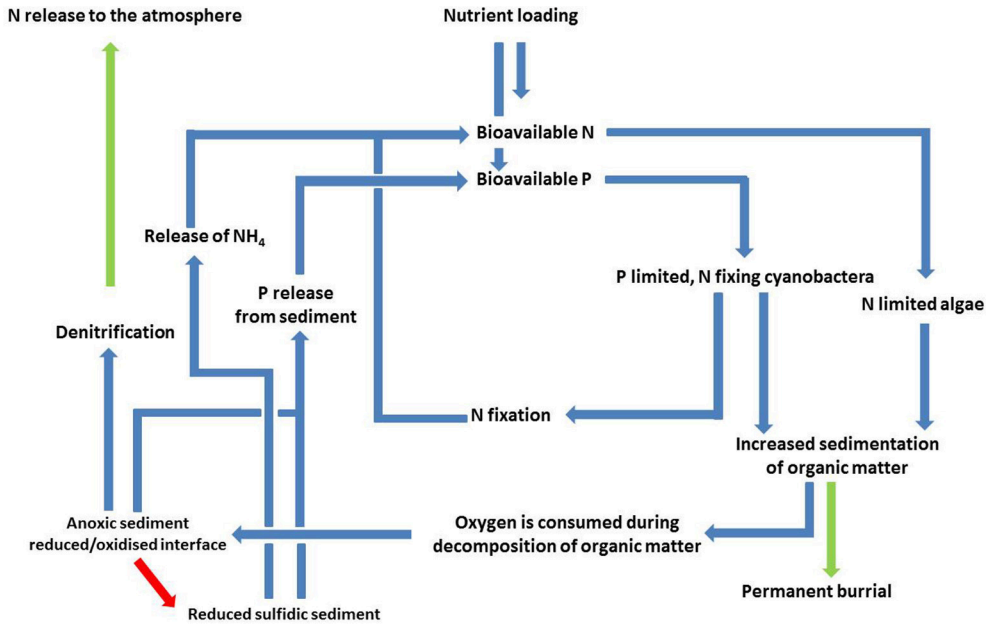

FIGURE 4 | A modified version of the vicious cycle presented in Tamminen and Andersen (2007) and Vahtera et al. (2007a) where the possible termination of denitrification has been added (red arrow). This takes place when the amount of organic matter is large enough to reduce both the sediment and bottom water, leading to a stop in the oxidation of ammonium (nitrification), which is a prerequisite for denitrificaiton to take place; however, denitrification higher in the water column may to some extent compensate for this (Dalsgaard et al., 2013). Both the quantity and quality (e.g., plankton community composition) of the spring bloom biomass may affect the magnitude of the nutrient sinks (green arrows).

of the spring bloom could affect this: with the shift toward a more dinoflagellate-dominated community (Wasmund and Uhlig, 2003; Klais et al., 2011), the sharp flux of diatom biomass to the sediment would diminish. This could have ecosystem-wide consequences as the organic material transport to the sediment affects both nitrogen and phosphorus cycles (Vahtera et al., 2007a). To some extent, the sedimentation pattern could be prolonged with more recycling in the euphotic zone (Tamelander et al., 2017), but at present we miss an understanding of how the observed shift in the spring phytoplankton community has on sedimentation and material fluxes on a large scale.

The pool of bioavailable P at the onset of summer is critical for the development of the cyanobacterial blooms later in the season. This has increased over large areas since the mid-1990s. In the Gulf of Finland and Baltic Proper the concentration may be as high as >0.5 μmol PO_4 L^{-1} after N sources have been depleted (**Figure 5**). In the Bothnian Sea the development is the same but with lower remaining P pool and Bothnian Bay is P limited and has an N surplus.

The two main cyanobacterial species: *Aphanizomenon flos-aquae* and *Nodularia spumigena* have different P uptake strategies. *A. flos-aquae* requires inorganic phosphate and can take up and store excess P for later growth (Larsson et al., 2001; Kangro et al., 2007), whereas *N. spumigena* has higher affinity for P uptake and relies more on recycled P (Hagström et al., 2001; Vahtera et al., 2007b). Under stable conditions there is also a spatial separation between the main summer cyanobacteria where *A. flos-aquae* typically remains lower in the water column whereas *N. spumigena* is found at the surface (Hajdu et al., 2007). *A. flos-aquae* is the main diazotroph in the Northern Baltic Proper, and in addition to *N. spumigena*, also *Dolichospermum* spp. contributes to the N-fixation (Klawonn et al., 2016). It is clear that cyanobacteria is benefitting from the oversupply of P (Raateoja et al., 2011), but several open questions remain. The dominant cyanobacterial species grow relatively slowly, in particular in water temperatures below 15°C (but *A. flos-aquae* is less temperature sensitive than *N. spumigena*), and there is typically a relatively short time window between the draw-down of bioavailable P and cyanobacteria growth, and it is not enough to satisfy the cyanobacterial need (Walve and Larsson, 2007; Nausch et al., 2008), so there must be other components in the plankton community that takes up the excess P. These could be other primary producers or heterotrophic bacteria (Nausch and Nausch, 2004). The prevailing N-limitation, limits growth of other phytoplankton and consequently inhibits their uptake of excess P. Heterotrophic bacteria is probably not limited by N, but might be limited by carbon (Lignell et al., 1992), at least their P uptake intensifies when they have a sufficient carbon source (Tamminen, 1989). To our knowledge, it is not clear what plankton groups takes up the excess P, but it does seem to accumulate in the particulate fraction and settle before the onset of dense cyanobacterial blooms (Nausch et al., 2008). It is evident that other P sources must exist for the cyanobacterial blooms (Raateoja et al., 2011), most likely through upwelling (Wasmund et al., 2012).

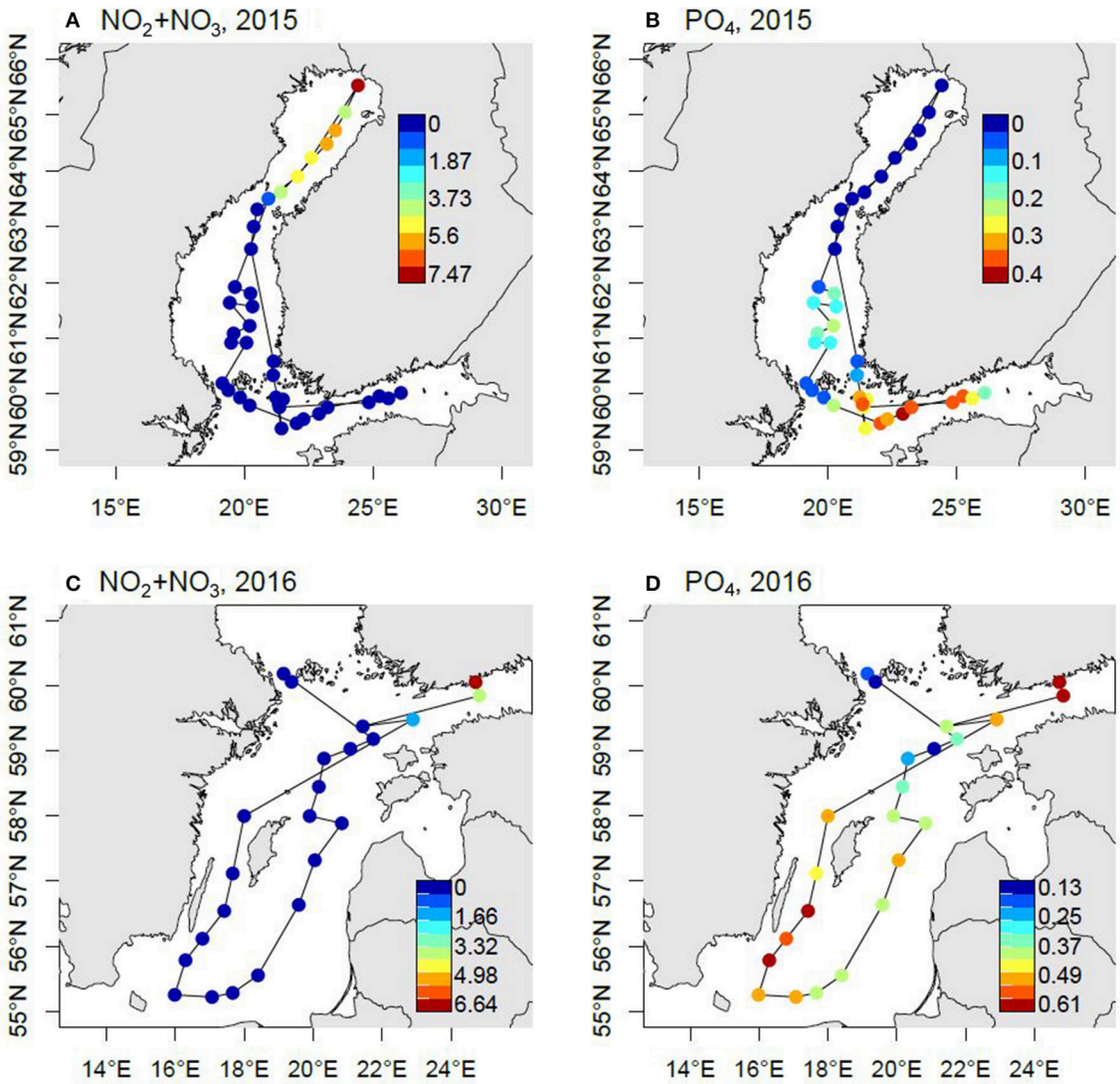

FIGURE 5 | Nutrient concentrations (μmol L^{-1}) at the surface (3 m depth) following the spring bloom. The samples were taken in May 2015 **(A,B)** and April 2016 **(C,D)** during the CFLUX15 and CFLUX16 research cruise, respectively, on board R/V Aranda. The maps have been modified from Spilling (2015) and Spilling (2016).

Role of Dissolved Organic Matter in Pelagic Nutrient Cycling

Due to the close connection with land with substantial freshwater input, the Baltic Sea has a large pool of dissolved organic matter (DOM) originating from outside the system, i.e., allochthonous DOM. In addition, there are several pathways from primary production into the DOM pool, such as direct release of exudates, lysis of cells, and sloppy feeding by grazers, i.e., autochthonous DOM. DOM is a potential source of carbon (DOC), nitrogen (DON) and phosphorus (DOP) for bacterial production, which may lead to remineralization of N and P back to inorganic forms available for phytoplankton. It may also provide organic matter to higher trophic levels through the microbial loop, although this is quite inefficient in trophic transfer (Anderson and Ducklow, 2001). Part of the allochthonous DOM, approximately 10% of DOC (Asmala et al., 2013), and ∼30% of DON and 75% of DOP (Stepanauskas et al., 2002) is taken up by bacteria. Photochemical degradation of allochthonous DOM can also support plankton production (Vähätalo et al., 2011), and in total, approximately 50% of the riverine DOM is removed (Seidel et al., 2017). The source of DOM can also be important as it may affect the phytoplankton community composition by favoring certain species (Jurgensone and Aigars, 2012). In the future, a warmer climate might lead to more precipitation and increased input of allochthonous DOM, in particular in the Northern Baltic Sea (Andersson et al., 2015), which might reduce light-dependent primary production and increase the importance of pelagic, heterotrophic bacteria (Wikner and Andersson, 2012; Andersson et al., 2018).

The input of autochthonous DOC from primary producers ranges from 2 to 50% of the fixed carbon in estuaries, averaging around 12% (Baines and Pace, 1991). In the Baltic Sea, there

is an increase of DOM during the productive season (Hoikkala et al., 2012), calculated to be 20–200 μmol DOC L^{-1} (Hoikkala et al., 2015). Only a part of the DOC from lysing cells is easily available for bacterial degradation, and in their review of different aquatic habitats, Søndergaard and Middelboe (1995) reported an average of 19% of the total dissolved organic carbon (DOC) pool to be labile in marine waters. However, higher percentages of 25–55% have been found in the Baltic Sea (Hoikkala et al., 2016), and Hoikkala et al. (2015) presented a conceptual model, where ∼50% of DOC produced by phytoplankton is rapidly degraded by bacteria. As the spring bloom depletes inorganic N sources in most of the sub basins of the Baltic Sea, autochthonous DON is an important component for primary and bacterial production (Korth et al., 2012). Later in the productive season N-fixing cyanobacteria is generally P limited, and DOP is potentially important. However, Nausch et al. (2008) studied the P pools in Baltic Proper and found a stable DOP pool suggesting that production and consumption was equal, and DOP was not a major P source for cyanobacteria.

After a dinoflagellate-dominated spring bloom, more DOC can be expected to be released in the pelagic zone, based on sedimentation studies (Heiskanen, 1998). However, diatoms are generally high DOC producers, and they can excrete organic compounds leading to even higher DOC concentrations than dinoflagellate-dominated blooms (Spilling et al., 2014). There are species-specific differences in DOC excretion, and at least a part of the heterotrophic bacterial community is affected by the phytoplankton community composition (Bunse et al., 2016), affecting also the responses in bacterial production (Camarena-Gómez et al., 2018). There is thus a potential link between the phytoplankton community composition during spring and the early summer DOM pool, with the potential to affect the cyanobacterial blooms during summer. This link has so far not received much attention, and it is currently not taken into account in model predictions of P availability and cascading effects on cyanobacterial bloom development.

A CONCEPTUAL MODEL

In the relatively shallow coastal and shelf ecosystems, the pelagic-benthic coupling is more important for ecosystem functioning than in the deep oceans. Changes in the phytoplankton communities may consequently lead to spatial and temporal differences in the quantity and quality of organic matter input to the seafloor, which in turn is the main driver for biogeochemical cycling of electron acceptors and nutrients. The conceptual model presented in **Figure 6** summarizes how different biogeochemical pathways may be altered by the phytoplankton community composition in the Baltic Sea, as described above. In particular, we represent the potential feedback mechanisms of changing plankton community in a typical site in the Gulf of Finland, characterized by seasonal sea ice and muddy, soft and oxic sediments inhabited by the two dominant macrozoobenthos species of soft bottom seabed, i.e., *Marenzelleria* spp. and *Macoma baltica*, which differentiate mostly by their different feeding habits, efficiency of bioturbation activities and location within sediments.

During harsh winters with a long ice season and thick ice cover, the sea-ice algal bloom typically dominated by diatoms is followed by a pelagic spring bloom of diatoms of similar species (e.g., *Chaetoceros* spp. *T. baltica*, and *A. taeniata* (**Figures 6A,B**). The bloom may be loosely grazed or degraded in the water column (up to 10%, Lignell et al., 1993), but most of it sinks to the seafloor. Under oxic sediment conditions, this large pool of organic matter may be efficiently consumed by the macrozoobenthos. With ample food supply, the macrozoobenthos community might increase and improve the oxygen conditions in the sediments through bioturbation (**Figure 6A**). However, if the amount of settling material exceeds the threshold of being efficiently consumed by the bottom communities, the result is aggravated oxygen consumption leading to permanent or seasonal hypoxia (Norkko et al., 2012). This, in turn, may cause the local fauna to perish with obvious loss of biodiversity, and may lead to an efflux of P from the anoxic sediments, further enhancing the summer bloom of cyanobacteria (**Figure 6B**), and fuelling the vicious cycle of Vahtera et al. (2007a) (**Figure 4**).

During mild winters, with a thin ice cover and short duration, winter mixing conditions in the water column may enhance the germination of dinoflagellates cysts (**Figure 6C**). Depending on snow thickness combined with photoperiod, the sea-ice diatom bloom may be enhanced or reduced compared to that of harsh winter (Tedesco et al., 2017). In the case of favorable light conditions (e.g., snow-free or little snow on the ice cover), the sea-ice diatom bloom may be coupled to an under ice bloom of germinated dinoflagellates after the sea ice has completely melted. If the spring bloom would be mostly composed of *P. catenata*, this would be mostly degraded in the water column, becoming part of the phyto-detritus available to the macrozoobenthos, in particular to *Marenzelleria*. On oxic sediments and at high abundances, *Marenzelleria* may help keep the deep sediments oxygenated and the sinking organic matter remineralized without passing any of the sediment thresholds (**Figure 6C**). However, there might be situations when the sinking material is not efficiently consumed with the risk of seasonal hypoxia/anoxia. In the case of a spring bloom dominated by *B. baltica*, about 40–50% of the sinking POC would be composed of not easily degradable cysts (**Figure 6D**). On oxic sediments, the remaining part would be available as a source of food for the macrofauna. Of this non-degradable carbon pool, only 10–20% of the cysts may germinate in the following winter (Kremp and Anderson, 2000), thus 40–45% of this spring production would be buried in the sediment. This would represent an effective long-term C sink in the sediments (**Figure 6D**), which has the potential to improve the environmental status of the Baltic Sea.

Marine ecosystem models are currently essential tools for exploring the responses of ecosystems for management actions and for exploitation, but these models can only be useful if the ecological processes are correctly described and the essential components are included. In order to develop and improve this approach, understanding the transfer of nutrients between pelagic and benthic systems from winter through spring and

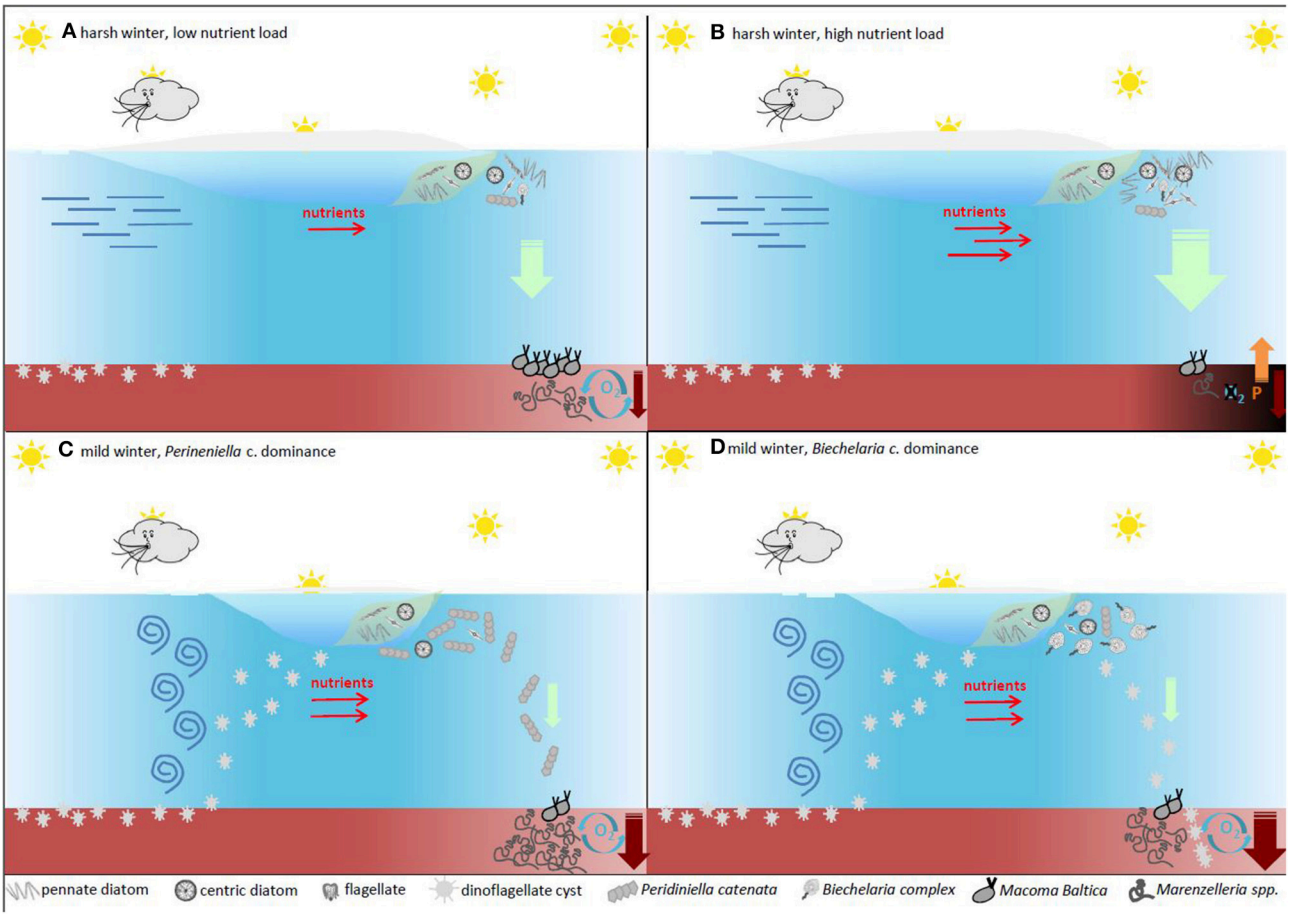

FIGURE 6 | A conceptual model of how the main spring phytoplankton groups affect sedimentation patterns and biogeochemical cycling of nutrients. The primary driver for the onset of the spring bloom is the availability of light, which is mainly governed by the mixing/stabilization of the upper parts of the water column. In the Baltic Sea large outflow of freshwater during spring creates patches of stratified water where the bloom initiates. After the spring bloom, diatoms tend to sink quickly to the seafloor where the biomass is remineralized. The sediment processes will depend on the amount of settling material and eutrophication have shifted the pristine state **(A)** towards a deteriorated environmental state with release of nutrients from the sediments **(B)**. Dinoflagellates on the other hand tend to lyse before reaching the sediment **(C)** with the exception of resting cysts **(D)**. These resting stages (some species of diatoms also produce large quantities of resting stages with the same function) are built for long term survival and are not remineralized in the sediment on a seasonal basis. Some of the resting stages are buried in the seafloor, providing a biological sink for organic nutrients. The size of this sink largely depends on the species composition of phytoplankton during the productive spring bloom.

into summer is needed. There are open questions related to the role of DOM in transfer of nutrients (quantity and quality), and the qualitative aspect of the sinking material, where changes in functional traits in the spring bloom community is important. The potential feedback mechanisms through changing plankton community composition have so far received relatively little attention, although community structure is known to play a major role for biogeochemical fluxes. The inherent difficulty in resolving causal connections from field observations calls for more dedicated experiments addressing the plankton community composition and the settling of phytoplankton in various forms under different environmental change scenarios.

Finally, as the Baltic Sea is facing increasing temperature associated with shorter ice season and thinner sea ice (Thomas et al., 2017), there are indications that climate change will weaken the magnitude, but prolong the duration of the spring bloom (Groetsch et al., 2016), which would directly affect the timing and flux of organic matter to the seafloor (Tamelander et al., 2017). Earlier stratification could benefit dinoflagellates, and the observed shift toward more dinoflagellate dominance in Gulf of Finland could continue and expand spatially. This would affect both the quantity and quality of the settling material and its mineralization at the seafloor, with less seabed enrichment in labile organic matter due to a more efficient pelagic microbial loop (**Figure 6C**). Dominance of species with high encystment rates and low germination success may enhance long-term burial of organic carbon as more resting stages are settling out of the water column (**Figure 6D**). This would functions as a biological sink and could be an underlying explanation for part of the unresolved N-burial (Jäntti and Hietanen, 2012), but this has not to our knowledge been tested before. Increasing

burial would diminish available nutrients in the ecosystem and would together with the realized reduction in nutrient loading counteract the observed spreading of the eutrophication. The increasing contribution of cyst-producing dinoflagellates could thus contribute to reversing eutrophication in the Baltic Sea.

AUTHOR CONTRIBUTIONS

The original idea for this manuscript came from a project involving KS, AK, and TiT. KO carried out data analysis on the Helsinki data (**Figures 2**, **3**). KO, AK, and RK formulated the phytoplankton species section and its development, and RK made **Figure 1** modified by KS. JL wrote the sediment process section and helped formulate the modified vicious cycle (**Figure 4**). LT, HP, KS, and TiT developed the conceptual model and LT made **Figure 5**. ToT reviewed and wrote about the trends in sedimentation. KS wrote the manuscript with contributions and/or comments from all co-authors.

FUNDING

This study was supported by the Academy of Finland (decisions no 259164 and 263376) and Estonian Research Council (no 1575P, KO). Further funding came from Walter and Andrée de Nottbeck Foundation (KS and ToT) and the Swedish Cultural Heritage (ToT). LT acknowledges support also from COCOA—Nutrient cocktail in coastal zones of the Baltic Sea—EU BONUS project.

ACKNOWLEDGMENTS

We are thankful to the City of Helsinki Environment Center (Finland) for providing the phytoplankton monitoring data.

REFERENCES

Adam, B., Klawonn, I., Svedén, J. B., Bergkvist, J., Nahar, N., Walve, J., et al. (2016). N_2-fixation, ammonium release and N-transfer to the microbial and classical food web within a plankton community. *ISME J.* 10, 450–459. doi: 10.1038/ismej.2015.126

Ahlgren, J., Reitzel, K., Tranvik, L., Gogoll, A., and Rydin, E. (2006). Degradation of organic phosphorus compounds in anoxic Baltic Sea sediments: a ^{31}P nuclear magnetic resonance study. *Limnol. Oceanogr.* 51, 2341–2348. doi: 10.4319/lo.2006.51.5.2341

Aigars, J., Poikane, R., Dalsgaard, T., Eglite, E., and Jansons, M. (2015). Biogeochemistry of N, P and Si in the Gulf of Riga surface sediments: implications of seasonally changing factors. *Cont. Shelf Res.* 105, 112–120. doi: 10.1016/j.csr.2015.06.008

Almroth-Rosell, E., Eilola, K., Kuznetsov, I., Hall, P. O. J., and Meier, H. E. M. (2015). A new approach to model oxygen dependent benthic phosphate fluxes in the Baltic Sea. *J. Mar. Syst.* 144, 127–141. doi: 10.1016/j.jmarsys.2014.11.007

Anderson, T. R., and Ducklow, H. W. (2001). Microbial loop carbon cycling in ocean environments studied using a simple steady-state model. *Aquat. Microb. Ecol.* 26, 37–49. doi: 10.3354/ame026037

Andersson, A., Brugel, S., Paczkowska, J., Rowe, O., Figueroa, D., Kratzer, S., et al. (2018). Influence of allochthonous dissolved organic matter on pelagic basal production in a northerly estuary. *Estuar. Coast. Shelf Sci.* 204, 225–235. doi: 10.1016/j.ecss.2018.02.032

Andersson, A., Meier, H. M., Ripszam, M., Rowe, O., Wikner, J., Haglund, P., et al. (2015). Projected future climate change and Baltic Sea ecosystem management. *Ambio* 44, 345–356. doi: 10.1007/s13280-015-0654-8

Asmala, E., Autio, R., Kaartokallio, H., Pitkänen, L., Stedmon, C., and Thomas, D. (2013). Bioavailability of riverine dissolved organic matter in three Baltic Sea estuaries and the effect of catchment land use. *Biogeosciences* 10, 6969–6986. doi: 10.5194/bg-10-6969-2013

BACCI (2015). Second *Assessment of Climate Change for the Baltic Sea Basin*. New York, NY: SpringerOpen.

Baines, S. B., and Pace, M. L. (1991). The production of dissolved organic matter by phytoplankton and its importance to bacteria: patterns across marine and freshwater systems. *Limnol. Oceanogr.* 36, 1078–1090. doi: 10.4319/lo.1991.36.6.1078

Belkin, I. M. (2009). Rapid warming of large marine ecosystems. *Prog. Oceanogr.* 81, 207–213. doi: 10.1016/j.pocean.2009.04.011

Berner, R. A. (1974). "Kinetic models for the early diagenesis of nitrogen, sulphur, phosphorus, and silicon in anoxic marine sediments," in *The Sea,* Vol. 5, *Marine Chemistry,* ed E. D. Goldberg (New York, NY: John Wiley and Sons), 427–450.

Blomqvist, S., Gunnars, A., and Elmgren, R. (2004). Why the limiting nutrient differs between temperate coastal seas and freshwater lakes: a matter of salt. *Limnol. Oceanogr.* 49, 2236–2241. doi: 10.4319/lo.2004.49.6.2236

Brzezinski, M. A., Olson, R. J., and Chisholm, S. W. (1990). Silicon availability and cell-cycle progression in marine diatoms. *Mar. Ecol. Prog. Ser.* 67, 83–96. doi: 10.3354/meps067083

Bunse, C., Bertos-Fortis, M., Sassenhagen, I., Sildever, S., Sjöqvist, C., Godhe, A., et al. (2016). Spatio-temporal interdependence of bacteria and phytoplankton during a Baltic Sea spring bloom. *Front. Microbiol.* 7:517. doi: 10.3389/fmicb.2016.00517

Camarena-Gómez, M. T., Lipsewers, T., Piiparinen, J., Eronen-Rasimus, E., Perez-Quemaliños, D., Hoikkala, L., et al. (2018). Shifts in phytoplankton community structure modify bacterial production, abundance and community composition. *Aquat. Microb. Ecol.* 81, 149–170. doi: 10.3354/ame01868

Canfield, D. E., Thamdrup, B., and Kristensen, E. (2005). Aquatic Geomicrobiology, Advances in Marine Biology. London: Elsevier Academic Press.

Carlsson, P., and Graneli, E. (1998). "Utilization of dissolved organic matter (DOM) by phytoplankton, including harmful species," in *Physiology of Harmful Algal Blooms. NATO ASI Series G41,* eds D. M. Anderson, A. D. Cembella, and G. M. Hallegraeff (Berlin: Springer-Verlag), 509–524.

Carstensen, J., Conley, D. J., Bonsdorff, E., Gustafsson, B. G., Hietanen, S., Janas, U., et al. (2014). Hypoxia in the Baltic Sea: biogeochemical cycles, benthic fauna, and management. *Ambio* 43, 26–36. doi: 10.1007/s13280-013-0474-7

Cloern, J. E. (2001). Our evolving conceptual model of the coastal eutrophication problem. *Mar. Ecol. Prog. Ser.* 210, 223–253. doi: 10.3354/meps210223

Conley, D. J., Carstensen, J., Aigars, J., Axe, P., Bonsdorff, E., Eremina, T., et al. (2011). Hypoxia is increasing in the coastal zone of the Baltic Sea. *Environ. Sci. Technol.* 45, 6777–6783. doi: 10.1021/es201212r

Conley, D. J., Humborg, C., Rahm, L., Savchuk, O. P., and Wulff, F. (2002). Hypoxia in the Baltic Sea and basin-scale changes in phosphorus biogeochemistry. *Environ. Sci. Technol.* 36, 5315–5320. doi: 10.1021/es025763w

Conley, D. J., Schelske, C. L., and Stoermer, E. F. (1993). Modification of the biogeochemical cycle of silica with eutrophication. *Mar. Ecol. Prog. Ser.* 101, 179–192. doi: 10.3354/meps101179

Dalsgaard, T., De Brabandere, L., and Hall, P. O. (2013). Denitrification in the water column of the central Baltic Sea. *Geochim. Cosmochim. Acta* 106, 247–260. doi: 10.1016/j.gca.2012.12.038

Danielsson, Å., Papush, L., and Rahm, L. (2008). Alterations in nutrient limitations — scenarios of a changing Baltic Sea. *J. Mar. Syst.* 73, 263–283. doi: 10.1016/j.jmarsys.2007.10.015

Darecki, M., and Stramski, D. (2004). An evaluation of MODIS and SeaWiFS bio-optical algorithms in the Baltic Sea. *Remote Sens. Environ.* 89, 326–350. doi: 10.1016/j.rse.2003.10.012

Doney, S. C. (1997). The ocean's productive deserts. *Nature* 389, 905–906. doi: 10.1038/39993

Duarte, C. M. (2014). Global change and the future ocean: a grand challenge for marine sciences. *Front. Mar. Sci.* 1:63. doi: 10.3389/fmars.2014.00063

Egge, J. K., and Aksnes, D. L. (1992). Silicate as regulating nutrient in phytoplankton competition. *Mar. Ecol. Prog. Ser.* 83, 281–289. doi: 10.3354/meps083281

Egger, M., Jilbert, T., Behrends, T., Rivard, C., and Slomp, C. P. (2015). Vivianite is a major sink for phosphorus in methanogenic coastal surface sediments. *Geochim. Cosmochim. Acta* 169, 217–235. doi: 10.1016/j.gca.2015.09.012

Einsele, W. (1938). Über chemische und kolloidchemische Vorgänge in Eisen-Phosphat-Systemen unter limnochemischen und limnogeologischen Gesichtspunkten. *Arch. Hydrobiol.* 33, 361–387.

Elmgren, R., Blenckner, T., and Andersson, A. (2015). Baltic Sea management: successes and failures. *Ambio* 44, 335–344. doi: 10.1007/s13280-015-0653-9

Fennel, W., and Neumann, T. (2014). *Introduction to the Modelling of Marine Ecosystems.* Amsterdam: Elsevier.

Froelich, P. N., Klinkhammer, G. P., Bender, M. L., Luedtke, N. A., Heath, G. R., Cullen, D., et al. (1979). Early oxidation of org. matter in pelagic sediments of the eastern equatorial Atlantic: suboxic diagenesis. *Geochim. Cosmochim. Acta* 43, 1075–1090. doi: 10.1016/0016-7037(79)90095-4

Gilpin, L. C., Davidson, K., and Roberts, E. (2004). The influence of changes in nitrogen: silicon ratios on diatom growth dynamics. *J. Sea Res.* 51, 21–35. doi: 10.1016/j.seares.2003.05.005

Groetsch, P. M. M., Simis, S. G. H., Eleveld, M. A., and Peters, S. W. M. (2016). Spring blooms in the Baltic Sea have weakened but lengthened from 2000 to 2014. *Biogeosciences* 13, 4959–4973. doi: 10.5194/bg-13-4959-2016

Gustafsson, B. G., Schenk, F., Blenckner, T., Eilola, K., Meier, H. M., Müller-Karulis, B., et al. (2012). Reconstructing the development of Baltic Sea eutrophication 1850–2006. *Ambio* 41, 534–548. doi: 10.1007/s13280-012-0318-x

Hagström, Å., Azam, F., Kuparinen, J., and Zweifel, U.-L. (2001). "Pelagic plankton growth and resource limitations in the Baltic Sea," in *A Systems Analysis of the Baltic Sea* (Berlin: Springer), 177–210.

Hajdu, S., Höglander, H., and Larsson, U. (2007). Phytoplankton vertical distributions and composition in Baltic Sea cyanobacterial blooms. *Harmful Algae* 6, 189–205. doi: 10.1016/j.hal.2006.07.006

Hallegraeff, G. M. (2010). Ocean climate change, phytoplankton community responses, and harmful algal blooms: a formidable predictive challenge. *J. Phycol.* 46, 220–235. doi: 10.1111/j.1529-8817.2010.00815.x

Halpern, B. S., Walbridge, S., Selkoe, K. A., Kappel, C. V., Micheli, F., D'Agrosa, C., et al. (2008). A global map of human impact on marine ecosystems. *Science* 319, 948–952. doi: 10.1126/science.1149345

Härnström, K., Ellegaard, M., Andersen, T. J., and Godhe, A. (2011). Hundred years of genetic structure in a sediment revived diatom population. *Proc. Natl. Acad. Sci. U.S.A.* 108, 4252–4257. doi: 10.1073/pnas.1013528108

Havenhand, J. N. (2012). How will ocean acidification affect Baltic Sea ecosystems? an assessment of plausible impacts on key functional groups. *Ambio* 41, 637–644. doi: 10.1007/s13280-012-0326-x

Heiskanen, A. S. (1993). Mass encystment and sinking of dinoflagellates during a spring bloom. *Mar. Biol.* 116, 161–167. doi: 10.1007/BF00350743

Heiskanen, A. S. (1995). Contamination of sediment trap fluxes by vertically migrating phototrophic microoranisms in the coastal Baltic Sea. *Mar. Ecol. Prog. Ser.* 122, 45–58. doi: 10.3354/meps122045

Heiskanen, A. S. (1998). Factors governing sedimentation and pelagic nutrient cycles in the northern Baltic Sea. *Monogr. Boreal. Env. Res.* 8, 1–80.

Heiskanen, A. S., and Kononen, K. (1994). Sedimentation of vernal and late summer phytoplankton communities in the coastal Baltic Sea. *Arch. Hydrobiol.* 131, 175–198.

HELCOM (2009). "Eutropication in the Baltic Sea - an integrated thematic assessment of the effects of nutrient enrichment and eutrophication in the Baltic Sea region," in *Baltic Sea Environment Proceedings* (Helsinki: Helsinki Commission).

HELCOM (2010). "Hazardous substances in the Baltic Sea – an integrated thematic assessment of hazardous substances in the Baltic Sea," in *Balt Sea Environment Proceedings* (Helsinki: Helsinki Commission).

Hietanen, S., and Kuparinen, J. (2008). Seasonal and short-term variation in denitrification and anammox at a coastal station on the Gulf of Finland, Baltic Sea. *Hydrobiologia* 596, 67–77. doi: 10.1007/s10750-007-9058-5

Hinder, S. L., Hays, G. C., Edwards, M., Roberts, E. C., Walne, A. W., and Gravenor, M. B. (2012). Changes in marine dinoflagellate and diatom abundance under climate change. *Nat. Clim. Change* 2, 271–275. doi: 10.1038/nclimate1388

Höglander, H., Larsson, U., and Hajdu, S. (2004). Vertical distribution and settling of spring phytoplankton in the offshore NW Baltic Sea proper. *Mar. Ecol. Prog. Ser.* 283, 15–27. doi: 10.3354/meps283015

Hoikkala, L., Kortelainen, P., Soinne, H., and Kuosa, H. (2015). Dissolved organic matter in the Baltic Sea. *J. Mar. Syst.* 142, 47–61. doi: 10.1016/j.jmarsys.2014.10.005

Hoikkala, L., Lahtinen, T., Perttilä, M., and Lignell, R. (2012). Seasonal dynamics of dissolved organic matter on a coastal salinity gradient in the northern Baltic Sea. *Cont. Shelf Res.* 45, 1–14. doi: 10.1016/j.csr.2012.04.008

Hoikkala, L., Tammert, H., Lignell, R., Eronen-Rasimus, E., Spilling, K., and Kisand, V. (2016). Autochthonous dissolved organic matter drives bacterial community composition during a bloom of filamentous cyanobacteria. *Front. Mar. Sci.* 3:111. doi: 10.3389/fmars.2016.00111

Hordoir, R., and Meier, H. (2012). Effect of climate change on the thermal stratification of the Baltic Sea: a sensitivity experiment. *Clim. Dyn.* 38, 1703–1713. doi: 10.1007/s00382-011-1036-y

Humborg, C., Smedberg, E., Medina, M. R., and Mörth, C.-M. (2008). Changes in dissolved silicate loads to the Baltic Sea—the effects of lakes and reservoirs. *J. Mar. Syst.* 73, 223–235. doi: 10.1016/j.jmarsys.2007.10.014

Ikävalko, J., and Thomsen, H. A. (1997). The Baltic Sea ice biota (March 1994): a study of the protistan community. *Eur. J. Protistol.* 33, 229–243. doi: 10.1016/S0932-4739(97)80001-6

Jaanus, A., Hajdu, S., Kaitala, S., Andersson, A., Kaljurand, K., Ledaine, I., et al. (2006). Distribution patterns of isomorphic cold-water dinoflagellates (*Scrippsiella/Woloszynskia* complex) causing 'red tides' in the Baltic Sea. *Hydrobiologia* 554, 137–146. doi: 10.1007/s10750-005-1014-7

Jäntti, H., and Hietanen, S. (2012). The effects of hypoxia on sediment nitrogen cycling in the Baltic Sea. *Ambio* 41, 161–169. doi: 10.1007/s13280-011-0233-6

Jilbert, T., Slomp, C. P., Gustafsson, B. G., and Boer, W. (2011). Beyond the Fe-P-redox connection: preferential regeneration of phosphorus from organic matter as a key control on Baltic Sea nutrient cycles. *Biogeosciences* 8, 1699–1720. doi: 10.5194/bg-8-1699-2011

Jurgensone, I., and Aigars, J. (2012). Bioavailability of riverine dissolved organic matter to phytoplankton in the marine coastal waters. *Estuar. Coast. Shelf Sci.* 107, 97–104. doi: 10.1016/j.ecss.2012.05.005

Kahru, M., Elmgren, R., and Savchuk, O. P. (2016). Changing seasonality of the Baltic Sea. *Biogeosciences* 13, 1009–1018. doi: 10.5194/bg-13-1009-2016

Kahru, M., Leppänen, J. M., Nõmmann, S., Passow, U., Postel, L., and Schulz, S. (1990). Spatio-temporal mosaic of the phytoplankton spring bloom in the open Baltic Sea in 1986. *Mar. Ecol. Prog. Ser.* 66, 301–309. doi: 10.3354/meps066301

Kahru, M., and Nõmmann, S. (1990). The phytoplankton spring bloom in the Baltic Sea in 1985, 1986 - multitude of spatiotemporal scales. *Cont. Shelf Res.* 10, 329–354. doi: 10.1016/0278-4343(90)90055-Q

Kangro, K., Olli, K., Tamminen, T., and Lignell, R. (2007). Species-specific responses of a cyanobacteria-dominated phytoplankton community to artificial nutrient limitation in the Baltic Sea. *Mar. Ecol. Prog. Ser.* 336, 15–27. doi: 10.3354/meps336015

Kazamia, E., Czesnick, H., Nguyen, T. T. V., Croft, M. T., Sherwood, E., Sasso, S., et al. (2012). Mutualistic interactions between vitamin B12-dependent algae and heterotrophic bacteria exhibit regulation. *Environ. Microbiol.* 14, 1466–1476. doi: 10.1111/j.1462-2920.2012.02733.x

Kiirikki, M., Lehtoranta, J., Inkala, A., Pitkänen, H., Hietanen, S., Hall, P. O. J., et al. (2006). A simple sediment process description suitable for 3D-ecosystem modelling — development and testing in the Gulf of Finland. *J. Mar. Syst.* 61, 55–66. doi: 10.1016/j.jmarsys.2006.02.008

Klais, R., Tamminen, T., Kremp, A., Spilling, K., An, B. W., Hajdu, S., et al. (2013). Spring phytoplankton communities shaped by interannual weather variability and dispersal limitation: mechanisms of climate change effects on key coastal primary producers. *Limnol. Oceanogr.* 58, 753–762. doi: 10.4319/lo.2013.58.2.0753

Klais, R., Tamminen, T., Kremp, A., Spilling, K., and Olli, K. (2011). Decadal-scale changes of dinoflagellates and diatoms in the anomalous Baltic Sea spring bloom. *PLoS ONE* 6:e21567. doi: 10.1371/journal.pone.0021567

Klawonn, I., Nahar, N., Walve, J., Andersson, B., Olofsson, M., Svedén, J., et al. (2016). Cell-specific nitrogen-and carbon-fixation of cyanobacteria in a temperate marine system (Baltic Sea). *Environ. Microbiol.* 18, 4596–4609. doi: 10.1111/1462-2920.13557

Korth, F., Deutsch, B., Liskow, I., and Voss, M. (2012). Uptake of dissolved organic nitrogen by size-fractionated plankton along a salinity gradient from the North Sea to the Baltic Sea. *Biogeochemistry* 111, 347–360. doi: 10.1007/s10533-011-9656-1

Kremp, A. (2000). Morphology and germination pattern of the resting cyst of *Peridiniella catenata* (Dinophycea) from the Baltic Sea. *Phycologia* 39, 183–186. doi: 10.2216/i0031-8884-39-3-183.1

Kremp, A., and Anderson, D. M. (2000). Factors regulating germination of resting cysts of the spring bloom dinoflagellate *Scrippsiella hangoei* from the northern Baltic Sea. *J. Plankton Res.* 22, 1311–1327. doi: 10.1093/plankt/22.7.1311

Kremp, A., Elbrächter, M., Schweikert, M., Wolny, J. L., and Gottschling, M. (2005). Woloszynskia halophila (Biecheler) comb. nov.: a bloom-forming cold-water dinoflagellate co-occurring with *Scrippsiella hangoei* (*Dinophyceae*) in the Baltic Sea. *J. Phycol.* 41, 629–642. doi: 10.1111/j.1529-8817.2005.00070.x

Kremp, A., Hinners, J., Klais, R., Leppänen, A.-P., and Kallio, A. (2018). Patterns of vertical cyst distribution and survival in 100-year-old sediment archives of three spring dinoflagellate species from the Northern Baltic Sea. *Eur. J. Phycol.* 53, 1–11. doi: 10.1080/09670262.2017.1386330

Kremp, A., Rengefors, K., and Montresorc, M. (2009). Species specific encystment patterns in three Baltic cold-water dinoflagellates: the role of multiple cues in resting cyst formation. *Limnol. Oceanogr.* 54, 1125–1138. doi: 10.4319/lo.2009.54.4.1125

Kremp, A., Tamminen, T., and Spilling, K. (2008). Dinoflagellate bloom formation in natural assemblages with diatoms: nutrient competition and growth strategies in Baltic spring phytoplankton. *Aquat. Microb. Ecol.* 50, 181–196. doi: 10.3354/ame01163

Kuosa, H., Autio, R., Kuuppo, P., Setala, O., and Tanskanen, S. (1997). Nitrogen, silicon and zooplankton controlling the Baltic spring bloom: an experimental study. *Estuar. Coast. Shelf Sci.* 45, 813–821. doi: 10.1006/ecss.1997.0241

Kuypers, M. M., Sliekers, A. O., Lavik, G., Schmid, M., Jørgensen, B. B., Kuenen, J. G., et al. (2003). Anaerobic ammonium oxidation by anammox bacteria in the Black Sea. *Nature* 422, 608–611. doi: 10.1038/nature01472

Larsen, J., Kuosa, H., Ikävalko, J., Kivi, K., and Hällfors, S. (1995). A redescription of *Scrippsiella hangoei* (Schiller) Comb-Nov - a red tide dinoflagellate from the northern Baltic. *Phycologia* 34, 135–144. doi: 10.2216/i0031-8884-34-2-135.1

Larsson, U., Hajdu, S., Walve, J., and Elmgren, R. (2001). Baltic Sea nitrogen fixation estimated from the summer increase in upper mixed layer total nitrogen. *Limnol. Oceanogr.* 46, 811–820. doi: 10.4319/lo.2001.46.4.0811

Legrand, C., and Carlsson, P. (1998). Uptake of high molecular weight dextran by the dinoflagellate *Alexandrium catenella*. *Aquat. Microb. Ecol.* 16, 81–86. doi: 10.3354/ame016081

Lehtoranta, J., Ekholm, P., and Pitkänen, H. (2008). Eutrophication-driven sediment microbial processes can explain the regional variation in phosphorus concentrations between Baltic Sea sub-basins. *J. Mar. Syst.* 74, 495–504. doi: 10.1016/j.jmarsys.2008.04.001

Lehtoranta, J., Ekholm, P., and Pitkänen, H. (2009). Coastal eutrophication thresholds: a matter of sediment microbial processes. *Ambio* 38, 303–308. doi: 10.1579/09-A-656.1

Lehtoranta, J., and Heiskanen, A. S. (2003). Dissolved iron: phosphate ratio as an indicator of phosphate release to oxic water of the inner and outer coastal Baltic Sea. *Hydrobiologia* 492, 69–84. doi: 10.1023/A:1024822013580

Lehtoranta, J., Savchuk, O. P., Elken, J., Dahlbo, K., Kuosa, H., Raateoja, M., et al. (2017). Atmospheric forcing controlling inter-annual nutrient dynamics in the open Gulf of Finland. *J. Mar. Syst.* 171, 4–20. doi: 10.1016/j.jmarsys.2017.02.001

Leterme, S. C., Edwards, M., Seuront, L., Attrill, M., Reid, P., and John, A. (2005). Decadal basin-scale changes in diatoms, dinoflagellates, and phytoplankton color across the North Atlantic. *Limnol. Oceanogr.* 50, 1244–1253. doi: 10.4319/lo.2005.50.4.1244

Lignell, R., Heiskanen, A. S., Kuosa, H., Gundersen, K., Kuuppo-Leinikki, P., Pajuniemi, R., et al. (1993). Fate of a phytoplankton spring bloom - sedimentation and carbon flow in the planktonic food web in the northern Baltic. *Mar. Ecol. Prog. Ser.* 94, 239–252. doi: 10.3354/meps094239

Lignell, R., Kaitala, S., and Kuosa, H. (1992). Factors controlling phyto- and bacterioplankton in late spring on a salinity gradient in the northern Baltic. *Mar. Ecol. Prog. Ser.* 84, 121–131. doi: 10.3354/meps084121

Litchman, E., and Klausmeier, C. A. (2008). Trait-based community ecology of phytoplankton. *Annu. Rev. Ecol. Evol. Syst.* 39, 615–639. doi: 10.1146/annurev.ecolsys.39.110707.173549

Lundberg, C., Jakobsson, B.-M., and Bonsdorff, E. (2009). The spreading of eutrophication in the eastern coast of the Gulf of Bothnia, northern Baltic Sea–an analysis in time and space. *Estuar. Coast. Shelf Sci.* 82, 152–160. doi: 10.1016/j.ecss.2009.01.005

Martin-Jézéquel, V., Hildebrand, M., and Brzezinski, M. A. (2000). Silicon metabolism in diatoms: implications for growth. *J. Phycol.* 36, 821–840. doi: 10.1046/j.1529-8817.2000.00019.x

Maximov, A., Bonsdorff, E., Eremina, T., Kauppi, L., Norkko, A., and Norkko, J. (2015). Context-dependent consequences of *Marenzelleria* spp. (Spionidae: Polychaeta) invasion for nutrient cycling in the Northern Baltic Sea. *Oceanologia* 57, 342–348. doi: 10.1016/j.oceano.2015.06.002

Meier, H. M., Andersson, H. C., Arheimer, B., Donnelly, C., Eilola, K., Gustafsson, B. G., et al. (2014). Ensemble modeling of the Baltic Sea ecosystem to provide scenarios for management. *Ambio* 43, 37–48. doi: 10.1007/s13280-013-0475-6

Mercado, J. M., Cortés, D., García, A., and Ramírez, T. (2007). Seasonal and inter-annual changes in the planktonic communities of the northwest Alboran Sea (Mediterranean Sea). *Prog. Oceanogr.* 74, 273–293. doi: 10.1016/j.pocean.2007.04.013

Moestrup, Ø., Lindberg, K., and Daugbjerg, N. (2009). Studies on woloszynskioid dinoflagellates IV: the genus *Biecheleria* gen. nov. *Phycol. Res.* 57, 203–220. doi: 10.1111/j.1440-1835.2009.00540.x

Mohrholz, V., Naumann, M., Nausch, G., Kruger, S., and Grawe, U. (2015). Fresh oxygen for the Baltic Sea - an exceptional saline inflow after a decade of stagnation. *J. Mar. Syst.* 148, 152–166. doi: 10.1016/j.jmarsys.2015.03.005

Nausch, M., and Nausch, G. (2004). Bacterial utilization of phosphorus pools after nitrogen and carbon amendment and its relation to alkaline phosphatase activity. *Aquat. Microb. Ecol.* 37, 237–245. doi: 10.3354/ame037237

Nausch, M., Nausch, G., Wasmund, N., and Nagel, K. (2008). Phosphorus pool variations and their relation to cyanobacteria development in the Baltic Sea: a three-year study. *J. Mar. Syst.* 71, 99–111. doi: 10.1016/j.jmarsys.2007.06.004

Niemi, Å. (1975). Ecology of phytoplankton in the Tvärminne area, SW coast of Finland. II. Primary production and environmental conditions in the archipelago and the sea zone. *Acta Bot. Fenn.* 105, 1–73.

Niemi, Å. (1979). Blue-green algal blooms and N:P ratio in the Baltic Sea. *Acta Bot. Fenn.* 110, 57–61.

Niiranen, S., Yletyinen, J., Tomczak, M. T., Blenckner, T., Hjerne, O., MacKenzie, B. R., et al. (2013). Combined effects of global climate change and regional ecosystem drivers on an exploited marine food web. *Glob. Change Biol.* 19, 3327–3342. doi: 10.1111/gcb.12309

Norkko, J., Reed, D. C., Timmermann, K., Norkko, A., Gustafsson, B. G., Bonsdorff, E., et al. (2012). A welcome can of worms? hypoxia mitigation by an invasive species. *Glob. Change Biol.* 18, 422–434. doi: 10.1111/j.1365-2486.2011.02513.x

Officer, C. B., and Ryther, J. H. (1980). The possible importance of silicon in marine eutrophication. *Mar. Ecol. Prog. Ser.* 3, 75–87. doi: 10.3354/meps003083

Olli, K., Clarke, A., Danielsson, Å., Aigars, J., Conley, D. J., and Tamminen, T. (2008). Diatom stratigraphy and long-term dissolved silica concentrations in the Baltic Sea. *J. Mar. Syst.* 73, 284–299. doi: 10.1016/j.jmarsys.2007.04.009

Olli, K., and Heiskanen, A.-S. (1999). Seasonal stages of phytoplankton community structure and sinking loss in the Gulf of Riga. *J. Mar. Syst.* 23, 165–184. doi: 10.1016/S0924-7963(99)00056-1

Olli, K., Heiskanen, A. S., and Lohikari, K. (1998). Vertical migration of autotrophic micro-organisms during a vernal bloom at the coastal Baltic Sea - coexistence through niche separation. *Hydrobiologia* 363, 179–189. doi: 10.1007/978-94-017-1493-8_14

Olli, K., Klais, R., Tamminen, T., Ptacnik, R., and Andersen, T. (2011). Long term changes in the Baltic Sea phytoplankton community. *Boreal Env. Res.* 16, 3–14.

Olli, K., and Trunov, K. (2010). Abundance and distribution of vernal bloom dinoflagellate cysts in the Gulf of Finland and Gulf of Riga (the Baltic Sea). *Deep Sea Res. II* 57, 235–242. doi: 10.1016/j.dsr2.2009.09.009

Olsen, S., and Paasche, E. (1986). Variable kinetics of silicon -limited growth in *Thalassiosira pseudonana* (*Bacillariophyceae*) in response to changed chemical composition of the growth medium. *Br. Phycol. J.* 21, 183–190. doi: 10.1080/00071618600650211

Omstedt, A., Humborg, C., Pempkowiak, J., Perttilä, M., Rutgersson, A., Schneider, B., et al. (2014). Biogeochemical control of the coupled CO_2-O_2 system of the Baltic Sea: a review of the results of Baltic-C. *Ambio* 43, 49–59. doi: 10.1007/s13280-013-0485-4

Papush, L., and Danielsson, Å. (2006). Silicon in the marine environment: dissolved silica trends in the Baltic Sea. *Estuar. Coast. Shelf Sci.* 67, 53–66. doi: 10.1016/j.ecss.2005.09.017

Papush, L., Danielsson, Å., and Rahm, L. (2009). Dissolved silica budget for the Baltic Sea. *J. Sea Res.* 62, 31–41. doi: 10.1016/j.seares.2009.03.001

Pitkänen, H., Lehtoranta, J., and Räike, A. (2001). Internal nutrient fluxes couteract decreases in external load: the case of the estuarial eastern Gulf of Finland, Baltic Sea. *Ambio* 30, 195–201. doi: 10.1579/0044-7447-30.4.195

Raateoja, M., Kuosa, H., and Hällfors, S. (2011). Fate of excess phosphorus in the Baltic Sea: a real driving force for cyanobacterial blooms? *J. Sea Res.* 65, 315–321. doi: 10.1016/j.seares.2011.01.004

Raateoja, M., Seppälä, J., Kuosa, H., and Myrberg, K. (2005). Recent changes in trophic state of the Baltic Sea along SW coast of Finland. *Ambio* 34, 188–191. doi: 10.1579/0044-7447-34.3.188

Reynolds, C. S. (2006). *Ecology of Phytoplankton.* Cambridge: Cambridge University Press. doi: 10.1017/CBO9780511542145

Rintala, J.-M., Spilling, K., and Blomster, J. (2007). Temporary cyst enables long-term dark survival of *Scrippsiella hangoei* (*Dinophyceae*). *Mar. Biol.* 152, 57–62. doi: 10.1007/s00227-007-0652-x

Rolff, C., and Elfwing, T. (2015). Increasing nitrogen limitation in the Bothnian Sea, potentially caused by inflow of phosphate-rich water from the Baltic Proper. *Ambio* 44, 601–611. doi: 10.1007/s13280-015-0675-3

Rysgaard, S., Fossing, H., and Jensen, M. M. (2001). Organic matter degradation through oxygen respiration, denitrification, and manganese, iron, and sulfate reduction in marine sediments (the Kattegat and the Skagerrak). *Ophelia* 55, 77–91. doi: 10.1080/00785236.2001.10409475

Savchuk, O. P. (2005). Resolving the Baltic Sea into seven subbasins: N and P budgets for 1991-1999. *J. Mar. Syst.* 56, 1–15. doi: 10.1016/j.jmarsys.2004.08.005

Schelske, C. L., and Stoermer, E. F. (1971). Eutrophication, silica depletion, and predicted changes in algal quality in Lake Michigan. *Science* 173, 423–424.

Seidel, M., Manecki, M., Herlemann, D. P., Deutsch, B., Schulz-Bull, D., Jürgens, K., et al. (2017). Composition and transformation of dissolved organic matter in the Baltic Sea. *Front. Earth Sci.* 5:31. doi: 10.3389/feart.2017.00031

Simis, S. G. H., Ylöstalo, P., Kallio, K., Spilling, K., and Kutser, T. (2017). Contrasting seasonality in optical-biogeochemical properties of the Baltic Sea. *PLoS ONE* 12:e0173357. doi: 10.1371/journal.pone.0173357

Sjöqvist, C., Godhe, A., Jonsson, P., Sundqvist, L., and Kremp, A. (2015). Local adaptation and oceanographic connectivity patterns explain genetic differentiation of a marine diatom across the North Sea–Baltic Sea salinity gradient. *Mol. Ecol.* 24, 2871–2885. doi: 10.1111/mec.13208

Slomp, C. P., Mort, H. P., Jilbert, T., Reed, D. C., Gustafsson, B. G., and Wolthers, M. (2013). Coupled dynamics of iron and phosphorus in sediments of an oligotrophic coastal basin and the impact of anaerobic oxidation of methane. *PLoS ONE* 8:e62386. doi: 10.1371/journal.pone.0062386

Smayda, T. J., and Reynolds, C. S. (2003). Strategies of marine dinoflagellate survival and some rules of assembly. *J. Sea Res.* 49, 95–106. doi: 10.1016/S1385-1101(02)00219-8

Smetacek, V. (1998). Biological oceanography - diatoms and the silicate factor. *Nature* 391, 224–225.

Søndergaard, M., and Middelboe, M. (1995). A cross-system analysis of labile dissolved organic carbon. *Mar. Ecol. Prog. Ser.* 118, 283–294. doi: 10.3354/meps118283

Spilling, K. (2007a). Dense sub-ice bloom of dinoflagellates in the Baltic Sea, potentially limited by high pH. *J. Plankton Res.* 29, 895–901. doi: 10.1093/plankt/fbm067

Spilling, K. (2007b). *On the Ecology of Cold-Water Phytoplankton in the Baltic Sea*. Ph.D, University of Helsinki.

Spilling, K. (2015). *Cruise Report for RV Aranda, CFLUX15 Cruise 4-15 May 2015*. Available online at: http://www.syke.fi/download/noname/%7BFB64C225-33DC-46E6-800A-FB04606AB5B6%7D/113092

Spilling, K. (2016). *Cruise report for RV Aranda, CFLUX16 Cruise 4-15 April 2016*. Available online at: http://www.syke.fi/download/noname/%7B86C061C0-1C16-4F0F-BCFA-7778513729E9%7D/121054

Spilling, K., Kremp, A., Klais, R., Olli, K., and Tamminen, T. (2014). Spring bloom community change modifies carbon pathways and C: N: P: Chl *a* stoichiometry of coastal material fluxes. *Biogeosciences* 11, 7275–7289. doi: 10.5194/bg-11-7275-2014

Spilling, K., Kremp, A., and Tamelander, T. (2006). Vertical distribution and cyst production of *Peridiniella catenata* (*Dinophyceae*) during a spring bloom in the Baltic Sea. *J. Plankton Res.* 28, 659–665. doi: 10.1093/plankt/fbi149

Spilling, K., and Lindström, M. (2008). Phytoplankton life cycle transformation lead to species-specific effects on sediment processes in the Baltic Sea. *Cont. Shelf Res.* 28, 2488–2495. doi: 10.1016/j.csr.2008.07.004

Spilling, K., and Markager, S. (2008). Ecophysiological growth characteristics and modeling of the onset of the spring bloom in the Baltic Sea. *J. Mar. Syst.* 73, 323–337. doi: 10.1016/j.jmarsys.2006.10.012

Spilling, K., Tamminen, T., Andersen, T., and Kremp, A. (2010). Nutrient kinetics modeled from time series of substrate depletion and growth: dissolved silicate uptake of Baltic Sea spring diatoms. *Mar. Biol.* 157, 427–436. doi: 10.1007/s00227-009-1329-4

Stepanauskas, R., Jørgensen, N. O., Eigaard, O. R., Žvikas, A., Tranvik, L. J., and Leonardson, L. (2002). Summer inputs of riverine nutrients to the Baltic Sea: bioavailability and eutrophication relevance. *Ecol. Monogr.* 72, 579–597. doi: 10.1890/0012-9615(2002)072[0579:SIORNT]2.0.CO;2

Stigebrandt, A., Rahm, L., Viktorsson, L., Ödalen, M., Hall, P. O., and Liljebladh, B. (2014). A new phosphorus paradigm for the Baltic proper. *Ambio* 43, 634–643. doi: 10.1007/s13280-013-0441-3

Stipa, T. (2004). The vernal bloom in heterogeneous convection: a numerical study of Baltic restratification. *J. Mar. Syst.* 44, 19–30. doi: 10.1016/j.jmarsys.2003.08.006

Stolpovsky, K., Dale, A. W., and Wallmann, K. (2015). Toward a parameterization of global-scale organic carbon mineralization kinetics in surface marine sediments. *Glob. Biogeochem. Cycles* 29, 812–829. doi: 10.1002/2015GB005087

Stolpovsky, K., Dale, A. W., and Wallmann, K. (2018). A new look at the multi-G model for organic carbon degradation in surface marine sediments for coupled benthic–pelagic simulations of the global ocean. *Biogeosciences* 15, 3391–3407. doi: 10.5194/bg-15-3391-2018

Sundström, A. M., Kremp, A., Daugbjerg, N., Moestrup, Ø., Ellegaard, M., Hansen, R., et al. (2009). Gymnodinium corollarium sp. nov. *(Dinophyceae)* — a new cold-water dinoflagellate responsible for cyst sedimentation events in the Baltic Sea. *J. Phycol.* 45, 938–952. doi: 10.1111/j.1529-8817.2009.00712.x

Svedén, J. B., Adam, B., Walve, J., Nahar, N., Musat, N., Lavik, G., et al. (2015). High cell-specific rates of nitrogen and carbon fixation by the cyanobacterium *Aphanizomenon* sp. at low temperatures in the Baltic Sea. *FEMS Microbiol. Ecol.* 91:fiv131. doi: 10.1093/femsec/fiv131

Tallberg, P., and Heiskanen, A.-S. (1998). Species-specific phytoplankton sedimentation in relation to primary production along an inshore—offshore gradient in the Baltic Sea. *J. Plankton Res.* 20, 2053–2070. doi: 10.1093/plankt/20.11.2053

Tallberg, P., Heiskanen, A.-S., Niemistö, J., Hall, P. O., and Lehtoranta, J. (2017). Are benthic fluxes important for the availability of Si in the Gulf of Finland? *J. Mar. Syst.* 171, 89–100. doi: 10.1016/j.jmarsys.2017.01.010

Tamelander, T., and Heiskanen, A. S. (2004). Effects of spring bloom phytoplankton dynamics and hydrography on the composition of settling material in the coastal northern Baltic Sea. *J. Mar. Syst.* 52, 217–234. doi: 10.1016/j.jmarsys.2004.02.001

Tamelander, T., Spilling, K., and Winder, M. (2017). Organic matter export to the seafloor in the Baltic Sea: drivers of change and future projections. *Ambio* 46, 842–851. doi: 10.1007/s13280-017-0930-x

Tamminen, T. (1989). Dissolved organic phosphorus regeneration by bacterioplankton: 5'-nucleotidase activity and subsequent phosphate uptake in a mesocosm enrichment experiment. *Mar. Ecol. Prog. Ser.* 58, 89–100. doi: 10.3354/meps058089

Tamminen, T. (1995). Nitrate and ammonium depletion rates and preferences during a Baltic spring bloom. *Mar. Ecol. Prog. Ser.* 120, 123–133. doi: 10.3354/meps120123

Tamminen, T., and Andersen, T. (2007). Seasonal phytoplankton nutrient limitation patterns as revealed by bioassays over Baltic Sea gradients

of salinity and eutrophication. *Mar. Ecol. Prog. Ser.* 340, 121–138. doi: 10.3354/meps340121

Tedesco, L., Miettunen, E., An, B. W., Haapala, J., and Kaartokallio, H. (2017). Long-term mesoscale variability of modelled sea-ice primary production in the northern Baltic Sea. *Elem. Sci. Anth.* 5:29. doi: 10.1525/elementa.223

Thomas, D. N., Kaartokallio, H., Tedesco, L., Majaneva, M., Piiparinen, J., Eronen-Rasimus, E., et al. (2017). "Life associated with Baltic Sea ice," in *Biological Oceanography of the Baltic Sea* (Dordrecht: Springer), 333–357.

Thornton, D. C. (2014). Dissolved organic matter (DOM) release by phytoplankton in the contemporary and future ocean. *Eur. J. Phycol.* 49, 20–46. doi: 10.1080/09670262.2013.875596

Vähätalo, A. V., Aarnos, H., Hoikkala, L., and Lignell, R. (2011). Photochemical transformation of terrestrial dissolved organic matter supports hetero-and autotrophic production in coastal waters. *Mar. Ecol. Prog. Ser.* 423, 1–14. doi: 10.3354/meps09010

Vahtera, E., Conley, D., Gustafsson, B., Kuosa, H., Pitkänen, H., Savchuk, O., et al. (2007a). Internal ecosystem feedbacks enhance nitrogen-fixing cyanobacteria blooms and complicate management in the Baltic Sea. *Ambio* 36, 186–194. doi: 10.1579/0044-7447(2007)36[186:IEFENC]2.0.CO;2

Vahtera, E., Laamanen, M., and Rintala, J. (2007b). Use of different phosphorus sources by the bloom-forming cyanobacteria *Aphanizomenon flos-aquae* and *Nodularia spumigena*. *Aquat. Microb. Ecol.* 46, 225–237. doi: 10.3354/ame046225

Vehmaa, A., Kremp, A., Tamminen, T., Hogfors, H., Spilling, K., and Engström-Öst, J. (2011). Copepod reproductive success in spring-bloom communities with modified diatom and dinoflagellate dominance. *ICES J. Mar. Sci.* 69, 351–357. doi: 10.1093/icesjms/fsr138

Walve, J., and Larsson, U. (2007). Blooms of Baltic Sea Aphanizomenon sp.(*Cyanobacteria*) collapse after internal phosphorus depletion. *Aquat. Microb. Ecol.* 49, 57–69. doi: 10.3354/ame01130

Warns, A., Hense, I., and Kremp, A. (2012). Modelling the life cycle of dinoflagellates: a case study with *Biecheleria baltica*. *J. Plankton Res.* 35, 379–392. doi: 10.1093/plankt/fbs095

Warns, A., Hense, I., and Kremp, A. (2013). Encystment of a cold-water dinoflagellate—from *in vitro* to *in silico*. *J. Mar. Syst.* 125, 54–60. doi: 10.1016/j.jmarsys.2012.10.003

Wasmund, N., Kownacka, J., Göbel, J., Jaanus, A., Johansen, M., Jurgensone, I., et al. (2017). The diatom/dinoflagellate index as an indicator of ecosystem changes in the Baltic Sea. 1. Principle and handling instruction. *Front. Mar. Sci.* 4:22. doi: 10.3389/fmars.2017.00022

Wasmund, N., Nausch, G., and Feistel, R. (2013). Silicate consumption: an indicator for long-term trends in spring diatom development in the Baltic Sea. *J. Plankton Res.* 35, 393–406. doi: 10.1093/plankt/fbs101

Wasmund, N., Nausch, G., and Matthaus, W. (1998). Phytoplankton spring blooms in the southern Baltic Sea - spatio-temporal development and long-term trends. *J. Plankton Res.* 20, 1099–1117. doi: 10.1093/plankt/20.6.1099

Wasmund, N., Nausch, G., Schneider, B., Nagel, K., and Voss, M. (2005). Comparison of nitrogen fixation rates determined with different methods: a study in the Baltic Proper. *Mar. Ecol. Prog. Ser.* 297, 23–31. doi: 10.3354/meps297023

Wasmund, N., Nausch, G., and Voss, M. (2012). Upwelling events may cause cyanobacteria blooms in the Baltic Sea. *J. Mar. Syst.* 90, 67–76. doi: 10.1016/j.jmarsys.2011.09.001

Wasmund, N., and Uhlig, S. (2003). Phytoplankton trends in the Baltic Sea. *ICES J. Mar. Sci.* 60, 177–186. doi: 10.1016/S1054-3139(02)00280-1

Wikner, J., and Andersson, A. (2012). Increased freshwater discharge shifts the trophic balance in the coastal zone of the northern Baltic Sea. *Glob. Change Biol.* 18, 2509–2519. doi: 10.1111/j.1365-2486.2012.02718.x

Witak, M., Dunder, J., and Leśniewska, M. (2011). *Chaetoceros* resting spores as indicators of Holocene paleoenvironmental changes in the Gulf of Gdansk, southern Baltic Sea. *Oceanol. Hydrobiol. Stud.* 40, 21–29. doi: 10.2478/s13545-011-0037-0

Wulff, F. V., Rahm, L., and Larsson, P. (2001). *A Systems Analysis of the Baltic Sea.* Berlin: Springer Verlag. doi: 10.1007/978-3-662-04453-7

Zlotnik, I., and Dubinsky, Z. (1989). The effect of light and temperature on DOC excretion by phytoplankton. *Limnol. Oceanogr.* 34, 831–839. doi: 10.4319/lo.1989.34.5.0831

Conflict of Interest Statement: The authors declare that the research was conducted in the absence of any commercial or financial relationships that could be construed as a potential conflict of interest.

frontiers in Marine Science

REVIEW
published: 15 November 2018
doi: 10.3389/fmars.2018.00434

Drivers of Cyanobacterial Blooms in a Hypertrophic Lagoon

Marco Bartoli[1,2], Mindaugas Zilius[2], Mariano Bresciani[3], Diana Vaiciute[2], Irma Vybernaite-Lubiene[2], Jolita Petkuviene[2], Gianmarco Giordani[1,2], Darius Daunys[2], Tomas Ruginis[2], Sara Benelli[4], Claudia Giardino[3], Paul A. Bukaveckas[5], Petras Zemlys[2], Evelina Griniene[2], Zita R. Gasiunaite[2], Jurate Lesutiene[2], Renata Pilkaitytė[2] and Arturas Baziukas-Razinkovas[2]*

[1] Department of Chemistry, Life Sciences and Environmental Sustainability, University of Parma, Parma, Italy, [2] Marine Research Institute, University of Klaipeda, Klaipeda, Lithuania, [3] Optical Remote Sensing Group, CNR-IREA, Milan, Italy, [4] Department of Life Sciences and Biotechnology, University of Ferrara, Ferrara, Italy, [5] Department of Biology and Center for Environmental Studies, Virginia Commonwealth University, Richmond, VA, United States

The Curonian Lagoon is Europe's largest lagoon and one of the most seriously impacted by harmful blooms of cyanobacteria. Intensive studies over the past 20 years have allowed us to identify the major drivers determining the composition and spatial extent of hyperblooms in this system. We summarize and discuss the main outcomes of these studies and provide an updated, conceptual scheme of the multiple interactions between climatic and hydrologic factors, and their influence on internal and external processes that promote cyanobacterial blooms. Retrospective analysis of remote sensed images demonstrated the variability of blooms in terms of timing, extension and intensity, suggesting that they occur only under specific circumstances. Monthly analysis of nutrient loads and stoichiometry from the principal tributary (Nemunas River) revealed large interannual differences in the delivery of key elements, but summer months were always characterized by a strong dissolved inorganic N (and Si) limitation, that depresses diatoms and favors the dominance of cyanobacteria. Cyanobacteria blooms occurred during high water temperatures, long water residence time and low-wind conditions. The blooms induce transient (night-time) hypoxia, which stimulates the release of iron-bound P, producing a positive feedback for blooms of N-fixing cyanobacteria. Consumer-mediated nutrient recycling by dreissenid mussels, chironomid larvae, cyprinids and large bird colonies, may also affect P availability, but their role as drivers of cyanobacteria blooms is understudied.

Keywords: Curonian Lagoon, nitrogen, phosphorus, silica, fluxes, stoichiometry, remote sensing, cyanobacteria

OPEN ACCESS

Edited by:
Riina Klais,
University of Tartu, Estonia

Reviewed by:
Sai Elangovan S,
National Institute of Oceanography (CSIR), India
Franziska Wemheuer,
University of New South Wales, Australia

****Correspondence:***
Marco Bartoli
marco.bartoli@unipr.it

Specialty section:
This article was submitted to Marine Ecosystem Ecology, a section of the journal Frontiers in Marine Science

Received: *13 May 2018*
Accepted: *30 October 2018*
Published: *15 November 2018*

Citation:
Bartoli M, Zilius M, Bresciani M, Vaiciute D, Vybernaite-Lubiene I, Petkuviene J, Giordani G, Daunys D, Ruginis T, Benelli S, Giardino C, Bukaveckas PA, Zemlys P, Griniene E, Gasiunaite ZR, Lesutiene J, Pilkaitytė R and Baziukas-Razinkovas A (2018) Drivers of Cyanobacterial Blooms in a Hypertrophic Lagoon. Front. Mar. Sci. 5:434. doi: 10.3389/fmars.2018.00434

INTRODUCTION

Human activities impact biogeochemical cycles, biological communities and ecosystem functioning of inland and coastal waters on a global scale (Bernot and Dodds, 2005; Muhlolland et al., 2008; Paerl, 2009; Han and Allan, 2012). Estuaries and lagoons have become enriched with nutrients due to wastewater discharge, aquaculture, and agriculture (Galloway et al., 2008; Paerl, 2009). Excess nutrients result in blooms, where algal biomass accumulates and exceeds the mineralization capacity of the heterotrophic community (Valiela et al., 1997). In fresh-brackish waters, algal

blooms may include one or more types of harmful cyanobacteria, resulting in the presence of cyanotoxins. The development of hypoxic or anoxic conditions can lead to die-offs of fish and benthic organisms (Norkko and Bonsdorff, 1996; Ye et al., 2011). In addition, changes in food web structure brought about by invasive species may accelerate eutrophication by reducing grazing pressure and allowing the proliferation of algae, including toxic forms (Carpenter et al., 1998; Rabalais et al., 2002). The alteration of nutrient stoichiometry (*sensu* Redfield) and changes in climate (e.g., warmer temperatures, precipitation timing and intensity) have also received attention as potential drivers of harmful algal blooms (Cloern, 2001; Yunev et al., 2007; Moore et al., 2008; Howarth et al., 2011). In this review, we analyze the drivers of algal blooms in the Curonian Lagoon, a hypereutrophic freshwater estuary. We discuss the relevance of nutrient loads and their stoichiometry on algal blooms, we analyze how algal blooms affect the ecosystem functioning (e.g., nutrient mass balances) and provide a mechanistic interpretation for positive feedbacks promoting the dominance of cyanobacteria.

THE CURONIAN LAGOON: GENERAL FEATURES OF A HYPERTROPHIC FRESHWATER ESTUARY

The Curonian Lagoon is a large (surface area = 1500 km^2), shallow (mean depth = 3.5 m) waterbody located along the south-eastern portion of the Baltic Sea (**Figure 1**). The Curonian Spit (a UNESCO heritage site) divides the lagoon from the Baltic Sea. The main source of water and nutrients is the Nemunas River, although the lagoon also exchanges water with the Baltic Sea via the narrow Klaipeda Strait (Vybernaite-Lubiene et al., 2017). Exchange of water through the strait is episodic; during wind-driven forcing events, the salinity of the lagoon rises to ∼7. The principal tributary (Nemunas River) bisects the lagoon such that the northern lagoon is subject to greater fluvial (and marine) influence, whereas the southern portion of the lagoon is more lentic, and has a longer water residence time (Umgiesser et al., 2016). The lagoon has a relatively small hydrologic loading factor (ratio of watershed area to surface area), which makes this system similar to a flow-through reactor, and provides an opportunity for mass balance studies (Bresciani et al., 2012; Zilius et al., 2014; Vybernaite-Lubiene et al., 2017). Prior work by our multidisciplinary and multinational team has included assessment of nutrient loads from the Nemunas watershed, application of hydraulic models to simulate water circulation in response to changing discharge and wind conditions, investigation of seasonal dynamics of biogeochemical cycles, and use of satellite remote sensing to monitor phytoplankton blooms (Vaičiūtė et al., 2015; Petkuviene et al., 2016; Umgiesser et al., 2016; Vybernaite-Lubiene et al., 2017, 2018). Our work at this site has also benefitted from long-term monitoring carried out by the Marine Research Department of the Lithuanian Ministry of Environment.

Data arising from these efforts have helped to guide management of the Curonian Lagoon via a number of national and international programs (HELCOM Baltic Sea Action Plan, European Water Framework Directive, various habitat and bird conservation initiatives). Despite the intensive studies carried out in the lagoon, there remains the question whether and how cyanobacteria blooms can be mitigated. These blooms extend over large areas of the lagoon and negatively impact ecosystem functions, including tourism and recreational activities, as well as local fisheries (Giardino et al., 2010; Belykh et al., 2013; Šulčius et al., 2015). The use of science for informing management decisions is dependent upon the interpretation and integration of available data, which is the focus of this paper.

SEASONAL SUCCESSION OF PHYTOPLANKTON

Detailed studies of plankton communities in the Curonian Lagoon have examined seasonal patterns, species interactions, production of cyanotoxins and the role of phytoplankton in food web energetics (e.g., Pilkaitytė and Razinkovas, 2006, Razinkovas, 2007; Lesutienė et al., 2014; Bukaveckas et al., 2017). Diatoms dominate the spring phytoplankton community, after which, following a short clear-water phase, cyanobacteria biomass increases (Gasiūnaitė et al., 2005; Pilkaitytė and Razinkovas, 2007). Fresh-brackish species dominate the phytoplankton community of the Curonian Lagoon. *Stephanodiscus hantzschii, Diatoma tenuis, Aulacoseira islandica, Asterionella formosa* are the dominant diatom species during spring while the N-fixing cyanobacteria *Aphanizomenon flosaquae, Dolichospermum affine*, *D. flosaquae,* as well as other cyanobacteria such as *Microcystis aeruginosa, M. wesenbergii*, *M. viridis*, and *Planktothrix agardhii* contribute to the summer biomass peak (Pilkaitytė and Razinkovas, 2007; Gasiūnaitė et al., 2008). According to long-term monitoring data (2001–2012), monthly average chlorophyll *a* (chl-a) concentrations reach 47 ± 14 mg m^{-3} during the spring diatom bloom and 96 ± 56 mg m^{-3} during the summer bloom (Marine Research Department of the Lithuanian Ministry of Environment).

WIND EFFECTS ON ALGAL BLOOM DEVELOPMENT

Algal blooms in the Curonian Lagoon have been tracked since the 1930's via synoptic sampling (Schmidt-Ries, 1940). More recently, satellite remote sensing has substantially improved our ability to track the spatial and temporal dynamics of bloom events and draw links to local weather conditions. The first attempt to map algal blooms in the Curonian Lagoon utilized the MEdium Resolution Imaging Spectrometer (MERIS) on board the Envisat-1 satellite (Giardino et al., 2010; Bresciani et al., 2012; Vaičiūtė et al., 2015). The combination of high spatial resolution (300 m) and short revisit time (2–3 days) greatly enhanced our ability to map chl-a. More recently, the Operational Land Imager (OLI, on board Landsat-8) and Multispectral Instrument (MSI, on board Sentinel-2A/B) have further enhanced spatial resolution (10–30 m) and allowed us

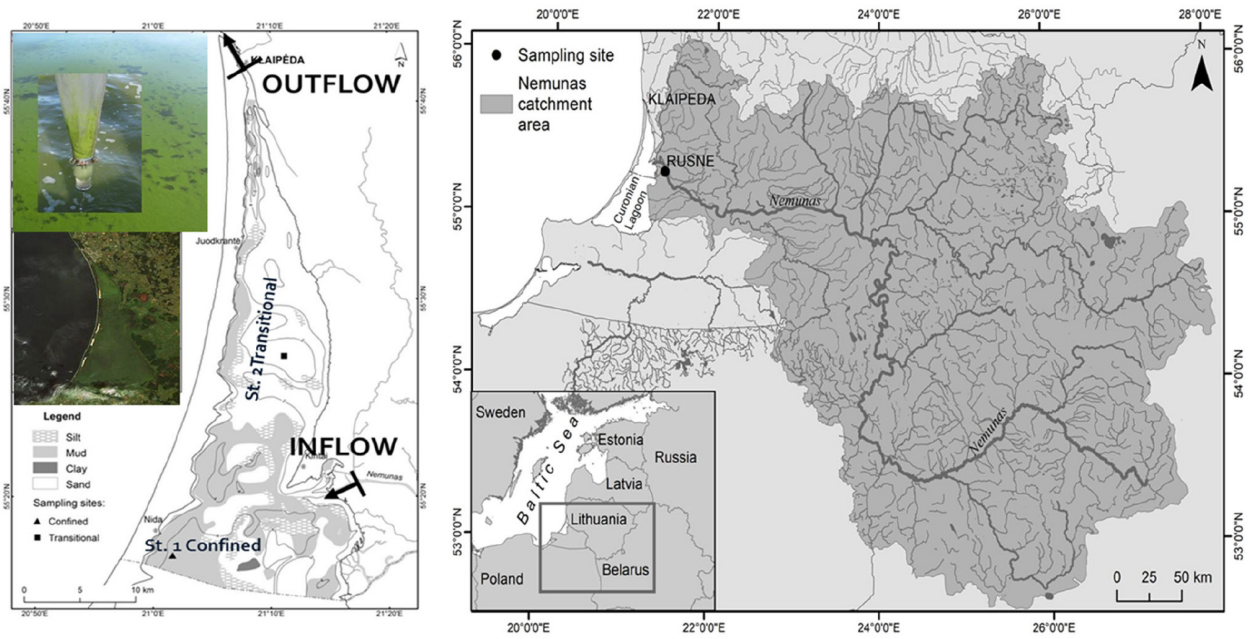

FIGURE 1 | Maps of the Nemunas River watershed (right) and the Lithuanian part of the Curonian Lagoon (left). The lagoon map includes water sampling stations at the lagoon inlet and outlet, and the main sediment sampling sites located at the confined muddy and transitional sandy areas. Color photos show the Curonian Lagoon during a summer cyanobacteria bloom.

to investigate the patchy distribution of cyanobacteria blooms (INFORM, 2017).

Results based on a large number of images from 2004 to 2016 revealed temporal variability and small-scale spatial patchiness of chl-a (Bresciani et al., 2012, 2014; Vaičiūtė et al., 2015). The southern part of the lagoon exhibited high chl-a (up to 500 mg m^{-3}) while the northern areas were characterized by lower values (∼50 mg m^{-3}) (Bresciani et al., 2012; **Figure 2**). Differences between the northern and southern portions of the lagoon were documented by earlier studies (Olenina, 1998; Krevs et al., 2007). However, the use of satellite images allowed us to identify hot spots of chl-a (up to 400 mg m^{-3}) and the presence of surface scums (e.g., Bresciani et al., 2014; **Figure 2**). Highest concentrations were coincident with prevailing wind conditions, suggesting that wind speed and direction was a significant driver for spatial distribution of positively buoyant cyanobacteria (Bresciani et al., 2014).

Wind speed affects not only the spatial distribution of cyanobacteria, but also influences water column mixing. Wind speeds less than 2 m s^{-1} are common and allow for the development of transient (daytime) thermal gradients within the water column (Zilius et al., 2014). The lagoon, though shallow, is relatively turbid and it is thought that stagnant conditions associated with low wind allow positively buoyant cyanobacteria to obtain favorable, near-surface light conditions. The combination of remote sensing, *in situ* biogeochemical studies, and local meteorological data allowed us to investigate these linkages over large spatial scales. Measurements of benthic and pelagic oxygen metabolism along with spatial patterns of MERIS-derived chl-a showed that 60–95% of the area of the lagoon was vulnerable to transient hypoxia when blooms coincide with calm conditions (Zilius et al., 2014).

HYDRODYNAMIC FACTORS AS DRIVERS OF BLOOMS

Freshwater inputs to the lagoon are dominated by the Nemunas River, which has an annual average discharge of 21.8 km^3, and accounts for 96% of total inputs (Jakimavičius and Kriaučiūnienė, 2013). The Nemunas River discharges into the central part of lagoon, dividing the system in a northern and a southern region that differ in water renewal time (Umgiesser et al., 2016). The northern part of the lagoon is characterized by strong riverine influence and short renewal time (< 80 days), which result in limited accumulation of suspended matter (Ferrarin et al., 2008; Remeikaitė-Nikienė et al., 2016). The southern part of the lagoon has a longer water residence time (> 190 days) with minimal fluvial influence. The latest efforts to analyze the water exchange within the Curonian Lagoon (Umgiesser et al., 2016) revealed different seasonal patterns of residence time, primarily driven by changes in hydrographic forcing by the Nemunas River. During elevated spring discharge, the entire lagoon is strongly flushed by Nemunas River. During summer, river discharge decreases, resulting in increased water residence time, particularly in the southern lagoon. Summer stagnation has implications for water temperature, stratification, nutrient availability and stoichiometry, and phytoplankton abundance and composition. In summer, wind forcing appears to be the most important factor influencing water column mixing and

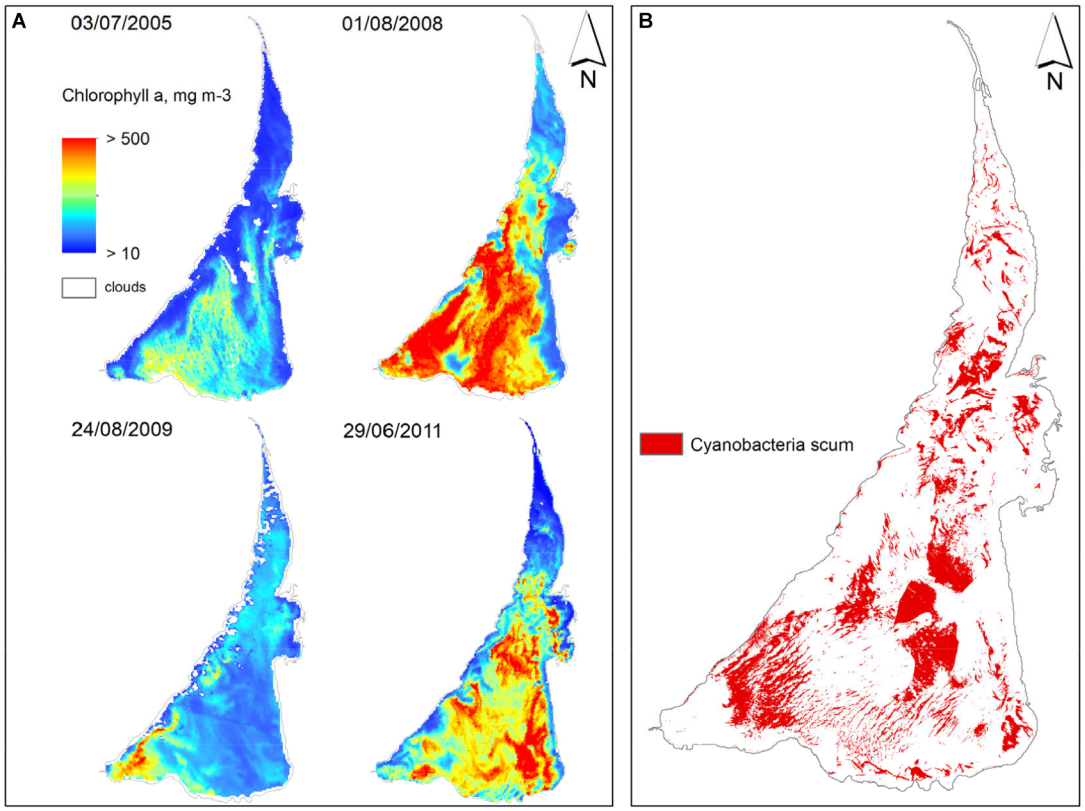

FIGURE 2 | Maps of Chl-a concentrations in the Curonian Lagoon from MERIS images **(A)** and cyanobacteria surface accumulations as retrieved by Landsat-8 OLI and Sentinel-2 MSI during June-September 2013-2016 **(B)**.

exchange between the southern and the northern part of the lagoon (Umgiesser et al., 2016).

NUTRIENT LOADS AND THEIR ECOLOGICAL STOICHIOMETRY

A study coupling the Curonian Lagoon with its watershed was started in 2012 to better characterize the timing of nutrient inputs and their stoichiometry. From 2012, on at least a monthly basis and more frequent (weekly) during high discharge periods, discharge and water chemistry (including all dissolved and particulate forms of N, Si, and P) were monitored near the inflow of the Nemunas River to the lagoon (Vybernaite-Lubiene et al., 2017; **Figure 1**). Discharge and nutrient concentrations displayed strong seasonality. Nitrate and reactive Si concentrations decreased by two orders of magnitude from spring to summer (e.g., NO_3^- from > 300 μM to < 1, SiO_2 from > 200 to < 1 μM) while reactive P concentrations showed comparatively smaller changes (from 0.2 to 4 μM). These seasonal patterns resulted in reduced DIN:DSi and DIN:DIP ratios, which shift the lagoon from an excess of N and Si in colder months, to P excess (DIN:DIP < 16) in warmer months (**Figure 3**). These findings support the hypothesis that cyanobacterial blooms are favored during summer by the limited

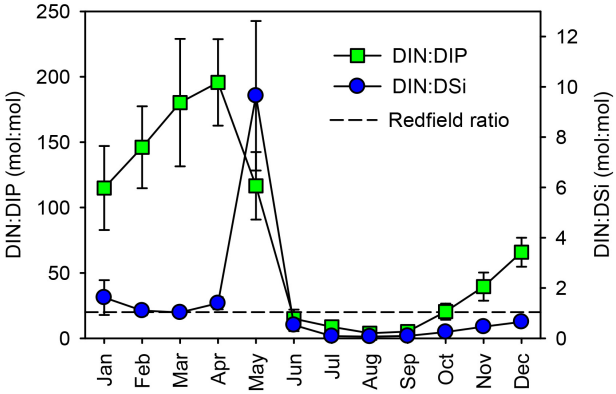

FIGURE 3 | The stoichiometric DIN:DIP and DIN:DSi ratios during 2012–2016 at the Nemunas River gaging station. Dashed lines indicate the theoretical Redfield ratio (DIN:DSi = 16:15 and DIN:DIP = 16:1). Averages ± standard deviations (n = 6) are reported.

N and Si supply via riverine inputs (Pilkaitytė and Razinkovas, 2007).

Our analyses of nutrient loads showed that recent (2012–2016) N export from the Nemunas River basin is similar to historical data (1986–2002), whereas P loads have declined by

nearly 60 % as a result of sewage treatment plant improvements (Vybernaite-Lubiene et al., 2018). Despite reductions in P loads, the lagoon remains imbalanced with an excess of P relative to N, thereby favoring the growth of N-fixing cyanobacteria. Further P reductions are needed to promote- limitation or co- limitation and thereby diminish the dominance of cyanobacteria. It is also important to stress that despite strong N limitation in the lagoon, hyperblooms of cyanobacteria do not occur every summer due to the influence of other factors that regulate blooms.

SEDIMENTS AND BENTHIC PROCESSES AS DRIVERS OF BLOOMS

The distribution of sediment types in the Curonian Lagoon is determined by hydrodynamic factors and by contributions from autochthonous and allochthonous materials (Pustelnikovas, 1994; Ferrarin et al., 2008). Curonian Lagoon sediments include a broad spectrum of deposits, from sand-dominated in the northern (riverine-influenced) sector to silt-dominated in the southern (more lentic) area (Trimonis et al., 2003). Declines in external (riverine) loads during the transition from spring to summer enhances the importance of internal recycling from the benthic compartment as a nutrient source for pelagic primary production. Studies of sedimentary processes revealed a shift in dominant microbial processes and benthic fluxes from spring to summer (Zilius et al., 2012, 2014; Petkuviene et al., 2016). For example, net N_2 production suggests the dominance of denitrification over N-fixation during spring; however N_2 fluxes are reversed during summer, suggesting net N import to the benthic compartment (Zilius et al., 2018).

Since 2009, oxygen penetration depth, total and diffusive sedimentary oxygen demand, pore water chemical environments, sedimentary pools and benthic fluxes were measured or calculated at sites representative of dominant sedimentary environments including littoral, pelagic transitional and confined zones (Zilius et al., 2012; **Figure 1**). In this turbid system, benthic photosynthesis was measurable only in shallow littoral illuminated sediments (∼1 m depth) representing a minor fraction (5%) of the total lagoon surface (Benelli et al., 2018). Here, benthic algae oxidize the upper sediment layer and efficiently retain nutrients, thereby impeding regeneration to the water column (Zilius et al., 2012; Benelli et al., 2018). Deeper sites were always heterotrophic and their seasonal oxygen metabolism and nutrient regeneration was driven by water temperature and phytoplankton blooms; recently settled fresh phytoplankton resulted in significantly higher oxygen uptake, limited oxygen penetration in sediments ($<$ 1 mm), and high rates of anaerobic to aerobic metabolism (Zilius et al., 2012, 2016).

The mechanisms underlying P release from sediments were analyzed in detail, as they contribute to lower inorganic DIN:DIP ratio in the water column and favor cyanobacteria (Zilius et al., 2014, 2015, 2016; Petkuviene et al., 2016). The distribution of sedimentary pools of P, Fe, Mn and S in the Curonian Lagoon was related to riverine influence; sandy sediments adjacent the Nemunas delta were oxidized and have a large geochemical buffer capacity against the effects of anoxia, with limited accumulation of free sulfide (Petkuviene et al., 2016). Muddy areas along the western and southern portion of the lagoon had chemically reduced sediments where the reduction of iron may result in large P release (Petkuviene et al., 2016). In manipulative experimental studies, simulated deposition of phytoplankton material, primarily composed of cyanobacteria, resulted in an increase of dissimilative nitrate reduction over denitrification and large methane production, but with limited reactive P release (Zilius et al., 2016). Experimental manipulations of intact cores, targeting short-term effects of anoxia, revealed that pools of detritial Ca bound P ($>$ 70 % of inorganic P) and oxidized Fe and Mn, prevent or buffer redox-dependent reactive P release from sediments (Zilius et al., 2015). However, seasonal measurements of reactive P fluxes at sandy and muddy areas revealed large summer P release at muddy sites coinciding with the occurrence of cyanobacterial blooms, and the onset of hypoxia and anoxia in the water column (Zilius et al., 2014; Petkuviene et al., 2016). These events occurred under specific conditions during prolonged stable weather, with no wind and high water temperature. Benthic P release occurred when the oxidized pools of metals within sediments were exhausted and contributed to the imbalanced stoichiometry by further lowering the DIN:DIP ratio. P regeneration from sediment, despite occurring over short period, had a significant effect on the lagoon P budget, resulting in a large export of P (Petkuviene et al., 2016).

TOP-DOWN DRIVERS OF BLOOMS

Zooplankton

The shift from diatom- to cyanobacteria- dominated phytoplankton communities was accompanied by a decline in relative zooplankton grazing. During the spring diatom bloom, maximum consumption by zooplankton corresponded to 34% of NPP (324 $\mu gCL^{-1}d^{-1}$), whereas during the summer cyanobacteria bloom grazing decreased to 8 % of NNP (470 $\mu gCL^{-1}d^{-1}$) (**Figure 4**). A similar pattern was observed in the southern part of the lagoon where zooplankton grazing declined from 60% of phytoplankton production during spring to 4 % in summer (Semenova and Aleksandrov, 2009). Despite reduced grazing rates, stable isotope studies show that cyanobacteria blooms support secondary production in a diverse group of benthic and pelagic consumers within the lagoon (Lesutienė et al., 2014). Our studies also show that cyanotoxins (microcystin) are found in tissues of fish and shellfish, indicating that cyanobacteria production supports higher trophic levels in this system (Bukaveckas et al., 2017).

Grazing by zooplankton may be an important driver of cyanobacteria bloom development. During winter, ciliate growth is limited by low biomass of phytoplankton. In the early spring, when small-sized phytoplankton are dominant, the ciliate assemblage was dominated by small naked oligotrichs and prostomatids. After the late spring diatom bloom, the ciliate assemblage shifted to medium sized tintinnids, which feed on the same nano-fraction of phytoplankton or/and heterotrophic flagellates as ciliates. The summer/autumn phase was characterized by increased taxonomical and functional

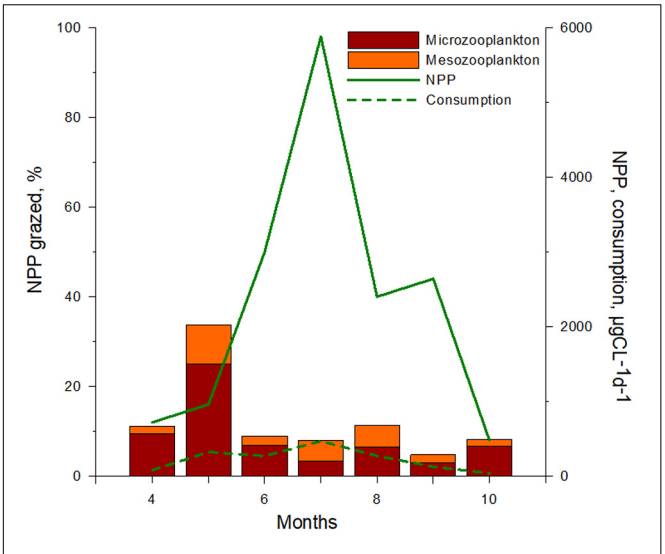

FIGURE 4 | Dynamics of net primary production and consumption by zooplankton (NPP, consumption, $\mu gCL^{-1}d^{-1}$), and estimated grazed NPP (%) by micro- and mesozooplankton during vegetative season in the Curonian Lagoon.

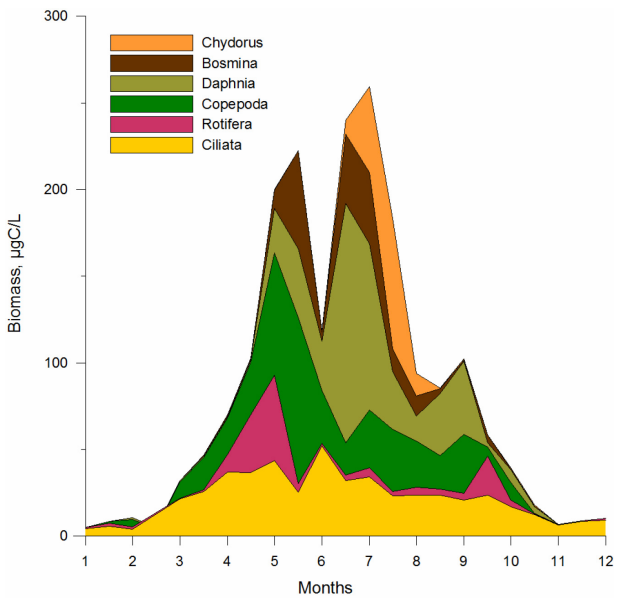

FIGURE 5 | Seasonal dynamics of zooplankton biomass in the Curonian Lagoon.

diversity of ciliates indicating exploitation of a wide size range of food. Small sized naked oligotrichs (*Strobilidium* spp.) and peritrichs (*Vorticella* spp.) (mainly bacterivorous ciliates) dominated in summer, indicating a shift from algal food to bacteria (Grinienė, 2013; Grinienė et al., 2016). The shift from large *Daphnia* to small-bodied *Chydorus sphaericus* coincides with the dominance of cyanobacteria (Gasiūnaitė and Razinkovas, 2004; **Figure 5**). *Chydorus* graze on smaller algae and therefore give an advantage to large cyanobacteria (Gasiūnaitė and Olenina, 1997). In addition, the presence of large filamentous colonies and toxic strains may foster the dominance of bloom forming cyanobacteria (Pilkaitytė and Razinkovas, 2007).

Macrofauna

Excluding the littoral zone, sediments of the Curonian Lagoon host few macrofauna species due to high organic content and poor oxygen conditions (Zettler and Daunys, 2007). Among them, oligochaetes, chironomid larvae and freshwater mussels, including native unionids and invasive dreissenids, are dominant groups (Daunys, 2001). Chironomid larvae and mussel aggregations may, due to their high densities, influence phytoplankton composition and abundance (Dame et al., 1980; Officer et al., 1982; Gili and Coma, 1998). We discuss here if and under which circumstances macrofauna may favor the onset of cyanobacterial blooms in the Curonian Lagoon.

In the lagoon, periods of short water residence time may impede efficient removal of particulate matter by suspension feeding. In spring (average residence time 7 days) only 10 % of particulate matter was removed by zebra mussels, while in summer (average residence time up to 15 days), the proportion of particulate matter removed increased to 30% (Daunys et al., 2006). Chironomid larvae and mussels may exert a top-down control of pelagic primary production but they may simultaneously excrete large amount of nutrients. Their activities also enhance the organic matter content of sediment via biodeposition, stimulating microbial activity and re-mineralization (Caraco et al., 1997; Stief, 2013; Ruginis et al., 2014; Benelli et al., 2017). It is unclear whether the net effect of phytoplankton removal via grazing is offset by nutrient regeneration via excretion and whether these processes have a specific benefit to cyanobacteria. *Dreissena polymorpha* was intensively studied due to its top-down control on phytoplankton and the possible management of its biomass to reverse eutrophication. However, such top-down control on pelagic primary production resulted to be site-specific and context-dependent (e.g., in shallow, well-mixed environments with low nutrient background more than in deep, stratified ecosystems with high nutrient inputs) (Conroy et al., 2005; Caraco et al., 2006). Furthermore, dreissenids excrete large amounts of reactive P and different authors have suggested that these mussels may change nutrient stoichiometry, via P mobilization and by enhancing N removal via denitrification (Zhang et al., 2008; Ruginis et al., 2014). The inability of zebra mussels to graze on larger forms of cyanobacteria may provide a competitive advantage over other algae, which, in combination with increased rates of reactive P re-cycling, enhances the potential for cyanobacteria blooms. These aspects need further study, but suggest that the presence of dreissenids mussels on the Curonian Lagoon may exacerbate the effects of nutrient loading, and favor increased dominance by cyanobacteria.

Birds

The Curonian Lagoon hosts a large bird community, including tufted ducks and common pochards with 24,500–54,700 and 1,800–41,000 individuals, respectively (Stanevičius et al., 2009),

goosanders (Žydelis, 2001), cormorants, with more than 10,000 breading birds (Švažas et al., 2011; Dagys and Zarankaitė, 2013), mallards, geese (3,000–6,500 ind/day) and little and black-headed gulls (1,000–1,500 ind./day). High densities of water birds are vectors of seeds, invertebrates, bacteria and phytoplankton (Tobiessen and Wheat, 2000), and also contribute to nutrient loads (Manny et al., 1994; Hahn et al., 2007; Green and Elmberg, 2014; Han et al., 2017).

During nesting, breeding and roosting periods, water birds enrich the water with guano (Klimaszyk et al., 2015). In enclosed aquatic ecosystems bird feces may contribute 50–69%, 27–40%, and 70–75% of total C, N, and P loads, respectively (Manny et al., 1994; Post et al., 1998; Boros et al., 2008; Gwiazda et al., 2014). Bird feces have low N:P, implying that water bird excretions may strengthen N limitation and promote cyanobacteria blooms (Rönicke et al., 2008; Han et al., 2017). Birds also have indirect effects on nutrient cycling by removing macrophytes, invertebrates and fish. Herbivorous birds, by removing plants, remove those elements that trap nutrients in the benthic compartment, provide shelter for zooplankton and allow sediment oxidation via radial oxygen loss. While grazing on macrophytes, birds resuspend sediments and mobilize pore water nutrients (Klimaszyk et al., 2015; Klimaszyk and Rzymski, 2016). Furthermore, a large fraction of macrophyte-associated P is released to the water column in the reactive form and is readily available to phytoplankton. The mechanisms that regulate P mobility in sediments are redox-dependent such that the removal of roots and macrofauna, together with particle resuspension, has the potential to mobilize sediment sources of P. In the Curonian Lagoon herbivorous birds represent the second largest water bird group, peaking in spring and distributed throughout the Nemunas River deltaic area and the littoral zone.

Benthivorous birds, feeding on macrofauna, produce an effect on the benthic system similar to that of fishes, removing animals that may keep the sediment oxidized and resuspending sediments and nutrients (Werner et al., 2005; Sánchez et al., 2006; Rodríguez-Pérez et al., 2007; Matuszak et al., 2014). Piscivorous birds convert fish-associated P into reactive P (Pūtys and Zarankaitė, 2010). Large colonies of cormorants have their peak activity during summer. The large bird community in the Curonian Lagoon may therefore affect by various direct and indirect mechanisms the cycling of nutrients and that of P in particular.

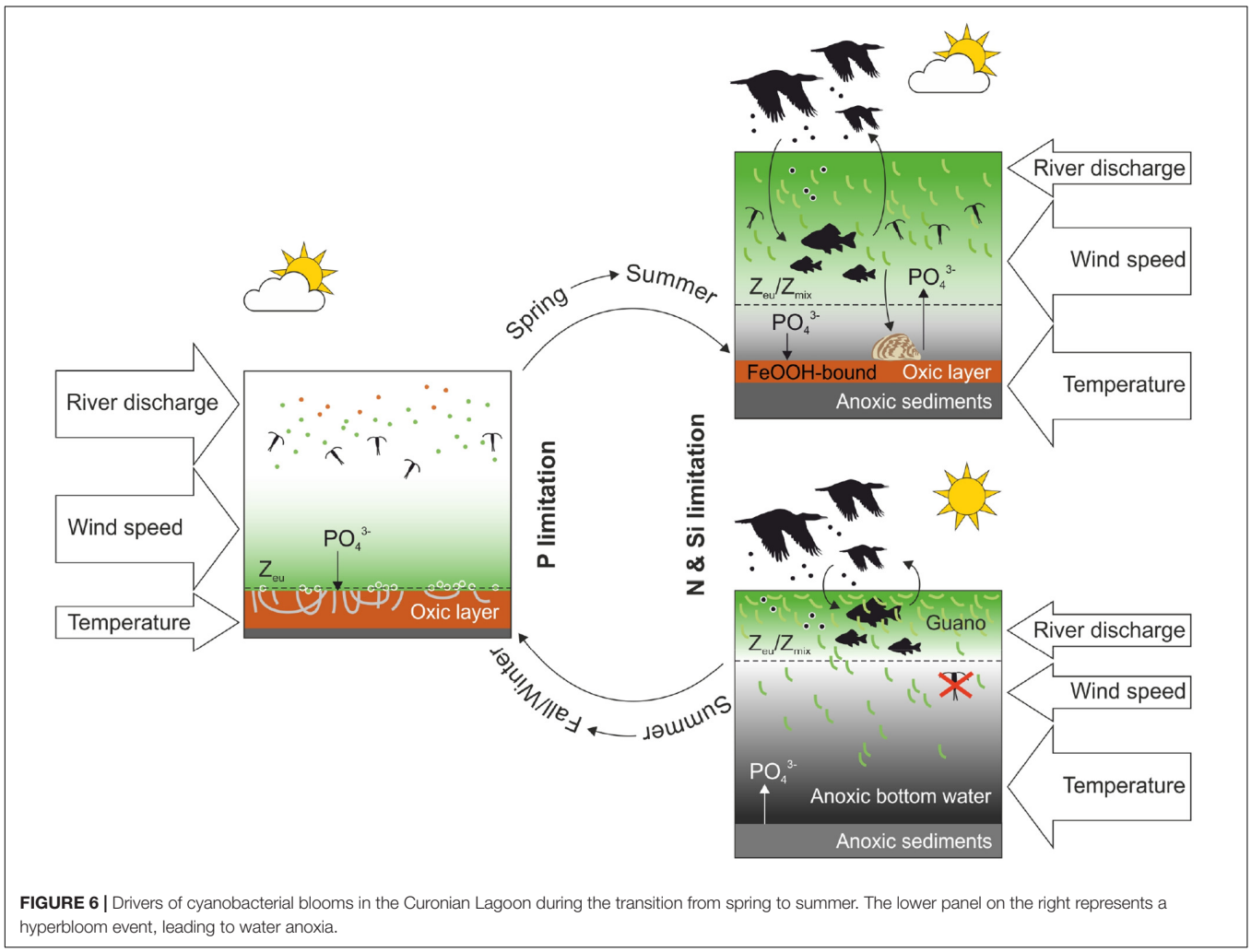

FIGURE 6 | Drivers of cyanobacterial blooms in the Curonian Lagoon during the transition from spring to summer. The lower panel on the right represents a hyperbloom event, leading to water anoxia.

Fish

Benthivorous fish, including carp, roach, bream and perch, represent the dominant fish component in the Curonian Lagoon (Cline et al., 1994; Persson and Svensson, 2006; Lithuanian Environmental Protection Agency (EPA), 2008; Adámek and Maršálek, 2013). Fish may produce both top-down (e.g., removal of grazers and competitors) and bottom-up effects (nutrient mobilization) that favor eutrophic conditions and cyanobacterial blooms (Shormann and Cotner, 1997; Roozen et al., 2007). The diet of benthivorous fish in the Curonian Lagoon includes mussels, chironomidae larvae, detritus, zooplankton and plants (Bubinas and Ložys, 2000). Benthivorous fish may impact the water quality, leading to nutrient accumulation and algal growth, by suspending the sediments and by feeding on filter-feeding zooplankton, burrowing macrofauna and macrophytes (Zambrano and Hinojosa, 1999; Williams et al., 2002; Parkos et al., 2003). Sediment resuspension by the benthic fish community increases water turbidity, limits light penetration and rooted macrophytes and favors P release and cyanobacteria growth (Hellström, 1991; Breukelaar et al., 1994). By removing invertebrates from the sediments, benthivorous fishes mobilize nutrients from the pore water (Tarvainen et al., 2002; Phan-Van et al., 2008). Resuspension itself may oxidize sediments, but this is a short-term and local effect, while reductions in invertebrate abundance impacts N removal via denitrification and P sequestration. Moreover, fish predation reduces zooplankton populations, resulting in low grazing on phytoplankton (Jeppesen et al., 1999). Fish excretions are very soluble and rich in N and P which stimulate periphyton growth and negatively affect macrophytes (Tarvainen et al., 2002; Williams et al., 2002). Excreted nutrients are dispersed horizontally and vertically and from littoral to pelagic areas (Schindler et al., 1996; Persson and Svensson, 2006).

SYNTHESIS

Cyanobacterial blooms in the Curonian Lagoon arise from multiple interacting factors, which include external forcing (riverine discharge and wind conditions) and internal processes (consumer-mediated nutrient cycling and sediment-water nutrient exchange). We summarize the information discussed in this review through a graphical representation of the multiple mechanisms that drive cyanobacterial blooms in the Curonian Lagoon (**Figure 6**).

During spring, the lagoon is diatom-dominated due to a combination of low water temperatures, high river discharge and availability of inorganic N and Si, in excess to P. The system alternates phases with clear and turbid water depending on the intensity of the spring diatom bloom and the occurrence of wind-associated sediment resuspension events. During spring, light penetration may attain 1–2 m and grazers exert appreciable control of algal biomass accrual. The water column is generally well mixed and normoxic; under these circumstances the upper sediment layer is oxidized and acts as a nutrient sink.

The spring-summer transition is marked by a decline in discharge of the Nemunas River, which is accompanied by the depletion of N and Si within the lagoon. Reductions in external loadings, together with processes occurring within the lagoon (high spring denitrification rates and Si sequestration via uptake and accumulation in sediment), result in the onset of N and Si limitation. Cyanobacteria become dominant, resulting in a series of cascade effects that include increased algal-associated turbidity and water stratification. Positive feedbacks arise as large colonies of cyanobacteria limit the capacity of grazers to control biomass accrual and high respiration rates promote oxygen under-saturation. Climatic conditions, which are highly variable, play an important role, as low wind conditions may further push the system toward hyperbloom events, with extensive surface scums (**Figure 7**). Water column respiration, not sediment oxygen demand, promote oxygen depletion in the system, due to the large availability of labile organic matter from decaying algal cells. By this mechanism, hyperblooms promote their persistence as hypoxia results in sediment P release. Other factors that may contribute to these large periodic outbreaks include the presence of waterbirds. Large colonies of cormorants settle in spring along the Curonian Spit and have their most intense period of activity during summer. Cormorants, through the production of guano, make large amounts of P available in surface water. Besides cormorants, colonies of seagulls, swans and duck have large numbers and may contribute to make fish or macrophyte P pools readily available to cyanobacteria. Other biological agents supporting algal blooms include the invasive freshwater mussel (*D. polymorpha*), which excretes large amounts of reactive P relative to the native unionid mussels and may therefore contribute to the low DIN:DIP ratio in the lagoon.

FIGURE 7 | Cyanobacteria hyperbloom with scum formation in the Curonian Lagoon, August 2013.

MANAGEMENT POLICIES AND PERSPECTIVES

The Curonian Lagoon ecosystem provides a number of provisioning and cultural ecosystem services, most directly linked to the main economic activities in the lagoon area – recreation and fishery (Rashleigh et al., 2012; Razinkovas-Baziukas et al., 2012). The lagoon also provides ecosystem services of relevance to the Baltic Sea region such as denitrification and phosphorus burial. Management efforts to improve water quality in the Curonian Lagoon have targeted reductions of nitrogen loads by 15 % and phosphorus by 8%. Model simulations (Ertürk et al., 2016) revealed that reductions of nitrogen loads by 14 % and phosphorus loads by 6%, will bring about a 10% reduction in the abundance of cyanobacteria (Razinkovas et al., 2008). Further reductions in riverine nutrient loads (40% decrease in both N and P) produced only a 10% decrease in peak chl-a concentrations (Razinkovas et al., 2008). Further efforts to improve water quality may require within-system bioengineering solutions (biomanipulations, mussels, reed harvesting).

Climate change projections for the Curonian Lagoon (Jakimavičius et al., 2018) indicate an increase of average water temperature up to 1.7–2°C by the middle of this century, consistent with trends observed during the last three decades (Dailidienė et al., 2011). According to this modeling study, the increase in water temperature was mostly confined to the summer-early autumn period, which may therefore favor the development of cyanobacteria blooms. Biogeochemical cycles of the Curonian Lagoon will be affected by changes in the water balance of the lagoon. A decline in contributions from Nemunas River coupled with an increase in Baltic water intrusions (due to sea level rise) will alter the water balance during the winter–spring period. A shift in the timing of peak discharge from spring to winter, as observed in recent decades (Dailidienė et al., 2011), may diminish algal blooms if a larger proportion of the nitrogen load from the Nemunas River passes through the Curonian Lagoon during the period of low phytoplankton productivity. However, the predicted decrease of ice cover is expected to reduce winter hypoxia, which would result in reductions in denitrification. Despite the intensive studies of this system, we are not able to predict whether climate change will exacerbate or mitigate cyanobacteria blooms. However, it is apparent that further management actions are needed to reduce nutrient loads and restore ecosystem services. There is a need for additional studies, both at the watershed-scale and the lagoon scale, to facilitate science-based management decision. At the watershed scale, long-term monitoring is needed to better understand the effectiveness of improved agricultural practices and water treatment on N, Si, and P export from the Nemunas basin to the Curonian Lagoon. Watershed practices may differentially affect the three elements further modifying their ecological stoichiometry, with implication for algal blooms (Yunev et al., 2007; Bresciani et al., 2014; Vybernaite-Lubiene et al., 2017).

CONCLUSION

This review analyzes the available information on the mechanisms driving cyanobacterial blooms in the Curonian Lagoon. Results from our analysis suggest that blooms are a consequence of multiple, interplaying factors, producing a cascade of processes and positive feedbacks. The hot moment for cyanobacteria blooms is the summer, due to combination of favorable nutrient stoichiometry (N and Si limitation), elevated water temperature, low wind speed, unbalanced internal recycling (P > N) and low grazing pressure. The hot spots of cyanobacteria are stagnant areas where limited water circulation and stratification provide these organisms a competitive advantage. These hot spots may serve as bloom initiation areas from which cyanobacteria are dispersed by prevailing winds. Ecological interactions among aquatic organisms, and how these respond to changes in climate and to species invasions remain understudied. The combination of satellite remote sensing, traditional monitoring of environmental parameters, detailed analysis of processes at the macro and microscale and the application of ecological network models, have proved to be useful tools for understanding the mechanisms underlying the development of cyanobacteria blooms. Our further efforts seek to improve our capacity to predict the occurrence and severity of algal blooms and guide prevention measures.

AUTHOR CONTRIBUTIONS

MBa collected and homogenized the material with the help of MZ, who realized the conceptual scheme of **Figure 6** and PB, who organized the different sections and improved the clarity of the paper. All authors contributed to the writing.

FUNDING

MBr, JP, and DV were supported by Research Council of Lithuania (LMT) grant "Phosphorus as driver of cyanobacterial hyperblooms in the Curonian Lagoon (Patchy)" (Agreement No. S-MIP-17-11), MZ was supported by LMT grant "The role of atmospheric nitrogen fixation in the largest eutroficated European lagoon (NitFix)" (Agreement No. P-MIP-17-126), IV-L and AR-B were supported by the BONUS project "Nutrient Cocktails in Coastal zones of the Baltic Sea (COCOA)" (No. BONUS-2/2014). This work was partly funded by the European Community's Seventh Framework Program (FP7/2007-2013) under Grant 606865 (INFORM) and by the EOMORES project belonging to the European Union's Horizon 2020 research and innovation Program (grant agreement n° 730066). Participation in this research effort by PB was aided by a Fulbright award.

REFERENCES

Adámek, Z., and Maršálek, B. (2013). Bioturbation of sediments by benthic macroinvertebrates and fish and its implication for pond ecosystems: a review. *Aquac. Int.* 21, 1–17. doi: 10.1007/s10499-012-9527-3

Belykh, O. I., Dmitrieva, O. A., Gladkikh, A. S., and Sorokovikova, E. G. (2013). Identification of toxigenic Cyanobacteria of the genus *Microcystis* in the Curonian Lagoon (Baltic Sea). *Oceanology* 53, 71–79. doi: 10.1134/S0001437013010025

Benelli, S., Bartoli, M., Racchetti, E., Moraes, P. C., Zilius, M., Lubiene, I., et al. (2017). Rare but large bivalves alter benthic respiration and nutrient recycling in riverine sediments. *Aquat. Ecol.* 51, 1–16. doi: 10.1007/s10452-016-9590-3

Benelli, S., Bartoli, M., Zilius, M., Vybernaite-Lubiene, I., Ruginis, T., Petkuviene, J., et al. (2018). Microphytobenthos and chironomid larvae attenuate nutrient recycling in shallow-water sediments. *Freshw. Biol.* 63, 187–201. doi: 10.1111/fwb.13052

Bernot, M. J., and Dodds, W. K. (2005). Nitrogen retention, removal, and saturation in lotic ecosystems. *Ecosystems* 8, 442–453. doi: 10.1007/s10021-003-0143-y

Boros, E., Nagy, T., Pigniczki, C., Kotymán, L., Balogh, K. V., and Vörös, L. (2008). The effect of aquatic birds on the nutrient load and water quality of soda pans in Hungary. *Acta Zool. Acad. Sci. Hung.* 54(Suppl. 1), 207–224.

Bresciani, M., Adamo, M., De Carolis, G., Matta, E., Pasquariello, G., Vaičiūtė, D., et al. (2014). Monitoring blooms and surface accumulation of Cyanobacteria in the Curonian Lagoon by combining MERIS and ASAR data. *Remote Sens. Environ.* 146, 124–135. doi: 10.1016/j.rse.2013.07.040

Bresciani, M., Giardino, C., Stroppiana, D., Pilkaitytė, R., Bartoli, M., and Razinkovas, A. (2012). Retrospective analysis of spatial and temporal variability of chlorophyll-a in the Curonian Lagoon. *J. Coast. Conserv.* 16, 511–519. doi: 10.1007/s11852-012-0192-5

Breukelaar, A. W., Lammens, E. H. R. R., Klein Breteler, J. G. P., and Ta'trai, I. (1994). Effects of benthivorous bream (*Abramis brama*) and carp (*Cyprinus carpio*) on sediment resuspension and concentrations of nutrients and chlorophyll a. *Freshw. Biol.* 32, 113–121. doi: 10.1111/j.1365-2427.1994.tb00871.x

Bubinas, A., and Ložys, L. (2000). The nutrition of fish in the Curonian lagoon and the coastal zone of the Baltic sea. *Acta Zool. Litu.* 10, 56–67. doi: 10.1080/13921657.2000.10512346

Bukaveckas, P. A., Lesutienė, J., Gasiūnaitė, Z. R., Ložys, L., Olenina, I., Pilkaitytė, R., et al. (2017). Microcystin in aquatic food webs of the Baltic and Chesapeake Bay regions. *Estuar. Coast. Shelf Sci.* 191, 50–59. doi: 10.1016/j.ecss.2017.04.016

Caraco, N. F., Cole, J. J., Raymond, P. A., Strayer, D. L., Pace, M. L., Findlay, S. E., et al. (1997). Zebra mussel invasion in a large, turbid river: phytoplankton response to increased grazing. *Ecology* 78, 588–602. doi: 10.1890/0012-9658(1997)078[0588:ZMIIAL]2.0.CO;2

Caraco, N. F., Cole, J. J., and Strayer, D. L. (2006). Top-down control from the bottom: regulation of eutrophication in a large river by benthic grazing. *Limnol. Oceanogr.* 51, 664–670. doi: 10.4319/lo.2006.51.1_part_2.0664

Carpenter, S. R., Caraco, N. F., Correll, D. L., Howarth, R. W., Sharpley, A. N., and Smith, V. H. (1998). Nonpoint pollution of surface waters with phosphorus and nitrogen. *Ecol. Appl.* 8, 559–568. doi: 10.1890/1051-0761(1998)008[0559:NPOSWW]2.0.CO;2

Cline, J. M., East, T. L., and Threlkeld, S. T. (1994). Fish interactions with the sediment–water interface. *Hydrobiologia* 275, 301–311. doi: 10.1007/BF00026721

Cloern, J. E. (2001). Our evolving conceptual model of the coastal eutrophication problem. *Mar. Ecol. Prog. Ser.* 210, 223–253. doi: 10.3354/meps210223

Conroy, J. D., Edwards, W. J., Pontius, R. A., Kane, D. D., Zhang, H., Shea, J. F., et al. (2005). Soluble nitrogen and phosphorus excretion of exotic freshwater mussels (*Dreissena* spp.): potential impacts for nutrient remineralisation in western Lake Erie. *Freshw. Biol.* 50, 1146–1162. doi: 10.1111/j.1365-2427.2005.01392.x

Dagys, M., and Zarankaitė, J. (2013). "Status of the breeding population of Great Cormorants in Lithuania in 2012," in *National Reports from the 2012 Breeding Census of Great Cormorants Phalacrocorax carbo in Parts of the Western Palearctic. IUCN-Wetlands International Cormorant Research Group Report. Technical Report from DCE –Danish Centre for Environment and Energy*, eds T. Bregnballe, J. Lynch, R. Parz-Gollner, L. Marion, S. Volponi, J.-Y. Paquet, et al. (Aarhus: Aarhus University), 69–71.

Dailidienė, I., Baudler, H., Chubarenko, B., and Navrotskaya, S. (2011). Long term water level and surface temperature changes in the lagoons of the southern and eastern Baltic. *Oceanologia* 53, 293–308. doi: 10.5697/oc.53-1-TI.293

Dame, R., Zingmark, R., Stevenson, R., and Nelson, D. (1980). "Filter feeder coupling between the estuarine water column and benthic subsystems," in *Estuarine Perspectives*, ed. V. S. Kennedy (San Diego, CA: Academic Press), 521–526. doi: 10.1016/B978-0-12-404060-1.50048-4

Daunys, D. (2001). *Patterns of Bottom Macrofauna Variability and its Role in the Shallow Coastal Lagoon*. Doctoral dissertation, Klaipeda, Klaipeda University.

Daunys, D., Zemlys, P., Olenin, S., Zaiko, A., and Ferrarin, C. (2006). Impact of the zebra mussel *Dreissena polymorpha* invasion on the budget of suspended material in a shallow lagoon ecosystem. *Helgol. Mar. Res.* 60, 113–120. doi: 10.1007/s10152-006-0028-5

Ertürk, A., Razinkovas-Baziukas, A., Zemlys, P., and Umgiesser, G. (2016). Linking carbon-nitrogen-phosphorus cycle and foodweb models of an estuarine lagoon ecosystem. *Comput. Sci. Tech.* 3, 350–412. doi: 10.15181/csat.v3i1.1093

Ferrarin, C., Razinkovas, A., Gulbinskas, S., Umgiesser, G., and Bliūdžiutė, L. (2008). Hydraulic regime-based zonation scheme of the Curonian Lagoon. *Hydrobiologia* 611, 133–146. doi: 10.1007/s10750-008-9454-5

Galloway, J. N., Townsend, A. R., Erisman, J. W., Bekunda, M., Cai, Z., Freney, J. R., et al. (2008). Transformation of the nitrogen cycle: recent trends, questions, and potential solutions. *Science* 320, 889–892. doi: 10.1126/science.1136674

Gasiūnaitė, Z. R., Cardoso, A. C., Heiskanen, A. S., Henriksen, P., Kauppila, P., Olenina, I., et al. (2005). Seasonality of coastal phytoplankton in the Baltic Sea: influence of salinity and eutrophication. *Estuar. Coast. Shelf Sci.* 65, 239–252. doi: 10.1016/j.ecss.2005.05.018

Gasiūnaitė, Z. R., Daunys, D., Olenin, S., and Razinkovas, A. (2008). "The Curonian lagoon," in *Ecology of Baltic Coastal Waters*, ed. U. Schiewer (Berlin: Springer).

Gasiūnaitė, Z. R., and Olenina, I. (1997). Zooplankton-phytoplankton interactions: a possible explanation of the seasonal succession in the Kursiu Marios lagoon. *Hydrobiologia* 363, 333–339. doi: 10.1023/A:1003161319026

Gasiūnaitė, Z. R., and Razinkovas, A. (2004). Temporal and spatial patterns of crustacean zooplankton dynamics in a transitional lagoon ecosystem. *Hydrobiologia* 514, 139–149. doi: 10.1023/B:hydr.0000018214.93205.32

Giardino, C., Bresciani, M., Pilkaitytė, R., Bartoli, M., and Razinkovas, A. (2010). *In situ* measurements and satellite remote sensing of case 2 waters: preliminary results from the Curonian Lagoon. *Oceanologia* 52, 197–210. doi: 10.5697/oc.52-2.197

Gili, J. M., and Coma, R. (1998). Benthic suspension feeders: their paramount role in littoral marine food webs. *Trends Ecol. Evol.* 13, 316–321. doi: 10.1016/S0169-5347(98)01365-2

Green, A. J., and Elmberg, J. (2014). Ecosystem services provided by waterbirds. *Biol. Rev.* 89, 105–122. doi: 10.1111/brv.12045

Grinienė, E. (2013). *Functional Role of Plankton Ciliates in a Eutrophic Coastal Lagoon*. Ph.D. thesis, Klaipėda, Klaipėda University: 123.

Grinienė, E., Šulčius, S., and Kuosa, H. (2016). Size-selective microzooplankton grazing on the phytoplankton in the Curonian Lagoon (SE Baltic Sea). *Oceanologia* 58, 292–301. doi: 10.1016/j.oceano.2016.05.002

Gwiazda, R., Woźnica, A., Łozowski, B., Kostecki, M., and Flis, A. (2014). Impact of waterbirds on chemical and biological features of water and sediments of a large, shallow dam reservoir. *Oceanol. Hydrobiol. Stud.* 43, 418–426. doi: 10.2478/s13545-014-0160-9

Hahn, S., Bauer, S., and Klaassen, M. (2007). Estimating the contribution of carnivorous waterbirds to nutrient loading in freshwater habitats. *Freshw. Biol.* 52, 2421–2433. doi: 10.1111/j.1365-2427.2007.01838.x

Han, H., and Allan, J. D. (2012). Uneven rise in N inputs to the Lake Michigan Basin over the 20th century corresponds to agricultural and societal transitions. *Biogeochemistry* 109, 175–187. doi: 10.1007/s10533-011-9618-7

Han, I., Yoo, K., Wee, G. N., No, J. H., Park, J., Min, S. J., et al. (2017). Short-term effects of great cormorant droppings on water quality and microbial community of an artificial agricultural reservoir. *J. Environ. Qual.* 46, 470–476. doi: 10.2134/jeq2016.11.0459

Hellström, T. (1991). The effect of resuspension on algal production in a shallow lake. *Hydrobiologia* 213, 183–190. doi: 10.1007/BF00016421

Howarth, R., Chan, F., Conley, D. J., Garnier, J., Doney, S., Marino, R., et al. (2011). Coupled biogeochemical cycles: eutrophication and hypoxia in temperate

estuaries and coastal marine ecosystems. *Front. Ecol. Environ.* 9, 18–26. doi: 10.1890/100008

INFORM (2017). *INFORM Prototype/Algorithms Validation Report Update, version 1.0*.

Jakimavičius, D., and Kriaučiūnienė, J. (2013). The climate change impact on the water balance of the Curonian Lagoon. *Water Resour.* 40, 120–132. doi: 10.1134/S0097807813020097

Jakimavičius, D., Kriaučiūnienė, J., and Šarauskienė, D. (2018). Impact of climate change on the Curonian Lagoon water balance components, salinity and water temperature in the 21st century. *Oceanologia* 60, 378–389. doi: 10.1016/j.oceano.2018.02.003

Jeppesen, E., Jensen, J. P., Søndergaard, M., and Lauridsen, T. (1999). Trophic dynamics in turbid and clearwater lakes with special emphasis on the role of zooplankton for water clarity. *Hydrobiologia* 408–409, 217–231. doi: 10.1007/978-94-017-2986-4_24

Klimaszyk, P., Brzeg, A., Rzymski, P., and Piotrowicz, R. (2015). Black spots for aquatic and terrestrial ecosystems: impact of a perennial cormorant colony on the environment. *Sci. Total Environ.* 517, 222–231. doi: 10.1016/j.scitotenv.2015.02.067

Klimaszyk, P., and Rzymski, P. (2016). The complexity of ecological impacts induced by great cormorants. *Hydrobiologia* 771, 13–30. doi: 10.1007/s10750-015-2618-1

Krevs, A., Koreiviene, J., Paskauskas, R., and Sulijiene, R. (2007). Phytoplankton production and community respiration in different zones of the Curonian lagoon during the midsummer vegetation period. *Transl. Waters Bull.* 1, 17–26. doi: 10.1285/i1825229Xv1n1p17

Lesutienė, J., Bukaveckas, P. A., Gasiūnaitė, Z. R., Pilkaitytė, R., and Razinkovas-Baziukas, A. (2014). Tracing the isotopic signal of a Cyanobacteria bloom through the food web of a Baltic Sea coastal lagoon. *Estuar. Coast. Shelf Sci.* 138, 47–56. doi: 10.1016/j.ecss.2013.12.017

Lithuanian Environmental Protection Agency (EPA) (2008). *The Assessment of Ichtiofauna Research and Ecological State According to Fish Indicators in the Curonian Lagoon and Baltic Sea*. Available at: http://vanduo.gamta.lt/files/2008m_tyrimu_rezultatu_analizes_ataskaita_Kursiu_mariose_ir_Baltijos_juroje.pdf

Manny, B. A., Johnson, W. C., and Wetzel, R. G. (1994). Nutrient additions by waterfowl to lakes and reservoirs: predicting their effects on productivity and water quality. *Hydrobiologia* 279–280, 121–132. doi: 10.1007/BF00027847

Matuszak, A., Mörtl, M., Quillfeldt, P., and Bauer, H. G. (2014). Macrophyte-associated macroinvertebrates as an important food source for wintering waterbirds at Lake Constance. *Limnology* 15, 69–76. doi: 10.1007/s10201-013-0414-z

Moore, S. K., Trainer, V. L., Mantua, N. J., Parker, M. S., Laws, E. A., Backer, L. C., et al. (2008). Impacts of climate variability and future climate change on harmful algal blooms and human health. *Environ. Health* 7(Suppl. 2):S4. doi: 10.1186/1476-069X-7-S2-S4

Muhlolland, P. J., Helton, A. M., Poole, G. C., Hall, R. O., Hamilton, S. K., Peterson, B. J., et al. (2008). Stream denitrification across biomes and its response to anthropogenic nitrate loading. *Nature* 452, 203–205. doi: 10.1038/nature06686

Norkko, A., and Bonsdorff, E. (1996). Population responses of coastal zoobenthos to stress induced by drifting algal mats. *Mar. Ecol. Prog. Ser.* 140, 141–151. doi: 10.3354/meps140141

Officer, C. B., Smayda, T. J., and Mann, R. (1982). Benthic filter feeding: a natural eutrophication control. *Mar. Ecol. Prog. Ser.* 9, 203–210. doi: 10.3354/meps009203

Olenina, I. (1998). Long-term changes in the Kuršiø Marios Lagoon: eutrophication and phytoplankton response. *Ekologija* 1, 56–65.

Paerl, H. W. (2009). Controlling eutrophication along the freshwater-marine continuum: dual nutrient (N and P) reductions are essential. *Estuaries Coast.* 32, 593–601. doi: 10.1007/s12237-009-9158-8

Parkos, J. J. III, Santucci, V. J. Jr., and Wahl, D. H. (2003). Effects of adult common carp (*Cyprinus carpio*) on multiple trophic levels in shallow mesocosms. *Can. J. Fish. Aquat. Sci.* 60, 182–192. doi: 10.1139/f03-011

Persson, A., and Svensson, J. M. (2006). Effects of benthivorous fish on biogeochemical processes in lake sediments. *Freshw. Biol.* 51, 1298–1309. doi: 10.1111/j.1365-2427.2006.01569.x

Petkuviene, J., Žilius, M., Lubiene, I., Ruginis, T., Giordani, G., Razinkovas-Baziukas, A., et al. (2016). Phosphorus cycling in a freshwater estuary impacted by cyanobacterial blooms. *Estuaries Coast.* 39, 1386–1402. doi: 10.1007/s12237-016-0078-0

Phan-Van, M., Rousseau, D., and De Pauw, N. (2008). Effects of fish bioturbation on the vertical distribution of water temperature and dissolved oxygen in a fish culture-integrated waste stabilization pond system in Vietnam. *Aquaculture* 281, 28–33. doi: 10.1016/j.aquaculture.2008.04.033

Pilkaitytė, R., and Razinkovas, A. (2006). Factors controlling phytoplankton blooms in a temperate estuary: nutrient limitation and physical forcing. *Hydrobiologia* 555, 41–48. doi: 10.1007/s10750-005-1104-6

Pilkaitytė, R., and Razinkovas, A. (2007). Seasonal changes in phytoplankton composition and nutrient limitation in a shallow Baltic lagoon. *Boreal Environ. Res.* 12, 551–559. doi: 10.1007/s11274-015-1903-5

Post, D. M., Taylor, J. P., Kitchell, J. F., Olson, M. H., Schindler, D. E., and Herwig, B. R. (1998). The role of migratory waterfowl as nutrient vectors in a managed wetland. *Conserv. Biol.* 12, 910–920. doi: 10.1046/j.1523-1739.1998.97112.x

Pustelnikovas, O. (1994). Transport and accumulation of sediment and contaminants in the Lagoon of Kuršiu marios (Lithuania) and Baltic Sea. *Neth. J. Aquat. Ecol.* 28, 405–411. doi: 10.1007/BF02334210

Pūtys, Ž., and Zarankaitė, J. (2010). Diet of the great cormorant (*Phalacrocorax carbo sinensis*) at the Juodkrantė colony, Lithuania. *Acta Zool. Litu.* 20, 179–189. doi: 10.2478/v10043-010-0031-6

Rabalais, N. N., Turner, R. E., and Wiseman, W. J. (2002). Gulf of Mexico hypoxia, AKA "The dead zone". *Annu. Rev. Ecol. Syst.* 33, 235–263. doi: 10.1146/annurev.ecolsys.33.010802.150513

Rashleigh, B., Razinkovas, A., and Pilkaitytė, R. (2012). Ecosystem services assessment of the Nemunas River delta. *Transl. Waters Bull.* 5, 75–84. doi: 10.1285/i1825229Xv5n2p75

Razinkovas, A., Dailidienė, I., and Pilkaitytė, R. (2008). "Reduction of the land-based discharges to the Curonian Lagoon in a view of a climate change perspective," in *Sustainable Use and Development of Watersheds, NATO Science for Peace and Security Series (Series C: Environmental Security)*, eds Ý. E. Gönenç, A. Vadineanu, J. P. Wolflin, and R. C. Russo (Dordrecht: Springer), 403–413.

Razinkovas-Baziukas, A., Margoński, P., and Povilanskas, R. (2012). "Management challenges for the South Baltic transboundary transitional waters," in *Transboundary Management of Transitional Waters – Code of Conduct and Good Practice Examples*, eds H. Nilsson, R. Povilanskas, and N. Stybel (Warnemünde: EUCC), 25–37.

Remeikaitė-Nikienė, N., Lujanienė, G., Malejevas, V., Barisevičiūtė, R., Žilius, M., Garnaga-Budrė, G., et al. (2016). Distribution and sources of organic matter in sediments of the south-eastern Baltic Sea. *J. Mar. Syst.* 157, 75–81. doi: 10.1016/j.jmarsys.2015.12.011

Rodríguez-Pérez, H., Green, A. J., and Figuerola, J. (2007). Effects of Greater flamingo *Phoenicopterus ruber* on macrophytes, chironomids and turbidity in natural marshes in Doñana, SW Spain. *Fundam. Appl. Limnol.* 170, 167–175. doi: 10.1127/1863-9135/2007/0170-0167

Rönicke, H., Doerffer, R., Siewers, H., Büttner, O., Lindenschmidt, K. E., Herzsprung, P., et al. (2008). Phosphorus input by nordic geese to the eutrophic Lake Arendsee, Germany. *Fundam. Appl. Limnol.* 172, 111–119. doi: 10.1127/1863-9135/2008/0172-0111

Roozen, F. C., Lürling, M., Vlek, H., Van Der Pouw Kraan, E. A., Ibelings, B. W., and Scheffer, M. (2007). Resuspension of algal cells by benthivorous fish boosts phytoplankton biomass and alters community structure in shallow lakes. *Freshw. Biol.* 52, 977–987. doi: 10.1111/j.1365-2427.2007.01729.x

Ruginis, T., Bartoli, M., Petkuviene, J., Zilius, M., Lubiene, I., Laini, A., et al. (2014). Benthic respiration and stoichiometry of regenerated nutrients in lake sediments with *Dreissena polymorpha*. *Aquat. Sci.* 76, 405–417. doi: 10.1007/s00027-014-0343-x

Sánchez, M. I., Green, A. J., and Alejandre, R. (2006). Shorebird predation affects density, biomass, and size distribution of benthic chironomids in salt pans: an exclosure experiment. *J. North Am. Benthol. Soc.* 25, 9–18. doi: 10.1899/0887-3593(2006)25[9:SPADBA]2.0.CO;2

Schindler, D. E., Carpenter, S. R., Cottingham, K. L., He, X., Hodgson, J. R., Kitchell, J. F., et al. (1996). "Food web structure and littoral zone coupling to pelagic trophic cascades," in *Food Webs: Integration of Pattern and Dynamics*, eds G. A. Polis and K. O. Winemiller (Boston, MA: Springer), 96–105. doi: 10.1007/978-1-4615-7007-3_9

Schmidt-Ries, H. (1940). Untersuchung zur kenntnis des pelagials eines strand gewassers (Kurisches Haff). *Z. Fischerei Deren Hilfswissenschaften B* 37:330.

Semenova, A. S., and Aleksandrov, S. V. (2009). The zooplankton consumption of primary production and an assessment of the waterbody trophic state on the basis of its structural and functional characteristics. *Inland Water Biol.* 2, 57–63. doi: 10.1134/S1995082909040099

Shormann, D. E., and Cotner, J. B. (1997). The effects of benthivorous smallmouth buffalo (*Ictiobus bubalus*) on water quality and nutrient cycling in a shallow floodplain lake. *Lake Reserv. Manage.* 13, 270–278. doi: 10.1080/07438149709354318

Stanevičius, V., Švažas, S., Raudonikis, L., and Gražulevičius, G. (2009). Non-breeding concentrations of the Tufted Duck *Aythya fuligula* in Lithuania. *Ekologija* 55, 29–39. doi: 10.2478/v10055-009-0004-x

Stief, P. (2013). Stimulation of microbial nitrogen cycling in aquatic ecosystems by benthic macrofauna: mechanisms and environmental implications. *Biogeosciences* 10, 7829–7846. doi: 10.5194/bg-10-7829-2013

Šulčius, S., Pilkaitytė, R., Mazur-Marzec, H., Kasperovièienë, J., Ezhova, E., Błaszczyk, A., et al. (2015). Increased risk of exposure to microcystins in the scum of the filamentous cyanobacterium Aphanizomenon flos-aquae accumulated on the western shoreline of the Curonian Lagoon. *Mar. Pollut. Bull.* 99, 264–270. doi: 10.1016/j.marpolbul.2015.07.057

Švažas, S., Chukalova, N., Grishanov, G., Pūtys, Ž., Sruoga, A., Butkauskas, D., et al. (2011). The role of Great Cormorant (*Phalacrocorax carbo sinensis*) for fish stock and dispersal of helminthes parasites in the Curonian Lagoon area. *Vet. Med. Zoot.* 55, 79–85.

Tarvainen, M., Sarvala, J., and Helminen, H. (2002). The role of phosphorus release by roach [*Rutilus rutilus* (L.)] in the water quality changes of a biomanipulated lake. *Freshw. Biol.* 47, 2325–2336. doi: 10.1046/j.1365-2427.2002.00992.x

Tobiessen, P., and Wheat, E. (2000). Long and short term effects of waterfowl on Collins Lake, an urban lake in upstate New York. *Lake Reserv. Manage.* 16, 340–344. doi: 10.1080/07438140009354241

Trimonis, E., Gulbinskas, S., and Kuzavinis, M. (2003). The Curonian Lagoon bottom sediments in the Lithuanian water area. *Baltica* 16, 13–20.

Umgiesser, G., Zemlys, P., Erturk, A., Razinkova-Baziukas, A., Mezine, J., and Ferrarin, C. (2016). Seasonal renewal time variability in the Curonian Lagoon caused by atmospheric and hydrographical forcing. *Ocean Sci.* 12, 391–402. doi: 10.5194/os-12-391-2016

Vaičiūtė, D., Bresciani, M., Bartoli, M., Giardino, C., and Bučas, M. (2015). Spatial and temporal distribution of coloured dissolved organic matter in a hypertrophic freshwater lagoon. *J. Limnol.* 74, 572–583. doi: 10.4081/jlimnol.2015.1176

Valiela, I., McClelland, J., Hauxwell, J., Behr, P. J., Hersh, D., and Foreman, K. (1997). Macroalgal blooms in shallow estuaries: controls and ecophysiological and ecosystem consequences. *Limnol. Oceanogr.* 42, 1105–1118. doi: 10.4319/lo.1997.42.5_part_2.1105

Vybernaite-Lubiene, I., Žilius, M., Giordani, G., Petkuviene, J., Vaičiūtė, D., Bukaveckas, P. A., et al. (2017). Effect of algal blooms on retention of N, Si and P in Europe's largest coastal lagoon. *Estuar. Coast. Shelf Sci.* 194, 217–228. doi: 10.1016/j.ecss.2017.06.020

Vybernaite-Lubiene, I., Zilius, M., Saltyte-Vaisiauske, L., and Bartoli, M. (2018). Recent Trends (2012-2016) of N, Si, and P export from the Nemunas River Watershed: loads, unbalanced stoichiometry, and threats for downstream aquatic ecosystems. *Water* 10:1178. doi: 10.3390/w10091178

Werner, S., Moertl, M., Bauer, H. G., and Rothhaupt, K. O. (2005). Strong impact of wintering waterbirds on zebra mussel (*Dreissena polymorpha*) populations at Lake Constance, Germany. *Freshw. Biol.* 50, 1412–1426. doi: 10.1111/j.1365-2427.2005.01411.x

Williams, A. E., Moss, B., and Eaton, J. (2002). Fish induced macrophyte loss in shallow lakes: top–down and bottom–up processes in mesocosm experiments. *Freshw. Biol.* 47, 2216–2232. doi: 10.1046/j.1365-2427.2002.00963.x

Ye, N., Zhang, X., Mao, Y., Liang, C., Xu, D., Zou, J., et al. (2011). 'Green tides' are overwhelming the coastline of our blue planet: taking the world's largest example. *Ecol. Res.* 26, 477–485. doi: 10.1007/s11284-011-0821-8

Yunev, O. A., Carstensen, J., Moncheva, S., Khaliulin, A., Ærtebjerg, G., and Nixon, S. (2007). Nutrient and phytoplankton trends on the western Black Sea shelf in response to cultural eutrophication and climate changes. *Estuar. Coast. Shelf Sci.* 74, 63–76. doi: 10.1016/j.ecss.2007.03.030

Zambrano, L., and Hinojosa, D. (1999). Direct and indirect effects of carp (*Cyprinus carpio* L.) on macrophyte and benthic communities in experimental shallow ponds in central Mexico. *Hydrobiologia* 408, 131–138. doi: 10.1023/A:1017085129620

Zettler, M. L., and Daunys, D. (2007). Long-term macrozoobenthos changes in a shallow boreal lagoon: comparison of a recent biodiversity inventory with historical data. *Limnologica* 37, 170–185. doi: 10.1016/j.limno.2006.12.004

Zhang, H., Culver, D. A., and Boegman, L. (2008). A two-dimensional ecological model of Lake Erie: application to estimate dreissenid impacts on large lake plankton populations. *Ecol. Model.* 214, 219–241. doi: 10.1016/j.ecolmodel.2008.02.005

Zilius, M., Bartoli, M., Bresciani, M., Kataržytė, M., Ruginis, T., Petkuvienė, J., et al. (2014). Feedback mechanisms between cyanobacterial blooms, transient hypoxia, and benthic phosphorus regeneration in shallow coastal environments. *Estuar. Coast.* 37, 680–694. doi: 10.1007/s12237-013-9717-x

Zilius, M., Bartoli, M., Daunys, D., Pilkaityte, R., and Razinkovas, A. (2012). Patterns of benthic oxygen uptake in a hypertrophic lagoon: spatial variability and controlling factors. *Hydrobiologia* 699, 85–98. doi: 10.1007/s10750-012-1155-4

Zilius, M., De Wit, R., and Bartoli, M. (2016). Response of sedimentary processes to cyanobacteria loading. *J. Limnol.* 75, 236–247. doi: 10.4081/jlimnol.2015.1296

Zilius, M., Giordani, G., Petkuviene, J., Lubiene, I., Ruginis, T., and Bartoli, M. (2015). Phosphorus mobility under short-term anoxic conditions in two shallow eutrophic coastal systems (Curonian and Sacca di Goro lagoons). *Estuar. Coast. Shelf Sci.* 164, 134–146. doi: 10.1016/j.ecss.2015.07.004

Zilius, M., Vybernaite-Lubiene, I., Vaiciute, D., Petkuviene, J., Zemlys, P., Liskow, I., et al. (2018). The influence of cyanobacteria blooms on the attenuation of nitrogen throughputs in a Baltic coastal lagoon. *Biogeochemistry* 141, 143–165. doi: 10.1007/s10533-018-0508-0

Žydelis, R. (2001). Some remarks on effect of climatic parameters on wintering waterbirds in the eastern Baltic. *Acta Zool. Litu.* 11, 303–308. doi: 10.1080/13921657.2001.10512463

Conflict of Interest Statement: The authors declare that the research was conducted in the absence of any commercial or financial relationships that could be construed as a potential conflict of interest.

frontiers in Marine Science

ORIGINAL RESEARCH
published: 07 August 2018
doi: 10.3389/fmars.2018.00272

Phytoplankton Community Dynamic: A Driver for Ciliate Trophic Strategies

Lumi Haraguchi[1]*, *Hans H. Jakobsen*[1], *Nina Lundholm*[2] and *Jacob Carstensen*[1]

[1] Department of Bioscience, Aarhus University, Roskilde, Denmark, [2] National History Museum of Denmark, University of Copenhagen, Copenhagen, Denmark

Phytoplankton plays a key role as primary producers and mediating biogeochemical cycles in the water column. The understanding of the temporal dynamic of primary grazers channeling energy and carbon from primary producers is important for evaluating aquatic ecosystems functioning. This study investigates the coupling between phytoplankton and ciliates from live samples collected with approximately daily frequency during an almost 2-year cycle. The study site is a nutrient-rich temperate estuary, Roskilde Fjord (Denmark). Our aim is to evaluate the importance of protist grazers, especially ciliates, as predators on phytoplankton and to evaluate differences among multiple nutritional strategies through different seasons. The phytoplankton community, was mostly dominated by small organisms (<20 μm) with few observations of diatoms. In most of observations, heterotrophic dinoflagellates biomass was smaller than biomass of ciliates (<10%), indicating that ciliates are the main component of microzooplankton. Except for the spring 2016, the ciliate community closely followed the phytoplankton community, showing a tight coupling between the primary producers and grazers during all seasons. This somehow contradicts the general assumption that ciliate dominance is restricted to periods of nutrient limitation dominated by the microbial food web and suggests a year-round key role of ciliates as consumers of phytoplankton biomass. Biomasses of ciliates increased during spring and were highest during summer. Relative importance of mixotrophs were high due to occurrence of *Mesodinium rubrum* blooms as well as other mixotrophic ciliates in late spring/early summer. *M. rubrum* biomass had the opposite pattern of the cryptophyte prey *Teleaulax* spp., and the coupling between the two populations was very strong in late spring. Ciliates that grazed on selected phytoplankton, had a smaller potential grazing impact regarding their biomasses, likely due to food limitation; conversely ciliates that feed on diverse prey items were less constrained by food limitation, and their seasonality appear to be driven by other factors. These findings suggest that the ciliate community structure and dynamics is important in structuring the phytoplankton community on short and seasonal scale.

Keywords: phytoplankton community, ciliates, grazing rates, mixotrophy, trophic strategies

OPEN ACCESS

Edited by:
Riina Klais,
University of Tartu, Estonia

Reviewed by:
Urania Christaki,
Université du Littoral Côte d'Opale, France
Sai Elangovan S,
National Institute of Oceanography (CSIR), India

***Correspondence:**
Lumi Haraguchi
luh@bios.au.dk

Specialty section:
This article was submitted to Marine Ecosystem Ecology, a section of the journal Frontiers in Marine Science

Received: *27 April 2018*
Accepted: *18 July 2018*
Published: *07 August 2018*

Citation:
Haraguchi L, Jakobsen HH, Lundholm N and Carstensen J (2018) Phytoplankton Community Dynamic: A Driver for Ciliate Trophic Strategies. Front. Mar. Sci. 5:272. doi: 10.3389/fmars.2018.00272

INTRODUCTION

Phytoplankton primary production supports higher trophic levels and fuels microbial remineralization (Azam et al., 1983; Sherr and Sherr, 1988). The dominant pelagic grazers of phytoplankton are typically associated with distinct operating modes of the food web compartments and nutrient cycling. Heterotrophic protist grazers and microzooplankton dominance is usually associated with the microbial loop and regenerated production; while mesozooplankton is associated with a linear food chain and export production (Fenchel, 1988; Buitenhuis et al., 2006). Grazing on particulate primary production in the global ocean surface is ∼10–15% for mesozooplankton and 59–75% for microzooplankton (Behrenfeld and Falkowski, 1997; Calbet, 2001; Landry and Calbet, 2004; Buitenhuis et al., 2010), with estimates for coastal and estuarine systems usually in the a lower range (Landry and Calbet, 2004).

Ciliates constitute an important component of the microzooplankton community with preference for small-sized preys, in contrast to mesozooplankton, and many ciliate species are also grazed by mesozooplankton (Hansen et al., 1997). Thus, ciliates can be an important link between small cells and higher trophic levels (Nielsen and Kiørboe, 1994). Besides their significant role in carbon transfer, ciliates are also considered high quality food, as a source of proteinaceous compounds with a low C:N ratio in comparison to phytoplankton (Stoecker and Capuzzo, 1990; Gifford, 1991).

Although many ciliates are heterotrophs, a number of pelagic species are mixotrophic, combining both phagotrophic and phototrophic nutrition (Stoecker, 1998). The recognition of mixotrophy in the marine plankton food web has challenged the classical understanding of pelagic food webs, as autotrophy and heterotrophy are not necessarily two distinct functional compartments (Flynn et al., 2013). Classical understanding of ecological interactions among plankton, such as competition for nutrients, indicates that nutrient uptake affinity decreases with organism size (Edwards et al., 2012), favoring smaller sizes under resource limiting conditions. Mixotrophy is advantageous to organisms under nutrient limited conditions, allowing them to reduce direct competition by grazing on smaller prey and increase direct ingestion of nutrients (Mitra et al., 2014). Modeling results suggest that mixotrophy favors larger organisms, and therefore enhances trophic transfer efficiency (Mitra et al., 2014; Ward and Follows, 2016). On top of that, mixotrophy appears to be important over both, space and time, in marine systems (Leles et al., 2017), stressing the need for ecological field studies to further elucidate the role of mixotrophy.

Today, the importance of ciliates in the marine environment, including coastal and estuarine systems, is well recognized (Calbet and Landry, 2004). However, the role of ciliate nutrition mode and its impacts on ecosystem productivity is understudied for a number of reasons. One is that most plankton monitoring programs focus on analyzing phytoplankton and mesozooplankton only and similarly, many field studies do not include analyses of ciliates. Second, fixation can destroy cells and change their characteristics, such as color, size, and shape (Choi and Stoecker, 1989; Stoecker et al., 1994), constraining the distinction between mixotrophs and heterotrophs. In addition, even if ciliates are properly recorded, many studies employ monthly sampling, which hampers the investigation of ecosystem trophodynamics due to the fast growth responses of ciliates and phytoplankton.

The use of in-flow systems (e.g., flow cytometry) have routinely been used to assess plankton communities, including different size fractions (Dashkova et al., 2017). Using these technologies in high frequency monitoring of plankton has demonstrated that short-term events can be easily missed with sampling frequencies typically employed for monitoring (Thyssen et al., 2008; Campbell et al., 2013; Dugenne et al., 2014). Furthermore, in-flow systems allow analysis of live samples, avoiding loss and shrinkage of cells due to fixation (Jakobsen and Carstensen, 2011; Haraguchi et al., 2017). Thus, the use of in-flow systems can improve our knowledge on the coupled dynamics of phytoplankton and ciliates, by allowing a large number of samples to be analyzed in relatively short time.

This study aims to assess the temporal coupling between phytoplankton and its protist grazers in a temperate mesohaline estuary (Roskilde Fjord, Denmark), evaluating differences in potential grazing rates of distinct trophic strategies over different time scales. More specifically, this study seeks to answer the following questions: (1) Are ciliates the dominant pelagic grazers in Roskilde Fjord? (2) Do mixotrophic ciliates comprise a significant proportion of the total ciliate biomass and thereby contribute significantly to the transfer of energy to higher trophic levels?

MATERIALS AND METHODS

Study Area and Sampling

Roskilde Fjord (RF; see **Figure S1** for a map of the study area and sampling pier) is a mesohaline, shallow and well-mixed estuary with a long residence time (up to 2 years) due to low river discharge and low tidal influence (Kamp-Nielsen, 1992). The estuary consists of two larger broads connected by a long narrow channel oriented in a south-north direction. It receives relatively high nutrient inputs due to dominance of agriculture in the RF catchment, which enhance primary production (Staehr et al., 2017).

Surface water (2 L) was sampled with a bucket from the Risø pier (55°41′30.19″N, 12° 4′55.24″E; **Figure S1**) almost every day from 15 February 2016 until 01 November 2017. Samples were delivered to the laboratory for immediate analysis within 10 to 20 min after sampling. Temperature and salinity were measured with an YSI Professional Plus multiparameter handheld meter (YSI, USA). Phytoplankton was analyzed with a pulse shape recording flow cytometer, whereas ciliates were analyzed by a color FlowCAM IV (see below).

Laboratory Analysis

Nutrients

Dissolved inorganic nutrient samples were stored frozen in 30 ml acid-washed plastic bottles. The samples were analyzed on a San ++ Continuous Flow Analyser (Skalar Analytical B.V, Breda,

NL) as previously described (Grasshof, 1976; Kaas and Markager, 1998). Detection limits were 0.04, 0.1, and 0.3 μmol L^{-1} for NO_2^-, NO_3^-, NH_4^+. Dissolved inorganic nitrogen (DIN) concentrations were calculated as the sum of the concentrations of NO_2^-, NO_3^-, and NH_4^+.

FlowCAM

Ciliate abundances and body volumes were analyzed from live samples using a color FlowCAM IV (Fluid Imaging Technologies, USA), following Calbet et al. (2014). From 15 March 2016 until 20 February 2017, samples were analyzed using a 4x objective and a flow cell FC300, whereas samples from 21 February until 1 November 2017 were analyzed using a 10x objective and a flow cell FC100x2. User calibration with standard beads (polymer microspheres of 50 μm, Thermo scientific™) were done for both magnification to validate counts and volumes calibration. The instrument was run in auto image-mode for both magnifications, capturing all particles in the range of 15–1,000 μm. The analysis time for each sample was ca. 40 min. (4x) or ca. 3 h (10x), corresponding to the analyzed volume of 20 and 10 ml, respectively. During analysis, samples were gently stirred (approx. 3.14 rad s^{-1}) and kept under dim light at room temperature (about 15–20°C). We assumed that cell loss during the analysis was insignificant, as no differences were observed between cell numbers recorded at the start and end of the runs. After sample processing, recorded images were manually sorted into ciliate morphotypes and dinoflagellate trophy, based on features such as cell size, color, and general morphology. Equivalent Spherical Diameter (ESD) and body volume were estimated by the software package VISP 3.17 (FluidImagine™). Cell size was estimated by the area based diameter (ABD) algorithm of VISP 3.17 (Jakobsen and Carstensen, 2011), except for tintinnids. This group of loricated ciliates can have their volumes overestimated from FlowCAM images, thus their individual volume was calculated as a prolate spheroid with diameter equal to the lorica width, and the length as 120% of width. Carbon biomass was obtained by converting volume to biomass using a generic protist volume-to-carbon conversion formula (Menden-Deuer and Lessard, 2000). The higher magnification allowed for identification of more morphotypes, which were grouped when necessary to match the 4x morphotypes. In all samples non-identified blurred images of ciliates were present, however these accounted for <5% of the observations in all samples.

Flow Cytometer

We employed a pulse-shape recording flow cytometer (PFCM) (CytoSense, Cytobuoy, NL) to analyse phytoplankton. This technique is suitable for rapid analysis of the phytoplankton size spectra, providing cell counts comparable to those obtained with traditional microscopy and more reliable information for picoplankton (Haraguchi et al., 2017). Additionally, it also provides information on cell size and morphology due to its capacity to store the optical profile for each particle, recorded as they travel through the flow cell. The instrument has a 488 nm laser, fluorescence sensors (yellow/green ∼550 nm, orange ∼ 600–650 nm and red ∼650–700 nm) and two scatter sensors, for light scattered parallel (forward scatter) and orthogonal (sideward scatter) to the incident laser beam. All the optical sensors are duplicated (except for the forward scatter) but set to different sensitivity for precise recording of both larger and smaller particles. Optical particle profiles from live samples (500–1000 μL, sampled at a flow rate of 8 μL s^{-1}) were collected using the software CytoUSB (cytobuoy.com), with a lower threshold of 30 mV for the high sensitivity red fluorescence sensor. This trigger was set to include only particles containing chlorophyll *a* (phytoplankton cells). Recorded cells were clustered according to similarities in their optical properties [length and total Forward Scatter (FWS), total red fluorescence (FLR); total orange fluorescence (FLO); total Sideward Scatter (SWS)], using the software CytoClus3 (cytobuoy.com). Particles were assigned to one cluster only and the same clustering algorithm was employed for all samples. Taxonomical information was obtained for some of the clusters based on their optical characteristics and photos taken by the equipment, which were cross-referenced with qualitative information obtained from live samples examined by light microscopy. Carbon biomass was obtained by converting total FWS to volume by applying the empirical formula in Haraguchi et al. (2017) and then converting volume to biomass using a generic protist volume-to-carbon conversion formula (Menden-Deuer and Lessard, 2000). Note that for some characteristic and/or abundant groups (e.g., chains, pico-eukaryotes, *Teleaulax* spp.) group-specific clusters were identified based on cells characteristics (size, shape, fluorescence). Other clusters, like nano-flagellates and micro-phytoplankton, comprised multiple species with lower relative abundance and no specific clusters could be drawn. For those, cluster definition was based on general functional features such as size and fluorescence levels.

Ciliates Potential Grazing Rates

Ciliate Trophic Strategy Definitions

During the study, 13 different ciliate morphotypes were identified (**Figure 1**). Heterotrophs were divided into three groups: (i) herbivores that were always observed with the same type of food in vacuole; (ii) herbivores with varying food content; and (iii) carnivores (ciliates that can also feed on other ciliates). Mixotrophs were identified as ciliates with a strong colouration and chloroplasts located throughout the cell periphery, and were assigned into two different groups following Mitra et al. (2016). Based on compiled information from the literature (**Table 1**), the ciliate morphotypes were grouped into five trophic strategies:

1. Specialist Non-Constitutive Mixotroph (SNCM): ciliates that acquire their chloroplasts and obtain them from specific prey.
2. General Non-Constitutive Mixotroph (GNCM): ciliates that acquire their chloroplasts and obtain them from multiple prey.
3. Selective herbivore (SH): heterotrophs that ingest a narrow range of prey.
4. Generic herbivore (GH): heterotrophs that ingest a broad range of prey.
5. Carnivore (Cv): heterotrophs that ingest a broad range of prey, including other ciliates.

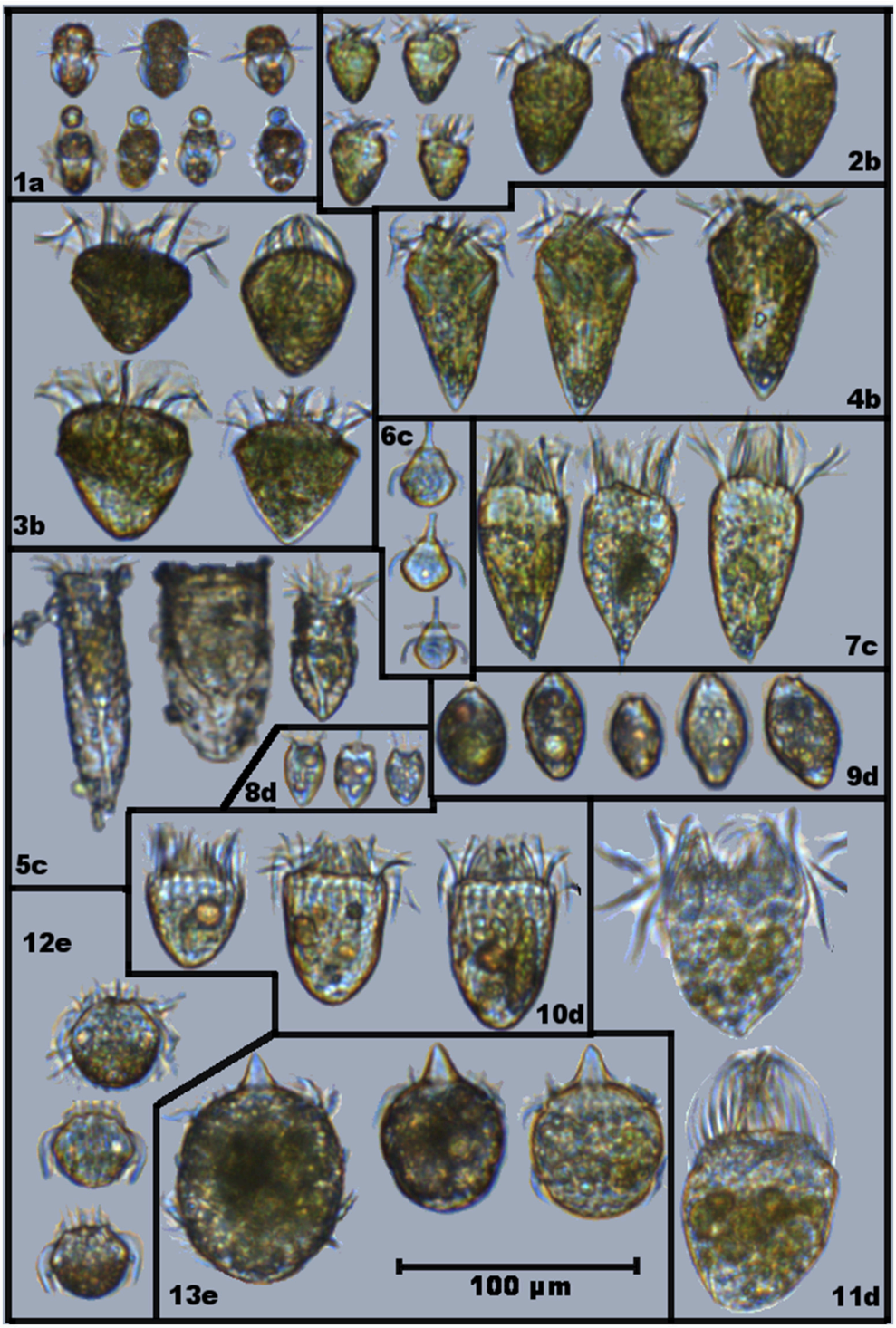

FIGURE 1 | Selected images showing different ciliates morphotypes found in Roskilde Fjord during the study period: (1) *Mesodinium rubrum*; (2) *Strombidium* spp; (3) *Strombidium* cf. *capitatum*; (4) *Strombidium* cf. *conicum*; (5) Tinitinnids; (6) *Mesodinium* cf. *velox*; (7) cf. *Pelagostrobilidium*; (8) *Balanion comatum*; (9) cf. *Urotricha*; (10) Choreotrichida; (11) Oligotrichida; (12) *Askenasia*; and (13) *Didinium*. Assigned trophy strategies are displayed as letters, accompanying the morphotypes numbers: (a) Specialist Non-Constitutive Mixotroph (SNCM); (b) General Non-Constitutive Mixotroph (GNCM); (c) Selective phagotroph (SP); (d) Generic phagotroph (GP); and (e) Carnivore (Cv). Note that some of displayed cells of *M. rubrum* (1a) are grabbing particles that are not their preferential prey (*Teleaulax* spp).

TABLE 1 | Ciliate morpho-types, trophy mode, their assigned potential preys in this study and references used to support preys assignment.

Number (Figure 1)	Ciliate morpho-type	Prey	References
SPECIALIST NON CONSTITUTIVE MIXOTROPH (SNCM)			
1	*Mesodinium rubrum*	*Teleaulax* spp.	Smith and Hansen, 2007; Peltomaa and Johnson, 2017
GENERALIST NON CONSTITUTIVE MIXOTROPH (GNCM)			
2	*Strombidium* spp	Pico eukaryotes and small nano-flagellates	Johnson, 2011; Schoener and McManus, 2012; this study
3	*Strombidium* cf. *capitatum*	Pico eukaryotes and small nano-flagellates	Johnson, 2011; Schoener and McManus, 2012; this study
4	*Strombidium* cf. *conicum*	Pico eukaryotes and small nano-flagellates	Johnson, 2011; Schoener and McManus, 2012; this study
SELECTIVE HERBIVORE (SH)			
5	Tintinnids	Pico eukaryotes and small nano-flagellates	Montagnes, 2012
6	*Mesodinium* cf. *velox*	Nanoflagellates	Tamar, 1986
7	cf. *Pelagostrombilidium*	Pico eukaryotes and small nano-flagellates	This study
GENERIC HERBIVORE (GH)			
8	*Balanion comatum*	5 μm <prey> 15 μm	Jakobsen and Montagnes, 1999
9	cf. *Urotricha*	10 μm <prey> 25 μm	This study
10	Choreotrichida	10 μm <prey> 25 μm	This study
11	Oligotrichida	10 μm <prey> 25 μm	This study
CARNIVORE (CV)			
12	*Askenasia*	15 μm <prey> 40 μm *M. rubrum*	Earland and Montagnes, 2002; this study
13	*Didinium*	15 μm<prey> 40 μm Including ciliates	Hewett, 1988

Prey Definition

FlowCAM IV allowed for identification of different ciliate morphotypes, and for the identification of prey items inside many of the ciliates. Food items were identified from food vacuoles, and based on their characteristics (size, shape, color), they were related to phytoplankton groups when possible. While some morphotypes were always observed with similar food vacuoles, others were observed with food vacuoles of different shapes, colors and sizes, indicating selective or generic prey preferences among ciliates types (**Figure 1**). Potential prey items used in the modeled grazing rates were assigned to each ciliate morphotype based on FlowCAM images (**Figure 1**; **Table 1**).

Potential Grazing

The potential grazing of different ciliate groups were estimated by calculating ingestion and clearance rates (see **Table 2** for nomenclature) following Hansen et al. (1997), with the exception of *Mesodinium rubrum* (see below). Generic maximum ingestions and clearance rates (normalized to predator volume) at standard temperature of 20°C were estimated from the volume of the ciliate cell using parameters from Hansen et al. (1997).

$$I_{max} = 50.1 \cdot {V_{cil}}^{-0.225} \quad (1)$$

$$C_{max} = 70.6 \cdot 10^{-6} \cdot {V_{cil}}^{-0.225} \quad (2)$$

From these, the half-saturation food density was found

$$K_m = \frac{I_{max}}{C_{max}} = 0.710 \cdot 10^6 \quad (3)$$

equivalent to 0.710 ppm. Cell-specific ingestion rates for the different ciliate groups were subsequently calculated as a function of food density of preferred prey (d) and water temperature (T) using the overall average Q_{10} =2.8 from Hansen et al. (1997).

$$I_{cell}(d, T, V_{cil}) = V_{cil} \cdot \frac{I_{max} \cdot d}{(K_m + d)} \cdot {Q_{10}}^{\frac{(T-20)}{10}} = V_{cil} \cdot \frac{50.1 \cdot {V_{cil}}^{-0.225} \cdot d}{(K_m + d)} \cdot {Q_{10}}^{\frac{(T-20)}{10}} \quad (4)$$

The ingestion rate for the entire ciliate group was found by summation across all cells within the group and accounting for the sampling volume

$$I(d, T, V_{cil}) = \frac{1}{V_{sample}} \cdot \sum I_{cell}(d, T, V_{cil}) \quad (5)$$

This volume-specific ingestion rate was subsequently converted into carbon units with a scaling factor ($r_{C:V}$), which was calculated from the volume-to-carbon conversion formula ($f()$) of Menden-Deuer and Lessard (2000) applied to the sample distribution of prey cell volumes (V_{prey})

$$\boldsymbol{r_{C:V}} = \frac{\sum \boldsymbol{cellcarbon}}{\sum \boldsymbol{cellvolume}} = \frac{\sum \boldsymbol{f(V_{prey})}}{\sum \boldsymbol{V_{prey}}} \quad (6)$$

When prey densities (d) were smaller than the half-saturation food density (K_m), potential food limitation is indicated. When food-limitation is observed, the prey ingested by a given ciliate is smaller than what it could potentially ingest based on its body volume, thus resulting grazing rates are smaller than expected for that ciliate.

For *M. rubrum*, potential grazing was defined based on cell counts, as daily specific prey intake has previously been reported to vary between 0.4 and 5 *Teleaulax* cells for each *Mesodinium* (Smith and Hansen, 2007). Three potential ingestion scenarios were estimated based on minimum (0.4 cryptophyte

TABLE 2 | Variables used for estimating ciliate grazing rates in Eq. 1–6.

Variables	Unit	Description
T	°C	Water temperature
V_{sample}	ml	Volume of the FlowCAM sample
V_{cil}	μm^3	Ciliate cell volume
V_{prey}	μm^3	Prey cell volume
d	$\mu m^3_{(prey)}$ ml^{-1}	Prey density
K_m	$\mu m^3_{(prey)}$ ml^{-1}	Half-saturation for food density
C_{max}	$\mu m^{-3}_{(predator)}$ $ml\ d^{-1}$	Volume-specific maximum clearance rate
I_{max}	$\mu m^3_{(prey)}$ $\mu m^{-3}_{(predator)}$ d^{-1}	Volume-specific maximum ingestion rate
$I_{cell}(d, T, V_{cil})$	$\mu m^3_{(prey)}$ d^{-1}	Volume-specific ingestion rate per ciliate cell
$I(d, T, V_{cil})$	$\mu m^3_{(prey)}$ ml^{-1} d^{-1}	Volume-specific ingestion rate for ciliate group

cells *Mesodinium*$^{-1}$ day^{-1}), maximum (5 cryptophyte cells *Mesodinium*$^{-1}$ day^{-1}), and average (2.7 cryptophyte cells *Mesodinium*$^{-1}$ day^{-1}). Daily intake rates (min, average, and max in cells L^{-1} d^{-1}) were calculated by scaling the cell-specific rates with the observed *M. rubrum* cell density. Finally, these daily intake rates were converted into carbon units by multiplying with the average individual cryptophyte C biomass of that particular sampling day.

STATISTICAL ANALYSIS

To evaluate the seasonality of the different ciliate morphotypes, a linear mixed model was fitted to quantify the biomass variation across months. Biomass observations were log-transformed to account for scale-dependent variability. The model included a random factor for the seasonal variation between the years and residual variation included an autoregressive process AR(1) to account for potential autocorrelation between the daily samples. The mixed effect models were fitted in R (R Core Team, 2017), using the nlme package (Pinheiro et al., 2017).

Prey-predator biomasses dynamics were quantified as the distance between consecutive observations, as the distance is proportional to differences in biomasses of both prey and predator. The distances were calculated as the Euclidean distance of log-transformed biomass data of phytoplankton and ciliates, which were separated according to the ciliates trophic strategies and their assigned preys (**Table 1**). Therefore, the Euclidean distance was used as a descriptor of the prey-predator dynamics, with longer distances associated with more variability in the biomasses of prey-predator pairs. As the study does not encompasses two full year cycles, differences between years were assessed considering only the productive season (15 March until 1 November).

To summarize the potential C flux through ciliates, simplified estimates of prey C biomass and potential grazing by the different trophic strategies were calculated as daily average for the productive season of each year.

RESULTS

Physical Environment

Water temperature in the study area varied seasonally from ∼4°C in winter to 20°C during summer, whereas salinity variation did not exhibit any consistent seasonal pattern, except for a small decrease during winter (**Figure 2A**). Although the 2 years appeared similar, subtle differences were observed: (i) spring warming was faster and summer temperatures remained at maximum level longer in 2016 than in 2017 (**Figure 2A**); (ii) salinity was lower in 2016 (**Figure 2A**). DIN varied seasonally, from $>20\,\mu M$ in winter to $<2\,\mu M$ in summer, as well as inter-annually with 2-fold higher winter concentrations observed in 2016 in comparison to 2017 (**Figure 2A**).

Phytoplankton and Microzooplankton Overall Dynamics

Interannual variations were observed, with considerably higher phytoplankton biomass in 2016 (**Figure 2B**), and higher ciliate biomass in 2017 (**Figure 2C**). The low phytoplankton biomass in 2017, compared to 2016, was mainly associated with lower abundance of cryptophytes, small nano-flagellates, and pico-eukaryotes in 2017 (data not shown). The average ciliate biomass for the entire study period was 22.3 $\mu g\ C\ L^{-1}$, and the average biomass during the productive season (March–November) was 12.3 and 55.8 $\mu g\ C\ L^{-1}$ in 2016 and 2017, respectively. Heterotrophic dinoflagellates were also more important in 2017 than in 2016 with average biomass during the productive season of 4.45 and 2.37 $\mu g\ C\ L^{-1}$, respectively. Overall, heterotrophic dinoflagellate biomass was much smaller than ciliate biomass, averaging 2.72 $\mu g\ C\ L^{-1}$ for the entire period, although biomass peaks could reach up to 40 $\mu g\ C\ L^{-1}$ (**Figure 2D**). Higher summer biomasses of heterotrophic dinoflagellates were associated with increased abundance of large-sized heterotrophic dinoflagellates, such as *Polykrikos*, *Protoperidinium*, and Warnowiids.

The higher ciliate biomass in 2017 was associated with increasing abundance of representatives of all trophic strategies (**Table 1**). The dominance of heterotrophs (herbivores + carnivores) was higher during spring and summer of 2016, while 2017 was characterized by slightly varying high biomass for most of the year (**Figure 3A**). Biomass of GNCM (mixotrophs excluding *M. rubrum*) was generally higher in 2017 than in 2016, with values peaking in late spring and summer for both years (**Figure 3B**). The biomass proportion between GNCM and heterotrophic ciliates was variable and higher contributions (up to 90% of the ciliates biomass, excluding *M. rubrum,* in 2017) of GNCM were recorded in summer (**Figure 3C**). Biomass of *M. rubrum* was also higher in 2017 and generally above 10 $\mu g\ C\ L^{-1}$ from April to October (**Figure 3D**).

Seasonality of Ciliate Morphotypes

Some ciliate morphotypes exhibited distinctive and recurring seasonal pattern (**Table 3**). cf. *Pelagostrombilidium* occurred during winter at temperatures <10°C, whereas *Askenasia* and *Strombidium* cf. *capitatum* were associated with higher

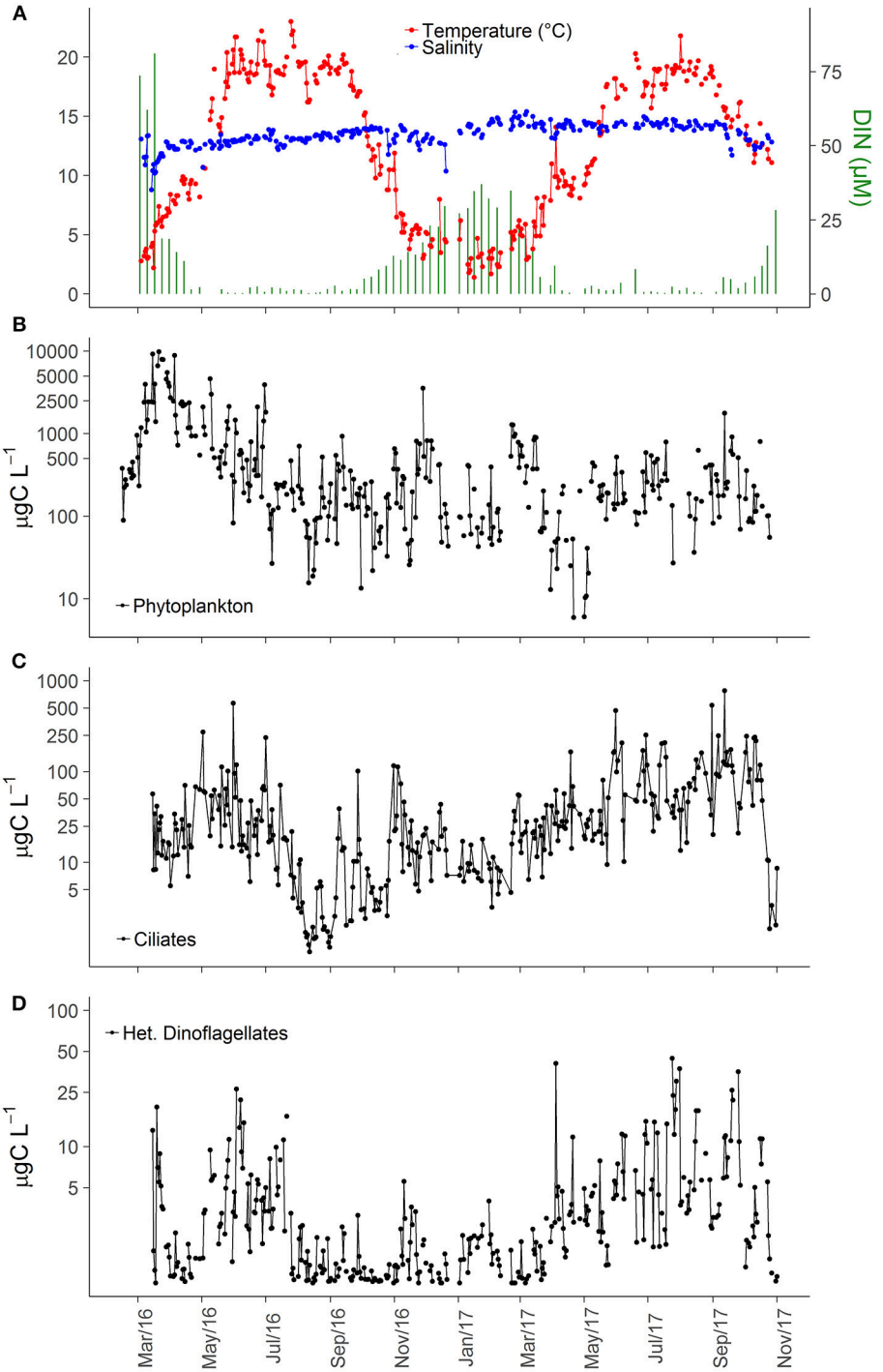

FIGURE 2 | Time series of abiotic variables **(A)**, carbon biomass of all phytoplankton cells **(B)**, all ciliate cells **(C)**, and all heterotrophic dinoflagellates cells **(D)** in inner Roskilde Fjord during the study period.

temperatures, mainly during late spring and summer (**Figures 4A–C**). Other ciliate morphotypes exhibited distinct seasonal patterns of high biomass, although their presence was not restricted to a specific seasonal window. *S.* cf. *conicum* and tinitinnids were most abundant during late spring and summer, but also found during autumn (**Figures 4D,E**). Other morphotypes, such as cf. *Urotricha* (**Figure 4F**), did not display any pronounced recurring seasonal pattern despite of the high

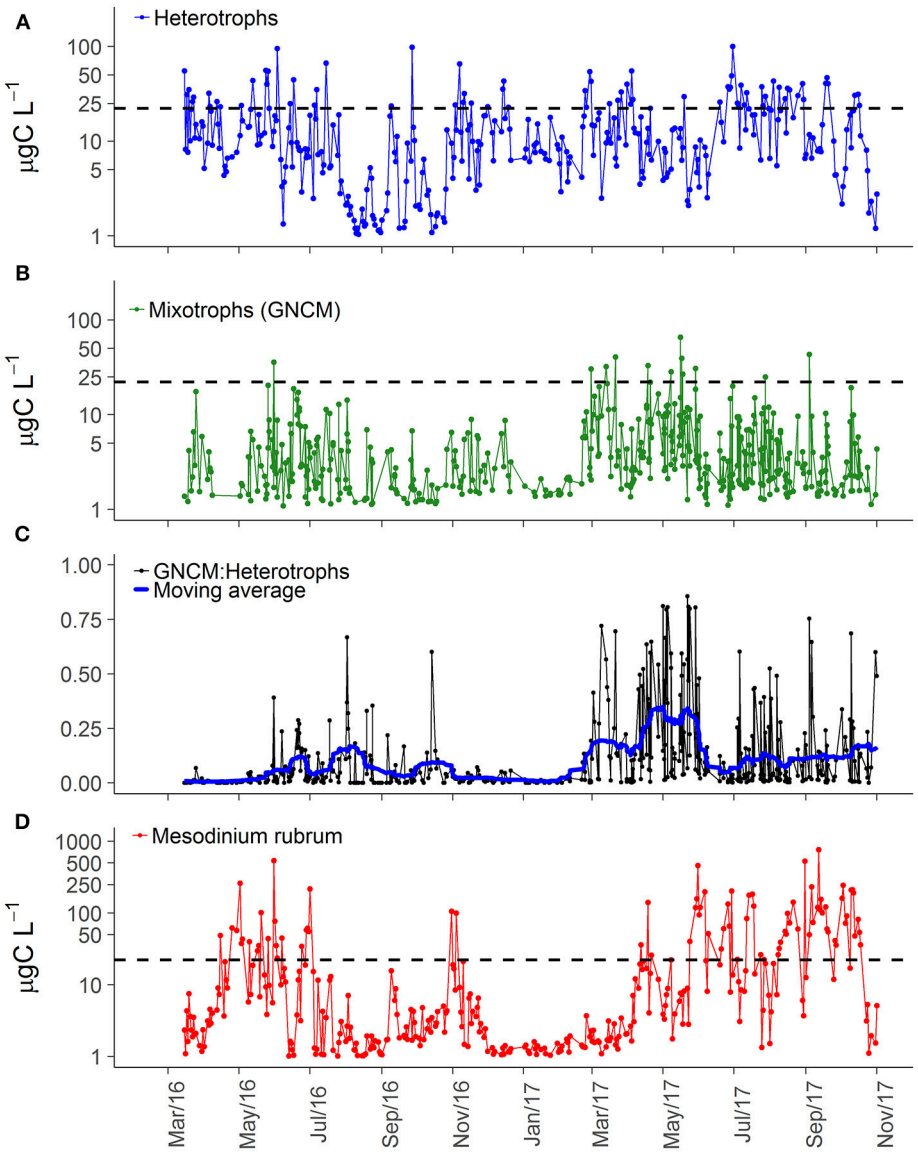

FIGURE 3 | Carbon biomass of three main ciliate groups in Roskilde Fjord **(A, B, D)** and the biomass proportion between GNCM and heterotrophic ciliates **(C)**. The black dashed horizontal lines in panels **(A, B, D)** represent the average of total ciliate biomass (22.26 µg C L^{-1}) over the entire study period. The thick blue line in panel c represents the centered moving average, using a 15 days window.

temporal variability. In spite of the significant differences among months (**Table 3**), some ciliates (*Didinium*, *Mesodinium* cf. *velox*, and Choreotrichida) did not have any clear occurrence pattern over the study period.

Potential Grazing by Ciliates

Potential grazing varied broadly over time for the five trophic strategies of ciliates and their associated preys (**Table 1**), displaying highly variable patterns of potential food limitation (**Figure 5**).

Temporal variations in biomass of *M. rubrum* (SNCM) and its cryptophyte prey were inversely related (**Figure 5A**). *Teleaulax* spp. was most abundant in winter when SNCM biomass was low, and decreased in late spring and summer when blooms of *M. rubrum* occurred. The seasonal pattern in SNCM biomass also shifted between the 2 years; the biomass was low in summer 2016, whereas it remained high from mid-April until late October in 2017.

GNCM ciliates attained similar biomass levels in 2016 and 2017, but their potential ingestion was lower in 2017 due to stronger food-limitation (**Figure 5B**), which was observed in 98% of the occasions in 2016 and in all observations in 2017. Consequently, biomass and potential ingestion observations were decoupled for this group. On the other hand, it also indicates strong grazing pressure on small phytoplankton cells by these ciliates during spring and summer (**Figure 5B**).

TABLE 3 | Seasonality test for the log-transform of carbon biomass of different ciliate morphotypes.

Ciliate morphotype	*P* (month)
Mesodinium rubrum	0.150
Strombidium spp.	0.464
Strombidium cf. *capitatum*	**<0.001**
Strombidium cf. *conicum*	**0.014**
Tintinnids	0.352
Mesodinium cf. *velox*	**<0.001**
cf. *Pelagostrombilidium*	**<0.001**
Balanion comatum	0.086
cf. *Urotricha*	0.577
Choreotrichida	**0.007**
Oligotrichida	**<0.001**
Askenasia	**0.006**
Didinium	**<0.001**

Significant variation (P < 0.05) among months are highlighted in bold.

SH ciliates were often food limited (82% of observations), even during winter and spring (**Figure 5C**). SH grazing impact varied interannually and was most intense from May to July in 2016, and from June to October in 2017. SH food limitation was observed more frequently in 2017 than in 2016 (60 and 77% of the observations in 2016 and 2017, respectively).

GH ciliates were food limited in 49 and 66% of the observations in 2016 and 2017, respectively (**Figure 5D**). The potential grazing for this group of ciliates seemed to be more intense in autumn 2017 compared to autumn 2016, and potential food limitation appeared to have started earlier in 2017 (around April) than 2016 (around June). A shift in the most abundant morphotype was observed between years, with Choreotrichida being the main GH morphotype in 2016, and cf. *Urotricha* in 2017. Together with SH, these ciliates appeared to be the main grazers during the winter period.

The carnivore ciliates (Cv) had high grazing rates during summer (**Figure 5E**), associated with high biomass of *Askenasia* (**Figure 4B**), but carnivores grazing can also be high in other periods, such as the spring bloom with high abundance of *Didinium* (**Figure 5E**). During 2016, potential grazing had higher peaks, observed in distinct periods of the year, while potential grazing rates had lower maximum values in 2017 but were consistently higher throughout a longer period (until autumn). Food limitation was observed in 32% of the observations (14% in 2016, and 55% in 2017), and as for the other trophic strategies, more frequent in 2017.

Interannual Differences in Prey-Predator Dynamics

Dynamics of prey-predator biomasses were analyzed for the productive season (15 March to 01 November) of each year (**Figure 6**). The arrows represent the distance between observations, and longer arrows can be used as a proxy for higher variability in the prey-predator relationships.

For the SNCM-prey coupling, the average distance between observations was lower in 2016 ($d = 1.19$) than in 2017 ($d = 1.36$), indicating higher variability in 2017. For this pair, variation between sampled days were higher (41% higher than the rest of productive season) during late spring to summer (day of year 110–200) in 2016 (**Figure 6A**). Distances in 2017 were more evenly distributed, with the distances found in late spring to summer, being only 8% longer than for the rest of the productive season (**Figure 6B**).

For GNCM-prey and SH-prey pairs, average distance between observations were higher in 2016 than in 2017, with $d_{2016} = 1.48$ and $d_{2017} = 0.74$ for GNCM; and $d_{2016} = 0.94$ and $d_{2017} = 0.85$ for SH (**Figures 6C–F**).

GH-prey dynamics did not appear to differ between years, with $d = 1.07$ and $d = 1.10$ for 2016 and 2017, respectively (**Figures 6G,H**). Similarly, Cv.-prey observations average distance did not vary between years ($d_{2016} = 1.22$ and $d_{2017} = 1.26$), however differences over specific periods of the productive season were observed for this group (**Figures 6I,J**). From spring to early summer (day of year 75–160) in 2016, distances were about 15% longer than for the rest of the period, while in 2017, distances in the same period were 58% longer than the rest of the productive season.

A simplified scheme (**Figure 7**) summarizes the daily average biomass for each group of phytoplankton preys and the potential daily C intake for the different ciliate trophic strategies during the productive season of each year. In 2016, biomasses of all phytoplankton prey groups were higher than in 2017, except for nano-flagellates (5–15 μm). The intake by ciliates was generally lower in 2016, with an overall relative removal of about 9% of phytoplankton daily standing biomass (**Figure 7A**). The potential grazing impact over the phytoplankton varied among the different trophic strategies, being low for SNCM and GH (∼3% of C prey biomass being grazed) and higher for GNCM and SH (about 19 and 14% of C prey biomass being grazed, respectively). In 2017, phytoplankton standing biomasses were modest when compared to the previous year, and potential grazing was higher for most ciliate trophic strategies (**Figure 7B**). The relative impact of grazing by the ciliates was about 31% of phytoplankton standing biomass in 2017, with GH being able to remove 12% of its prey biomass, while GNCM and SNCM being able to graze 37 and 46% of their preys standing biomasses daily.

DISCUSSION

Our results underline that microzooplankton, especially ciliates, can be an important component of the pelagic food web in temperate nutrient-rich estuaries at all times. On top of that, we also demonstrate that different components of the heterotrophic protist plankton have distinct ecological strategies, each affecting the phytoplankton community in its own way. Even though our results are based on standing biomasses and do not include any direct rate measurement (neither primary production nor grazing), we believe that the high temporal resolution data on both phytoplankton and microzooplankton support our findings. Furthermore, our results explore the diets of different ciliates in detail, revealing the existence of various prey-predator

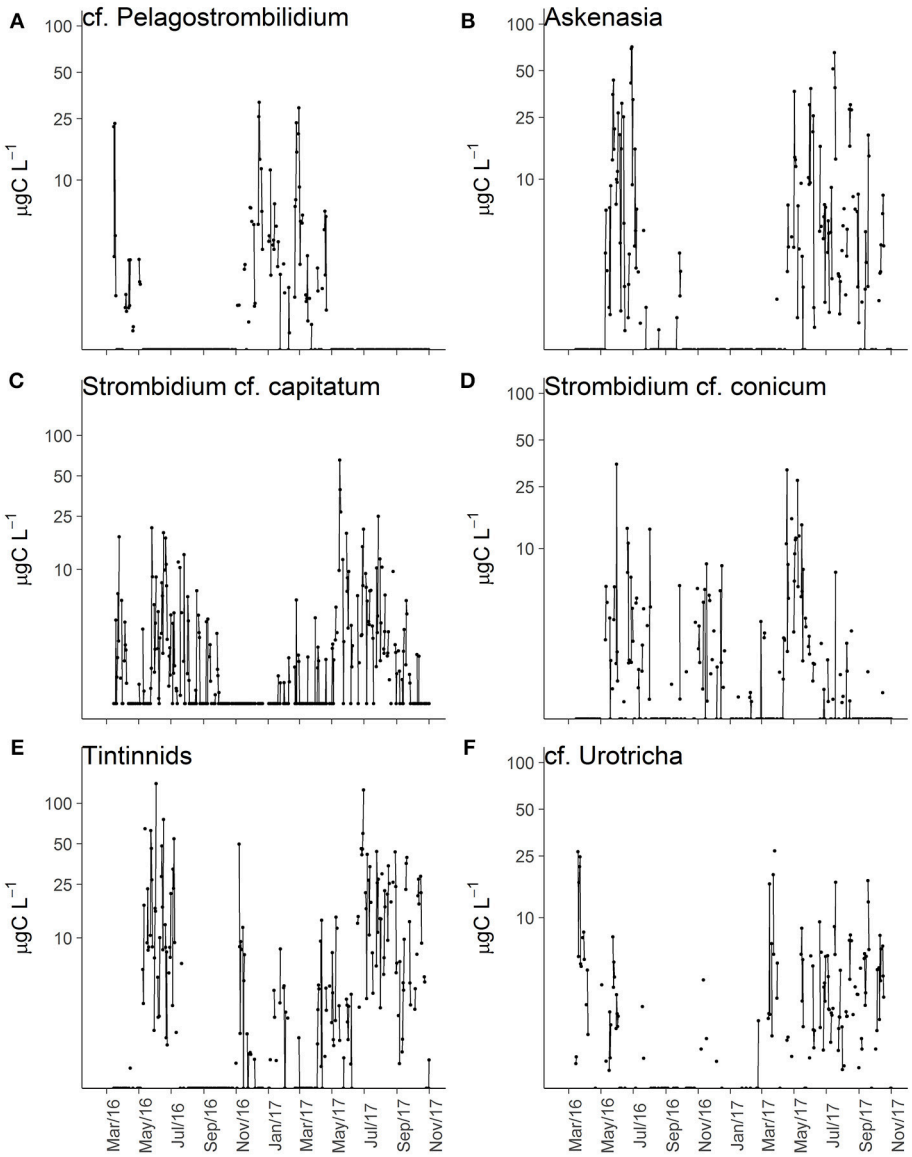

FIGURE 4 | Biomass variations over time for selected ciliates morphotypes: cf. *Pelagostrombilidium* **(A)**, *Askenasia* **(B)**, *Strombidium* cf. *capitatum* **(C)**, *S*. cf. *conicum* **(D)**, Tintinnids **(E)**, and cf. *Urotricha* **(F)**.

couplings that are likely to influence the community functioning in distinct ways. Additionally, we structured potential grazing calculations as proposed by Hansen et al. (1997), following the Michaelis-Menten kinetics, in contrast to the rectilinear model approach suggested by other authors, e.g., Zervoudaki et al. (2009). The Michaelis-Menten kinetics allow grazing estimation at varying prey concentrations, whereas a rectilinear model assumes a linear increase in ingestion rate until food saturation is reached, which can overestimate the potential grazing.

Classically, the relative importance of trophic pathways of phytoplankton primary production in any specific ecosystem is highly dependent on the balance between nutrient inputs and recycling, with increasing dominance of larger phytoplankton species and mesozooplankton in areas with higher input of new nutrients (Azam et al., 1983; Fenchel, 1988; Buitenhuis et al., 2006). Although Roskilde Fjord (RF) is a nutrient rich system (Staehr et al., 2017), its inner portion, which is also the area of interest in this study, has always been dominated by small phytoplankton organisms ($<20\,\mu m$), not diatoms, evidenced by the long term monitoring data. Besides microzooplankton, potential consumers of phytoplankton in RF are pelagic mesozooplankton and benthic filter feeders; however, benthic grazers were not sampled in this study, therefore we cannot compare directly the relative importance of pelagic vs. benthic grazing. We also acknowledge that protozooplankton

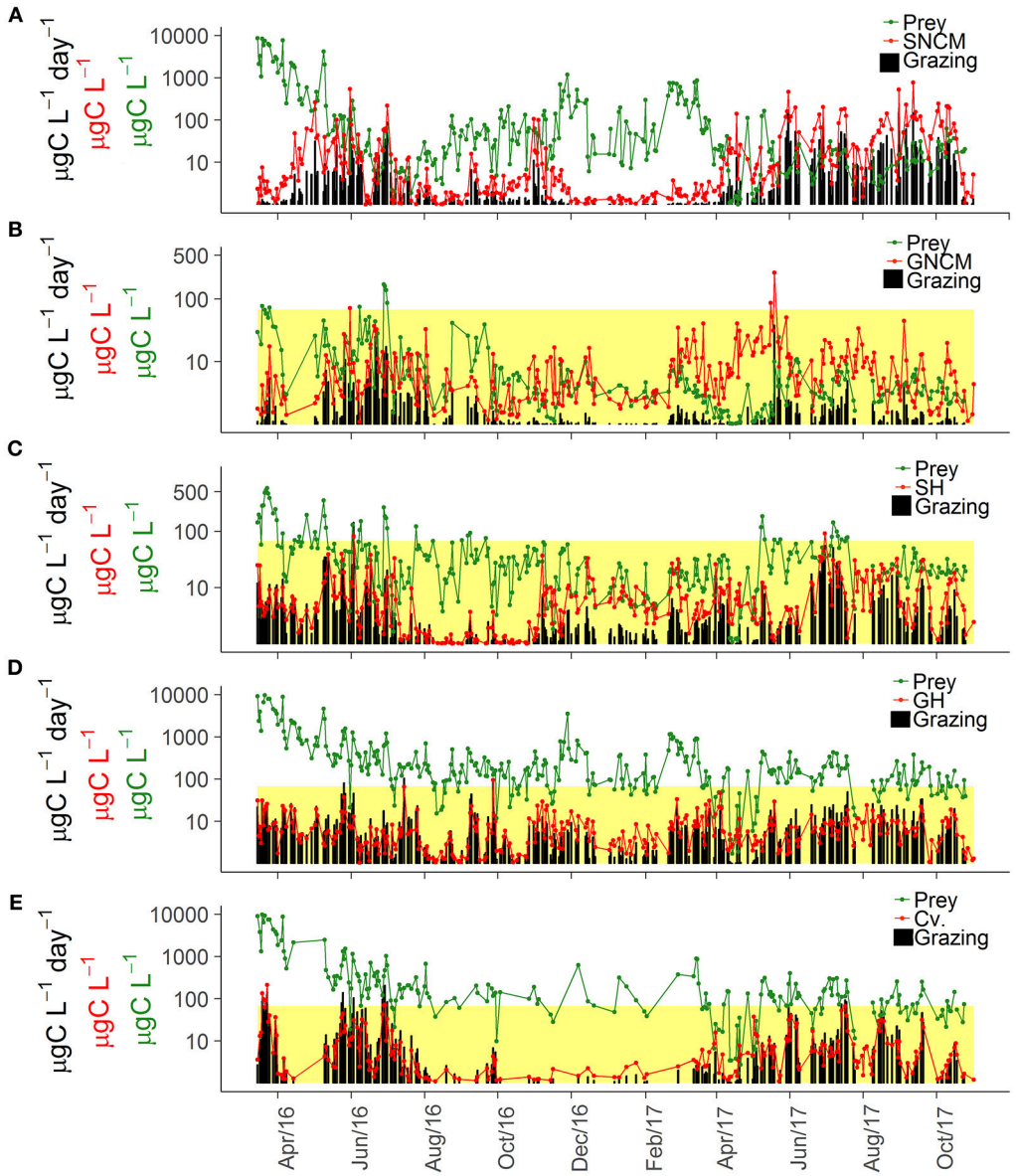

FIGURE 5 | Temporal dynamics of assigned phytoplankton prey, ciliate biomass, and potential grazing rates for the different trophic strategies: SNCM, Specialist Non Constitutive Mixotroph **(A)**, GNCM, Generalist Non Constitutive Mixotroph **(B)**, SH, Selective Herbivore **(C)**, GH, Generic Herbivore **(D)**, and Cv, Carnivore **(E)**. The upper limits of the yellow colored area indicate the half-saturation constant for food density (Km), thus when prey concentrations are smaller than Km (within the yellow area) it indicates potential food limitation. As SNCM potential grazing **(A)** was estimated in a distinct way, the Km criteria was not used for this trophic strategy. For further details on Km definition and calculation, see "Potential Grazing" in the section Materials and Methods.

grazing in RF was only calculated for larger protozooplankton (ciliates and heterotrophic dinoflagellates). Other organisms, such heterotrophic nano-flagellates and small heterotrophic dinoflagellates ($<15\,\mu m$), were not properly recorded by any of the methods used in this study, and likely increase the real contribution of protozooplankton grazing.

Heterotrophic dinoflagellates can be an important component of microzooplankton and microbial food webs (Sherr and Sherr, 2007), but their importance in RF seems low compared to ciliates. Heterotrophic dinoflagellates biomass was less than 10% of ciliate biomass in most samples, even though it was higher in a few instances. On top of that, dinoflagellates have lower growth and grazing rates than ciliates (Hansen, 1992; Jakobsen and Hansen, 1997), which indicates a minor role of this group for carbon cycling in RF. Seasonality of heterotrophic dinoflagellates was marked by the increased occurrence of large sized cells during summer. The observed increase in size of heterotrophic dinoflagellates is in agreement with what has previously been described for other open areas, such as Kattegat and Kiel Bight (Smetacek, 1981; Hansen, 1991), and might reflect an adaptation in the dinoflagellate assembly to the larger prey items. However, summer is also characterized by higher biomass of ciliates, and

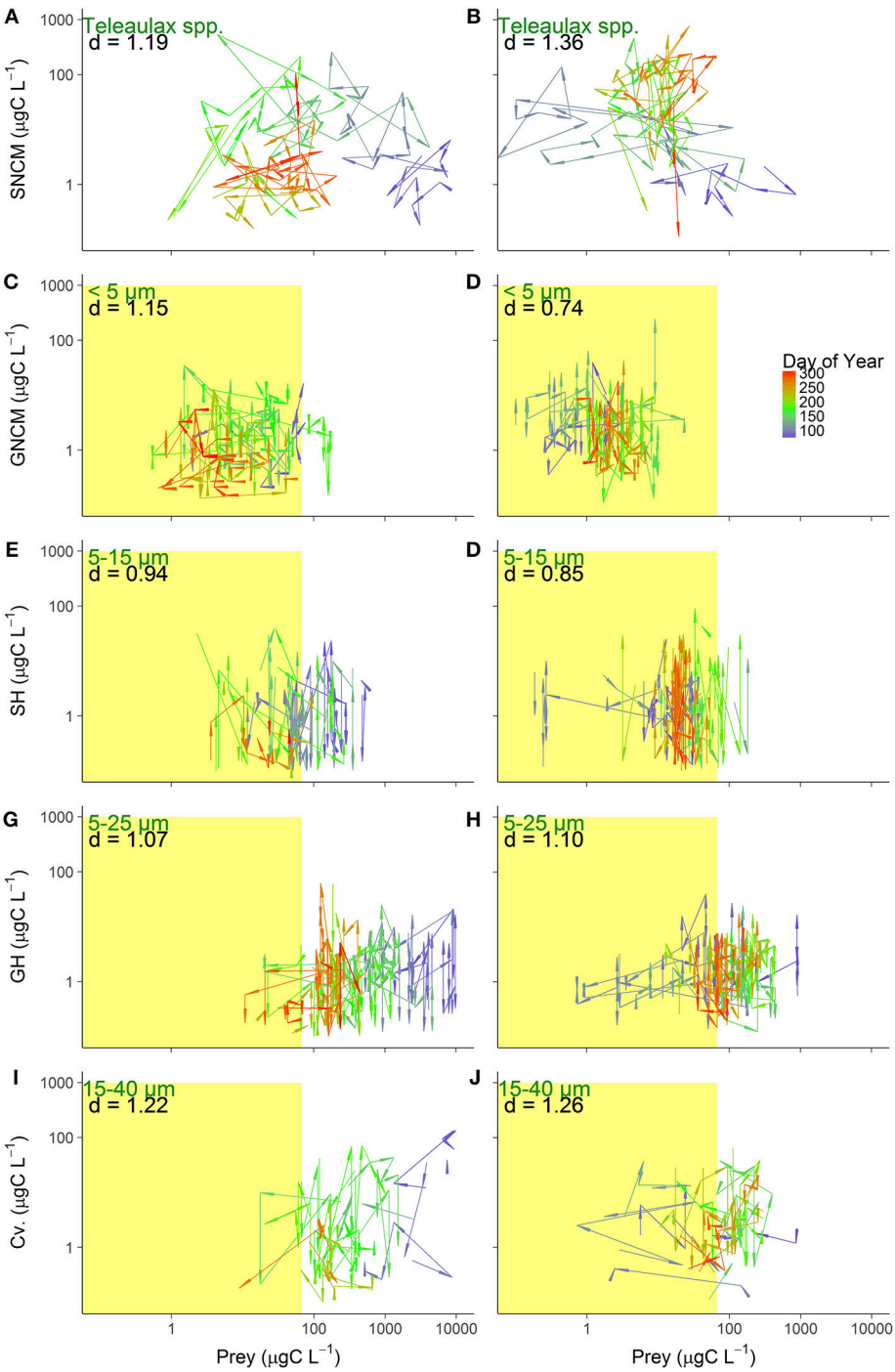

FIGURE 6 | Prey-predator biomass dynamics for the five trophic strategies in 2016 (left) and 2017 (right): SNCM, Specialist Non Constitutive Mixotroph **(A,B)**, GNCM, Generalist Non Constitutive Mixotroph **(C,D)**, SH, Selective Herbivore **(E,F)**, GH, Generic Herbivore **(G,H)**, and Cv, Carnivore **(I,J)**. Arrows represent the distance between observations (Euclidean distance) and color gradient indicate the day of year. Text depicts the phytoplankton prey assigned for each predator group (green), and the average Euclidean distance (d) between observation in the productive season of each year (black). Right limits of the yellow colored area indicate the half-saturation constant of food density (Km), and the observations to the left, within the colored area, indicate potential food limitation (except for SNCM, see explanation in **Figure 5**).

the increasing proportion of large heterotrophic dinoflagellates might indicate a change in ecological strategy which aims to avoid competition with ciliates that graze on smaller phytoplankton.

Salinity variations are mainly associated with freshwater discharges during winter, enhancing dissolved inorganic nitrogen (DIN) concentrations that are mainly consumed by

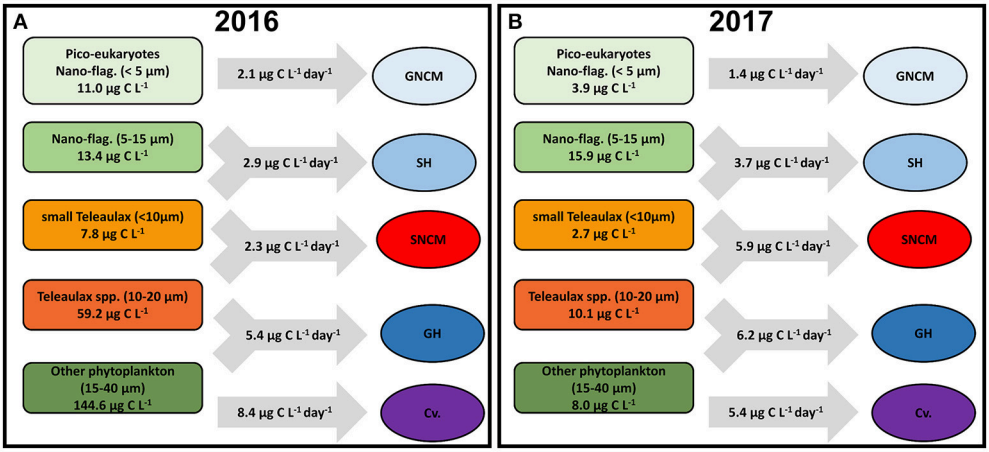

FIGURE 7 | Simplified scheme showing the daily average biomass of each phytoplankton prey group and the average grazing rates of each ciliate trophic strategy in 2016 **(A)** and 2017 **(B)**. Averages calculated only for the productive season (March to November).

phytoplankton during spring (Staehr et al., 2017). Although inter-annual differences in salinity were modest, DIN inputs were higher in 2016. This could explain the intense spring bloom observed in 2016 compared to the modest one in 2017, but it cannot explain entirely the consistently higher biomass of all ciliate types and heterotrophic dinoflagellates in 2017 compared to 2016. Differences in phytoplankton biomass could be due to the higher microzooplankton biomass in 2017 compared to 2016, indicating a more intense grazing in 2017. Thus, it is likely that phytoplankton is top-down controlled by microzooplankton in RF, and that due to fast turnover rates of both communities, primary production is higher despite relatively lower phytoplankton biomasses. Additionally, it is likely that the high DIN inputs in the winter of 2016 disrupted the coupling between phytoplankton and their ciliate predators that was better depicted in 2017. DIN concentrations were depleted to similar levels after the spring bloom in both years, indicating that higher concentrations in the winter of 2016 probably supported the larger bloom observed in this year. This large perturbation in the prey-predator coupling at the beginning of the productive season probably shaped also the rest of the year, causing interannual differences in prey-predator coupling, and reduced the number of observations with food-limitation in 2016. The prey-predator coupling varied among trophic strategies, resulting in the following contrasts between the studied years: (1) larger variation in the coupling in 2016 than in 2017 (for GNCM and SH); (2) differences in the timing when variations were observed during the productive season (SNCM and Cv.); and (3) changes in the dominance of the main morphotype (GH).

Previous studies have described various seasonal dynamics of ciliates in coastal and estuarine areas, and their importance in the trophic energy transfer. In Gulf of Maine, distinct ciliate assemblages were dominant at specific seasons, with larger ciliates found in spring, associated with larger preys, and smaller ciliates in other periods, when available prey were smaller (Montagnes et al., 1988). Conversely, ciliates in Coos Bay were reported to control small-sized phytoplankton throughout the year (Cowlishaw, 2004). In our study, ciliate biomass and their estimated potential grazing rates were in the same range as biomass of phytoplankton prey, especially for sizes $<15\,\mu m$ and cryptophytes, indicating selective pressure by ciliates grazing on small phytoplankton cells. The phytoplankton groups with lower standing biomass in 2017 compared to 2016 (cryptophytes, pico-eukaryotes, and small nano-flagellates) were subject to intense grazing pressure by different ciliate morphotypes, which probably substituted each other over the year in succession. These ciliate morphotypes also tended to be more food limited (GNCM and SH). Furthermore, as potential ingestion rates were modeled from standing biomass and not directly measured, it is likely that our grazing rates, especially for 2017, are underestimated due to intense grazing that resulted in low standing biomass of some phytoplankton groups. Yet, they provide valuable information on potential impact of ciliates, suggesting that ciliate grazing is an important driver for the phytoplankton succession, and that the microbial loop is a key pathway in the RF food web, despite of the high new nutrient input from land, which was assumed to promote the short-chain food web (Azam et al., 1983). Thus, ciliates might be a key player in the overall trophic transfer in RF, as an intermediate step between small-sized phytoplankton and mesozooplankton (Calbet and Saiz, 2005) and benthic filter feeders (Zeldis et al., 2004).

Organism with acquired phototrophy, including ciliates, are considered to have an increased gross growth efficiency, and therefore enhancing carbon export and nutrient cycling (Stoecker et al., 2009, 2017; Mitra et al., 2016). Experimental studies have shown that among non-constitutive mixotrophs, the acquired capability of photosynthesis can increase the specific growth rates. However, this should not be generalized, as specific growth rate varies among species, and for some mixotrophs, it can still be low compared to autotrophs or heterotrophs

(Jakobsen et al., 2000; Jakobsen and Strom, 2004; Schoener and McManus, 2012). Despite the fact that these organisms can often dominate microzooplankton communities and be responsible for a considerable proportion of primary production and/or grazing, *in situ* ecological data describing processes and importance of those organisms are still sparse (Stoecker et al., 2017). It is hypothesized that autotrophic and heterotrophic organisms dominate during the developmental phase of the ecosystems, while mixotrophs dominate in mature systems, benefiting from a flexible nutrition (Mitra et al., 2014). Our study shows that mixotrophic nutrition is increasingly important at the decline of spring bloom and during summer, when the system shifts from net autotrophy to net heterotrophy (Staehr et al., 2017). Additionally, our results demonstrated that mixotrophs (SNCM and GNCM, and even morphotypes among GNCM) have distinct temporal dynamics, reflecting different ecological strategies.

Mesodinium rubrum acquires its chloroplasts from specific prey (*Teleaulax* spp.), taking strong control over the photosynthetic apparatus of its prey, and being able to survive at low prey concentrations (Smith and Hansen, 2007; Peltomaa and Johnson, 2017). These organisms have been the focus of many ecophysiological studies. Blooms of *M. rubrum* are common in coastal areas and have been associated with occurrence of cryptophytes (Johnson et al., 2013; Hamilton et al., 2017; Lips and Lips, 2017). Our data shows that periods with high *M. rubrum* biomass are associated with low cryptophyte biomass, except for the spring bloom (March–April). Even though high biomass of *M. rubrum* occur around summer, *M. rubrum* was present in most (>95%) of samples during all seasons. Using the higher magnification of FlowCAM in 2017 allowed us to observe cell discolouration and size reduction of *M. rubrum* individuals during late summer/autumn, coinciding with the period of higher temperatures and low DIN in RF. At the same time, cells of *M. rubrum* were observed capturing particles other than cryptophytes with their oral tentacles (see **Figures 1,1a**-lower row). This emphasizes that the ecological flexibility of *M. rubrum* remains poorly understood, but that the flexibility could also explain the apparent success of *M. rubrum* in many environments and, in the case of RF, over the entire year.

In contrast to *M. rubrum*, oligotrichids that retain chloroplasts (GNCM), do not seem to be able to maintain them and need to feed at higher rates than *M. rubrum,* to replace aging plastids at higher rate (Jakobsen and Strom, 2004; Schoener and McManus, 2012). The plastid turnover rate depends on the availability of the plastid source, and GNCM usually use plastids of different origin, although they have a preferred type, depending on the species (Stoecker et al., 1988; Stoecker and Silver, 1990; Schoener and McManus, 2012). Under controlled conditions, *Strombidium rassoulzadegani* had newly acquired plastids positioned at the cell periphery within 30 min after being offered new prey, and it replaced all plastids after 2–3 days, yielding a plastid turnover rate slower than other *Strombidium* species (Stoecker and Silver, 1990; Schoener and McManus, 2012). Thus, GNCM can ingest phytoplankton prey at similar rates as heterotrophic ciliates (Jakobsen and Strom, 2004; Schoener and McManus, 2012), having a potential impact on carbon cycling, especially when larger species are present. GNCM in our study were composed of different species, with higher biomasses being associated with the proliferation of large morphotypes (*Strombidium* cf. *conicum* and *S.* cf. *capitatum*). These morphotypes were usually found during spring and summer, but higher biomasses were observed mainly in late spring. As those ciliates were food limited in most occasions (<95% of observations), their estimated grazing rates were around 10 times smaller than their potential ingestion based on cell volume. This indicates that despite of having a strong presence in RF, grazing imposed by mixotrophs is lower than by heterotrophic ciliates. On the other hand, mixotrophic nutrition supports their survival until suitable prey is encountered.

High volatility in the dominance of different types of ciliates was observed in this study. The temporal dynamics of the different trophic strategies demonstrated that mixotrophs (SNCM and GNCM) and carnivores exhibited strong seasonality in their occurrence and potential impact, predominating during summer. Conversely, herbivores (SH and GH) appeared to be widely distributed throughout the year, but apparently with different ecological strategies. GH types are present in low concentrations in most of the samples; whereas SH types occur with variable importance over the annual cycle (cf. *Pelagostrobilidium* in winter and tintinnids in summer), but together covering different seasons. This illustrates how complex and flexible ciliate communities can be, showing a great potential to control and drive changes of phytoplankton. We also observed a gradient in the prey-predator coupling among trophic strategies of ciliates, in which the more selective ciliates tend to be more efficient in removing their prey and are more often food limited, while the opposite is observed for ciliates that have a wider prey range, with exception of SNCM. However, those patterns are subjected to variability introduced by exogenous forcing (i.e., nutrient loads).

CONCLUSION

The use of in-flow techniques supports the analysis of phytoplankton and their microzooplankton grazers with high frequency. Additionally, the use of live samples further allows exploring trophic characteristics of ciliates, providing insights to the trophic strategies and specific prey classification. Ciliates are likely the main pelagic grazers in RF and probably play an essential role in the food web, linking primary production of small-celled organisms to higher trophic levels. Although ciliates are most abundant during summer, they are still important in other seasons. This is due to the range of different ecological strategies within the diverse ciliate community, combining different trophic strategies with different physiological adaptations. Thus, the ciliate community structure is highly complex and most likely an important driver for structuring the phytoplankton community.

AUTHOR CONTRIBUTIONS

LH, HJ, JC, and NL contributed conception and design of the study; LH and HJ collected the data and organized the database; LH, HJ, and JC performed the data analysis; LH wrote the first draft of the manuscript. All authors contributed to manuscript writing, revision, read and approved the submitted version.

FUNDING

LH was supported by a grant from the Brazilian program Science without Borders/CAPES (Grant No. 13581-13-9). This study is a contribution from the BONUS COCOA project (grant agreement 2112932-1) supported by Innovation Fund Denmark and the European Union.

SUPPLEMENTARY MATERIAL

The Supplementary Material for this article can be found online at: https://www.frontiersin.org/articles/10.3389/fmars.2018.00272/full#supplementary-material

Figure S1 | Map showing the sampled station location (red star) at Roskilde Fjord (Denmark).

REFERENCES

Azam, F., Fenchel, T., Field, J., Gray, J., Meyer-Reil, L., and Thingstad, F. (1983). The ecological role of water-column microbes in the sea. *Mar. Ecol. Prog. Ser.* 10, 257–263. doi: 10.3354/meps010257

Behrenfeld, M. J., and Falkowski, P. G. (1997). Photosynthetic rates derived from satellite-based chlorophyll concentration. *Limnol. Oceanogr.* 42, 1–20. doi: 10.4319/lo.1997.42.1.0001

Buitenhuis, E., Le Quéré, C., Aumont, O., Beaugrand, G., Bunker, A., Hirst, A., et al. (2006). Biogeochemical fluxes through mesozooplankton. *Global Biogeochem. Cycles* 20:GB2003. doi: 10.1029/2005GB002511

Buitenhuis, E. T., Rivkin, R. B., Séailley, S., and Le Quéré, C. (2010). Biogeochemical fluxes through microzooplankton. *Global Biogeochem. Cycles* 24:GB4015. doi: 10.1029/2009GB003601

Calbet, A. (2001). Mesozooplankton grazing effect on primary production: a global comparative analysis in marine ecosystems. *Limnol. Oceanogr.* 46, 1824–1830. doi: 10.4319/lo.2001.46.7.1824

Calbet, A., and Landry, M. R. (2004). Phytoplankton growth, microzooplankton grazing, and carbon cycling in marine systems. *Limnol. Oceanogr.* 49, 51–57. doi: 10.4319/lo.2004.49.1.0051

Calbet, A., and Saiz, E. (2005). The ciliate-copepod link in marine ecosystems. *Aquat. Microb. Ecol.* 38, 157–167. doi: 10.3354/ame038157

Calbet, A., Sazhin, A. F., Nejstgaard, J. C., Berger, S. A., Tait, Z. S., Olmos, L., et al. (2014). Future climate scenarios for a coastal productive planktonic food web resulting in microplankton phenology changes and decreased trophic transfer efficiency. *PLoS ONE* 9:e94388. doi: 10.1371/journal.pone.0094388

Campbell, L., Henrichs, D. W., Olson, R. J., and Sosik, H. M. (2013). Continuous automated imaging-in-flow cytometry for detection and early warning of *Karenia brevis* blooms in the Gulf of Mexico. *Environ. Sci. Pollut. Res.* 20, 6896–6902. doi: 10.1007/s11356-012-1437-4

Choi, J. W., and Stoecker, D. K. (1989). Effects of fixation on cell volume of marine planktonic protozoa. *Appl. Environ. Microbiol.* 55, 1761–1765.

Cowlishaw, R. J. (2004). Seasonal coupling between ciliate and phytoplankton standing stocks in the South Slough of Coos Bay, Oregon. *Estuaries* 27, 539–550. doi: 10.1007/BF02803545

Dashkova, V., Malashenkov, D., Poulton, N., Vorobjev, I., and Barteneva, N. S. (2017). Imaging flow cytometry for phytoplankton analysis. *Methods* 112, 188–200. doi: 10.1016/j.ymeth.2016.05.007

Dugenne, M., Thyssen, M., Nerini, D., Mante, C., Poggiale, J.-C., Garcia, N., et al. (2014). Consequence of a sudden wind event on the dynamics of a coastal phytoplankton community: an insight into specific population growth rates using a single cell high frequency approach. *Front. Microbiol.* 5:485. doi: 10.3389/fmicb.2014.00485

Earland, K. A., and Montagnes, D. J. S. (2002). Description of a new marine species of askenasia blochmann, 1895 (ciliophora, haptoria), with notes on its ecology. *J. Eukaryot. Microbiol.* 49, 423–427. doi: 10.1111/j.1550-7408.2002.tb00222.x

Edwards, K. F., Thomas, M. K., Klausmeier, C. A., and Litchman, E. (2012). Allometric scaling and taxonomic variation in nutrient utilization traits and maximum growth rate of phytoplankton. *Limnol. Oceanogr.* 57, 554–566. doi: 10.4319/lo.2012.57.2.0554

Fenchel, T. (1988). Marine plankton food chains. *Annu. Rev. Ecol. Syst.* 19, 19–38. doi: 10.1146/annurev.es.19.110188.000315

Flynn, K. J., Stoecker, D. K., Mitra, A., Raven, J. A., Glibert, P. M., Hansen, P. J., et al. (2013). Misuse of the phytoplankton–zooplankton dichotomy: the need to assign organisms as mixotrophs within plankton functional types. *J. Plankton Res.* 35, 3–11. doi: 10.1093/plankt/fbs062

Gifford, D. J. (1991). The protozoan-metazoan trophic link in pelagic ecosystems. *J. Protozool.* 38, 81–86. doi: 10.1111/j.1550-7408.1991.tb04806.x

Grasshof, K. (ed) (1976). *Methods of Seawater Analysis*. Weinheim: Verlag Chemie

Hamilton, M., Hennon, G. M. M., Morales, R., Needoba, J., Peterson, T. D., Schatz, M., et al. (2017). Dynamics of Teleaulax -like cryptophytes during the decline of a red water bloom in the Columbia river estuary. *J. Plankton Res.* 39, 589–599. doi: 10.1093/plankt/fbx029

Hansen, J. (1991). Quantitative importance and trophic role of heterotrophic dinoflagellates in a coastal pelagial food web. *Mar. Ecol. Prog. Ser.* 73, 253–261.

Hansen, J., Bjornsen, P. K., and Hansen, B. W. (1997). Zooplankton grazing and growth: scaling within the 2-2,000-mm body size range. *Limnol. Oceanogr.* 42, 687–704.

Hansen, P. J. (1992). Prey size selection, feeding rates and growth dynamics of heterotrophic dinoflagellates with special emphasis on Gyrodinium spirale. *Mar. Biol.* 114, 327–334. doi: 10.1007/BF00349535

Haraguchi, L., Jakobsen, H., Lundholm, N., and Carstensen, J. (2017). Monitoring natural phytoplankton communities: a comparison between traditional methods and pulse-shape recording flow cytometry. *Aquat. Microb. Ecol.* 80, 77–92. doi: 10.3354/ame01842

Hewett, S. W. (1988). Predation by *Didinium Nasutum*: effects of predator and prey size. *Ecology* 69, 135–145.

Jakobsen, H. H., and Carstensen, J. (2011). FlowCAM: sizing cells and understanding the impact of size distributions on biovolume of -planktonic community structure. *Aquat. Microb. Ecol.* 65, 75–87. doi: 10.3354/ame01539

Jakobsen, H. H., and Hansen, J. (1997). Prey size selection, grazing and growth response of the small heterotrophic dinoflagellate *Gymnodinium* sp. and the ciliate Balanion comatum-a comparative study. 158, 75–86.

Jakobsen, H. H., Hansen, P. J., and Larsen, J. (2000). Growth and grazing responses of two chloroplast-retaining dinoflagellates: effect of irradiance and prey species. *Mar. Ecol. Prog. Ser.* 201, 121–128. doi: 10.3354/meps201121

Jakobsen, H. H., and Montagnes, D. J. S. (1999). A redescription of balanion comatum wulff, 1919 (prorodontida, ciliophora), with notes on its cultivation and behaviour. *J. Eukaryot. Microbiol.* 46, 198–205. doi: 10.1111/j.1550-7408.1999.tb04604.x

Jakobsen, H. H., and Strom, S. L. (2004). Circadian cycles in growth and feeding rates of heterotrophic protist plankton. *Limnol. Oceanogr.* 49, 1915–1922. doi: 10.4319/lo.2004.49.6.1915

Johnson, M. D. (2011). Acquired phototrophy in ciliates: a review of cellular interactions and structural adaptations1. *J. Eukaryot. Microbiol.* 58, 185–195. doi: 10.1111/j.1550-7408.2011.00545.x

Johnson, M. D., Stoecker, D. K., and Marshall, H. G. (2013). Seasonal dynamics of *Mesodinium rubrum* in chesapeake Bay. *J. Plankton Res.* 35, 877–893. doi: 10.1093/plankt/fbt028

Kaas, H., and Markager, S. (1998). *Technical Guidelines for Marine Monitoring*. Available online at: http://bios.au.dk/raadgivning/fagdatacentre/fdcmarintny/tekniske-anvisninger-nova-1998/

Kamp-Nielsen, L. (1992). "Benthic-pelagic coupling of nutrient metabolism along an estuarine eutrophication gradient," in *Sediment/Water Interactions*, eds B. T. Hart and P. G. Sly (Dordrecht: Springer), 457–470.

Landry, M. R., and Calbet, A. (2004). Microzooplankton production in the oceans. *ICES J. Mar. Sci.* 61, 501–507. doi: 10.1016/j.icesjms.2004.03.011

Leles, S. G., Mitra, A., Flynn, K. J., Stoecker, D. K., Hansen, P. J., Calbet, A., et al. (2017). Oceanic protists with different forms of acquired phototrophy display contrasting biogeographies and abundance. *Proc. Biol. Sci.* 284:20170664. doi: 10.1098/rspb.2017.0664

Lips, I., and Lips, U. (2017). The importance of mesodinium rubrum at post-spring bloom nutrient and phytoplankton dynamics in the vertically stratified baltic sea. *Front. Mar. Sci.* 4:407. doi: 10.3389/fmars.2017.00407

Menden-Deuer, S., and Lessard, E. J. (2000). Carbon to volume relationships for dinoflagellates, diatoms, and other protist plankton. *Limnol. Oceanogr.* 45, 569–579. doi: 10.4319/lo.2000.45.3.0569

Mitra, A., Flynn, K. J., Burkholder, J. M., Berge, T., Calbet, A., Raven, J. A., et al. (2014). The role of mixotrophic protists in the biological carbon pump. *Biogeosciences* 11, 995–1005. doi: 10.5194/bg-11-995-2014

Mitra, A., Flynn, K. J., Tillmann, U., Raven, J. A., Caron, D., Stoecker, D. K., et al. (2016). Defining planktonic protist functional groups on mechanisms for energy and nutrient acquisition: incorporation of diverse mixotrophic strategies. *Protist* 167, 106–120. doi: 10.1016/j.protis.2016.01.003

Montagnes, D. J. S. (2012). "Ecophysiology and Behavior of Tintinnids," in *The Biology and Ecology of Tintinnid Ciliates*, eds J. R. Dolan, D. J. S. Montagnes, S. Agatha, D. W. Coats, and D. K. Stoecker (Chichester: John Wiley and Sons, Ltd), 85–121.

Montagnes, D. J. S., Lynn, D. H., Roff, J. C., and Taylor, W. D. (1988). The annual cycle of heterotrophic planktonic ciliates in the waters surrounding the Isles of Shoals, Gulf of Maine: an assessment of their trophic role. *Mar. Biol.* 99, 21–30. doi: 10.1007/BF00644973

Nielsen, T. G., and Kiørboe, T. (1994). Regulation of zooplankton biomass and production in a temperate, coastal ecosystem. 2. Ciliates. *Limnol. Oceanogr.* 39, 508–519. doi: 10.4319/lo.1994.39.3.0508

Peltomaa, E., and Johnson, M. (2017). *Mesodinium rubrum* exhibits genus-level but not species-level cryptophyte prey selection. *Aquat. Microb. Ecol.* 78, 147–159. doi: 10.3354/ame01809

Pinheiro, J., Bates, D., DebRoy, S., and Sarkar, D. (2017). *nlme: Linear and Nonlinear Mixed Effects Models*. Available online at: https://cran.r-project.org/package=nlme

R Core Team (2017). *R: A Language and Environment for Statistical Computing*. Available online at: http://www.r-project.org/

Schoener, D., and McManus, G. (2012). Plastid retention, use, and replacement in a kleptoplastidic ciliate. *Aquat. Microb. Ecol.* 67, 177–187. doi: 10.3354/ame01601

Sherr, E. B., and Sherr, B. F. (2007). Heterotrophic dinoflagellates: a significant component of microzooplankton biomass and major grazers of diatoms in the sea. *Mar. Ecol. Prog. Ser.* 352, 187–197. doi: 10.3354/meps07161

Sherr, E., and Sherr, B. (1988). Role of microbes in pelagic food webs: a revised concept. *Limnol. Oceanogr.* 33, 1225–1227. doi: 10.4319/lo.1988.33.5.1225

Smetacek, V. (1981). The annual cycle of protozooplankton in the Kiel Bight. *Mar. Biol.* 63, 1–11. doi: 10.1007/BF00394657

Smith, M., and Hansen, P. (2007). Interaction between *Mesodinium rubrum* and its prey: importance of prey concentration, irradiance and pH. *Mar. Ecol. Prog. Ser.* 338, 61–70. doi: 10.3354/meps338061

Staehr, P. A., Testa, J., and Carstensen, J. (2017). Decadal changes in water quality and net productivity of a shallow danish estuary following significant nutrient reductions. *Estuaries Coasts* 40, 63–79. doi: 10.1007/s12237-016-0117-x

Stoecker, D., Johnson, M., deVargas, C., and Not, F. (2009). Acquired phototrophy in aquatic protists. *Aquat. Microb. Ecol.* 57, 279–310. doi: 10.3354/ame01340

Stoecker, D. K. (1998). Conceptual models of mixotrophy in planktonic protists and some ecological and evolutionary implications. *Eur. J. Protistol.* 34, 281–290. doi: 10.1016/S0932-4739(98)80055-2

Stoecker, D. K., and Capuzzo, J. M. (1990). Predation on protozoa: its importance to zooplankton. *J. Plankton Res.* 12, 891–908. doi: 10.1093/plankt/12.5.891

Stoecker, D. K., Gifford, D. J., and Putt, M. (1994). Preservation of marine planktonic ciliates: losses and cell shrinkage during fixation. *Mar. Ecol. Prog. Ser.* 110, 293–299. doi: 10.3354/meps110293

Stoecker, D. K., Hansen, P. J., Caron, D. A., and Mitra, A. (2017). Mixotrophy in the marine plankton. *Ann. Rev. Mar. Sci.* 9, 311–335. doi: 10.1146/annurev-marine-010816-060617

Stoecker, D. K., and Silver, M. W. (1990). Replacement and aging of chloroplasts in *Strombidium capitatum* (Ciliophora: Oligotrichida). *Mar. Biol.* 107, 491–502. doi: 10.1007/BF01313434

Stoecker, D. K., Silver, M. W., Michaels, A. E., and Davis, L. H. (1988). Obligate mixotrophy in *Laboea strobila*, a ciliate which retains chloroplasts. *Mar. Biol.* 99, 415–423. doi: 10.1007/BF02112135

Tamar, H. (1986). Four marine species of Mesodinium (Ciliophora: Didiniidae). I. Mesodinium velox n. sp. *Trans. Am. Microsc. Soc.* 105, 130–140. doi: 10.2307/3226385

Thyssen, M., Mathieu, D., Garcia, N., and Denis, M. (2008). Short-term variation of phytoplankton assemblages in Mediterranean coastal waters recorded with an automated submerged flow cytometer. *J. Plankton Res.* 30, 1027–1040. doi: 10.1093/plankt/fbn054

Ward, B. A., and Follows, M. J. (2016). Marine mixotrophy increases trophic transfer efficiency, mean organism size, and vertical carbon flux. *Proc. Natl. Acad. Sci. U.S.A.* 113, 2958–2963. doi: 10.1073/pnas.1517118113

Zeldis, J., Robinson, K., Ross, A., and Hayden, B. (2004). First observations of predation by New Zealand Greenshell mussels (*Perna canaliculus*) on zooplankton. *J. Exp. Mar. Bio. Ecol.* 311, 287–299. doi: 10.1016/j.jembe.2004.05.019

Zervoudaki, S., Nielsen, T. G., and Carstensen, J. (2009). Seasonal succession and composition of the zooplankton community along an eutrophication and salinity gradient exemplified by Danish waters. *J. Plankton Res.* 31, 1475–1492. doi: 10.1093/plankt/fbp084

Conflict of Interest Statement: The authors declare that the research was conducted in the absence of any commercial or financial relationships that could be construed as a potential conflict of interest.

frontiers in Marine Science

ORIGINAL RESEARCH
published: 12 December 2017
doi: 10.3389/fmars.2017.00407

The Importance of *Mesodinium rubrum* at Post-Spring Bloom Nutrient and Phytoplankton Dynamics in the Vertically Stratified Baltic Sea

Inga Lips and Urmas Lips*

Department of Marine Systems, Tallinn University of Technology, Tallinn, Estonia

The inter-annual dynamics of the photosynthetic ciliate *Mesodinium rubrum* in the central Gulf of Finland in spring-summer continuum during 5 years were followed. The analysis was mainly based on high-resolution measurements and sampling in the surface layer along the ferry route Tallinn-Helsinki. The main purpose was to analyze the dynamics of *M. rubrum* biomass, its contribution to the photosynthetic plankton biomass, and the influence of water temperature and variations of inorganic nutrients in the surface and sub-surface layer on its dynamics. The analysis revealed that the outcome of the *M. rubrum* bloom in spring was largely related to the surface layer water temperature—in the years of earlier warming, the higher biomass of this species was formed. The photosynthetic ciliate was an important primary producer in all studied years during the late phase or post-spring bloom period in the Gulf of Finland. The maximum proportion of *M. rubrum* in the photosynthetic plankton community was estimated up to 88% in May and up to 91% in June. We relate the observed post-spring bloom decrease of phosphate concentrations in the surface layer to the dominance and growth of *M. rubrum*. We suggest that this link can be explained by the vertical migration behavior of *M. rubrum* and phosphate utilization in the surface layer coupled with inorganic nitrogen assimilation in the sub-surface layer. Thus, the dynamics of *M. rubrum* could strongly influence the amount of post-spring bloom excess PO_4^{3-} in the euphotic layer and the depth of nitracline in the Gulf of Finland.

Keywords: *Mesodinium rubrum*, spring bloom, nutrients, stratification, Baltic Sea

OPEN ACCESS

Edited by:
Riina Klais,
University of Tartu, Estonia

Reviewed by:
Matthew D. Johnson,
Woods Hole Oceanographic Institution, United States
Harri Kuosa,
Finnish Environment Institute, Finland

****Correspondence:***
Inga Lips
inga.lips@ttu.ee

Specialty section:
This article was submitted to Marine Ecosystem Ecology, a section of the journal Frontiers in Marine Science

Received: *21 September 2017*
Accepted: *29 November 2017*
Published: *12 December 2017*

Citation:
Lips I and Lips U (2017) The Importance of Mesodinium rubrum at Post-Spring Bloom Nutrient and Phytoplankton Dynamics in the Vertically Stratified Baltic Sea. Front. Mar. Sci. 4:407. doi: 10.3389/fmars.2017.00407

INTRODUCTION

Phytoplankton production, together with the terrestrial organic carbon load, is the largest primary source of organic carbon to the Baltic Sea (Kulinski and Pempkowiak, 2011). As total annual ecosystem respiration in temperate estuaries and estuarine type seas like Baltic Sea exceeds gross primary production, the temporary shift to autotrophy state only occurs during seasonal and episodic bloom events of photosynthetic plankton when photosynthesis exceeds total system respiration (Cloern et al., 2014). In the Baltic Sea, during the phytoplankton spring bloom, up to 60% of annual carbon fixation takes place, and 40–80% of this fixed carbon sinks out from the surface layer (Heiskanen, 1998; Tamelander and Heiskanen, 2004). The spring bloom

leads to depletion of inorganic nutrients in the euphotic layer and through the sedimentation of phytoplankton-derived organic carbon to the acceleration of benthic respiration and nutrient regeneration rates (Conley and Johnstone, 1995).

Spring bloom in the Baltic Sea is co-dominated by diatoms and dinoflagellates (e.g., Kononen and Niemi, 1984; Wasmund and Uhlig, 2003). The late phase of the spring bloom (in May) in the Gulf of Finland is dominated by vertically migrating dinoflagellates together with ciliates (Heiskanen, 1995; Höglander et al., 2004; Lips et al., 2014). Ciliates are an important trophic link between primary producers and metazoa consuming a significant fraction of small-sized phytoplankton and bacterioplankton production and are important in remineralization of macronutrients (Rivkin et al., 1999; Calbet and Landry, 2004). Besides this, ciliates can also be significant contributors to primary production through mixotrophy which is the occurrence of phagotrophy and phototrophy in the same organism. Mixotrophic oligotrichs have been reported both in freshwater and in seawater ecosystems (Esteban et al., 2010).

Mass occurrences of photosynthetic ciliate *Mesodinium rubrum* Lohmann 1908 (*Myrionecta rubra* Jankowski 1976) are reported around the world (e.g., Mackenzie and Gillespie, 1986; Crawford, 1989; Wilkerson and Grunseich, 1990; Cloern et al., 1994; Johnson et al., 2013; Kang et al., 2013). In the Baltic Sea, the highest abundances/biomasses and largest size distribution of *M. rubrum* are observed after the diatom-dinoflagellate dominated spring bloom, usually in May–June (Lindholm, 1985; Passow, 1991; Rychert, 2004; Thamm et al., 2004). The peak of *M. rubrum* biomass mostly coincides with the period when nitrates are exhausted from the upper mixed layer and the increase of photosynthetic biomass is mostly regarded to be based on regenerated nutrients (according to Dugdale and Goering, 1967).

M. rubrum is extremely mobile, known to be fastest autotroph in the sea with a swimming velocity that is reported to reach 8.5 mm s^{-1} (30 m h^{-1}; Smayda, 2010) and showing marked phototaxis and vertical migrations (Lindholm, 1985). Some studies already a long time ago demonstrated the very high rate of primary production of this species (e.g., Mackenzie and Gillespie, 1986; Crawford, 1989; Stoecker et al., 1991; review by Johnson, 2011). Increased temperature and water column stability, decreased salinity and depletion of dissolved inorganic nitrogen from the surface layer are known to have positive influence to the occurrence and abundance of *M. rubrum* (Lindholm and Mörk, 1990; Cloern et al., 1994; Montagnes et al., 2008; Johnson et al., 2013) in different locations worldwide. In several studies, the ability of directly utilize nitrate, ammonium, dissolved organic nitrogen (Lindholm and Mörk, 1990; Wilkerson and Grunseich, 1990; Tong et al., 2015) and phosphates (review by Lindholm, 1985; Tong et al., 2015) have been reported. *M. rubrum* mass occurrences tend to develop in a chemical environment where competing photosynthetic species are a resource (nutrient) limited or are not able to migrate vertically to exploit the pools of dissolved inorganic nutrients below the euphotic layer. Ability to migrate vertically complemented with efficient nutrient uptake has been considered to enable *M. rubrum* to compete with phytoplankters (Stoecker et al., 1991).

The main aim of this paper is to present the interannual dynamics of photosynthetic ciliate *M. rubrum* in the central Gulf of Finland in spring-summer continuum and to analyze how the increase in mixotrophic ciliate biomass affects the spatial distribution (both horizontal and vertical) and temporal variation of nutrients in the stratified water column. We hypothesize that the magnitude and intensity of *M. rubrum* bloom has a significant impact on the inorganic nutrient concentrations after the spring bloom and hence may influence the outcome of summer phytoplankton blooms. The analysis is based on high-resolution measurements and sampling in the surface layer along the ferry route Tallinn-Helsinki complemented with vertical profiling and sampling through the water column at one station close to the ferry line. We recognize that *M. rubrum* belongs to a species complex (Johnson et al., 2016) and that our data may include *M. major* and/or multiple variants of *M. rubrum*. However, since we did not measure the diversity of genetic variants, we will refer to all observed *Mesodinium* ciliates as *M. rubrum*.

MATERIALS AND METHODS

Study Region

The dataset analyzed was collected during 5 years (2009–2012, 2014) in the central part of the Gulf of Finland, the easternmost basin of the Baltic Sea (**Figure 1**). The Gulf of Finland is a stratified elongated estuarine basin where the general water movement in the surface layer is anticlockwise (Alenius et al., 1998) but the dynamics of water masses are very much meteorologically driven at the mesoscale. The surface layer salinity in the area is typically between 4 and 6 g kg^{-1}, decreasing from west to east due to the major river discharge at the eastern end of the Gulf and slightly from south to north due to the anti-clockwise general circulation. A seasonal variation of inorganic nutrient concentrations is observed in the Gulf of Finland upper layer—minimum values in summer and maximum in winter. Nitrogen is considered the limiting nutrient in the Baltic Sea, and after the development of thermal stratification in spring the nitrogen-rich deeper layers are separated from the nitrogen-depleted surface layer causing the rapid decline in the phytoplankton biomass co-dominated by diatoms and dinoflagellates. At the same time there can be observed the residual amounts of phosphates and silicates in the surface layer after the spring bloom (e.g., Tamelander and Heiskanen, 2004). In summer, the strong stratification and nitrogen limitation give competitive advantages for cyanobacteria (Lips and Lips, 2008) able to fix molecular nitrogen and photosynthetic species able to migrate vertically in the water column (Lips et al., 2011).

Measurements and Sample Analysis

Measurements were conducted using autonomous ferrybox system (-4H- Jena Engineering GmbH) installed on board the passenger ferry "Baltic Princess" (AS Tallink Grupp) plying between Tallinn and Helsinki (**Figure 1**) in 2009–2012 and 2014. Seawater was pumped through the measuring system from ∼4

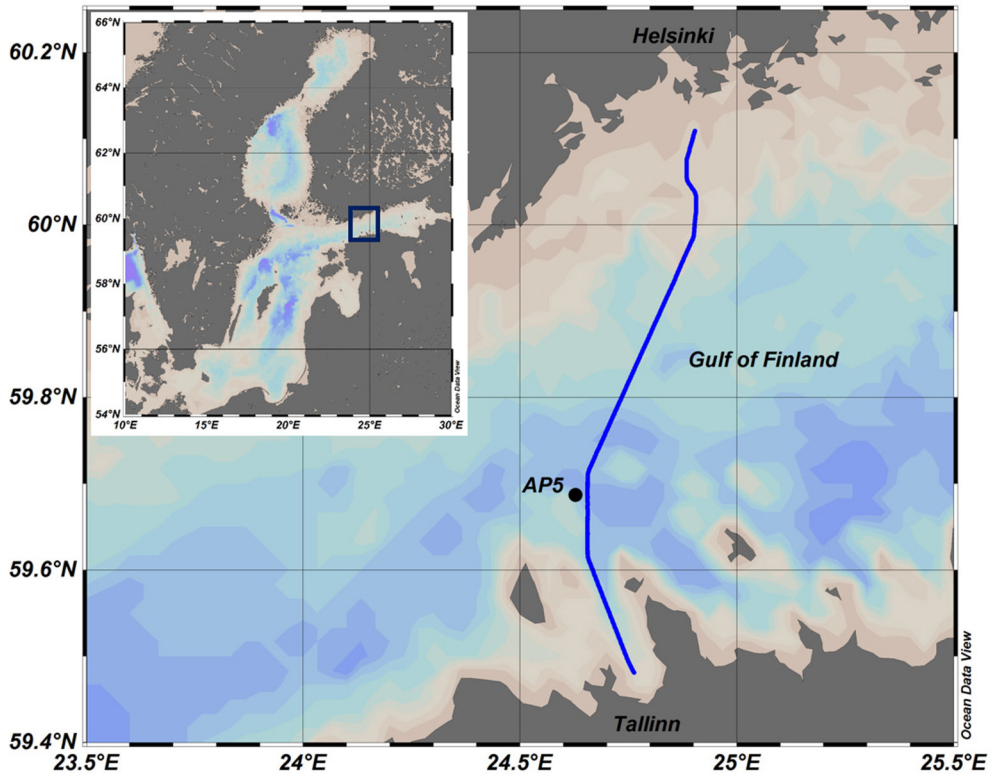

FIGURE 1 | Map of the Baltic Sea and the study area. Ferrybox route is shown as a solid line and Station AP5 as a black circle.

to 5 m depth while the ferry was moving at an average speed of 15–16 knots. The temperature, salinity, and chlorophyll *a* (Chl *a*) fluorescence were measured with the time resolution of 20 s corresponding approximately to a spatial resolution of 160 m.

Weekly-biweekly water sampling from up to 17 locations along the 75-km-long ferry route was conducted using an automatic refrigerating (4°C) sampler (Sigma 900 MAX), being part of the ferrybox system. Sampling dates and number of samples collected for nutrient and phytoplankton analyses on each date along the south-north transect are shown in **Table 1**. Altogether 753 samples were collected from the surface layer in five studied years and analyzed to determine the concentrations of PO_4^{3-}, $NO_2^- + NO_3^-$, Chl *a*, and phytoplankton species composition, wet weight, and carbon (C) biomass.

Sampling and measurements on board the research vessel SALME were performed at the station AP5 (**Figure 1**) in spring-summer 2010–2012 and 2014 (the sampling days and depths can be seen in **Figure 3**). CTD measurements using an Ocean Seven 320*plus* CTD probe (Idronaut S.r.l.) equipped with a Seapoint Chl *a* fluorometer were performed, and water samples with a vertical resolution from 5 to 10 m were collected. Collected water samples were analyzed to determine the same parameters as from ferrybox samples. On 20–21 May 2014, the 24 h campaign for measurements and sampling was performed. Vertical profiles of temperature, salinity, Chl *a* fluorescence and dissolved oxygen content were registered together with phytoplankton sampling with 2 h interval. Samples for nutrient analysis were collected with 6 h interval.

Inorganic nutrients were analyzed with the automatic nutrient analyzers μMac 1000 (Systea S.r.l.) and Lachat QuikChem 8500 Series 2 (Lachat Instruments, Hach Company). The nutrient analyses were performed according to the guidelines of the American Public Health Association (APHA, 1992; methods 4500-NO_3 and 4500-P for μMac 1000) and recommendations made by USEPA, ISO, and DIN standards (methods 31-107-04-1-D NO_3 (Egan, 2000) and 31-115-01-1-I PO_4 (Ammerman, 2001) for the Lachat instrument). The lower detection range for PO_4^{3-} and $NO_2^- + NO_3^-$ was 0.03 and 0.07 μM, respectively.

The Chl *a* concentration in the water samples was determined using Whatman GF/F glass fiber filters following extraction at room temperature in the dark with 96% ethanol for 24 h. The Chl *a* content from the extract was measured spectrophotometrically (Thermo Helios γ) in the laboratory (HELCOM, 1988). Chl *a* fluorescence measured on board the research vessel and by the ferrybox system was calibrated against Chl *a* measured in the water samples. For each device and season, a linear regression equation between fluorescence and Chl *a* was found and used to convert fluorescence values into Chl *a* content values.

Phytoplankton sub-samples (100 ml) were preserved and analyzed according to the HELCOM recommendations and EVS-EN 15972:2011 standard. The wet weight biomasses were calculated according to Olenina et al. (2006), and

TABLE 1 | Ferrybox sampling dates and number of samples (*n*) in different years.

2009	*n*	2010	*n*	2011	*n*	2012	*n*	2014	*n*
5.04.2009	17	4.04.2010	17			2.04.2012	12	06.04.2014	9
12.04.2009	17	12.04.2010	17	11.04.2011	16	9.04.2012	10	13.04.2014	9
19.04.2009	17	19.04.2010	17	17.04.2011	16	16.04.2012	12	22.04.2014	10
26.04.2009	17	27.04.2010	15	24.04.2011	17	23.04.2012	12	28.04.2014	10
3.05.2009	17	3.05.2010	17	2.05.2011	16	1.05.2012	12	04.05.2014	11
10.05.2009	17	10.05.2010	17	8.05.2011	17	7.05.2012	12	15.05.2014	11
17.05.2009	17	17.05.2010	17	15.05.2011	16	14.05.2012	12	20.05.2014	11
24.05.2009	17	24.05.2010	17	22.05.2011	17			25.05.2014	11
31.05.2009	17	31.05.2010	17	1.06.2011	9	28.05.2012	12	01.06.2014	11
		7.06.2010	16			7.06.2012	12		
14.06.2009	17	14.06.2010	17	12.06.2011	9			10.06.2014	11
21.06.2009	17	21.06.2010	17			17.06.2012	12		
28.06.2009	17	30.06.2010	16	26.06.2011	9	25.06.2012	12	25.06.2014	11

the phytoplankton carbon (C) content was calculated using C:biovolume factors according to Menden-Deuer and Lessard (2000). Carbon biomass of naked ciliates was calculated according to the method described by Putt and Stoecker (1989).

Calculations

For the years, when the autonomous profiler data were available, the stratification parameter P $\left[J\,m^{-3}\right]$ was estimated after Simpson et al. (1990) as

$$P = \frac{1}{h_2 - h_1}\int_{-h_2}^{-h_1}(\rho_A - \rho(z))\,gzdz,\ \rho_A = \frac{1}{h_2 - h_1}\int_{-h_2}^{-h_1}\rho(z)\,dz$$

where $\rho(z)$ is the density profile in the water layer between the depths h_1 and h_2. The obtained estimates of P characterize the strength of stratification between the depth of 40 m (h_2) where nutrients were always available and the ferrybox sampling depth of 4 m (h_1). The pre-processed CTD-profiles with a depth step of 0.5 m acquired at station AP5 were used.

All correlations between the data series are given as Pearson correlation coefficients. Only significant correlations are referred with a p-value < 0.05.

The consumption rate of phosphates was estimated as suggested by Lips et al. (2014) assuming that the temporal changes in phosphate concentrations, using a large enough number of analyses over the entire transect, were mostly related to the consumption. A linear regression equation between the measured phosphate concentrations and date (day of the year) was found for each post-spring bloom period using the least squares method. The slope of the found regression line was taken as the estimate of the consumption rate of PO_4^{3-} (units $\mu M\ day^{-1}$). The related need for $NO_2^- + NO_3^-$ was calculated according to the Redfield ratio (N:P ratio 16:1).

RESULTS

Inter-Annual Changes in Sea Surface Temperature and Salinity

The Gulf of Finland was partially ice-covered in 2009 and 2014, and ice-covered in 2010, 2011, and 2012; however, in 2012 the ice winter was 2 weeks shorter than on average. The spring warming of the surface layer differed in timing and rate of temperature increase in the studied years (**Figure 2**). The earliest warming was observed in 2014 when the average cross-gulf surface layer temperature exceeded 4°C by 21 April and 5°C 1 week later (see **Figure 2**, where relevant dates are marked with vertical red and black lines). The average cross-gulf surface layer temperature exceeded 4 and 5°C a few days earlier in 2009 compared with 2012 (**Table 2**). The warming of the surface layer in 2010 and 2011 was slower compared with other years, and spring 2011 was characterized by several warming-cooling periods in April-May. Due to several cooling periods in spring 2011, the average cross-gulf temperature stayed around 4°C until 21 May.

The surface layer salinity (**Figure 2**) in spring-early summer differed between the years, indicating the complex wind-driven circulation patterns and mixing in the Gulf of Finland surface layer in the studied years. On average, the lowest surface layer salinity was registered in 2009 and the highest in 2011. Most probably the high surface layer salinity in 2010 and 2011 was caused by intense vertical mixing in winters 2009–2010 and 2010–2011, respectively. For instance, in winter 2010–2011, there occurred two longer periods with westerly-southwesterly winds resulting in estuarine circulation reversals (eastward flow in the surface layer and westward flow in the deeper layers) that led to intense vertical mixing and a temporal collapse of vertical stratification (Liblik et al., 2013). The latter could also influence the concentrations of nutrients in the surface layer at the onset of the spring bloom.

A typical north-south gradient of the surface layer salinity (on average, salinity is higher near the Estonian coast than near the Finnish coast; e.g., (Kikas and Lips, 2016) was well seen in spring 2009. In spring 2012, a water tongue with slightly lower

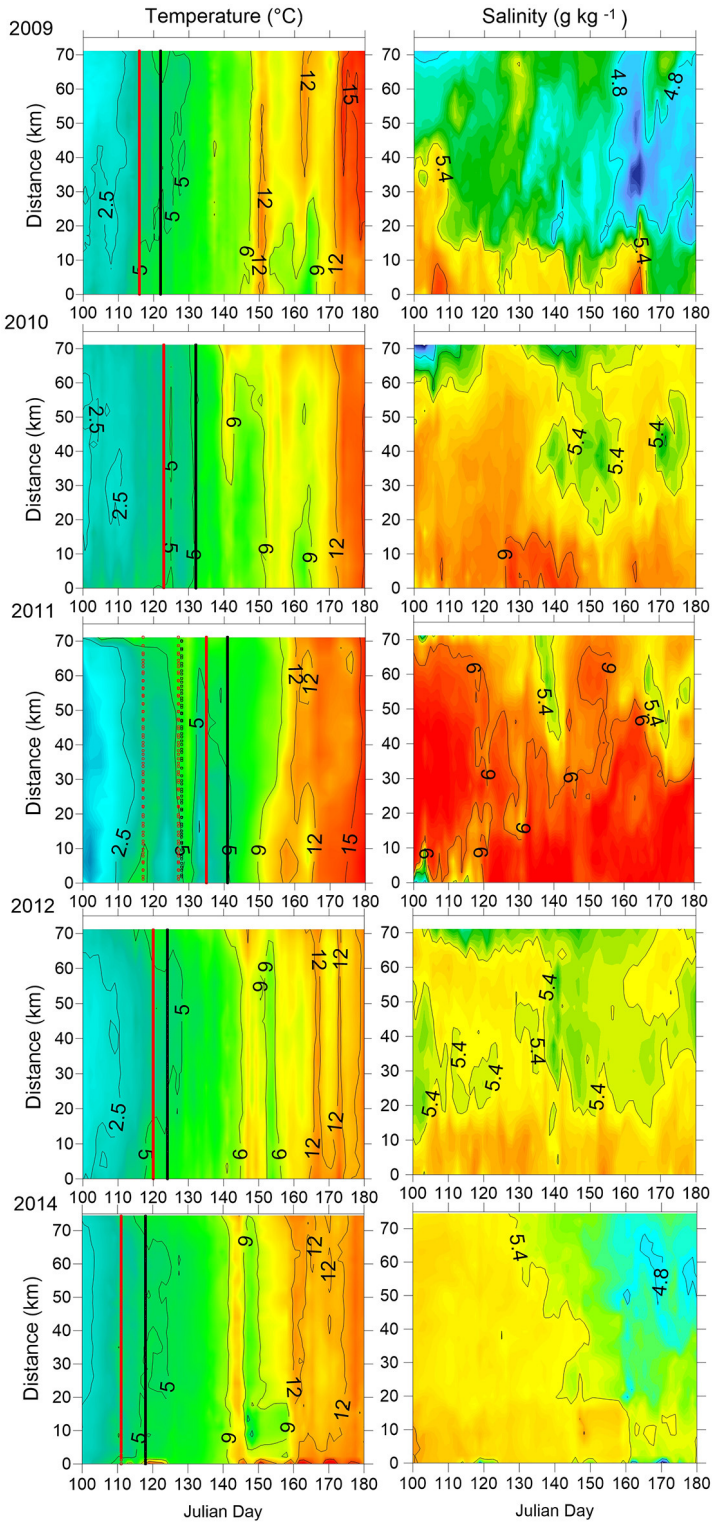

FIGURE 2 | The temporal variation of horizontal distribution of temperature and salinity in the surface layer along the cross-gulf section in the Gulf of Finland in 2009–2012 and 2014. Data of daily measurements with a spatial resolution of 160 m are used. Distance from the southern end of the study transect (see **Figure 1**) is plotted on the y-axis. The days when the average cross-gulf temperature exceeded 4°C (red line) and 5°C (black line) are indicated.

TABLE 2 | The warming of the surface layer: dates (Julian day) when the certain average cross-gulf temperature was reached and dates when maximum *M. rubrum* biomass was observed.

	2009	2010	2011	2012	2014
≥4°C	27.04 (117)	03.05 (123)	15.05* (135)	28.04 (119)	21.04 (111)
≥5°C	03.05 (123)	12.05 (132)	21.05** (141)	05.05 (126)	28.04 (118)
≥6°C	12.05 (132)	16.05 (136)	25.05** (145)	09.05 (130)	14.05 (134)
≥10°C	30.05 (150)	07.06 (158)	07.06 (158)	27.05 (148)	24.05 (144)
Max *MR* BM	17.05 (137)	14.06 (165)	01.06 (152)	01.05 (122)	15.05 (135)

**First warming was registered on 27.04., after that, several colder periods with water temperature around 4°C were registered.*

***Warming over 5°C registered on 08.-12.05.2011 was followed by lower water temperatures until 21.05.2011.*

salinity occurred in the central part of the Gulf. The horizontal distribution of salinity was uniform across the Gulf in March-April-May 2014, while slightly less saline waters appeared in the northern Gulf in June 2014 and the ordinary north-south salinity gradient was established.

Vertical stratification of the water column at low temperatures in April–early May is mostly controlled by the vertical distribution of salinity. The strongest stratification in the upper 40 m layer at station AP5 until mid-May was found in 2010 and 2012 (**Figure 3**) with stratification parameter varying from 32.5 to 45.7 J m^{-3} and from 34.5 to 46.9 J m^{-3}, respectively. At the same time, the stratification was weak in April–early May both in 2011 and 2014. The stratification parameter varied from 12.0 to 22.0 J m^{-3} in 2011 and from 12.4 to 24.6 J m^{-3} in 2014, although the surface layer salinity was clearly higher in 2011 than in 2014. In all studied years, vertical stratification strengthened in late May–June due to the formation of the seasonal thermocline. Vertical stratification in June was still stronger in 2010 and 2012 (stratification parameter exceeded 70 J m^{-3}) than in 2011 and 2014, but a change from a weak to strong stratification was also clear at the measurement site in June 2014 with the estimated stratification parameter up to 55.4 J m^{-3} in late June.

Inter-Annual Changes in Inorganic Nutrient Concentrations

Sampling for the analysis of inorganic nutrient concentrations started in the second week of April (during the phytoplankton spring bloom and was usually performed until the end of May-beginning of June when the $NO_2^-+NO_3^-$ concentrations were below or close to the detection limit (**Figure 4**). In April, during the development of phytoplankton spring bloom, the $NO_2^-+NO_3^-$ concentrations decreased weekly in all studied years. The highest initial $NO_2^-+NO_3^-$ concentrations were measured in 2011 among the all five spring periods. The $NO_2^-+NO_3^-$ concentrations were below or close to the detection limit by the 24 April in 2014, by the 2 May in 2011 and by the 7 May in 2012. In 2009 and 2010, the concentrations of $NO_2^-+NO_3^-$ fell close to detection limit by 10 May (except in the southern part of the study transect in 2010). A late spring increase in the surface layer $NO_2^-+NO_3^-$ concentration was detected in 2010 and 2011.

The measurements of $NO_2^-+NO_3^-$ concentrations at station AP5 in 2010–2012 and 2014 (**Figure 3**) were conducted during the same period as sampling along the ferry route, and the analysis results allow following the depletion of inorganic nitrogen in the surface and sub-surface layer and deepening of the nitracline with time. By mid-April in 2010, the $NO_2^-+NO_3^-$ concentrations in the upper 10 m layer were in the range of 0.2–0.4 μM whereas high levels were measured at the depths of 15 and 20 m (1.6 and 6.8 μM respectively). A significant deepening of the nitracline was observed at the beginning of May, and higher concentrations were reintroduced to the upper layer due to the rise of the pycnocline at the end of May (**Figure 3**). In 2011, the upper 10 m layer was depleted of $NO_2^-+NO_3^-$ by the start of sampling on 21 April whereas relatively high concentrations were measured at a depth of 15 and 20 m (0.7 and 1.9 μM respectively). The sharp deepening of the nitracline down to 25 m was observed at the beginning of May, and a similar rise of the pycnocline, as it was registered in 2010, took place by 18 May. Due to this process, higher $NO_2^-+NO_3^-$ concentrations were detected in the upper layer again in both years. The subsequent samplings in 2011 were conducted with an ∼2-week time lag, and probably the $NO_2^-+NO_3^-$ were depleted faster than seen from the interpolated field in **Figure 3**. In 2012, the deepening of the nitracline was observed from the beginning of May, and no significant rise in $NO_2^-+NO_3^-$ concentrations was detected in the second half of May at station AP5; instead, the continuous deepening of the nitracline down to 25–30 m was observed. In 2014, the $NO_2^-+NO_3^-$ were depleted down to the 25 m depth and, like in 2012, no significant rise in nitracline depth was revealed after the spring bloom.

After the depletion of $NO_2^-+NO_3^-$, there was always some PO_4^{3-} left in the surface layer (**Figure 4**) and the concentrations of excess PO_4^{3-} were quite different in the studied years. In 2009 and 2012, the average concentrations were 0.13 μM (in the range of 0.12–0.16 μM) and 0.18 μM (in the range of 0.08–0.24 μM), respectively. For the same period, the concentrations of PO_4^{3-} were on average 0.33 μM (in the range of 0.20–0.42 μM) and 0.37 μM (in the range of 0.23–0.48 μM) in 2010 and 2014 respectively, and 0.76 μM (in the range of 0.44–0.97 μM) in 2011. The observed late spring rise of the pycnocline increased the surface layer PO_4^{3-} concentrations in 2010 and 2011 remarkably (**Figures 3**, **4**).

Consumption of Inorganic Nutrients in May–June

The PO_4^{3-} was depleted in the surface layer by 31 May in 2009, an increase in concentration in the surface layer was observed in mid-June, and the PO_4^{3-} was depleted again by the end of the month. In 2010, the sampling for PO_4^{3-} analysis was performed until 14 June, and there was still on average 0.16 μM PO_4^{3-} left (range of 0.11–0.24 μM) in the surface layer. In 2011, the sampling period for nutrient analysis was shorter compared with other years in this study, but by 1 June, there was still on average 0.42 μM PO_4^{3-} left (range of 0.30–0.56 μM) in the surface layer along the cross-gulf study transect. In 2012, the sampling of nutrients was conducted until 7 June, and by that time, the

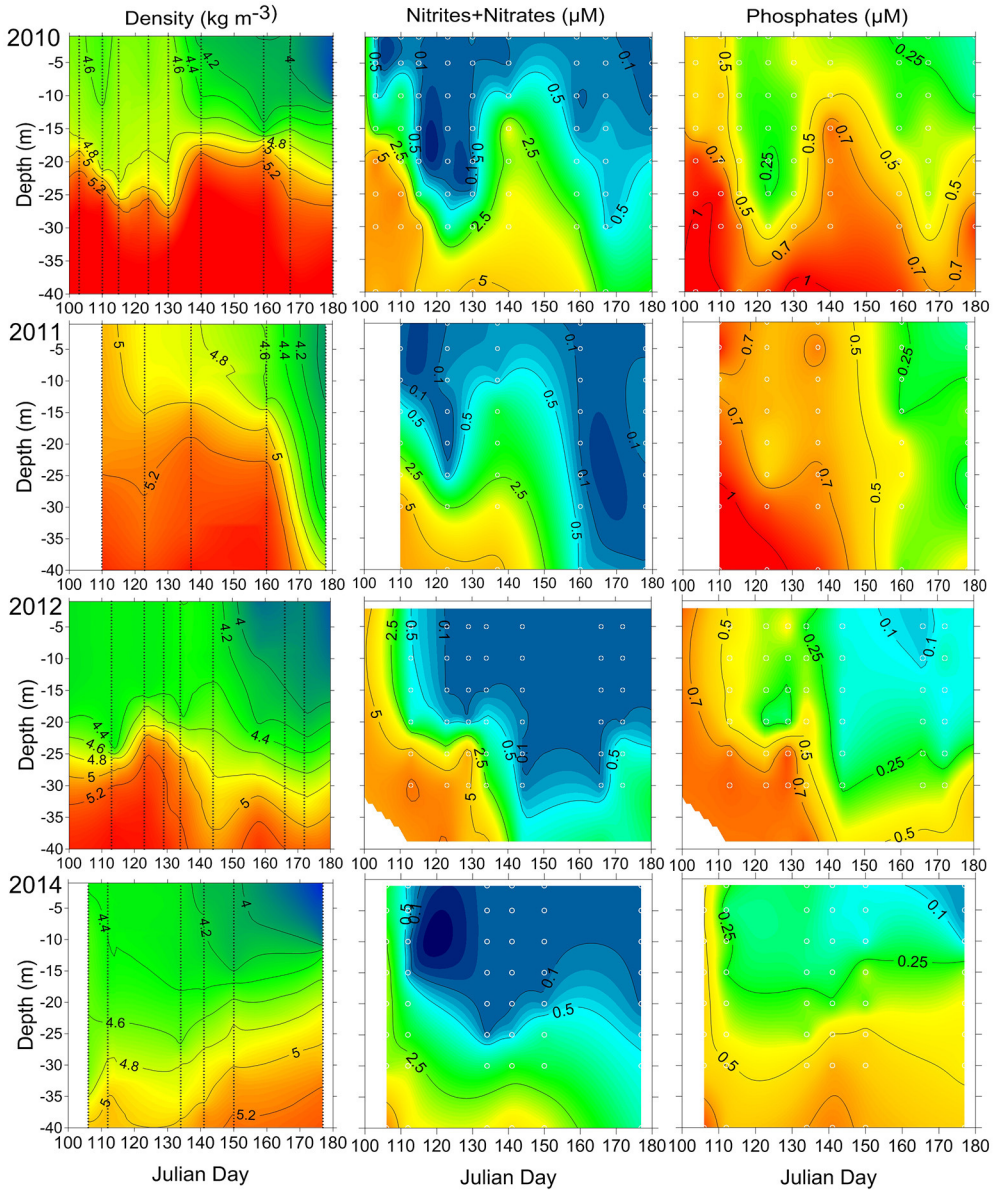

FIGURE 3 | The temporal variation of vertical distribution of density and inorganic nutrients at station AP5 in 2010–2012 and 2014. The sampling days are indicated with vertical lines, and sampling depths are shown as white circles.

phosphate concentrations in the surface layer were close to the detection limit. In 2014, nutrients were sampled until 25 June, and PO_4^{3-} levels were below detection limit by 10 June.

According to the availability of PO_4^{3-} in the surface layer after the depletion of $NO_2^- + NO_3^-$, the consumption of surplus PO_4^{3-} was estimated (**Table 3**). The consumption rates of PO_4^{3-} were estimated for the following periods: from 10 May until 31 May in 2009 (days 130–151), from 10 May until 14 June in 2010 (days 130–165), from 2 May until 1 June in 2011 (days 122–152), from 7 May until 7 June in 2012 (days 129–160), and from 4 May until 25 June in 2014 (days 125–146). The consumption of PO_4^{3-} within these periods was much lower compared with the consumption during the antedate phytoplankton spring bloom (data not presented). Relatively low consumption of PO_4^{3-} in the post-spring bloom period was found in 2009 and 2012, and the estimates were significantly higher in 2010, 2011, and 2014. The probable consumption/need of $NO_2^- + NO_3^-$, assuming that nutrients were consumed according to the N:P ratio of 16:1, was also estimated. Higher inorganic nitrogen needs to deplete surplus PO_4^{3-} from the surface layer were found in 2010, 2011, and 2014 compared with 2009 and 2012. The statistically significant relationship between the decrease of PO_4^{3-} and an increase of *M. rubrum* biomass in the surface layer was found ($R = 0.70$, $p < 0.01$, $n = 27$) for all springs except the year 2010.

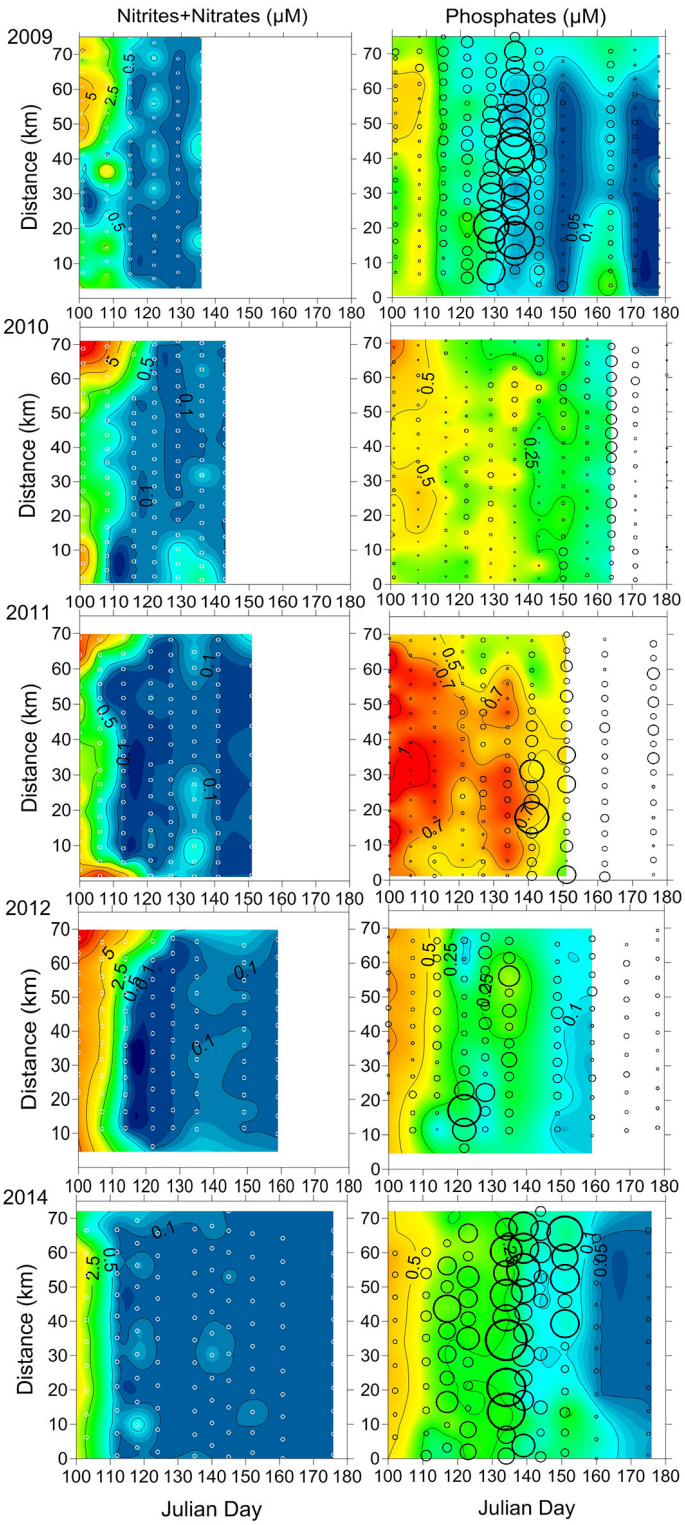

FIGURE 4 | The temporal variation of the horizontal distribution of inorganic nutrients in the surface layer along the cross-gulf section in the Gulf of Finland in 2009-2012 and 2014. Sampling sites are indicated as white circles on left panels. The open circles on right panels indicate the distribution and intensity of *M. rubrum* biomass ($\mu gC\ l^{-1}$; smallest circle = 0 $\mu gC\ l^{-1}$; biggest = 510 $\mu gC\ l^{-1}$).

TABLE 3 | Estimated consumption rates of PO_4^{3-} after the depletion of nitrites-nitrates in the surface layer (n = number of observations and R = correlation coefficient; for all series $p < 0.01$), standard errors of the estimates se_b, and calculated potential need for $NO_2^- + NO_3^-$ to consume the observed excess PO_4^{3-} according to the N:P ratio of 16:1.

	2009	2010	2011	2012	2014
consumption of PO_4^{3-} $\mu M\ day^{-1}$	−0.004 ($n = 68$; $R = 0.79$)	−0.007 ($n = 93$; $R = 0.79$)	−0.007 ($n = 83$; $R = 0.39$)	−0.005 ($n = 47$; $R = 0.69$)	−0.007 ($n = 43$; $R = 0.83$)
se_b $\mu M\ day^{-1}$	0.0003	0.0006	0.002	0.0007	0.0008
need for $NO_2^- + NO_3^-$ $\mu M\ day^{-1}$/ μM	0.064 1.28	0.112 4.0	0.112 2.56	0.080 1.44	0.112 3.52

Interannual Changes in *Mesodinium rubrum* Biomass in May–June

The ciliate *M. rubrum* was an important primary producer in all studied years during the late phase or post-spring bloom (dominated by diatoms and dinoflagellates) period in the Gulf of Finland. In April, during the spring bloom peak, its average contribution to the photosynthetic plankton community was low, on average 8% ($n = 213$) in all studied years, being the lowest in 2011 when it stayed around 4% ($n = 50$). The average contribution of *M. rubrum* to the photosynthetic plankton community in the sea area between Tallinn and Helsinki in May was very variable in studied years. The lowest contribution in 2010 and 2011 (11–13% with $n = 51$ and $n = 66$, respectively) and the highest in 2009 and 2014 (53–61% with $n = 81$ and $n = 44$, respectively) were registered. The average contribution to the photosynthetic plankton biomass in May 2012 was 28% ($n = 48$). Even the *M. rubrum* biomass seemed modest in spring-summer 2010 its proportion in the overall phytoplankton community was similar to the year 2012—on average 32% if the period from the beginning of May until the end of June was taken into account.

The most significant differences between the years were in the timing of the maximum contribution of *M. rubrum*. The highest proportion in the photosynthetic plankton community measured in May was in 2009 (81%, $n = 85$), 2012 (72%, $n = 48$), and 2014 (86%, $n = 44$). The highest contributions in June were observed in 2010 (97%, $n = 99$), 2011 (91%, $n = 27$), and 2014 (86%, $n = 33$). In addition, the remarkable differences in biomass and distribution of *M. rubrum* were observed (**Figure 4**). The most intensive blooms, distributed quite evenly across the Gulf, were registered in 2009 and 2014 when very high biomass values were measured at the first half of May – on 10 and 17 May (91–457 and 106.6–510.1 $\mu gC\ l^{-1}$, respectively) in 2009 and on 15 May (136–439 $\mu gC\ l^{-1}$) in 2014. The year 2014 is characterized by a longer period with high biomass values of *M. rubrum* either along the entire cross-gulf transect or in the different parts of it (28 April until 4 June, **Figure 4**). High values of *M. rubrum* biomass were also detected in 2011 and 2012 but the cross-gulf distribution was patchy and the intensive bloom period shorter with biomasses over 300 $\mu gC\ l^{-1}$ only at one sampling date, on 22 May in 2011 (9.5–508 $\mu gC\ l^{-1}$) and on 1 May in 2012 (24.2–479.4 $\mu gC\ l^{-1}$). Remarkably lower *M. rubrum* biomass values were observed in May–June 2010 when the highest values were measured a month later, compared with the other studied years, on 14 June (76–276 $\mu gC\ l^{-1}$).

A significant relationship ($R = 0.60$, $p < 0.01$, $n = 22$) was found between the start (a week with a noticeable increase in biomass compared with the previous sampling) of the *M. rubrum* bloom and warming of the sea surface layer. The clear increase in *M. rubrum* biomass was observed after the cross-gulf average surface layer temperature had reached over 4°C (**Figure 5**). The maximum *M. rubrum* biomass was higher and established earlier in warmer springs (2009 and 2014; **Table 2**). Also, the average cross-gulf biomass of *M. rubrum* in May was greater in the years characterized by earlier surface layer warming (2009–155 $\mu gC\ l^{-1}$, 2012–119 $\mu gC\ l^{-1}$, and 2014–193 $\mu gC\ l^{-1}$). Springs with slower surface layer warming or very dynamic temperature pattern were characterized by lower *M. rubrum* average biomass in May (2010–51 $\mu gC\ l^{-1}$ and 2011–62 $\mu gC\ l^{-1}$).

A moderate relationship was found with average cross-gulf surface layer salinity and *M. rubrum* biomass build up ($R = 0.40$, $p < 0.05$, $n = 28$).

A qualitative relationship between the vertical stratification and bloom outcome could be demonstrated based on the estimated stratification parameter at station AP5 (located at the distance of 22 km north from the southern end of the cross-gulf study transect; **Figure 3**) and *M. rubrum* biomass in the area. The lowest biomass of *M. rubrum* in spring was observed in 2010 when also the vertical stratification was very strong at station AP5. The highest biomass was found in spring 2014, characterized with the weak vertical stratification, and the decline of *M. rubrum* biomass in the southern part of the study transect coincided with the strengthening of stratification at station AP5 in late May 2014. Nevertheless, similar outcomes of the bloom with occasional high biomass of *M. rubrum* were registered in 2011 and 2012, although the vertical stratification differed significantly between these years—the stratification parameter varied from 12.0 to 35.6 J m^{-3} in 2011 and from 26.3 to 51.0 J m^{-3} (72.1 J m^{-3} in early July) in 2012.

Moderate but statistically not significant agreement of *M. rubrum* biomass in May with preceding period cryptophyte biomass was found (**Figure 6**). Still, the years with higher cryptophyte biomass in April showed the earlier establishment of the ciliate bloom, except in 2011 when the surface layer temperature was very variable in April. In addition, the decline of the *M. rubrum* bloom corresponds with the development of

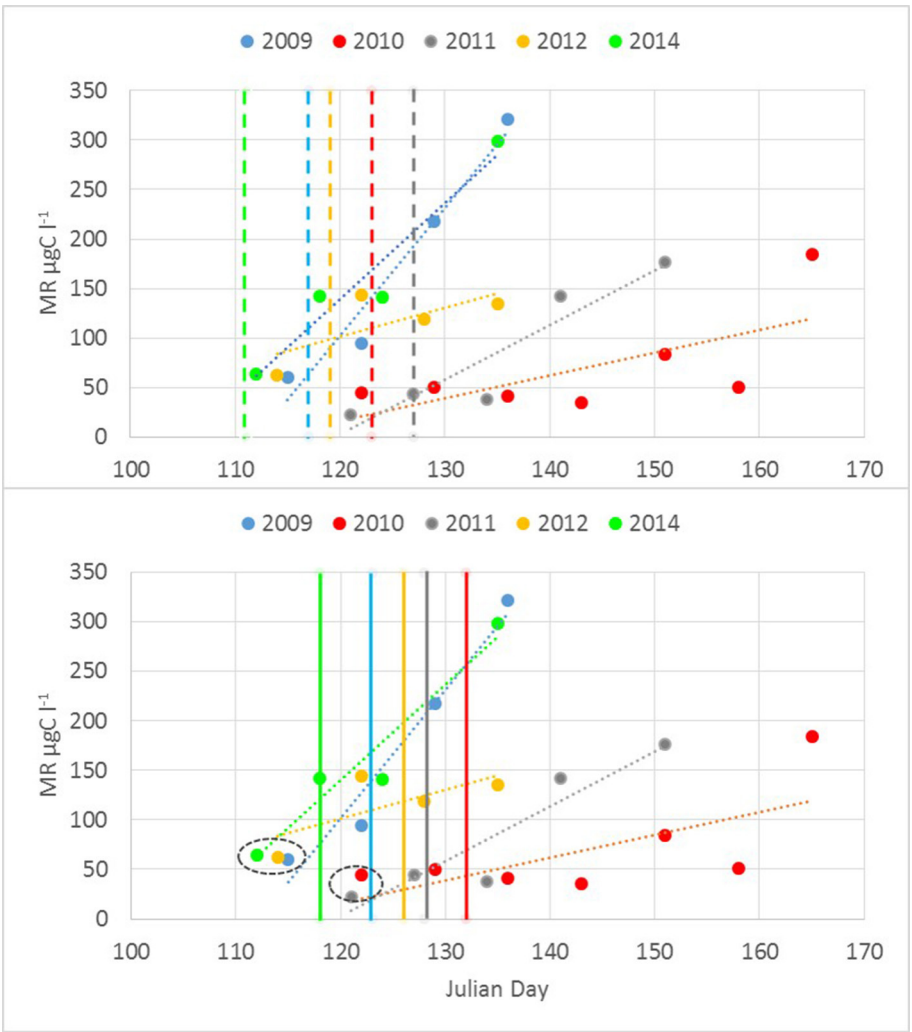

FIGURE 5 | *Mesodinium rubrum* biomass increase up to maximum concentration observed in relation to the average cross-gulf surface layer temperature. Color-coded vertical lines mark the days in different years when average surface layer temperature rose over 4°C (upper panel) and 5°C (lower panel).

Dinophysis acuminata (Claparède and Lachmann 1859) biomass increase in June (**Figure 6**; $R = 0.51$, $p < 0.05$, $n = 23$).

Diel Vertical Dynamics in *Mesodinium rubrum* Abundance in Spring 2014

On 21–22 May 2014, the 24 h measurement and sampling campaign was performed at station AP5. By this time, the water temperature in the upper 5 m layer was above 7°C (**Figure 7**). The surface layer salinity was about 5.45 g kg^{-1}, and a clear vertical salinity gradient was observed in the sub-surface layer below 20 m depth. The $NO_2^- + NO_3^-$ was depleted down to 20 m depth, but there was still some PO_4^{3-} left in the surface layer (**Figure 7**).

Phytoplankton sampling at 2 h intervals and 5 m vertical resolution allowed following the vertical displacement of *M. rubrum* cells (**Figure 7**). Although the highest abundances were usually obtained from the 1 m depth, the clear increase in abundance in the sub-surface layers can be observed at night. Cells started to descend after 7 p.m. (local time) and maximum abundances at 25–30 m depth were registered in the early morning between 1 and 7 a.m. Most of the descending cells did not migrate deeper than 20 m depth, where the start of nitracline was located. By 11 a.m. next day, the cells were again mainly concentrated in the upper 15 m layer.

DISCUSSION

The biomass of the photosynthetic ciliate *M. rubrum* had an evident influence on the primary production of plankton community and nutrient cycling. The inorganic nitrogen, accumulated in the upper layer in the Gulf of Finland during winter, is consumed on average by the beginning of May (**Figure 4**) by rapidly growing spring bloom diatoms and dinoflagellates (Lips et al., 2014). Due to the low N:P ratio

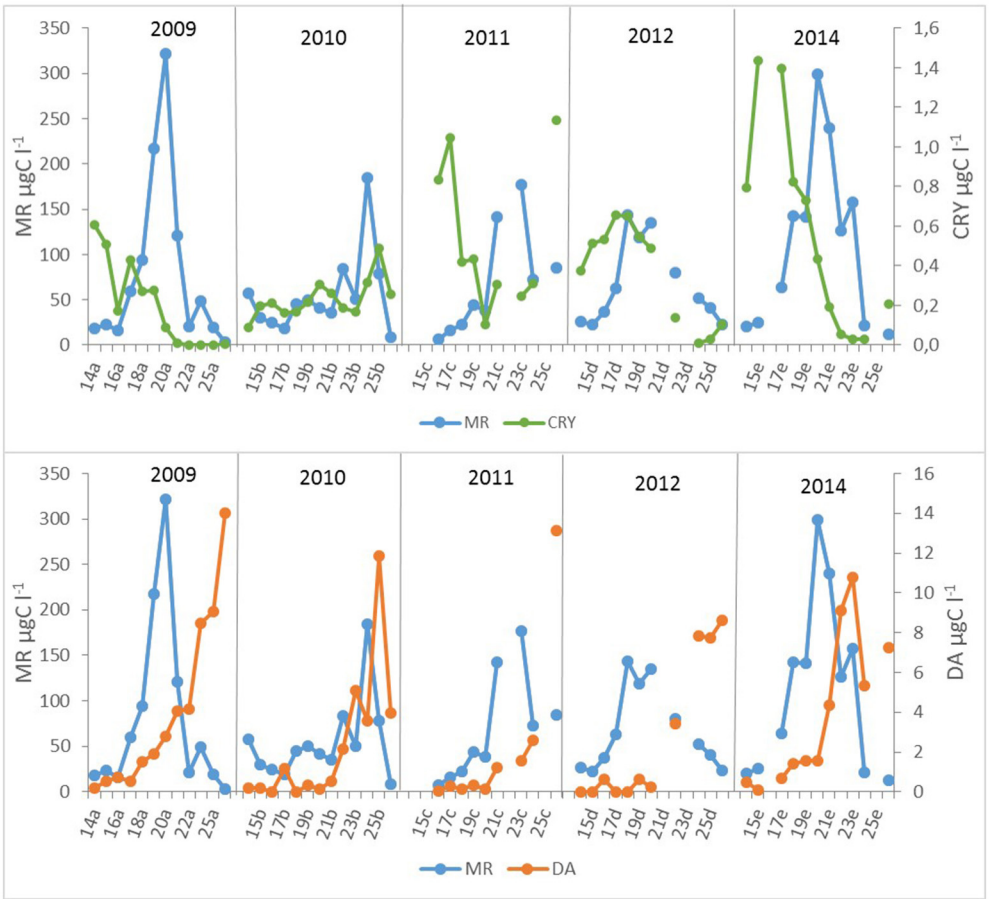

FIGURE 6 | *Mesodinium rubrum* (MR), cryptomonads (CRY), and *Dinophysis acuminata* (DA) biomass dynamics in different years (a–2009, b–2010, c–2011, d–2012, e–2014). The number of the week is shown on the x-axis.

in the winter pool of nutrients and nutrients in the sub-surface layer after the formation of stratification, vertical mixing, and/or advection introduces PO_4^{3-} into surface layer always in excess compared with nitrogen (Laanemets et al., 2011). The depletion of excess PO_4^{3-} in the surface layer before the increase of biomass of N-fixing cyanobacteria (at the end of June-beginning of July) was recognized in the present study.

The depletion of surplus PO_4^{3-} would need significant amounts of inorganic nitrogen which is depleted from the surface layer after the spring bloom. It is possible to roughly estimate the potential need for inorganic nitrogen (**Table 3**) and to predict biomass increase of photosynthetic plankton according to the Redfield ratio (C:N:P of 106:16:1) based on the available PO_4^{3-} in the surface layer and neglecting the remineralization process and consumption by bacteria. For example, the predicted increase in photosynthetic biomass in the surface layer for the period from 3 May to 17 May 2009 (after the depletion of $NO_2^- + NO_3^-$ in the surface layer; days 122–136) could be ~100 µgC l^{-1} taking into account the average concentration of available PO_4^{3-} (0.08 µM). The real measured biomass increase in photosynthetic plankton (including ciliate *M. rubrum*) was on average 42% higher. This discrepancy can be explained either by the fact that net community production may be underestimated if it is based on nutrient concentrations and Redfield ratios only because the contributions of recycled nutrients cannot be taken into account (Thomas et al., 1999) or there are other potential nutrient sources unnoticed when sampling only from the surface layer. In the present study, during the selected period, the shift to species able to migrate vertically in the stratified water column, took place. In fact, the main biomass increase was formed by phototrophic ciliate *M. rubrum*—the biomass increased more than two times from an average 95–220 µgC l^{-1} in the study area. During the first week (3–10 May), the total biomass of phytoplankton increased only by 50 µgC l^{-1} while the biomass of *M. rubrum* increased at the same time by 120 µgC l^{-1} (the difference is due to the disappearance of spring bloom species from the community after the inorganic nitrogen depletion from the surface layer). Within the next week (10–17 May), the average increase in total biomass of phototrophic plankton was 130 µgC l^{-1}, whereas, on average 100 µgC l^{-1} was due to the increase of biomass of *M. rubrum*. The estimated consumption

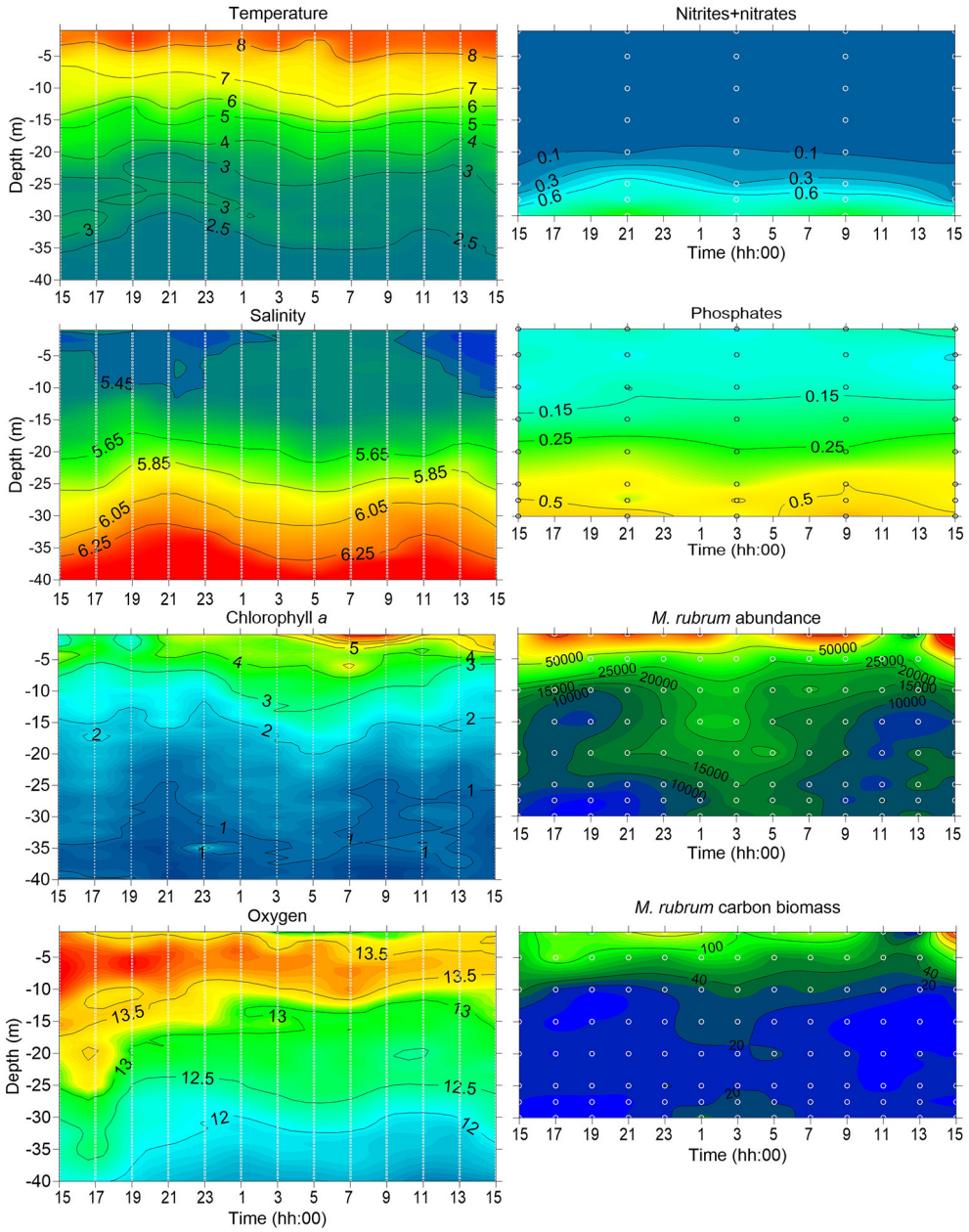

FIGURE 7 | Temporal changes in vertical distribution of temperature (°C), salinity (g kg^{-1}), chlorophyll *a* (μ l^{-1}) and dissolved oxygen (mg l^{-1}; left panels) measured at station AP5 during the 24 h experiment (2 h interval) on 20–21 May 2014. Temporal changes in vertical distribution of nutrients (nitrites-nitrates and phosphates; μM), *M. rubrum* abundance (units l^{-1}) and biomass (μ l^{-1}; right panels) sampled at 6 and 2 h intervals respectively at station AP5; sampling depths are indicated as white circles.

rate of PO_4^{3-} in the surface layer would have supported the total photosynthetic biomass increase approximately by 65 and 40 μgC l^{-1} only, respectively for these 2 weeks. Hence, the observed biomass increase in the whole period of 3–17 May was suggested to be mainly established due to the change in the photosynthetic plankton community composition and the ability of particular species to migrate to the sub-surface layers and assimilate nutrients (both nitrates and phosphates) necessary for their growth.

Still, there are other features and mechanisms to be considered. One should note the increase in $NO_2^-+NO_3^-$ concentration in the surface layer by 17 May 2009 (day 136, **Figure 4**). When the measured decrease of PO_4^{3-} in the surface layer for the period of 10–17 May was rather low (0.03 μM), the increase in $NO_2^-+NO_3^-$ concentration at the same time was remarkable (0.34 μM) and coincided with the highest *M. rubrum* biomass values measured in spring 2009 in the study area. If to assume that the increase of inorganic nitrogen concentration in

the surface layer was induced by the rise of pycnocline, as it was observed in May 2010 and 2011 (**Figure 3**; no vertical profiles available for spring 2009), there should have also been observed the increase in PO_4^{3-} concentration in the surface layer. Instead, the slight decrease in PO_4^{3-} concentration coincided with the increase in $NO_2^- + NO_3^-$ concentration and *M. rubrum* biomass. The first major increase in *M. rubrum* biomass (from 3 to 10 May) was proposed to be mainly related to the species ability to migrate to the lower layers and exploit nutrient reserves there to be able to multiply later in the surface layer. The N-depleted surface layer together with significant biomass increase support this assumption. The second biomass increase (from 10 to 17 May) of *M. rubrum* is most probably a combination of previous and following growth, and advection of water masses with lower salinity into the study area (**Figure 2**), which probably had higher inorganic nitrogen concentration. Hence, high-resolution measurements and sampling enable to see a more comprehensive picture.

Similar calculations were made for May-June 2014, a period when a decrease in PO_4^{3-} concentration in the surface layer during *M. rubrum* bloom was observed. The predicted average biomass increase of primary producers for a period from 22 April to 15 May ($\sim$100 μgC l^{-1}) was also lower than the average real outcome (155 μgC l^{-1}). It is important to note, that the increase of *M. rubrum* biomass was as high as 4.7 times during the considered period, increasing its contribution to the overall photosynthetic plankton biomass from 15 to 56%. These noticed simultaneous dynamics of nutrients and phototrophic plankton biomass suggest the assimilation of inorganic nutrients (both – nitrates and phosphates) in the sub-surface layers and their transport to the surface layer by vertically migrating *M. rubrum*.

The year 2010 was characterized with the lowest maximum biomass of *M. rubrum*. Calculations showed that in the period from 31 May to 14 June, the decrease of PO_4^{3-} by 0.11 μM could have supported the biomass increase according to the Redfield ratio approximately by 140 μgC l^{-1}, which was slightly lower but still quite close to the measured average biomass increase for this period (159 μgC l^{-1}). For the same period, the average increase in *M. rubrum* biomass was 100 μgC l^{-1}, and the contribution of this species to the total phototrophic plankton biomass was increasing within 2 weeks from 50 to 85%. The biomass increase seemed to be mostly based on the PO_4^{3-} left in the surface layer and assimilation of sub-surface $NO_2^- + NO_3^-$ after the rise of nitracline at the second half of May (**Figure 3**).

These kind of calculations, without taking into account all possible sources and sinks of inorganic nutrients, are very rough. In addition, dynamic mesoscale features on the background of meteorologically forced transport and mixing (as intensive horizontal flows of water masses with different salinity and/or nutrient concentration to or through the study area) make these simplified calculations/assessments complicated. At the same time, the decrease in the surface layer PO_4^{3-} concentration in spring is very often significantly associated with the *M. rubrum* biomass increase and dominance in the community. Hence, the contribution of this species to the dynamics of inorganic nutrients cannot be neglected. The biomass of photosynthetic plankton in the second half of May was dominated by *M. rubrum* (70%) in all studied years. As the main increase in total photosynthetic plankton biomass was due to the growth of this species, the significant amounts of available inorganic nutrients (both in horizontal and vertical scale) were consumed most probably by it.

The spring bloom is predominantly regarded as a new production according to the definition of Dugdale and Goering (1967). After the nitrate depletion and decline of the spring bloom, the primary production in the Baltic Sea is mostly assumed to be based on the availability of regenerated nutrients (e.g., Kivi et al., 1993). Earlier studies (Jimenez and Intriago, 1987; Lindholm and Mörk, 1990and references therein, Crawford and Lindholm, 1997; Lips and Lips, 2014) are supporting the results of the present study about the importance of vertical migration to the nutrient dynamics and autotrophic growth in periods characterized by inorganic nutrient limitation in the surface layer. The remarkable growth of *M. rubrum* and formation of red tides in different seasons are based on new nutrients introduced to the surface layer either by physical processes (rise of the thermocline/pycnocline, advection of surface layer water masses, upwelling) or biological capabilities (vertical migration through pycnoclines). The dominance of photosynthetic ciliate *M. rubrum* after the spring bloom not only increases the retention time of newly produced material in the nutrient-limited euphotic layer (Lips et al., 2014) but its contribution to the overall photosynthetic community and primary production can be outstanding. Leppänen and Bruun (1986) estimated that *Mesodinium* contributed about 10% of primary production in spring (April-May) in the open Northern Baltic Proper having at the same time on average only 2% of the total biomass of primary producers. Three decades later the overall contribution of this photosynthetic ciliate to the spring primary producers biomass seems to be increased significantly allowing the estimation on average 8–38% of total primary producers for the same period. Hence, 4–19 times higher contribution to the spring primary production can be expected, and the even greater contribution due to the overall climate change and an increase in sea surface temperature can be foreseen.

The very dynamic nature of *M. rubrum* blooms in spring would make difficult predictions of impact to the other trophic levels without knowledge of this species ecological preferences. Considering the regulating factors in dynamics of plankton community, limiting factors affecting population growth directly and controlling factors influencing the outcome of growth processes exist (Thingstad and Sakshaug, 1990). Johnson et al. (2013) have shown a significant positive correlation of *M. rubrum* field population with temperature in spring. Also, Montagnes et al. (2008) demonstrated a significant effect of temperature on *M. rubrum* abundance; the one-degree increase would increase the mean abundance by 1.42, and explained it with a decreased growth rate at low temperature. The limitation of cellular metabolic capacity by the thermal stress (Moeller et al., 2011) and a decrease in swimming velocity with decreasing temperatures (Riisgård and Larsen, 2009) have also been suggested. The motion of *M. rubrum* is characterized by jumping after shorter or longer periods of motionless, but it is also capable of sustained swimming (Fenchel and Hansen, 2006). Besides escape from

predators, the jumping is necessary to create fluid motion surrounding the ciliate to increase the contribution of advective transport in nutrient uptake (Jiang, 2011). Slow warming (**Figure 2**, **Table 2**) in the study area at the end of April in 2010 probably created a physical environment not supporting the intensive growth and active motions, including the vertical migrations to assimilate nitrates from deeper layers, of *M. rubrum* compared with other studied years. Hence, when migratory capabilities were reduced, the competitive advantages over other migrating photosynthetic plankton were downgraded. The other important factor in combination with the low surface water temperature to influence the growth of *M. rubrum* is the low position of nitracline (below 20 m already by the end of April) in 2010 (**Figure 3**). Although the ability of *M. rubrum* to migrate through the density gradients is well-documented (e.g., Figueroa et al., 1998), the present results suggest that vertical stratification could notably influence the growth and bloom outcome of this species. The latter is also supported by the data from spring 2014. The observed clear decrease of *M. rubrum* biomass in late May 2014 in the southern part of the transect (**Figure 4**) coincided with the strengthening of vertical stratification (**Figure 3**).

M. rubrum is an obligate phototroph obtaining most of its carbon from photosynthesis, and only one cryptophyte prey per cell is required to maintain its maximum growth (Hansen and Fenchel, 2006). The suitable prey and predator relationships are hypothesized to support the *M. rubrum* surface bloom formation (Stoecker et al., 2009). Cryptophytes-*M. rubrum* relationships can also be followed in the data set of studied years with significant bloom maximum in 2009, 2011–2012, and 2014 (**Figure 6**), but the same does not hold for the year 2010 when the initial biomass of cryptophytes was several times lower in April compared with other years. Most probably, the combination of regulating factors (both limiting and controlling) influenced the *M. rubrum* biomass outcome in 2010.

Complex migratory patterns observed in the present study and described by others (e.g., review by (Crawford, 1989) might be related to a combination of requirements for light, cryptophyte prey, and nutrients, especially nitrates. The migrations in response to nutrient and light conditions in the stratified sea can lead to a vertical distribution in which the majority of the population may be concentrated close to the surface during the day and in deeper layers at night. Most commonly, only part of the populations are performing such daily migrations (Pérez et al., 1999; Rychert, 2004), but getting a more realistic picture of the extent of such migrations temporally very high-resolution measurements are needed. The suggested vertical migrations of *M. rubrum* between the surface layer and the nitracline should create incidents when during the high biomass period of this ciliate in the plankton community the Chl *a* concentrations could occasionally be elevated in the sub-surface layer. Sub-surface maxima have been reported earlier in the Gulf of Finland in summer in the cases when the dinoflagellate *Heterocapsa triquetra* (Ehrenberg) Stein 1883 was present in the community in high abundances (Lips et al., 2011; Lips and Lips, 2014). The high-resolution measurements with a profiling mooring and a towed undulating vehicle (data not presented here) registered the sub-surface Chl *a* maxima in spring 2012. During the period of the high biomass of *M. rubrum* in the first half of May, thin layers of relatively high Chl *a* values were observed on several occasions. In the frame of the present study, the vertical sampling conducted at 2 h intervals and resolution of 5 m might have been too low as *M. rubrum* could have theoretically made several migrations within 2 h or was missed in the depths not sampled. Still, the integrated biomass values increased slightly from 21 p.m. until 1 a.m. (240–380 $\mu C\ l^{-1}$) and decreased again afterwards, indicating the high probability of success in sampling during the active migration. The high swimming speed allows *M. rubrum* to descend to the nitracline in the evening, stay there to assimilate nutrients and migrate back to the well-lit surface layer by midday. From the presented 24-h study, the observed migration pattern allows suggesting the diurnal vertical migrations of this species. Still, extensive studies should be made in the future to see the longer pattern and regularity of such migrations and assess more precisely the influence not only to the horizontal but also to the vertical distribution of inorganic nutrients. The ability to migrate vertically and exploit the nutrient pools from the lower layers may significantly influence the nutricline depth after the development of stratification in spring. Interestingly, even the nitracline was located at 20 m depth in May 2014, part of the *M. rubrum* cells migrated deeper—down to 25 and 30 m depth.

The photosynthetic ciliate *M. rubrum* might be a key player in the trophic transfer of energy after the decline of spring bloom and establishment of late summer phytoplankton blooms. This phototrophic ciliate not only prolongs the autotrophic production in the nutrient-depleted surface layer but also acts as an important food supply to other organisms (e.g., Park et al., 2006; Fileman et al., 2007; Lee et al., 2014; **Figure 6**). Also, the excretion of nutrients through mineralization and cell explosion can be a significant source of nitrogen (Lindholm, 1985; Miller et al., 1995) to phytoplankton species present in the surface layer community. High nitrate and phosphate assimilation rates reported in previous studies (Dugdale et al., 1987; Jiang, 2011; Tong et al., 2015), support the assumption that inorganic nitrogen available in spring-summer continuum, either brought close to the surface through pycnocline rise or from adjacent areas, will be mostly assimilated by dominating *M. rubrum* if the other environmental conditions support its growth. Also, the dominance of *M. rubrum* in May-June, its migration behavior, and phosphate utilization in the surface layer is strongly influencing the amount of excess PO_4^{3-} that is usually regarded to support the summer cyanobacterial bloom development (e.g., Janssen et al., 2004; Laanemets et al., 2006; Raateoja et al., 2011). The years, when PO_4^{3-} was depleted or close to the depletion by the end of our study period, are characterized by lower cyanobacterial biomass development and *vice versa* (Kahru and Elmgren, 2014). Hence, the dynamics and intensity of *M. rubrum* blooms in May-June have, besides nutrient distribution, the significant impact also on the late summer phytoplankton communities. The interactions between *M. rubrum* biomass development and other phytoplankton groups should be studied further as its contribution to the total photosynthetic biomass has increased in all seasons in the Baltic Sea (Jaanus et al., 2011). Thamm et al. (2004) have demonstrated the shift of the peak occurrence of this species from spring (in 1987) over spring/summer (in 1990) to summer (in 1997).

CONCLUSIONS

The clear relationship between the start and outcome of the *M. rubrum* bloom and average cross-gulf surface layer temperature emphasize the potentially high impact of this species to the spring–early summer plankton community in the background of overall climate change and continuous increase in sea surface temperature. The very high proportion of *M. rubrum* in the phototrophic plankton community has created the shift from, previously acknowledged, regenerated production toward new production at the period between spring bloom and summer cyanobacterial bloom in the Baltic Sea. The dominance of *M. rubrum* after the spring bloom in vertically stratified Gulf of Finland strongly influences the amount of excess phosphates in the surface layer and vertical inorganic nutrient dynamics. Within present study, comprising sampling with high temporal and spatial resolution, the understanding of dynamics and possible impacts of spring *M. rubrum* blooms to the Gulf of Finland ecosystem was increased.

AUTHOR CONTRIBUTIONS

UL organized and partly conducted the measurements and sampling in the study area. IL conducted all phytoplankton and partly the nutrient analysis. Both authors contributed to the data analysis and manuscript writing.

FUNDING

The present work was supported by institutional research funding IUT (IUT19-6) of the Estonian Ministry of Education and Research, by the Estonian Science Foundation grant no. 8930 and by EU Regional Development Foundation, Environmental Conservation and Environmental Technology R&D Programme project VeeOBS (3.2.0802.11-0043).

ACKNOWLEDGMENTS

We appreciate the help of crew and colleagues during sampling and analysis.

REFERENCES

Alenius, P., Myrberg, K., and Nekrasov, A. (1998). Physical oceanography of the Gulf of Finland: a review. *Boreal Environ. Res.* 3, 97–125.

Ammerman, J. (2001). *QuikChem® Method 31-115-01-1-I – Determination of Orthophosphate by Flow Injection Analysis*. Lachat Instruments.

APHA (1992). *APHA, AWWA, and WPCF Standard Methods for the Examination of Water and Wastewater, 18th Edn*. Washington, DC: Am. Public Health Assoc.

Calbet, A., and Landry, M. R. (2004). Phytoplankton growth, microzooplankton grazing, and carbon cycling in marine systems. *Limnol. Oceanogr.* 49, 51–57. doi: 10.4319/lo.2004.49.1.0051

Cloern, J. E., Cole, B. E., and Hager, S. W. (1994). Notes on *Mesodinium rubrum* red tides in San Francisco Bay (California, USA). *J. Plankton Res.* 16, 1269–1276. doi: 10.1093/plankt/16.9.1269

Cloern, J. E., Foster, S. Q., and Kleckner, A. E. (2014). Phytoplankton primary production in the world's estuarine-coastal ecosystems. *Biogeosciences* 11, 2477–2501. doi: 10.5194/bg-11-2477-2014

Conley, D. J., and Johnstone, R. W. (1995). Biogeochemistry of N, P and Si in Baltic Sea sediments: response to a simulated deposition of a spring diatom bloom. *Mar. Ecol. Prog. Ser.* 122, 265–276. doi: 10.3354/meps122265

Crawford, D. (1989). *Mesodinium rubrum*: the phytoplankter that wasn't. *Mar. Ecol. Prog. Ser.* 58, 161–174. doi: 10.3354/meps058161

Crawford, D. W., and Lindholm, T. (1997). Some observations on vertical distribution and migration of the phototrophic ciliate *Mesodinium rubrum* (=*Myrionecta rubra*) in a stratified brackish inlet. *Aquat. Microb. Ecol.* 13, 267–274. doi: 10.3354/ame013267

Dugdale, R. C., and Goering, J. J. (1967). Uptake of new and regenerated forms of nitrogen in primary productivity. *Limnol. Oceanogr.* 12, 196–206. doi: 10.4319/lo.1967.12.2.0196

Dugdale, R. C., Wilkerson, F. P., Barber, R. T., Blasco, D., and Packard, T. T. (1987). Changes in nutrients, pH, light penetration and heat budget by migrating photosynthetic organisms. *Oceanol. Acta* SP, 103–107.

Egan, L. (2000). *QuikChem® Method 31-107-04-1-D – Determination of Nitrate and/or Nitrite in Brackish Waters by Flow Injection Analysis*. Lachat Instruments.

Esteban, G. F., Fenchel, T., and Finlay, B. J. (2010). Mixotrophy in ciliates. *Protist* 161, 621–641. doi: 10.1016/j.protis.2010.08.002

Fenchel, T., and Hansen, P. J. (2006). Motile behaviour of the bloom-forming ciliate *Mesodinium rubrum*. *Mar. Biol. Res.* 2, 169–177. doi: 10.1080/17451000600571044

Figueroa, F. L., Niell, F. X., Figueiras, F. G., and Villarino, M. L. (1998). Diel migration of phytoplankton and spectral light field in the Ria de Vigo (NW Spain). *Mar. Biol.* 130, 491–499. doi: 10.1007/s002270050269

Fileman, E., Smith, T., and Harris, R. (2007). Grazing by *Calanus helgolandicus* and *Para-Pseudocalanus* spp. *o*n phytoplankton and protozooplankton during the spring bloom in the Celtic Sea. *J. Exp. Mar. Biol. Ecol.* 348, 70–84. doi: 10.1016/j.jembe.2007.04.003

Hansen, P. J., and Fenchel, T. (2006). The bloom-forming ciliate *Mesodinium rubrum* harbours a single permanent endosymbiont. *Mar. Biol. Res.* 2, 169–177. doi: 10.1080/17451000600719577

Heiskanen, A.-S. (1995). Contamination of sediment trap fluxes by vertically migrating phototrophic microorganisms in the coastal Baltic sea. *Mar. Ecol. Prog. Ser.* 122, 45–58. doi: 10.3354/meps122045

Heiskanen, A.-S. (1998). Factors governing sedimentation and pelagic nutrient cycles in the northern Baltic Sea. *Boreal Environ. Res.* 8:80.

HELCOM (1988). Guidelines for the Baltic monitoring programme for the third stage. Biological determinants. *Balt. Sea Environ. Proc.* 27D, 1–161.

Höglander, H., Larsson, U., and Hajdu, S. (2004). Vertical distribution and settling of spring phytoplankton in the offshore NW Baltic Sea Proper. *Mar. Ecol. Prog. Ser.* 283, 15–27. doi: 10.3354/meps283015

Jaanus, A., Andersson, A., Olenina, I., Toming, K., and Kaljurand, K. (2011). Changes in phytoplankton communities along a north-south gradient in the Baltic Sea between 1990 and 2008. *Boreal Environ. Res.* 16, 191–208.

Janssen, F., Neumann, T., and Schmidt, M. (2004). Inter-annual variability in cyanobacteria blooms in the Baltic Sea controlled by wintertime hydrographic conditions. *Mar. Ecol. Prog. Ser.* 275, 59–68. doi: 10.3354/meps275059

Jiang, H. (2011). Why does the jumping ciliate *Mesodinium rubrum* possess an equatorially located propulsive ciliary belt? *J. Plankton Res.* 33, 998–1011. doi: 10.1093/plankt/fbr007

Jimenez, R., and Intriago, P. (1987). Observations on blooms of *Mesodinium rubrum* in the upwelling area off Ecuador. *Oceanol. Acta SP*. 145–154.

Johnson, M. D. (2011). Acquired phototrophy in ciliates: a review of cellular interactions and structural adaptations. *J. Eukar. Microb.* 58, 185–195. doi: 10.1111/j.1550-7408.2011.00545.x

Johnson, M. D., Beaudoin, D. J., Laza-Martinez, A., Dyhrman, S. T., Fensin, E., Lin, S., et al. (2016). The genetic diversity of *Mesodinium* and associated cryptophytes. *Front. Microbiol.* 7:2017. doi: 10.3389/fmicb.2016.02017

Johnson, M. D., Stoecker, D. K., and Marshall, H. G. (2013). Seasonal dynamics of *Mesodinium rubrum* in Chesapeake Bay. *J. Plankton Res.* 35, 877–893. doi: 10.1093/plankt/fbt028

Kahru, M., and Elmgren, R. (2014). Multidecadal time series of satellite-detected accumulations of cyanobacteria in the Baltic Sea. *Biogeosciences* 11, 3619–3633. doi: 10.5194/bg-11-3619-2014

Kang, N. S., Lee, K. H., Jeong, H. J., Yoo, Y. D., Seong, K. A., Potvin, É., et al. (2013). Red tides in Shiwha Bay, western Korea: a huge dike and tidal power plant established in a semi-enclosed embayment system. *Harmful Algae* 30, S114–S130. doi: 10.1016/j.hal.2013.10.011

Kikas, V., and Lips, U. (2016). Upwelling characteristics in the Gulf of Finland (Baltic Sea) as revealed by Ferrybox measurements in 2007-2013. *Ocean Sci*. 12, 843–859. doi: 10.5194/os-12-843-2016

Kivi, K., Kaitala, S., Kuosa, H., Kuparinen, J., Leskinen, E., Lignell, R., et al. (1993). Nutrient limitation and grazing control of the Baltic plankton community during annual succession. *Limnol. Oceanogr.* 38, 893–905. doi: 10.4319/lo.1993.38.5.0893

Kononen, K., and Niemi, Å. (1984). Long-term variation of the phytoplankton composition at the entrance of the Gulf of Finland. *Ophelia Suppl.* 3, 101–110.

Kulinski, K., and Pempkowiak, J. (2011). The carbon budget of the Baltic Sea. *Biogeosciences* 8, 3219–3230. doi: 10.5194/bg-8-3219-2011

Laanemets, J., Lilover, M. J., Raudsepp, U., Autio, R., Vahtera, E., Lips, I., et al. (2006). A fuzzy logic model to describe the cyanobacteria *Nodularia spumigena* blooms in the Gulf of Finland, Baltic Sea. *Hydrobiologia* 554, 31–45. doi: 10.1007/s10750-005-1004-x

Laanemets, J., Väli, G., Zhurbas, V., Elken, J., Lips, I., and Lips, U. (2011). Simulation of mesoscale structures and nutrient transport during summer upwelling events in the Gulf of Finland in 2006. *Boreal Environ. Res.* 16, 15–26.

Lee, K. H., Jeong, H. J., Yoon, E. Y., Jang, S. H., Kim, H. S., and Yih, W. (2014). Feeding by common heterotrophic dinoflagellates and a ciliate on the red-tide ciliate *Mesodinium rubrum*. *Algae* 29, 153–163. doi: 10.4490/algae.2014.29.2.153

Leppänen, J.-M., and Bruun, J.-E. (1986). The role of pelagic ciliates including *Mesodinium* during the spring bloom of 1982. in the open northern Baltic Proper *Ophelia Suppl.* 4, 147–157.

Liblik, T., Laanemets, J., Raudsepp, U., Elken, J., and Suhhova, I. (2013). Estuarine circulation reversals and related rapid changes in winter near-bottom oxygen conditions in the Gulf of Finland, Baltic Sea. *Ocean Sci.* 9, 917–930. doi: 10.5194/os-9-917-2013

Lindholm, T. (1985). *Mesodinium rubrum* - a unique photosynthetic ciliate. *Adv. Aquat. Microbiol*. 3, 1–48.

Lindholm, T., and Mörk, A. C. (1990). Depth maxima of *Mesodinium rubrum* (Lohmann) hamburger and buddenbrock - examples from a stratified Baltic Sea Inlet. *Sarsia* 75, 53–64. doi: 10.1080/00364827.1990.10413441

Lips, I., and Lips, U. (2008). Abiotic factors influencing cyanobacterial bloom development in the Gulf of Finland (Baltic Sea). (2008). *Hydrobiologia* 614, 133–140. doi: 10.1007/s10750-008-9449-2

Lips, I., Rünk, N., Kikas, V., Meerits, A., and Lips, U. (2014). High-resolution dynamics of the spring bloom in the Gulf of Finland of the Baltic Sea. *J. Mar. Syst*. 129, 135–149. doi: 10.1016/j.jmarsys.2013.06.002

Lips, U., and Lips, I. (2014). Bimodal distribution patterns of motile phytoplankton in relation to physical processes and stratification (Gulf of Finland, Baltic Sea). *Deep Sea Res. Part II Top. Stud. Oceanogr.* 101, 107–119. doi: 10.1016/j.dsr2.2013.05.029

Lips, U., Lips, I., Liblik, T., Kikas, V., Altoja, K., Buhhalko, N., et al. (2011). Vertical dynamics of summer phytoplankton in a stratified estuary (Gulf of Finland, Baltic Sea). *Ocean Dyn.* 61, 903–915. doi: 10.1007/s10236-011-0421-8

Mackenzie, A. L., and Gillespie, P. A. (1986). Plankton ecology and productivity, nutrient chemistry, and hydrography of Tasman Bay, New Zealand, 1982–1984, New Zealand. *J. Mar. Freshw. Res.* 20, 365–395. doi: 10.1080/00288330.1986.9516158

Menden-Deuer, S., and Lessard, E. J. (2000). Carbon to volume relationships for dinoflagellates, diatoms, and other protist plankton. *Limnol. Oceanogr*. 45, 569–579. doi: 10.4319/lo.2000.45.3.0569

Miller, C. A., Penry, D. L., and Glibert, P. M. (1995). The impact of trophic interactions on rates of nitrogen regeneration and grazing in Chesapeake Bay. *Limnol. Oceanogr.* 40, 1005–1011. doi: 10.4319/lo.1995.40.5.1005

Moeller, H. V., Johnson, M. D., and Falkowski, P. G. (2011). Photoacclimation in the phototrophic marine ciliate *Mesodinium rubrum* (ciliophora). *J. Phycol.* 47, 324–332. doi: 10.1111/j.1529-8817.2010.00954.x

Montagnes, D. J. S., Allen, J., Brown, L., Bulit, C., Davidson, R., Díaz-Ávalos, C., et al. (2008). Factors controlling the abundance and size distribution of the phototrophic ciliate *Myrionecta rubra* in open waters of the North Atlantic. *J. Eukaryot. Microbiol*. 55, 457–465. doi: 10.1111/j.1550-7408.2008.00344.x

Olenina, I., Hajdu, S., Edler, L., Andersson, A., Wasmund, N., Busch, S., et al. (2006). Biovolumes and size-classes of phytoplankton in the Baltic Sea. *Balt. Sea Environ. Proc*. 104:144.

Park, M. G., Kim, S., Kim, H. S., Myung, G., Kang, Y. G., and Yih, W. (2006). First successful culture of the marine dinoflagellate *Dinophysis acuminata*. *Aquat. Microb. Ecol*. 45, 101–106. doi: 10.3354/ame045101

Passow, U. (1991). Vertical migration of *Gonyaulax catenata* and *Mesodinium rubrum*. *Mar. Biol*. 110, 455–463. doi: 10.1007/BF01344364

Pérez, M. T., Dolan, J. R., Vidussi, F., and Fukai, E. (1999). Diel vertical distribution of planktonic ciliates within the surface layer of the NW Mediterranean (May 1995). *Deep Res. Part I Oceanogr. Res. Pap*. 47, 479–503. doi: 10.1016/S0967-0637(99)00099-0

Putt, M., and Stoecker, D. K. (1989). An experimentally determined carbon : volume ratio for marine "oligotrichous" ciliates from estuarine and coastal waters. *Limnol. Oceanogr.* 34, 1097–1103. doi: 10.4319/lo.1989.34.6.1097

Raateoja, M., Kuosa, H., and Hällfors, S. (2011). Fate of excess phosphorus in the Baltic Sea: a real driving force for cyanobacterial blooms? *J. Sea Res*. 65, 315–321. doi: 10.1016/j.seares.2011.01.004

Riisgård, H. U., and Larsen, P. S. (2009). Ciliary-propelling mechanism, effect of temperature and viscosity on swimming speed, and adaptive significance of "jumping" in the ciliate *Mesodinium rubrum*. *Mar. Biol. Res*. 5, 585–595. doi: 10.1080/17451000902729704

Rivkin, R. B., Putland, J. N., Anderson, M. R., and Deibel, D. (1999). Microzooplankton bacterivory and herbivory in the NE subarctic Pacific. *Deep Sea Res. Part II Top. Stud. Oceanogr*. 46, 2579–2618. doi: 10.1016/S0967-0645(99)00077-6

Rychert, K. (2004). The size structure of the *Mesodinium rubrum* population in the Gdansk Basin. *Oceanologia* 46, 439–444.

Simpson, J. H., Brown, J., Matthews, J., and Allen, G. (1990). Tidal straining, density currents and mixing in the control of estuarine stratification. *Estuar. Coasts* 13, 125–132. doi: 10.2307/1351581

Smayda, T. J. (2010). Adaptations and selections of harmful and other dinoflagellate species in upwelling systems. 2. Motility and migratory behaviour. *Progr. Oceanogr*. 85, 71–91. doi: 10.1016/j.pocean.2010.02.005

Stoecker, D. K., Johnson, M. D., De Vargas, C., and Not, F. (2009). Acquired phototrophy in aquatic protists. *Aquat. Microb. Ecol.* 57, 279–310. doi: 10.3354/ame01340

Stoecker, D. K., Putt, M., Davis, L. H., and Michaels, A. E. (1991). Photosynthesis in *Mesodinium rubrum*: species-specific measurements and comparison to community rates. *Mar. Ecol. Prog. Ser.* 73, 245–252. doi: 10.3354/meps073245

Tamelander, T., and Heiskanen, A. S. (2004). Effects of spring bloom phytoplankton dynamics and hydrography on the composition of settling material in the coastal northern Baltic Sea. *J. Mar. Syst*. 52, 217–234. doi: 10.1016/j.jmarsys.2004.02.001

Thamm, R., Schernewski, G., Wasmund, N., and Neumann, T. (2004). Spatial phytoplankton pattern in the Baltic Sea. *Balt. Sea Typol. Coastline Rep.* 4, 928–2734.

Thingstad, T. F., and Sakshaug, E. (1990). Control of phytoplankton growth in nutrient recycling ecosystems. Theory and terminology. *Mar. Ecol. Prog. Ser.* 63, 261–272. doi: 10.3354/meps063261

Thomas, H., Ittekkot, V., Osterroht, C., and Schneider, B. (1999). Preferential recycling of nutrients – the ocean's way to increase new production and to pass nutrient limitation? *Limnol. Oceanogr.* 44, 1999–2004. doi: 10.4319/lo.1999.44.8.1999

Tong, M., Smith, J., Kulis, D., and Anderson, D. (2015). Role of dissolved nitrate and phosphate in isolates of *Mesodinium rubrum* and toxin-producing *Dinophysis acuminata*. *Aquat. Microb. Ecol.* 75, 169–185. doi: 10.3354/ame01757

Wasmund, N., and Uhlig, S. (2003). Phytoplankton trends in the Baltic Sea. *ICES J. Mar. Sci.* 60, 177–186. doi: 10.1016/S1054-3139(02)00280-1

Wilkerson, F. P., and Grunseich, G. (1990). Formation of blooms by the symbiotic ciliate *Mesodinium rubrum* - the significance of nitrogen uptake. *J. Plankton Res*. 12, 973–989. doi: 10.1093/plankt/12.5.973

Conflict of Interest Statement: The authors declare that the research was conducted in the absence of any commercial or financial relationships that could be construed as a potential conflict of interest.

frontiers in Marine Science

ORIGINAL RESEARCH
published: 13 November 2018
doi: 10.3389/fmars.2018.00408

Ecosystem Effects of Morphological and Life History Traits in Two Divergent Zooplankton Populations

Konrad Karlsson and Monika Winder*

Department of Ecology Environment and Plant Sciences, Stockholm University, Stockholm, Sweden

Little is known about the ecosystem effects of locally adapted populations. The filter feeding copepod *Eurytemora affinis* is an abundant and important zooplankton in coastal waters that consist of a cryptic species complex with locally adapted populations. We used a mesocosm setup to investigate population and ecosystem interactions of two populations from the Baltic Sea with different morphology and life history traits. One population is laterally wider, larger-sized, more fecund, and have higher growth rate than the other. The experimental ecosystems varied in algae community (pelagic algae, and pelagic algae + benthic diatoms) with two resource supply scenarios. Results showed that the large-sized population is a more effective grazer. In low resource supply the small-sized population starved, whereas the large-sized population was unaffected, resulting in a larger population increase of both nauplii and copepodites than for the small-sized population. Addition of benthic diatoms to the pelagic algae community had much more negative effects on the reproduction of the large-sized population. This suggests that the large-sized population feeds near benthic to a greater extent than the small-sized population, and that filamentous benthic diatoms interfere with the grazing process. Despite the negative effects of benthic diatoms, the large-sized population could maintain similar or higher reproduction than the small-sized population. In addition, the high grazing efficiency of the large-sized population resulted in a different community composition of algae. Specifically, flagellated species and small sized benthic diatoms were more grazed upon by the large-sized population. Our results show that morphologically divergent, yet phylogenetically closely related zooplankton populations can have different ecosystem functions, and in turn have different population increase in response to resource supply and algae community.

Keywords: local adaptation, common gardening experiment, intraspecific variation, ecological-evolutionary dynamics, resource specialization, morphological divergence, niche partitioning, size efficiency

OPEN ACCESS

Edited by:
Riina Klais,
University of Tartu, Estonia

Reviewed by:
Sami Souissi,
Lille University of Science and Technology, France
Ana Marta Gonçalves,
University of Coimbra, Portugal

****Correspondence:***
Konrad Karlsson
konrad.karlsson@su.se

Specialty section:
This article was submitted to Marine Ecosystem Ecology, a section of the journal Frontiers in Marine Science

Received: *29 April 2018*
Accepted: *15 October 2018*
Published: *13 November 2018*

Citation:
Karlsson K and Winder M (2018) Ecosystem Effects of Morphological and Life History Traits in Two Divergent Zooplankton Populations. Front. Mar. Sci. 5:408. doi: 10.3389/fmars.2018.00408

1. INTRODUCTION

The number of species in an ecosystem and their traits affect diverse ecosystem processes (Hooper et al., 2005). A key question is whether the species or their traits are the best predictor of ecosystem functions because variation within species, such as differences in resource specialization and life history traits (e.g., growth and fecundity) can affect ecosystem processes (Harmon et al., 2009; Bassar et al., 2010; Walsh et al., 2012). Consequently, variation in ecosystem processes can be larger

within species than between species (Gianuca et al., 2016) and not all conspecifics can be regarded as ecologically equal (Bolnick et al., 2002). Furthermore, interactions of species and ecosystems are bilateral so that species may diverge depending on the type of habitat (Marklund et al., 2018).

Many species exhibits adaptations dependent on attributes in their local habitat. Differences between locally adapted populations can be quantified by rearing populations in a common *garden* where the environments are identical for all individuals (Falconer and Mackay, 1996), thereby the environmental source of phenotypic variance between populations can be eliminated. Hence the phenotypic variance of a quantified trait is caused by genetic variance when the environment is identical. In addition, locally adapted populations may have different ecological effects (Schoener, 2011), which can be estimated by common *gardening* experiments. The difference between a common garden and a common gardening experiment is the switch of focal point. In the former the focus is on the environmental effects on phenotypes. In the latter the focus is on the effect of phenotypes on the environment. Therefore, there are two focal points for delineating evolutionary diversification: the effect of ecology on phenotypes, and the effect of phenotypes on ecology. By constructing common gardening experiments, where one put specific phenotypes (e.g., populations) in replicated ecosystems, it is possible to quantify both of these effects (Matthews et al., 2011b, 2014).

Overlooking divergence within species results in loss of information about how organisms interact with and shape their ecosystems. A common procedure when conceptualizing ecosystems is to use a trait-based approach (Litchman et al., 2013; Colina et al., 2016). However, to describe trait diversity correctly one has to acknowledge that traits diverge also within species. For instance, in a fish species when averaging consumption of benthic and pelagic resources it seems as if fish are connectors of the pelagic and benthic food webs (Schindler and Scheuerell, 2002; Vander Zanden and Vadeboncoeur, 2002). However, when accounting for that fish can specialize for either benthic or pelagic resources it seems as if they disconnect these two food webs (Quevedo et al., 2009). In fish, there are many examples of how adaptive radiations and plastic specializations in resource use have caused intra-specific morphological variation, which results in different ecosystem effects by the different morphotypes (Harmon et al., 2009; Palkovacs and Post, 2009; Post and Palkovacs, 2009; Lundsgaard-Hansen et al., 2014). In addition to morphological traits, life history traits such as divergence in populations' growth rates and fecundity can affect ecosystem processes differently (Bassar et al., 2010; Walsh et al., 2012). Furthermore, traits that diverge under artificial selection can have different effects in experimental ecosystems (Becks et al., 2010; Pantel et al., 2015), giving a direct link from adaptation to ecosystem effects.

The focal species in the present study is the calanoid copepod *Eurytemora affinis* (Poppe, 1880), a dominant zooplankton species in estuaries in the northern hemisphere and an important grazer and prey for fish (Hernroth and Ackefors, 1979; Diekmann et al., 2012; Rajasilta et al., 2014). It consists of a cryptic species complex (Lee and Frost, 2002) and inter-population crosses have shown that certain populations cannot reproduce further than two generations (Lee, 2000). Specifically, in the Baltic Sea the great morphological variation in *E. affinis* have led to past taxonomic confusion and classification into invalid species (Lee and Frost, 2002; Sukhikh et al., 2016) because the females of some populations can be larger, laterally wider, and carry more eggs than others do (Gurney, 1931).

Revisions of the *E. affinis* species complex have been ongoing since it was first described by Poppe (1880) and Gurney (1931). Recently, a new species within the complex, *Eurytemora carolleeae*, was described (Alekseev and Souissi, 2011). This species originate from the North American east coast and is listed as an invasive species in the Baltic Sea, with occurrences in the Gulf of Finland and the Gulf of Riga (Alekseev and Souissi, 2011; Sukhikh et al., 2013). The morphological traits used to discriminate between *E. affinis* and *E. carolleeae* are non-adaptive (Alekseev and Souissi, 2011; Sukhikh et al., 2013; Lajus et al., 2015), and thus unlikely to have any ecosystem effects (Matthews et al., 2011a). Furthermore, taxonomic classification based on morphology alone is not distinct because some key traits overlap between the two species (Sukhikh et al., 2013; Vasquez et al., 2016) and differentiate between *E. affinis* populations (Sukhikh et al., 2016). Therefore, we use the *E. affinis* species name throughout and refer to the *E. affinis* species complex in the present study.

A previous common garden experiment revealed differences in development time as a response to temperature between Baltic Sea *E. affinis* populations, where a population from the Gulf of Riga (Pärnu Bay) had similar (12 and 17°C) or shorter (22.5°C) development time than a population from the Swedish coast (Stockholm Archipelago) (Karlsson and Winder, unpublished data). Females from the Gulf of Riga population also appeared to have a larger body size than the Swedish coast population, which was however not quantified. For copepods in general, development time increase with species size and fecundity (Allan, 1976; Gillooly, 2000), thus this large-sized population breaks this norm. The trait differences between the two populations' may affect ecosystem processes, such as differences in prey size spectra, prey selection, and grazing efficiency (Bassar et al., 2010; Walsh et al., 2012; Gianuca et al., 2016).

The aim of this study is to (i) describe and quantify morphology and fecundity in a common garden experiment and (ii) quantify ecosystem responses and reciprocal effects in a common gardening experiment (mesocosms) of these two *E. affinis* populations from the Baltic Sea. We constructed mesocosm environments with two types of algae (prey) community and two types of resource supplies. To investigate if the described trait differences affect feeding efficiency and algae community, and the reciprocal effects of algae community and resource supply on population growth, female prosome length, and clutch size. Algae community included two treatments one with pelagic species and one with pelagic species plus benthic diatoms, resource supply included two levels of nutrients. The mesocosm experiment lasted for 14 days, which corresponds to approximately one generation time for both populations at the experimental temperature of 17°C (Karlsson and Winder,

unpublished data). We hypothesized that populations would differentiate over the algae treatment if they diverged in their feeding behavior and resource specialization, and differentiate over the resource supply treatment if they diverge in their demand for food and feeding efficiency.

2. MATERIALS AND METHODS

2.1. Sampling and Rearing of Cultures

No specific ethical permits were needed for research on invertebrate crustaceans. This study does not include vulnerable populations and endangered animal species. Populations were sampled in spring 2014 in the Stockholm archipelago at Askö monitoring station B1 (hereafter referred to as STHLM) 58°48.19′,17°37.52′ (latitude, longitude) and in summer 2014 in the Pärnu Bay a shallow inner part of Gulf of Riga (hereafter referred to as GOR) 58°21.67′, 24°30.83' by vertical tow nets. More than 300 adult copepods were taken from the samples and used to start stock cultures. Before measurements of morphology and clutch size (number of eggs), stock cultures were kept for a minimum of three generations to reduce imprints of maternal effects (Sanford and Kelly, 2010) in 3 L (Exo Terra^{TM}) aquariums at 17°C and 7 PSU and fed with the cryptophyte *Rhodomonas salina*. Aquariums were aeriated by gently stirring the water once a day. Before the mesocosm experiment, cultures were kept for at least three generations in 45 L plastic tubs at 15°C and 7 PSU and fed with the cryptophyte *Rhinomonas nottbecki*. The two experiments were separated in time by 2 years, from 2014 to 2016 and during this time we predict that approximately 42 generations have past, given a generation time of 17 days at 15°C (Karlsson and Winder, unpublished data).

The zooplankton were at all times kept in tap water that had been circulated for about a week in an aquarium with gravel from a freshwater stream to condition the water for aquatic organisms (reduce chlorine and excessive gas); to adjust the right salinity we used Instant Ocean^{TM} sea salt.

2.2. Common Garden Experiment: Measurements of Morphology and Clutch Size

In autumn 2014 we started up 5 cultures per population by taking 10 egg carrying females from our stock cultures into 3 L aquariums with GF/F Whatman^{TM} filtered aquarium water of 2 PSU. The copepods were fed *ad libitum* of the cryptophyte *Rhodomonas salina* (100,000–200,000 cells ml^{-1}). More than 27,000 cells ml^{-1} did not increase egg production (a proxy for growth in adult female copepods) in *Acartia tonsa* (Kiørboe et al., 1985) a copepod of similar size as *E. affinis*. As soon as the daughters of the inoculated females had developed egg sacks they were picked out to be photographed dorsal or ventral side, measured (prosome length), and the number of eggs in each female clutch were counted. We sampled 50 females per population, 10 from each culture.

We measured shape and size of the females' prosomen with 14 landmark data points from the digitized images. To visualize shape of the two populations we ran a principal component analysis with the landmark data (14 x and 14 y coordinates, in pixel units), made by R package `geomorph` (Adams and Otarola-Castillo, 2013), and depicted the individuals of each population that had minimum and maximum values on principal component 1 (**Figures 1**, **2**). We computed landmarks with the software packages `tpsUtil` and `tpsDig2` (Rohlf, 2011b, 2013). We computed partial warps, uniform variables, and centroids with `tpsRegr` (Rohlf, 2011a). To test if shape differed between populations we used a MANCOVA with partial warps (11 x and 11 y) and uniform variables (1 x and 1 y) as response, size (centroid of each specimen) was included as covariate, and population as explanatory variable. The centroid size is calculated in pixel units as the square root of the sum of squared landmark distances to the centroid, which is a two-dimensional measure of size (1 pixel correspond to ca 0.89 μm). The interaction of population and size was not significant, thereby we concluded that the size and shape slopes of both populations do not differ, and therefore removed the interaction and use size as covariate (Engqvist, 2005). We used a two-way ANOVA to test the interaction of prosome length and population on clutch size. Furthermore, we followed up this analysis with a one-way ANOVA to test for differences in prosome length between populations.

2.3. Common Gardening Experiment: Set Up and Treatments

For the common gardening experiment, we used three types of factors each with two levels of treatment: two zooplankton

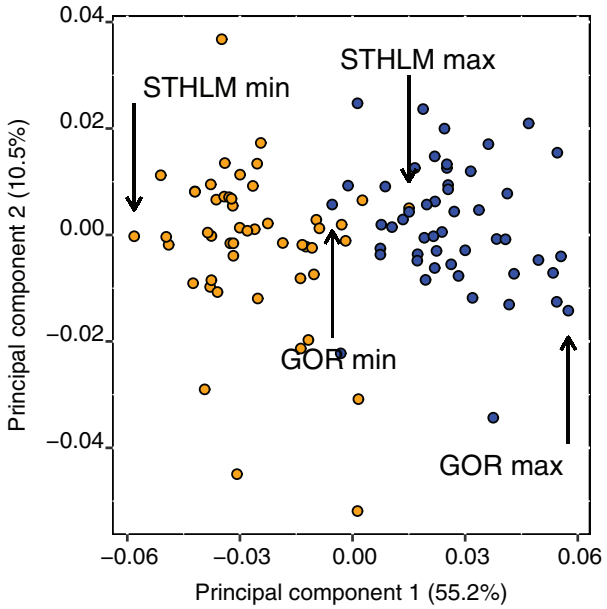

FIGURE 1 | Principal component axes 1 and 2 of shape variation of Procrustes aligned specimens for the STHLM (orange) and GOR (blue) *E. affinis* populations, individuals with minimum and maximum value on principal component 1 from the respective population are marked out. These individuals are depicted in **Figure 2**.

populations (STHLM and GOR), two nutrient treatments (low and high), and two types of algae community (pelagic and pelagic + benthic diatoms). We replicated each factor combination 10 times, summing up to 80 mesocosms ($2 \times 2 \times 2 \times 10$). For control treatments we used factor combinations of nutrient levels and algae community without zooplankton, replicated 5 times, summing up to 20 control mesocosms ($2 \times 2 \times 5$).

The mesocosms were 3 L plastic aquariums (Exo Terra^{TM}) filled with GF/F Whatman^{TM} filtered aquarium water, placed in a rooftop greenhouse at the Department of Ecology, Environment and Plant Sciences at Stockholm University. The mesocosms received natural light as well as light from metal halide lamps in 12:12 h night:day cycle, with an average 55.8 (range 16.7, 202.1) µmol m^{-2} s^{-1} on the bottom of the mesocoms. Average temperature during the experiment was 17.0°C, but oscillated during the night day cycle and was highest just before lamps turned off (average 18.8°C, range 16.8–20.6°C) and lowest just before lights turned on (average 14.9°C, range 13.6–15.9°C). We added nutrients and Instant Ocean^{TM} sea salt while the water was separated into two containers one for low and one for high resource supply treatment, water was later portioned out to the mesocosm after thorough mixing. We added 57.6 µmol L^{-1} SiO_4, 28.4 µmol L^{-1} of NO_3, and 2.4 µmoles L^{-1} PO_4 to the high resource supply treatment, for the low nutrient treatment the respective concentrations were 30.6, 12.9, and 1.1 µmol L^{-1}. Ratios of Si:N:P were similar for the high and low resource supply treatment with 24:12:1 and 28:12:1, respectively. We further added micronutrients, B vitamins, and peat extract (**Table S1**). Concentrations of NO_2 + NO_3 and SiO_4 (**Figure S1**) were higher than deliberately, suggesting that additional nutrients came into the mesocosm from either the algae or zooplankton cultures. Either way, the contrasts of resource supply treatments were clearly visible and quantifiable. We added salt to reach a salinity of 10 PSU, which was a salinity where both zooplankton and algae could coexist.

The two communities of algae consisted of either five pelagic species or the same pelagic species plus an addition of three benthic species (**Table S2**). The pelagic species were: the pooled sample of *R. nottbecki* and *R. salina* referred to as cryptophytes, *Heterocapsa triquetra*, *Pseudoscourfeldia marina*, *Skeletonema marinoi*, and *Isochrysis* sp. The benthic species where the pooled sample of *Nitzschia aurariae* and *Navicula perminuta*, *Melosira* sp., and *Fragilaria* sp. We selected algae species that belonged to some of the commonly found taxonomic classes in the Baltic Sea, with the compromise that they should be readily cultured in lab conditions on the same growth media (**Table S1**) and at the same salinity (10 PSU). We added the pelagic species in equal amounts to all mesocosms and the benthic species in equal amounts to half of the mesocosms. Therefore, at the beginning of the experiment the benthic treatment contained more food than the pelagic, but over time the amount of food was constrained to the concentration of nutrients. We inoculated the mesocosms by adding 1 ml from the same homogenized culture to each mesocosm for each species of algae. The inoculation concentrations were measured on the start day (October 4th) from Lugol-preserved samples diluted 10 times and placed in a tubular plankton chamber. We then took pictures by inverted light microscopy at specific locations in the chamber and calculated the number of cells per picture by `EBImage` R package (Pau et al., 2010), these numbers were calculated back to cells ml^{-1} algae ml^{-1} algae culture (**Table S2**).

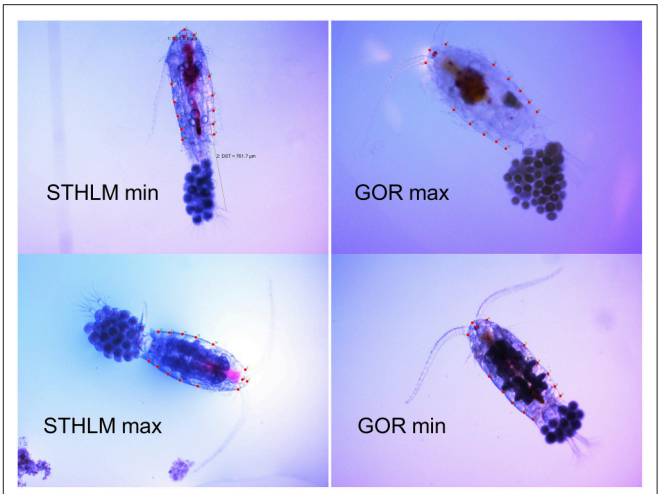

FIGURE 2 | Pictures of *E. affinis* individuals with minimum and maximum value on principal component 1 from the respective population, these individuals are marked out in **Figure 1**. Pictures include locations of the 14 landmarks used in the principal component analysis. The prosome lengths of the individuals depicted are 833 and 776 µm for STHLM min and max, and 833 and 923 µm for GOR min and max, respectively. Note that the pictures are meant to show variation in shape and not in size and length. The scale of the pictures are 2,300 µm wide and 1,725 µm high.

One day after mesocosm setup, we added zooplankton from the stock cultures that consisted of similar ratios of nauplii, copepodites, and adults for both populations. Zooplankton were added by taking aliquots of the thoroughly mixed stock cultures to each mesocosm. We added slightly less individuals from the GOR population since these individuals are larger to get similar zooplankton bio-volumes for both populations. Aliquots (n =10) of the starting concentrations for each population were put in 4% formalin to be counted and measured. For these samples we counted the number of nauplii in stage 1–3 and 4–6 and copepodites in stage 1–3 and 4–6 (where stage 6 are the adults), and made measurements of length, width, and depth of the prosome body for all individual life stages. We then calculated the average bio-volume for an individual within one of these four groups by using the volume of an ellipse and multiplied the bio-volume with the number of individuals in the corresponding life-stage interval. Subsequently, we used the bio-volume sum in each sample to test if initial volumes were different for the two populations by a t-test.

2.4. Common Gardening Experiment: Sampling and Sample Analysis

We took two types of algae samples, one to measure relative fluorescence units (RFU) and one to count and identify the algae. We took samples directly after the mesocosms were gently stirred. RFU samples were measured in a Trilogy^{TM} fluorometer

(Turner design), samples for counts were preserved in acidic Lugol, and were counted with an inverted light microscope.

We counted cryptophytes, *H. triquetra*, *Fragilaria* sp., and *Melosira* sp. in continuous transects (field of view) over the full diameter of the chamber at 100 times magnification. We counted *N. aurariae* and *N. perminuta* in a continuous transect in 400 times magnification, and the smallest species *P. marina*, *Isochrysis* sp., and *S. marinoi* in 20 fields of view in a transect at 1,000 times magnification. We took samples of both RFU and Lugol on day 2, 6, 10, and 14. For RFU we measured all 100 mesocoms at each sampling occasion. Samples for counts of the pelagic species were 5, 2, 5, and 2 samples per treatment combination (including controls) and respective day. Samples for counts of the benthic species were 5, 2, 5, and 2 per treatment combination of the controls; and 5, 4, 7, and 2 per treatment combination with zooplankton.

At the same days as algae sampling we took two samples per treatment combination of free phosphate (PO_4), nitrite + nitrate ($NO_2 + NO_3$), ammonia (NH_4), and silicate (SiO_4) by filtering 10 ml water through a 0.45 µm filter and then analyzing the filtrate in a segmented flow analysis (**Figure S1**).

At the end of the experiment on day 15 (14 days after copepod innoculation), which corresponds to the development time for one generation (given *ad libitum* food conditions and 17°C, Karlsson and Winder, unpublished data), the mesocosms were poured through a 45 µm net and all inhabiting zooplankton were filtered out and put in 4% formalin. From these samples we counted the number of nauplii and the pooled number of copepodites and adults. Two egg-carrying females from each sample (mesocosm) were picked at random and their prosome lengths were measured and clutch size counted. We expected the nauplii to have been born in the mesocosm during the experiment, and that the copepodites and adults mainly to be part of the individuals inoculated at the beginning.

2.5. Statistical Analyses of the Common Gardening Experiment

We used R for all analyzes (R Core Team, 2017). The response variables: counts of nauplii (N1-N6) and copepodites + adults (C1-C6), prosome length of females, and female clutch size, were fitted as Gaussian response models by functions `lme` or `gls` from the `nlme` (Pinheiro et al., 2017) package. When there was more than one observation per mesocosm we used mesocosm ID as random effect in the linear mixed effect models (`lme`), and when variances in the different treatments were unequal we fitted extended linear models with power covariates in the linear models (`gls`). Models were evaluated by starting with a full model containing all treatment interactions (population, algae, and nutrients) and subsequently removing non-significant interactions, based on AIC. We only included the highest order of significant interactions or main effects in the running text, full model outputs can be found in the **Supplementary Material**.

RFU and species counts were analyzed by extended linear mixed models (function `lme`), with power covariates to control for the increasing residual variation due to algal growth. For both RFU and species counts we omitted the control to test for the difference between populations. The pelagic species occurred both with and without benthic diatoms, whereas the benthic diatoms only occurred with pelagic species, and hence the main effect of the addition of benthic diatoms was only estimated for the pelagic species. The RFU analysis was split up between pelagic and pelagic + benthic algae treatments as we expected the emitted fluorescence to differ between pelagic flagellates and benthic diatoms, and therefore a direct comparison could be spurious. The effects of resource supply were estimated for both RFU and species counts. We included a third degree polynomial of time as an interaction with the treatments (population, algae, resource supply) in both the RFU and the species counts models. This tests if the polynomial relationship with time differs between treatment contrasts. However, we did not include the estimates of the treatment main effects (i.e., time = 0), and the main effect of time in the results as it is not the focus of this study.

3. RESULTS

3.1. Common Garden Experiment: Morphology and Clutch Size

The shape of the females prosomen differed significantly between the populations [MANCOVA, $F_{(24, 74)} = 5.19$, $p < 0.001$] the GOR population was wider and rounder than the more laterally compressed STHLM population (**Figures 1**, **2**) and the size of the prosomen had no significant effect on shape [MANCOVA, $F_{(24,74)} = 1.51$, $p = 0.090$].

We found a significant interaction of population and prosome length on clutch size [two-way ANOVA, $F_{(1, 96)} = 6.68$,

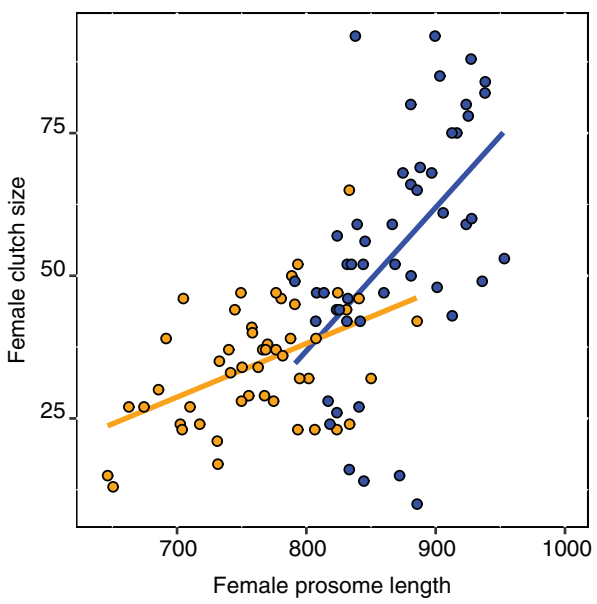

FIGURE 3 | Relationship of female clutch sizes and prosome lengths for the STHLM (orange) and GOR (blue) *E. affinis* populations. Points are observed values and lines are fitted values from a two-way analysis of variance.

$p = 0.011$]. Hence, the relationship between prosome length and clutch size differs between the two populations (**Figure 3**), and a 1 μm increase in length increased clutch size with 0.25 and 0.09 eggs for the GOR and STHLM populations respectively. Furthermore, the main effects of population [two-way ANOVA, $F_{(1, 96)} = 48.06$, $p < 0.001$] and prosome length [two-way ANOVA, $F_{(1, 96)} = 25.64$, $p < 0.001$] were significant, the average clutch sizes were 34.6 (28.1, 41.0; 95% CI) for the STHLM population and 54.4 (49.8, 58.9) eggs female^{-1} for the GOR population. Furthermore, the females' prosome length differed between populations [one-way ANOVA, $F_{(1, 98)} = 124$, $p < 0.001$] and was on average 762.1 (743.1, 781.1; 95% CI) for the STHLM population and 869.8 (856.4, 883.3) μm for the GOR population.

3.2. Common Gardening Experiment

The averages of zooplankton bio-volumes at the start of the experiment were not significantly different between the populations [t-test, $t_{(18)} = -0.541$, $p = 0.595$] and was 3.08 (± 0.24, SE) for the STHLM population and 2.91 (± 0.22) mm^{-3} for the GOR population. Number of individuals per stage at the start of the experiment (averages rounded to whole numbers) were for the STHLM population, N1-N3: 105 (86–116, range), N4-N6: 10 (3–22), C1-C3: 9 (1–17), C4-C6: 30 (18–49). Respective numbers for the GOR population were, N1-N3: 69 (51–92), N4-N6: 28 (15–38), C1-C3: 14 (5–20) and C4-C6: 17 (10–27).

Algae concentrations measured as RFU were significantly lower with the GOR population than with the STHLM population. The lower values for the GOR population were consistent over both resource supply and algae treatments, suggesting that this population is a more efficient grazer than the STHLM population (**Figure 4**, **Table 1**).

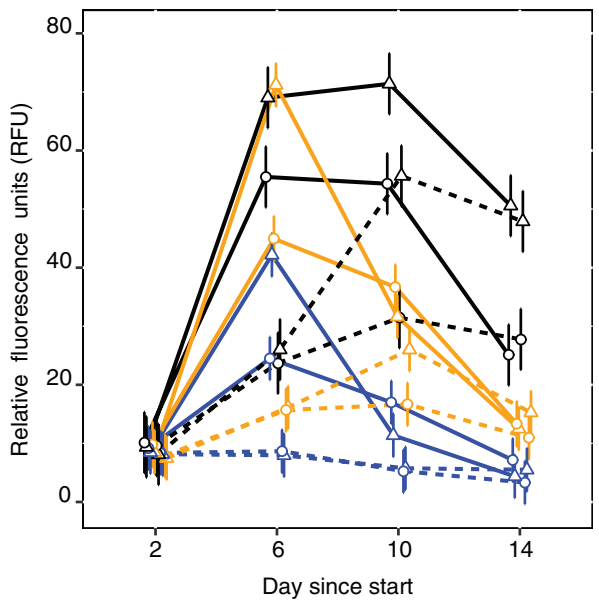

FIGURE 4 | Relative fluorescence units as proxy for algal biomass for the control (black), STHLM (orange) and GOR (blue) *E. affinis* populations. Solid and dotted lines are respective high and low nutrient treatments, triangles and circles are respective pelagic and benthic treatments. Estimates and 95% CI are fitted by restricted maximum likelihood.

Concentrations of all the pelagic species (cryptophytes, *H. triquetra*, *Isochrysis* sp., and *P. marina*) were significantly lower with the GOR population than the STHLM population, whereas for *S. marinoi* there was no difference between the populations (**Figure 5**, **Table 2**). Concentrations of the large filamentous benthic diatoms *Fragilaria* sp. and *Melosira* sp. did not differ between the populations, while the smaller single celled benthic diatoms *N. aurariae* + *N. perminuta* were significantly lower with the GOR population than the STHLM population (**Figure 5**, **Table 3**).

The addition of benthic diatoms had a negative effects on the concentrations of all the pelagic species except *H. triquetra* (**Figure 5**, **Table 2**). Addition of nutrients had positive effects on the concentrations of all species except *H. triquetra* and *Fragilaria* sp. (**Figure 5**, **Tables 2**, **3**).

The numbers of nauplii at the end of the experiment depended on the interaction of algae treatment and population [$t_{(5, 72)} = 3.15$, $p = 0.002$] and on the interaction of population and resource supply [$t_{(5, 72)} = 2.66$, $p = 0.001$]. The GOR population was more negatively affected by benthic algae than the STHLM population, and the STHLM population was more negatively affected by low resource supplies (**Figure 6A**, **Table S3**).

For copepodites + adults we found a significant interaction of population origin and resource supply [$t_{(4, 73)} = 5.24$, $p < 0.001$], where low resources led to a striking decrease in numbers for the STHLM population, but not for the GOR population. Furthermore, we found a significant main effect of algae treatment [$t_{(4, 73)} = 3.88$, $p < 0.001$] indicating that the addition of benthic diatoms had weak negative effects for both populations (**Figure 6B**, **Table S4**).

The females clutch sizes depended on the three-way interaction of population x resource supply x algae [$t_{(69)} = 3.02$, $p = 0.004$]. For the STHLM population, clutch sizes were unaffected by algae treatment but smaller in low resource supply. For the GOR population, clutch sizes differed between algae treatments in low resource supplies (**Figure 7A**, **Table S5**). For female prosome length (**Figure 7B**) we found no

TABLE 1 | ANOVA output from the mixed models on the relative fluorescence units.

	numDF	denDF	*F*-value	*p*-value
PELAGIC ALGAE				
Population * time	3	111.00	44.55	<0.001
Nutrients * time	3	111.00	216.41	<0.001
PELAGIC ALGAE + DIATOMS				
Population * time	3	111.00	25.24	<0.001
Nutrients * time	3	111.00	47.11	<0.001

The interactions tests for differences in the trend over time for the treatments: population and resource supply. Output of the treatments main effects, and the main effect of time are omitted.

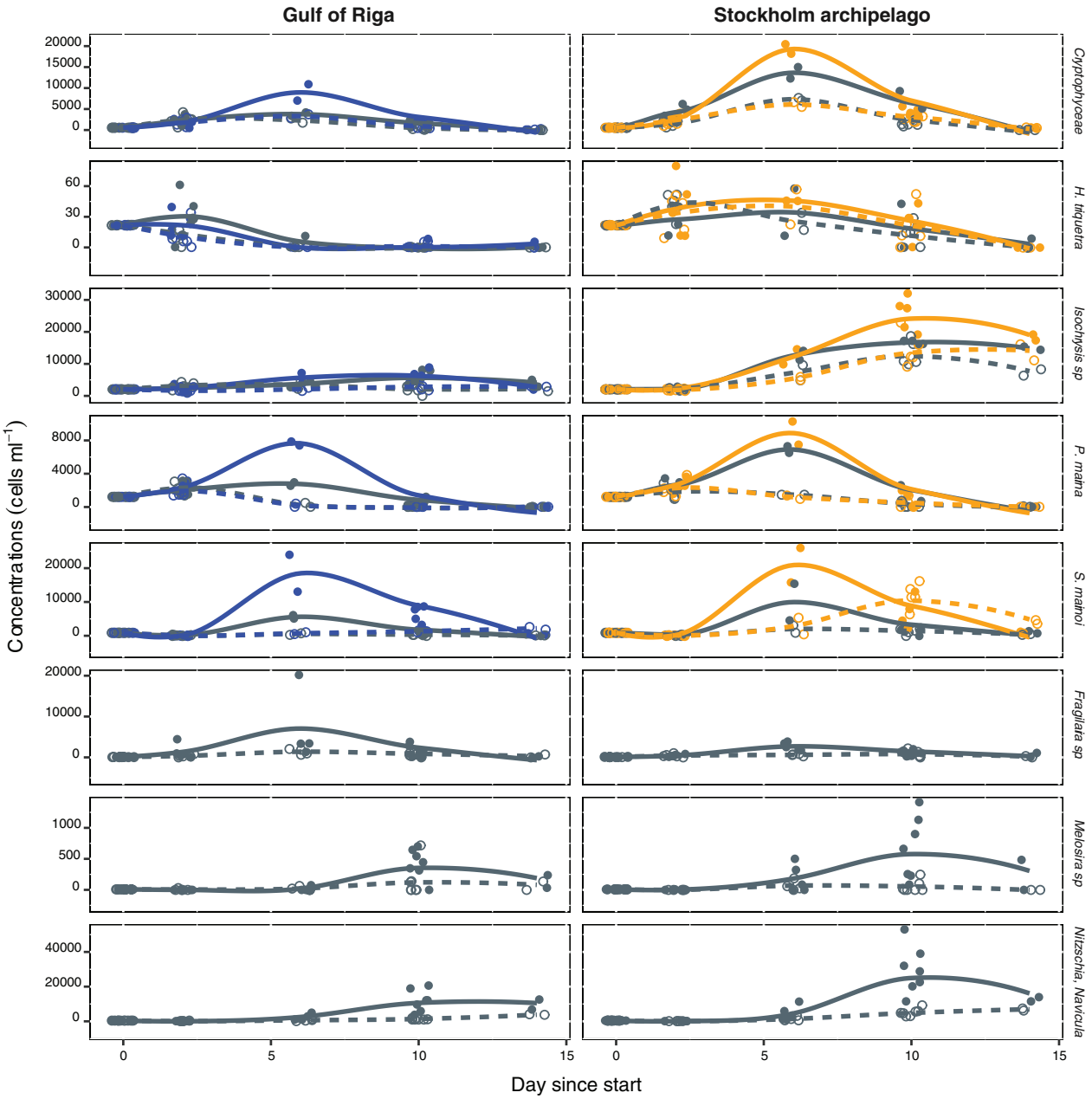

FIGURE 5 | Concentrations in cells ml^{-1} of the different algae species over time (days) in the common gardening experiment, for the treatments: algae community, nutrient level, and zooplankton population, figure head shows the *E. affinis* populations. Color, line-type, and point shape codes are: blue and orange are respective GOR and STHLM population in the pelagic algae treatment, gray is the pelagic + benthic diatom treatment (same for both populations), solid and dashed lines are respective high and low nutrient treatment, filled and open circles are respective high and low nutrient treatment. Lines are fitted by local regression by the R package `ggplot2` (Wickham, 2009), points are observed values.

interactive effects, but both the main effects of population [$t_{(74)} = 14.45$, $p < 0.001$] and resource supply were significant [$t_{(74)} = 3.87$, $p < 0.001$], whereas the effect of algae was not [$t_{(74)} = 0.19$ $p = 0.848$]. Females were generally smaller in the STHLM population compared to the GOR population, and in low resource supply compared to high resource supply.

4. DISCUSSION

In the common garden experiment we could show that the two *E. affinis* populations from the Baltic Sea differentiate genetically in female morphology and clutch size. These trait differences further affect how the populations interact with

TABLE 2 | ANOVA output from the mixed models on the pelagic algae.

	numDF	denDF	*F*-value	*p*-value
Cryptophyceae				
Population * time	3	59	25.38	< 0.001
Algae * time	3	59	23.08	0.005
Nutrients * time	3	59	4.66	< 0.001
H. tiquetra				
Population * time	3	59	9.74	< 0.001
Algae * time	3	59	0.89	0.452
Nutrients * time	3	59	0.14	0.935
***Isochrysis* sp.**				
Population * time	3	59	66.45	< 0.001
Algae * time	3	59	3.30	0.026
Nutrients * time	3	59	13.14	< 0.001
P. marina				
Population * time	3	59	6.77	< 0.001
Algae * time	3	59	6.26	< 0.001
Nutrients * time	3	59	71.38	< 0.001
S. marinoi				
Population * time	3	59	2.63	0.058
Algae * time	3	59	14.08	< 0.001
Nutrients * time	3	59	42.80	< 0.001

The interactions tests for differences in the trend over time for the treatments: population, algae, and nutrients. Output of the treatments main effects, and the main effect of time are omitted.

TABLE 3 | ANOVA output from the mixed models on the benthic algae.

	numDF	denDF	*F*-value	*p*-value
***Fragilaria* sp.**				
Population * time	3	36	1.30	0.288
Nutrients * time	3	36	2.66	0.063
***Melosira* sp.**				
Population * time	3	36	1.98	0.134
Nutrients * time	3	36	5.05	0.005
N. aurariae* + *N. perminuta				
Population * time	3	36	4.95	0.005
Nutrients * time	3	36	13.00	< 0.001

The interactions tests for differences in the trend over time for the treatments: population and nutrients. Output of the treatments main effects, and the main effect of time are omitted.

various experimental ecosystems. In general, the small-sized STHLM population was more sensitive to resource supply, whereas the large-sized GOR population was more sensitive to the type of algal community.

4.1. Common Garden Experiment: Morphology and Clutch Size

The two populations clearly differentiated in females' average shape, length, and clutch size. The differences in average length persisted from the first common garden experiment and throughout the mesocosm experiment made 2 years and ca 42 generations later. Thus, there should be little doubt that these differences are due to genetic differentiation. A previous study by Winkler et al. (2011) found neutral (mitochondrial DNA) genetic differentiation between populations from the Gulf of Riga and the Swedish Baltic coast. Our study confirms this by showing genetic differentiation in quantitative traits. There were however large individual variation within populations and individuals from the two populations overlap in shape, length and clutch size. This large morphological variation implies that whenever these two morphotypes coexists complete discrimination of the two will be difficult. The morphological variation in *E. affinis* has led to previous confusion in species classification. In Northern European estuaries two species of *Eurytemora* were described in the nineteenth century, *E. affinis* (Poppe, 1880) and *E. hirundoides* (Nordqvist, 1888). According to the taxonomic key provided by Gurney (1931) the small-sized population from the Stockholm Archipelago (STHLM) corresponds to a morphotype that was described as *E. hirundoides*. Our study shows that classification of *Eurytemora* by prosome length and fecundity can be spurious. Because these traits overlap between individuals even in genetically distinct populations in a controlled environment. Furthermore, prosome length and egg production in zooplankton are highly plastic traits that can be affected by both food conditions and temperature (Ban, 1994), which can further impede discrimination of the two populations unless they are reared under common conditions (Falconer and Mackay, 1996; Sanford and Kelly, 2010).

4.2. Common Gardening Experiment

Based on the populations different effect on RFU we concluded that the GOR population were more efficient grazers than the STHLM population, which was expected because of their larger size. We found that the pelagic flagellates and the benthic diatoms *N. aurariae* + *N. perminuta* were in lower concentrations with the GOR population than with the STHLM population. Whereas there was no difference in the concentration of the pelagic diatom *S. marinoi* between populations. Perhaps this is due to that motile flagellates can escape the copepods feeding current (Jakobsen, 2002) whereas non-motile diatoms probably cannot. In general, larger copepods have a stronger feeding current (Peters and Downing, 1984) which could be harder for flagellates to evade and explain why the GOR population is more efficient in feeding on flagellates. Given that *N. aurariae* + *N. perminuta* settle on the bottom, their lower concentrations with the GOR population suggest that this population occupy the bottom of the mesocosms to a greater extent than the STHLM population. Furthermore, the concentrations of the two largest filamentous diatoms *Melosira* sp. and *Fragilaria* sp. did not differ between the populations. Our results suggest that there is no difference in the size spectrum of resource use between the populations, despite the populations' difference in size.

We found contrasting effects on the amount of nauplii and copepodites + adults for the two populations at the end of the experiment, which depended on resource supply and algae treatment. The large-sized GOR population was a more efficient

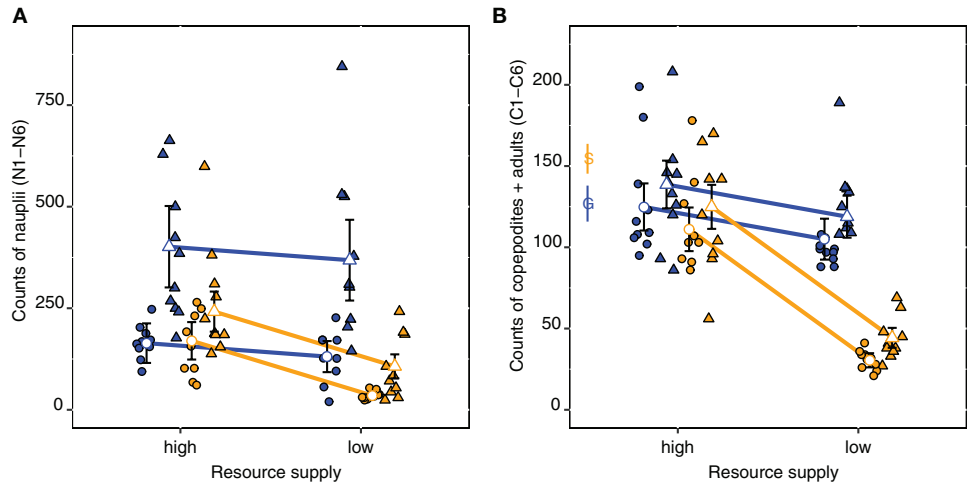

FIGURE 6 | Nauplii **(A)** and copepodites + adults **(B)** counts for the STHLM (orange) and GOR (blue) *E. affinis* populations at the end of the experiment. Triangles and circles are respective pelagic and benthic treatments, the resource supply treatment is shown on the x-axis. Estimates and 95% CI are from generalized least square models fitted with a power covariate to control for unequal variances. Observations are included as points. In **(B)** average number of individuals at start are shown with 95% CI for the STHLM and GOR populations, denoted by the letters S and G.

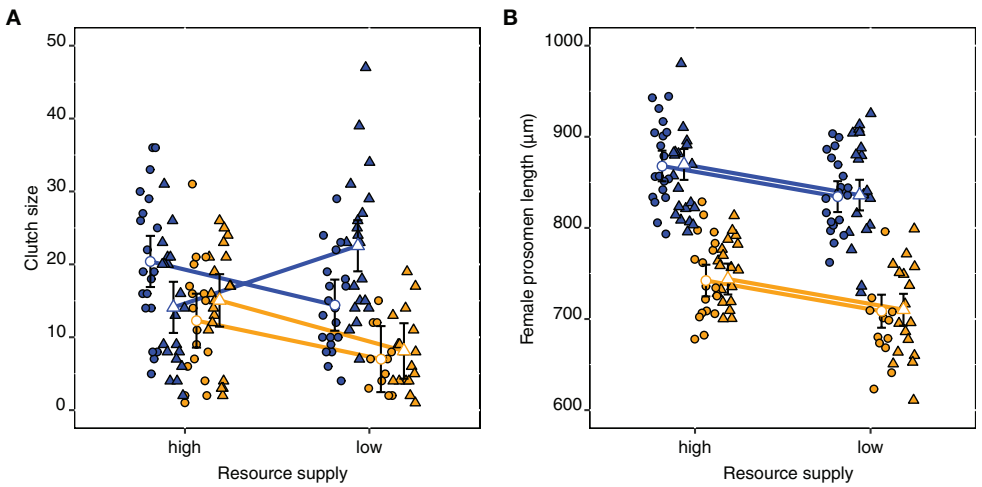

FIGURE 7 | Clutch sizes **(A)** and females prosome lengths **(B)** for the STHLM (orange) and the GOR (blue) *E. affinis* populations at the end of the experiment. Triangles and circles are respective pelagic and benthic treatments, the resource supply treatment is shown on the x-axis. Observations are included as points. Estimates and 95% CI are fitted by restricted maximum likelihood.

grazer and could therefore acquire the amount of resources needed even in low resource concentrations, which allowed them to maintain a similar population size in both high and low resource supply (**Figure 4**). In contrast, for the small-sized STHLM population, less resources resulted in a notable decrease in nauplii and copepodites + adults (**Figures 6A,B**). Larger animals are in general more efficient in resource acquisition and can feed on a wider size range of resources than smaller ones (Wilson, 1975; Gianuca et al., 2016), therefore the GOR population have a competitive advantage over the STHLM population. The STHLM population starved in the low nutrient treatment, probably because metabolic demand relative to body size is higher for smaller-sized zooplankton (Hansen et al., 1997), while both filtration and feeding rates of zooplankton increase with increasing size (Peters and Downing, 1984; Gianuca et al., 2016). Thus, the STHLM population acquires fewer resources while needing relatively more, and hence performs poorly at low resource concentrations. Our results suggest that a larger body size enables copepods to graze more efficiently and mitigate starvation at low resource concentrations.

The addition of benthic diatoms had a greater effect on the number of nauplii than on the number of copepodites +

adults, with a stronger negative effect in the presence of benthic diatoms for the GOR population than for the STHLM population. For calanoid copepods feeding on large aggregates is difficult compared to smaller particled food and can result in starvation (Koski et al., 2017). Thus, large filamentous diatoms may have disturbed the feeding process and reduced the copepods feeding efficiency. Because the GOR population was more negatively affected by benthic diatoms than the STHLM population , it suggests that females of the GOR population feed more from the bottom of the mesocosm where the filaments settled.

Differences in habitat use of *E. affinis* populations have been reported in the past and according to Gurney (1931) the GOR morphotype corresponds to "Buchtenplankton" (bay plankton) while the STHLM morphotype corresponds to "Kustenplankton" (coastal plankton). This is in agreement with the habitats where the populations were sampled. Similarly, two clades of *E. affinis* are reported from the St. Lawrence estuary. One clade mainly inhabits the inner reaches of the estuary and has invaded the Great Lakes (Winkler et al., 2008; Favier and Winkler, 2014), and has been reported as epi-benthic in the lakes (Torke, 2001). The clade in the Great Lakes have been classified as *E. carolleeae* by Vasquez et al. (2016). The other clade in St. Lawrence is mainly found in the middle parts of the estuary, suggesting that it occupies the pelagic habitat (Winkler et al., 2008; Favier and Winkler, 2014). Furthermore, epi-benthic zooplankton are often larger than pelagic zooplankton because a large size in a pelagic habitat increases the risk of predation by planktivorous fish (Brooks and Dodson, 1965). For the GOR population the larger sized females are likely prevented to enter the pelagic because of their conspicuousness, while nauplii and copepodites in the low stages likely stay closer to the surface, which is the general pattern for copepods (Irigoien et al., 2004; Casper and Thorp, 2007). This suggests that apart from morphological differences, the populations' behavior also differ.

Comparisons showed considerably smaller female clutch sizes of a European *E. affinis* population from the Seine than of two North American east coast populations assumed to be *E. carolleeae* from the St. Lawrence and the Chesapeake Bay (Beyrend-Dur et al., 2009; Devreker et al., 2012). Hence, the larger clutch size and epi-benthic behavior of the GOR population, similar to what has been reported in North American clades, suggest that this population could be the invasive *E. carolleeae*. In contrast, similar trait differences as observed in the present study have been reported between European *E. affinis* populations since the beginning of the 20th century (Gurney, 1931 and references therein, Sukhikh et al., 2016). The species name *E. carolleeae* has not been fully applied by researchers in the field. Regardless, if one categorize the *E. affinis* complex into clades (e.g., Favier and Winkler, 2014; Lee, 2016) or species (e.g., Sukhikh et al., 2013), it is important to focus on the contrasting ecological effects (e.g., freshwater invasions, habitat preferences) of adaptive variation within the *E. affinis* species complex.

Competition for nutrients between benthic diatoms and flagellates led to lower concentrations of flagellated species. However, we do not believe the lower concentrations of flagellates in the benthic algae treatment is the cause for the decline in nauplii for the GOR population. Because the resource supply treatment had no effect even in the treatments without benthic diatoms (**Figure 6A**). In contrast, the STHLM population was sensitive to resource supply, and for this population a reduction in flagellates caused by competition with benthic diatoms could explain why the nauplii count is lower when benthic diatoms were added.

4.3. Conclusion

Our study indicates that the large-sized GOR population of *E. affinis* is a superior competitor in low resource supply mainly because they can feed more efficiently on motile flagellates, than the small-sized population. However, when the resource supply is high and benthic diatoms are present, their competitive advantage disappears. We suggest that the benthic diatoms used in our study interfere in the feeding process and reduce their filtration efficiency. These results suggest that the GOR population exhibits a close relation to benthic habitats and that this morphotype is mainly found in shallow bay areas of the Baltic Sea. Apart from the morphological differences, the populations diverge in habitat choice rather than in resource specialization. We suggest that adaptive radiation in resource use is not the driver of morphological variation in *E. affinis*, but rather the trade-off between size-efficiency and vulnerability to predators. Perhaps the GOR population can afford to have a larger size because the adults stay close to the bottom. An important question for further research is to address the effects of planktivorous fish on zooplankton of different size and behavior, in pelagic vs. benthic habitats. This would highlight if the shallow littoral zone acts as a refugium for large epi-benthic morphotypes of *E. affinis*, whereas smaller morphotypes inhabit the coastal pelagic waters.

The past and current eutrophic state of the Baltic Sea (Andersen et al., 2017) may have been more advantageous for the small-sized STHLM population than the large-sized GOR population because the small-sized population has a positive response to increased resource supply. In addition eutrophication has reduced the extent of the littoral zone (Ojaveer et al., 2010) and thus the habitat for the larger-sized population. Given the area of suitable habitats, we assume that the small-sized population is by far the most common in the Baltic Sea. For example, we have only found the small-sized morphotype (i.e., none of the large extremes indicates a large-size morphotype) in samples from the central parts of Bothnian Bay, Bothnian Sea, Gulf of Finland, Gulf of Riga and the Baltic Proper (Karlsson, *personal observation*). We speculate that the large-sized morphotype is not unique to the Pärnu Bay in the Gulf of Riga, but can probably be found in similar shallow bays with outlets of freshwater along the eastern and southern Baltic Proper.

Our results show that morphologically divergent, yet phylogenetically closely related zooplankton populations can have different effects on ecosystem functions, and in turn have different population increase in response to resource supply and algae community. These results underline that the two *E. affinis* morphotypes cannot be regarded as ecologically equal in their interaction with algae communities. Furthermore, their different

habitat choice implies that the pelagic morphotype are more important for pelagic feeding fish such as herring and sprat, whereas the benthic morphotype is more important for fish species that feed in more complex littoral habitats such as perch and sticklebacks. This highlights the large morphological and life history variation in the *E. affinis* species complex and that populations affect ecosystem properties in different ways.

DATA AVAILABILITY STATEMENT

The raw data supporting the conclusions of this manuscript will be made available by the authors, without undue reservation, to any qualified researcher.

AUTHOR CONTRIBUTIONS

KK performed the experiments, analyzed the data, and wrote a first draft of the manuscript. KK and MW wrote the manuscript.

FUNDING

This is a contribution to the BONUS BIO-C3 project and was supported by BONUS (Art 185), funded jointly by the EU and the Swedish Research Council FORMAS.

ACKNOWLEDGMENTS

We thank Marilyn Kalaus and Henn Ojaveer for field collection of zooplankton, and Erika Hedlund for taking mesocosm samples. We thank the two reviewers for their comments, which improved an earlier version of this manuscript.

SUPPLEMENTARY MATERIAL

The Supplementary Material for this article can be found online at: https://www.frontiersin.org/articles/10.3389/fmars.2018.00408/full#supplementary-material

REFERENCES

Adams, D., and Otarola-Castillo, E. (2013). geomorph: an r package for the collection and analysis of geometric morphometric shape data. *Methods Ecol. Evol.* 4, 393–399. doi: 10.1111/2041-210X.12035

Alekseev, V. R., and Souissi, A. (2011). A new species within the eurytemora affinis complex (copepoda: Calanoida) from the atlantic coast of usa, with observations on eight morphologically different european populations. *Zootaxa* 2767, 41–56.

Allan, J. D. (1976). Life history patterns in zooplankton. *Am. Nat.* 110, 165–180. doi: 10.1086/283056

Andersen, J. H., Carstensen, J., Conley, D. J., Dromph, K., Fleming-Lehtinen, V., Gustafsson, B. G., et al. (2017). Long-term temporal and spatial trends in eutrophication status of the baltic sea. *Biol. Rev.* 92, 135–149. doi: 10.1111/brv.12221

Ban, S. (1994). Effect of temperature and food concentration on post-embryonic development, egg production and adult body size of calanoid copepod eurytemora affinis. *J. Plankton Res.* 16, 721–735. doi: 10.1093/plankt/16.6.721

Bassar, R. D., Marshall, M. C., López-Sepulcre, A., Zandonà, E., Auer, S. K., Travis, J., et al. (2010). Local adaptation in trinidadian guppies alters ecosystem processes. *Proc. Natl. Acad. Sci. U.S.A.* 107, 3616–3621. doi: 10.1073/pnas.0908023107

Becks, L., Ellner, S. P., Jones, L. E., and Hairston Jr, N. G. (2010). Reduction of adaptive genetic diversity radically alters eco-evolutionary community dynamics. *Ecol. Lett.* 13, 989–997. doi: 10.1111/j.1461-0248.2010.01490.x

Beyrend-Dur, D., Souissi, S., Devreker, D., Winkler, G., and Hwang, J -S. (2009). Life cycle traits of two transatlantic populations of eurytemora affinis (copepoda: Calanoida): salinity effects. *J. Plankton Res.* 31, 713–728. doi: 10.1093/plankt/fbp020

Bolnick, D. I., Svanbäck, R., Fordyce, J. A., Yang, L. H., Davis, J. M., Hulsey, C. D., et al. (2002). The ecology of individuals: incidence and implications of individual specialization. *Am. Nat.* 161, 1–28. doi: 10.1086/343878

Brooks, J. L., and Dodson, S. I. (1965). Predation, body size, and composition of plankton. *Science* 150, 28–35. doi: 10.1126/science.150.3692.28

Casper, A. F., and Thorp, J. H. (2007). Diel and lateral patterns of zooplankton distribution in the st. lawrence river. *River Res. Appl.* 23, 73–85. doi: 10.1002/rra.966

Colina, M., Calliari, D., Carballo, C., and Kruk, C. (2016). A trait-based approach to summarize zooplankton–phytoplankton interactions in freshwaters. *Hydrobiologia* 767, 221–233. doi: 10.1007/s10750-015-2503-y

Devreker, D., Pierson, J. J., Souissi, S., Kimmel, D. G., and Roman, M. R. (2012). An experimental approach to estimate egg production and development rate of the calanoid copepod eurytemora affinis in chesapeake bay, usa. *J. Exp. Mar. Biol. Ecol.* 416, 72–83. doi: 10.1016/j.jembe.2012.02.010

Diekmann, A. B. S., Clemmesen, C., John, M. A. S., Paulsen, M., and Peck, M. A. (2012). Environmental cues and constraints affecting the seasonality of dominant calanoid copepods in brackish, coastal waters: a case study of acartia, temora and eurytemora species in the south-west baltic. *Mar. Biol.* 159, 2399–2414. doi: 10.1007/s00227-012-1955-0

Engqvist, L. (2005). The mistreatment of covariate interaction terms in linear model analyses of behavioural and evolutionary ecology studies. *Anim. Behav.* 70, 967–971. doi: 10.1016/j.anbehav.2005.01.016

Falconer, D. S., and Mackay, T. F. C. (1996). *Introduction to Quantitative Genetics, 4th Edn*. Harlow: Longman.

Favier, J -B., and Winkler, G. (2014). Coexistence, distribution patterns and habitat utilization of the sibling species complex eurytemora affinis in the st lawrence estuarine transition zone. *J. Plankton Res.* 36, 1247–1261. doi: 10.1093/plankt/fbu063

Gianuca, A. T., Pantel, J. H., and De Meester, L. (2016). Disentangling the effect of body size and phylogenetic distances on zooplankton top-down control of algae. *Proc. R. Soc. B* 283:20160487. doi: 10.1098/rspb.2016.0487

Gillooly, J. F. (2000). Effect of body size and temperature on generation time in zooplankton. *J. Plankton Res.* 22, 241–251. doi: 10.1093/plankt/22.2.241

Gurney, R. (1931). *British Fresh-Water Copepoda*, Vol. 1. London: Ray Society.

Hansen, P. J., Bjørnsen, P. K., and Hansen, B. W. (1997). Zooplankton grazing and growth: scaling within the 2-2,-μm body size range. *Limnol. Oceanogr.* 42, 687–704. doi: 10.4319/lo.1997.42.4.0687

Harmon, L. J., Matthews, B., Des Roches, S., Chase, J. M., Shurin, J. B., and Schluter, D. (2009). Evolutionary diversification in stickleback affects ecosystem functioning. *Nature* 458, 1167–1170. doi: 10.1038/nature07974

Hernroth, L., and Ackefors, H. (1979). The zooplankton of the baltic proper: a long-term investigation of the fauna, its biology and ecology. *Swed. Board Fish. Inst. Mar. Res.* 20:60.

Hooper, D. U., Chapin, F., Ewel, J., Hector, A., Inchausti, P., Lavorel, S., et al. (2005). Effects of biodiversity on ecosystem functioning: a consensus of current knowledge. *Ecol. Monogr.* 75, 3–35. doi: 10.1890/04-0922

Irigoien, X., Conway, D. V., and Harris, R. P. (2004). Flexible diel vertical migration behaviour of zooplankton in the irish sea. *Mar. Ecol. Progr. Ser.* 267, 85–97. doi: 10.3354/meps267085

Jakobsen, H. H. (2002). Escape of protists in predator-generated feeding currents. *Aquat. Microb. Ecol.* 26, 271–281. doi: 10.3354/ame026271

Kiørboe, T., Møhlenberg, F., and Hamburger, K. (1985). Bioenergetics of the planktonic copepod acartia tonsa: relation between feeding, egg production and respiration, and composition of specific dynamic action. *Mar. Ecol. Progr. Ser.* 26, 85–97. doi: 10.3354/meps026085

Koski, M., Boutorh, J., and de la Rocha, C. (2017). Feeding on dispersed vs. aggregated particles: the effect of zooplankton feeding behavior on vertical flux. *PLoS ONE* 12:e0177958. doi: 10.1371/journal.pone.0177958

Lajus, D., Sukhikh, N., and Alekseev, V. (2015). Cryptic or pseudocryptic: can morphological methods inform copepod taxonomy? An analysis of publications and a case study of the eurytemora affinis species complex. *Ecol. Evol.* 5, 2374–2385. doi: 10.1002/ece3.1521

Lee, C. E. (2000). Global phylogeography of a cryptic copepod species complex and reproductive isolation between genetically proximate "populations". *Evolution* 54, 2014–2027. doi: 10.1111/j.0014-3820.2000.tb01245.x

Lee, C. E. (2016). Evolutionary mechanisms of habitat invasions, using the copepod eurytemora affinis as a model system. *Evol. Appl.* 9, 248–270. doi: 10.1111/eva.12334

Lee, C. E., and Frost, B. W. (2002). Morphological stasis in the eurytemora affinis species complex (copepoda: Temoridae). *Hydrobiologia* 480, 111–128. doi: 10.1023/A:1021293203512

Litchman, E., Ohman, M. D., and Kiørboe, T. (2013). Trait-based approaches to zooplankton communities. *J. Plankton Res.* 35, 473–484. doi: 10.1093/plankt/fbt019

Lundsgaard-Hansen, B., Matthews, B., and Seehausen, O. (2014). Ecological speciation and phenotypic plasticity affect ecosystems. *Ecology* 95, 2723–2735. doi: 10.1890/13-2338.1

Marklund, M. H., Svanbäck, R., Zha, Y., Scharnweber, K., and Eklöv, P. (2018). The influence of habitat accessibility on the dietary and morphological specialisation of an aquatic predator. *Oikos* 127, 160–169. doi: 10.1111/oik.04094

Matthews, B., De Meester, L., Jones, C. G., Ibelings, B. W., Bouma, T. J., Nuutinen, V., et al. (2014). Under niche construction: an operational bridge between ecology, evolution, and ecosystem science. *Ecol. Monogr.* 84, 245–263. doi: 10.1890/13-0953.1

Matthews, B., Hausch, S., Winter, C., Suttle, C. A., and Shurin, J. B. (2011a). Contrasting ecosystem-effects of morphologically similar copepods. *PLoS ONE* 6:e26700. doi: 10.1371/journal.pone.0026700

Matthews, B., Narwani, A., Hausch, S., Nonaka, E., Peter, H., Yamamichi, M., et al. (2011b). Toward an integration of evolutionary biology and ecosystem science. *Ecol. Lett.* 14, 690–701. doi: 10.1111/j.1461-0248.2011.01627.x

Nordqvist, O. (1888). *Die Calaniden Finlands, Vol. 47*. Helsingfors: Druckerei der Finnischen Litteratur-Gesellschaft.

Ojaveer, H., Jaanus, A., MacKenzie, B. R., Martin, G., Olenin, S., Radziejewska, T., et al. (2010). Status of biodiversity in the baltic sea. *PLoS ONE* 5:e12467. doi: 10.1371/journal.pone.0012467

Palkovacs, E. P., and Post, D. M. (2009). Experimental evidence that phenotypic divergence in predators drives community divergence in prey. *Ecology* 90, 300–305. doi: 10.1890/08-1673.1

Pantel, J. H., Duvivier, C., and Meester, L. D. (2015). Rapid local adaptation mediates zooplankton community assembly in experimental mesocosms. *Ecol. Lett.* 18, 992–1000. doi: 10.1111/ele.12480

Pau, G., Fuchs, F., Sklyar, O., Boutros, M., and Huber, W. (2010). Ebimage—an R package for image processing with applications to cellular phenotypes. *Bioinformatics* 26, 979–981. doi: 10.1093/bioinformatics/btq046

Peters, R. H., and Downing, J. A. (1984). Empirical analysis of zooplankton filtering and feeding rates. *Limnol. Oceanogr.* 29, 763–784. doi: 10.4319/lo.1984.29.4.0763

Pinheiro, J., Bates, D., DebRoy, S., Sarkar, D., and R Core Team (2017). *nlme: Linear and Nonlinear Mixed Effects Models*. R package version 3.1-131.

Poppe, S. A. (1880). Über eine neue art der calaniden-gattung Temora, Baird. *Abhandlungen-Naturwissenschaftlichen Verein zu Bremen*. 7, 55–60.

Post, D. M., and Palkovacs, E. P. (2009). Eco-evolutionary feedbacks in community and ecosystem ecology: interactions between the ecological theatre and the evolutionary play. *Proc. R. Soc. B* 364, 1629–1640. doi: 10.1098/rstb.2009.0012

Quevedo, M., Svanbäck, R., and Eklöv, P. (2009). Intrapopulation niche partitioning in a generalist predator limits food web connectivity. *Ecology* 90, 2263–2274. doi: 10.1890/07-1580.1

R Core Team (2017). *R: A Language and Environment for Statistical Computing*. Vienna: R Foundation for Statistical Computing.

Rajasilta, M., Hänninen, J., and Vuorinen, I. (2014). Decreasing salinity improves the feeding conditions of the baltic herring (clupea harengus membras) during spring in the bothnian sea, northern baltic. *ICES J. Mar. Sci.* 71, 1148–1152. doi: 10.1093/icesjms/fsu047

Rohlf, J. (2011a). *tpsRegr, Shape Regression, version 1.40*. New York, NY: Department of Ecology and Evolution, State University of New York at Stony Brook.

Rohlf, J. (2011b). *tpsUtil, File Utility Program. version 1.58*. New York, NY: Department of Ecology and Evolution, State University of New York at Stony Brook.

Rohlf, J. (2013). *tpsDig, Digitize Landmarks and Outlines, version 2.12*. New York, NY: Department of Ecology and Evolution, State University of New York at Stony Brook.

Sanford, E., and Kelly, M. W. (2010). Local adaptation in marine invertebrates. *Annu. Rev. Mar. Sci.* 3, 509–535. doi: 10.1146/annurev-marine-120709-142756

Schindler, D. E., and Scheuerell, M. D. (2002). Habitat coupling in lake ecosystems. *Oikos* 98, 177–189. doi: 10.1034/j.1600-0706.2002.980201.x

Schoener, T. W. (2011). The newest synthesis: understanding the interplay of evolutionary and ecological dynamics. *Science* 331, 426–429. doi: 10.1126/science.1193954

Sukhikh, N., Souissi, A., Souissi, S., and Alekseev, V. (2013). Invasion of eurytemora sibling species (copepoda: Temoridae) from north america into the baltic sea and european atlantic coast estuaries. *J. Nat. Hist.* 47, 753–767. doi: 10.1080/00222933.2012.716865

Sukhikh, N., Souissi, A., Souissi, S., Winkler, G., Castric, V., Holl, A. C., et al. (2016). Genetic and morphological heterogeneity among populations of eurytemora affinis (crustacea: Copepoda: Temoridae) in european waters. *C. R. Biol.* 339, 197–206. doi: 10.1016/j.crvi.2016.03.004

Torke, B. (2001). The distribution of calanoid copepods in the plankton of wisconsin lakes. *Hydrobiologia* 453, 351–365. doi: 10.1023/A:1013185916287

Vander Zanden, M. J., and Vadeboncoeur, Y. (2002). Fishes as integrators of benthic and pelagic food webs in lakes. *Ecology* 83, 2152–2161. doi: 10.2307/3072047

Vasquez, A. A., Hudson, P. L., Fujimoto, M., Keeler, K., Armenio, P. M., and Ram, J. L. (2016). Eurytemora carolleeae in the laurentian great lakes revealed by phylogenetic and morphological analysis. *J. Great Lakes Res.* 42:802. doi: 10.1016/j.jglr.2016.04.001

Walsh, M. R., DeLong, J. P., Hanley, T. C., and Post, D. M. (2012). A cascade of evolutionary change alters consumer-resource dynamics and ecosystem function. *Proc. R. Soc. B* 279, 3184–3192. doi: 10.1098/rspb.2012.0496

Wickham, H. (2009). *ggplot2: Elegant Graphics for Data Analysis*. New York, NY: Springer-Verlag.

Wilson, D. S. (1975). The adequacy of body size as a niche difference. *Am. Nat.* 109, 769–784. doi: 10.1086/283042

Winkler, G., Dodson, J. J., and Lee, C. E. (2008). Heterogeneity within the native range: population genetic analyses of sympatric invasive and noninvasive clades of the freshwater invading copepod eurytemora affinis. *Mol. Ecol.* 17, 415–430. doi: 10.1111/j.1365-294X.2007.03480.x

Winkler, G., Souissi, S., Poux, C., and Castric, V. (2011). Genetic heterogeneity among eurytemora affinis populations in western europe. *Mar. Biol.* 158, 1841–1856. doi: 10.1007/s00227-011-1696-5

Conflict of Interest Statement: The authors declare that the research was conducted in the absence of any commercial or financial relationships that could be construed as a potential conflict of interest.

frontiers in Marine Science

REVIEW
published: 12 February 2019
doi: 10.3389/fmars.2019.00040

Measures and Approaches in Trait-Based Phytoplankton Community Ecology – From Freshwater to Marine Ecosystems

Guntram Weithoff[1]* *and Beatrix E. Beisner*[2]

[1] *Department Ecology and Ecosystem Modelling, University of Potsdam, Potsdam, Germany,* [2] *Department of Biological Sciences, University of Québec à Montreal and Groupe de Recherche Interuniversitaire en Limnologie et en Environnement Aquatique, Montreal, QC, Canada*

Trait-based approaches to investigate (short- and long-term) phytoplankton dynamics and community assembly have become increasingly popular in freshwater and marine science. Although the nature of the pelagic habitat and the main phytoplankton taxa and ecology are relatively similar in both marine and freshwater systems, the lines of research have evolved, at least in part, separately. We compare and contrast the approaches adopted in marine and freshwater ecosystems with respect to phytoplankton functional traits. We note differences in study goals relating to functional trait use that assess community assembly and those that relate to ecosystem processes and biogeochemical cycling that affect the type of characteristics assigned as traits to phytoplankton taxa. Specific phytoplankton traits relevant for ecological function are examined in relation to herbivory, amplitude of environmental change and spatial and temporal scales of study. Major differences are identified, including the shorter time scale for regular environmental change in freshwater ecosystems compared to that in the open oceans as well as the type of sampling done by researchers based on site-accessibility. Overall, we encourage researchers to better motivate why they apply trait-based analyses to their studies and to make use of process-driven approaches, which are more common in marine studies. We further propose fully comparative trait studies conducted along the habitat gradient spanning freshwater to brackish to marine systems, or along geographic gradients. Such studies will benefit from the combined strength of both fields.

Keywords: algae, functional traits, ocean, lake, biogeochemistry, community assembly

OPEN ACCESS

Edited by:
Kalle Olli,
University of Tartu, Estonia

Reviewed by:
Alberto Basset,
University of Salento, Italy
Franziska Wemheuer,
University of New South Wales, Australia

***Correspondence:**
Guntram Weithoff
weithoff@uni-potsdam.de

Specialty section:
This article was submitted to Marine Ecosystem Ecology, a section of the journal Frontiers in Marine Science

Received: *30 April 2018*
Accepted: *28 January 2019*
Published: *12 February 2019*

Citation:
Weithoff G and Beisner BE (2019) Measures and Approaches in Trait-Based Phytoplankton Community Ecology – From Freshwater to Marine Ecosystems. Front. Mar. Sci. 6:40. doi: 10.3389/fmars.2019.00040

INTRODUCTION AND SOME HISTORY OF TRAIT-BASED APPROACHES IN PHYTOPLANKTON ECOLOGY

Phytoplankton has been studied for a very long time, starting with the description and identification of the diverse plethora of species. The linkage between phenotypically-based taxonomy and evolutionary history led to an initial scientifically sound categorization. Since a number of traits are linked to phylogeny, this phylogenetic categorization inherently incorporated a (weak) trait-based component (Bruggeman, 2011; Narwani et al., 2015). Moreover, long before trait-based approaches became popular, what are currently considered phytoplankton traits (e.g., edible or motile)

were commonly referred to, without explicitly using the term "trait." A good example is the conceptual narrative PEG model for seasonal lake plankton community succession that emerged as early as the 1980s (Sommer et al., 1986). This oft-referred to lake model is essentially trait-based, without using the term trait. The roots of trait-based thinking about phytoplankton are in Ramon Margalef's original work describing the "life-forms" and "functional morphologies" favorable to remaining in the water column under different nutrient conditions, irrespective of whether one considers freshwater or marine environments (Margalef, 1978). Margalef's Mandala, as it has become known, underlies much thinking on phytoplankton community assembly based on traits. Margalef's thinking formed a strong undercurrent in the pillar of the development of trait-based approaches to phytoplankton community assembly in freshwaters. Subsequently, in the 1980s, Colin Reynolds established a functional classification of lake phytoplankton assemblages based on observations from field data (summarized in Reynolds, 1997 and elaborated further in Reynolds et al., 2002). Using this classification scheme, characteristic phytoplankton communities comprised of key species were identified and related to specific environmental conditions, including season, lake trophy, lake morphometry, light availability. Within each assemblage, functionally different groups were usually represented, demonstrating that for a particular environment, complementarity through different ecological strategies or trait combinations enable thriving communities. It is from these sources that the application of trait-based thinking and theory with respect to phytoplankton has its roots, and from which it is currently rapidly expanding.

PHYTOPLANKTON TRAIT TYPES

Traits for phytoplankton have been fairly well-explored and described for both marine and freshwater ecosystem types. In freshwaters, the focus has been on lake phytoplankton, and the conceptual link back to Reynold's earlier work on functional groups (see previous section) can be directly traced in many cases. There are now essentially two schools of thought, although they are highly related. One "explicitly" defines traits as categorical, nominal or continuous and the other groups organisms by morphometric features into functional groups sometimes called "morphospecies," continuing more directly Reynold's classification. The first is common to both marine and freshwater studies while the morphospecies classification has been more commonly used only in freshwater studies, likely owing to the tradition of studying seasonal succession in these environments and less focus on biogeochemical cycling that preclude the need for high quality physiological processing rates.

Explicitly-Defined Traits

Using explicitly defined traits lends itself well to the estimation of functional diversity indicators (such as functional dispersion, richness, diversity and evenness; Weithoff, 2003; Villéger et al., 2008; Laliberté and Legendre, 2010) as well as community weighted means to characterize functional composition of communities (e.g., Beisner and Longhi, 2013; Moser et al., 2017). It also enables the examination of trade-offs between different continuously measured traits such as those associated with nutrient uptake and storage (Litchman et al., 2007; Edwards et al., 2012). All of these indicators are relevant to questions of competitive interaction between phytoplankton, interaction with predators, and thus community assembly. Explicitly-defined traits will also characterize ecosystem functioning, including processes such as primary production, trophic transfer (biomass) and nutrient cycling and this has been addressed mainly in studies relating biodiversity to ecosystem function (BEF studies) (e.g., Zwart et al., 2015; Abonyi et al., 2018).

Generally, trait matrices are created for communities of interest whereby each species is characterized by a series of explicit traits. The traits used reflect both functions related to resource acquisition (bottom–up processes) and predation (top–down processes). In the explicit framework, commonly used traits are classified by type (Litchman and Klausmeier, 2008) as follows:

> First: *Morphological*: size, biovolume, mucilage presence/absence, biological form (unicellular/colonial/coenobium/sincoenobium/filament/chains).
> Second: *Physiological*: (a) presence/absence of silica demand, heterocysts (N_2-fixation), mixotrophy, toxin production, resting stages; (b) dominant pigment type; (c) nutrient and/or light uptake parameters; (d) temperature optima.
> Third: *Behavioral*: presence/absence of flagella, aerotypes.

Generally many of these traits are based on literature or expert knowledge to classify traits, although many gaps still exist. There are new and evolving techniques to fill the data gaps on traits, mainly through the use of phylogenetic relationships (e.g., Bruggeman, 2011).

An important potential drawback with this approach, that assigns static traits to species, is that the actual expression of traits in phytoplankton may depend heavily on local (spatial and temporal) environmental conditions (but see section "Study of Communities vs. Selected Taxonomic Groups" on phenotypic plasticity). However (Violle et al., 2007), based on trait-based approaches in plants, argue that traits should be measurable on individuals independently of the environmental conditions. It is clear that such arguments do not necessarily apply in the case of the short-generation time and fast response times characteristic of phytoplankton. Notably, phytoplankton traits related to physiology may not always be expressed to the same degree, nor even active at all– for example classifying a species as a nitrogen-fixer does not characterize temporal variability in this trait that may occur in a changing environment. The next step in functional trait consideration of phytoplankton communities will be to better characterize *in situ* trait expression using genetic, biochemical or physiological probes. The challenge is doing so at the community level for the wide range of phytoplankton taxa and cells potentially present.

Morphospecies Classification

This approach is also commonly used, mainly in freshwater ecosystems in which it has roots (Reynolds et al., 2002), specifically in Reynolds (1997) trait-based "response group" classification of lake phytoplankton. Response group classification was based largely on how communities changed reliably year-to-year during seasonal succession. The morphospecies approach in particular counts, among other things, on the fact that shape (including size) affects buoyancy, uptake parameters and predator handling time and thus simplifies the original classification proposed by Reynolds (1988).

Morphospecies classification assumes that the empirical observation of the morphology of phytoplankton community constituents reflects the environmental and biotic interaction constraints on the community as well as the physiology of the organisms. It relies heavily on the idea that the morphometry of taxa reflect their autecology (physiology and functioning) (Kruk et al., 2010). Thus, like the response group approach of Reynolds (1988, 1997), it differs from the explicit trait approach in that it considers trait-mediated effects that arise from species interactions (by empirically assessing group composition) (Abonyi et al., 2018). Summarily, clusters of taxa based entirely on morphological features can be defined statistically and should represent meaningful functional phytoplankton groups.

In many ways, the original morphospecies classification resembles a reduced version of the explicitly-defined traits (Kruk et al., 2010). It was based originally on nine morphological traits including many that overlap with the previous classification: volume, maximum linear dimension, surface area, and the presence of mucilage, flagella, gas vesicles (or aero-topes), heterocysts or siliceous exoskeletal structures. Essentially, what is not found explicitly in the morphospecies approach is any explicit reference to physiological parameter rates – these are assumed (and were shown by Kruk et al., 2010) to be correlated with the morphological traits and group classification. The other difference from the explicitly-defined trait approach, is that instead of creating a *species x trait* matrix, then used to estimate functional composition or diversity, the focus here is on creating morphologically based functional groups (MBFGs) using clustering techniques. The groups thus created can then be related to environmental gradients or ecosystem functioning. In this approach, a potential short-coming however is the need to translate these morpho-groups into fitness (Naselli-Flores and Barone, 2011).

"Master" Traits

There has been a large focus on cell or body size as a "master" trait – so-called because of the large number of physiological and morphometric features that are regulated by body size. Also feedbacks with the environment are related to body size, as evident in the metabolic theory of ecology (e.g., Brown et al., 2004), which demonstrates the theoretical link between body size and ecosystem processes. Furthermore, it is recognized that body size and body size distribution (e.g., biomass size spectra) in phytoplankton communities can reflect many environmental factors such as vertical water dynamics and depth, trophic state, predation, and factors affecting growth (reviewed in Mouillot et al., 2006; Litchman and Klausmeier, 2008). It should be noted that the use of biomass size spectra has a long history in both marine and freshwater plankton studies: with older studies usually focused on estimating food web transfer efficiencies (e.g., Kerr, 1974; Gaedke, 1993; Sprules and Goyke, 1994) and not to prediction of other functional traits important for community assembly within specific groups like the phytoplankton themselves. More recent work has directly considered the relations between size spectra and effect traits such as nutrient recycling rates and in response to environmental conditions in aquatic ecosystems (e.g., Rodríguez et al., 2001) as is currently done in more explicit trait-based approaches. In phytoplankton body size is usually estimated as cell size along the maximum linear dimension (abbreviated as MLD or GALD: greatest axial linear dimension). The use of cell size is common to both the explicit trait and morphospecies frameworks and lends itself well to ecosystem modeling (e.g., Acevedo-Trejos et al., 2016).

Elemental stoichiometry of phytoplankton cells could be considered a type of "master trait" because, like size, these relationships are subject to biophysical rules that link growth rates with environments, food web interactions and thus biogeochemical cycles (Finkel et al., 2010). This consideration stems originally and largely from marine studies of phytoplankton (Finkel et al., 2010; Litchman et al., 2015), in large part due to the longer focus on biogeochemical cycles and feedbacks with phytoplankton (e.g., Follows and Dutkiewicz, 2011). Phytoplankton taxa have distinct stoichiometric ratios in both the macronutrients (e.g., C:P, N:P), but also in relation to micronutrients such as Cu, Fe, Zn, Co, Cd, and Mn; relationships that have evolved over time (reviewed in Litchman et al., 2015). Because of the strong potential effect of changes in stoichometry that would accompany changes in phytoplankton communities driven by environmental factors (other than biogeochemical ones), it is argued that the stoichiometric properties or traits of altered communities could inform on how biogeochemical processes are likely to be altered.

More recently, and in a different context, an interest in using phytoplankton to produce biofuel has lead to a fuller investigation of the stoichiometric traits in freshwater phytoplankton as well (Shurin et al., 2013, 2014). The goal has been to optimize long-term culture conditions for commercial-grade algal biofuels through the manipulation of C:N:P ratios that best optimize desired phytoplankton biomass production based on organismal requirements (stoichiometric traits).

Other Trait Types

There are a series of other trait types being developed, some focusing on more aggregate properties of communities (i.e., defined at the community and not individual level) and others focussing directly on the many individual phytoplankton present in a community. We will describe these briefly working from the aggregate community to the individual level.

Remotely-Sensed Traits

In marine ecosystems, researchers have begun to use optical properties measured from satellites to estimate overall phytoplankton community structure. Essentially, from MERIS wavelengths, bio-optical traits (BOTs) have been derived to characterize phytoplankton functional types (PFTs) (Aiken et al., 2007, 2008). Such PFTs can then be linked to the global carbon cycle using bio-mechanistic models (Aiken et al., 2008). As with other trait-based methods, estimating the functional type (PFT) from remotely sensed oceanographic data requires that a specific BOT exist for each taxon. Bio-optical traits are derived more specifically from a suite of variables: Chl-a concentration; accessory pigments (Chl-b, Chl-c, carotenoids, phycobillins); pigment ratios (TChl-a/AP, TChl-a/TP, PPC/TC); phytoplankton absorption at 443 nm ($a_{ph}443$), and the spectral slope of a_{ph}.

Pigments as Traits

Using high performance liquid chromatography (HPLC), it is possible to characterize phytoplankton communities by their pigments (e.g., Zhao and Quigg, 2014). Post-processing of HPLC results enables observation of changes in communities in terms of often highly phylogenetically conserved pigment groups. Because taxa with different pigments respond differently to the light environment, their pigment profiles can be considered as functional traits.

Cell Chemotyping for Macromolecular Traits

This method relies on the fact that there are conserved strategies in energy and C partitioning amongst phytoplankton species that can then be used to characterize their growth rate traits. Cell chemotyping can be done using Fourier transform infrared (FTIR)-spectroscopy to obtain biochemical signatures in phytoplankton cells (Fanesi et al., 2017). In this study, the authors demonstrated that the macromolecular (FTIR absorption peaks of proteins, lipids, carbohydrates, and phosphorylated compounds) composition of phytoplankton cells was able to better characterize details of cell physiology related to growth rates. In this way, a common set of physiological traits can be used to define species and it has the potential to apply to *in situ* estimates of functioning of cells, even in dynamic environments.

Scanning Flow Cytometry Traits

Another recent method applies to characterizing individual cells in a community, rather than assigning traits to all individuals in the same taxon. Thus, the focus is on intra-specific variation. The idea is to scan communities using flow cytometry to obtain a series of parameter estimates (traits) for all individual cells present in a community (Fontana et al., 2014). These traits characterize morphology (length, area) as well as fluorescence characters (chlorophyll a, accessory and degraded pigments) on the individual level, thereby allowing for intra-specific variation in these traits to be estimated.

Trait Concept Standardization

To better integrate the various ways in which traits have been defined and used for phytoplankton, recent developments have been underway to better harmonize data and allow for its interoperability (e.g., exchange between computer platforms or software). In particular the development of thesauri is occurring generally in ecology, to standardize the semantic properties for trait labels, including their definitions. For phytoplankton, the PhytoTraits thesaurus has recently been created[1] (Rosati et al., 2017). This thesaurus creates a standard definition of phytoplankton traits and their measurements that will permit better data integration across studies. A thesaurus ensures the integration amongst different datasets that use different terms for the same concept (for example biomass, weight, or dry weight; Rosati et al., 2017). Thesaurus construction uses eco-informatics approaches to acquire, integrate and analyze trait terms, developing a standard terminology or "controlled vocabulary" to which the scientific community can refer. Each term or concept obtains its own Uniform Resource Identifier (URI that is a unique, persistent internet label). New terms can then be added to thesauri such as PhytoTrait via a portal and traits labeled differently but referring to the same concept can be identified and properly classified.

Traits Used in Marine and Freshwater Research

Due to the similar nature of marine and freshwater habitats, relevant phytoplankton traits are also very similar between marine and freshwater species. The master trait size is commonly used independently of the habitat under consideration, being a unifying trait (Litchman and Klausmeier, 2008). Other, less frequently used traits, are resource use traits, e.g., nitrate acquisition (N-fixation), mixotrophy or traits related to light harvesting (Barton et al., 2013; Edwards et al., 2013). In freshwater studies, size is often expanded to a more complex measure of shape, taking morpho-functional differences between species into account (e.g., Kruk et al., 2010), often in combination with phylogenetic/taxonomic relatedness (Huszar and Caraco, 1998; Cellamare et al., 2013; Segura et al., 2013). In studies investigating the vertical structure of lakes, the pigment composition (Beisner and Longhi, 2013) and the motility of cells (by gas vacuoles or flagella) are further relevant traits (e.g., Pomati et al., 2012), likely less important in the well-mixed surface layer of the open ocean.

LITERATURE SURVEY

To better compare how trait-based approaches have been used in phytoplankton ecological research in marine and freshwater studies, we performed a literature search using the criteria "phytoplankton" AND "trait*" in the Web of Science (Clarivate Analytics) on March 7, 2018. A total of 631 entries matched our criteria; the oldest one is from 1976 (Vladimirskaya et al., 1976), taking 15 years until the next papers appeared. From that point onwards, the number of contributions increased rapidly with a total of 243 papers published in 2015–2017 on phytoplankton and trait*. We discarded > 300 papers from our subsequent analysis because the term trait was not at all related to phytoplankton or because the study did not fit into

[1] http://thesauri.lifewatchitaly.eu/PhytoTraits/index.php

the context of phytoplankton trait-based ecology. Another ca. 150 were also removed because of a lack of a community context, dealing with only a single trait or a single species, or a particular measurement technique. A total of 150 papers remained and these were grouped into marine or freshwater (lakes and rivers) studies, then classified according to study type (field observational surveys, experimental, mathematical modeling and conceptual/review) and according their research question (community assembly, response to environmental change or relations with biogeochemical cycling). A substantial number of the papers could not assigned clearly to each category, because research questions were overarching or the themes were only loosely related to our categories. Thus, the exact numbers we present are debatable, but they do indicate some overall tendencies. From the subset of 150 articles, we found an almost equal share of marine (67) and freshwater (76) studies (**Figure 1** and **Table 1**). Furthermore, there were several modeling or conceptual/review studies that were either not specific to one habitat type or explicitly dealt with both. Grouping these articles into field surveys, experimental, mathematical modeling and conceptual/review studies, it became obvious that experimental studies were underrepresented, while field surveys and mathematical modeling studies dominate the literature. Mathematical modeling studies were more commonly applied to marine ecosystems, while field studies were more often conducted in freshwater studies. This might reflect the accessibility and higher sampling frequencies of freshwater sites, but also the goal of the respective studies (see section "Comparing Freshwater and Marine Trait Studies: Assembly vs. Biogeochemistry"). This literature survey better enabled us to determine the different ways in which traits have been incorporated into the study of phytoplankton ecology in both freshwater and marine environments, which we now elaborate with some examples.

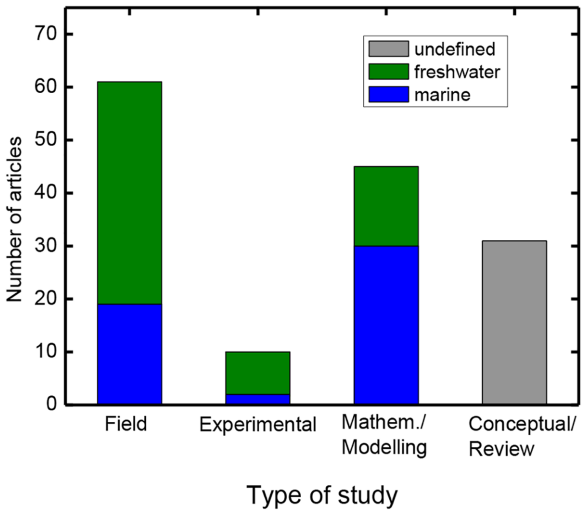

FIGURE 1 | Results of the literature search using "phytoplankton" AND "trait*." From a total 631 articles, 150 were selected that used a trait-based approach to study phytoplankton ecology. The remaining studies were assigned to four different types according to their predominant approach and according to ecosystem type. The conceptual/review articles were often not specific to a habitat type, so no further distinctions were made.

STUDY OF COMMUNITIES vs. SELECTED TAXONOMIC GROUPS

Trait-based phytoplankton studies generally consider either the whole community or focus on responses in certain phylogenetic groups such as the diatoms or other major phyla. Whole community studies from freshwater sites typically analyze seasonal dynamics or a component of temporal variation, such as the spring bloom, using classical phylogenetic (taxonomic) approaches. A trait component, such as cell size as a master trait, or some measures of functional diversity based on functional traits is sometimes added to broaden the view. However, such studies do not focus on a trait-based approach *per se* making it difficult to group them unambiguously into our categories.

Another aspect in community studies is the analysis of spatial (mostly vertical) differences in communities from stratified environments (e.g., Longhi and Beisner, 2010; Santana et al., 2017). Often the response to environmental changes or a detailed analysis of the traits within a particular taxonomic group (representing a particular set of traits) has been the focus. For example, diatoms represent a phylogenetic group common to both marine and freshwater studies. They are abundant in lakes, rivers and oceans alike, and play an important role in food webs and the biogeochemical cycles. As a result, their trait distribution and the consequences for diatom dynamics have been commonly studied in both ecosystem types (e.g., Terseleer et al., 2014; B-Béres et al., 2017; Taherzadeh et al., 2017). Diatoms come with the added advantage that they preserve in sediments and can thus be the focus of longer-term paleo-limnological or paleo-oceanographic analyses (Smol et al., 2005; McKay et al., 2012). In marine studies dinoflagellates and coccolithophores represent other target groups. For dinoflagellates, important traits relate either to toxin production or to mixotrophy, for coccolithophores relevant traits relate to the tolerance to ocean acidification (see section "Genotypic Trait Plasticity").

TRAIT VARIABILITY: GENOTYPIC vs. PHENOTYPIC

An important, though often neglected, aspect in the quantification of traits is the phenotypic and genotypic plasticity of traits. Plasticity or trait variation is difficult to measure, but it is important for the parametrization of mathematical models and for the understanding of community processes on timescales relevant for phytoplankton ecology.

Phenotypic Trait Plasticity

Many traits can vary substantially according to environmental conditions. While some traits can be measured on individuals (e.g., body size), some are more amenable to measurement at the community level, representing the average of a population of

TABLE 1 | Summary of the focus of the 73 trait-based studies examining entire (or a majority of groups within) phytoplankton communities.

Research perspective	Marine	Freshwater	Marine/freshwater	Estuaries
Effects of the environment on trait assembly or dynamics	8	29	1	3
Trait interactions on community structure or dynamics	7	6	3	0
Traits on ecosystem function or its biogeography	8	3	2	0
Other topics	1	1	1	0
Total	24	39	7	3

Note in some studies, the focus could not clearly assigned to one of the categories.

individuals, such as nutrient ratios or physiological traits. Size, as a master trait (see section "Phytoplankton Trait Types"), is related to many ecological processes, but it can also be highly variable. To account for cell size variation within a phytoplankton population or community and over extended periods, modern techniques now exist, although not regularly utilized to assess size variation, including flow cytometry or related systems that also provide images (e.g., Flow-CAM, CytoBOT).

Body size variation, in addition to being easy to measure, is ecological very relevant in phytoplankton and thus often considered in ecological studies. For example, because zooplankton herbivory is often size-selective, a selective pressure on distinct prey size classes is introduced, thereby changing the size distribution of a population or community (Sommer et al., 2001; Lewandowska et al., 2014). Furthermore, in freshwater ecosystems, it has been observed that the mere presence of the herbivore *Daphnia*, can induce changes in the colony size of their algal prey driven by kairomones, even without any herbivory (Hessen and VanDonk, 1993). In another example, the physiological status of phytoplankton cells can also drive their body sizes and thus the variation observed in a population or community: during the regular cell growth cycle the size of the cells might vary by a factor of two or even more (Massie et al., 2010). With increasing nutrient limitation, the cell cycle arrests at a certain limiting nutrient concentration and it continues only under nutrient replete conditions, which may synchronize a population's cell size to a smaller value (Massie et al., 2010). Body size in diatoms is a particularly interesting case of size variation. Diatoms reduce their average cell size through progressive population growth, because after cell division the newly-built theca is formed from the inner (smaller) part of the mother theca leading to a continuous cell size reduction of one of the daughter cells (Lee, 1999). Associated to a smaller body size is an increase in the surface to volume ratio, facilitating the nutrient uptake per unit of volume (Reynolds, 1997).

Physiological traits also vary in response to environmental changes. A common strategy is the optimization of resource use efficiency. This includes an increase in chlorophyll-*a* or other photosynthetic pigments by phytoplankton cells to better collect photons at low light availabilities or spectral discontinuities (Richardson et al., 1981; Falkowski and LaRoche, 1991). Another example is the production of the enzyme nitrogenase under nitrogen limiting conditions, which enables the fixation of elementary nitrogen. An increasing nitrogenase activity is typically found with increasing duration of nitrogen-depleted conditions (e.g., Paerl, 1988).

Genotypic Trait Plasticity

Traits and trait values not only vary in response to environmental factors but also among different genotypes within a population. Information on genotypic trait variation is surprisingly rare and often stems from research in other fields than trait-based ecology. We can draw on several examples involving phytoplankton. First, with respect to toxicity, different strains of potentially toxic algae have been analyzed to understand the mechanisms and physiological costs behind toxin production. In marine habitats, dinoflagellates (e.g., *Alexandrium*) are the most prominent toxic group, while cyanobacteria (e.g., *Microcystis* and others) are the main toxin producers in freshwaters. Within one species, the ability and magnitude of toxin production among different strains varies considerably, making it difficult to assign this trait to a species (Ichimi et al., 2002; Kardinaal et al., 2007; Touzet et al., 2008). Another source for information on trait plasticity comes from invasion biology: invasive species usually regarded as species with a high genotypic plasticity facilitating their establishment in newly invaded habitats. For the invasive cyanobacterium *Cylindrospermopsis,* high genotypic trait variability is notable (Willis et al., 2016; Bolius et al., 2017). Genotypic variation in phytoplankton also comes from global change research as it is related to ocean acidification. The response of coccolithophores to declining pH-levels has been shown to be strain-specific (Müller et al., 2015; Rickaby et al., 2016) and varies at different times scales (Meyer and Riebesell, 2015; Schlüter et al., 2016). Differentiating between such short-term strain-specific acclimation and long-term adaptation makes it difficult to predict community responses to ocean acidification.

Consequences for Trait-Based Modeling

For several applications of trait-based approaches, trait variability might not be a serious disadvantage, as for example with respect to aspects of community assembly in relatively stable environments. However, for modeling ecosystem processes or species interactions more directly and on shorter timescales, the variability in traits may be critical. However, not only does the variability itself complicate trait-based modeling (Coutinho et al., 2016), but the shape of the trait distribution also plays an important role (Gaedke and Klauschies, 2018). The shape of the trait distribution determines the potential for adaptive responses to environmental change. For example, when environmental forces act specifically on a certain trait and a distinct range of the trait values, a bimodal trait distribution might permit a more sustainable response option relative to a normal trait distribution, especially if the pressure is imposed around the mean. A great

deal more work will be necessary to establish the distributions of highly variable individual phytoplankton traits to inform these modeling approaches.

COMPARING FRESHWATER AND MARINE TRAIT STUDIES: ASSEMBLY vs. BIOGEOCHEMISTRY

Narrowing our literature survey subset of 150 articles further, by including only those studies that had either a broad spatial (many samples over a broader area) or temporal scale (time series data), as well as those that considered the entire (or a substantial part of the) phytoplankton community under a trait-based view, 73 articles remained. The majority were freshwater studies, with 29 dealing mostly with environmental factors driving community assembly or temporal dynamics when assessed using traits (perspective 1, **Table 1** and **Supplementary Table S1**). Other studies at the community level examined trait distributions more directly by focusing on interactions between them and how this could influence community structure or dynamics (without explicit consideration of environmental variation). This group (perspective 2, **Table 1**) was more evenly split between marine and freshwater environments (6–7 per environment). On the other hand, studies that focused more directly on ecosystem consequences of traits (perspective 3, **Table 1**), including ecosystem biogeography and biogeochemical processes including stoichiometry, were much less numerous (total of 13), with the majority (8) from marine environments and another two combining freshwater and marine. Irrespective of research perspective, a total of seven studies used trait-based approaches in marine and freshwaters together, and three considered estuaries.

Generally speaking, for phytoplankton, the nature of the pelagic habitat as well as the main representative phyla and their ecology are relatively similar across both marine and freshwater ecosystems. Despite this similarity, research questions and approaches have evolved, at least in part, separately, in the two environments. One crucial difference between these ecosystem types is the accessibility and the possibility to take frequent samples. For many lakes, routine sampling campaigns are regularly conducted, either by local authorities or scientific institutes and universities. Thus, many data sets with some temporal resolution and good physico-chemical background data exist. In comparison, less data exists for coastal regions, and regular, high temporal resolution biological sampling in open ocean sites is very rare (but see Buitenhuis et al., 2013; Brun et al., 2015).

Traditionally, much ecological research was performed at field stations investigating the on-site environment. This is particularly the case for freshwater biological stations, many of which were established to combine monitoring and research, often in relation to water utilities and providers related to drinking water, fisheries or recreational uses. For these purposes, water quality and phytoplankton community composition has been extensively studied, with frequent and regular sampling of the pelagic food web, to ensure the management of drinking water quality and quantity or of fish harvest. At marine biological stations, local sites have also been sampled, although they have served primarily as entry points to understanding the open ocean, for which cruises are expensive and do not allow for regular sampling.

These different ecosystem accessibility and scientific histories are mirrored in the different research questions addressed in phytoplankton trait-based studies in freshwater and marine systems. Trait-based studies from the open ocean preferentially investigate biogeographic trait patterns (Acevedo-Trejos et al., 2013; Barton et al., 2013) or they have a strong biogeochemical focus aiming for the quantification of globally important processes related to primary production such as carbon-dioxide acquisition, nitrogen fixation (Breton et al., 2017), or oceanic stoichiometry and biochemistry (Litchman et al., 2007, 2015; Strom, 2008; Finkel et al., 2010; Bonachela et al., 2016), but also on phytoplankton dynamics (Alexander et al., 2015) (**Figure 2**). In oceanography, many studies model trait-based processes, aiming for broad-scale extrapolation of these globally (Smith et al., 2016; Vallina et al., 2017). From a conceptual point of view, marine research considers how traits and trait distribution drive processes determining the environmental conditions (e.g., biogeochemistry).

In the more accessible coastal or freshwater sites such as lakes, the conceptual view is often in the opposite direction (**Figure 2**), considering instead how phytoplankton communities respond to the environment and which environmental factors drive the trait-based community assembly. Answers to these research questions rely on a sampling regime with a high temporal resolution. A prominent example for a coastal long-term sampling site is the Western Channel Observatory site in the English Channel off the coast of Plymouth, United Kingdom (Edwards et al., 2013; Mutshinda et al., 2017). Coastal sites that are influenced by the tide or estuaries are subjected to rapid environmental changes so that the response to such changes became into the focus of the investigations (Aubry et al., 2017; Klais et al., 2017; Moser et al., 2017). On a similar time-scale, lakes (and rivers) are also characterized by rapid environmental changes and studies on these systems thus often deal with trait-driven responses to these by the community. Longer-term studies that consider several

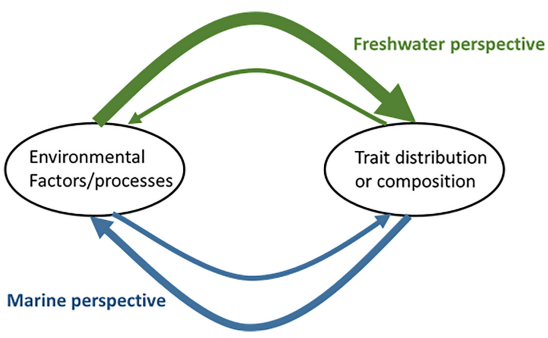

FIGURE 2 | Schematic of the pre-dominant perspectives in marine and freshwater phytoplankton trait-based research. Line thickness indicates the relative number of studies.

months or years are highly suitable to these types of questions, especially when similar environmental changes are repeated during the investigation, representing a form of temporal replication (Pomati et al., 2012; Edwards et al., 2013; Tsai et al., 2014; Weithoff et al., 2015; Bortolini et al., 2016; Weithoff and Gaedke, 2017). Alternatively, instead of temporal replication, trait-based approaches also enable a space-for-time substitution in which many sites receiving a similar environmental signal (e.g., sites along a coastal or river stretch or lakes within the same region) are sampled only once or a very few times (Longhi and Beisner, 2010; Machado et al., 2016; Santana et al., 2017; Vadrucci et al., 2017). Trait-based approaches become particularly helpful in such cases, as they are ataxonomic, facilitating the detection of common response patterns within these potentially disparate communities. Another aspect of freshwater trait-based studies is the analysis of the vertical distribution of phytoplankton (Pomati et al., 2012; Beisner and Longhi, 2013; Santana et al., 2017), when steep physical-chemical gradients exist. One drawback we noted in several studies is that they lack a clear rationale as to why they use trait-based approaches in relation to the ecological goals (as also argued by Hébert et al., 2017 for zooplankton). Clearly outlined goals related to improved understanding of community assembly vs. contributions of phytoplankton to biogeochemical cycles should be a part of every study that uses trait-based approaches.

RECOMMENDATIONS AND CONCLUSION

Similarities and differences in phytoplankton trait-based approaches between marine and freshwater studies can be identified by the ways in which traits are assigned and the focus of the primary research questions to which traits are applied. With respect to trait assignment, two related schools of thought exist, either "explicitly" defining several species' traits simultaneously so that there is little overlap between taxa, or by restricting classification to "morphospecies" types, continuing more directly Reynold's earlier classification. Explicitly-defined traits are commonly used in both marine and freshwater studies, while morphospecies classification has been more commonly used in freshwater habitats. We attribute this difference to the tradition of studying seasonal succession and community assembly under varying environmental conditions in highly accessible freshwater environments that preempts the need for higher resolution physiological processing rates. Marine studies often focus on globally relevant biogeochemical cycles, for which key process-related traits are studied on the most abundant taxa, especially coccolithophores, diatoms, dinoflagellates and prochlorophytes. In general, researchers are encouraged to better motivate, why they apply trait-based analyses to their studies. They will benefit from applying the strong process-driven approaches used in most marine studies to investigate the relationship between traits and biogeochemical processes. Marine researchers might benefit from the mechanistic approaches used by freshwater researchers to better understand community assembly using traits, if more resolved time-series data can be obtained through autonomous buoys or remote sensing. As another avenue of future research, we propose fully comparative trait studies conducted along the habitat gradient spanning freshwater to brackish to marine systems. Such studies can combine the strengths of both fields and would be of general ecological interest. Other comparative studies could analyze latitudinal, altitudinal, or trophic gradients using phytoplankton traits as a common currency to assess community structure. In some cases, data likely already exist to conduct these studies. Given the low number of experimental studies we noted in our literature survey, it would be very useful to test the field survey patterns more explicitly in manipulated experiments, such as in mesocosms, to ascertain mechanisms influencing trait distribution and expression. Last, but not least, a common challenge for future research in both systems remains to account for within-species trait variation, a critical component to trait-based studies in all aquatic habitats, especially in an era of rapid environmental change.

AUTHOR CONTRIBUTIONS

All authors listed have made a substantial, direct and intellectual contribution to the work, and approved it for publication.

FUNDING

BEB was supported by the Alexander von Humboldt-Stiftung.

SUPPLEMENTARY MATERIAL

The Supplementary Material for this article can be found online at: https://www.frontiersin.org/articles/10.3389/fmars.2019.00040/full#supplementary-material

TABLE S1 | List of articles that had either a broad spatial (many samples over a broader area) or temporal scale (time series data), as well as those that considered the entire (or a substantial part of the) phytoplankton community under a trait-based view; sorted by year.

REFERENCES

Abonyi, A., Horvath, Z., and Ptacnik, R. (2018). Functional richness outperforms taxonomic richness in predicting ecosystem functioning in natural phytoplankton communities. *Freshwat. Biol.* 63, 178–186. doi: 10.1111/fwb.13051

Acevedo-Trejos, E., Brandt, G., Merico, A., and Smith, S. L. (2013). Biogeographical patterns of phytoplankton community size structure in the oceans. *Glob. Ecol. Biogeogr.* 22, 1060–1070. doi: 10.1038/srep08918

Acevedo-Trejos, E., Brandt, G., Smith, S. L., and Merico, A. (2016). PhytoSFDM version 1.0.0: phytoplankton size and functional diversity model. *Geosci. Model. Dev.* 9, 4071–4085. doi: 10.5194/gmd-9-4071-2016

Aiken, J., Fishwick, J. R., Lavender, S., Barlow, R., Moore, G. F., Sessions, H., et al. (2007). Validation of MERIS reflectance and chlorophyll during the BENCAL cruise October 2002: preliminary validation of new demonstration products

for phytoplankton functional types and photosynthetic parameters. *Internat. J. Rem. Sens.* 28, 497–516. doi: 10.1080/01431160600821036

Aiken, J., Hardman-Mountford, N. J., Barlow, R., Fishwick, J., Hirata, T., and Smyth, T. (2008). Functional links between bioenergetics and bio-optical traits of phytoplankton taxonomic groups: an overarching hypothesis with applications for ocean colour remote sensing. *J. Plankton Res.* 30, 165–181. doi: 10.1093/plankt/fbm098

Alexander, H., Rouco, M., Haley, S. T., Wilson, S. T., Karl, D. M., and Dyhrman, S. T. (2015). Functional group-specific traits drive phytoplankton dynamics in the oligotrophic ocean. *Proc. Natl. Acad. Sci. U.S.A.* 112, E5972–E5979. doi: 10.1073/pnas.1518165112

Aubry, F. B., Pugnetti, A., Roselli, L., Stanca, E., Acri, F., Finotto, S., et al. (2017). Phytoplankton morphological traits in a nutrient-enriched, turbulent mediterranean microtidal lagoon. *J. Plankton Res.* 39, 564–576. doi: 10.1093/plankt/fbx008

Barton, A. D., Pershing, A. J., Litchman, E., Record, N. R., Edwards, K. F., Finkel, Z. V., et al. (2013). The biogeography of marine plankton traits. *Ecol. Lett.* 16, 522–534. doi: 10.1111/ele.12063

B-Béres, V., Török, P., Kókai, Z., Lukács, A., T-Krasznai, E., Tóthmérészc, B., et al. (2017). Ecological background of diatom functional groups: comparability of classification systems. *Ecol. Indic.* 82, 183–188. doi: 10.1016/j.ecolind.2017.07.007

Beisner, B. E., and Longhi, M. L. (2013). Spatial overlap in lake phytoplankton: relations with environmental factors and consequences for diversity. *Limnol. Oceanogr.* 58, 1419–1430. doi: 10.4319/lo.2013.58.4.1419

Bolius, S., Wiedner, C., and Weithoff, G. (2017). High local trait variability in a globally invasive cyanobacterium. *Freshwat. Biol.* 62, 1879–1890. doi: 10.1111/fwb.13028

Bonachela, J. A., Klausmeier, C. A., Edwards, K. F., Litchman, E., and Levin, S. A. (2016). The role of phytoplankton diversity in the emergent oceanic stoichiometry. *J. Plankton Res.* 38, 1021–1035. doi: 10.1093/plankt/fbv087

Bortolini, J. C., Moresco, G. A., de Paula, A. C. M., Jati, S., and Rodrigues, L. C. (2016). Functional approach based on morphology as a model of phytoplankton variability in a subtropical floodplain lake: a long-term study. *Hydrobiologia* 767, 151–163. doi: 10.1007/s10750-015-2490-z

Breton, E., Christaki, U., Bonato, S., Didry, M., and Artigas, L. F. (2017). Functional trait variation and nitrogen use efficiency in temperate coastal phytoplankton. *Mar. Ecol. Prog. Ser.* 563, 35–49. doi: 10.3354/meps11974

Brown, J. H., Gillooly, J. F., Allen, A. P., Savage, V. M., and West, G. B. (2004). Towards a metabolic theory in ecology. *Ecology* 85, 1771–1789. doi: 10.1890/03-9000

Bruggeman, J. (2011). A phylogenetic approach to the estimation of phytoplankton traits. *J. Phycol.* 47, 52–65. doi: 10.1111/j.1529-8817.2010.00946.x

Brun, P., Vogt, M., Payne, M. R., Gruber, N., O'Brien, C. J., Buitenhuis, E. T., et al. (2015). Ecological niches of open ocean phytoplankton taxa. *Earth Syst. Sci. Data* 5, 227–239. doi: 10.3389/fmicb.2012.00362

Buitenhuis, E. T., Vogt, M., Moriarty, R., Bednaršek, N., Dones, J. C., Leblanc, L., et al. (2013). MAREDAT: towards a world atlas to MARin ecosystem DATa. *Earth Syst. Sci. Data* 5, 227–239. doi: 10.5194/essd-5-227-2013

Cellamare, M., de Tezanos Pinto, P., Leitão, M., Coste, M., Boutry, S., and Haury, J. (2013). Using functional approaches to study phytoplankton communities in a temperate region exposed to tropical species dispersal. *Hydrobiologia* 702, 267–282. doi: 10.1007/s10750-012-1330-7

Coutinho, R. M., Klauschies, T., and Gaedke, U. (2016). Bimodal trait distributions with large variances question the reliability of trait-based aggregate models. *Theor. Ecol.* 9, 389–408. doi: 10.1007/s12080-016-0297-9

Edwards, K. F., Litchman, E., and Klausmeier, C. A. (2013). Functional traits explain phytoplankton community structure and seasonal dynamics in a marine ecosystem. *Ecol. Lett.* 16, 56–63. doi: 10.1111/ele.12012

Edwards, K. F., Thomas, M. K., Klausmeier, C. A., and Litchman, E. (2012). Allometric scaling and taxonomic variation in nutrient utilization traits and maximum growth rate of phytoplankton. *Limnol. Oceanogr.* 57, 554–566. doi: 10.4319/lo.2012.57.2.0554

Falkowski, P. G., and LaRoche, J. (1991). Acclimation to spectral irradiance in algae. *J. Phycol.* 27, 8–14. doi: 10.1111/j.0022-3646.1991.00008.x

Fanesi, A., Wagner, H., and Wilhelm, C. (2017). Phytoplankton growth rate modelling: can spectroscopic cell chemotyping be superior to physiological predictors? *Proc. R. Soc. B.* 284:20161956. doi: 10.1098/rspb.2016.1956

Finkel, Z. V., Beardall, J., Flynn, K. J., Quigg, A., Rees, T. A. V., and Raven, J. A. (2010). Phytoplankton in a changing world: cell size and elemental stoichiometry. *J. Plankton Res.* 32, 119–137. doi: 10.1093/plankt/fbp098

Follows, M. J., and Dutkiewicz, S. (2011). Modeling diverse communities of marine microbes. *Ann. Rev. Mar. Sci.* 3, 427–451. doi: 10.1146/annurev-marine-120709-142848

Fontana, S., Jokela, J., and Pomati, F. (2014). Opportunities and challenges in deriving phytoplankton diversity measures from individual trait-based data obtained by scanning flow-cytometry. *Front. Microbiol.* 5:324. doi: 10.3389/fmicb.2014.00324

Gaedke, U. (1993). Ecosystem analysis based on biomass size distribution – a case study of a plankton community in a large lake. *Limnol. Oceanogr.* 38, 112–127. doi: 10.4319/lo.1993.38.1.0112

Gaedke, U., and Klauschies, T. (2018). Analyzing the shape of observed trait distributions enables a data-based moment closure of aggregate models. *Limnol. Oceanogr. Methods* 15, 979–994. doi: 10.1002/lom3.10218

Hébert, M.-P., Beisner, B. E., and Maranger, R. (2017). Linking zooplankton communities to ecosystem functioning: toward an effect-trait framework. *J. Plankton Res.* 39, 3–12. doi: 10.1093/plankt/fbw068

Hessen, D. O., and VanDonk, E. (1993). Morphological changes in *Scenedesmus* induced by substances released by *Daphnia*. *Arch. Hydrobiol.* 127, 129–140.

Huszar, V. L. M., and Caraco, N. (1998). The relationship between phytoplankton composition and physical-chemical variables: a comparison of taxonomic and morphological-functional approaches in six temperate lakes. *Freshwat. Biol.* 40, 679–696. doi: 10.1046/j.1365-2427.1998.00369.x

Ichimi, K., Suzuki, T., and Ito, A. (2002). Variety of PSP toxin profiles in various culture strains of *Alexandrium tamarense* and change of toxin profile in natural A. tamarense population. *J. Exp. Mar. Biol. Ecol.* 273, 51–60. doi: 10.1016/S0022-0981(02)00137-5

Kardinaal, W. E. A., Tonk, L., Janse, I., Hol, S., Slot, P., Huisman, J., et al. (2007). Competition for light between toxic and nontoxic strains of the harmful cyanobacterium *Microcystis*. *Appl. Environm. Microbiol.* 73, 2939–2946. doi: 10.1128/AEM.02892-06

Kerr, S. R. (1974). Theory of size distribution in ecological communities. *J. Fish. Res. Board Canada* 31, 1859–1862. doi: 10.1139/f74-241

Klais, R., Norros, V., Lehtinen, S., Tamminen, T., and Olli, K. (2017). Community assembly and drivers of phytoplankton functional structure. *Funct. Ecol.* 31, 760–767. doi: 10.1111/1365-2435.12784

Kruk, C., Huszar, V. L. M., Peeters, E. T. H. M., Bonilla, S., Costa, L., Lürling, M., et al. (2010). A morphological classification capturing functional variation in phytoplankton. *Freshwat. Biol.* 55, 614–627. doi: 10.1111/j.1365-2427.2009.02298.x

Laliberté, E., and Legendre, P. (2010). A distance-based framework for measuring functional diversity from multiple traits. *Ecology* 91, 299–305. doi: 10.1890/08-2244.1

Lee, R. E. (1999). *Phycology*. Cambridge: Cambridge University Press.

Lewandowska, A. M., Hillebrand, H., Lengfellner, K., and Sommer, U. (2014). Temperature effects on phytoplankton diversity - The zooplankton link. *J. Sea Res.* 85, 359–364. doi: 10.1016/j.seares.2013.07.003

Litchman, E., and Klausmeier, C. A. (2008). Trait-based community ecology of phytoplankton. *Ann. Rev. Ecol. Evol. Syst.* 39, 615–639. doi: 10.1146/annurev.ecolsys.39.110707.173549

Litchman, E., Klausmeier, C. A., Schofield, O. M., and Falkowski, P. G. (2007). The role of functional traits and trade-offs in structuring phytoplankton communities: scaling from cellular to ecosystem level. *Ecol. Lett.* 10, 1170–1181. doi: 10.1111/j.1461-0248.2007.01117.x

Litchman, E., Pinto, P. D., Edwards, K. F., Klausmeier, C. A., Kremer, C. T., and Thomas, M. K. (2015). Global biogeochemical impacts of phytoplankton: a trait-based perspective. *J. Ecol.* 103, 1384–1396. doi: 10.1111/1365-2745.12438

Longhi, M. L., and Beisner, B. E. (2010). Patterns in taxonomic and functional diversity of lake phytoplankton. *Freshwat. Biol.* 55, 1349–1366. doi: 10.1111/j.1365-2427.2009.02359.x

Machado, K. B., Teresa, F. B., Vieira, L. C. G., Huszar, V. L. D., and Nabout, J. C. (2016). Comparing the effects of landscape and local environmental variables on taxonomic and functional composition of phytoplankton communities. *J. Plankton Res.* 38, 1334–1346. doi: 10.1093/plankt/fbw062

Margalef, R. (1978). Life forms of phytoplankton as survival alternatives in an unstable environment. *Oceanologia Acta* 1, 493–509.

Massie, T. M., Blasius, B., Weithoff, G., Gaedke, U., and Fussmann, G. F. (2010). Cycles, phase synchronization, and entrainment in single-species phytoplankton populations. *Proc. Natl. Acad. Sci. U.S.A.* 107, 4236–4241. doi: 10.1073/pnas.0908725107

McKay, R., Naish, T., Carter, L., Riesselmann, C., Dunbar, R., Sjunneskog, C., et al. (2012). Antarctic and Southern Ocean influences on Late Pliocene global cooling. *Proc. Natl. Acad. Sci. U.S.A.* 109, 6423–6428. doi: 10.1073/pnas.1112248109

Meyer, J., and Riebesell, U. (2015). Reviews and syntheses: responses of coccolithophores to ocean acidification: a meta-analysis. *Biogeosciences* 12, 1671–1682. doi: 10.5194/bg-12-1671-2015

Moser, G. A. O., Piedras, F. R., Oaquim, A. B. J., Souza, D. S., Leles, S. G., de Lima, D. T., et al. (2017). Tidal effects on phytoplankton assemblages in a near-pristine estuary: a trait-based approach for the case of a shallow tropical ecosystem in Brazil. *Mar. Ecol.* 38:4. doi: 10.1111/maec.12450

Mouillot, D., Spatharis, S., Reizopoulou, S., Laugier, T., Sabetta, L., Basset, A., et al. (2006). Alternatives to taxonomic-based approaches to assess changes in transitional water communities. *Aquat. Conserv. Mar. Freshw. Syst.* 16, 469–482. doi: 10.1002/aqc.769

Müller, M. N., Trull, T. W., and Hallegraeff, G. M. (2015). Differing responses of three Southern Ocean *Emiliania huxleyi* ecotypes to changing seawater carbonate chemistry. *Mar. Ecol. Prog. Ser.* 531, 81–90. doi: 10.3354/meps11309

Mutshinda, C. M., Finkel, Z. V., Widdicombe, C. E., and Irwin, A. J. (2017). Phytoplankton traits from long-term oceanographic time-series. *Mar. Ecol. Prog. Ser.* 576, 11–25. doi: 10.3354/meps12220

Narwani, A., Alexandrou, M. A., Herrin, J., Vouaux, A., Zhou, C., Oakley, T. H., et al. (2015). Common ancestry is a poor predictor of competitive traits in freshwater green algae. *PLoS One* 10:9. doi: 10.1371/journal.pone.0137085

Naselli-Flores, L., and Barone, R. (2011). Fight on plankton! Or, phytoplankton shape and size as adaptive tools to get ahead in the struggle for life. *Cryptogam. Algol.* 32, 157–204. doi: 10.7872/crya.v32.iss2.2011.157

Paerl, H. W. (1988). "Growth and reproductive strategies of freshwater blue-green algae (Cyanobacteria)," in *Growth and Reproductive Strategies in Freshwater Phytoplankton*, ed. C. D. Sandgren (Cambridge: Cambridge University Press), 261–315.

Pomati, F., Matthews, B., Jokela, J., Schildknecht, A., and Ibelings, B. (2012). Effects of re-oligotrophication and climate warming on plankton richness and community structure in a deep mesotrophic lake. *Oikos* 121, 1317–1327. doi: 10.1111/j.1600-0706.2011.20055.x

Reynolds, C. S. (1988). "Functional morphology and the adaptive strategies of freshwater phytoplankton," in *Growth and Reproductive Strategies in Freshwater Phytoplankton*, ed. C. D. Sandgren (Cambridge: Cambridge University Press), 388–433.

Reynolds, C. S. (1997). *Vegetation Processes in the Pelagic: A Model for Ecosystem Theory*. Luhe: Ecology Institute.

Reynolds, C. S., Huszar, V., Kruk, C., Naselli-Flores, L., and Melo, S. (2002). Towards a functional classification of the freshwater phytoplankton. *J. Plankton Res.* 24, 417–428. doi: 10.1093/plankt/24.5.417

Richardson, K., Beardall, J., and Raven, J. A. (1981). Adaptation of unicellular algae to irradiance: an analysis of strategies. *New Phytol.* 93, 157–191. doi: 10.1111/j.1469-8137.1983.tb03422.x

Rickaby, R. E. M., Hermoso, M., Lee, R. B. Y., Rae, B. D., Heureux, A. M. C., Balestreri, C., et al. (2016). Environmental carbonate chemistry selects for phenotype of recently isolated strains of *Emiliania huxleyi*. *Deep Sea Res. II* 127, 28–40. doi: 10.1016/j.dsr2.2016.02.010

Rodríguez, J., Tintoré, J., Allen, J. T., Blanco, J. M., Gomis, D., Reul, A., et al. (2001). Mesoscale vertical motion and the size structure of phytoplankton in the ocean. *Nature* 410, 360–363. doi: 10.1038/35066560

Rosati, I., Bergami, C., Stanca, E., Roselli, L., Tagliolato, P., Oggioni, A., et al. (2017). A thesaurus for phytoplankton trait-based approaches: development and applicability. *Ecol. Inform.* 42, 129–138. doi: 10.1016/j.ecoinf.2017.10.014

Santana, L. M., Weithoff, G., and Ferragut, C. (2017). Seasonal and spatial functional shifts in phytoplankton communities of five tropical reservoirs. *Aquat. Ecol.* 51, 531–543. doi: 10.1007/s10452-017-9634-3

Schlüter, L., Lohbeck, K. T., Gröger, J. P., Riebesell, U., and Reusch, T. B. H. (2016). Long-term dynamics of adaptive evolution in a globally important phytoplankton species to ocean acidification. *Sci. Adv.* 2:e1501660. doi: 10.1126/sciadv.1501660

Segura, A. M., Kruk, C., Calliari, D., and Fort, H. (2013). Use of morphology-based functional approach to model phytoplankton community succession in a shallow subtropical lake. *Freshw. Biol.* 58, 504–512. doi: 10.1111/j.1365-2427.2012.02867.x

Shurin, J. B., Abbott, R. L., Deal, M. S., Kwan, G. T., Litchman, E., McBride, R. C., et al. (2013). Industrial-strength ecology: trade-offs and opportunities in algal biofuel production. *Ecol. Lett.* 16, 1393–1404. doi: 10.1111/ele.12176

Shurin, J. B., Mandal, S., and Abbott, R. L. (2014). Trait diversity enhances yield in algal biofuel assemblages. *J. Appl. Phycol.* 51, 603–611. doi: 10.1111/1365-2664.12242

Smith, S. L., Pahlow, M., Merico, A., Acevedo-Trejos, E., Sasai, Y., Yoshikawa, C., et al. (2016). Flexible phytoplankton functional type (FlexPFT) model: size-scaling of traits and optimal growth. *J. Plankton Res.* 38, 977–992. doi: 10.1093/plankt/fbv038

Smol, J. P., Wolfe, A. P., Birks, H. J. B., Douglas, M. S. V., Jones, V. J., Korhola, A., et al. (2005). Climate-driven regime shift in the biological communities of arctic lakes. *Proc. Natl. Acad. Sci. U.S.A.* 102, 4397–4402. doi: 10.1073/pnas.0500245102

Sommer, U., Gliwicz, Z. M., Lampert, W., and Duncan, A. (1986). The PEG-model of seasonal succession of planktonic events in fresh waters. *Arch. Hydrobiol.* 106, 433–471.

Sommer, U., Sommer, F., Santer, B., Jamieson, C., Boersma, M., Becker, C., et al. (2001). Complementary impact of copepods and cladocerans on phytoplankton. *Ecol. Lett.* 4, 545–550. doi: 10.1046/j.1461-0248.2001.00263.x

Sprules, W. G., and Goyke, A. P. (1994). Size-based structure and production in the pelagia of Lakes Ontario and Michigan. *Can. J. Fish. Aquat. Sci.* 51, 2603–2611. doi: 10.1139/f94-260

Strom, S. L. (2008). Microbial ecology of ocean biogeochemistry: a community perspective. *Science* 320, 1043–1045. doi: 10.1126/science.1153527

Taherzadeh, N., Kerimoglu, O., and Wirtz, K. W. (2017). Can we predict phytoplankton community size structure using size scalings of eco-physiological traits? *Ecol. Model.* 360, 279–289. doi: 10.1016/j.ecolmodel.2017.07.008

Terseleer, N., Bruggeman, J., Lancelot, C., and Gypens, N. (2014). Trait-based representation of diatom functional diversity in a plankton functional type model of the eutrophied southern North Sea. *Limnol. Oceanogr.* 59, 1958–1972. doi: 10.4319/lo.2014.59.6.1958

Touzet, N., Franco, J. M., and Raine, R. (2008). Morphogenetic diversity and biotoxin composition of *Alexandrium* (Dinophyceae) in Irish coastal waters. *Harmful Algae* 7, 782–797. doi: 10.1016/j.hal.2008.04.001

Tsai, C.-H., Miki, T., Chang, C.-W., Ishikava, K., Ichise, S., Kumagai, M., et al. (2014). Phytoplankton functional group dynamics explain species abundance distribution in a directionally changing environment. *Ecology* 95, 3335–3343. doi: 10.1890/13-1946.1

Vadrucci, M. R., Barbone, E., Ungaro, N., Romano, A., and Bucci, R. (2017). Application of taxonomic and morpho-functional properties of phytoplankton communities to water quality assessment for artificial lakes in the Mediterranean Ecoregion. *J. Plankton Res.* 39, 550–563. doi: 10.1093/plankt/fbx011

Vallina, S. M., Cermeno, P., Dutkiewicz, S., Loreau, M., and Montoya, J. M. (2017). Phytoplankton functional diversity increases ecosystem productivity and stability. *Ecol. Model.* 361, 184–196. doi: 10.1016/j.ecolmodel.2017.06.020

Villéger, S., Mason, N. W. H., and Mouillot, D. (2008). New multidimensional functional indices for a multifaceted framework in functional ecology. *Ecology* 89, 2290–2301. doi: 10.1890/07-1206.1

Violle, C., Navas, M.-L., Vile, D., Kazakou, E., Fortunel, C., Hummel, I., et al. (2007). Let the concept of trait be functional! *Oikos* 116, 882–892. doi: 10.1111/j.0030-1299.2007.15559.x

Vladimirskaya, E. V., Makarov, R. R., Maslennikov, V. V., and Movchan, O. A. (1976). Some traits of phytoplankton distribution. *Okeanologyia* 16, 1069–1075.

Weithoff, G. (2003). The concepts of 'plant functional types' and 'functional dversity' in lake phytoplankton – a new understanding of phytoplankton ecology? *Freshwat. Biol.* 48, 1669–1675. doi: 10.1046/j.1365-2427.2003.01116.x

Weithoff, G., and Gaedke, U. (2017). Mean functional traits of lake phytoplankton reflect seasonal and inter-annual changes in nutrients, climate and herbivory. *J. Plankton Res.* 39, 509–517.

Weithoff, G., Rocha, M. R., and Gaedke, U. (2015). Comparing seasonal dynamics of functional and taxonomic diversity reveals the driving forces underlying phytoplankton community structure. *Freshw. Biol.* 60, 758–767. doi: 10.1111/fwb.12527

Willis, A., Chuang, A. W., Woodhouse, J. N., Neilan, B. A., and Burford, M. A. (2016). Intraspecific variation in growth, morphology and toxin quotas for the cyanobacterium, *Cylindrospermopsis raciborskii*. *Toxicon* 119, 307–310. doi: 10.1016/j.toxicon.2016.07.005

Zhao, Y., and Quigg, A. (2014). Nutrient Limitation in Northern Gulf of Mexico (NGOM): phytoplankton communities and photosynthesis respond to nutrient pulse. *PLoS One* 9:e88732. doi: 10.1371/journal.pone.0088732

Zwart, J. A., Solomon, C. T., and Jones, S. E. (2015). Phytoplankton traits predict ecosystem function in a global set of lakes. *Ecology* 96, 2257–2264. doi: 10.1890/14-2102.1

Conflict of Interest Statement: The authors declare that the research was conducted in the absence of any commercial or financial relationships that could be construed as a potential conflict of interest.

frontiers in Marine Science

METHODS
published: 27 September 2017
doi: 10.3389/fmars.2017.00317

Manipulation of Non-random Species Loss in Natural Phytoplankton: Qualitative and Quantitative Evaluation of Different Approaches

Friederike G. Engel[1], Aleksandra M. Lewandowska[2], Sarah L. Eggers[3] and Birte Matthiessen[1]*

[1] Experimental Ecology-Food Webs, Marine Ecology, GEOMAR Helmholtz Centre for Ocean Research, Kiel, Germany, [2] Institute for Chemistry and Biology of the Marine Environment, Carl von Ossietzky University of Oldenburg, Oldenburg, Germany, [3] Hustedt Diatom Study Centre, Polar Biological Oceanography, Alfred Wegener Institute Helmholtz Centre for Polar and Marine Research, Bremerhaven, Germany

Ecological research in recent decades revealed that species loss has a predominantly negative effect on ecosystem functioning and stability. Most of these studies were based on random species loss scenarios, but extinctions in nature are not random. Recent experimental studies using macroscopic communities largely advanced knowledge about the effects of non-random species loss. However, in microscopic communities like the phytoplankton, implementing realistic species loss scenarios is challenging and experimental data are scarce. Creating more realistic experiments to study the role of phytoplankton diversity for ecosystem functioning is particularly important, as they provide up to 50% of global primary productivity, form the basis of all pelagic food webs, and are important for biogeochemical cycling. In this study, we experimentally tested and evaluated three methods for non-random species loss in a natural marine phytoplankton community. Dilution, filtration, and heat stress removed the targeted rare, large, and sensitive species, respectively. All these species groups are extremely vulnerable to extinction in future climate scenarios and play important roles in the communities. Dilution and filtration with a fine mesh additionally decreased initial biomass, which increased the variability of species left in the respective replicates. The methods tested in this study can be used to non-randomly manipulate phytoplankton species diversity in communities used for experiments. However, in studies where species identities are more important than species richness, the dilution and filtration methods should be modified to eliminate the effect of decreasing initial biomass.

Keywords: phytoplankton, non-random species loss, realistic species loss, species loss manipulation, extinction

OPEN ACCESS

Edited by:
Kristian Spilling, Finnish Environment Institute (SYKE), Finland

Reviewed by:
Maria Stockenreiter, Fakultät für Biologie, Ludwig-Maximilians-Universität München, Germany
Punyasloke Bhadury, Indian Institute of Science Education and Research Kolkata, India

****Correspondence:***
Friederike G. Engel
fengel@geomar.de

Specialty section:
This article was submitted to Marine Ecosystem Ecology, a section of the journal Frontiers in Marine Science

Received: *20 July 2017*
Accepted: *19 September 2017*
Published: *27 September 2017*

Citation:
Engel FG, Lewandowska AM, Eggers SL and Matthiessen B (2017) Manipulation of Non-random Species Loss in Natural Phytoplankton: Qualitative and Quantitative Evaluation of Different Approaches. Front. Mar. Sci. 4:317. doi: 10.3389/fmars.2017.00317

INTRODUCTION

Over the last centuries, humans have increasingly influenced and modified all ecosystems on planet Earth. Habitat destruction, the emission of greenhouse gases, and the introduction of non-native species led to species loss rates comparable to historic mass extinction events (Barnosky et al., 2011). A large number of experimental studies tested the effects of species loss on different ecosystem processes. They uncovered a generally negative effect of species loss on ecosystem functioning

and stability (Hooper et al., 2005; Cardinale et al., 2012). Depending on the magnitude of species loss, its effect size on ecosystem functioning is comparable to those arising from direct effects of environmental factors, such as acidification or nutrient pollution (Hooper et al., 2012). To date, in most diversity manipulation experiments, researchers altered species richness by randomly adding species to or excluding them from communities (Bracken and Low, 2012; Mensens et al., 2015; Radchuk et al., 2015). However, loss of species in natural communities is not random, but depends on a multitude of factors including population size (i.e., rarity), body size, and sensitivity to environmental stress (Gross and Cardinale, 2005). Previous research showed that the effects of biodiversity loss on ecosystem functioning can largely differ in randomly assembled communities compared to communities experiencing non-random species loss (Solan et al., 2004; Bracken et al., 2008; Mensens et al., 2015).

Manually removing or adding target species is feasible in communities with larger and substrate-bounded organisms, such as in grasslands (Zavaleta and Hulvey, 2004; Selmants et al., 2012, 2014) or the marine benthos (Bracken et al., 2008; Stachowicz et al., 2008; Bracken and Low, 2012). However, in microbial communities, such as phytoplankton, the manipulation of non-random species loss from natural communities is particularly challenging. A recent laboratory experiment with freshwater phytoplankton showed that it is possible to create communities with distinct species richness gradients using different levels of dilution and disturbance (Hammerstein et al., 2017). Nevertheless, technically it is nearly impossible to remove certain target species or groups from a natural microbial community without significantly altering the overall organism density. Hence, such diversity manipulations are prone to be confounded with a hidden density treatment, which can have two major consequences. First, it can directly affect the total biomass which is often used as a measure for ecosystem functioning. Second, it can enhance the variability of which species are remaining in a treated community and thus indirectly affect ecosystem functioning. To date the latter problem remains largely unquantified, so that the effects of realistic changes in phytoplankton diversity on ecosystem functioning in experiments remain essentially unknown (Gamfeldt et al., 2015).

Even though extinctions in the oceans are not as common as on land, and direct extinctions caused by humans were less often recorded for marine organisms, the influence humans have on aquatic ecosystems is immense and will likely continue to increase (McCauley et al., 2015). In particular for marine phytoplankton, that contribute almost 50% to global primary production (Field et al., 1998) and play an important role in biogeochemical cycling (Falkowski et al., 1998), future changes in biodiversity remain speculative.

In the present study, we tested different methods to non-randomly remove rare, large and sensitive species from natural phytoplankton communities. These methods can be employed to manipulate community composition before the onset of an experiment or they can be used as factors in the experiment to create different levels of species composition. In the following section we elaborate on the rationale behind focusing on these particular groups.

Loss of Rare Species

Rare species are often characterized by small population sizes, narrow geographical ranges and little genetic variation within populations (Rabinowitz, 1981; Frankham, 2005; Harnik et al., 2012). These characteristics in combination with stochastic processes make rare species more likely to go extinct than common species (Lande, 1993; Frankham, 2005; O'Grady et al., 2006; Leitão et al., 2016). Due to numerical disadvantages, rarity is often accompanied by competitive inferiority which can lead to extinction by competitive exclusion. An example of competitive inferiority can be seen in the context of priority effects, where the first colonizers exhibit a numerical advantage such that they can exclude later arriving species by monopolizing shared resources (Urban and De Meester, 2009; de Meester et al., 2016). Priority effects can also happen at the onset of a phytoplankton bloom. Eggers and Matthiessen (2013) showed experimentally that the initial structure of a phytoplankton community influenced the identity of the respective dominant species at bloom peak.

Despite their increased risk of extinction, rare species are important in communities because they can maintain ecosystem functions under changing environmental conditions when they substitute for dominant species that are lost or decline in numbers (Walker et al., 1999; Norberg et al., 2001; Elmqvist et al., 2003; Lyons et al., 2005; Mouillot et al., 2013; Jain et al., 2014; Leitão et al., 2016; Jousset et al., 2017). Hence, manipulating the loss of rare species in bloom building phytoplankton can provide important information about possible future scenarios, in which these species might be lost at disproportionally high rates.

Loss of Large Species

Experiments and observations have shown that rising seawater temperatures lead to the reduction of average cell size in phytoplankton communities (Morán et al., 2010; Peter and Sommer, 2012; Sommer et al., 2012). Though the underlying reasons are not completely understood yet, current research suggests that it is partly driven by decreased nutrient availability in the euphotic layer of the oceans due to stronger stratification under warmer conditions (Hofmann et al., 2011; Winder and Sommer, 2012; Acevedo-Trejos et al., 2014; Lewandowska et al., 2014). This situation benefits smaller-sized cells. Small cells have more efficient nutrient uptake rates because they have more favorable surface area to volume ratios (Aksnes and Egge, 1991; Raven, 1998; Mara-ón, 2014). Additionally, experiments have attributed the increase in smaller phytoplankton cell sizes with warming to trophic interactions. Depending on the preferred size spectrum of the prey, more intense grazing by zooplankton under higher temperatures can lead to the reduction in average phytoplankton cell size in a community (Sommer and Lewandowska, 2011). Since smaller cell size has been proposed to be one of the universal responses to global warming for aquatic organisms (Daufresne et al., 2009), testing the effect of losing larger species from phytoplankton communities can be very important for future phytoplankton diversity experiments.

Loss of Sensitive Species and Potential Interaction with Rarity

Species are considered sensitive when they have a narrow environmental optimum and therefore steep reaction norms. They are generally very susceptible to changes in the environment including a variety of biotic and abiotic factors, such as salinity, pH, and temperature. In this study, we tested the effect of losing heat sensitive species, because one of the major changes in the future ocean is predicted to be an increase in the average surface ocean temperature (IPCC, 2014). Many species that are sensitive to environmental change are at the same time low in their abundance, because they have very specialized habitat requirements (Davies et al., 2004). Therefore, we additionally combined the loss of sensitive and rare species as one of the treatments, a valuable addition to the experimental design as it can improve our understanding of the mechanisms underlying sensitive species loss.

The aim of this study was to test the immediate effects of the above described non-random species loss scenarios on a natural phytoplankton community and to evaluate their impact on diversity change at bloom peak. Additionally, we aimed to qualitatively analyze how far the manipulations led to increased variability in species identities present in the communities (i.e., whether the methods manipulated the loss of the same species among replicates).

MATERIALS AND METHODS

Experimental Set-Up

The experimental units consisted of white polypropylene buckets filled with 25 L of sterile filtered (0.2 μm) seawater that we collected from the Kiel Fjord (Kiel, Germany) in March 2013. At that time it was possible to obtain nutrient-rich winter water with dissolved inorganic nutrient concentrations of 30.73 μmol L^{-1} nitrate and nitrite ($NO_3 + NO_2$), 0.77 μmol L^{-1} phosphate (PO_4), and 34.77 μmol L^{-1} silicate (SiO_4).

We distributed the experimental units randomly in two temperature controlled rooms (10°C) that were equipped with computer-programmed ceiling light units (Econlux, Hibay LED 100 W, full sun-light spectrum) providing light from above and creating an underwater light intensity of 130 μmol m^{-2} s^{-1} and a light-dark cycle of 16:8 h. This corresponded to the local irradiance levels in Kiel Fjord at the time of the year the experiment was conducted (Brock, 1981).

Depending on the treatment, we inoculated the experimental units with different volumes of a natural phytoplankton stock community that was collected shortly before the experimental start from surface waters of the Kiel Fjord, Germany in April 2013 at the onset of spring bloom. To exclude meso-grazers (copepods) from the experiment, we pre-filtered the stock community with a 200 μm sieve. For a detailed description of treatment application see section Manipulation of Different Species Loss Scenarios and **Table 1**.

We stirred the water body of each experimental unit carefully once per day to ensure a homogenous distribution of the phytoplankton in the experimental units. To prevent airborne particle transport into the experimental units, but still allowing for oxygen exchange and light penetration, we loosely covered the buckets with transparent polyethylene foil.

Manipulation of Different Species Loss Scenarios

We applied three methods (dilution, filtration, and heat stress), resulting in five treatments (**Table 1**): **control** (*Co*–no manipulation), **dilution** to remove rare species (two levels: *D1*–weak dilution, *D2*–strong dilution), **filtration** to remove large species (two levels: *F1*–coarse filtration, *F2*–fine filtration), **heat stressed** (*S*) to remove heat sensitive species, and **dilution of heat stressed** to simultaneously remove sensitive and rare species (two levels: *SxD1*–weak dilution of heat stressed, *SxD2*–strong dilution of heat stressed). Each treatment level and combination was 4-fold replicated which resulted in 32 experimental units in total.

In order to lose temperature sensitive species prior to the experimental onset, we separated the collected and pre-filtered stock community into two temperature treatments (control (10°C) = non-heated stock community; heat stress (22°C) = heated stock community). We chose 22°C, because it represents a critical temperature for many Baltic Sea auto- and heterotrophs (Reusch et al., 2005; Eggers et al., 2012; Werner et al., 2016). The stock communities were stored in closed glass bottles (Duran, 2,500 mL) in climate cabinets for 24 h. After 24 h, we inoculated

TABLE 1 | Overview of the experimental design with treatment names and levels, abbreviations, and how the treatments were realized.

Treatment name	Treatment level	Abbrev.	Treatment description	Added inoculum	Target species
Control		(*Co*)	No manipulation	10 mL of non-heated stock community	none
Dilution	weak	(*D1*)	10% concentration of control inoculum	1 mL of non-heated stock community	rare
	strong	(*D2*)	1% concentration of control inoculum	0.1 mL of non-heated stock community	rare
Filtration	coarse	(*F1*)	Filtration through 100 μm sieve	10 mL of filtered non-heated stock community	large
	fine	(*F2*)	Filtration through 20 μm sieve	10 mL of filtered non-heated stock community	large
Heat stressed		(*S*)	Heat stressed with 22°C for 24 h	10 mL of heat stressed stock community	sensitive
Dilution of heat stressed	weak	(*SxD1*)	10% concentration of heat stressed inoculum	1 mL of heat stressed stock community	rare and sensitive
	strong	(*SxD2*)	1% concentration of heat stressed inoculum	0.1 mL of heat stressed stock community	rare and sensitive

The last column shows which species groups were targeted for removal.

the experimental units according to the different treatments (**Table 1**). For the control (*Co*), we added 10 mL of the non-heated stock community. We applied the two levels of the dilution treatment by adding inocula of 1 and 0.1 mL of the non-heated stock community, resulting in 10% (*D1*) and 1% (*D2*) of the control concentrations, respectively. For the two levels of the filtration treatment, we filtered the non-heated stock community with 100 µm (*F1*) and 20 µm (*F2*) sieves, respectively. 10 mL of the respective filtrates were added to the experimental units. For the heat stressed treatment (*S*), we added 10 mL of the heated stock community to the experimental units. To prepare the combined treatment of heat stress and dilution, we added inocula of 1 and 0.1 mL of the heated stock community to achieve 10% (*SxD1*) and 1% (*SxD2*) concentrations of the heat stressed treatment, respectively. For an overview of all treatments, treatment levels and combinations as well as their respective inocula volumes see **Table 1**.

To assess if the targeted species were actually lost due to the specific diversity manipulations, we classified each species as at least one of the following four categories: common, rare, large, and sensitive (**Table 2**, **Figure 1**). We based these categorizations on species abundances (common or rare species) and cell sizes (large species) obtained microscopically from a 100 mL sample of the non-heated stock community. Additionally, we microscopically determined species abundances in a 100 mL sample of the heated stock community to define sensitive species. For a detailed overview of the categorizations see **Table 2**.

Because phytoplankton species often belong to more than one of the above defined four categories, overlapping species were placed as shown in **Figure 1**. Since the sample that we initially analyzed for the control treatment already represented a dilution of the total species pool present in the stock community, it did not contain the full set of phytoplankton species at the onset of the experiment. More precisely, we found single individuals of some species in initial samples of specific treatments but not in the control. We defined these species as rare (**Figure 1**). Resulting from this, we based the qualitative assessment of the initial loss of target species caused by the treatments on the total species pool of 30 species. In addition, we related the quantitative assessment of how many species were effectively lost in the treatments to the control.

TABLE 2 | Categorization of species into separate groups based on 100 mL samples analyzed of the control (non-heated stock community) and heat stressed treatment (heated stock community).

Category	Abbrev.	Criteria for grouping	Reference sample
Common	C	>1% contribution to total community biomass and >100 cells	control
Rare	R	<1% contribution to total community biomass and <100 cells	control
Large	L	average of largest cell dimension exceeds 20 µm (corresponding to the mesh size of the fine filtration sieve)	control
Sensitive	Se	At least 75% decrease in species biomass compared to the control	heat stressed

Sampling and Analysis

We sampled phytoplankton twice over the course of the experiment: at the onset of the experiment (initial), and after the community had reached stationary phase (bloom peak). To determine when each community had reached the stationary phase, we took daily fluorescence measurements with a fluorometer (Turner Designs 10AU^{TM} Field Fluorometer). We applied a sigmoidal growth model (Equation 1) to confirm the exact developmental stage of the bloom:

$$f_t = \frac{a}{1 + \left[\frac{a-b}{b}\right] e^{-\mu t}} \quad (1)$$

where f_t is the relative fluorescence after t days, a is the maximum relative fluorescence (carrying capacity), b is the starting relative fluorescence, and µ is the growth rate. The treatments reached their termination point when the growth curve of at least one replicate of that treatment significantly fit the model for three consecutive days. At this time, the other replicates of the treatment had reached stationary phase and we sampled all replicates of the same treatment. We took the last samples 18 days after starting the experiment, corresponding to approximately 9–18 microalgae generations. We preserved the phytoplankton samples in Lugol's iodine solution and stored them in the dark until further processing. To determine phytoplankton cell numbers and biovolume, we counted the samples using an inverted microscope after Utermöhl (1958). For the initial samples (i.e., at the onset of the experiment), we examined a 100 mL sample of each treatment. This corresponded to cell abundances ranging from approximately 200 (*D2*, *SxD2*) to over 14,000 (*Co*, *S*) cells counted (see Supplementary Table 1). Identifications were made to the species level when

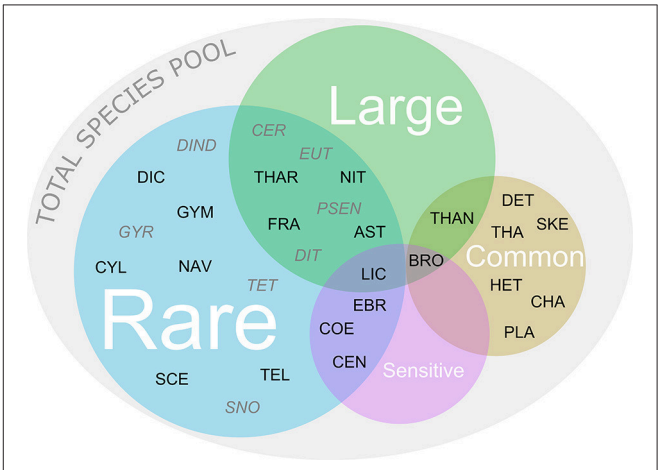

FIGURE 1 | Categorization of common, rare, sensitive, and large species initially present in the total species pool. Combinations of more than one category are displayed as overlapping areas in the Venn diagram. For abbreviations of species names and their initial relative biomass in each treatment see Supplementary Table 2. The black letters show species that were initially present in the control. The gray italic letters show species that were initially not present in the control but found in other treatments.

possible, otherwise genera were determined. Based on procedures described in Hillebrand et al. (1999), we calculated species-specific cell biovolume by approximating cell shapes to simple geometric bodies. By summing up species specific biovolumes, we calculated the total biovolume of a sample, which is used as a proxy for total biomass hereafter.

To compare phytoplankton communities, we calculated species richness, Pielou's evenness (Pielou, 1966) and Bray-Curtis dissimilarity (Bray and Curtis, 1957; Clarke et al., 2006) using the *vegan* package in R version 3.2.3 (Oksanen et al., 2017; R Core Team, 2017). The latter two were calculated based on species-specific biomass data. For the bloom peak samples, we computed Bray-Curtis dissimilarity both as average within (B-C_{intra}) and between (B-C_{inter}) treatments. For the initial samples, we could only calculate B-C_{inter}, because we did not have any replication of the inocula. Therefore, the initial samples could only be compared quantitatively. Taking multiple sub-samples at this point would have led to pseudo-replication. To compare treatments at bloom peak, we performed a multi-factorial ANOVA in R 3.2.3 (R Core Team, 2017). We tested the main effects of the categorical factors dilution, filtration and heat stress as well as the interaction of dilution and heat stress on species richness, Pielou's evenness (J'), and within-treatment variation (B-C_{intra}). Evenness and dissimilarity data were log-transformed to increase normality and account for non-homogenous variance distribution, respectively. We performed *post-hoc* tests (Tukey HSD) to specify which treatments significantly differed from one another. Finally, we created multi-dimensional scaling (MDS) plots based on the Bray-Curtis dissimilarity matrix in Primer 6 (Clarke and Gorley, 2006).

RESULTS

Initial Treatment Effects

All diversity manipulations initially decreased species richness by at least two species compared to the control (**Figure 2A**). We found the strongest declines in initial richness in the dilution

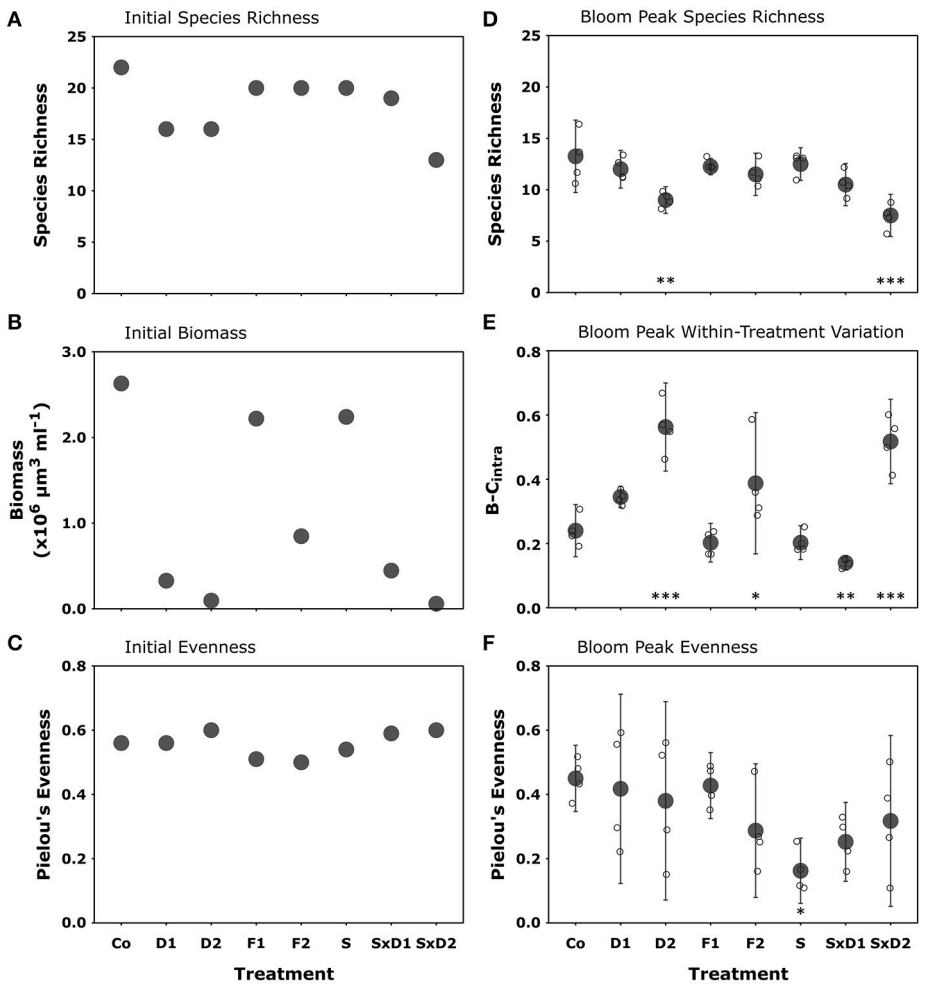

FIGURE 2 | Initial species richness **(A)**, total biomass (shown as biovolume; **B**), and Pielou's evenness (J'; **C**); bloom peak species richness **(D)**; within treatment variation (as Bray-Curtis dissimilarity (B-C_{intra}); **E**), and Pielou's evenness (J′, **F**). Filled gray dots represent treatment means (±95% CI), while open dots show the single replicates of the bloom peak samples. Asterisks denote statistically significant differences from the control detected with Tukey HSD tests (*$p < 0.05$, **$p < 0.01$, ***$p < 0.001$).

treatment (*D1* and *D2*) and in the strong dilution of stressed treatment (*SxD2*). Compared to the control, the decreases were six and nine species, respectively (**Figure 2A**). Both filtration treatment levels, as well as the heat stressed treatment (*S*), reduced initial richness by two species compared to the control (**Figure 2A**).

The total species pool in the initial samples consisted of 30 species, of which 22 were present in the control treatment (*Co*) (**Figures 1**, **2A**, **3**). Generally, the vast majority (i.e., 22) of the species in the total pool was rare, including 12 species that were additionally large and/or sensitive (**Figures 1**, **3**).

Dilution successfully implemented the loss of rare species. In both levels of the dilution treatment (*D1* and *D2*), 14 species were absent from the total species pool, of which 13 were initially defined as rare (**Figure 3**). Likewise, in the two levels of the dilution of stressed treatment (*SxD1* and *SxD2*) almost only rare species were absent from the total species pool. That is, in the weak dilution of stressed treatment (*SxD1*), 11 species were missing from the total species pool, of which 10 were rare. In the strong dilution of stressed treatment (*SxD2*), 15 of the 17 missing species were rare (**Figure 3**).

Filtration only partially removed large species. In both levels (*F1* and *F2*), five of the ten species that were missing from the total species pool were large (**Figure 3**). However, six species that we initially categorized as large species were still found in both levels of the filtration treatment (**Figure 3**). All of them appeared in low abundances in the fine filtration (*F2*), but some of them were frequent in the coarse filtration (*F1*). As a side effect, both filtration treatment levels also removed five small rare species (**Figure 3**). This is comparable to the absence of rare species in the control treatment and can be attributed to detection limits (i.e., not all species were found in the sub-sample of the initial communities).

Heat stress successfully removed sensitive species. Ten species from the total species pool were missing in the heat stressed treatment (*S*), of which four were sensitive (Se; **Figure 3**). Considering the fact that we initially defined five species as sensitive (**Figure 1**), a high proportion of sensitive species were effectively lost with heat stress. Similarly, in the two levels of the dilution of heat stressed treatment, three out of five sensitive species were missing (**Figure 3**). All but one of the remaining missing species in the heat stressed treatment (S) were rare (**Figure 3**).

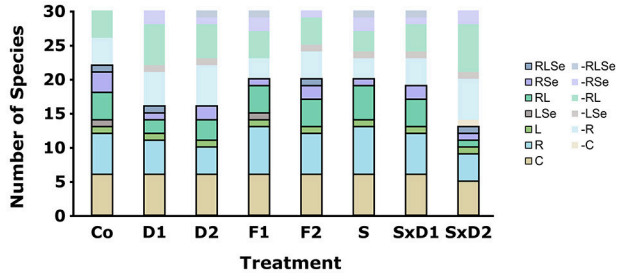

FIGURE 3 | Initial number of species belonging to the different categories. Species were defined as common (C), rare (R), large (L), rare large (RL), rare sensitive (RSe), large sensitive (LSe) or rare large sensitive (RLSe) as seen in **Figure 1** and abbreviated as in **Table 2**. Opaque bars framed by black lines depict the number of species present in each category while transparent bars show categories of species missing from the total species pool of 30 species.

The treatments differentially affected initial total biomass. Reduction of total biomass in the strong dilutions (*D2* and *SxD2*) was highest (99% compared to the control; **Figure 2B**). The heat stressed treatment (*S*) and the coarse filtration (*F1*) reduced total initial biomass by 15% compared to the control (**Figure 2B**). Reduction in the fine filtration (*F2*) and weak dilutions (*D1* and *SxD1*) was intermediate ranging from 68 to 88% (**Figure 2B**).

Those treatments that substantially reduced the initial total biomass (i.e., *F2*, *D1 SxD1*, *D2*, *SxD2*; **Figure 2B**) had the biggest influence on community composition which is reflected in the alignment of the community similarities along the initial biomass dilution gradient (**Figure 4A**). Whereas, the community composition of the heat stressed treatment (*S*) and the coarse filtration (*F1*) remained very close to the control (60% similarity in community structure, **Figure 4A**), the strong dilutions (*D2* and *SxD2*) were least similar in their community structures to all other treatments (<20% similarity, **Figure 4A**).

Initially, *Thalassiosira sp.* (THA) was the dominant species in most treatments according to biomass data, followed by *Skeletonema costatum* (SKE) and *Detonula confervaceae* (DET). These three species together contributed over 70% to total biomass in nearly all treatments. Only the strongly diluted treatments (*D2* and *SxD2*) were dominated by other species. In the strong dilution (*D2*), *Ceratium fusus* (CER) was the dominant species (41% contribution to total biomass) and in the strong dilution of stressed treatment (*SxD2*), the primarily benthic diatom *Licmophora sp.* (LIC) was the most dominant species (45% biomass; **Figure 4A**, Supplementary Table 2). This was caused by the extremely large cell-size of individual CER and LIC in relation to the here concurrently diluted contribution to biomass of smaller-sized THA and DET. Though community compositions largely differed between the treatments, initial Pielou's evenness remained similar in all species loss scenarios (between 0.5 and 0.6; **Figure 2C**).

Treatment Effects at Bloom Peak

Compared to the initial values, species richness, evenness, community composition, and hence similarity between the communities changed in all treatments, including the control. In the control, the average species richness at bloom peak was 13 (**Figure 2D**), a decrease by nine species compared to experimental onset (**Figure 2A**). Likewise, evenness at bloom peak decreased by 0.11 in the control compared to the initial value (**Figure 2C**), resulting in an average value of 0.45 (**Figure 2F**). Since a decrease in species richness and Pielou's evenness was apparent in all treatments, the control remained the most species rich and evenly distributed treatment at bloom peak (**Figures 2D,F**).

The strongly diluted treatments (*D2* and *SxD2*), that initially led to the strongest species loss, still showed a significantly lower species richness at bloom peak compared to the control (**Figure 2D**). In the strong dilution (*D2*), richness declined by

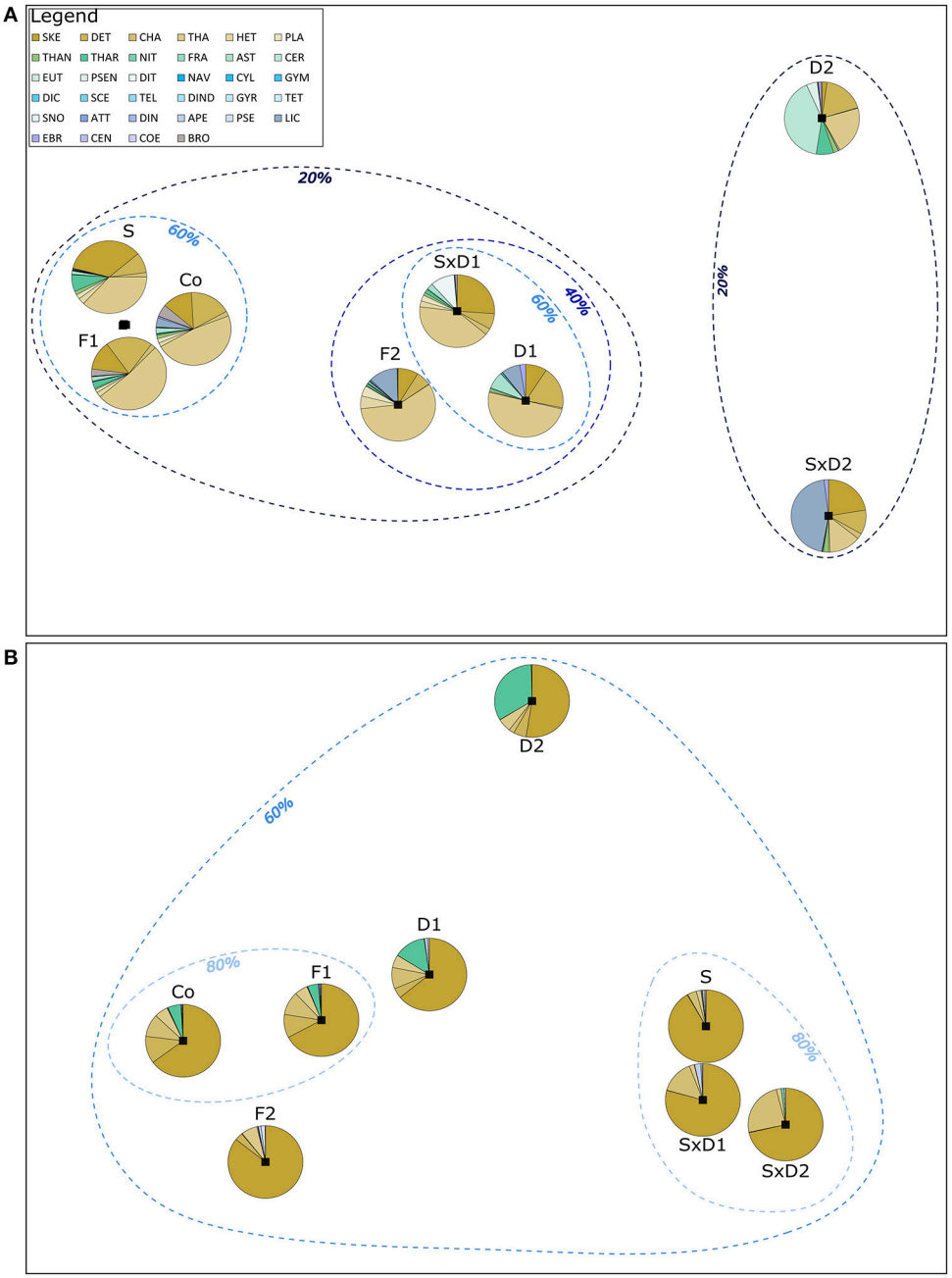

FIGURE 4 | Schematic representation of community similarities between the different treatments. The distances are based on MDS plots that were obtained by calculating a Bray-Curtis dissimilarity matrix (B-C_{inter}) between the replicates of each treatment. The overlain pie charts show initial **(A)** and bloom peak **(B)** species composition in the different treatments. The dashed lines depict percentages of community composition similarities between different treatments. Pie diagrams represent average species composition based on biomass data. In **(A)**, the pie charts for *S*, *F1*, and *Co* correspond to highly similar data points overlapping in between these three pie charts. *F1* and *Co* of the initial samples had a similarity of more than 80%, but this could not be represented graphically. Legend with color-coded species abbreviations is valid for both, *a* and *b*. 2D stress for **(A,B)**: 0.01.

four species and in the combination of heat stress and strong dilution (*SxD2*) it declined by six species (**Figure 2D**; Tukey HSD: $p = 0.002$ and < 0.001, respectively; for ANOVA results see **Table 3**). The latter effect seemed largely driven by the strong dilution because heat stress alone did not result in a significant species loss at bloom peak compared to the control (**Figure 2D**; Tukey HSD: $p = 0.99$; ANOVA results in **Table 3**). Filtration did not have a lasting significant effect on species richness at bloom peak [**Figure 2D**, Tukey HSD: $p = 0.95$ (*F1*) and $p = 0.55$ (*F2*); ANOVA results in **Table 3**].

TABLE 3 | ANOVA results showing the effects of the factors dilution, filtration, heat stress and the interaction between dilution and heat stress on species richness, Pielou's Evenness (J'), and within-treatment variation (B-C_{intra}) at bloom peak.

Response	Factor	df	Sums of squares	Mean squares	F	*p*-value
Richness	whole model	7,24	106.40	15.20	9.23	**<0.001**
	dilution	2	91.13	45.56	27.68	**<0.001**
	filtration	2	5.13	2.56	1.56	0.231
	stress	1	9.37	9.37	5.70	**0.025**
	dilution:stress	2	0.75	0.38	0.23	0.798
J′	whole model	7,24	3.44	0.49	2.56	**0.040**
	dilution	2	0.01	<0.01	0.02	0.986
	filtration	2	0.68	0.34	1.76	0.194
	stress	1	1.97	1.97	10.26	**0.004**
	dilution:stress	2	0.79	0.40	2.07	0.149
B-C_{intra}	whole model	7,24	6.78	0.97	28.63	**<0.001**
	dilution	2	4.10	2.05	60.65	**<0.001**
	filtration	2	0.97	0.49	14.38	**<0.001**
	stress	1	0.89	0.89	26.16	**<0.001**
	dilution:stress	2	0.82	0.41	12.10	**<0.001**

Statistically significant results ($p < 0.05$) are displayed in bold letters.

At bloom peak, the treatments were more equal in their species composition compared to the initial samples. Whereas, similarity of the community structure of some treatments were initially <20% (**Figure 4A**), similarity at bloom peak was more than 60% between all treatments (**Figure 4B**). This was mainly caused by the dominance of SKE that contributed at least 52% to total biomass in all treatments at bloom peak (**Figure 4B**, Supplementary Table 3).

Generally, community composition of the treatments at bloom peak was no longer mainly influenced by the dilution gradient; instead the level of heat stress had the most pronounced effect on community composition and similarity between treatments (**Figure 4B**). This effect was driven by even stronger dominance (90%) of SKE in the heat stressed treatment compared to the control (65%), and by the strong joined dominance of SKE and CHA in the dilution of stressed communities (**Figure 4B**, Supplementary Table 3). Even though heat stress did not affect Pielou's evenness initially (**Figure 2C**), the strong dominance of SKE in the heat stressed community significantly decreased evenness at bloom peak (J' = 0.16) compared to the control (J' = 0.45; **Figure 2F**; Tukey HSD: $p = 0.038$; ANOVA results in **Table 3**). SKE is a species that has been observed to have higher growth rates under warmer conditions and performs best in temperatures between 20 and 24°C (Sanchez et al., 1995). The initial effects of filtration (*F1* and *F2*) and weak dilution (*D1*) on community composition (**Figure 4A**) were not mirrored at bloom peak. Thus, community compositions in these treatments were similar to the control (**Figure 4B**).

Within-Treatment Variation

As an important side-effect, we observed high within-treatment variation (dissimilarity between replicates of a treatment, B-C_{intra}) in most dilutions (D1, *D2*, and *SxD2*) and in the fine filtration (*F2)* treatment (**Figure 2E**). Random effects, such as differing species-specific relative contribution to total biomass, or the absence and presence of certain species in replicates of the same treatment (Supplementary Figure 1), could manifest themselves in the treatments that initially decreased total biomass (**Figure 2B**). More precisely, the weak dilution (*D1*) had two pairs of replicates that were alike but differed from the other two replicates (Supplementary Figure 1). The strong dilution (*D2*) had one replicate that contained a large biomass of *Thalassiosira rotula* (THAR), contributing 40% to total biomass, while the other three replicates did not contain any THAR at all. In the strong dilution of stressed treatment (*SxD2*), two replicates had very high proportions (47 and 61%) of *Chaetoceros spp*. (CHA), while the other two replicates had minimal amounts of CHA (0.8 and 3.2%). In the strong filtration treatment (*F2*), one replicate differed from the rest in that it contained a larger proportion of THA and DET compared to the other three replicates (Supplementary Figure 1). Consequently, as stated above, B-C_{intra} clearly coincided with the amount of initially removed biomass in the different treatments. The only exception to this pattern was the weak dilution of stressed treatment (*SxD1*), in which the replicates were very homogenous at bloom peak (Supplementary Figure 1), resulting in a significantly lower B-C_{intra} value than in the control (**Figure 2E**).

DISCUSSION

Using non-random species loss scenarios for experiments in community ecology is becoming increasingly important, because it allows for a more realistic approach to predict phytoplankton communities' functional reaction to changing environmental conditions. The here tested methods advance the marine sciences in two ways: first, they give the opportunity for more realistic experiments in phytoplankton community ecology and second, they allow a quantification of the hidden treatment effect due to initial variation of phytoplankton density. Certainly, these two factors are linked—in that the dilutive manipulations always alter both species richness and species identities simultaneously.

Essentially, all three treatments (dilution, heat stress, and filtration) reduced richness of the targeted species groups. That is, dilution effectively removed rare (decrease by 93% compared to the total species pool) and heat stress sensitive species (decrease by 80% compared to the total species pool). Filtration removed some of the large species, but the success rate was only 50% removal compared to the total species pool.

Effects of Dilution

Successful decrease of species richness due to dilution at the onset of the bloom (**Figure 2A**) translated into lower species richness at bloom peak (**Figure 2D**), but did not significantly influence Pielou's evenness at bloom peak (**Figure 2F**). Since rare species are statistically more likely to be excluded from a smaller inoculum, we expected an initial decrease in species richness. Problematic is that even though dilution lead to the effective loss of rare species, it was not possible to control which species were lost in replicates of the same

treatment. This lead to a high variability of species present at bloom peak, causing more heterogeneous responses in species composition and evenness between replicates of the same treatment (**Figure 2F**, Supplementary Figure 1). In experiments studying the effect of species loss on ecosystem processes, the high variability of species causes problems, because the effects observed in these experiments cannot clearly be attributed to the decrease in richness. It could just as likely be an effect of species identity carrying certain functional traits. Furthermore, in many experiments—especially those focusing on species traits—species identity is of great importance. For example, in grazing experiments it is essential to distinguish whether edible or inedible species are lost. In certain climate change studies, it is of great interest if calcifying coccolithophores or silicifying diatoms are lost. In these cases, our methods of non-random species loss should be modified (e.g., by using other stress factors) or might not be suited at all.

To eliminate the problem of not only decreasing species numbers, but also losing random species traits in different replicates of the same treatment, the inoculum size could be adjusted so that starting densities between treatments would be more comparable. In culture experiments with bacteria, this is already practiced (Franklin et al., 2001; Hol et al., 2015). For this, the diluted community is allowed to grow for several days such that an increase in biomass can be achieved before the start of the experiment. However, to the best of our knowledge, this method has not been used for phytoplankton and therefore should be tested experimentally. It has to be confirmed that rare phytoplankton species are actually removed from the culture in the long run and cannot grow back to original numbers if the inoculum is re-grown.

Nevertheless, for experiments that only focus on species richness, dilution is a good method to create non-randomly assembled communities. With dilution, distinct gradients of species richness can be created (Roger et al., 2016; Hammerstein et al., 2017), which is a large improvement over traditional culture experiments with randomly assembled communities. Furthermore, some experimental ecologists have used this side effect of dilution to their advantage. Trommer et al. (2012) for example, aimed at reaching high variation within treatments to increase ecological noise and make the community response broader. In addition to being an experimental manipulation method, the dilution treatment can be useful for other applications, such as long-term phytoplankton evolution experiments. In these experiments, researchers use semi-continuous culturing approaches where each new culture is established as a (diluted) inoculum of the former (Lohbeck et al., 2012; Schlüter et al., 2014). For these types of experiments, the tested levels of dilution allow to estimate the potential loss of genotypes at each step.

In general, dilution can be used as a standard method to lose rare species or genotypes in natural phytoplankton communities, for experiments that only manipulate richness. For experiments with an additional focus on species identities, some adjustments should be made to the dilution method and within-treatment variation should be considered.

Effects of Heat Stress

Heat stress successfully decreased species richness of sensitive species (**Figure 2A**). This did not have an immediate effect on community composition (**Figure 4A**), but was reflected at bloom peak by the extreme dominance of a warm-adapted species (**Figure 4B**). For this manipulation it is helpful to have a good knowledge of the community present at the onset of the experiment, because that allows for fine-tuning of the heat stress treatment (e.g., setting a specific target temperature or exposing species to a certain temperature for a specific time frame). Other methods to target different types of sensitive species are also feasible. Hammerstein et al. (2017) used a mechanical disturbance by shaking the cultures to create communities with distinct gradients of species richness with the goal to lose sensitive species. Summarizing, heat stress can be one successful method to lose sensitive species in natural phytoplankton communities.

Effects of Filtration

In this study, fine filtration (20 μm) successfully decreased initial richness (**Figure 2A**), and similarly to the dilution treatment, reduced initial biomass (**Figure 2B**). The observed effects on within-treatment variability at bloom peak were also comparable to dilution (**Figure 2E**). This problem can easily be mitigated by adjusting the inoculum volume of the filtration treatment so that it contains comparable phytoplankton densities to the control.

A disadvantage of the filtration method was that it did not completely remove all large species. Many large species are long and thin, which means that individuals could still pass through the sieve if they reach it in the right angle. This can create a bias in size class categorization (Graham and Jones, 2007). Sieving the samples multiple times could minimize this problem. In contrast to this, cells of some species that were not defined as large were filtered out in this treatment. This included genera like *Skeletonema*, *Chaetoceros*, and *Detonula*, which are chain-forming and therefore accumulate to a greater size (Round et al., 1990). The individual cell size, however, can be smaller than the colony size. In this case, it has to be clarified whether an individual cell or the entire colony is categorized in a specific size class. Related to this, the special morphology of some genera, including *Chaetoceros,* can also lead to a size class bias. *Chaetoceros* cells themselves may not have an average dimension exceeding 20 μm, but many species of this genus are conspicuous due to long spines protruding from the valves (Round et al., 1990). We also observed this in the present study: the overall largest cell dimension including spines often exceeded 20 μm and therefore fewer cells of this genus were found in the filtration treatment. The morphology and life history of species has to be considered when targeting specific species for removal.

Another challenge to the accuracy of the filtration treatment in our experiment is based on the definition for large species that we employed (i.e., the largest cell dimension exceeds 20 μm). We chose this definition due to the scarcity of species exceeding 100 μm in size. We still found several species initially categorized as large in the coarse filtration treatment (*F1*), for which we had used the 100 μm sieve (**Figure 2**). In

other studies, the definition of large species might be chosen differently as there may be predominantly species in larger size classes, depending on the sampling location and time of the year.

If all these complications are considered, filtration can be a successful method to test the ecosystem consequences of manipulating the "master trait" cell size in experimental phytoplankton communities.

CONCLUSION

In general, the tested manipulations of non-random species loss allow to assess the effects of realistic phytoplankton diversity change. These methods can be used to manipulate species composition for a wide variety of biodiversity experiments independent of their scale (i.e., micro- and mesocosm) or location (i.e., outdoor and indoor). However, researchers should take special care to avoid the pitfalls of the dilution and filtration methods, especially when species identities are important for the experimental outcome. All in all, these methods are a valuable improvement for hitherto artificially assembled phytoplankton communities in biodiversity—ecosystem functioning experiments, simply because non-random species loss is more realistic (Gamfeldt et al., 2015).

AUTHOR CONTRIBUTIONS

BM, AL, and SE conceived the study. FE conducted the experiment and analyzed the data. FE, BM, AL, and SE wrote the manuscript. All authors agree on the final version of this manuscript and agree to be accountable for all aspects of this work.

FUNDING

The research was funded by internal grants from the GEOMAR Helmholtz Centre for Ocean Research Kiel.

ACKNOWLEDGMENTS

We thank Thomas Hansen and Bente Gardeler for technical assistance and two reviewers for their helpful comments on the manuscript.

SUPPLEMENTARY MATERIAL

The Supplementary Material for this article can be found online at: http://journal.frontiersin.org/article/10.3389/fmars.2017.00317/full#supplementary-material

REFERENCES

Acevedo-Trejos, E., Brandt, G., Bruggeman, J., and Merico, A. (2014). Mechanisms shaping size structure and functional diversity of phytoplankton communities in the ocean. *Sci. Rep.* 5:8918. doi: 10.1038/srep08918

Aksnes, D. L., and Egge, J. K. (1991). A theoretical model for nutrient uptake in phytoplankton. *Mar. Ecol. Prog. Ser.* 70, 65–72. doi: 10.3354/meps070065

Barnosky, A. D., Matzke, N., Tomiya, S., Wogan, G. O. U., Swartz, B., Quental, T. B., et al. (2011). Has the Earth's sixth mass extinction already arrived? *Nature* 471, 51–57. doi: 10.1038/nature09678

Bracken, M. E. S., Friberg, S. E., Gonzalez-Dorantes, C. A., and Williams, S. L. (2008). Functional consequences of realistic biodiversity changes in a marine ecosystem. *Proc. Natl. Acad. Sci. U.S.A.* 105, 924–928. doi: 10.1073/pnas.0704103105

Bracken, M. E. S., and Low, N. H. N. (2012). Realistic losses of rare species disproportionately impact higher trophic levels. *Ecol. Lett.* 15, 461–467. doi: 10.1111/j.1461-0248.2012.01758.x

Bray, J. R., and Curtis, J. T. (1957). An ordination of the upland forest communities of Southern Wisconsin. *Ecol. Monogr.* 27, 325–349. doi: 10.2307/1942268

Brock, T. D. (1981). Calculating solar radiation for ecological studies. *Ecol. Modell.* 14, 1–19. doi: 10.1016/0304-3800(81)90011-9

Cardinale, B. J., Duffy, J. E., Gonzalez, A., Hooper, D. U., Perrings, C., Venail, P., et al. (2012). Biodiversity loss and its impact on humanity. *Nature* 486, 59–67. doi: 10.1038/nature11148

Clarke, K. R., Somerfield, P. J., and Chapman, M. G. (2006). On resemblance measures for ecological studies, including taxonomic dissimilarities and a zero-adjusted Bray-Curtis coefficient for denuded assemblages. *J. Exp. Mar. Biol. Ecol.* 330, 55–80. doi: 10.1016/j.jembe.2005.12.017

Daufresne, M., Lengfellner, K., and Sommer, U. (2009). Global warming benefits the small in aquatic ecosystems. *Proc. Natl. Acad. Sci. U.S.A.* 106, 12788–12793. doi: 10.1073/pnas.0902080106

Davies, K. F., Margules, C. R., and Lawrence, J. F. (2004). A synergistic effect puts rare, specialized species at greater risk of extinction. *Ecology* 85, 265–271. doi: 10.1890/03-0110

de Meester, L., Vanoverbeke, J., Kilsdonk, L. J., and Urban, M. C. (2016). Evolving perspectives on monopolization and priority effects. *Trends Ecol. Evol.* 31, 136–146. doi: 10.1016/j.tree.2015.12.009

Eggers, S. L., Eriksson, B. K., and Matthiessen, B. (2012). A heat wave and dispersal cause dominance shift and decrease biomass in experimental metacommunities. *Oikos* 121, 721–733. doi: 10.1111/j.1600-0706.2011.19714.x

Eggers, S. L., and Matthiessen, B. (2013). Initial dominance in coccolithophore communities affects community structure but does not translate into altered community functioning. *Mar. Ecol. Prog. Ser.* 473, 67–77. doi: 10.3354/meps10064

Elmqvist, T., Folke, C., Nyström, M., Peterson, G., Bengtsson, J., Walker, B., et al. (2003). Response diversity, ecosystem change, and resilience. *Front. Ecol. Environ.* 1, 488–494. doi: 10.1890/1540-9295(2003)001[0488:RDECAR]2.0.CO;2

Falkowski, P. G., Barber, R. T., and Smetacek, V. (1998). Biogeochemical controls and feedbacks on ocean primary production. *Science* 281, 200–206. doi: 10.1126/science.281.5374.200

Field, C. B., Behrenfeld, M. J., Randerson, J. T., and Falkowski, P. (1998). Primary production of the biosphere: integrating terrestrial and oceanic components. *Science* 281, 237–240. doi: 10.1126/science.281.5374.237

Frankham, R. (2005). Genetics and extinction. *Biol. Conserv.* 126, 131–140. doi: 10.1016/j.biocon.2005.05.002

Franklin, R. B., Garland, J. L., Bolster, C. H., and Mills, A. L. (2001). Impact of dilution on microbial community structure and functional potential: comparison of numerical simulations and batch culture experiments. *Appl. Environ. Microbiol.* 67, 702–712. doi: 10.1128/AEM.67.2.702-712.2001

Gamfeldt, L., Lefcheck, J. S., Byrnes, J. E. K., Cardinale, B. J., Duffy, J. E., and Griffin, J. N. (2015). Marine biodiversity and ecosystem functioning: what's known and what's next? *Oikos* 124, 252–265. doi: 10.1111/oik.01549

Graham, J. L., and Jones, J. R. (2007). Microcystin distribution in physical size class separations of natural plankton communities. *Lake Reserv. Manag.* 23, 161–168. doi: 10.1080/07438140709353919

Gross, K., and Cardinale, B. J. (2005). The functional consequences of random vs. ordered species extinctions. *Ecol. Lett.* 8, 409–418. doi: 10.1111/j.1461-0248.2005.00733.x

Hammerstein, S. K., Stockenreiter, M., and Stibor, H. (2017). Directed diversity manipulations within natural phytoplankton communities. *Limnol. Oceanogr. Methods* 15, 653–662. doi: 10.1002/lom3.10190

Harnik, P. G., Simpson, C., and Payne, J. L. (2012). Long-term differences in extinction risk among the seven forms of rarity. *Proc. R. Soc. B* 279, 4969–4976. doi: 10.1098/rspb.2012.1902

Hillebrand, H. Dürselen, C.-D., Kirschtel, D., Pollingher, U., and Zohary, T. (1999). Biovolume calculation for pelagic and benthic microalgae. *J. Phycol.* 424, 403–424. doi: 10.1046/j.1529-8817.1999.3520403.x

Hofmann, M., Worm, B., Rahmstorf, S., and Schellnhuber, H. J. (2011). Declining ocean chlorophyll under unabated anthropogenic CO_2 emissions. *Environ. Res. Lett.* 6:34035. doi: 10.1088/1748-9326/6/3/034035

Hol, W. H. G., Garbeva, P., Hordijk, C. A., Hundscheid, M. P. J., Klein Gunnewiek, P. J. A., van Agtmaal, M., et al. (2015). Non-random species loss in bacterial communities reduces antifungal volatile production. *Ecology* 96, 2042–2048. doi: 10.1890/14-2359.1

Hooper, D. U., Adair, E. C., Cardinale, B. J., Byrnes, J. E. K., Hungate, B. A., Matulich, K. L., et al. (2012). A global synthesis reveals biodiversity loss as a major driver of ecosystem change. *Nature* 486, 105–108. doi: 10.1038/nature11118

Hooper, D. U., Chapin, F. S. III., and Ewel, J. J. (2005). Effects of biodiversity on ecosystem functioning: a consensus of current knowledge. *Ecol. Monogr.* 75, 3–35. doi: 10.1890/04-0922

IPCC (2014). *Climate Change 2014. Synthesis Report. Contribution of Working Groups I, II and III to the Fifth Assessment Report of the Intergovernmental Panel on Climate Change*. eds R. K. Pachauri and L. A. Meyer (Geneva: IPCC).

Jain, M., Flynn, D. F. B., Prager, C. M., Hart, G. M., Devan, C. M., Ahrestani, F. S., et al. (2014). The importance of rare species: a trait-based assessment of rare species contributions to functional diversity and possible ecosystem function in tall-grass prairies. *Ecol. Evol.* 4, 104–112. doi: 10.1002/ece3.915

Jousset, A., Bienhold, C., Chatzinotas, A., Gallien, L., Gobet, A., Kurm, V., et al. (2017). Where less may be more: how the rare biosphere pulls ecosystems strings. *ISME J.* 11, 853–862. doi: 10.1038/ismej.2016.174

Lande, R. (1993). Risks of population extinction from demographic and environmental stochasticity and random catastrophes. *Am. Nat.* 142, 911–927. doi: 10.1086/285580

Leitão, R. P., Zuanon, J., Villéger, S., Williams, S. E., Baraloto, C., Fortunel, C., et al. (2016). Rare species contribute disproportionately to the functional structure of species assemblages. *Proc. R. Soc. B* 283:20160084. doi: 10.1098/rspb.2016.0084

Lewandowska, A. M., Boyce, D. G., Hofmann, M., Matthiessen, B., Sommer, U., and Worm, B. (2014). Effects of sea surface warming on marine plankton. *Ecol. Lett.* 17, 614–623. doi: 10.1111/ele.12265

Lohbeck, K. T., Riebesell, U., and Reusch, T. B. H. (2012). Adaptive evolution of a key phytoplankton species to ocean acidification. *Nat. Geosci.* 5, 346–351. doi: 10.1038/ngeo1441

Lyons, K. G., Brigham, C. A., Traut, B. H., and Schwartz, M. W. (2005). Rare species and ecosystem functioning. *Conserv. Biol.* 19, 1019–1024. doi: 10.1111/j.1523-1739.2005.00106.x

Mara-ón, E. (2014). Cell size as a key determinant of phytoplankton metabolism and community structure. *Ann. Rev. Mar. Sci.* 7, 241–264. doi: 10.1146/annurev-marine-010814-015955

McCauley, D. J., Pinsky, M. L., Palumbi, S. R., Estes, J. A., Joyce, F. H., and Warner, R. R. (2015). Marine defaunation: animal loss in the global ocean. *Science* 347:1255641. doi: 10.1126/science.1255641

Mensens, C., De Laender, F., Janssen, C. R., Sabbe, K., and De Troch, M. (2015). Stressor-induced biodiversity gradients: revisiting biodiversity-ecosystem functioning relationships. *Oikos* 124, 677–684. doi: 10.1111/oik.01904

Morán, X. A. G., López-Urrutia, Á., Calvo-Díaz, A., and Li, W. K. W. (2010). Increasing importance of small phytoplankton in a warmer ocean. *Glob. Chang. Biol.* 16, 1137–1144. doi: 10.1111/j.1365-2486.2009.01960.x

Mouillot, D., Bellwood, D. R., Baraloto, C., Chave, J., Galzin, R., Harmelin-Vivien, M., et al. (2013). Rare species support vulnerable functions in high-diversity ecosystems. *PLoS Biol.* 11:e1001569. doi: 10.1371/journal.pbio.1001569

Norberg, J., Swaney, D. P., Dushoff, J., Lin, J., Casagrandi, R., and Levin, S. A. (2001). Phenotypic diversity and ecosystem functioning in changing environments: a theoretical framework. *Proc. Natl. Acad. Sci. U.S.A.* 98, 11376–11381. doi: 10.1073/pnas.171315998

O'Grady, J. J., Brook, B. W., Reed, D. H., Ballou, J. D., Tonkyn, D. W., and Frankham, R. (2006). Realistic levels of inbreeding depression strongly affect extinction risk in wild populations. *Biol. Conserv.* 133, 42–51. doi: 10.1016/j.biocon.2006.05.016

Oksanen, J., Blanchet, F. G., Friendly, M., Kindt, R., Legendre, P., McGlinn, D., et al. (2017). *Vegan: Community Ecology Package*. R package version 2.4-4. Available online at: https://CRAN.R-project.org/package=vegan

Peter, K. H., and Sommer, U. (2012). Phytoplankton cell size: intra- and interspecific effects of warming and grazing. *PLoS ONE* 7:e49632. doi: 10.1371/journal.pone.0049632

Pielou, E. C. (1966). The measurement of diversity in different types of biological collections. *J. Theor. Biol.* 13, 131–144. doi: 10.1016/0022-5193(66)90013-0

Clarke, K. R., and Gorley, R. N. (2006). *PRIMER v6: User Manual/Tutorial*. PRIMER-E, Plymouth.

Rabinowitz, D. (1981). "Seven forms of rarity," in *The Biological Aspects of Rare Plant Conservation*, ed H. Synge (Chichester: John Wiley), 205–217.

Radchuk, V., De Laender, F., Van den Brink, P. J., and Grimm, V. (2015). Biodiversity and ecosystem functioning decoupled: invariant ecosystem functioning despite non-random reductions in consumer diversity. *Oikos* 125, 424–433. doi: 10.1111/oik.02220

Raven, J. A. (1998). The twelfth tansley lecture. small is beautiful: the picophytoplankton. *Funct. Ecol.* 12, 503–513. doi: 10.1046/j.1365-2435.1998.00233.x

R Core Team (2017). *R: A Language and Environment for Statistical Computing*. Vienna: R Foundation for Statistical Computing.

Reusch, T. B. H., Ehlers, A., Hämmerli, A., and Worm, B. (2005). Ecosystem recovery after climatic extremes enhanced by genotypic diversity. *Proc. Natl. Acad. Sci. U.S.A.* 102, 2826–2831. doi: 10.1073/pnas.0500008102

Roger, F., Bertilsson, S., Langenheder, S., Osman, O. A., and Gamfeldt, L. (2016). Effects of multiple dimensions of bacterial diversity on functioning, stability and multifunctionality. *Ecology* 97, 2716–2728. doi: 10.1002/ecy.1518

Round, F. E., Crawford, R. M., and Mann, D. G. (1990). *The Diatoms: Biology and Morphology of the Genera*. Cambridge: Cambridge University Press.

Sanchez, S., Martinez, M. E., Molina, E., and de la Casa, J. A. (1995). The influence of temperature on the growth and fatty acid composition of *Skeletonema costatum* in a batch photobioreactor. *J. Chem. Technol. Biotechnol.* 62, 148–152. doi: 10.1002/jctb.280620206

Schlüter, L., Lohbeck, K. T., Gutowska, M. A., Groger, J. P., Riebesell, U., and Reusch, T. B. H. (2014). Adaptation of a globally important coccolithophore to ocean warming and acidification. *Nat. Clim. Chang.* 4, 1024–1030. doi: 10.1038/nclimate2379

Selmants, P. C., Zavaleta, E. S., Pasari, J. R., and Hernandez, D. L. (2012). Realistic plant species losses reduce invasion resistance in a California serpentine grassland. *J. Ecol.* 100, 723–731. doi: 10.1111/j.1365-2745.2011.01949.x

Selmants, P. C., Zavaleta, E. S., and Wolf, A. A. (2014). Realistic diversity loss and variation in soil depth independently affect community-level plant nitrogen use. *Ecology* 95, 88–97. doi: 10.1890/13-1192.1

Solan, M., Cardinale, B. J., Downing, A. L. A., Engelhardt, K. M., Ruesink, J. L., and Srivastava, D. S. (2004). Extinction and ecosystem function in the marine benthos. *Science* 306, 1177–1180. doi: 10.1126/science.1103960

Sommer, U., Aberle, N., Lengfellner, K., and Lewandowska, A. (2012). The baltic sea spring phytoplankton bloom in a changing climate: an experimental approach. *Mar. Biol.* 159, 2479–2490. doi: 10.1007/s00227-012-1897-6

Sommer, U., and Lewandowska, A. (2011). Climate change and the phytoplankton spring bloom: warming and overwintering zooplankton have similar effects on phytoplankton. *Glob. Chang. Biol.* 17, 154–162. doi: 10.1111/j.1365-2486.2010.02182.x

Stachowicz, J. J., Best, R. J., Bracken, M. E. S., and Graham, M. H. (2008). Complementarity in marine biodiversity manipulations: reconciling divergent evidence from field and mesocosm experiments. *Proc. Natl. Acad. Sci. U.S.A.* 105, 18842–18847. doi: 10.1073/pnas.0806425105

Trommer, G., Pondaven, P., Siccha, M., and Stibor, H. (2012). Zooplankton-mediated nutrient limitation patterns in marine phytoplankton: an experimental approach with natural communities. *Mar. Ecol. Prog. Ser.* 449, 83–94. doi: 10.3354/meps09508

Urban, M. C., and De Meester, L. (2009). Community monopolization: local adaptation enhances priority effects in an evolving metacommunity. *Proc. R. Soc. B* 276, 4129–4138. doi: 10.1098/rspb.2009.1382

Utermöhl, H. (1958). Zur Vervollkommnung der quantitativen Phytoplankton Methodik. *Mitteilungen Int. Vereinigung Theor. Angew. Limnol.* 9, 263–272.

Walker, B., Kinzig, A., and Langridge, J. (1999). Attribute diversity, resilience, and ecosystem function: the nature and significance of dominant and minor species. *Ecosystems* 2, 95–113. doi: 10.1007/s100219900062

Werner, F. J., Graiff, A., and Matthiessen, B. (2016). Temperature effects on seaweed-sustaining top-down control vary with season. *Oecologia* 180, 889–901. doi: 10.1007/s00442-015-3489-x

Winder, M., and Sommer, U. (2012). Phytoplankton response to a changing climate. *Hydrobiologia* 698, 5–16. doi: 10.1007/s10750-012-1149-2

Zavaleta, E. S., and Hulvey, K. B. (2004). Realistic species losses disproportionately reduce grassland resistance to biological invaders. *Science* 306, 1175–1177. doi: 10.1126/science.1102643

Conflict of Interest Statement: The authors declare that the research was conducted in the absence of any commercial or financial relationships that could be construed as a potential conflict of interest.

Advantages of publishing in Frontiers

OPEN ACCESS
Articles are free to read for greatest visibility and readership

FAST PUBLICATION
Around 90 days from submission to decision

HIGH QUALITY PEER-REVIEW
Rigorous, collaborative, and constructive peer-review

TRANSPARENT PEER-REVIEW
Editors and reviewers acknowledged by name on published articles

Frontiers
Avenue du Tribunal-Fédéral 34
1005 Lausanne | Switzerland

Visit us: www.frontiersin.org
Contact us: info@frontiersin.org | +41 21 510 17 00

REPRODUCIBILITY OF RESEARCH
Support open data and methods to enhance research reproducibility

DIGITAL PUBLISHING
Articles designed for optimal readership across devices

FOLLOW US
@frontiersin

IMPACT METRICS
Advanced article metrics track visibility across digital media

EXTENSIVE PROMOTION
Marketing and promotion of impactful research

LOOP RESEARCH NETWORK
Our network increases your article's readership